

SYNTHESIS AND REACTIVITY OF π -CONJUGATED TRIAZENES

by

HORACIO ENRIQUE BARRAGAN PEYRANI

Presented to the Faculty of the Graduate School of
The University of Texas at Arlington in Partial Fulfillment
of the Requirements
for the Degree of

DOCTOR OF PHILOSOPHY

THE UNIVERSITY OF TEXAS AT ARLINGTON

May 2019

Copyright © by Horacio Enrique Barragan Peyrani 2019

All Rights Reserved



Acknowledgements

I would like to express my deep gratitude to my supervisor, Dr. Alejandro Bugarin for his excellent mentorship and support during all these years. I greatly appreciate the time he spent sharing his knowledge with me and also encouraging me to pursue my scientific interests, leading by example to motivate me to keep working hard and pushing myself to overcome my limits. Overall, I feel very proud for having been a member of Dr. Bugarin's research group.

I am also very thankful to all my Dissertation Committee Members: Dr. Carl Lovely, Dr. Frank Foss and Dr. Saiful Chowdhury for their guidance and suggestions to improve the quality of my work. I would also like to thank Dr. Junha Jeon who, along with the other Organic Division professors, gave me valuable advice and recommendations to improve my research during our Division Meeting Presentations.

I owe a great debt of gratitude to my research colleagues in the Organic Division and other research labs for all their support, suggestions, invaluable discussions and friendship. I would like to thank Dr. Xiaoyun Huang, Anurag Noonikara Poyil, Olatunji Ojo, Alena Trinidad, Gerardo Yopez, Ravi Singh, Dr. Diego Lopez, Dr. Pawan Thapa, Dr. Parham Asgari, Thiru Avullala, Udaya Dakarapu, Hiep Nguyen, Paola Sotelo and Susana Aguirre-Medel. Thank you all for supporting me when I most needed it.

I would also like to extend my gratitude to UT Arlington's fantastic staff because without their help, all of this would have not been possible. I would like to thank the Administrative Assistants, Mrs. Jill Howard, Mrs. Debbie Cooke and the Graduate Program Coordinator, Stephanie Henry for all their kind help. My great appreciation also goes to Dr. Brian Edwards, Dr. Roy McDougal and Dr. Chuck Savage for their training and great help with the instrumentation I used. I would also like to thank our Undergraduate Lab Coordinators, Dr. William Cleaver and Cynthia Griffith for their support and advice on teaching duties; as

well as the Stockroom Supervisors, Mrs. Beth Klimek, Mr. Jason Lloyd and Mr. James Garner for always kindly providing me with all the supplies I required.

Special thanks to my research collaborators, Dr. Siddappa Patil, whose research helped me to start my own projects, as well as Dr. Haobin Wang and Dr. Chou-Hsun Yang for their excellent computational studies.

I am also enormously thankful to my parents, Elizabeth Peyrani and Horacio Barragan, as well as my grandmothers Esthela Garza and Emma Treviño for being incredible to me and always being there when I needed them; to my dear Cinthya Reyes, whose love and understanding always motivates me to push forward; and to my dear friends: Gerardo Juarez, Arturo Obregon, Miguel Hinojosa, Pana Garza, Esteban Ibarra, Rosaena Garza, Mario Martinez, Gabriela Ramos, Manuel Perera, Diana Sanchez and Luis Garcia for being like my brothers and sisters, for inspiring me and helping me out in more ways than I can count throughout this adventure.

March 7th, 2019

Abstract

SYNTHESIS AND REACTIVITY OF π -CONJUGATED TRIAZENES

Horacio Enrique Barragan Peyrani, PhD

The University of Texas at Arlington, 2019

Supervising Professor: Alejandro Bugarin

The triazene functional group has found numerous applications in organic and medicinal chemistry, with several important chemotherapeutic drugs containing this functionality. In spite of this, the reactivity of π -conjugated triazenes has been scarcely explored. The work described in this dissertation investigates the synthesis and new reactions of π -conjugated triazenes developed in our group, demonstrating the versatility of these molecules that allow access to several functionalities which can serve as building blocks for more complex structures.

Chapter 1 surveys the prior literature of π -conjugated triazenes, describing their known synthesis and reactivity .

In **Chapter 2**, new oxidation and substitution reactions of organic azides through the intermediacy of π -conjugated triazenes are discussed. Oxidation reactions are performed utilizing organic azides, imidazolium salts, and potassium *tert*-butoxide in DMSO to form a triazene intermediate, which readily undergoes oxidation under mild, acid-catalyzed conditions. Additionally, by replacing DMSO for other nucleophiles such as; alcohols or thiols, substitution reactions occur instead which generate ethers and thioethers respectively.

Chapter 3 presents a transition-metal-free aryl-aryl cross-coupling reaction between π -conjugated triazenes and arenes or heteroarenes under UV irradiation (350 nm) in acidic conditions. The biaryls or heterobiaryls are obtained in a straightforward fashion at room temperature and in short reaction times. The reaction can also be performed using sunlight as radiation source. Computational studies suggest that the reaction proceeds through photoisomerization of the triazene to the *Z*-isomer which readily decomposes to produce a reactive aryl cation, which undergoes coupling with its corresponding (hetero)arene.

Finally, in **Chapter 4**, the formation of amides by reacting aryl π -conjugated triazenes with nitriles under UV irradiation (350 nm) is described. Studies with ^{15}N labeled molecules suggest that the reaction involves nucleophilic attack by the nitrile nitrogen to an aryl cation derived from the arene. Due to the similarity in the reaction conditions with the aryl-aryl cross-coupling reaction introduced in the previous chapter, these two methods can be performed in one-pot, introducing both an amide as well as a biaryl group in the same step. This was demonstrated by synthesizing an immunosuppressant using this combined reaction, highlighting the potential synthetic utility of these transformations.

Table of Contents

Acknowledgements	iii
Abstract	v
List of Illustrations	ix
List of Tables	xi
Chapter 1 Introduction and previous works	1
1.1 Introduction to triazenes	1
1.2 Synthesis of π -conjugated triazenes	3
1.3 Previous studies of π -conjugated triazene reactivity	9
1.3.1 Thermally-induced N_2 extrusion	9
1.3.2 Conversion of π -conjugated triazenes to guanidines	11
1.3.3 Diazo and azide transfer reactions	12
1.3.4 Alkylation of π -conjugated triazenes.....	13
1.3.5 π -conjugated triazenes as diazonium sources and as photochemically activated bases	14
Chapter 2 Oxidation and Substitution Reactions	18
2.1 Introduction and initial observations.	18
2.2 Optimization of the reaction conditions	19
2.3 Substrate scope.....	21
2.4 Proposed mechanism for the oxidation reaction	23
2.5 Nucleophilic substitution reactions of π -conjugated triazenes	24
Chapter 3 Photochemically-Activated Aryl-Aryl Cross-Coupling Reactions	31
3.1 Introduction	31
3.2 Reaction design and optimization	33

3.3 Triazene synthesis and substrate scope	36
3.3 Mechanistic and computational studies	42
Chapter 4 Amide Synthesis	52
4.1 Introduction	52
4.2 Initial observation and reaction optimization	54
4.3 Reaction scope	57
4.4 Proposed mechanism	61
Chapter 5 Experimental procedures for Chapter 2	66
Chapter 6 Experimental procedures for Chapters 3 and 4	77
Appendix A List of abbreviations	112
Appendix B ^1H and ^{13}C NMR Spectra	115
References	215
Biographical information	224

List of Illustrations

Figure 1-1 Classes and examples and of triazenes.....	2
Figure 1-2 First synthesis of π -conjugated triazenes.....	3
Figure 1-3 Triazene synthesis using imidazolium salts and azides	4
Figure 1-4 Synthesis of triazene from a free carbene.....	4
Figure 1-5 Synthesis and UV/Vis analysis of benzimidazole-derived triazenes	6
Figure 1-6 Synthesis of aromatic triazenes.....	7
Figure 1-7 Azide scope for triazene synthesis	8
Figure 1-8 Thermally-induced nitrogen extrusion in triazenes.....	10
Figure 1-9 Proposed mechanism for the thermal N ₂ extrusion in triazenes	10
Figure 1-10 Guanidine synthesis from carbene	11
Figure 1-11 Guanidine synthesis from a free carbene.....	11
Figure 1-12 Guanidine and guanidinium salt synthesis from triazene	12
Figure 1-13 Diazo and azide transfer reactions using triazenes	12
Figure 1-14 Alkylation of π -conjugated triazenes	13
Figure 1-15 Synthesis of water-soluble triazenes.....	15
Figure 1-16 Synthesis of azo dyes from triazenes.....	15
Figure 1-17 Photoisomerization and basicity change of triazenes	16
Figure 1-18 π -conjugated triazenes over the years.....	17
Figure 2-1 Initial observation.....	19
Figure 2-2 Proposed mechanism for the oxidation reaction	24
Figure 2-3 Proposed mechanism for the oxidation under basic conditions	29
Figure 3-1 Representative syntheses of biaryl compounds.....	33
Figure 3-2 Synthesis of immunosuppressant 86	42

Figure 3-3 Byproduct identification	43
Figure 3-4 Plausible mechanistic pathways for the aryl-aryl cross-coupling reaction	46
Figure 3-5 Projection of the force for N1-H ⁺ and N3-H ⁺	47
Figure 3-6 B3LYP/6-31G* Reaction energy diagram for the cross-coupling of triazene 84d to form biphenyl 85d and phenol 85d'	49
Figure 4-1 Representative methods for amide synthesis	54
Figure 4-2 Initial observation of amide formation.....	55
Figure 4-3 Proposed mechanism for amide synthesis.....	62
Figure 4-4 Experiments with isotopically-labelled molecules.....	63
Figure 4-5 Synthesis of biologically-active compounds	65

List of Tables

Table 2-1 Optimization of reaction conditions.....	20
Table 2-2 Optimization of NHC precursor.....	21
Table 2-3 Scope of the oxidation reaction.....	23
Table 2-4 Scope of substitution reaction.....	25
Table 2-5 Oxidation under basic conditions.....	28
Table 3-1 Optimization of reaction conditions.....	35
Table 3-2 NHC precursor optimization.....	36
Table 3-3 Synthesis of aryl π -conjugated triazenes.....	38
Table 3-4 Synthesis of biphenyls.....	39
Table 3-5 Synthesis of biphenyls and heterobiaryls.....	41
Table 4-1 Optimization of amide synthesis.....	56
Table 4-2 Reaction scope for amide formation.....	58
Table 4-3 Reaction scope with different nitriles.....	60
Table 6-1 PCM ground state energy difference between N1-H ⁺ and N3-H ⁺	93
Table 6-2 Electronic energy difference between the protonated and unprotonated triazenes at the PCM ground electronic state.....	94
Table 6-3 Calculated absorption wavelength for the first bright state.....	95
Table 6-4 Electronic coupling between the ground and first bright excited state for the 1-Z configuration of N3-H ⁺	96
Table 6-5 Energy of dissociation reaction between 1-E and 1-Z of N3-H ⁺	97
Table 6-6 Difference of binding energy (BE) between path A and B.....	98
Table 6-7 Binding energy (BE) between path B and C.....	99
Table 6-8 Energy difference between final products of path A and B.....	100

Table 6-9 Relative free energies and enthalpies for species involved in the Ar-Ar-Cross-coupling of triazene 84d	101
---	-----

Notes

Portions of this thesis have been taken, with permission, from the following publications:

- Barragan, E.; Bugarin A. π -Conjugated Triazenes: Intermediates that Undergo Oxidation and Substitution Reactions. *J. Org. Chem.* **2017**, *82*, 1499-1506. **Reprinted with permission from Copyright 2017 American Chemical Society.**
- Barragan, E.; Noonikara Poyil, A.; Chou-Hsun, Y.; Wang, H.; Bugarin, A. Metal-free cross-coupling of π -conjugated triazenes with unactivated arenes via photoactivation. *Org. Chem. Front.* **2019**, *6*, 152-161. **Reproduced with permission from The Royal Society of Chemistry.**

Chapter 1

Introduction and previous works

1.1 Introduction to triazenes

Nitrogen-containing organic molecules represent one of the most important classes of organic substances in existence.¹ Nitrogen-containing organic compounds are essential for life since they are indispensable components in biological systems: amino acids form the basis of all proteins, nitrogen is also abundantly present in the structure of nucleic acids, it is also a fundamental part of the structures of natural products, such as alkaloids and other biologically-active compounds that have been used as medicinal drugs, etc.¹ In fact, nitrogen-containing molecules are so abundant in nature that they comprise the second most abundant source of nitrogen on Earth, second only to the nitrogen in the atmosphere.¹ Due to the great abundance and importance of nitrogen-containing compounds, the discovery, synthesis and reactivity of new nitrogen-containing compounds is currently one of the most active research areas in organic chemistry.²

Among the vast diversity of nitrogen-containing organic molecules, a particularly interesting class are compounds containing the triazene group. Triazenes are nitrogen-containing molecules that possess an arrangement of three nitrogen atoms in sequence with a double bond between the first and second nitrogen atoms. The first synthesis of a triazene was reported more than 150 years ago by Martius and Griess who synthesized 1,3-diphenyltriazene in 1866.³ Among organic triazenes there exist three main categories. Linear, cyclic and π -conjugated triazenes (Figure 1-1). Linear triazenes are usually prepared through the reaction of an amine with an aniline or alkyl azide.⁴ A number of compounds in this family have demonstrated biological activity functioning as DNA-methylating agents,⁵ with some compounds even becoming prominent anticancer drugs based on this mechanism of action such as dacarbazine,⁶ a drug commonly prescribed for

the treatment of melanoma.⁷ Linear triazenes have also been used as cleavable linkers for DNA-directed reactions,⁸ as aromatic amine protecting groups,⁹ polymer synthesis and formation of heterocycles.¹⁰ Cyclic triazenes are prepared in a similar manner to linear triazenes albeit the reaction is carried out in an intramolecular fashion.⁴ This class of triazenes have found extensive use as chemotherapeutic drugs such as temozolamide, used for treating aggressive brain tumors such as glioblastoma.¹¹

π -Conjugated triazenes, in contrast to their linear and cyclic varieties, have been scarcely explored since their first reported synthesis more than fifty years ago by Winberg and Coffman.¹² Nevertheless, applications of this triazene class have arisen, especially as multifunctional linkers in polymer synthesis,¹³ as intermediates in the synthesis of azo dyes through generating diazonium intermediates.¹⁴ In addition, π -conjugated triazenes have recently been used as photochemically-activated basic catalysts.¹⁵

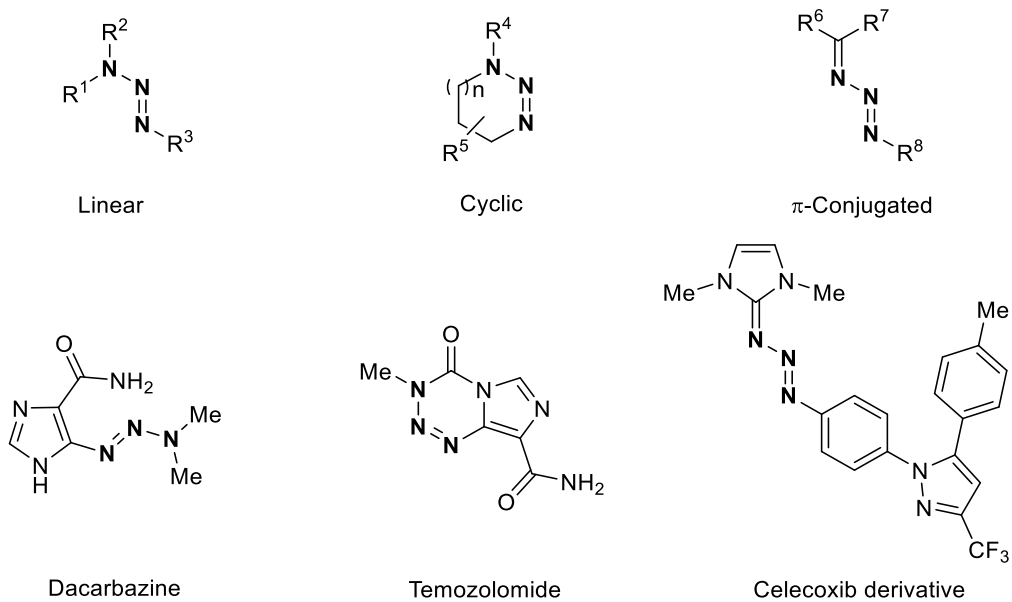


Figure 1-1 Classes and examples and of triazenes

1.2 Synthesis of π -conjugated triazenes

The first reported synthesis of a π -conjugated triazene dates back to 1965 by Winberg and Coffman¹² who prepared three different triazenes in one step from bis(imidazolidine) **1** by reacting it in cold benzene with *p*-toluenesulfonyl azide, *p*-nitrophenyl azide and diphenyl phosphonyl azide (**2-4**) respectively, yielding π -conjugated compounds (**5-7**) in modest yields around 35%. Although the yields obtained were not ideal, this experiment provided the basis to perform all subsequent research on π -conjugated triazenes (Figure 1-2).

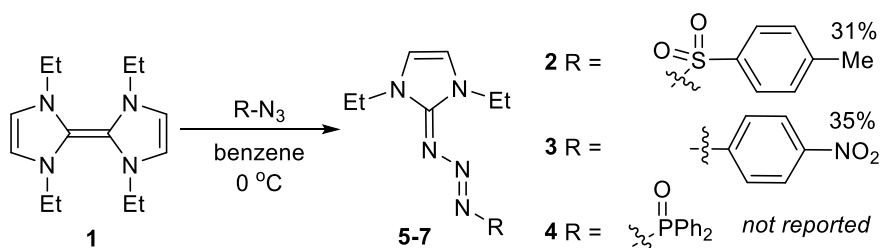


Figure 1-2 First synthesis of π -conjugated triazenes

The next development in the synthesis of π -conjugated triazenes was reported forty years later by Bielawski and co-workers.¹⁶ The strategy they employed consisted in the use of imidazolium-derived *N*-heterocyclic carbene (NHC) precursors **8**. Then, through deprotonation with sodium hydride or potassium *tert*-butoxide, the free carbene is formed *in situ* and then reacted with an azide **9** to afford the corresponding π -conjugated triazene **10**. The scope of this reaction was subsequently explored and the reaction conditions were tested using methyl, mesityl and isopropyl *N*-substituted imidazolium salts and seven different azides in THF. All triazene products were obtained in good to excellent yields (from 54 to 94%).(Figure 1-3a).¹⁶

In addition, upon X-ray diffraction analysis of a crystallized sample of 1-benzyl-3-(1,3-dimesitylimidazol-2-ylidene)triazene **11**, the *Z*-isomer of the triazene was observed.

(Figure 1-3b) Interestingly, this has been the only record so far of the *Z*-isomer of a triazene derived from an aliphatic azide. Further trials by the same group to try to repeat this observation resulted in the formation of crystals of the *E*-isomer exclusively.¹⁶

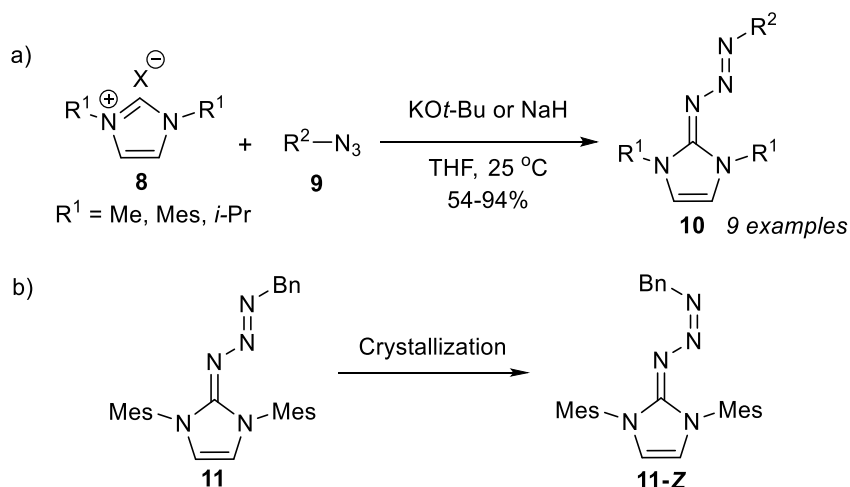


Figure 1-3 Triazene synthesis using imidazolium salts and azides

Bielawski's group also compared the formation of a π -conjugated triazene using a free carbene versus resorting to the deprotonation of the NHC precursor salt.¹⁶ In this work they reacted the free carbene 1,3-di-*tert*-butylimidazol-2-ylidene **12** with benzyl azide in THF at room temperature, obtaining the corresponding triazene **13** in quantitative yield. Subsequently, they deprotonated 1,3-di-*tert*-butylimidazolium chloride with both sodium hydride and potassium *tert*-butoxide to generate the carbene *in situ* and reacted it with benzyl azide to also afford triazene **13**, showing no significant difference in yield compared to the free carbene reaction (Figure 1-4).¹⁶

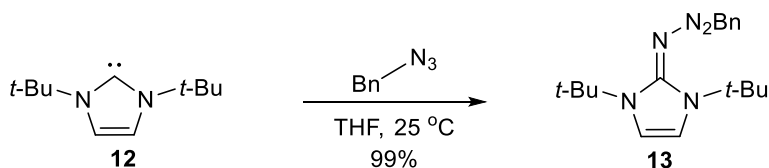


Figure 1-4 Synthesis of triazene from a free carbene

In order to expand the scope of the synthesis of π -conjugated triazenes and to try to improve the stability of the synthesized molecules, Bielawski's group prepared nine new π -conjugated triazenes by using benzimidazole derived carbenes and **14** aryl azides **15** in THF at room temperature. All triazenes **16** were obtained in nearly quantitative yields (Figure 1-5a). Furthermore, UV/Vis spectroscopic analysis and X-ray crystallography of the synthesized triazenes revealed bond alteration patterns characteristic of donor-acceptor molecules, as well as electron delocalization in all molecules due to stereoelectronic effects from the functional groups present on the azide moiety or the NHC, with triazenes possessing λ_{\max} values ranging from 364 to 467 nm. From this data it follows that the λ_{\max} of these π -conjugated triazenes can be tuned by selecting the appropriate combination of NHC and organic azide. In general, triazenes derived from electron-rich NHC's and electron-poor azides exhibit the largest λ_{\max} values (Figure 1-5b).¹⁷

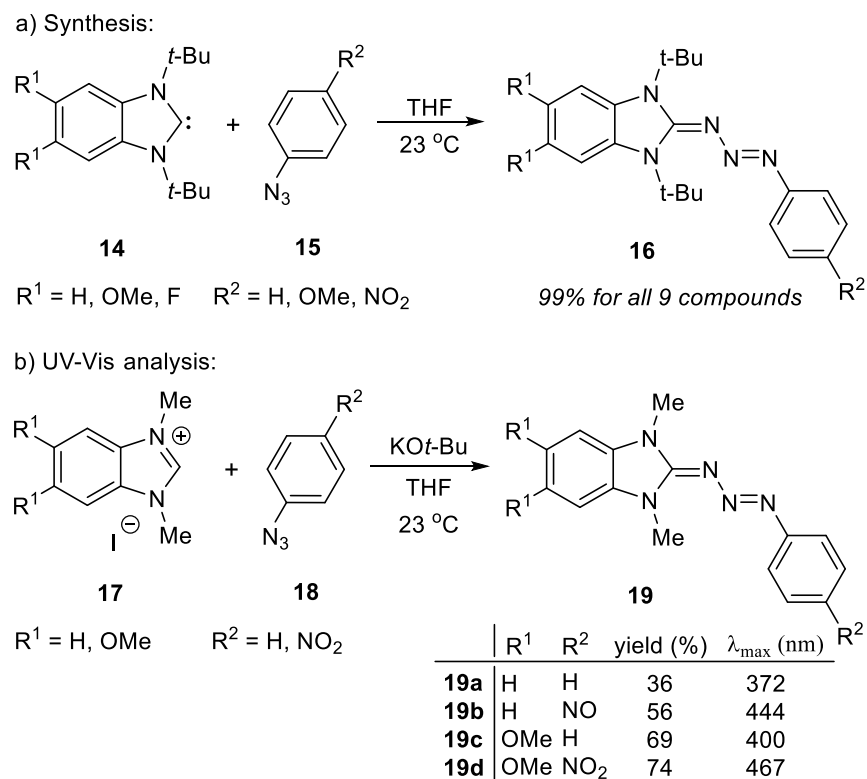


Figure 1-5 Synthesis and UV/Vis analysis of benzimidazole-derived triazenes

In contrast to the excellent results obtained in the synthesis of π -conjugated triazenes by using benzimidazole derived carbenes with bulky *N* substituents like *tert*-butyl, the use of *N*-methyl substituted benzimidazolium salts **17** resulted in triazenes **19a-d** that presented the same electron-delocalization patterns but that were obtained in considerably lower yields (between 36 and 74%) even under the same conditions used to generate the bulkier benzimidazole-2-ylidenes (Figure 1-5b).¹⁷ This decrease in the obtained yields was attributed by the researchers to the rapid dimerization of the *N*-methyl substituted carbenes to form tetraaminoethylenes, followed by oxidation under aerobic conditions.¹⁸

More recently, our group reported several air- and moisture-stable π -conjugated triazene dyes.¹⁹ These triazenes were prepared using Bielawski's method using a small carbene derived from *N*-methylimidazolium iodide **21** and a variety of organic azides **22**

(alkyl, vinyl, aryl and heteroaryl). The π -conjugated triazenes **23-25** were obtained in moderate to excellent yields (Figures 1-6 and 1-7). The carbene was generated in situ by deprotonation of the imidazolium salt with sodium hydride in THF and reacted with the corresponding azide at room temperature. The synthesized triazenes were analyzed with UV/Vis spectroscopy to study the electron delocalization between the coupled NHC and azide moieties. All triazene dyes are brightly colored and were found to have a UV/Vis absorption bands between 294 and 450 nm with the exception of the aliphatic triazene **27d** where no absorption band was observed over that wavelength range.¹⁹ An expected result since there is no π -system over which the electrons can be delocalized in the azide moiety.

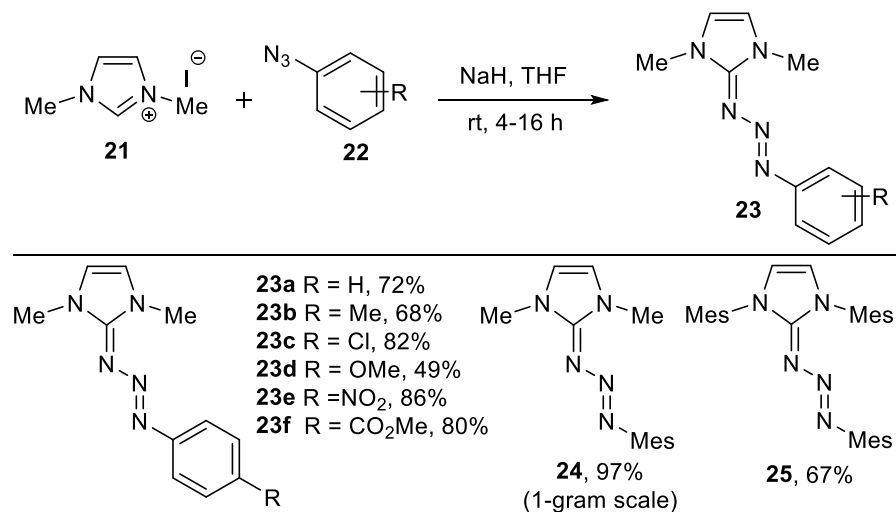


Figure 1-6 Synthesis of aromatic triazenes

Using this approach with the small carbene precursor **21**, our group was able to obtain π -conjugated triazenes **27a-e** derived from vinyl, phosphoryl, aliphatic and heteroaromatic azides as well as a triazene derivative of Celecoxib **27f**, a non-steroidal anti-inflammatory drug often prescribed to treat the pain of several kinds of arthritis, which was obtained in 48% yield.¹⁹

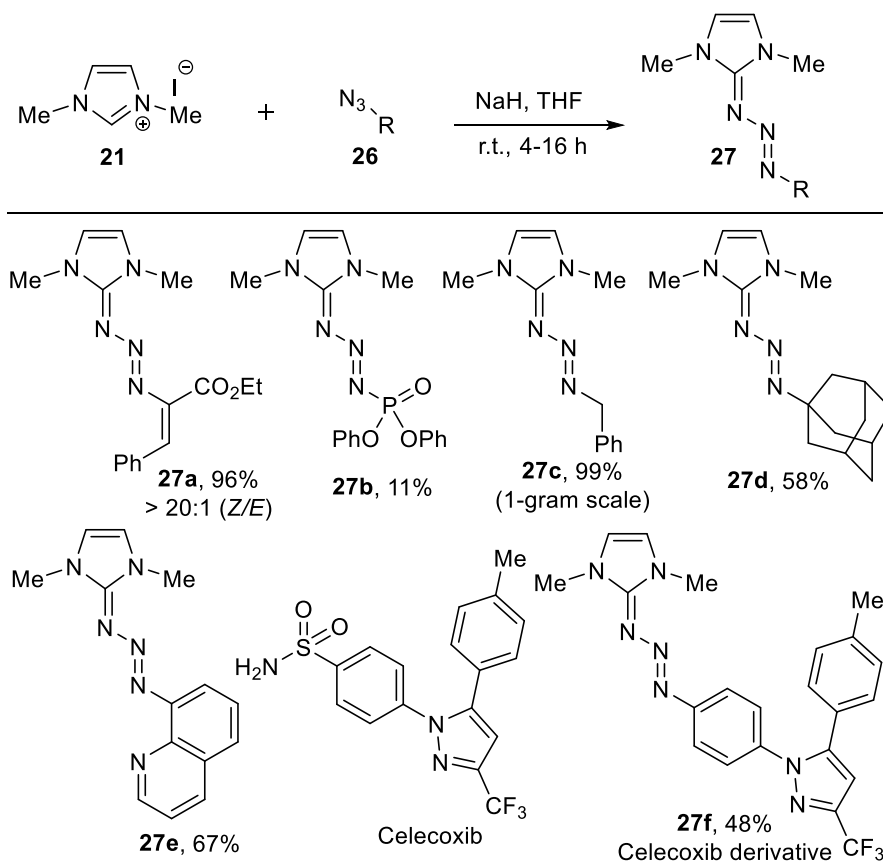


Figure 1-7 Azide scope for triazene synthesis

X-ray analysis of the obtained triazenes **23c** and **23e** demonstrated the near-planar structure of the molecules which facilitates orbital overlap and electron delocalization. Similar to most of Bielawski's trials,¹⁷ both molecules were only observed as the *E*-isomer exclusively (X-ray crystal structures not shown, but they are available in our publications).¹⁹⁻²⁰

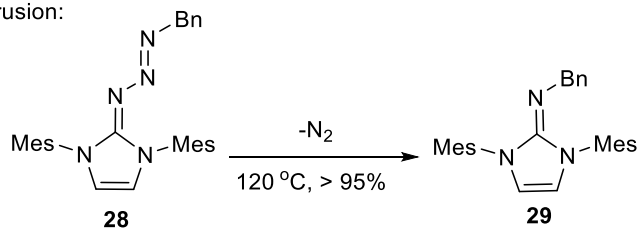
1.3 Previous studies of π -conjugated triazene reactivity

1.3.1 Thermally-induced N_2 extrusion

Aside from previous developments in the synthesis and determination of structural properties of π -conjugated triazenes, although not thoroughly explored, there have been a few studies that explore the reactivity of this class of compounds which will be discussed in this section.

While studying the thermal stability of π -conjugated triazenes in 2005, Bielawski identified a guanidine decomposition product **29**, which arises from the loss of molecular nitrogen from the triazene molecule upon heating in DMSO- d_6 (Figure 1-8a).¹⁶ In order to further study this transformation, Bielawski and co-workers analyzed a series of π -conjugated triazenes **30a-g** using thermogravimetric analysis under a N_2 atmosphere.¹⁷ The results of this study demonstrated that increasing the bulk of the *N*-substituents in the NHC moiety increases the thermal stability of the triazene. The thermal stability of the triazenes is also significantly influenced by the electronic properties of the azide moiety. This is showcased in Bielawski's study, where it was observed that triazene **30e** containing an electron donating group (OMe) suffered decomposition at 35 °C less than triazene **30f** containing an electron-withdrawing group (NO_2) (Figure 1-8b). These observations suggest that in order to design a triazene with high thermal stability, it is required to use a carbene precursor with bulky substituents in combination with an electron-deficient azide. Our own observations support this conclusion since our electron-rich triazenes have readily decomposed in solution upon heating or even by just staying in solution for a few hours at room temperature. Meanwhile, the electron-deficient triazenes we have prepared can resist temperatures of even 120 °C for 24 hours without any appreciable decomposition to the guanidine product.¹⁹

a) N₂ extrusion:



b) Thermal stability:

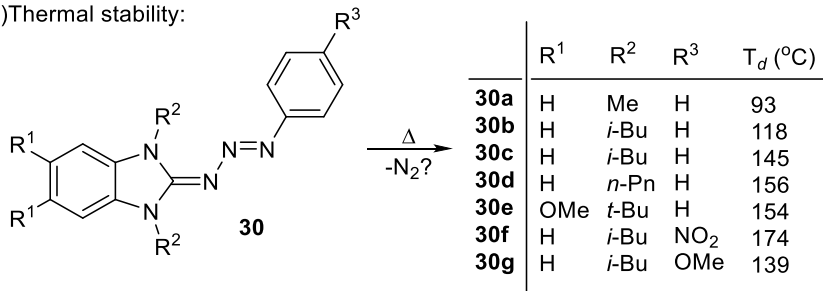


Figure 1-8 Thermally-induced nitrogen extrusion in triazenes

In order to elucidate the mechanism of this thermally-induced nitrogen extrusion, Bielawski's group prepared ¹⁵N-labeled triazene **31** and heated it to 170 °C in solution, yielding the ¹⁵N-containing guanidine **33** as the major product.¹⁷ In light of this observation, Bielawski proposed a mechanism in which the ¹⁵N atom attacks the NHC carbon to form a four-membered ring intermediate **32**, which then undergoes loss of N₂ to afford guanidine **33** (Figure 1-9).²¹ This proposed mechanism is analogous to that of the Staudinger reaction, in which an organic azide and a phosphine react to give an phosphazene intermediate, with the difference between the two mechanisms being that the electrophile in the Staudinger reaction is a phosphorus atom, while in the triazene nitrogen extrusion, the electrophile is a carbon atom.²¹

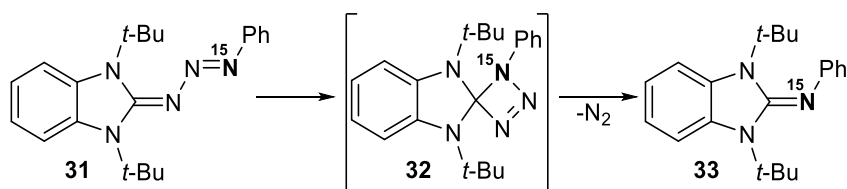


Figure 1-9 Proposed mechanism for the thermal N₂ extrusion in triazenes

1.3.2 Conversion of π -conjugated triazenes to guanidines

In 2001, Clyburne and co-workers reported their work in the synthesis of 2,3-diazabutadienes by reaction of NHC's with different diazoalkanes. In this work they reported a single example of the synthesis of guanidine **35** in 24% yield from the reaction of the free carbene **34** and azidotrimethylsilane (Figure 1-10).²² The reaction is presumed to occur through a triazene intermediate. However, the researchers were not able to isolate said intermediate and did not propose a mechanism in this report, leaving the matter open to the reader's interpretation.

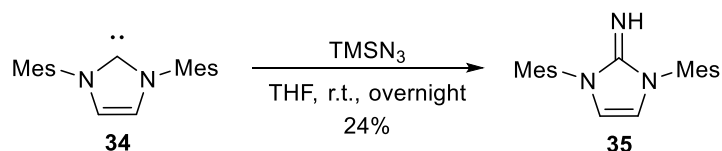


Figure 1-10 Guanidine synthesis from carbene

Later in 2009, Lyapkalo and co-workers managed to isolate the triazene intermediates **37a-c** in their reaction of free carbenes **36a-c** with *tert*-butyl azide. The isolated triazenes readily furnished guanidinium salts **38a-c** upon mild acidic treatment with ammonium tetrafluoroborate, extruding molecular nitrogen as well as 2-methylpropene (Figure 1-11).²³

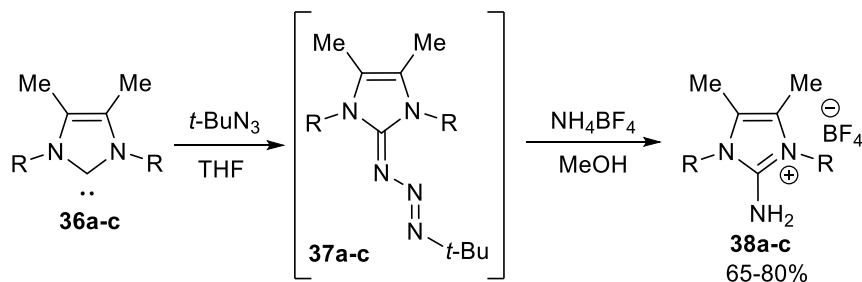


Figure 1-11 Guanidine synthesis from a free carbene

A similar reaction was performed by Tamm and co-workers who prepared guanidinium salt **41** and guanidine **40** using a triazene intermediate **39**. The guanidine salts

41 was obtained under similar conditions to those used by Lyapkalo, followed by treatment with sodium hydroxide solution to yield the free guanidine **40**. Guanidine **40** can also be synthesized by simply stirring triazene **39** in methanol overnight.²⁴

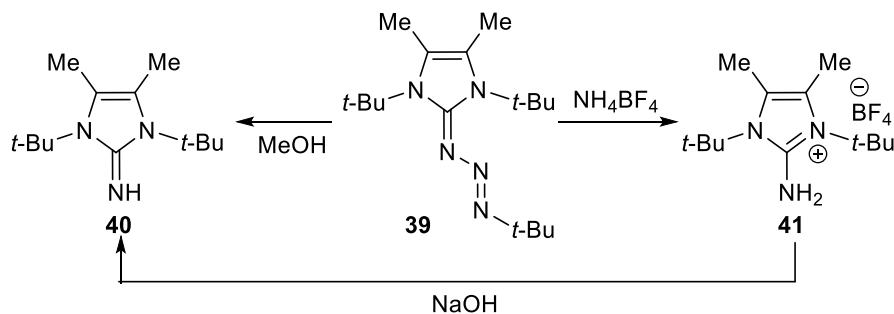


Figure 1-12 Guanidine and guanidinium salt synthesis from triazene

1.3.3 Diazo and azide transfer reactions

Another example of π -conjugated triazene reactivity is the use of triazenes as diazo and azide transfer reagents.²⁵ The Kitamura group developed triazene derived reagents that can transfer a diazo²⁶ or azide moiety.²⁷ 2-Azido-1,3-dimethylimidazolium chloride **42** was found to effect diazo-transfer to 1,3-dicarbonyl compounds efficiently, as well as to convert primary anilines into aromatic azides. After the transfer, the imidazolium moiety is converted into a urea **45** or a guanidine **48** respectively (Figure 1-13).

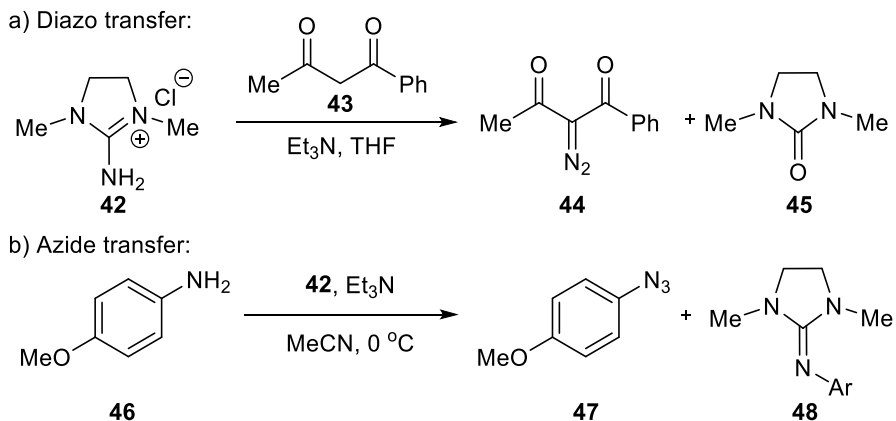


Figure 1-13 Diazo and azide transfer reactions using triazenes

1.3.4 Alkylation of π -conjugated triazenes

Katritzky and co-workers synthesized different donor-acceptor triazenes from triazolium salts using potassium *tert*-butoxide to generate the carbenes *in situ* in the presence of 4-nitroazidobenzene.²⁸ These triazolium-derived π -conjugated triazenes are obtained as ionic salts that undergo *N*-alkylation when reacted with methyl iodide or benzyl bromide, indicating the nucleophilicity of the electron-rich nitrogen on the side chain of the NHC moiety. Additionally, alkylation reactions on neutral triazenes were also performed by Bielawski²⁹ and Katritzky²⁸ on benzimidazole and imidazole-derived triazenes respectively. For both kinds of triazenes, the reaction with methyl iodide generated the *N*-methylated product **52** in quantitative yield. (Figure 1-14). All of these triazenes showed methylation exclusively on the nitrogen directly connected to the aryl group, evidencing the increased nucleophilicity of this particular nitrogen among the others within these molecules. The nucleophilicity of this nitrogen is believed to originate due to the push-pull electronic character of these molecules resulting in an increase of the electron density on this atom.

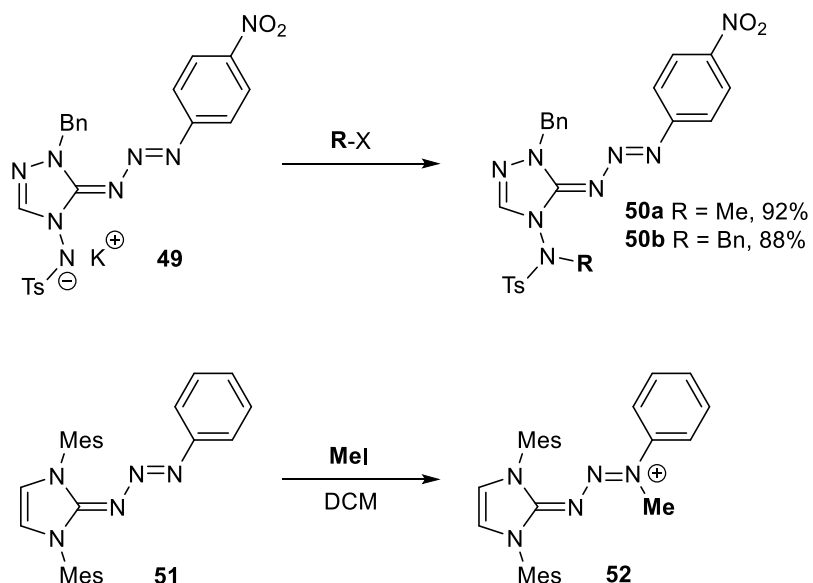


Figure 1-14 Alkylation of π -conjugated triazenes

1.3.5 π -conjugated triazenes as diazonium sources and as photochemically activated bases

Recently, diazonium ion generation from π -conjugated triazenes was reported by Jewett and co-workers who synthesized a series of water-soluble triazenes to test their reactivity under physiologically relevant conditions.¹⁴ Jewett's approach consisted on using zwitterionic NHC precursors in order to generate anionic triazenes that would be soluble in water. For the synthesis of these triazenes, *N*-methylimidazole and *N*-mesitylimidazole **53** were treated with 1,3-propanesultone **54** to produce zwitterionic NHC precursor **55**. Deprotonation of the NHC precursor with potassium *tert*-butoxide and treatment with several aromatic azides **56** furnished triazenes **57** in modest to excellent yields (Figure 1-15).¹⁴ The bulky mesityl triazenes were found to be considerably more stable in aqueous solution than the small methyl triazenes. Stability experiments performed under a constant pH of 6 supported the trend observed by previous researchers that triazenes derived from electron-deficient azides are more stable than triazenes derived from electron-rich azides. During stability trials in water for these triazenes, a change of pH was observed over time. A closer examination of this observation revealed that the triazenes were decomposing into diazonium ions over time. These diazonium ions were captured by addition of phenol derivatives to afford diazo compounds **59a** and **59b**.¹⁴ Additionally, the organic dye Sudan orange G **59c** was obtained in 68% yield by trapping the diazonium intermediate derived from triazene **57a** using resorcinol (Figure 1-16).¹⁴ The capability of these π -conjugated triazenes to not only be water soluble but also to afford diazonium ions under physiologically relevant conditions highlights the potential applicability of this class of compounds for biochemical and drug development applications in the future.

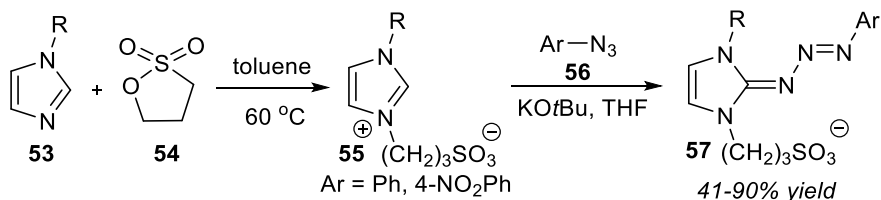


Figure 1-15 Synthesis of water-soluble triazenes

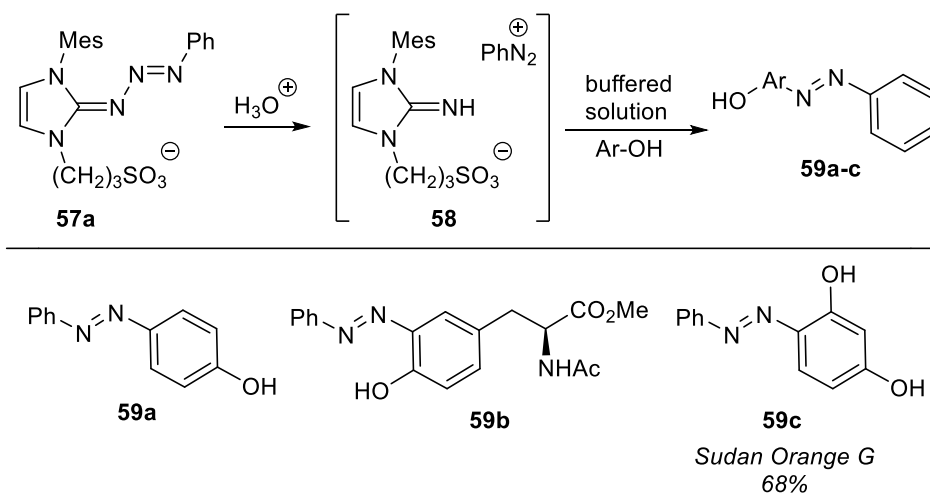


Figure 1-16 Synthesis of azo dyes from triazenes

Jewett and co-workers also investigated the effect that UV irradiation has on triazenes and its relationship with pH. To test this, a buffered aqueous solution of triazene **60-E** with a constant pH of 9 was irradiated using a handheld UV lamp with a wavelength around 350 nm. After a few hours, complete decomposition of the triazene was observed. In contrast, a non-irradiated solution of the same triazene was stable for days. These observations suggested that a photochemical reaction was taking place, most likely an *E* to *Z* photoisomerization, with the resulting triazene isomer being significantly less stable. By changing the solvent from water to DMSO, the reaction was able to be monitored by NMR. By analyzing the reaction using NOESY experiments, the *Z*-isomer of the triazene **60-Z** was identified in the reaction mixture. Since both *E* and *Z* isomers were observed by NMR, a solution of the triazene in DMSO was irradiated until an *E/Z* ratio of 7:3 was

observed and then the sample was treated with AcOH. As expected, the *Z*-isomer NMR signal disappeared within two minutes, supporting the lower stability of this isomer. Moreover, it was also observed that during irradiation, the pH of the solution increased with time. Initially the solution pH was 9 and upon UV irradiation it increased to 9.8 in minutes as the triazene converted to its *Z*-isomer. The authors explained that upon isomerization, the planarity of the molecule is lost to reduce strain, breaking the conjugation with the phenyl group due to poor orbital alignment, thus localizing electron density on nitrogen 1 making it more basic. This change in basicity of the triazene molecule suggested a possible application of these molecules as photochemically activated bases. In order to test this, Jewett and co-workers performed a Henry reaction between 4-nitrobenzaldehyde and nitroethane using π -conjugated triazene **60-E** as the basic catalyst under UV irradiation at 350 nm. The nitroalcohol product was obtained in 90% yield using 25 mol% of the catalyst, suggesting that indeed, π -conjugated triazenes can be utilized as photobasic catalysts.¹⁵

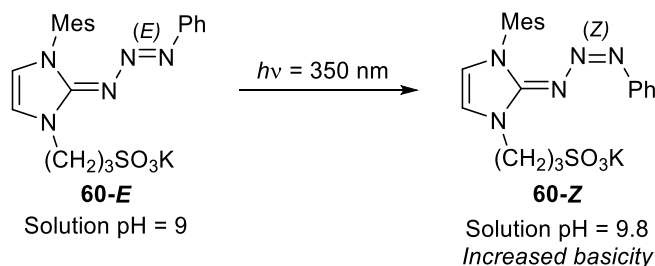


Figure 1-17 Photoisomerization and basicity change of triazenes

In summary, π -conjugated triazenes are a class of organic molecules that although being first synthesized over fifty years ago,³ have so far only been investigated by a handful of research groups (Figure 1-18) and their reactivity has only been superficially explored. The aim of this work is to contribute to the developing knowledge of π -conjugated triazene reactivity and in the following chapters novel reactions will be discussed which allow the conversion of these triazene molecules to different functional groups such as: aldehydes,

ketones, ethers, thioethers, biaryls, and amides. Accessing all these functionalities from azides through π -conjugated triazenes demonstrates the versatility of these molecules and proves convenient to the preparation of building blocks which can be used in the synthesis of more complex molecular structures.

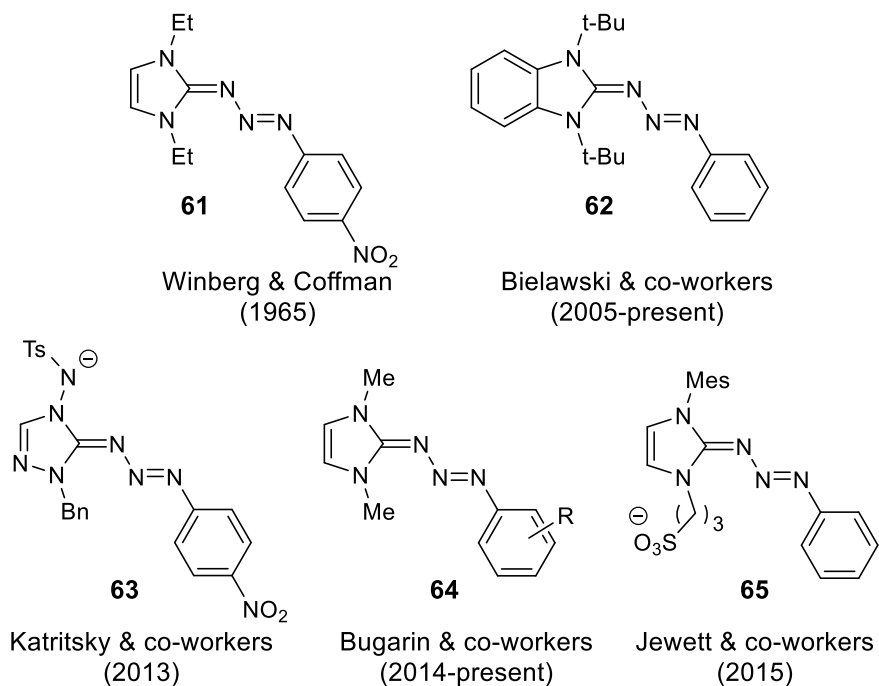


Figure 1-18 π -conjugated triazenes over the years

Chapter 2

Oxidation and Substitution Reactions

2.1 Introduction and initial observations.

Versatile molecules, or molecules that can undergo different classes of reactions to allow access to different functional groups have been remarkable staples of synthetic organic chemistry. Well-known examples of such molecules are: allenylsilanes,³⁰ arylsulfonium salts,³¹ hypervalent iodine,³² dimethyl sulfoxide,³³ dimethylformamide,³⁴ and organic azides.³⁵ All of these molecules can be derivatized to different products through various pathways. In addition, the fact that these molecules can also function as reagents, intermediates, or catalysts for many transformations renders them as useful synthetic tools for the organic chemist. Among these versatile molecules, organic azides are among the most widely used compounds, as exemplified in click chemistry,³⁶ natural product total synthesis,³⁷ heterocycles,³⁸ Staudinger reaction,³⁹ and nitrene precursors.⁴⁰

Recently, we observed that π -conjugated triazenes, synthesized from azides and *N*-heterocyclic carbenes (NHCs),¹⁹ provide potentially valuable new intermediates for use in organic syntheses.³ Initially, we investigated the thermal stability of these π -conjugated triazenes, which were stable at 60 °C for 2 h. However, when Dr. Patil heated these same triazenes at 120 °C in DMSO-*d*₆, consumption of triazene **66** was observed.¹⁹ Identification of the byproducts from the reaction revealed them to be iminoimidazole **67** and benzaldehyde **68** in a 4:1 ratio (Figure 2-1). These initial observations, have led us to document an unprecedented, simple, two step protocol that commences from readily available organic azides to provide syntheses of aldehydes, ketones, ethers, and sulfides via π -conjugated triazene intermediates. Furthermore, the method is compatible with a wide-range of nucleophiles, including oxygen, and sulfur nucleophiles, and achieved under mild reaction conditions. These results reveal the exceptional reactivity of these scarcely

studied molecules, which should may now merit consideration as new members of the versatile molecule club.

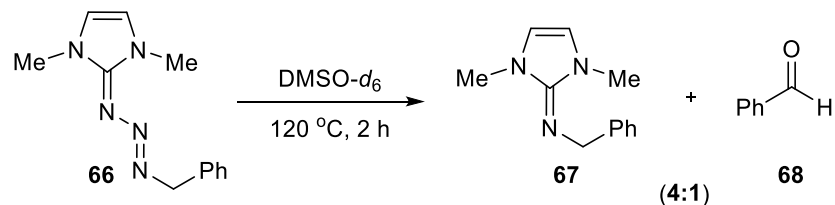
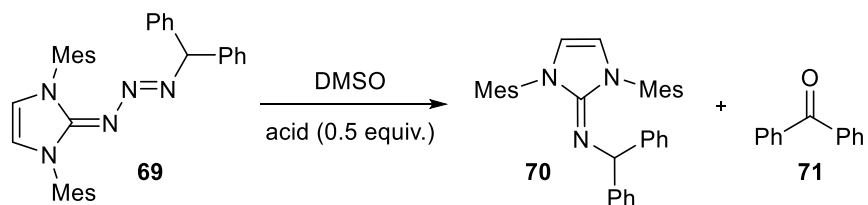


Figure 2-1 Initial observation

2.2 Optimization of the reaction conditions

To help optimize reaction conditions, triazene **69** was synthesized (Table 2-1). This selection was based on the consideration that triazene **69** produces benzophenone **70** instead of the more volatile benzaldehyde **69**, thus easing isolation by minimizing product losses due to evaporation. Heating of triazene **69** at 120 °C for 2 h in DMSO, without any additive, afforded benzophenone **70** in 20% yield (entry 1). Increasing the reaction time did not improve the reaction yield (entry 2), indicating that the triazene is the reacting substrate and not the iminoimidazole byproduct **71**, which remains intact after 12 h of heating. Based on this observation, to further activate triazene **69**, we screened several Lewis and Brønsted acids (entries 3–8), and it was clearly established that the stronger the Lewis acid the higher the yield. In fact, SnCl₄ furnished the product in 72% yield even at room temperature (entry 6). Nonetheless, among all screened Lewis and Brønsted acids, TsOH afforded the product with the highest yield (89%) at room temperature, in only 30 min (entry 7), in addition to being significantly easier to handle than SnCl₄. Based on this result, we decided to use TsOH for further experiments.

Table 2-1 Optimization of reaction conditions

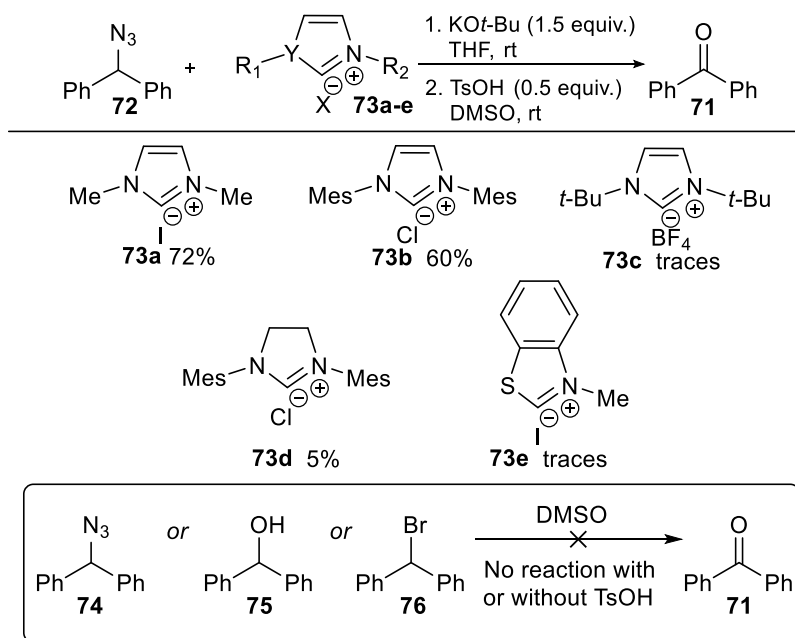


entry	acid	temp (°C)	time (h)	NMR ratio 70/71	NMR yield of 71 (%)
1	none	120	2	4:1	20
2	none	120	12	4:1	21
3	PdCl ₂	120	2	1:1	43
4	ZnCl ₂	120	2	1:3	58
5	CuSO ₄	120	2	1:3	62
6	SnCl ₄	rt	5	1:4	72
7	TsOH	rt	0.5	1:9	89
8	TFA	rt	0.5	1:2	39

Having optimized conditions for the conversion of a π -conjugated triazene to a carbonyl compound, we next investigated the scope of converting benzhydryl azide **72** to benzophenone **71** in a two-step, one-pot protocol (Table 2-2) in order to demonstrate a net conversion of organic azides into carbonyl compounds via a triazene intermediate. Examining this protocol presented two challenges. First, the formation of the triazene intermediate is dependent on the NHC precursor used (e.g., **73c**, **73d**, and **73e** did not provide a significant yield of their respective triazene intermediate). Second, the TsOH–DMSO-catalyzed oxidation, in the second step, is affected by steric effects of the triazene intermediate (e.g., **73b** is more steric hindered than **73a**). This size difference makes **73b** more stable and, therefore, less responsive to Brønsted acid activation. In

contrast, **73a** produces a less sterically hindered or more reactive triazene intermediate, which afforded benzophenone **71** in 72% yield after two-step, one-pot reaction versus a 60% yield using **73b**. Thus, these results establish 1,3-dimethylimidazolium iodide **73a** as the best NHC precursor, among those tested, to accomplish this transformation. Furthermore, azide **74**, alcohol **75**, and alkyl bromide **76** counterparts were reacted under the same reaction conditions, with or without the Brønsted acid, and no reaction was observed for any of the substrates at room temperature. This indicates that the observed reaction is due to formation of the triazene and not a direct oxidation reaction of the azide (Table 2-2).⁴¹

Table 2-2 Optimization of NHC precursor

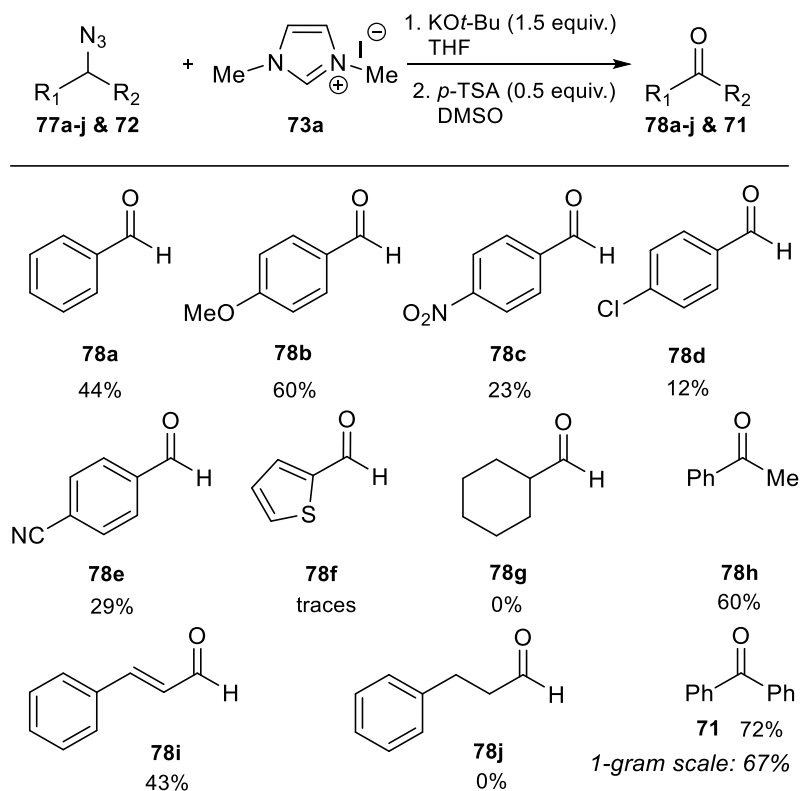


2.3 Substrate scope

With the optimal conditions for the two-step, one-pot procedure in hand, we subsequently explored the scope of this new transformation (Table 2-3) by surveying the reactivity of freshly prepared organic azides (**77a-j** and **71**) and 1,3-dimethylimidazolium

iodide **73a** using KO^tBu and THF at room temperature. All reactions were terminated after 12 h (the standard time for triazene formation) for comparison purposes. THF was then removed under reduced pressure, and a catalytic amount of TsOH (50 mol%) in DMSO was added to the reaction mixture. The reaction mixture was quenched after only 30 min, and the product was isolated using silica gel flash chromatography. From this study, it was observed that secondary azides afford their products in higher yields (e.g., **71** and **78h** were obtained in 72% and 60% yield, respectively). The system is also efficient for the allylic azide **78i**, affording *trans*-cinnamaldehyde **78i** in moderate yield (43%). Two classes of primary azides were investigated: benzylic azides and aliphatic azides. Unfortunately, aliphatic azides proved to be unreactive toward our reaction conditions and did not create the expected aldehyde products (e.g., **78g** and **78j**). Nonetheless, the other class of primary azides (benzylic) exhibited high sensitivity to electronic effects. The electron-rich 4-methoxybenzaldehyde **78b** was obtained in a good yield (60%), whereas benzaldehyde **78c** was obtained in a moderate yield (44%), and the electron-poor 4-nitrobenzaldehyde **78c** was obtained in relatively small yield (23%). Finally, several heterocycles containing a benzylic azide were investigated, including 2-(azidomethyl)thiophene **77f**, but unfortunately, only traces of thiophene-2-carbaldehyde **78f** were observed. This presumably indicates Brønsted acid protonation of the heterocycle itself instead of activation of a nitrogen atom on the triazene moiety, leading to unknown decomposition pathways. Overall, although the yields are modest, it is worth noting that this is a two-step, one-pot procedure and represents the net conversion of an azide to a carbonyl compound under mild reaction conditions, in other words, an unprecedented transformation.

Table 2-3 Scope of the oxidation reaction



2.4 Proposed mechanism for the oxidation reaction

In order to understand the mechanistic details of this novel transformation, we turned our attention to the data obtained during the azide survey (Table 2-3), the reagents employed (TsOH and DMSO), and the detection of dimethyl sulfide **79f** as a byproduct. From Table 2-3, it is clear that secondary azides are the best substrates, followed by allylic azides, benzylic azides, and finally primary aliphatic azides, which do not work. Based on this information, we proposed a S_N1 -like mechanism where triazene **79** is first protonated by TsOH followed by fast triazene disintegration into three fragments. These fragments are nitrogen gas (bubbles observed), iminoimidazole **79b**, and carbocation **79c**. After carbocation **79c** is released, DMSO quickly traps it, forming the alkoxy-sulfonium

intermediate **79e**. Finally, **79e** undergoes a Kornblum-type mechanism,⁴² which releases dimethyl sulfide **79f** (observed) and the expected benzophenone **71**. An alternative, less likely, mechanism is the direct attack of DMSO to protonated triazene **79a** (S_N2). However, the data from Table 2-3 suggest that substrates that produce more stable carbocations (secondary azides, as well as substrates containing electron-donating groups) generated higher yields, supporting the proposed S_N1 mechanism (Figure 2-2).

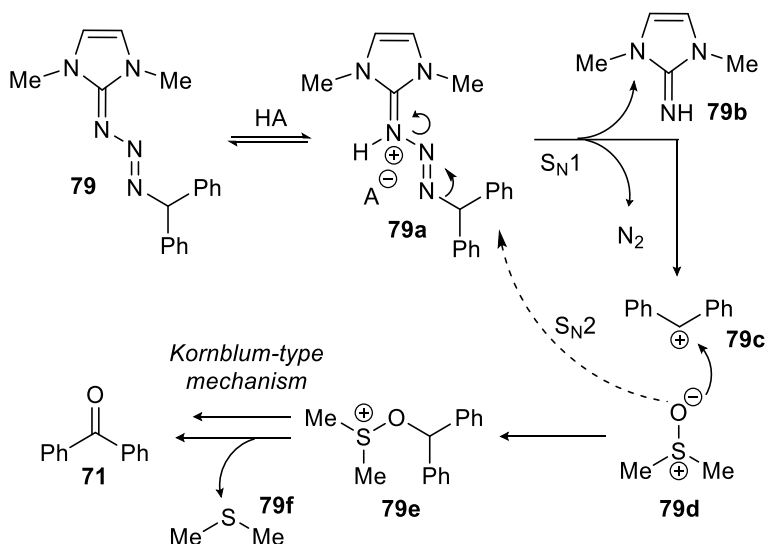


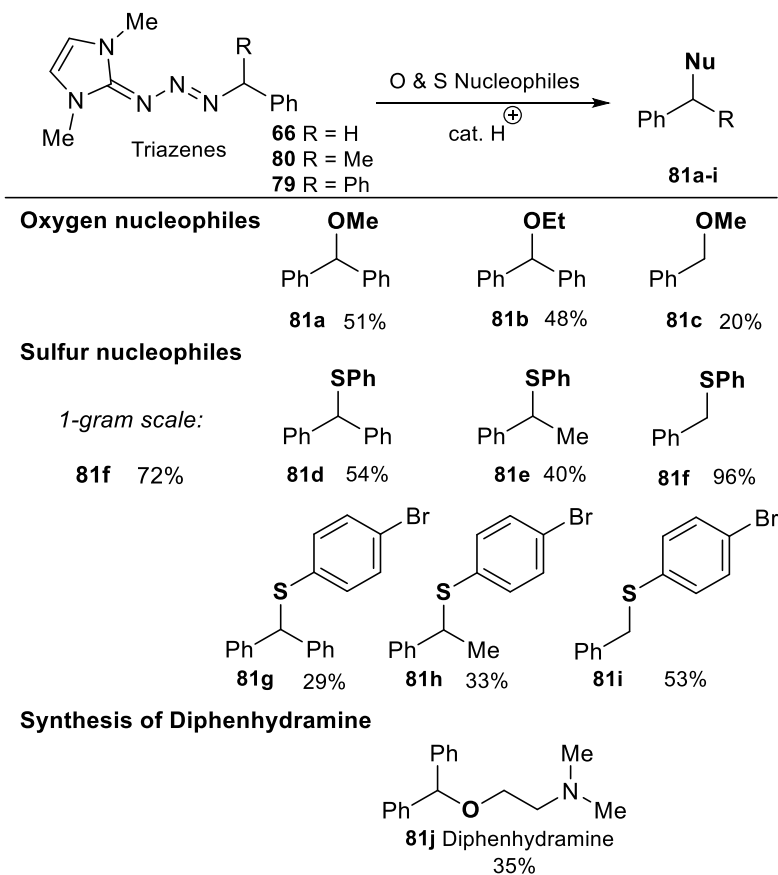
Figure 2-2 Proposed mechanism for the oxidation reaction

2.5 Nucleophilic substitution reactions of π -conjugated triazenes

Considering the proposed Figure 2-2 mechanism, it was hypothesized that nucleophiles, other than DMSO, could attack the protonated triazene intermediate **79a**. If this is correct, this would allow access to a variety of organic compounds from common triazene intermediates. To test this hypothesis, we synthesized triazenes **66**, **80**, and **79** and subjected them to reaction conditions described in Table 2-4 in the presence of oxygen and sulfur nucleophiles. Since the reactions cannot be run in DMSO due to competition with oxidation, a brief solvent screening was performed using catalytic TsOH and 50 equiv of methanol as nucleophile. Unfortunately, low yields were observed with other solvents

(e.g., DMF, acetone, THF, EtOAc, and CH₂Cl₂). However, when thiophenol was investigated as both solvent and nucleophile, we observed an excellent yield (96%) of sulfide **81f** without an external Brønsted acid (Table 2-4). This result indicates that thiophenol can serve as both nucleophile and Brønsted acid, thus catalyzing its own reaction. In addition, two more sulfides derived from thiophenol were also synthesized and afforded the desired products **81d** and **81e** in 54% and 40% yield, respectively (Table 2-4). To our gratification, using 4-bromothiophenol as nucleophile in THF also afforded the sulfide adducts **81g** (from **79**), **81h** (from **80**), and **81i** (from **66**) in 29%, 33%, and 53% yield, respectively.

Table 2-4 Scope of substitution reaction



Encouraged by these results, and because ethers and their corresponding derivatives are valuable synthetic intermediates,⁴³ we next explored the compatibility of the thiophenol-mediated nucleophilic substitution using oxygen-containing nucleophiles. We were pleased to discover that our approach is viable for use with nucleophiles other than thiols. For example, good results were obtained with methanol and ethanol, using only 5 mol % of thiophenol as Brønsted acid. Triazene **79** afforded ethers **81a** and **81b** in 51% and 48% yield, respectively, while triazene **66** gave benzylmethyl ether **81c** in 20% yield. The low yield of **81c** is apparently due to the higher activation energy required to liberate the primary benzyl carbocation intermediate from triazene **66** compared to the secondary benzylic carbocation derivative of triazene **79** (Table 2-4). It is also possible that for the stronger sulfur nucleophiles reacting in thiophenol, an S_N2 mechanism is operating instead considering the opposite trend observed in the yields compared to the weaker O nucleophiles which follow the expected S_N1 trend.

To further demonstrate the synthetic utility and practicality of this transformation, we applied our methodology to the synthesis of the antihistaminic drug diphenhydramine (**81j**, Benadryl®),⁴⁴ depicted on the bottom of Table 2-4. The synthesis of **81j** was accomplished using triazene **79** and 2-(dimethylamino)ethanol, as nucleophile, at 60 °C for 36 h, with a modest 35% yield. The lower yield obtained in this case is the result of incomplete reaction due to the nature of the starting material (very polar oxygen nucleophile); extended reaction times or recycling may provide increased yields.

Overall, the data in Tables 2-3 and 2-4 establish that this method can be used to prepare selectively substituted ketones and aldehydes, structural motifs present in a plethora of important compounds as illustrated with the above-noted synthesis of the ether-containing drug Benadryl®. The notable feature of our new carbonyl synthesis is the use of acidic conditions to accomplish the oxidation (Figure 2-2) instead of the well-known basic

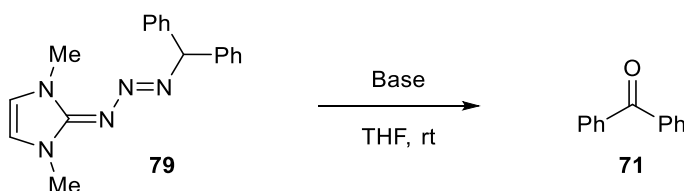
conditions used for other reported DMSO oxidations (e.g., Kornblum⁴² and Swern⁴⁵). This method thus enables the synthesis of ketones and aldehydes from azides without the need for oxalyl chloride addition and under acidic media, a current limitation of the Kornblum and Swern oxidations. Reactions which also require different substrates such as alkyl halides and alcohols respectively.⁴⁶

During the synthesis of triazene **79** with a small excess of base (1.5 equiv of KO-*t*-Bu), trace amounts of benzophenone **71** were observed, indicating that an oxidation of benzhydryl azide **74** was occurring. In order to understand the origin of this transformation and to elucidate the mechanism of this reaction, a comprehensive set of experiments was performed as follows (Table 2-5): Triazene **79** was subjected to an excess of different bases (20.0 equiv) and stirred at room temperature for 3 h. From this study, it was found that organic bases such as DBU did not promote this oxidation (entry 2). On the other hand, CsCO₃, KO-*t*-Bu, and NaH provided the adduct **71** in 55%, 56%, and 58% yield, respectively (entries 3–5). Since these reactions were performed under an air atmosphere and oxygen is known to promote alcohol oxidations under basic conditions,⁴⁷ we carried out an oxygen-free reaction by purging THF with argon and stirring the reaction mixture under an argon atmosphere (entry 6). Surprisingly, the yield was comparable under both argon (57%) and air (58%), and the absence of base did not produce benzophenone **71** (entry 1).

Subsequently, we performed a two-step, one-pot procedure, without the isolation of triazene **79** from NHC precursor **73a** and benzhydryl azide **74**, under basic conditions (entry 7). This also provided benzophenone **71** in similar yield (50%), supporting the convenience of using a one-pot procedure. Finally, according to a previous report, the oxidation of benzylic azides to carbonyl compounds has been observed in DMSO under basic conditions.⁴⁸ Therefore, to determine if this known reaction was responsible for the formation of the product during the *in situ* formation of triazene **79**, benzhydryl azide **74**

was also subjected to 20 equiv. of sodium hydride, in both air and argon atmosphere, resulting in no reaction (Table 5, entries 8 and 9). These results are in accordance to the previous report which establishes that the direct oxidation of azides to carbonyl compounds only occurs readily in highly polar solvents like DMF and DMSO and not in less polar solvents like MeCN.⁴⁸ Since we are using THF which is even less polar, this indicates that azide **74** does not react under said conditions and thus triazene **79** is the reactive species in this transformation.

Table 2-5 Oxidation under basic conditions



entry	substrate	base	atmosphere	time (h)	yield of 71 (%)
1	79	none	argon	3	0
2	79	DBU	O ₂ /air	3	0
3	79	CsCO ₃	O ₂ /air	3	55
4	79	KO ^t -Bu	O ₂ /air	3	56
5	79	NaH	O ₂ /air	3	58
6	79	NaH	argon	3	57
7	73a + 74	NaH	O ₂ /air	3	50
8	74	NaH	argon	3	0
9	74	NaH	O ₂ /air	3	0

In an effort to extend the scope of this transformation using basic conditions, all azide precursors of aldehydes and ketones from Table 2-3 were screened. Unfortunately, only benzophenone **71** was observed in 50% yield (Table 2-5, entry 7) and 4-cyanobenzaldehyde **77e** in less than 10% yield. We propose that product formation, under basic conditions, proceeds via a polar mechanism (Figure 2-3). First, a benzylic deprotonation takes place to form triazene anion **79a'**, followed by a selective protonation to form intermediate **79b'**. Thereafter, **79b'** decomposes to NHC **79c'** and imine **79d'** (observed), with nitrogen extrusion providing the driving force. Finally, hydrolysis of the imine produces benzophenone **71**. However, it should be noted that a radical mechanism is also plausible. Additional studies are required to either refute or support this hypothesis.

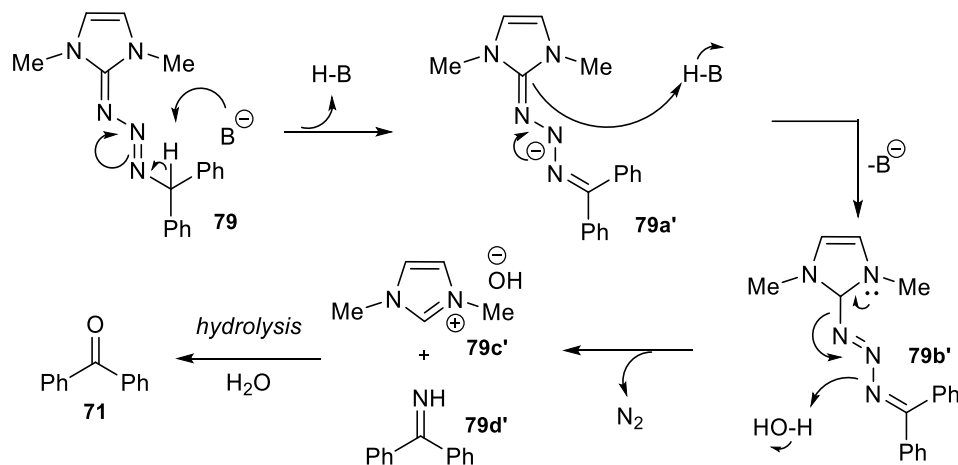


Figure 2-3 Proposed mechanism for the oxidation under basic conditions

In summary, in this chapter we have documented three new reactions of π -conjugated triazenes, specifically, oxidation and substitution reactions both carried under mild reaction conditions. The transformations described above establish the use of organic azides as useful synthetic scaffolds for the synthesis of aldehydes, ketones, ethers, and sulfides compounds via π -conjugated triazene intermediates which can be considered as versatile molecules. The products were observed in moderate to excellent yields, with

sulfur nucleophiles generally giving better results than weaker oxygen nucleophiles. Overall, this methodology not only broadens the known reactivity of traditional organic azides but also provides straightforward access to multiple functional groups starting from highly abundant amines for rapidly building organic frameworks, an important consideration in many synthetic studies.

Chapter 3

Photochemically-Activated Aryl-Aryl Cross-Coupling Reactions

3.1 Introduction

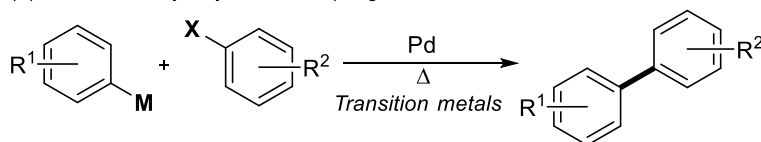
Photochemistry is the study of chemical processes that occur due to absorption of electromagnetic radiation (light). Since its formal discovery and initial development near the turn of the twentieth century, this science has developed attractive and milder alternatives to traditional thermal reactions.⁴⁹ As early as 1912, one of the main photochemistry pioneers, Giacomo Ciamician, envisioned a future where photochemical, and especially sunlight-driven chemical processes, would be prevalent and thus a world where human civilization was powered primarily by sunlight.⁵⁰ Noticing that the coal-dependent industries of his time would not be perpetually sustainable as the non-renewable resource would be depleted over time, he indicated the need to eventually replace fossil fuels with renewable alternatives like sunlight. In particular, with respect to chemical processes, he recognized that photochemical reactions typically involve milder reaction conditions compared to thermal methods, therefore providing a sustainable alternative.⁵⁰ In general, photons in the ultraviolet and visible regions of the electromagnetic spectrum hold sufficient energy to promote molecules to excited electronic states, which in turn can lead to complementary mechanistic pathways that are inaccessible to molecules in the ground state.⁵¹ For example, chemists around the globe have achieved a multitude of challenging transformations, under mild photochemical conditions, that are often impossible without the use of high temperatures or aggressive reagents, such as oxidations,⁵² isomerizations,⁵³ cycloadditions,⁵⁴ deprotections,⁵⁵ and cross-couplings.⁵⁶ Among the former, aryl-aryl cross-coupling is one of the most challenging organic transformations in synthetic chemistry.⁵⁷ This class of reaction is of paramount value in organic chemistry because they provide access to a variety of valuable chemical scaffolds

required to complete syntheses of numerous compounds, including many key biologically-active molecules.⁵⁷ Traditionally, aryl–aryl cross-coupling reactions are mostly achieved using Pd-catalyzed methods such as: Suzuki,⁵⁸ Negishi,⁵⁹ Stille,⁶⁰ or Hiyama⁶¹ couplings (Figure 3-1, eq (1)). Although these methods typically provide the desired adducts in high yields, they often involve the use of stoichiometric toxic heavy metals, such as organic Zn or Sn species, which require specialized procedures for their synthesis, purification, recovery, and disposal.⁶² In addition, significant major limitations encountered in these transition-metal catalyzed cross-coupling reactions are high temperatures, that limit functional group tolerance, and long reaction times, which rise operation costs.⁶³ Alternately, milder synthetic methods, that employ unactivated arenes for the preparation of biaryls, have been reported, albeit still using high temperatures (Figure 3-1, eq (2)).⁶⁴ Among these methods, the most reliable procedures take advantage of highly reactive species such as aryl-iodonium salts,⁶⁵ aryl-diazotates,⁶⁶ and aryl-diazonium salts⁶⁶ in the presence of catalytic amounts of transition metals at high temperatures. Aryl–aryl cross-couplings that take advantage of aryl-diazonium salts are perhaps the mildest approach thus far reported since they release molecular nitrogen, as the clean by-product.⁶⁷ In addition, aryl-diazonium salts are versatile intermediates since they can generate aryl cations⁶⁴⁻⁶⁵ or aryl radicals depending on the reaction conditions.⁶⁸ A major disadvantage of aryl-diazonium salts is their instability, making them less desirable at large scales since they are known to be explosive.⁶⁹ Therefore, it is clear that a milder and straightforward approach to aryl–aryl cross-couplings is still highly desired.

In this chapter we continue exploring the reactivity of π -conjugated triazenes^{19-20,}
⁷⁰ with a particular emphasis on their capability of providing *in situ* generation of aryl-diazonium salts, thus avoiding potential explosions, while maintaining mild reaction conditions. We will discuss π -conjugated triazenes as aryl-diazonium reservoirs⁷¹ that can

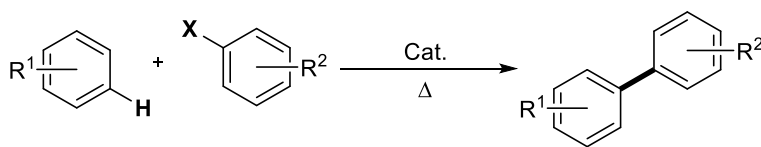
be delivered under photoirradiation at room temperature to produce biaryl adducts (Figure 3-1, eq (3)), in short reaction times. To achieve better results, we take advantage of our previous observation that Brønsted acids can increase the reactivity of π -conjugated triazenes⁷⁰ and Jewett's report on photo-isomerization of triazenes.¹⁴⁻¹⁵

(1) Traditional aryl-aryl cross-coupling reactions:



$\text{M} = \text{Sn, Zn, B, Si}$ $\text{X} = \text{Cl, Br, I, OTf}$

(2) Cross-coupling reactions using unactivated arenes:



Cat. = Fe, Ag, Rh, Cu, Pd, TBP, ^tBuOK

X = B, Br, CHO, CO₂H, diazo, & iodonium salts

(3) Metal-free aryl-aryl cross-coupling at room temperature: **This work**

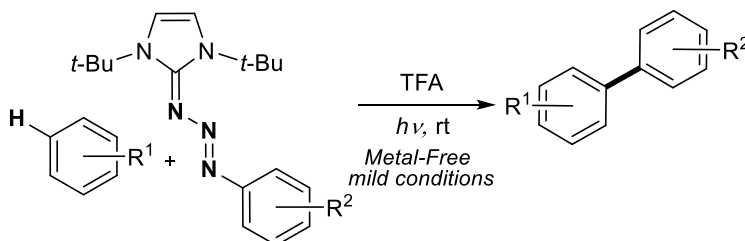


Figure 3-1 Representative syntheses of biaryl compounds

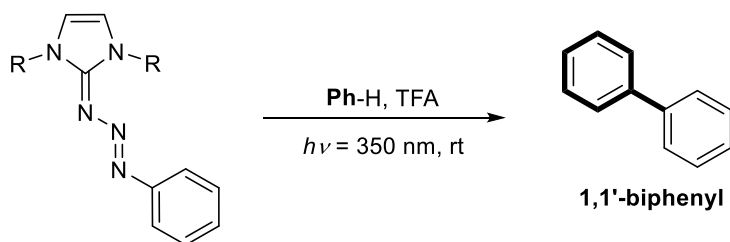
3.2 Reaction design and optimization

Initially, we investigated the conversion of two π -conjugated triazenes derived from methyl and *tert*-butyl imidazolium salts into 1,1'-biphenyl (Table 3-1). In order to find the best reaction conditions, the photochemical transformation was studied using different Brønsted acids and the impact that time and Brønsted acid's stoichiometry have on the product yield. From these experiments, trifluoroacetic acid (TFA) was identified as a superior catalyst over other acids such as: HCl, TsOH, H₂SO₄, and AcOH that only

generated small amounts of the desired biaryl product. With TFA as the optimal Brønsted acid on hand, the reaction time was studied, using 1.0 equivalents of TFA (Table 3-1, entries 1–4). From these results, it was noticed that the reaction virtually halts after 2 h (entry 2), with relatively small increments up to reaction times of 24 h (entries 3 and 4). Therefore, 2 h was selected as a satisfactory reaction time for this transformation. Optimization of TFA's stoichiometry in the reaction media was then investigated using 0.1 to 10 equivalents of TFA (entries 5 to 8). A catalytic amount (0.1 equiv.) of TFA, resulted in only trace amount of product formation (entry 5), while the maximum yield (33%) was observed using 10 equiv. (entry 8). However, since using lower TFA loading (5 equiv.) led to an essentially similar yield (31%), this latter amount was employed as a preferred loading (entry 7). Subsequently, using a different triazene derived from *di**tert*-butylimidazolium tetrafluoroborate (**82c**), we observed a substantial increase in yield (59%) (entry 9). The reaction was also performed under thermal conditions (65 °C) without UV irradiation, affording the expected product in only 3% yield, thus highlighting the power of photochemical induction (entry 10). Also, as a control experiment, we ran the reaction at room temperature, without applying heat or UV irradiation, under which conditions no product was obtained (entry 11), thereby providing additional support for the need of photoactivation to produce the desired adduct.

With the best reaction conditions on hand, and aware of the potential effect of the triazene structure on reaction yields, we synthesized more triazenes using different *N*-heterocyclic carbene (NHC) precursors and azidobenzene to evaluate their effectiveness for the cross-coupling reaction. As depicted in Table 3-2, reaction yields are highly dependent on the stability of the triazene.^{3, 19, 70}

Table 3-1 Optimization of reaction conditions

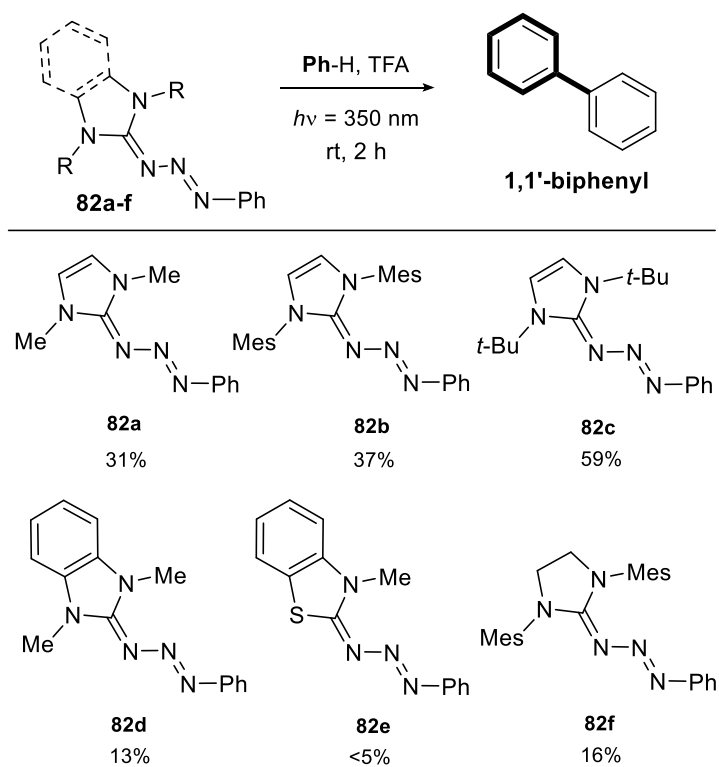


entry	R	TFA (equiv.)	time (h)	yield (%)
1	Me	1	1	7
2	Me	1	2	18
3	Me	1	4	20
4	Me	1	24	22
5	Me	0.1	2	Traces
6	Me	2	2	20
7	Me	5	2	31
8	Me	10	2	33
9	<i>t</i>-Bu	5	2	59
10	<i>t</i> -Bu	5	2	3
11	<i>t</i> -Bu	5	2	0

For example, the highly stable triazene **82f** doesn't react well under these reaction conditions (16%). On the other hand, highly unstable triazenes **82d** and **82e** decomposed too quickly into many by-products, affording the expected product in low yield, 13% and <5%, respectively. Importantly, we also synthesized triazenes that possess moderate stability (**82a-c**), which release the phenyldiazonium ion slow enough to be captured by the unactivated arene. The yields of triazenes **82a-c** are proportional to the size of the nitrogen

substituents on the imidazolium moiety, going from 31% for methyl (**82a**), 37% for mesityl (**82b**), to a significantly higher yield of 59% for tert-butyl (**82c**). This trend is perhaps due to increased steric interactions between the nitrogen substituents and the phenyl moiety that develop during the triazene *E/Z* isomerization upon photo-irradiation, making the triazene derived from **82c** the best choice for this aryl–aryl coupling.^{67b}

Table 3-2 NHC precursor optimization



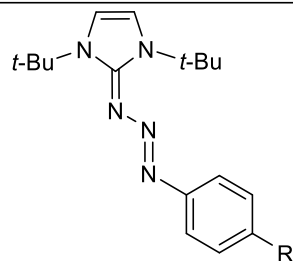
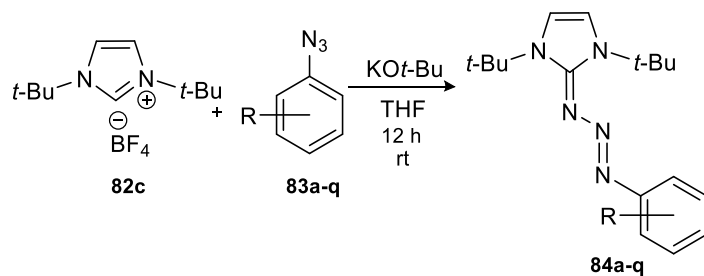
3.3 Triazene synthesis and substrate scope

Having identified *tert*-butylimidazolium tetrafluoroborate **82c** as the most effective NHC partner, we proceeded to synthesize several π -conjugated triazenes by reacting the NHC precursor **82c** with miscellaneous aromatic azides **83a-q**, following our previously established protocol,^{19, 70} to afford seventeen new triazenes **84a-q** with good to excellent yields (Table 3-3). This relatively large set of triazenes includes, electron-donating and

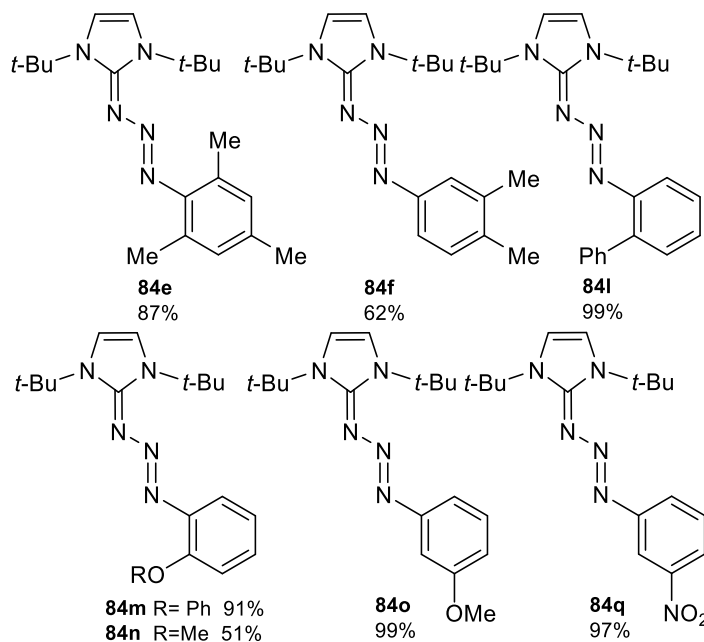
electron-withdrawing substituents. In addition, steric hindrance was also considered. For this purpose, we prepared *para*, *ortho*, and *meta* substituted triazenes with yields up to 99% (Table 3-3). Interestingly, synthesis of triazene **84e** required the use of sodium hydride instead of the commonly used potassium *tert*-butoxide. This observation suggests that the extra benzylic protons in the mesityl moiety might further react with *t*-BuOK via radicals,⁷² whereas NaH doesn't appear to.

To study the scope and limitations of the aryl–aryl cross-coupling reaction, the freshly prepared triazenes **84a–q** were subjected to UV-irradiation (350 nm) for 2 h periods (Table 3-4). Data obtained from these experiments suggest that the electronic character of the substituents on the phenyl ring of the triazene profoundly influence the reaction yield. The neutral triazene **84d** gave the highest yield (59%), whereas triazenes bearing weak electron-withdrawing or weak electron-donating groups such as: alkyl (**84b** & **84c**) or halides (**84a** & **84p**) afforded moderate yields. In addition, triazenes possessing strong electron-withdrawing groups through resonance afforded lower yields. For example, 4-cyanobiphenyl triazene **84h**, gave only 10% yield and 4-nitrobiphenyl triazene **84j** did not react at all, and nearly stoichiometric amount of unreacted starting material, triazene **84j**, was recovered (Table 3-4). This observation is in agreement with our previous observations^{19, 70} as well as Bielawski's,¹⁷ who reported that electron-poor triazenes are particularly stable. This stability renders such triazenes unreactive under our reaction conditions. On the other hand, electron-rich triazenes are highly reactive and readily undergo decomposition to side products, which accounts for the low yield (18%) of 2-methoxybiaryl **85n**.

Table 3-3 Synthesis of aryl π -conjugated triazenes

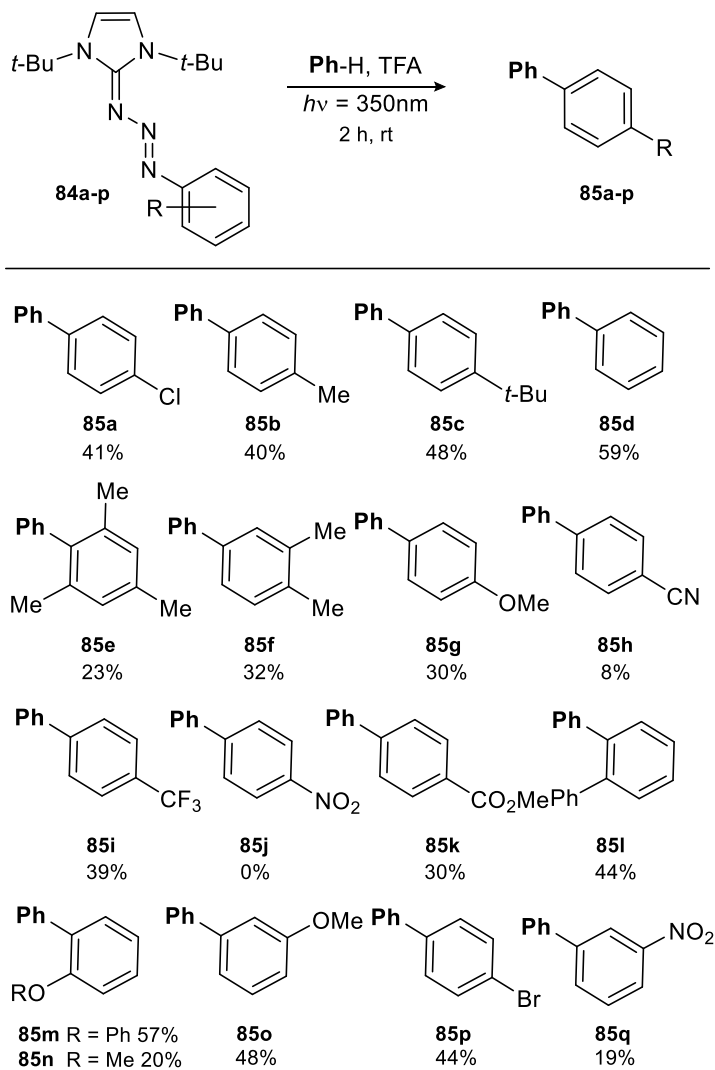


- 84a** R = Cl, 66%
- 84b** R = Me, 48%
- 84c** R = *t*-Bu, 89%
- 84d** R = H, 87%
- 84g** R = OMe, 70%
- 84h** R = CN, 74%
- 84i** R = CF₃, 94%
- 84j** R = NO₂, 90%
- 84k** R = CO₂Me, 69%
- 84p** R = Br, 89%



However, changing the substituent of the triazene from 2-methoxy **84n** to 2-phenoxy **84m** increases its stability due to its weaker electron-donating character, thus helping afford bisaryl adduct **85m** in a higher yield (57%). Finally, the highly steric hindered triazene **84e**, afforded the product **85e**, albeit only in 20% yield.

Table 3-4 Synthesis of biphenyls

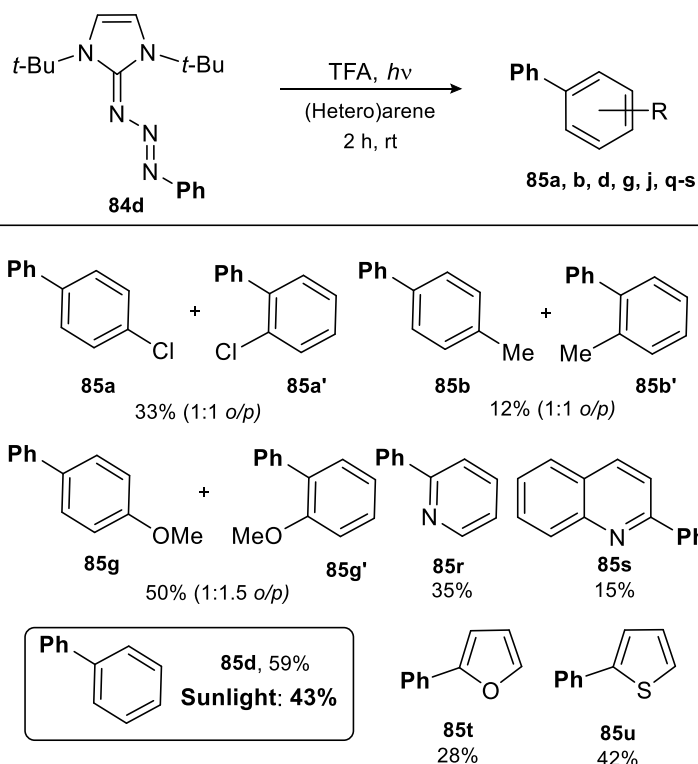


We speculate that the low yield of **85e** is due to the higher energy required for nucleophilic attack by benzene, on the sterically-encumbered carbocation intermediate. Although, most of the yields are moderate, it is worth noting that the reaction tolerates different functional groups including; halides (Cl & Br), electron-poor (CF_3 , NO_2 , CO_2Me , & CN), electron-rich (OMe & OPh), and hindered substrates such as mesityl triazene and

ortho substituted triazenes (Me, OMe & OPh), and most important, none of the substrates produced additional regioisomers (Table 3-4).

To further evaluate the general applicability of this transformation, two different sets of arenes were selected; (1) substituted arenes to investigate their regioselectivity, and (2) heteroarenes, to check their suitability for the preparation of heteroaromatic biaryls, an often-challenging task (Table 3-5).⁶⁶ Arenes such as chlorobenzene and toluene showed product formation but no regioselectivity (1:1, *ortho/para*), whereas anisole exhibited some preference for the most nucleophilic position, the *ortho* regioisomer **4g** (1.5:1, *ortho/para*). In terms of the following heteroarenes: pyridine, quinoline, furan, and thiophene the outcome was encouraging since all the products were isolated as single regioisomers, albeit in moderate yields (Table 3-5). The observed regioselectivity towards *ortho* and *para* positions, with no *meta* product formed suggests that there is a phenyl cation, derived from the triazene, formed during the reaction steps, and it is in agreement with the known selectivity of electrophilic aromatic substitutions.⁷³ However, the adducts isolated from heteroarenes suggest that a phenyl radical is also plausible, since 2-phenylquinoline **85s** was observed (Table 3-5). Because of the two potential mechanistic pathways, we investigated both possibilities further and the details are presented below. Of significant relevance, we note that our transformation can also be performed under even milder conditions using sunlight in lieu of UV-radiation albeit for a longer period of time (9 h in sunlight vs 2 h with UV). For example, the biphenyl adduct **85d** was obtained in 43% yield (as highlighted in Table 3-5).

Table 3-5 Synthesis of biphenyls and heterobiaryls



To demonstrate the practical utility of our method to synthesize bioactive molecules, the known immunosuppressant compound **86** was synthesized in two-steps from stable triazene **84p**. Using our mild reaction conditions, the new brominated biaryl **85v** was generated from triazene **84p** and *p*-xylene in 36%. A 12 h reaction time was required, for the maximum yield, since *p*-xylene is more sterically hindered than benzene. Subsequently, freshly prepared intermediate **85v** was coupled with commercially available 2,3-difluorobenzamide, following the reaction conditions previously reported by Greaney,⁶⁵ to produce the final compound **86** in 90% yield (Figure 3-2).

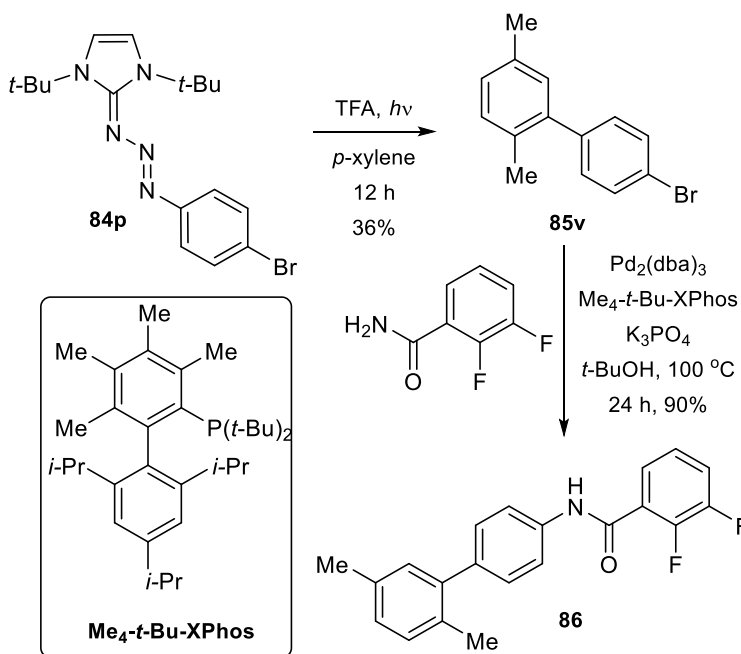


Figure 3-2 Synthesis of immunosuppressant **86**

3.3 Mechanistic and computational studies

After analyzing all the previous results, and to attempt to gain a better understanding of the reaction mechanism, we proceeded to search for any byproducts present in these reactions (Figure 3-3). Our objective was to find an explanation for the modest yields obtained for some of the substrates.

For this purpose, we selected three triazenes (**84c**, **84m**, and **84p**) and subjected them to our standard reaction conditions, with the exception that benzene and benzene- d_6 were employed without drying (Figure 3-3). To our surprise, phenols **85c'**, **85m'**, and **85p'** were isolated in approximately 1:1 ratio with respect to the usual biaryl products. The benzene- d_6 experiment helped us to more closely monitor the reaction and revealed that only the expected biaryl product and the phenolic by-product were present in approximating a 1:1 ratio, with a total yield of 95% (Figure 3-3, eq (2)). These results suggest that water is competing by capturing the proposed aryl cation that is formed *in situ*. This strongly

suggests an ionic mechanism. However, a radical mechanism cannot be ruled out since aryl radicals have been observed during aryldiazonium decomposition.^{67b} After closer analysis of our compiled results, most of the previous reactions presented phenol by-products when wet solvents or reagents were used. However, adding extra water did not affect yields and ratios and our best efforts to perform our reaction under anhydrous conditions did not improve the aryl-aryl cross-coupling yields, since minimum amount of water has a profound effect on the phenyl cation intermediate as will be discussed in the following sections (Figure 3-6).

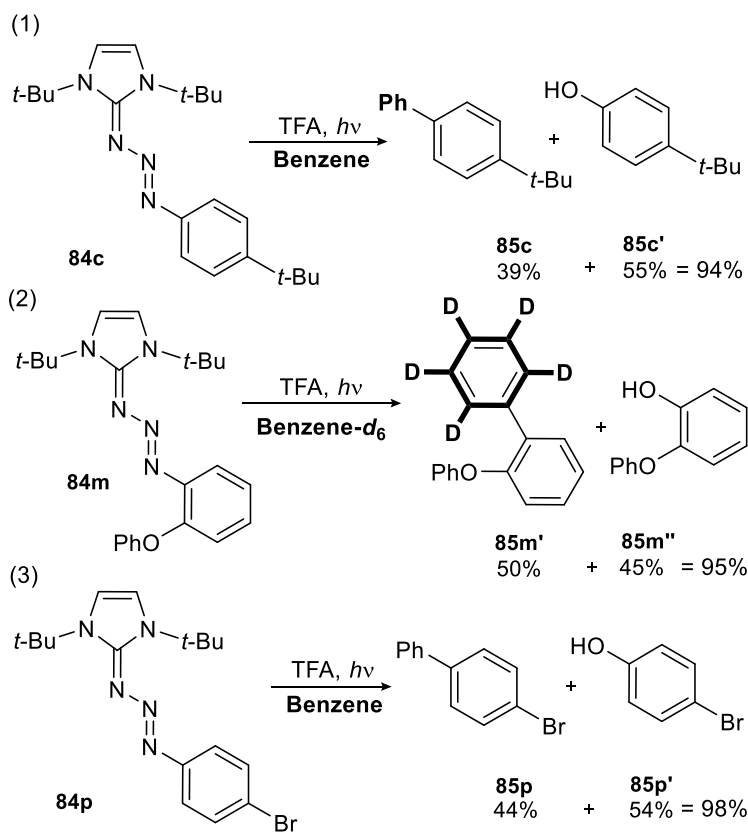


Figure 3-3 Byproduct identification

With all experimental information on hand, we proceeded to consider plausible mechanistic pathways that encompass all the observed results (Figure 3-4). Additionally,

to explore further possible mechanistic pathways, density functional theory (DFT) was employed by Dr. Haobin Wang and Dr. Chou-Hsun Yang at the University of Colorado Denver to examine model compounds discussed in this paper. All of the detailed data obtained from the computational studies can be found in Chapter 6 in Tables 6-1 to 6-9. All calculations were performed using the quantum chemistry program package Q-Chem 5.0⁷⁴ with the hybrid functional B3LYP. Geometry optimizations were carried out using the basis set 6-31G* to find the ground state minima. Then, single point electronic energies were obtained using basis set 6-31+G* (i.e., including diffuse functions), whereas test calculations employing a larger basis set 6-31+G* or 6-311++G** produced relatively smaller differences. Linear response time-dependent DFT (TD-DFT)/TDA calculations were used to calculate the vertical excitation energies and to optimize the excited state structures. Solvent (benzene) effects were approximated using the conductor-like polarizable continuum model (cPCM) model.⁷⁵ To gauge the accuracy of the DFT calculations, we also used the auxiliary basis set (resolution- of-identity) second order Møller–Plesset perturbation theory (RI-MP2)⁷⁶ method to calculate ground state energies for all the triazene compounds (Table 6-1). The benchmark RI-MP2 values are consistent with those from the DFT calculations, suggesting that DFT is adequate for investigating the compounds in this paper.

The first reaction step in Figure 3-4 concerns the protonation of **84d-E**, which involves two main possible sites: N1 and N3, calculations show that the ground state energy of N1-H⁺ is lower than N3-H⁺ for all molecules, as shown in Table 6-2. As reported Table 6-2 our calculations, under our experimental conditions, indicate that the neutral molecules have electronic energies lower than the protonated triazenes (N1-H⁺ by 10–20 kcal mol⁻¹, and N3-H⁺ by 20–30 kcal mol⁻¹). These results were obtained using cPCM model in (dilute) benzene solution, which has a small dielectric constant ($\epsilon = 2.27$). On the

other hand, the energy differences between the neutral and protonated triazenes are significantly reduced when the solvent dielectric constant is increased. Under the actual experimental condition, where trifluoroacetic acid ($\epsilon = 8.55$) is present, protonated species are favored to undergo subsequent photoexcitation processes (Table 6-3). The minimum energy geometries for the protonated N3-H⁺ and unprotonated triazene complexes in their first bright excited states correspond to **84d-Z** configurations. On the other hand, the protonated N1-H⁺ complexes are still in **84d-E** configurations, which suggest that photoisomerization occurs readily for triazenes protonated on N3, but not for those protonated on N1 (Figure 3-4).

The subsequent reaction step for the photoexcited molecules is the ultrafast internal conversion down to their ground states. In principle, the internal conversion competes with the fluorescent decay. To distinguish between the radiative (fluorescent) and non-radiative decay, we estimated the electronic coupling elements (for non-radiative decay) between the ground and excited state using the generalized Mulliken–Hush method (Table 6-4).⁷⁷ Our calculations indicate that internal conversion is the dominant transition. After the non-radiative internal conversion, the electronic energy is transferred into the vibrational energy of the molecule. The specific partition of the converted energy is determined by the vibronic coupling. Under the linear response approximation, this is represented by the ground state gradient at the geometry of vertical de-excitation. While the magnitude of the force reflects the strength of the vibronic coupling, the direction of it can be used to indicate the reaction coordinate (Figure 3-5). Our results show that the vibronic couplings involve primarily the displacement of three nitrogen atoms for the N3-H⁺ complexes, but involve more atoms for N1-H⁺. This suggests that photoexcitation and subsequent internal conversion facilitate the dissociation reaction for N3-H⁺ with a *Z* configuration, but not for N1-H⁺ with an *E* configuration.

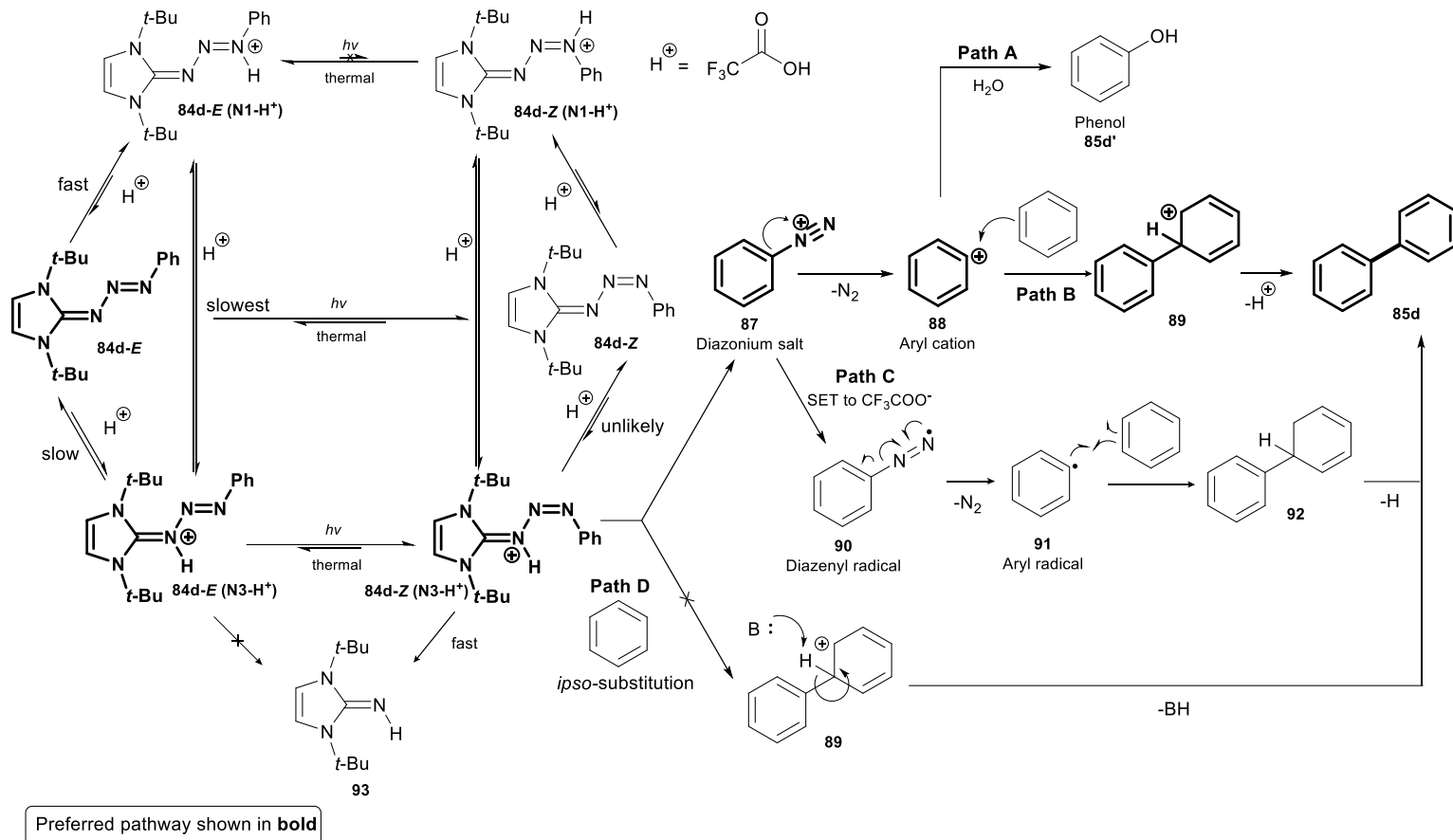


Figure 3-4 Plausible mechanistic pathways for the aryl-aryl cross-coupling reaction

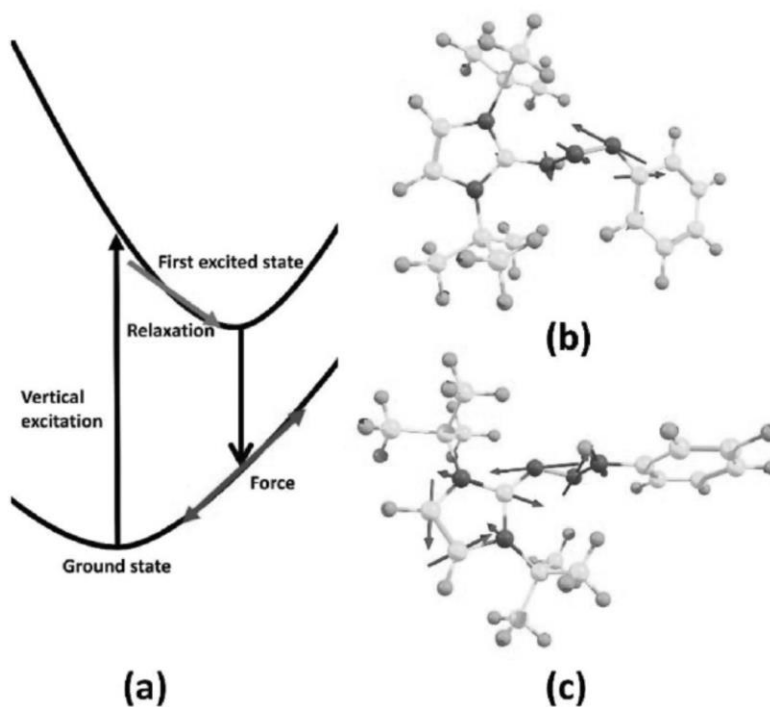


Figure 3-5 Projection of the force for N1-H⁺ and N3-H⁺

At this point in the mechanistic discussion, though the formation of the aryldiazonium intermediate seems plausible, the possibility of direct aromatic *ipso* substitution by the aromatic molecule on the protonated triazene cannot be discarded (Figure 3-4, Path D). Therefore, to obtain experimental data that would allow us to clarify if *ipso* substitution is part of the mechanism, we attempted the capture of the aryldiazonium intermediate, by means of a Sandmeyer reaction, under our conditions.⁷⁸ We subjected triazene **84p** in dichloromethane to reaction with 2.0 equiv. of tetrabutylammonium bromide, 1 mol% of CuBr, and 5.0 equiv. of TFA under UV irradiation at 350 nm. After 2 h, we observed formation of *p*-dibromobenzene in 23% yield, which supports the presence of the phenyldiazonium intermediate upon photo-activation of the triazene **84p** under acidic conditions, suggesting that *ipso* substitution is not occurring (Figure 3-4, Path D).

To discuss thermodynamics of forming the expected product in the final reaction step, there are three possible pathways; two for the aryl cation in Paths A and B, and one for the aryl radical as seen in Path C (Figure 3-4 and Fig. 3-6). For A and B pathways, we performed calculations on two complexes, the aryl cation with water and benzene, and compared their binding energies (Table 6-6). For most species, the electronic energy of the aryl cation with water is higher than that with benzene, within a few kcal per mol. This implies that forming the aryl cation with the benzene complex is slightly more favorable than with the water complex (Figure 3-6).

We also compared the binding energies between Path B and Path C, (Table 6-7). The calculations show that the energy of Path B is much lower than Path C, by around 40–60 kcal mol⁻¹. This indicates that forming the aryl radical complex requires more energy. Therefore, Path C is not favorable in the final reaction step. Finally, the energy of the final products following Path A are slightly higher than Path B, within 5 kcal mol⁻¹, which indicates that both reactions can occur (Figures 3-4 and 3-6).

Finally, we calculated the relative free energies of starting materials, intermediates and products for the aryl–aryl cross-coupling reaction of triazene **84d** (Table 6-9) and constructed the reaction energy diagram shown in Figure 3-4. The total free energy includes the electronic energy, the gas phase entropic contribution and the solvent free energy in the standard state. As can be seen from this diagram, the energies of the ground state protonated triazenes on N1 and N3 are only 15 kcal mol⁻¹ apart in dilute benzene (and 5 kcal mol⁻¹ in THF, $\epsilon = 7.8$). Under experimental conditions and considering subsequent reactions, the two species are likely in equilibrium with one another. Both the unprotonated triazene **84d-E** and the N1 protonated triazene can be photochemically promoted to their respective excited states, but both relax through non-radiative processes back to the ground state (Figure 3-6). On the other hand, once the N3 protonated triazene

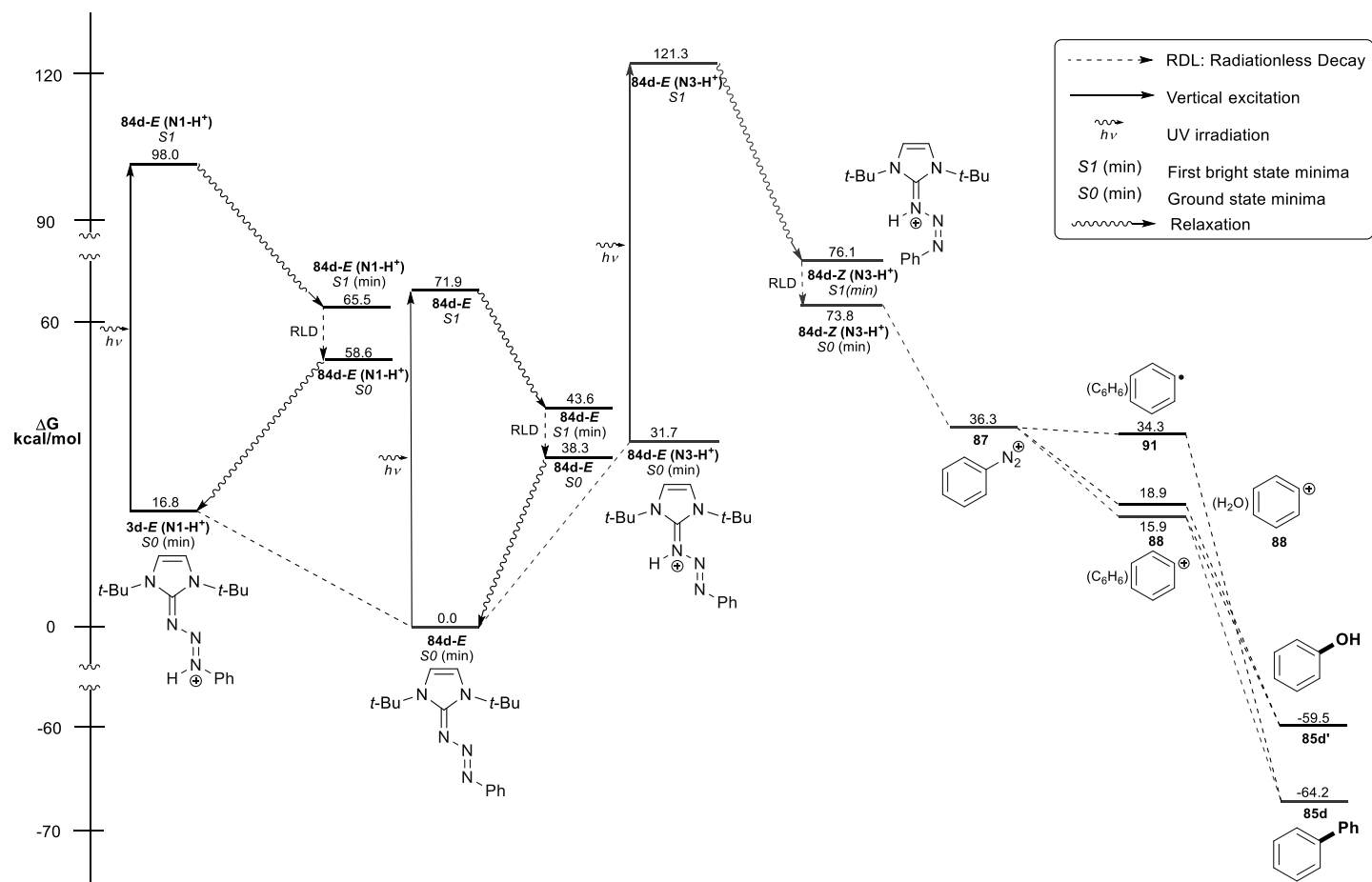


Figure 3-6 B3LYP/6-31G* Reaction energy diagram for the cross-coupling of triazene **84d** to form biphenyl **85d** and phenol **85d'**

is promoted to the excited state it will preferentially isomerize to its respective *Z* isomer **84d-Z**, which can then decompose exergonically to the diazonium ion **87** (Figure 3-6). From that point, the next reaction intermediate is most likely the aryl cation **88**, since in the presence of solvating water its energy is 17 kcal mol⁻¹ lower than **87** and 20 kcal mol⁻¹ lower in benzene (Figure 3-6). The possibility of an *ipso* substitution by benzene at this step, instead of the aryl cation formation, cannot be discounted; however, our calculations didn't find it likely. According to existing literature, the true mechanism might lie somewhere in between aryl cation and aryl radical processes.^{58c, 76b} Finally, the formation of biphenyl **85d** and phenol **85d'** are both likely due to the closeness of their energies, which correlates to the good yields and ratios obtained (Figure 3-3).

In summary, the energy of the ground state for N1-H⁺ is more stable than N3-H⁺; the excitation energies of first bright state of deprotonated and protonated triazene complexes are in the ultraviolet region (Table 6-3). The ultrafast internal conversion for N3-H⁺ in 1-*Z* configuration promotes the subsequent dissociation reaction; whereas for N1-H⁺ there is no such mechanism. The free energies of the aryl cations with water are lower than those with benzene; the free energies of the aryl radical are higher than the aryl cation and the free energies of the final products show biphenyl as slightly more stable than phenol. Therefore, based on the experimental data and the computational analysis, we believe that the most plausible reaction mechanism for the metal-free photochemically-activated cross coupling follows a cationic pathway (Path B), starting with the protonation of the triazene, followed by *E/Z* photoisomerization under UV light irradiation, which activates the triazene for decomposition into an aryldiazonium salt. This aryldiazonium ion loses nitrogen to generate an aryl cation which, in turn, can either react with an aromatic molecule to form the biaryl product or be captured by a molecule of water to produce the corresponding phenol. These two competitive processes which tend to slightly favor the phenolic product

during the final step are likely the cause for the modest yields in our reactions and previous unexplained low yields reported in many different aryl–aryl cross couplings articles.^{58c, 64, 66, 79} Therefore, we have found new reactivity for π -conjugated triazenes and our studies are expected to positively impact aryl-aryl transformations thus significantly helping to contribute to enhanced milder and more sustainable approaches in many chemical reactions and synthetic processes.

Chapter 4

Amide Synthesis

4.1 Introduction

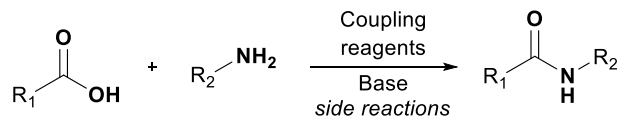
It is well known that the amide functional group is of utmost importance in both chemistry and biochemistry.⁸⁰ For example, amide bonds are fundamental moieties in the structure and function of proteins and enzymes that regulate all metabolic processes of living organisms.⁸¹ Amides are also present in a plethora of natural and synthetic bioactive molecules; for instance, Ghose and Viswandhan reported that amides, along with alcohols and tertiary aliphatic amines are the top functional groups present in the compounds listed in the Comprehensive Medicinal Chemistry drug database.⁸² In view of the prevalence of amide bonds in therapeutic drugs, the ACS Green Chem. Institute Pharmaceutical Roundtable, with representatives of several of the most prominent global pharmaceutical corporations, identified the search for greener amide formation methodologies as their number one priority area of research in 2007.⁸³ Notably, over a decade later, the search for general, greener alternatives still continues.⁸⁴

Amides have been synthesized using a plethora of diverse approaches (Figure 4-1). For example, because a direct acyl substitution reaction between an amine and a carboxylic acid is thermodynamically unfavorable,⁸⁵ most of the traditional methods to prepare amides involve the activation of the carboxylic acid first. This generates reactive species such as: acyl halides,⁸⁶ anhydrides,⁸⁷ acyl azides,⁸⁸ esters,⁸⁹ acylimidazoles,⁹⁰ etc.⁹¹ This resulting activated intermediates can then undergo an acyl substitution with its corresponding amine to form the desired amide bond.⁹¹ Some limitations of these traditional methods include the propensity for some activated species, such as acyl chlorides, to undergo hydrolysis, cleavage of existing protecting groups, and other side reactions.⁹² Other activated intermediates like acyl azides can also produce unwanted

isocyanate by-products via Curtius rearrangement.⁹³ Finally, the use of some activated species such as anhydrides results in the waste of half of the equivalents of carboxylic acid used (Figure 4-1, eq. 1).⁹¹ As a response to the limitations of traditional amide syntheses, new methodologies have emerged that attempt to circumvent these issues. For example, using boronic acids as catalysts to achieve the direct condensation of carboxylic acids and amines to amides (Figure 4-1, eq. 2);⁹⁴ oxidative coupling of alcohols and amines by using ruthenium catalysts (Figure 4-1, eq. 3);⁹⁵ the reaction of thioacids with amine surrogates such as isonitriles,⁹⁶ isocyanates,⁹⁷ azides,⁹⁸ and sulphonamides (Figure 4-1, eq. 4);⁹⁹ and the Buchwald cross-coupling amidation.¹⁰⁰ These methods, though promising alternatives to conventional amide syntheses, still require harsh conditions and, in most cases, the use of heavy metal catalysts, high temperatures, and long reaction times,¹⁰¹ which makes them less desirable from a Green Chem. perspective (Figure 4-1).

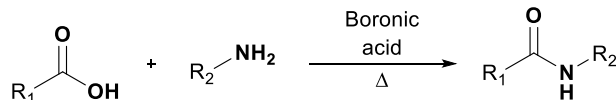
In our continued effort to develop greener alternatives for carbon-carbon and carbon-heteroatom bond forming transformation, we have achieved and reported mild methods that produce aldehydes, ketones, thiols, alcohols, allenols, miscellaneous allylic compounds, and biaryls.^{70, 102} In the previous chapter, we described a mild photoinduced cross-coupling reactions of π -conjugated triazenes with unactivated arenes.^{102b} This aryl-aryl cross coupling served as the foundation to the design of a greener alternative for the efficient synthesis of amides, achieved under metal-free and simple photoactivation of π -conjugated triazenes in the presence of aliphatic and aromatic nitriles under mild conditions (Fig. 1, eq. 5). This also represents a further development of the reactivity of π -conjugated triazenes, adding the amide group to the list of functional groups that can be accessed through these versatile molecules.

(1) Conventional amide formation by acid activation:

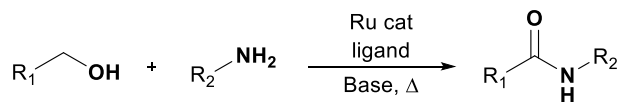


Coupling reagents: SOCl₂, H₂NN₂H, CDI, DCC, etc.

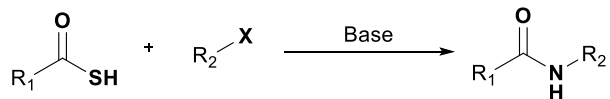
(2) Direct condensation with boronic acid catalysts:



(3) Ru-mediated oxidative coupling of alcohols and amines:



(4) Reaction with thioacids with amine surrogates:



$\text{X} = \text{NC}, \text{NCO}, \text{ArSO}_2\text{NH}, \text{N}_3$

(5) Photoreaction of π -conjugated triazenes with nitriles. **This work:**

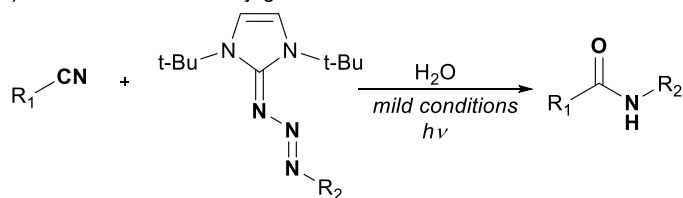


Figure 4-1 Representative methods for amide synthesis

4.2 Initial observation and reaction optimization

In the previous chapter we demonstrated that π -conjugated triazenes can be photoactivated easily in the presence of a Brønsted acid.^{102b} During those studies and while trying aryl-aryl cross-coupling reaction in different solvents we discovered an unknown product formed when triazene **84c** was reacted under UV light in acidic acetonitrile. We isolated this product and identified as amide **94d** which was initially obtained in 48% yield (Figure 4-2).

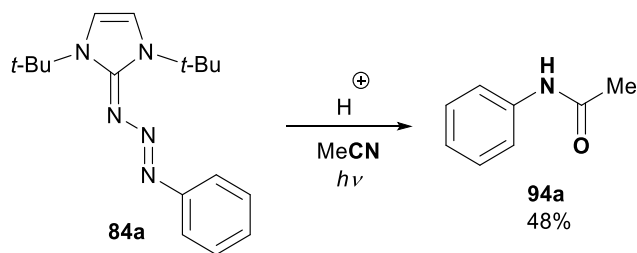
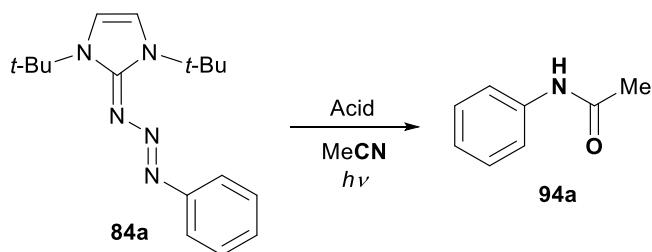


Figure 4-2 Initial observation of amide formation

Intrigued by this transformation, we decided to explore this mode of reactivity further. At time, we had already determined that *tert*-butylimidazolium tetrafluoroborate **82c** as the best *N*-heterocyclic carbene precursor to enhance the reactivity of triazenes. Therefore, we investigated the direct conversion of π -conjugated triazene **84a** into amide **94a** (Table 4-1). Initially, and to optimize the reaction conditions, different Brønsted acids were screened; including trifluoroacetic acid (TFA), TsOH, HCl, and H₂SO₄ (entries 1 to 5). H₂SO₄ proved to be too harsh and unidentified byproducts were observed (entry 1), whereas TFA afforded a 61% yield (entry 5). Encouraged by this result, TFA's stoichiometry was investigated using 1.0 to 10 equivalents of TFA, using photo-irradiation at 350 nm during 4 h (entries 5 to 7). It was found that 5.0 equivalents of TFA were optimal to efficiently promote this transformation (entry 5). The impact of reaction time was also studied (entries 5, 8 to 10). It was noted that the reaction practically halts after 4 h (entry 5), with a very small differences even at 12 h (entry 10). Therefore, 4 h was chosen as the best reaction time for this transformation. Important to note that all reactions were performed open to the atmosphere, and the expected product was still obtained in 43% yield using dry acetonitrile (entry 11), presumably due to moisture in the air and traces amount of water present in TFA. For comparative purposes, two reactions were simultaneously performed, one using ACS grade acetonitrile (entry 5) and the second using dry acetonitrile with 10 equivalents of water (entry 12). Both reaction afforded the product

in similar yields (61% vs 60%, respectively). Finally, the reaction was done at room temperature without applying UV irradiation, under which conditions no reaction was observed, even after 12 h (entry 13), thereby supporting our hypothesis that photoactivation is required to produce the desired amides.

Table 4-1 Optimization of amide synthesis



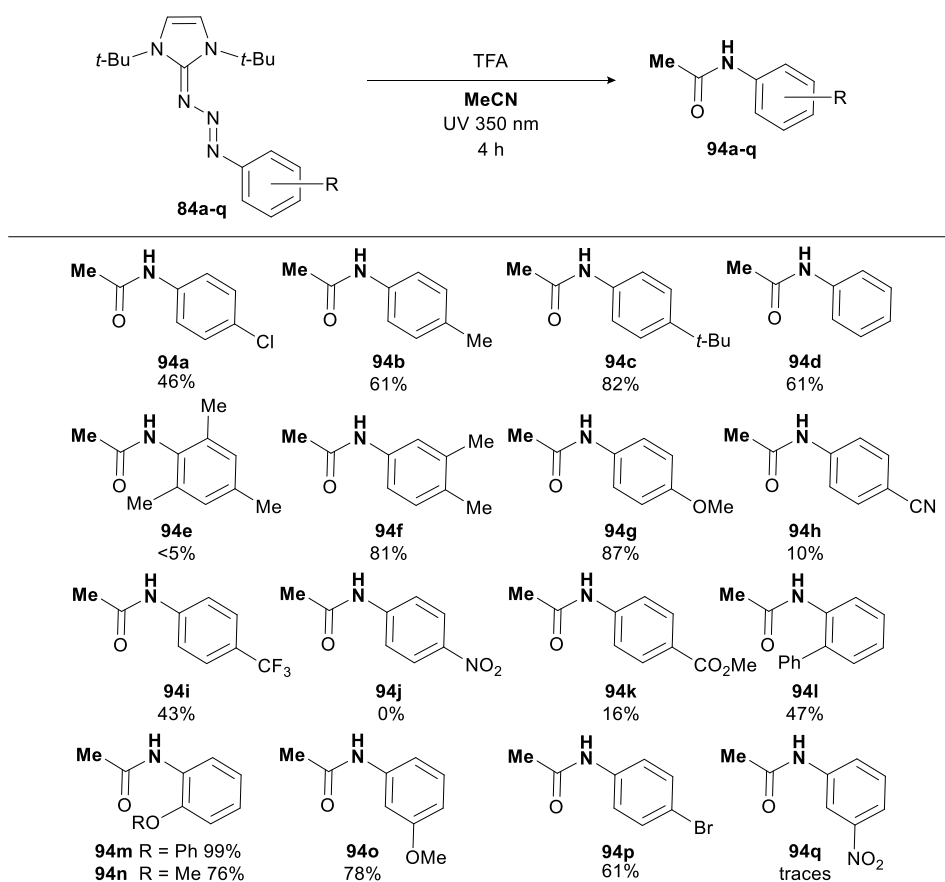
entry	acid	acid equiv.	time (h)	yield (%)
1	none	0	4	No Rxn
2	H ₂ SO ₄	5	4	8
3	HCl	5	4	40
4	TsOH	5	4	44
5	TFA	5	4	61
6	TFA	1	4	17
7	TFA	10	4	60
8	TFA	5	2	33
9	TFA	5	8	62
10	TFA	5	12	62
11	TFA	5	4	43
12	TFA	5	4	57
13	TFA	5	12	No Rxn

4.3 Reaction scope

With the optimal conditions established, we proceeded to explore the overall potential and scope of our new synthetic transformation. For this purpose, we utilized the same set of π -conjugated triazenes **84a-q** that we tested in the previous chapter. With this diverse set of triazenes, the direct conversion of these freshly prepared triazenes into acetamides was investigated employing UV irradiation and TFA (Table 4-2). The results indicated that our transformation has a strong dependence on steric and electronic effects of the aromatic azide moiety (Table 4-2). For instance, the standard triazene **84d**, which is derived from benzene, afforded the expected product **94d** in 61% yield, whereas triazenes with aromatic rings having weak electron-donating alkyl groups (i.e., toluene **84b**, 1,2-xylene **84f**, and 4-*tert*-butylbenzene **84c**), afforded 61%, 81%, and 82% yields, respectively. However, when triazene bearing a mesityl group **84e** was subjected to the same reaction condition, only <5% of product **94d** was observed, presumably due to the steric repulsion caused by the two *ortho* methyl groups. The prior statement is also supported by the fact that biphenyl amide **94l** adduct, that has an *ortho* phenyl group, was obtained in only 47% yield. On the other hand, electron-rich triazenes bearing strong electron-donating substituents in the *ortho* position, such as phenoxy **84m** and methoxy **84n** groups, led to excellent yields, with the phenoxy derivative **84m** delivering the expected product in 99% yield. In addition, when comparing the anisole derivatives (*para* **84g**, *meta* **84o**, and *ortho* **84n**) a slight preference for the *para* position over the *ortho* and *meta* isomers was observed, indicating that both steric and electronic effects play an important role in the reaction mechanism. Furthermore, the reaction tolerated halides, the chloro **84a** and bromo **84p** adducts were obtained in 46% and 61% yields, respectively. Moreover, electron-withdrawing groups such as; nitro (both *meta* **84m**, and *para* **84j**), cyano **94h** and methyl ester **94k** substituents led to poor yields or even no formation of

products. Nonetheless, it is important to note that strong electron-poor triazenes don't decompose easily.^{3, 19} Therefore, unreacted triazene can be recovered from the reaction mixtures. Fortunately, the moderate electron-poor triazene **84i** produced the expected benzamide adduct **94i** in 43% yield (Table 4-2). All this evidence suggests that a positively charged intermediate, most likely an aryl cation is involved in the formation of the amides, which can be stabilized by electron-donating groups. However, steric hindrance and electron-withdrawing substituents decrease the reaction yield.

Table 4-2 Reaction scope for amide formation

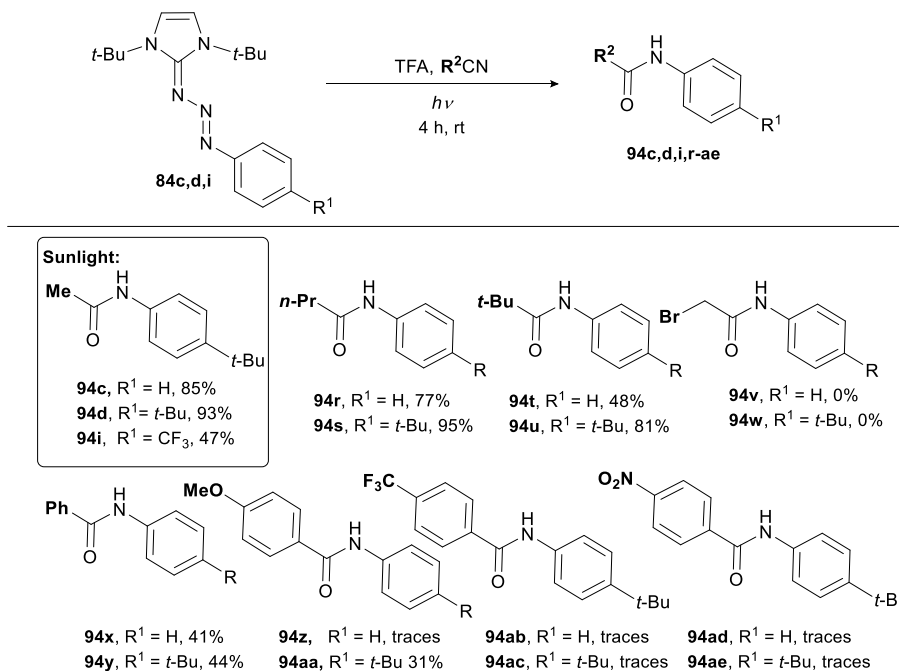


With the triazene scope established, we proceeded to evaluate other alkyl and aryl nitriles as suitable reagents for the amidation reaction (Table 4-3). We reacted various alkyl

and aryl nitriles with three triazenes (**84c**, **84d**, and **94i**), under our optimal reaction conditions. The results of these experiments are summarized in Table 4-3. While comparing acetonitrile reactivity with those three triazenes (Table 4-2), it was found that triazene **84i** gave the lowest yield (43% of amide **94i**), whereas triazenes **84c** deliver adduct **94c** with the highest yield (82%). The alkyl nitriles butyronitrile and trimethylacetonitrile followed the same pattern, with yields up to 95%, see adduct **94s** (Table 4-3). Unfortunately, bromoacetonitrile was not suitable for this transformation and only triazene decomposition was observed **94v-w**, perhaps due to the easily cleavable bromine group. On the other hand, aromatic nitriles resulted in modest yields (i.e., **94x** 41%, **94y** 44%, and **94aa** 31%) to only traces (e.g., **94ae**). These results can be rationalized by the lower nucleophilicity of aryl vs alkyl nitriles due to electron delocalization over the aromatic system. Nonetheless, it is also worth mentioning that in contrast to the experiments performed in benzonitrile as the solvent (**94x** and **94y**), the solids *p*-nitrobenzonitrile, *p*-(trifluoromethyl)benzonitrile, and anisonitrile were dissolved in 2 mL of dichloromethane (DCM) and subjected to the reaction conditions (Table 4-3). Importantly, once again, it was observed that the electron-rich anisonitrile was a suitable reagent to produce the expected adduct **94aa** in 31%, due to its high nucleophilicity. In contrast, electron-poor benzonitriles produced only traces of the expected compounds, further accentuating the importance of the nucleophilicity of the nitrile species on the overall reaction.

In all experiments, the largest triazene **84c** proved to be the best substrate, indicating a correlation between the stability of the triazene and the product yield (Tables 4-2 & 4-3). The results have shown that highly stable triazenes do not react (e.g., **84j**), whereas unstable or sterically hindered triazenes decomposed to unknown byproducts (e.g., **94e**).

Table 4-3 Reaction scope with different nitriles



In order to further explore the power of photochemistry and to test our transformation as a potential greener alternative for amide synthesis, we performed a couple of reactions under natural sunlight (Table 4-3). We were delighted to see the expected product formed in good to excellent yields. The sunlight results followed a similar trend as the standard procedure, wherein electron-deficient benzamide **94i** was produced in 47%, neutral benzamide **94c** in 85%, and the weak, electron-rich 4-*tert*-butylbenzamide **94d** in 93% yield (Table 4-3 inside the box). It is worth noting that these yields are from 4 to 24% higher than those obtained from the standard conditions, albeit achieved in 9 h instead of 4 h. Furthermore, two unproductive nitriles from the standard conditions [bromoacetonitrile and *p*-(trifluoromethyl)benzonitrile] were subjected to sunlight irradiation, unfortunately, the outcome was the same, no adduct was observed. Although, some nitriles are not suitable for this transformation, we have demonstrated that natural sunlight is very

efficient for the direct conversion of triazenes into amides. We believe that the remaining substrates, from Tables 4-2 and 4-3, can be certainly produced employing sunlight irradiation. However, sunlight intensity is not the same around the year or around the globe. Therefore, presumably yields will be different for reactions performed here in Texas compared to those observed in other climates.

4.4 Proposed mechanism

Considering our parallel work,^{102b} the data obtained, and the trends observed, we propose a reaction mechanism, illustrated in Figure 4-3. During the initial step, triazene **84d** is protonated by TFA, this protonated triazene subsequently undergoes photoisomerization from the (*E*)-isomer to the (*Z*)-isomer. Then, the (*Z*)-protonated triazene easily decomposes into guanidine **93** and aryl diazonium salt **87**, which quickly loses nitrogen gas to produce aryl cation **88**. Subsequent nucleophilic attack to the carbocation **88** by the nitrile results in the formation of a nitrilium ion intermediate **95**, which is captured by water, to form the expected benzamide product **94d**. Overall, our proposed mechanism can be considered an analogue to the Ritter reaction¹⁰³ with an aryl cation intermediate instead of the known alkyl carbocation that serves as the electrophile.¹⁰³ In this reaction, the triazene would act as a photochemically-activated source for the diazonium ion,¹⁰⁴ such diazonium ions are known precursors of aryl cations.¹⁰⁵

Alternatively to the depicted proposed mechanism (Figure 4-3), it is important to consider that π -conjugated triazenes can also act as nucleophiles, as previously reported by Bielawski, during S_N2 studies.²⁹ This alternative mechanism could involve a direct attack from the aniline nitrogen of the triazene to a protonated nitrile. To examine this potential alternative pathway, we conducted additional experiments using isotopically-labelled molecules. First, we reacted triazene **84c** with acetonitrile- d_3 and, as expected, the new deuterated amide **94c'** was obtained in 65%, using the standard procedure (Figure 4-4, eq.

1). Then, and in order to determine whether the nitrogen atom of the amide product originated from the triazene or from the nitrile, we prepared ^{15}N -labeled triazene **84c'**. When reacting this isotopically-labelled triazene **84c'** with acetonitrile, the product **94c** was isolated in 71% (Figure 4-4, eq 2). However, its ^{15}N NMR spectrum didn't present any peaks, thus indicating that the nitrogen did not originate from the triazene molecule. In contrast, when the non-labelled triazene **84c** was reacted with ^{15}N -labelled benzonitrile, the resulting amide **94y'** showed a clear ^{15}N NMR peak at 121.5 ppm (Figure 4-4, eq 3). This signal is distinct from that of the ^{15}N -labelled benzonitrile starting material, which appears at 250.1 ppm. Therefore, these results clearly indicate that the nitrogen on the amide indeed originates from the nitrile, which would be in accord with the mechanism we propose in Figure 4-3.

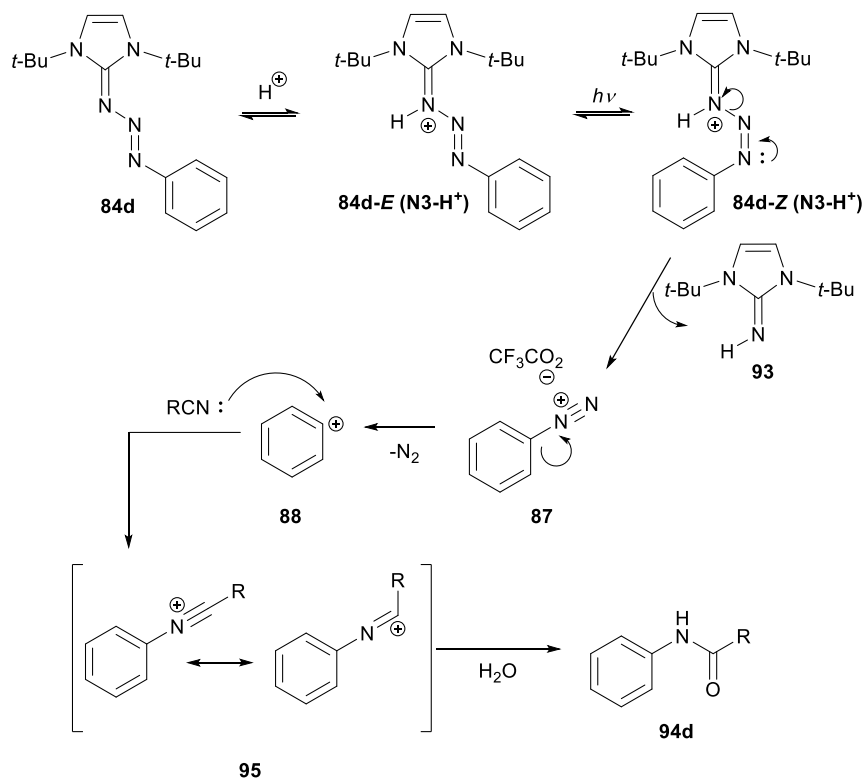


Figure 4-3 Proposed mechanism for amide synthesis

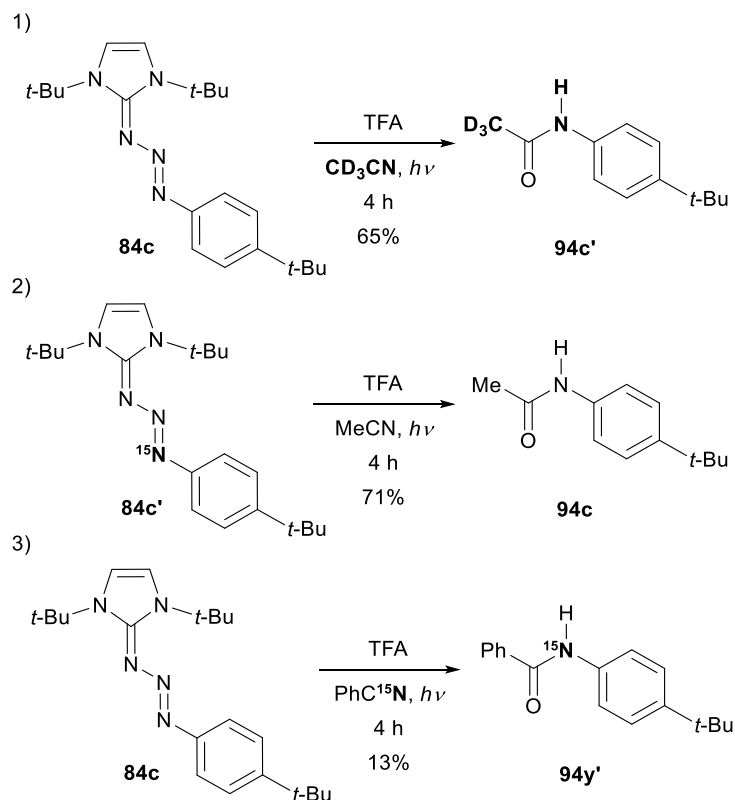


Figure 4-4 Experiments with isotopically-labelled molecules

Finally, to further test the synthetic utility of this new green, and more straightforward amide bond-forming reaction, we synthesized two important, biologically active molecules (Figure 4-5). We used this new approach to synthesize biaryl-containing amide compound **86**, (shown on the previous chapter) which has been shown to inhibit interleukin-2 cytokine, suppressing the immunological processes of cells.⁶⁵ To achieve the synthesis of this bioactive molecule **86**, we took advantage of our parallel report described on Chapter 3 that utilized a green strategy to photochemically promote aryl-aryl cross-coupling reactions of π -conjugated triazenes with arenes,^{102b} in a tandem process with this amide bond formation reaction (Figure 4-5). First, triazene **84r** was synthesized in 63% yield by the coupling of di-*tert*-butylimidazolium tetrafluoroborate **82c** with 1,4-

diazidobenzene **83r**, using potassium *tert*-butoxide as a base (Figure 4-5, top). Then, a 2:1 mixture of *p*-xylene and 2,3-difluorobenzonitrile (DFBN) were added to the freshly prepared triazene **84r** and photoirradiated at 350 nm for 4 h. We were thrilled to obtain the desired compound **11** in 45% yield. We believe this is an impressive accomplishment, since two of the most critical transformations were performed simultaneously in one pot, under mild reaction conditions. The second biologically active compound, acetaminophen (Tylenol®), was readily prepared in two synthetic steps from triazene **84g**. Step one involved our standard amidation reaction conditions to produce benzamide **94g** in 87%. The second step involved demethylation using BBr₃.¹⁰⁶ Acetaminophen was isolated in 53% yield (Figure 4-5, bottom).

In summary, we have presented yet another example of previously unknown π -conjugated triazene reactivity that allows access to amides under mild photochemical conditions. This transformation along with the aryl-aryl cross-coupling described in Chapter 3, opens up the possibility of introducing two of the most important functional groups (biaryl and amide) in a simple, single-step reaction as demonstrated in the synthesis of immunosuppressant molecule **86**. This highlights the potential that π -conjugated triazenes have as versatile molecules and the perspective of future discoveries when continuing to explore their still relatively unknown reactivity.

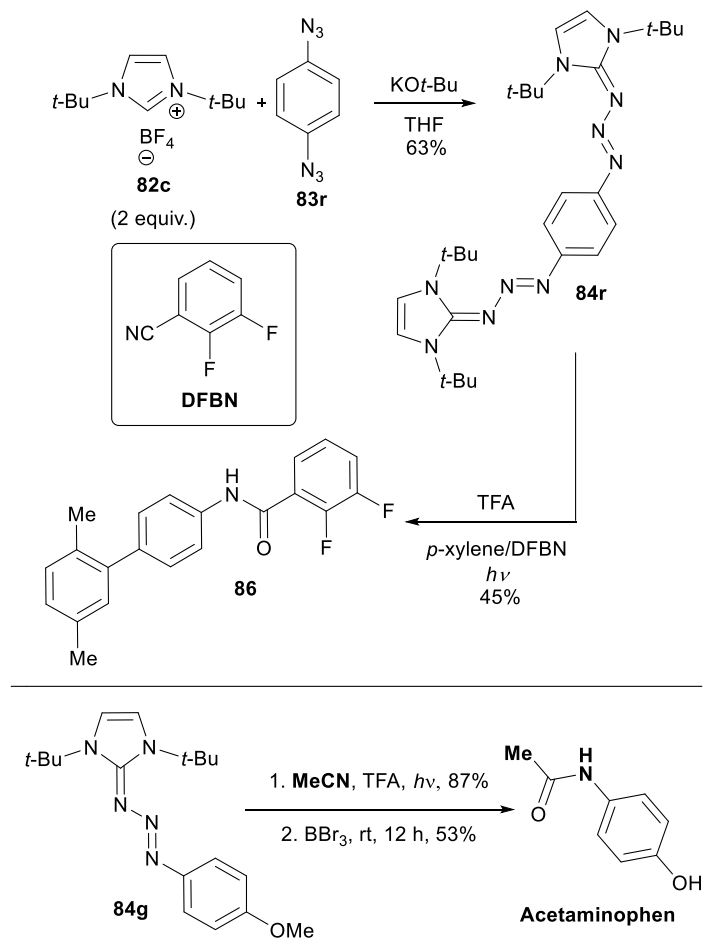


Figure 4-5 Synthesis of biologically-active compounds

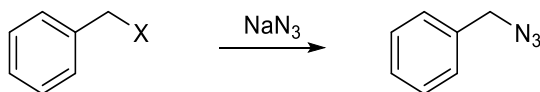
Chapter 5

Experimental procedures for Chapter 2

General Information

All reactions were carried out in oven-dried glassware with magnetic stirring. All NHC precursors were commercially obtained and used as received. Solvents were dried and degassed from a JC Meyer company solvent purification system. Heating was accomplished by oil bath. Purification of reaction products was carried out by flash column chromatography using silica gel 60 (230-400 mesh). TLC visualization was accompanied with UV light and KMnO₄ and iodine stains. The removal of volatile solvent was accomplished using a rotary evaporator attached to a dry diaphragm pump (10-15 mm Hg) followed by pumping to a constant weight with an oil pump (<300 mTorr). ¹H NMR spectra were recorded at 500 MHz and 300 MHz, and are reported relative to CDCl₃ (δ 7.25), DMSO (δ 2.50) or CD₃OD (δ 3.31). ¹H NMR coupling constants (*J*) are reported in Hertz (Hz) and multiplicities are indicated as follows: s (singlet), d (doublet), t (triplet), m (multiplet). Proton-decoupled ¹³C NMR spectra were recorded at 125 MHz and 75 MHz and reported relative to CDCl₃ (δ 77.0), DMSO (δ 39.5) or CD₃OD (δ 49.0) IR experiments were recorded with neat samples on a Bruker Alpha instruments fitted with diamond ATR sample plate. High-resolution (HR) mass spectra were recorded at the Shimadzu Center Laboratory for Advance Analytical Chemistry at UTA.

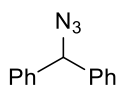
General Procedure for the Synthesis of Azides (73)



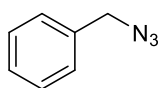
Method A. The corresponding halide (1 equiv.) was dissolved in DMF (0.5 M). Sodium azide (1.2 equiv.) was then added and the resulting mixture was stirred at 80 °C for 4 h. Then, the mixture was allowed to cool to room temperature and water was added. Two extractions were then performed with Et₂O, the organic layer was washed with brine dried over Na₂SO₄ and evaporated under reduced pressure to yield products **73a**, **73b**, **73d**, **73e**, **73g**, **73h** and **73j**.

Method B. *p*-nitro benzyl chloride (1 mmol), sodium azide (1.2 mmol) and 30 mL of DMSO were added to a light-shielded reaction flask. The mixture was then stirred at room temperature for 1 h. 30 mL of water were then added. The mixture was extracted with ethyl acetate (3 x 15 mL), the organic layer was washed with brine (2 x 15 mL), dried over Na₂SO₄ and evaporated under reduced pressure to yield **73c**.

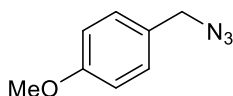
Method C. To a vigorously stirred solution of NaI (4 mmol) and furfuryl alcohol (2 mmol) in 2 mL of acetonitrile under argon was added methanesulfonic acid (4 mmol) at room temperature. The reaction mixture was stirred for 15 minutes. Then, anhydrous aluminum chloride (0.2 mmol) and sodium azide (6 mmol) were added and the reaction mixture was heated to reflux and stirred for 5 h. Then, the mixture was allowed to cool to room temperature and quenched with water. Three extractions were then performed with Et₂O, the organic layer was washed with 10% sodium sulfate solution, dried over Na₂SO₄ and evaporated under reduced pressure to yield crude products. The crude products were purified by column chromatography on silica gel, using hexanes as mobile phase yielding product **73f**.



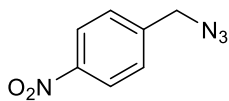
(Azidomethylene)dibenzene (71)¹⁰⁷ Colorless liquid (146 mg, 70% yield) ¹H NMR (500 MHz, CDCl₃) δ 7.46-7.36- (m, 10H), 5.79 (s, 1H); ¹³C NMR (125 MHz, CDCl₃) δ 139.8, 128.9, 128.3, 127.6, 68.7



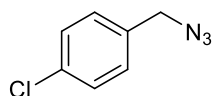
(Azidomethyl)benzene (73a)¹⁰⁷ Colorless liquid (109 mg, 82% yield) ¹H NMR (500 MHz, CDCl₃) δ 7.49-7.39 (m, 5H), 4.37 (s, 2H); ¹³C NMR (125 MHz, CDCl₃) δ 135.6, 129.0, 128.5, 128.4, 54.9



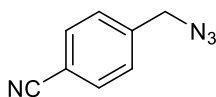
1-(azidomethyl)-4-methoxybenzene (73b)¹⁰⁷ Colorless liquid (98 mg, 60% yield) ¹H NMR (500 MHz, CDCl₃) δ 7.26 (d, *J* = 8.6 Hz, 2H), 6.93 (d, *J* = 8.6 Hz, 2H), 4.26 (s, 2H), 3.80 (s, 3H); ¹³C NMR (125 MHz, CDCl₃) δ 159.8, 129.9, 127.6, 114.3, 55.3, 54.5



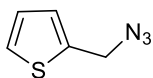
1-(azidomethyl)-4-nitrobenzene (73c)¹⁰⁸ Colorless liquid (98 mg, 55% yield) ¹H NMR (500 MHz, CDCl₃) δ 8.21 (dd, *J*_d = 9.16 Hz, *J*_d = 2.29 Hz, 2H), 7.48 (d, *J* = 8.59 Hz, 2H), 4.49 (s, 2H); ¹³C NMR (125 MHz, CDCl₃) δ 147.8, 142.9, 128.7, 124.1, 53.8.



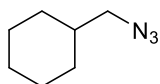
1-(azidomethyl)-4-chlorobenzene (73d)¹⁰⁹ Colorless liquid (144 mg, 86% yield) ¹H NMR (300 MHz, CDCl₃) δ 7.36 (d, *J* = 8.6 Hz, 2H), 7.25 (d, *J* = 8.6 Hz, 2H), 4.31 (s, 2H); ¹³C NMR (75 MHz, CDCl₃) δ 134.3, 134.1, 129.7, 129.1, 54.1.



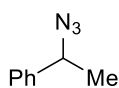
4-(azidomethyl)benzonitrile (73e)¹⁰⁷ Colorless liquid (123 mg, 78% yield) ¹H NMR (500 MHz, CDCl₃) δ 7.65 (d, *J* = 8.59 Hz, 2H), 7.42 (d, *J* = 8.59 Hz, 2H), 4.43 (s, 2H); ¹³C NMR (125 MHz, CDCl₃) δ 140.9, 132.7, 128.6, 118.6, 112.2, 54.1.



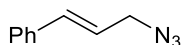
2-(azidomethyl)thiophene (73f)¹¹⁰ Colorless liquid (60 mg, 43% yield) ¹H NMR (500 MHz, CDCl₃) δ 7.33 (dd, *J*_d = 5.15 Hz, *J*_d = 1.15 Hz, 1H), 7.06 (d, *J* = 3.44 Hz, 1H), 7.03-7.01 (m, 1H), 4.49 (s, 2H); ¹³C NMR (125 MHz, CDCl₃) δ 137.4, 127.5, 127.3, 126.6, 49.2



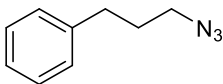
(Azidomethyl)cyclohexane (73g)¹¹¹ Colorless liquid (84 mg, 60% yield) ¹H NMR (500 MHz, CDCl₃) δ 3.08 (d *J* = 6.30 Hz, 2H), 1.76-1.70 (m, 4H), 1.57-1.48 (s, 1H), 1.28-1.09 (m, 3H), 0.98-0.90 (m, 2H); ¹³C NMR (125 MHz, CDCl₃) δ 58.1, 38.1, 30.7, 26.3, 25.8



2-azidoethylbenzene (73h)¹⁰⁷ Colorless liquid (130 mg, 88% yield) ¹H NMR (500 MHz, CDCl₃) δ 7.45-7.36 (m, 5H), 4.66 (q, *J* = 6.9 Hz, 1H), 1.58 (d, *J* = 6.9 Hz, 3H); ¹³C NMR (125 MHz, CDCl₃) δ 141.1, 128.9, 128.3, 126.6, 61.3, 21.7

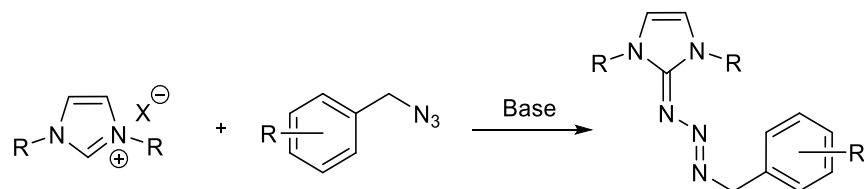


Trans-cinnamyl azide (73i)¹¹² To a solution of allylbenzene in 20 mL of CHCl₃, Br₂ was added at 0 °C. The mixture was stirred at 0 °C for 10 min, then the solvent was evaporated at reduced pressure to afford the crude dibromide intermediate. This intermediate was dissolved in 20 mL of DMSO and NaN₃ (12 mmol) and DBU (20 mmol) were added. The resulting mixture was stirred at room temperature for 1 h. Then water was added and the mixture was extracted with ethyl acetate (3 x 10 mL), the organic layer was dried over Na₂SO₄ and the solvent was evaporated at reduced pressure to afford the crude product. This crude product was purified by column chromatography to afford compound **73i** as a colorless liquid (107 mg, 67% yield) ¹H NMR (500 MHz, CDCl₃) δ 7.48-7.26 (m, 5H), 6.65 (d, *J* = 15.8 Hz, 1H), 6.24 (dt, *J*_d = 15.8 Hz, *J*_t = 6.8 Hz, 1H), 3.94 (d, *J* = 6.3 Hz, 2H); ¹³C NMR (125 MHz, CDCl₃) δ 136.1, 134.7, 128.8, 128.3, 126.8, 122.5, 53.1

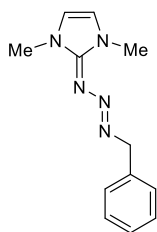


(3-azidopropyl)benzene (73j)¹¹¹ Colorless liquid (137 mg, 85% yield) ¹H NMR (500 MHz, CDCl₃) δ 7.40-7.26 (m, 5H), 3.34 (t, *J* = 6.9 Hz, 2H), 2.78 (t, *J* = 7.8 Hz, 2H), 1.98 (tt, *J*_t = 7.5 Hz, *J*_t = 6.9 Hz, 2H) ¹³C NMR (125 MHz, CDCl₃) δ 141.1, 128.7, 128.64 126.32 50.8, 32.9, 30.6

General Procedure for the Synthesis of Triazenes (66,69,79,&80).

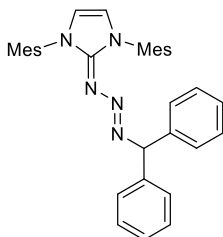


Following our previously reported procedure, to a suspension of the corresponding NHC precursor (1.5 mmol) in THF (20 mL) was added the respective azide (1 mmol) and left stirring for 5 min. KO^tBu (1.5 mmol) was added to the mixture and left stirring a room temperature for 12 h. To the resulting mixture 5 mL of hexanes were added and the solids were filtered through Celite. The volatiles were evaporated at reduced pressure to afford an oily product. This crude product was washed with hexanes (3 x 20 mL) and dried *in vacuo* to afford the solid products **66**, **66**, **69**, **79** and **80**. **Note:** The melting points of the triazenes could not be determined due to decomposition of the compounds when heated to around 125 °C.



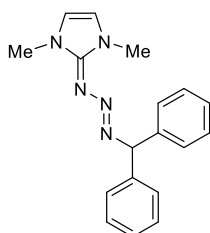
(*E*)-1-benzyl-3-(1,3-dimethylimidazol-2-ylidene)triazene (**66**)¹⁹.

Red solid. (211 mg, 92% yield). ¹H NMR (500 MHz, CDCl₃): δ 7.34 (d, *J* = 7.4 Hz, 2H), 7.28 (t, *J* = 7.6 Hz, 2H), 7.20 (t, *J* = 7.4 Hz, 1H), 6.30 (s, 2H), 4.83 (s, 2H), 3.52 (s, 6H). ¹³C NMR (125 MHz, CDCl₃): δ 152.7, 139.1, 129.0, 128.2, 126.6, 115.7, 65.3, 35.5



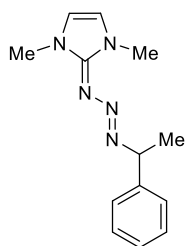
(*E*)-1-benzhydryl-3-(1,3-dimesitylimidazol-2-ylidene)triazene

(**69**). Pale orange solid. (370 mg, 72% yield). IR (neat) ν 3173, 1541, 1489, 1409, 1232, 698 cm⁻¹. ¹H NMR (300 MHz, CDCl₃): δ 7.20-7.05 (m, 10 H), 6.87 (s, 4 H), 6.44 (s, 2 H), 4.64 (s, 1 H), 2.31 (s, 6 H), 2.11 (s, 12 H). ¹³C NMR (75 MHz, CDCl₃): δ 152.5, 143.3, 138.3, 135.6, 134.5, 128.9, 128.3, 127.9, 126.3, 116.2, 21.2, 18.2. HRMS (ESI) calcd. for C₃₄H₃₆N₅ [M+H]⁺: 514.2965, found: 514.2963



(E)-1-benzhydryl-3-(1,3-dimethylimidazol-2-ylidene)triazene

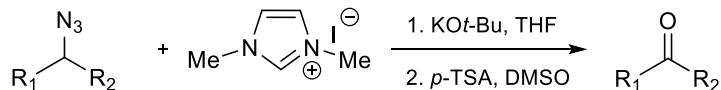
(79). Orange solid. (168 mg, 55% yield). IR (neat) ν 3119, 2099, 1555, 1492, 1403, 1260, 694 cm^{-1} . ^1H NMR (300 MHz, CDCl_3): 7.39 (d, $J = 7.2$ Hz, 4H), 7.30-7.20 (m, 4H), 7.19-7.11 (m, 2H), 6.24 (s, 2H), 5.76 (s, 1H), 3.45 (s, 6H) ^{13}C NMR (75 MHz, CDCl_3): δ .152.78, 143.62, 128.48, 128.26, 126.62, 115.94, 35.61 HRMS (ESI) calcd. for $\text{C}_{18}\text{H}_{20}\text{N}_5$ $[\text{M}+\text{H}]^+$:306.1713, found: 306.1708



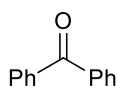
(E)-1-(1-phenylethyl)-3-(1,3-dimethylimidazol-2-

ylidene)triazene (80). Brown oil. (124 mg, 51% yield). IR (neat) ν 3114, 1660, 1559, 1502, 1418, 1243, 701 cm^{-1} . ^1H NMR (300 MHz, CD_3OD): 7.33-7.24 (m, 4H), 7.19-7.16 (m, 1H), 6.62 (s, 2H) 4.69 (q, $J = 6.9$ Hz, 1H), 1H) 3.46 (s, 6H) 1.53 (d, $J = 6.9$ Hz, 3H) ^{13}C NMR (75 MHz, CD_3OD): δ 152.24, 144.39, 128.04, 127.01, 126.46, 116.40, 68.07, 34.40, 20.74; HRMS (ESI) calcd. for $\text{C}_{13}\text{H}_{18}\text{N}_5$ $[\text{M}+\text{H}]^+$: 244.1550, found: 244.1555

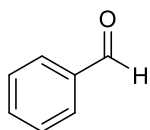
General Procedure for Oxidation Reactions.



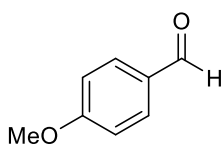
Dimethylimidazolium iodide (0.75 mmol,) and KO-*t*-Bu (0.75 mmol) were suspended in THF (1.0 mL) and stirred under argon at room temperature for 15 min. To this suspension was added the corresponding azide (0.5 mmol), and the suspension was stirred at room temperature for 12 h. The volatiles were then removed under reduced pressure. This was followed by addition of DMSO (1.0 mL) and TsOH (0.25 mmol) and stirred at room temperature for 30 min. The crude mixture was then purified using column chromatography with silica gel and hexanes/ethyl acetate (9:1) as mobile phase to afford products **72** and **81a-i**.



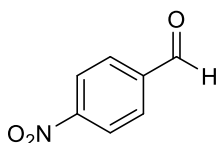
Benzophenone (72)¹¹³ Colorless liquid. (66 mg, 72% yield) ¹H NMR (300 MHz, CDCl₃) δ 7.81-7.78 (m, 4H), 7.59-7.54 (m, 2H), 7.49-7.43 (m, 4H); ¹³C NMR (75 MHz, CDCl₃) δ 196.8, 137.7, 132.6, 130.2, 128.4; 1 g scale (547 mg, 67% yield).



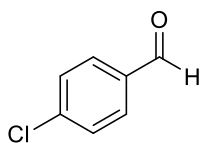
Benzaldehyde (81a)¹¹⁴ Colorless liquid. (23 mg, 44% yield) ¹H NMR (300 MHz, CDCl₃) δ 9.82 (s, 1H), 7.71-7.67 (m, 2H), 7.45-7.25 (m, 3H); ¹³C NMR (75 MHz, CDCl₃) δ 192.5, 136.4, 134.5, 129.7, 129.0.



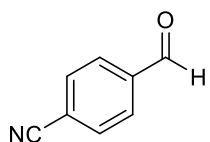
4-methoxybenzaldehyde (81b)¹¹⁵ Colorless liquid. (41 mg, 60% yield) ¹H NMR (300 MHz, CDCl₃) δ 9.78 (s, 1H), 7.74 (d, *J* = 8.9 Hz, 2H), 6.91 (d, *J* = 8.9 Hz, 2H), 3.79 (s, 3H); ¹³C NMR (75 MHz, CDCl₃) δ 190.9, 164.7, 132.0, 130.0, 114.4, 55.6.



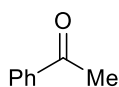
4-nitrobenzaldehyde (81c)¹¹⁵ Pale yellow solid. (17 mg, 23% yield) ¹H NMR (300 MHz, CDCl₃) δ 10.13 (s, 1H), 8.34 (d, *J* = 8.6 Hz, 2H), 8.05 (d, *J* = 8.6 Hz, 2H); ¹³C NMR (75 MHz, CDCl₃) δ 190.6, 151.2, 140.1, 130.6, 124.4.



4-chlorobenzaldehyde (81d)¹¹⁵ White solid (8 mg, 12% yield) ¹H NMR (300 MHz, CDCl₃) δ 9.80 (s, 1H), 7.63 (d, *J* = 8.6 Hz, 2H), 7.29 (d, *J* = 8.3 Hz, 2H); ¹³C NMR (75 MHz, CDCl₃) δ 190.8, 140.6, 134.7, 130.8, 129.3.

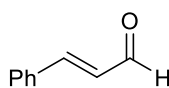


4-formylbenzonitrile (81e)¹¹⁶ White solid (19 mg, 29% yield) ¹H NMR (300 MHz, CDCl₃) δ 10.05 (s, 1H), 7.96 (d, *J* = 8.3 Hz, 2H), 7.81 (d, *J* = 8.3 Hz, 2H); ¹³C NMR (75 MHz, CDCl₃) δ 190.9, 138.8, 133.0, 130.0, 117.9, 117.6.



Acetophenone (81h)¹¹⁴ Colorless liquid. (36 mg, 60% yield) ¹H

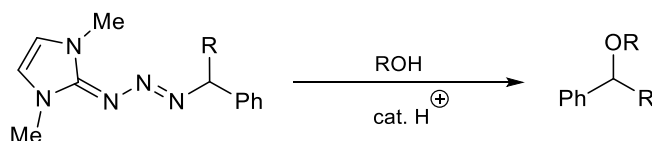
NMR (300 MHz, CDCl₃) δ 7.86 (d, *J* = 7.2 Hz, 2H), 7.47-7.45 (m, 1H), 7.37-7.32 (m, 2H), 2.48 (s, 3H); ¹³C NMR (75 MHz, CDCl₃) δ 198.0, 137.1, 133.1, 128.6, 128.3, 26.6.



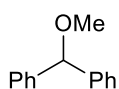
Trans-cinnamaldehyde (81i)¹¹⁷ Yellow oil. (28 mg, 43% yield) ¹H

NMR (500 MHz, CDCl₃) δ 9.60 (d, *J* = 7.9 Hz, 1H), 7.47-7.44 (m, 2H), 7.38-7.30 (m, 4H), 6.64-6.57 (m, 1H); ¹³C NMR (125 MHz, CDCl₃) δ 193.8, 152.9, 134.1, 131.4, 129.2, 128.6, 128.5.

General Procedure for the Synthesis of Ethers (81a-c)

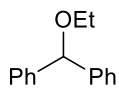


The corresponding triazene (0.3 mmol) was dissolved in 0.5 mL of the respective alcohol (methanol for **81a** and **81c** or ethanol for **81b**), PhSH (0.015 mmol) was added, and the mixture was stirred at 55 °C for 4 h. The volatiles were then removed under reduced pressure, and the crude mixture was purified using column chromatography with silica gel and hexanes/ethyl acetate (9:1) as mobile phase to afford products **81a-c**.



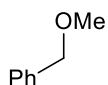
(Methoxymethylene)dibenzene (81a)¹¹⁸ Colorless oil (30 mg, 51%

yield) ¹H NMR (300 MHz, CDCl₃) δ 7.43-7.29 (m, 10H), 5.30 (s, 1H), 3.44 (s, 3H); ¹³C NMR (75 MHz, CDCl₃) δ 142.2, 128.6, 127.6, 127.1, 85.6, 57.2.



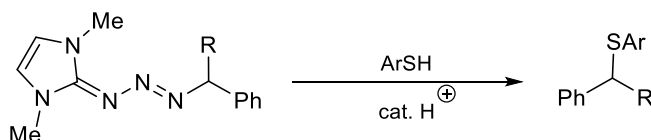
(Ethoxymethylene)dibenzene (81b)¹¹⁹ Colorless oil (31 mg, 48%

yield) ¹H NMR (300 MHz, CDCl₃) δ 7.43-7.28 (m, 10H), 5.41 (s, 1H), 3.57 (q, *J* = 6.9 Hz, 2H) 1.32 (t, *J* = 6.9 Hz, 3H); ¹³C NMR (75 MHz, CDCl₃) δ 142.7, 128.5, 127.5, 127.1, 83.6, 64.7, 15.5.

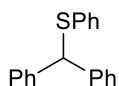


(Methoxymethylene)benzene (81c)¹²⁰ Colorless oil (7 mg, 20% yield) ¹H NMR (300 MHz, CDCl₃) δ 7.40-7.32 (m, 5H), 4.50 (s, 2H), 3.43 (s, 3H); ¹³C NMR (75 MHz, CDCl₃) 138.4, 128.6, 127.9, 127.8, 74.8, 58.2.

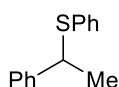
General Procedure for the Synthesis of Thiophenol Derivatives (81d-f)



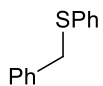
The respective triazene (0.3 mmol) was dissolved in thiophenol (0.3 mL) and stirred at room temperature for 1 h. Then ethyl acetate (15 mL) was added to the mixture, which was then washed with 10% NaOH solution (3 × 10 mL). The organic layer was dried over Na₂SO₄, and the volatiles were removed under reduced pressure. The crude mixture was then purified using column chromatography with silica gel and hexanes/dichloromethane (1:1) as mobile phase to afford products **15d-f**.



Benzhydryl(phenyl)sulfane (81d)¹²¹ White solid (45 mg, 54% yield) ¹H NMR (300 MHz, CDCl₃) δ 7.44-7.23 (m, 15H), 5.58 (s, 1H); ¹³C NMR (75 MHz, CDCl₃) δ 141.1, 136.2, 130.6, 128.8, 128.7, 128.5, 127.4, 126.7, 57.5.

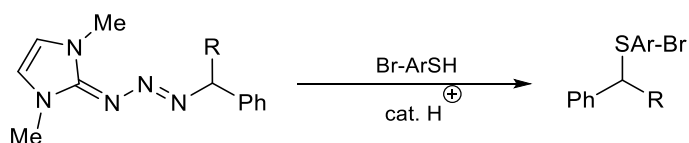


Phenyl(1-phenylethyl)sulfane (81e)¹²² Pale yellow oil. (26 mg, 40% yield) ¹H NMR (300 MHz, CDCl₃) δ 7.45-7.30 (m, 10H), 4.48 (q, *J* = 6.9 Hz, 1H), 1.76 (d, *J* = 6.9 Hz, 3H); ¹³C NMR (75 MHz, CDCl₃) δ 143.4, 135.4, 132.7, 129.0, 128.7, 127.5, 127.4, 127.3, 48.2, 22.6.

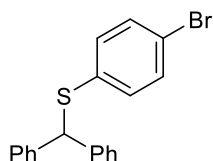


Benzyl(phenyl)sulfane (81f)¹²³ White solid. (58 mg, 96% yield) ¹H NMR (300 MHz, CDCl₃) δ 7.37-7.21 (m, 10H), 4.16 (s, 2H); ¹³C NMR (75 MHz, CDCl₃) δ 137.6, 136.5, 129.9, 129.0, 128.6, 127.3, 126.5, 39.1; 1 g scale (629 mg, 71% yield).

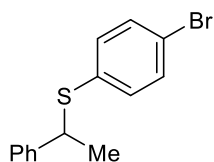
General Procedure for the Synthesis of 4-Bromothiophenol Derivatives (81g-i)



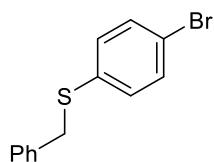
The respective triazene (0.3 mmol) and 4-bromothiophenol (0.6 mmol) were dissolved in THF (0.5 mL), and the mixture was stirred at room temperature for 1 h. The volatiles were then removed under reduced pressure, and ethyl acetate (15 mL) was added. The solution was washed with 10% NaOH solution (3 × 10 mL). The organic layer was dried over Na₂SO₄, and the volatiles were removed under reduced pressure. The crude mixture was then purified using column chromatography with silica gel and hexanes/dichloromethane (1:1) as mobile phase to afford products **81g-i**.



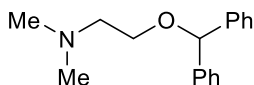
Benzhydryl(4-bromophenyl)sulfane (81g). White solid (31 mg, 29% yield) IR (neat) ν 3076, 1561, 1489, 694 cm^{-1} . ¹H NMR (300 MHz, CDCl₃) δ 7.45-7.40 (m, 4H), 7.34-7.21 (m, 8H), 7.11-7.07 (m, 2H), 5.52 (s, 1H); ¹³C NMR (75 MHz, CDCl₃) δ 140.6, 135.3, 132.1, 131.9, 128.8, 128.5, 127.6, 120.8, 57.6; HRMS (ESI) calcd. for C₁₉H₁₆BrS [M+H]⁺: 355.0151, found: 355.0158



(4-bromophenyl)(1-phenylethyl)sulfane (81h). Colorless oil (29 mg, 33% yield) IR (neat) ν , 3085, 1570, 1470, 697 cm^{-1} . ¹H NMR (300 MHz, CDCl₃) δ 7.52 (d, J = 2.1 Hz, 4H), 7.43-7.31 (m, 5H), 5.09 (q, J = 6.9 Hz, 1H), 1.85 (d, J = 6.5 Hz, 3H) ¹³C NMR (75 MHz, CDCl₃) δ 142.9, 134.3, 134.1, 131.9, 128.6, 127.4, 127.3, 121.4, 48.2, 22.3; HRMS (ESI) calcd. for C₁₄H₁₂BrS [M-H]⁺: 290.9838, found: 290.9840



Benzyl(4-bromophenyl)sulfane (81i)¹²⁴ White solid (44 mg, 53% yield) ¹H NMR (300 MHz, CDCl₃) δ 7.37 (d, *J* = 8.6 Hz, 2H), 7.30-7.26 (m, 5H), 7.15 (d, *J* = 8.6 Hz, 2H), 4.09 (s, 2H); ¹³C NMR (75 MHz, CDCl₃) δ 137.1, 135.5, 132.0, 131.6, 128.9, 128.7, 127.4, 120.4, 39.2.



Diphenhydramine (81j). Triazene **14** (0.3 mmol) and TsOH (0.15 mmol) were dissolved in (dimethylamino)ethanol (0.5 mL) and stirred at 60 °C for 36 h. The crude mixture was then purified using column chromatography with silica gel and ethyl acetate/methanol (9:1) as mobile phase to afford product **81j** as a colorless oil (27 mg, 35% yield) IR (neat) ν 3061, 2941, 1492, 1452, 1102, 696 cm⁻¹. ¹H NMR (300 MHz, CDCl₃) δ 7.46-7.28 (m, 10H), 5.46 (s, 1H), 3.67 (t, *J* = 5.8 Hz, 2H), 2.71 (t, *J* = 5.8 Hz, 2H), 2.37 (s, 6H); ¹³C NMR (75 MHz, CDCl₃) δ 142.4, 128.6, 127.6, 127.2, 84.2, 67.6, 59.1, 46.2; HRMS (ESI) calcd. for C₁₇H₂₂NO [M+H]⁺: 256.1696, found: 256.170

Chapter 6

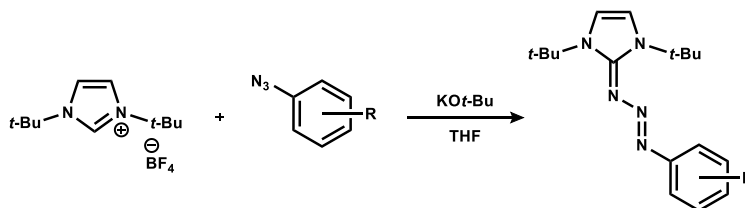
Experimental procedures for Chapters 3 and 4

General Information

All photochemical reactions were carried out in quartz tubes using a Rayonet photochemical reactor with 350 nm UV lamps. All commercially obtained reagents were used as received. Solvents were dried, degassed and obtained from a JC Meyer company solvent purification system. Heating was accomplished by either a heating mantle or silicone oil bath. Purification of reaction products was carried out by flash column chromatography using silica gel 60 (230-400 mesh). TLC visualization was accompanied with UV light. Concentration in vacuo refers to the removal of volatile solvent using a rotary evaporator attached to a dry diaphragm pump (10-15 mm Hg) followed by pumping to a constant weight with an oil pump (<300 mTorr).

^1H NMR spectra were recorded at 500 MHz and are reported relative to CDCl_3 (δ 7.26), DMSO (δ 2.50) or CD_3OD (δ 3.31). ^1H NMR coupling constants (J) are reported in Hertz (Hz) and multiplicities are indicated as follows: s (singlet), d (doublet), t (triplet), m (multiplet). Proton-decoupled ^{13}C NMR spectra were recorded at 125 MHz and reported relative to CDCl_3 (δ 77.0), DMSO (δ 39.5) or CD_3OD (δ 49.0). IR experiments were recorded with neat samples on a Bruker Alpha instruments fitted with diamond ATR sample plate. High-resolution (HR) mass spectra were recorded at the Shimadzu Center for Advanced Analytical Chemistry at UTA.

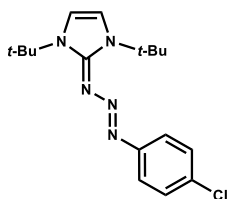
General Methods for the Preparation of Triazenes (84)



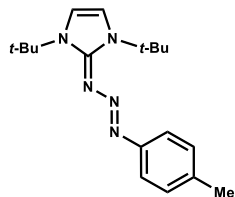
Method A. To a flask containing 1,3-di-*tert*-butylimidazolium tetrafluoroborate (1.1 mmol), potassium *tert*-butoxide (1.3 mmol) and dry THF was added (10 mL) under Ar. The resulting suspension was stirred for 15 minutes, followed by dropwise addition of aromatic azide (1.1 mmol). The resulting mixture was left stirring at room temperature for 12 h. After this time, hexanes (10 mL) were added and the resulting solid precipitate filtered. The filtered solid was dissolved in DCM (20 mL) and the precipitated salts filtered. The resulting solution was then concentrated *in vacuo* and dried under high vacuum, affording the pure triazene.

Method B. Same procedure for method A but using NaH instead of potassium *tert*-butoxide. This method was used to prepare triazenes **84e** and **84g**. **Note:** The melting points of the triazenes could not be determined due to decomposition of the compounds when heated to around 125 °C.

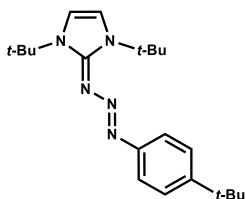
(*E*)-2-((4-chlorophenyl)triaz-2-en-1-ylidene)-1,3-di-*tert*-butyl-2,3-



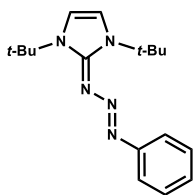
dihydro-1H-imidazole (84a): Prepared from 4-chloroazidobenzene (169 mg, 1.1 mmol) according to the general procedure A, obtained as a yellow solid (242 mg, 66%). IR (neat) ν 3095, 1473, 1449, 1257, 699 cm^{-1} ; ^1H NMR (CDCl_3 , 500 MHz): δ 7.48 (d, $J = 8.6$ Hz, 2H), 7.25 (d, $J = 8.6$ Hz, 2H), 6.92 (s, 2H), 1.63 (s, 18H); ^{13}C NMR (CDCl_3 , 125 MHz): δ 153.95, 151.51, 128.97, 128.52, 121.71, 112.65, 59.35, 30.19; HRMS (ESI) m/z 334.1798, calcd for $\text{C}_{17}\text{H}_{25}\text{N}_5\text{Cl}$ [$\text{M} + \text{H}$] $^+$ 334.1793.



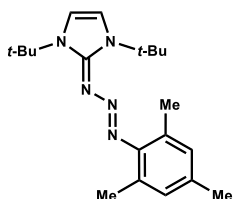
(E)-2-((4-methylphenyl)triaz-2-en-1-ylidene)-1,3-di-tert-butyl-2,3-dihydro-1H-imidazole (84b): Prepared from 4-methylazidobenzene (149 mg, 1.1 mmol) according to the general procedure A, obtained as an orange solid (228 mg, 48%). IR (neat) ν 3088, 1491, 1448, 1266, 694 cm^{-1} ; ^1H NMR (CDCl_3 , 500 MHz): δ 7.44 (d, $J = 8.6$ Hz, 2H), 7.10 (d, $J = 8.0$ Hz, 2H), 6.85 (s, 2H), 2.31 (s, 3H), 1.63 (s, 18H); ^{13}C NMR (CDCl_3 , 125 MHz): δ 153.97, 150.51, 133.57, 129.07, 120.58, 112.24, 58.99, 30.10, 20.93; HRMS (ESI) m/z 314.2335, calcd for $\text{C}_{18}\text{H}_{28}\text{N}_5$ $[\text{M} + \text{H}]^+$ 314.2339.



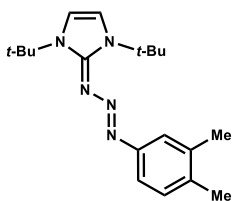
(E)-2-((4-tert-butylphenyl)triaz-2-en-1-ylidene)-1,3-di-tert-butyl-2,3-dihydro-1H-imidazole (84c): Prepared from 4-tert-butylazidobenzene (193 mg, 1.1 mmol) according to the general procedure A, obtained as a yellow solid (348 mg, 89%). IR (neat) ν 3032, 1493, 1447, 1260, 687 cm^{-1} ; ^1H NMR (CDCl_3 , 500 MHz): δ 7.49 (d, $J = 8.6$ Hz, 2H), 7.32 (d, $J = 8.6$ Hz, 2H), 6.86 (s, 2H), 1.64 (s, 18H), 1.31 (s, 9H); ^{13}C NMR (CDCl_3 , 125 MHz): δ 153.98, 150.26, 146.84, 125.35, 120.22, 112.29, 59.05, 34.31, 31.46, 30.15; HRMS (ESI) m/z 356.2812, calcd for $\text{C}_{21}\text{H}_{34}\text{N}_5$ $[\text{M} + \text{H}]^+$ 356.2809.



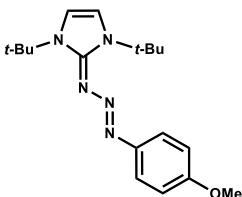
(E)-2-((phenyl)triaz-2-en-1-ylidene)-1,3-di-tert-butyl-2,3-dihydro-1H-imidazole (84d): Prepared from azidobenzene (131 mg, 1.1 mmol) according to the general procedure A, obtained as a yellow solid (287 mg, 87%). IR (neat) ν 3179, 1475, 1449, 1263, 693 cm^{-1} ; ^1H NMR (CDCl_3 , 500 MHz): δ 7.53 (dd, $J = 8.6$ Hz, $J = 1.2$ Hz, 2H), 7.31-7.28 (m, 2H), 7.09-7.06 (m, 1H), 6.85 (s, 2H), 1.64 (s, 18H); ^{13}C NMR (CDCl_3 , 125 MHz): δ 154.05, 152.78, 128.44, 124.05, 120.70, 112.44, 59.17, 30.16; HRMS (ESI) m/z 300.2178, calcd for $\text{C}_{17}\text{H}_{26}\text{N}_5$ [$\text{M} + \text{H}$] $^+$ 300.2183.



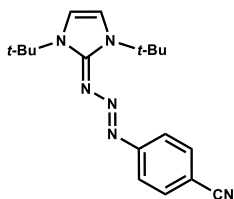
(E)-2-((2,4,6-trimethylphenyl)triaz-2-en-1-ylidene)-1,3-di-tert-butyl-2,3-dihydro-1H-imidazole (84e): Prepared from 2,4,6-trimethylazidobenzene (177 mg, 1.1 mmol) according to the general procedure B, obtained as a yellow solid (327 mg, 87%). IR (neat) ν 3132, 1477, 1427, 1265, 674 cm^{-1} ; ^1H NMR ($\text{DMSO}-d_6$, 500 MHz): δ 7.12 (s, 2H), 6.75 (s, 2H), 2.18 (s, 3H), 1.60 (s, 6H), 1.50 (s, 18H); ^{13}C NMR ($\text{DMSO}-d_6$, 125 MHz): δ 154.01, 148.68, 131.45, 128.62, 120.47, 113.14, 58.23, 29.35, 20.43, 18.62; HRMS (ESI) m/z 342.2655, calcd for $\text{C}_{20}\text{H}_{32}\text{N}_5$ [$\text{M} + \text{H}$] $^+$ 342.2658.



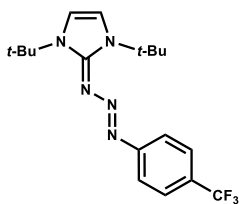
(E)-2-((3,4-dimethylphenyl)triaz-2-en-1-ylidene)-1,3-di-tert-butyl-2,3-dihydro-1H-imidazole (84f): Prepared from 3,4-dimethylazidobenzene (162 mg, 1.1 mmol) according to the general procedure A, obtained as a yellow solid (223 mg, 62%). IR (neat) ν 3077, 1478, 1433, 1261, 650 cm^{-1} ; ^1H NMR (CDCl_3 , 500 MHz): δ 7.34 (s, 1H), 7.28-7.27 (m, 1H), 7.05 (d, $J = 8.0$ Hz, 1H), 6.80 (s, 2H), 2.24 (s, 6H), 1.63 (s, 18H); ^{13}C NMR (CDCl_3 , 125 MHz): δ 153.85, 150.59, 136.40, 132.35, 129.65, 122.19, 117.91, 112.25, 59.01, 30.10, 19.97, 19.27; HRMS (ESI) m/z 328.2499, calcd for $\text{C}_{19}\text{H}_{30}\text{N}_5$ [$\text{M} + \text{H}$] $^+$ 328.2501.



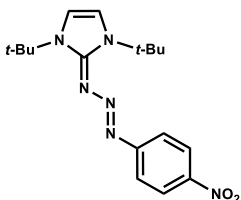
(E)-2-((4-methoxyphenyl)triaz-2-en-1-ylidene)-1,3-di-tert-butyl-2,3-dihydro-1H-imidazole (84g): Prepared from 4-methoxyazidobenzene (164 mg, 1.1 mmol) according to the general procedure B, obtained as a yellow solid (254 mg, 70%). IR (neat) ν 3091, 1491, 1434, 1267, 698 cm^{-1} ; ^1H NMR (CDCl_3 , 500 MHz): δ 7.47 (d, $J = 9.2$ Hz, 2H), 6.85 (d, $J = 9.2$ Hz, 2H), 6.78 (s, 2H), 3.79 (s, 3H), 1.63 (s, 18H); ^{13}C NMR (CDCl_3 , 125 MHz): δ 156.87, 153.71, 146.29, 121.55, 113.80, 112.28, 59.04, 55.38, 30.28; HRMS (ESI) m/z 330.2285, calcd for $\text{C}_{18}\text{H}_{26}\text{N}_5\text{O}$ [$\text{M} + \text{H}$] $^+$ 330.2288.



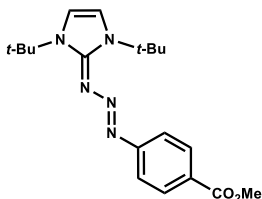
(E)-2-((4-cyanophenyl)triaz-2-en-1-ylidene)-1,3-di-tert-butyl-2,3-dihydro-1H-imidazole (84h): Prepared from 4-cyanoazidobenzene (159 mg, 1.1 mmol) according to the general procedure A, obtained as an orange solid (264 mg, 74%). IR (neat) ν 3099, 1481, 1444, 1254, 670 cm^{-1} ; ^1H NMR (CDCl_3 , 500 MHz): δ 7.51 (s, 4H), 6.94 (s, 2H), 1.61 (s, 18H); ^{13}C NMR (CDCl_3 , 125 MHz): δ 156.73, 153.62, 132.75, 120.50, 120.27, 113.34, 105.47, 59.80, 30.19; HRMS (ESI) m/z 325.2132, calcd for $\text{C}_{18}\text{H}_{25}\text{N}_6$ [$\text{M} + \text{H}$] $^+$ 325.2135.



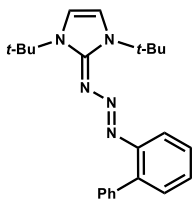
(E)-2-((4-trifluorophenyl)triaz-2-en-1-ylidene)-1,3-di-tert-butyl-2,3-dihydro-1H-imidazole (84i): Prepared from 4-(trifluoromethyl)azidobenzene (206 mg, 1.1 mmol) according to the general procedure A, obtained as a yellow solid (430 mg, 94%). IR (neat) ν 3094, 1488, 1450, 1249, 678 cm^{-1} ; ^1H NMR (CDCl_3 , 500 MHz): δ 7.56-7.50 (m, 4H), 6.88 (s, 2H), 1.63 (s, 18H); ^{13}C NMR (CDCl_3 , 125 MHz): δ 155.84, 153.95, 124.84 (m), 125.66 (q, $J_{\text{CF}} = 3.6$ Hz), 125.05 (m), 120.26, 112.97, 59.56, 30.20; HRMS (ESI) m/z 368.2052, calcd for $\text{C}_{18}\text{H}_{25}\text{N}_6\text{F}_3$ $[\text{M} + \text{H}]^+$ 368.2057.



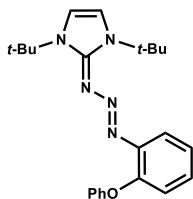
(E)-2-((4-nitrophenyl)triaz-2-en-1-ylidene)-1,3-di-tert-butyl-2,3-dihydro-1H-imidazole (84j): Prepared from 4-nitroazidobenzene (181 mg, 1.1 mmol) according to the general procedure A, obtained as a red solid (341 mg, 90%). IR (neat) ν 3099, 1492, 1454, 1238, 697 cm^{-1} ; ^1H NMR (CDCl_3 , 500 MHz): δ 8.15 (d, $J = 9.2$ Hz, 2H), 7.62 (d, $J = 9.2$ Hz, 2H), 7.09 (s, 2H), 1.63 (s, 18H); ^{13}C NMR (CDCl_3 , 125 MHz): δ 158.94, 153.24, 143.23, 124.87, 119.80, 113.60, 60.02, 30.21; HRMS (ESI) m/z 345.2030, calcd for $\text{C}_{17}\text{H}_{25}\text{N}_6\text{O}_2$ $[\text{M} + \text{H}]^+$ 345.2034.



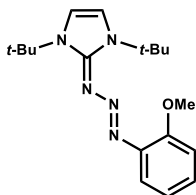
(E)-2-((4-methyl 4-azidobenzoate)triaz-2-en-1-ylidene)-1,3-di-tert-butyl-2,3-dihydro-1H-imidazole (84k): Prepared from methyl 4-azidobenzoate (195 mg, 1.1 mmol) according to the general procedure A, obtained as a red solid (271 mg, 69%). IR (neat) ν 3164, 1711, 1480, 1451, 1271, 697 cm^{-1} ; ^1H NMR (CDCl_3 , 500 MHz): δ 7.94 (d, $J = 8.6$ Hz, 2H), 7.51 (d, $J = 8.6$ Hz, 2H), 6.90 (s, 2H), 3.85 (s, 3H), 1.61 (s, 18H); ^{13}C NMR (CDCl_3 , 125 MHz): δ 167.40, 157.05, 153.81, 130.33, 124.68, 119.98, 113.02, 59.56, 51.65, 30.15; HRMS (ESI) m/z 358.2240, calcd for $\text{C}_{19}\text{H}_{28}\text{N}_5\text{O}_2$ $[\text{M} + \text{H}]^+$ 358.2238.



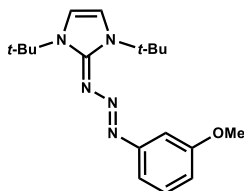
(E)-2-((2-phenylphenyl)triaz-2-en-1-ylidene)-1,3-di-tert-butyl-2,3-dihydro-1H-imidazole (84l): Prepared from 2-phenylazidobenzene (215 mg, 1.1 mmol) according to the general procedure A, obtained as a yellow solid (409 mg, 99%). IR (neat) ν 3088, 1497, 1470, 1236 692 cm^{-1} ; ^1H NMR (CDCl_3 , 500 MHz): δ 7.51 (d, $J = 7.5$ Hz, 2H), 7.38-7.35 (m, 2H), 7.32-7.29 (m, 2H), 7.27-7.20 (m, 2H), 7.16 (t, $J = 7.5$ Hz, 1H), 6.82 (s, 2H), 1.62 (s, 18H); ^{13}C NMR (CDCl_3 , 125 MHz): δ 152.34, 149.53, 140.42, 136.57, 130.93, 130.42, 127.67, 127.53, 126.28, 125.42, 118.55, 116.29, 35.63, 30.01; HRMS (ESI) m/z 376.2491, calcd for $\text{C}_{23}\text{H}_{30}\text{N}_5$ $[\text{M} + \text{H}]^+$ 376.2496.



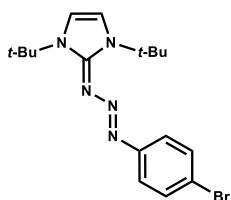
(E)-2-((2-phenyloxyphenyl)triaz-2-en-1-ylidene)-1,3-di-tert-butyl-2,3-dihydro-1H-imidazole (84m): Prepared from 2-phenyloxyazidobenzene (232 mg, 1.1 mmol) according to the general procedure A, obtained as a brown solid (332 mg, 77%). IR (neat) ν 3066, 1488, 1448, 1235, 688 cm^{-1} ; ^1H NMR (CDCl_3 , 500 MHz): δ 7.42-7.40 (m, 1H), 7.21-7.18 (m, 2H), 7.06-7.01 (m, 2H), 6.98-6.91 (m, 4H), 6.81 (s, 2H), 1.56 (s, 18H); ^{13}C NMR (CDCl_3 , 125 MHz): δ 159.04, 154.29, 149.28, 145.49, 129.01, 124.54, 123.99, 121.46, 120.96, 119.47, 117.86, 112.57, 59.22, 30.09; HRMS (ESI) m/z 392.2447, calcd for $\text{C}_{23}\text{H}_{30}\text{N}_5\text{O}$ $[\text{M} + \text{H}]^+$ 392.2445.



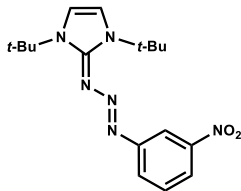
(E)-2-((2-methoxyphenyl)triaz-2-en-1-ylidene)-1,3-di-tert-butyl-2,3-dihydro-1H-imidazole (84n): Prepared from 2-methoxyazidobenzene (164 mg, 1.1 mmol) according to the general procedure A, obtained as a yellow solid (185 mg, 51%). IR (neat) ν 3097, 1480, 1433, 1256, 676 cm^{-1} ; ^1H NMR (DMSO- d_6 , 500 MHz): δ 7.20-7.18 (m, 3H), 6.99-6.95 (m, 2H), 6.81-6.78 (m, 1H), 3.78 (s, 3H), 1.55 (s, 18H); ^{13}C NMR (DMSO- d_6 , 125 MHz): δ 153.14, 152.74, 142.21, 124.46, 120.47, 116.75, 113.61, 112.39, 58.64, 55.49, 29.51; HRMS (ESI) m/z 330.2293, calcd for $\text{C}_{18}\text{H}_{28}\text{N}_5\text{O}$ [$\text{M} + \text{H}$] $^+$ 330.2294.



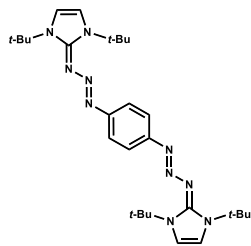
(E)-2-((3-methoxyphenyl)triaz-2-en-1-ylidene)-1,3-di-tert-butyl-2,3-dihydro-1H-imidazole (84o): Prepared from 3-methoxyazidobenzene (164 mg, 1.1 mmol) according to the general procedure A, obtained as a yellow solid (359 mg, 99%). IR (neat) ν 3090, 1494, 1433, 1270, 675 cm^{-1} ; ^1H NMR (DMSO- d_6 , 500 MHz): δ 7.23 (s, 2H), 7.15 (t, $J = 8.0$ Hz, 1H), 6.89-6.88 (m, 2H), 6.59-6.57 (m, 1H), 3.71 (s, 3H), 1.56 (s, 18H); ^{13}C NMR (DMSO- d_6 , 125 MHz): δ 154.18, 153.35, 142.25, 124.76, 120.25, 117.61, 112.28, 111.57, 59.14, 55.69, 30.21; HRMS (ESI) m/z 330.2296, calcd for $\text{C}_{18}\text{H}_{28}\text{N}_5\text{O}$ [$\text{M} + \text{H}$] $^+$ 330.2294.



(E)-2-((2-bromophenyl)triaz-2-en-1-ylidene)-1,3-di-tert-butyl-2,3-dihydro-1H-imidazole (84p): Prepared from 4-bromoazidobenzene (218 mg, 1.1 mmol) according to the general procedure A, obtained as a yellow solid (370 mg, 89%). IR (neat) ν 3092, 1496, 1435, 1260, 641 cm^{-1} ; ^1H NMR (CDCl_3 , 500 MHz): δ 7.45 (d, $J = 8.9$ Hz, 2H), 7.39 (d, $J = 8.9$ Hz, 2H), 6.97 (s, 2H), 1.62 (s, 18H); ^{13}C NMR (CDCl_3 , 125 MHz): δ 153.91, 151.99, 131.40, 122.10, 116.76, 112.66, 59.31, 30.15; HRMS (ESI) m/z 378.1291, calcd for $\text{C}_{17}\text{H}_{25}\text{BrN}_5$ [$\text{M} + \text{H}$] $^+$ 378.1293.



(E)-2-((3-nitrophenyl)triaz-2-en-1-ylidene)-1,3-di-tert-butyl-2,3-dihydro-1H-imidazole (84q): Prepared from 3-nitroazidobenzene (181 mg, 1.1 mmol) according to the general procedure A, obtained as a yellow solid (367 mg, 97%). IR (neat) ν 3096, 1496, 1435, 1256, 678 cm^{-1} ; ^1H NMR (CDCl_3 , 500 MHz): δ 8.30 (t, $J = 2.0$ Hz, 1H), 7.86-7.82 (m, 2H), 7.41 (t, $J = 8.0$ Hz, 1H), 6.94 (s, 2H), 1.64 (s, 18H); ^{13}C NMR (CDCl_3 , 125 MHz): δ 154.44, 153.70, 148.91, 129.02, 127.76, 117.75, 113.21, 113.16, 59.69, 30.16; HRMS (ESI) m/z 345.2036, calcd for $\text{C}_{17}\text{H}_{25}\text{N}_6\text{O}_2$ $[\text{M} + \text{H}]^+$ 345.2039.

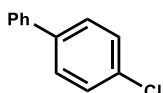
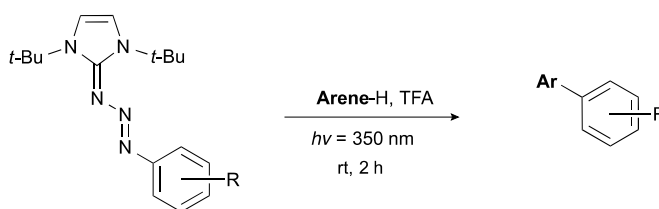


1,4-bis((E)-1,3-di-tert-butyl-1H-imidazol-2(3H)-ylidene)triaz-1-en-1-yl)benzene (84r): Prepared from 1,6-diazidobenzene (320 mg, 2.0 mmol) according to the general procedure A with double the amount of di-tert-butylimidazolium tetrafluoroborate, obtained as a dark orange solid (66 mg, 63%). IR (neat) ν 3070, 1502, 1363, 1147, 707 cm^{-1} ; ^1H NMR ($\text{DMSO}-d_6$, 500 MHz): δ 7.23 (s, 2H), 7.17 (s, 2H), 3.34 (s, 4H), 1.56 (s, 18H); ^{13}C NMR ($\text{DMSO}-d_6$, 125 MHz): δ 153.27, 149.96, 120.74, 113.92, 58.99, 29.95

General Method for the Preparation of Biaryl Compounds (4)

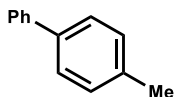
To a quartz tube containing triazene (0.2 mmol) was added aromatic solvent (2 mL). Then, the tube was capped and TFA (1.0 mmol) was added with a syringe. Next, the mixture was left to stir inside a photoreactor under UV irradiation (350 nm) for 2 h. After 2 h the resulting mixture was concentrated *in vacuo*. Purification by flash chromatography (SiO₂, EtOAc/hexanes mixtures) provided the pure biaryl compound.

Sunlight Reactions Variation: Conditions are identical as for the general method but using natural sunlight as radiation source instead of photoreactor. Reactions were exposed to natural sunlight for 9 h.



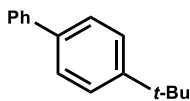
4-chlorobiphenyl (85a):¹²⁵ Prepared from triazene **84a** (67 mg,

0.2 mmol) according to the general procedure, obtained as a colorless solid (17 mg, 38%). ¹H NMR (CDCl₃, 500 MHz): δ 7.57-7.52 (m, 4H), 7.47-7.41 (m, 4H), 7.38-7.37 (m, 1H); ¹³C NMR (CDCl₃, 125 MHz): δ 139.97, 139.64, 133.35, 128.89, 128.86, 128.37, 127.57, 126.97.

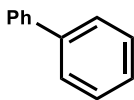


4-methylbiphenyl (85b):¹²⁶ Prepared from triazene **84b** (73 mg,

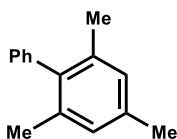
0.2 mmol) according to the general procedure, obtained as a colorless solid (16 mg, 40%). ¹H NMR (CDCl₃, 500 MHz): δ 7.60 (d, $J = 7.5$ Hz, 2H), 7.51 (d, $J = 8.6$ Hz, 2H), 7.44 (t, $J = 7.5$ Hz, 2H), 7.34 (t, $J = 7.5$ Hz, 1H), 7.27 (d, $J = 8.0$ Hz, 2H), 2.41 (s, 3H); ¹³C NMR (CDCl₃, 125 MHz): δ 141.13, 138.32, 136.99, 129.45, 128.69, 126.97, 126.95 (2C), 21.08.



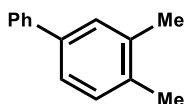
4-tert-butylbiphenyl (85c):¹²⁷ Prepared from triazene **84c** (71 mg, 0.2 mmol) according to the general procedure, obtained as a colorless solid (25 mg, 48%). ¹H NMR (CDCl₃, 500 MHz): δ 7.61 (d, *J* = 7.5 Hz, 2H), 7.56 (d, *J* = 8.0 Hz, 2H), 7.49 (d, *J* = 8.0 Hz, 2H), 7.44 (m, 2H), 7.34 (t, *J* = 7.5 Hz, 1H), 1.39 (s, 9H); ¹³C NMR (CDCl₃, 125 MHz): δ 150.22, 141.03, 138.29, 128.67, 127.00, 126.95, 126.76, 125.68, 34.51, 31.35.



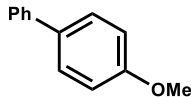
Biphenyl (85d):¹²⁶ Prepared from triazene **84d** (69 mg, 0.2 mmol) according to the general procedure, obtained as a colorless solid (21 mg, 59%). ¹H NMR (CDCl₃, 500 MHz): δ 7.70 (d, *J* = 8.0 Hz, 4H), 7.54 (t, *J* = 8.0 Hz, 4H), 7.45 (t, *J* = 7.5 Hz, 2H); ¹³C NMR (CDCl₃, 125 MHz): δ 141.18, 128.72, 127.21, 127.12. Sunlight: (15 mg, 43%).



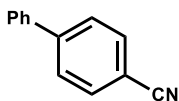
2,4,6-trimethylbiphenyl (85e):¹²⁸ Prepared from triazene **84e** (68 mg, 0.2 mmol) according to the general procedure, obtained as a colorless solid (9 mg, 20%). ¹H NMR (CDCl₃, 500 MHz): δ 7.42 (t, *J* = 7.5 Hz, 2H), 7.32 (t, *J* = 7.5 Hz, 1H), 7.15-7.13 (m, 2H), 6.95 (s, 2H), 2.34 (s, 3H), 2.00 (s, 6H); ¹³C NMR (CDCl₃, 125 MHz): δ 141.05, 139.03, 136.53, 135.95, 129.27, 128.33, 128.01, 126.47, 21.00, 20.71.



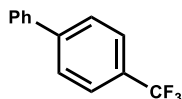
3,4-dimethylbiphenyl (85f):¹²⁹ Prepared from triazene **84f** (65 mg, 0.2 mmol) according to the general procedure, obtained as a colorless solid (13 mg, 31%). ¹H NMR (CDCl₃, 500 MHz): δ 7.59 (d, *J* = 6.9 Hz, 2H), 7.45-7.42 (m, 2H), 7.39 (s, 1H), 7.36-7.32 (m, 2H), 7.22 (d, *J* = 7.5 Hz, 1H), 2.35 (s, 3H), 2.32 (s, 3H); ¹³C NMR (CDCl₃, 125 MHz): δ 141.26, 138.84, 136.88, 135.69, 130.03, 128.64, 128.42, 126.98, 126.87, 124.49, 19.93, 19.43.



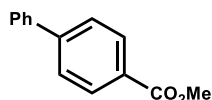
4-methoxybiphenyl (85g):¹³⁰ Prepared from triazene **84g** (66 mg, 0.2 mmol) according to the general procedure, obtained as a colorless solid (13 mg, 30%). ¹H NMR (CDCl₃, 500 MHz): 7.58-7.53 (m, 4H), 7.43 (m, 2H), 7.32 (t, *J* = 7.5 Hz, 1H), 6.99 (d, *J* = 8.6 Hz, 2H), 3.86 (s, 3H); δ; ¹³C NMR (CDCl₃, 125 MHz): δ 159.11, 140.80, 133.74, 128.70, 128.14, 126.71, 126.64, 114.17, 55.32.



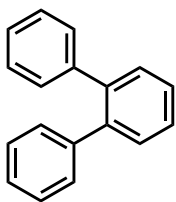
4-cyanobiphenyl (85h):¹³⁰ Prepared from triazene **84h** (65 mg, 0.2 mmol) according to the general procedure, obtained as a colorless solid (4 mg, 10%). ¹H NMR (CDCl₃, 500 MHz): δ 7.73 (d, *J* = 8.6 Hz, 2H), 7.69 (d, *J* = 8.6 Hz, 2H), 7.59 (d, *J* = 6.9 Hz, 2H), 7.49 (t, *J* = 7.5 Hz, 2H), 7.43 (t, *J* = 7.5 Hz, 1H); ¹³C NMR (CDCl₃, 125 MHz): δ 145.67, 139.17, 132.59, 129.10, 128.65, 127.73, 127.22, 118.95, 110.89.



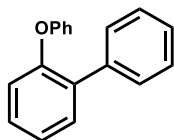
4-(trifluoromethyl)biphenyl (85i):¹²⁶ Prepared from triazene **84i** (73 mg, 0.2 mmol) according to the general procedure, obtained as a colorless solid (15 mg, 28%). ¹H NMR (CDCl₃, 500 MHz): δ 7.70 (s, 4H), 7.62-7.60 (m, 2H), 7.50-7.47 (m, 2H), 7.43-7.39 (m, 1H); ¹³C NMR (CDCl₃, 125 MHz): δ 144.71, 139.75, 129.31 (m), 128.97, 128.16, 127.41, 127.27, 125.69 (q, *J*_{CF} = 3.6 Hz), 124.29 (m)



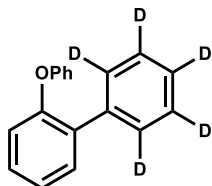
Methyl 4-phenylbenzoate (85k):¹³⁰ Prepared from triazene **84k** (71 mg, 0.2 mmol) according to the general procedure, obtained as a colorless solid (13 mg, 26%). ¹H NMR (CDCl₃, 500 MHz): δ 8.11 (d, *J* = 8.6 Hz, 2H), 7.67-7.62 (m, 4H), 7.47 (t, *J* = 7.5 Hz, 2H), 7.41-7.39 (m, 1H), 3.95 (s, 3H); ¹³C NMR (CDCl₃, 125 MHz): δ 166.99, 145.61, 139.98, 130.08, 128.90, 128.86, 128.12, 127.26, 127.03, 52.12.



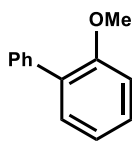
1,2-diphenylbenzene (85l):^{58d} Prepared from triazene **84l** (87 mg, 0.2 mmol) according to the general procedure, obtained as a colorless solid (18 mg, 34%). ¹H NMR (CDCl₃, 500 MHz): δ 7.46-7.44 (m, 4H), 7.25-7.21 (m, 6H), 7.17-7.16 (m, 4H); ¹³C NMR (CDCl₃, 125 MHz): δ 141.48, 140.54, 130.58, 129.87, 127.83, 127.45, 126.42.



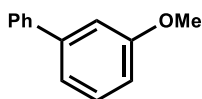
2-phenoxybiphenyl (85m):¹³¹ Prepared from triazene **84m** (78 mg, 0.2 mmol) according to the general procedure, obtained as a colorless solid (33 mg, 57%). ¹H NMR (CDCl₃, 500 MHz): δ 7.55 (d, *J* = 6.8 Hz, 2H), 7.47 (dd *J* = 7.5 Hz, *J* = 1.72 Hz, 1H), 7.38-7.35 (m, 3H), 7.31-7.25 (m, 3H), 7.23-7.20 (m, 1H), 7.02-7.00 (m, 2H), 6.94 (dd, *J* = 8.6 Hz, *J* = 1.2 Hz, 2H); ¹³C NMR (CDCl₃, 125 MHz): δ 157.77, 153.56, 137.70, 133.66, 131.26, 129.57, 129.18, 128.65, 128.09, 127.17, 124.01, 122.60, 120.09, 118.15.



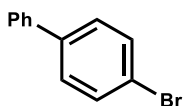
2'-phenoxy-1-1'-biphenyl-2,3,4,5,6-d₅ (85m'): Prepared from triazene **84m** (78 mg, 0.2 mmol) according to the general procedure, obtained as a colorless solid (25 mg, 50%). ¹H NMR (CDCl₃, 500 MHz): δ 7.48 (dd *J* = 8.0 Hz, *J* = 1.7 Hz, 1H), 7.33-7.20 (m, 4 H), 7.05-7.02 (m, 2H), 6.96-6.94 (m, 2H); ¹³C NMR (CDCl₃, 125 MHz): δ 157.78, 153.57, 137.51, 133.63, 131.25, 129.57, 128.76 (t, *J*_{CD} = 24.0 Hz), 128.64, 127.57 (t, *J*_{CD} = 24.0 Hz), 126.66 (t, *J*_{CD} = 24.0 Hz), 124.02, 122.59, 120.11, 118.14.



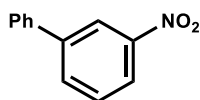
2-methoxybiphenyl (85n):¹³² Prepared from triazene **84n** (76 mg, 0.2 mmol) according to the general procedure, obtained as a yellow oil (8 mg, 18%). ¹H NMR (CDCl₃, 500 MHz): δ 7.55-7.53 (m, 2H), 7.42 (t, *J* = 7.5 Hz, 2H), 7.35-7.32 (m, 3H), 7.06-6.99 (m, 2H), 3.82 (s, 3H); ¹³C NMR CDCl₃, 125 MHz): δ 156.43, 138.50, 130.87, 130.68, 129.52, 128.58, 127.95, 126.90, 120.79, 111.18, 55.52.



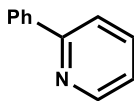
3-methoxybiphenyl (85o):¹³³ Prepared from triazene **84o** (76 mg, 0.2 mmol) according to the general procedure, obtained as a yellow oil (18 mg, 41%). ¹H NMR (CDCl₃, 500 MHz): δ 7.61 (d, *J* = 7.5 Hz, 2H), 7.45 (t, *J* = 7.5 Hz, 2H), 7.39-7.36 (m, 2H), 7.21-7.19 (m, 1H), 7.15-7.14 (m, 1H), 6.93-6.91 (m, 1H), 3.88 (s, 3H); ¹³C NMR (CDCl₃, 125 MHz): δ 159.91, 142.75, 141.08, 129.73, 128.71, 127.39, 127.18, 119.67, 112.87, 112.65, 55.28.



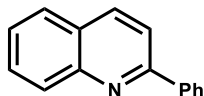
4-bromobiphenyl (85p):¹³⁰ Prepared from triazene **84p** (76 mg, 0.2 mmol) according to the general procedure, obtained as a colorless solid (24 mg, 44%). ¹H NMR (CDCl₃, 500 MHz): δ 7.58-7.55 (m, 4H), 7.48-7.44 (m, 4H), 7.39-7.36 (m, 1H); ¹³C NMR (CDCl₃, 125 MHz): δ 140.11, 139.97, 131.84, 128.88, 128.73, 127.62, 126.92, 121.52.



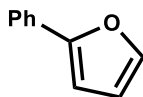
3-nitrobiphenyl (85q):¹²⁵ Prepared from triazene **84q** (80 mg, 0.2 mmol) according to the general procedure, obtained as a colorless solid (6 mg, 13%). ¹H NMR (CDCl₃, 500 MHz): δ 8.47-8.46 (m, 1H), 8.22-8.20 (m, 1H), 7.92 (d, *J* = 7.5 Hz, 1H), 7.64-7.60 (m, 3H), 7.52-7.44 (m, 3H); ¹³C NMR (CDCl₃, 125 MHz): δ 148.72, 142.87, 138.67, 133.04, 129.70, 129.16, 128.53, 127.15, 122.03, 121.96



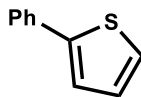
2-phenylpyridine (85r):¹³⁴ Prepared from triazene **84d** (69 mg, 0.2 mmol) according to the general procedure, obtained as a colorless solid (13 mg, 35%). ¹H NMR (CDCl₃, 500 MHz): δ 8.72 (d, *J* = 4.6 Hz, 1H), 8.00 (d, *J* = 6.9 Hz, 2H), 7.81-7.74 (m, 2H), 7.51-7.42 (m, 3H), 7.28-7.26 (m, 1H); ¹³C NMR (CDCl₃, 125 MHz): δ 157.22, 149.16, 137.29, 129.50, 129.18, 128.81, 127.01, 122.23, 120.89.



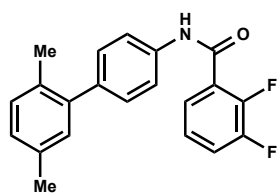
2-phenylquinoline (85s):¹³⁵ Prepared from triazene **84d** (69 mg, 0.2 mmol) according to the general procedure, obtained as a colorless solid (7 mg, 15%). ¹H NMR (CDCl₃, 500 MHz): δ 8.24 (d, *J* = 8.6 Hz, 1H), 8.18 (d, *J* = 6.9 Hz, 3H), 7.89 (d, *J* = 8.6 Hz, 1H), 7.84 (d, *J* = 8.0 Hz, 1H), 7.74 (t, *J* = 8.6 Hz, 1H), 7.54 (t, *J* = 7.5 Hz, 3H), 7.48 (t, *J* = 7.5 Hz, 1H); ¹³C NMR (CDCl₃, 125 MHz): δ 157.28, 148.86, 139.64, 136.97, 129.87, 129.47, 129.12, 128.87, 127.68, 127.47, 127.15, 126.43, 119.10.



2-phenylfuran (85t):¹³⁶ Prepared from triazene **84d** (69 mg, 0.2 mmol) according to the general procedure, obtained as a colorless solid (9 mg, 28%). ¹H NMR (CDCl₃, 500 MHz): δ 7.68 (d, *J* = 8.3 Hz, 2H), 7.47 (d, *J* = 1.2 Hz, 1H), 7.38 (t, *J* = 8.0 Hz, 2H), 7.27-7.22 (m, 1H), 6.66 (d, *J* = 3.4 Hz, 1H), 6.48-6.47 (m, 1H); ¹³C NMR (CDCl₃, 125 MHz): δ 154.12, 142.03, 130.86, 128.64, 127.30, 123.76, 111.61, 104.92.



2-phenylthiophene (85u):¹³⁷ Prepared from triazene **84d** (69 mg, 0.2 mmol) according to the general procedure, obtained as a colorless solid (16 mg, 42%). ¹H NMR (CDCl₃, 500 MHz): δ 7.64-7.60 (m, 2H), 7.40-7.37 (m, 2H), 7.33-7.27 (m, 3H), 7.10-7.08 (m, 1H); ¹³C NMR (CDCl₃, 125 MHz): δ 144.37, 134.20, 128.86, 128.74, 127.98, 127.44, 125.94, 123.06.

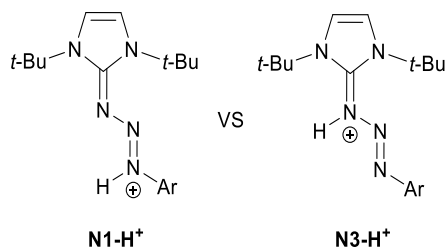


***N*-(2,5'-dimethyl-[1,1'-biphenyl]-4-yl)-2,3-difluorobenzamide**

(86):⁶⁵ Prepared from triazene **84p** (180 mg, 0.5 mmol), obtained as a pale-yellow solid (54 mg, 32%). ¹H NMR (CDCl₃, 500 MHz): δ 8.33 (d, *J* = 13.2 Hz, 1H), 7.94-7.91 (m, 1H), 7.70 (d, *J* = 8.6 Hz, 2H), 7.39-7.34 (m, 4H), 7.17 (d, *J* = 7.5 Hz, 1H), 7.09-7.06 (m, 2H), 2.36 (s, 3H), 2.25 (s, 3H); ¹³C NMR (CDCl₃, 125 MHz): δ 160.28 (m), 150.64 (m), 148.81 (m), 140.95, 138.96, 136.01, 135.27, 132.21, 130.49, 130.32, 129.91, 128.03, 126.66 (d, *J*_{CF} = 3.6 Hz), 124.87 (m), 123.62 (d, *J*_{CF} = 9.6 Hz), 120.62 (m), 120.24, 20.92, 19.98.

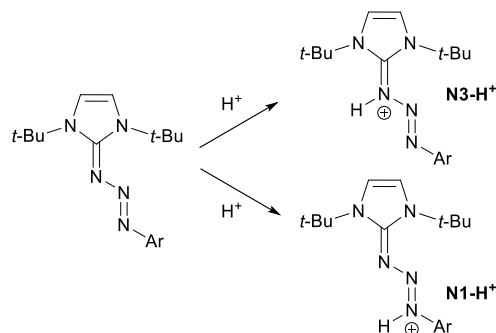
Computational Data Tables

Table 6-1 PCM ground state energy difference between N1-H⁺ and N3-H⁺, calculated using DFT-B3LYP and RI-MP2 (Basis set: 6-31+G* and cc-pVTZ basis set, respectively)



Compound	B3LYP (kcal/mol)	RI-MP2 (kcal/mol)	Ar
84a	-4.5	-3.2	4-CIPh
84b	-5.0	-3.7	4-MePh
84c	-14.9	-10.7	4- <i>t</i> -BuPh
84d	-14.9	-10.3	Ph
84e	-14.2	-8.4	Mes
84f	-5.2	-3.9	2,3-MePh
84g	-14.6	-11.5	4-OMePh
84h	-4.9	-3.4	4-CNPh
84i	-5.0	-3.6	4-CF ₃ Ph
84j	-5.0	-3.2	4-NO ₂ Ph
84k	-5.5	-3.7	4-CO ₂ MePh
84l	-16.2	-11.4	2-PhPh
84m	-7.9	-4.9	2-OPhPh
84n	-16.4	-9.9	2-OMePh
84o	-5.6	-4.0	3-OMePh
84p	-4.4	-3.2	4-BrPh
84q	-4.3	-3.8	3-NO ₂ Ph

Table 6-2 Electronic energy difference between the protonated and unprotonated triazenes at the PCM ground electronic state

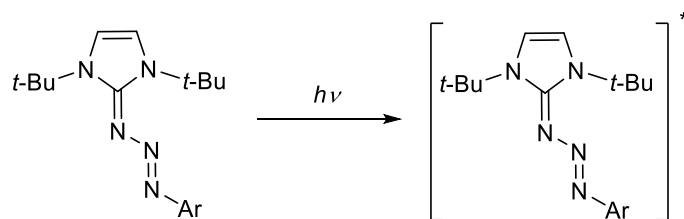


Compound	N1-H ⁺ (kcal/mol)	N3-H ⁺ (kcal/mol)
84a	17.8	22.2
84b	14.5	19.4
84c	14.2	29.2
84d	15.3	30.1
84e	13.3	27.5
84f	13.8	19.0
84g	14.3	28.9
84h	21.2	26.0
84i	19.6	24.7
84j	22.9	27.9
84k	18.1	23.7
84l	14.0	30.3
84m	13.5	21.3
84n	11.2	27.7
84o	14.3	19.9
84p	17.9	22.3
84q	21.1	25.5

In summary: The title reaction has a positive reaction energy. However, it is acid dependent.

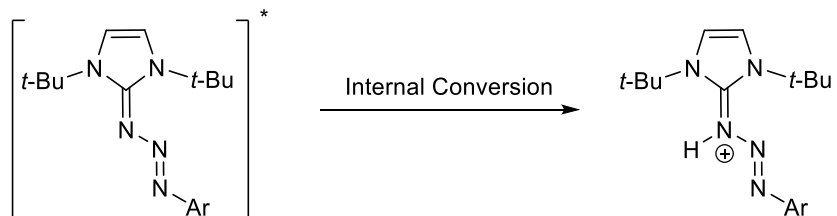
Here was calculated for TFA.

Table 6-3 Calculated absorption wavelength for the first bright state



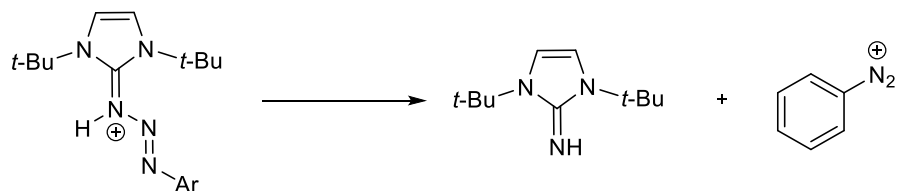
Compound	N1-H ⁺ (nm)	N3-H ⁺ (nm)	Unprotonated (nm)
84a	357	319	400
84b	358	316	395
84c	356	332	396
84d	349	318	396
84e	358	348	391
84f	357	321	395
84g	376	352	395
84h	354	324	420
84i	347	319	407
84j	376	339	477
84k	356	325	420
84l	370	336	401
84m	393	399	403
84n	379	340	402
84o	375	359	393
84p	354	323	400
84q	356	329	529

Table 6-4 Electronic coupling between the ground and first bright excited state, calculated at the Frank-Condon geometry (absorption) for the 1-Z configuration of N3-H⁺



Compound	Coupling (cm ⁻¹)
84a	14
84b	37
84c	146
84d	514
84e	53
84f	2713
84g	5
84h	35
84i	9
84j	24
84k	5
84l	9
84m	520
84n	6
84o	2000
84p	7
84q	9

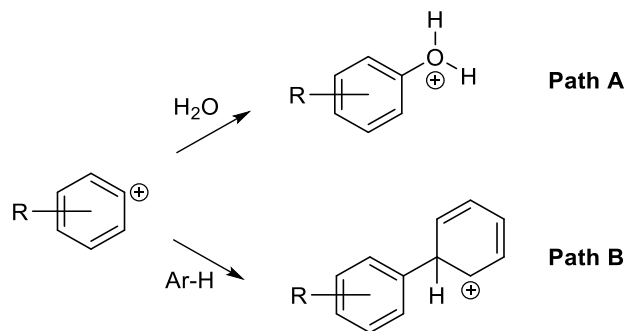
Table 6-5 Energy of dissociation reaction between 1-*E* and 1-*Z* of N3-H⁺



Compound	1- <i>E</i> (kcal/mol)	1- <i>Z</i> (kcal/mol)	Ar
84a	31.6	-20.5	4-ClPh
84b	26.8	-26.0	4-MePh
84c	16.2	-26.7	4- <i>t</i> -BuPh
84d	19.8	-32.5	Ph
84e	8.7	-38.4	Mes
84f	25.3	-26.9	2,3-MePh
84g	13.2	-32.7	4-OMePh
84h	37.3	-17.7	4-CNPh
84i	35.8	-17.4	4-CF ₃ Ph
84j	39.6	-25.0	4-NO ₂ Ph
84k	32.8	-26.3	4-CO ₂ MePh
84l	15.4	-28.3	2-PhPh
84m	23.5	-34.6	2-OPhPh
84n	14.5	-40.4	2-OMePh
84o	28.9	-39.8	3-OMePh
84p	31.5	-31.6	4-BrPh
84q	38.7	-28.5	3-NO ₂ Ph

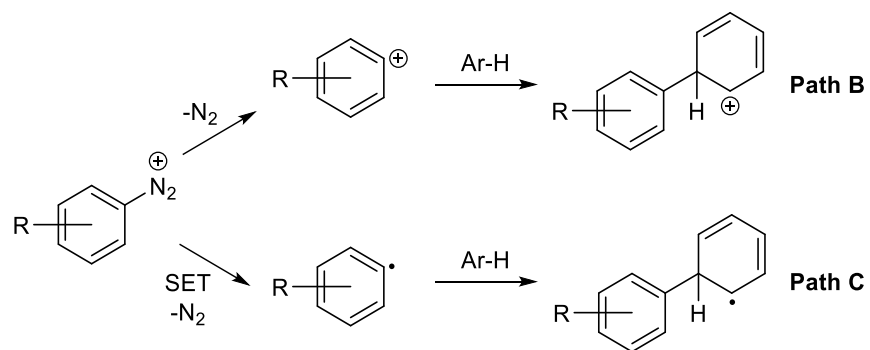
Table 6-6 Difference of binding energy (BE) between path A and B. The difference is

BE(pathA)- BE(pathB)



Aryldiazonium Salt	BE Difference(kcal/mol)
84a	4.4
84b	8.3
84c	-2.5
84d	2.7
84e	-2.0
84f	1.6
84g	2.2
84h	5.9
84i	5.2
84j	7.4
84k	4.2
84l	0.2
84m	3.0
84n	2.4
84o	2.4
84p	4.3
84q	6.8

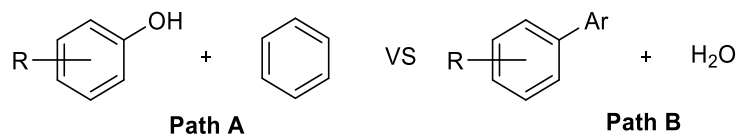
Table 6-7 Binding energy (BE) between path B and C. The difference is BE(pathB)-BE(pathC)



Compound	Energy Difference(kcal/mol)
84a	-61.0
84b	-60.2
84c	-48.5
84d	-55.2
84e	-42.5
84f	-51.3
84g	-56.8
84h	-63.6
84i	-62.3
84j	-66.3
84k	-58.6
84l	-50.0
84m	-44.7
84n	-62.3
84o	-52.9
84p	-60.7
84q	-66.6

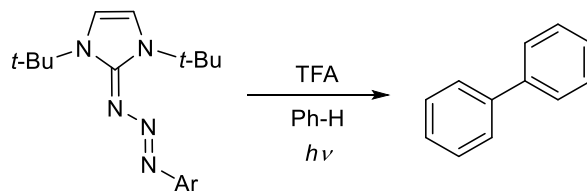
Table 6-8 Energy difference between final products of path A and B. The difference is E(pathA)-

E(pathB)



Compound	Energy Difference (kcal/mol)
84a	6.0
84b	6.1
84c	5.9
84d	5.6
84e	2.0
84f	6.0
84g	7.2
84h	4.7
84i	4.9
84j	4.3
84k	4.6
84l	2.4
84m	3.2
84n	6.2
84o	5.4
84p	5.9
84q	5.7

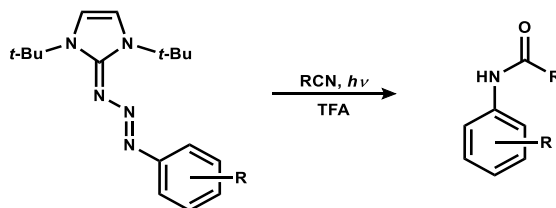
Table 6-9 Relative free energies and enthalpies for species involved in the Ar-Ar-Cross-coupling
of triazene **84d**



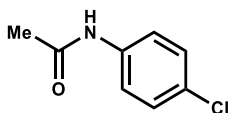
Compound	ΔG (kcal/mol)	ΔH (kcal/mol)
84d-E S0(min)	0.0	0.0
84d-E (N1-H⁺) S0(min)	16.8	0.0
84d-E (N3-H⁺) S0(min)	31.7	-0.3
84d-E S1	71.9	0.0
84d-E (N1-H⁺) S1	98.0	-0.1
84d-E (N3-H⁺) S1	121.3	-0.3
84d-Z (N3-H⁺) S1(min)	76.1	-3.3
84d-E (N1-H⁺) S1(min)	65.5	-0.1
84d-E S1(min)	43.6	0.0
84d-Z (N3-H⁺) S0	73.8	-3.3
84d-E (N1-H⁺) S0	58.6	-0.1
84d-E S0	38.3	0.0
87	36.3	-2.8
88 (H₂O)	18.9	-2.3
88 (C₆H₆)	15.9	-3.3
93	34.3	-5.5
85d	-64.2	-1.2
85d'	-59.5	-0.9

min = minima

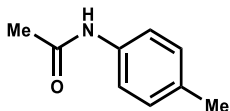
General Method for the Preparation of Aromatic Amides (94)



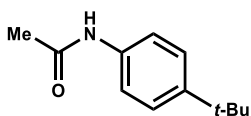
To a quartz tube containing triazene (0.2 mmol) was added the corresponding nitrile (2 mL). Then, the tube was capped and TFA (1.0 mmol) was added with a syringe. Next, the mixture was left to stir inside a photoreactor under UV irradiation (350 nm) for 4 h. After this time, the resulting mixture was concentrated *in vacuo*. Purification by flash chromatography (SiO₂, EtOAc/hexanes mixtures) provided the pure aromatic amide.



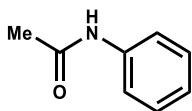
N-(4-(chloro)phenyl)acetamide (94a):¹³⁸ Prepared from triazene **84a** (77 mg, 0.2 mmol) according to the general procedure, obtained as a pale yellow solid (18 mg, 46%). ¹H NMR (CDCl₃, 500 MHz): δ 7.45 (d, *J* = 8.9 Hz, 2H), 7.28 (d, *J* = 8.9 Hz, 2H), 2.18 (s, 3H); ¹³C NMR (CDCl₃, 125 MHz): δ 168.42, 136.33, 129.34, 129.00, 121.11, 24.58



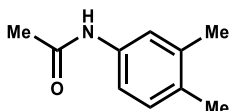
N-(4-(methyl)phenyl)acetamide (94b):¹³⁹ Prepared from triazene **84b** (73 mg, 0.2 mmol) according to the general procedure, obtained as a pale yellow solid (21 mg, 61%). ¹H NMR (CDCl₃, 500 MHz): δ 7.50 (s, 1H), 7.43 (d, *J* = 8.3 Hz, 2H), 7.10 (d, *J* = 8.3 Hz, 2H), 2.30 (s, 3H), 2.15 (s, 3H); ¹³C NMR (CDCl₃, 125 MHz): δ 168.57, 135.18, 134.03, 129.43, 120.13, 24.37, 20.83



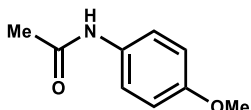
N-(4-(*tert*-butyl)phenyl)acetamide (94c):¹⁴⁰ Prepared from triazene **84c** (82 mg, 0.2 mmol) according to the general procedure, obtained as a pale yellow solid (36 mg, 82%). ¹H NMR (CDCl₃, 500 MHz): δ 7.96 (s, 1H), 7.42 (d, *J* = 8.6 Hz, 2H), 7.31 (d, *J* = 8.6 Hz, 2H), 2.16 (s, 3H), 1.29 (s, 9H); ¹³C NMR (CDCl₃, 125 MHz): δ 169.09, 147.45, 135.03, 125.69, 120.08, 34.31, 31.28, 24.15



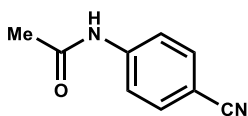
N-phenylacetamide (94d):¹⁴⁰ Prepared from triazene **84d** (69 mg, 0.2 mmol) according to the general procedure, obtained as a pale yellow solid (19 mg, 61%). ¹H NMR (CDCl₃, 500 MHz): δ 7.74 (s, 1H), 7.48 (d, *J* = 7.5 Hz, 2H), 7.31 (t, *J* = 8.0 Hz, 2H), 7.13 (t, *J* = 7.4 Hz, 1H), 2.20 (s, 3H); ¹³C NMR (CDCl₃, 125 MHz): δ 169.82, 137.26, 129.00, 124.87, 120.42, 24.15



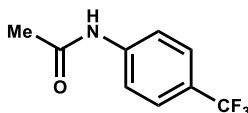
N-(2,2-(dimethyl)phenyl)acetamide (94f):¹⁴¹ Prepared from triazene **84f** (76 mg, 0.2 mmol) according to the general procedure, obtained as a pale yellow solid (31 mg, 81%). ¹H NMR (CDCl₃, 500 MHz): δ 8.02 (s, 1H), 7.27 (s, 1H), 7.21 (d, *J* = 7.7 Hz, 1H), 7.04 (d, *J* = 7.7 Hz, 1H), 2.21 (s, 3H), 2.20 (s, 3H), 2.19 (s, 3H); ¹³C NMR (CDCl₃, 125 MHz): δ 169.24, 137.16, 135.13, 133.09, 129.86, 121.76, 117.95, 24.08, 19.82, 19.15



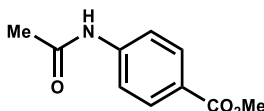
N-(4-(methoxy)phenyl)acetamide (94g):¹⁴⁰ Prepared from triazene **84g** (76 mg, 0.2 mmol) according to the general procedure, obtained as a pale yellow solid (33 mg, 87%). ¹H NMR (CDCl₃, 500 MHz): δ 7.86 (s, 1H), 7.38 (d, 8.9 Hz, 2H), 6.82 (d, *J* = 8.9 Hz, 2H), 3.76 (s, 3H), 2.13 (s, 3H); ¹³C NMR (CDCl₃, 125 MHz): δ 168.75, 156.40, 130.90, 122.07, 113.99, 55.40, 24.06



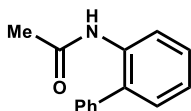
N-(4-(cyano)phenyl)acetamide (94h):¹⁴² Prepared from triazene **84h** (75 mg, 0.2 mmol) according to the general procedure, obtained as a pale yellow solid (4 mg, 10%). ¹H NMR (CDCl₃, 500 MHz): δ 7.65 (d, *J* = 8.9 Hz, 2H), 7.61 (d, *J* = 8.9 Hz, 2H), 7.43 (s, 1H), 2.22 (s, 3H); ¹³C NMR (CDCl₃, 125 MHz): δ 168.52, 141.85, 133.31, 119.40, 118.79, 107.14, 24.80



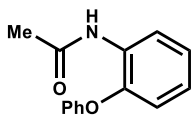
N-(4-(trifluoromethyl)phenyl)acetamide (94i):¹⁴³ Prepared from triazene **84i** (85 mg, 0.2 mmol) according to the general procedure, obtained as a pale yellow solid (20 mg, 43%). ¹H NMR (CDCl₃, 500 MHz): δ 7.63 (d, *J* = 8.6 Hz, 2H), 7.56 (d, *J* = 8.6 Hz, 2H), 2.21 (s, 3H); ¹³C NMR (CDCl₃, 125 MHz): δ 168.64, 140.84, 126.24 (d, *J* = 3.6 Hz), 125.09, 122.93, 119.30, 24.66



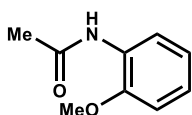
Methyl 4-acetamidobenzoate (94k):¹⁴⁴ Prepared from triazene **84k** (83 mg, 0.2 mmol) according to the general procedure, obtained as a pale yellow solid (7 mg, 16%). ¹H NMR (CDCl₃, 500 MHz): δ 7.96 (d, *J* = 8.9 Hz, 2H), 6.87 (d, *J* = 8.9 Hz, 2H), 3.89 (s, 3H); ¹³C NMR (CDCl₃, 125 MHz): δ 166.98, 159.79, 131.91, 122.68, 117.46, 115.17, 51.97, 29.69



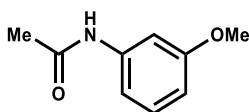
N-(2-(phenyl)phenyl)acetamide (94l):¹⁴⁵ Prepared from triazene **84l** (87 mg, 0.2 mmol) according to the general procedure, obtained as a pale yellow solid (23 mg, 47%). ¹H NMR (CDCl₃, 500 MHz): δ 8.24 (d, *J* = 8.3 Hz, 1H), 7.49-7.32 (m, 7H), 7.26-7.18 (m, 1H), 2.03 (s, 3H); ¹³C NMR (CDCl₃, 125 MHz): δ 168.50, 138.05, 134.48, 130.04, 129.17, 129.05, 128.38, 127.94, 124.47, 121.76, 24.48



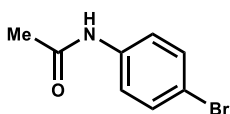
N-(2-(phenoxy)phenyl)acetamide (94m):¹⁴⁶ Prepared from triazene **84m** (91 mg, 0.2 mmol) according to the general procedure, obtained as a pale yellow solid (52 mg, 99%). ¹H NMR (CDCl₃, 500 MHz): δ 8.41 (d, *J* = 8.0 Hz, 1H), 7.81 (s, 1H), 7.37 (t, *J* = 7.5 Hz, 2H), 7.18-7.10 (m, 2H), 7.03-7.00 (m, 3H), 6.84 (d, *J* = 8.6 Hz, 1H), 2.20 (s, 3H); ¹³C NMR (CDCl₃, 125 MHz): δ 168.95, 156.25, 145.64, 129.98, 124.20, 123.99, 123.95, 121.01, 118.70, 117.54, 24.74



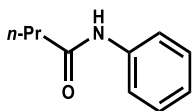
N-(2-(methoxy)phenyl)acetamide (94n):¹³⁹ Prepared from triazene **84n** (76 mg, 0.2 mmol) according to the general procedure, obtained as a pale yellow solid (29 mg, 76%). ¹H NMR (CDCl₃, 500 MHz): δ 8.32 (dd, *J* = 8.0 Hz, *J* = 1.1 Hz, 1H), 7.83 (s, 1H), 7.05 (td, *J*_t = 8.0 Hz, *J*_d = 1.2 Hz, 1H), 6.96 (td, *J*_t = 7.2, *J*_d = 1.2 Hz, 1H), 6.88 (d, *J* = 8.0 Hz, 1H), 3.88 (s, 3H), 2.23 (s, 3H); ¹³C NMR (CDCl₃, 125 MHz): δ 168.81, 147.72, 127.32, 123.91, 121.06, 119.86, 55.62, 24.74



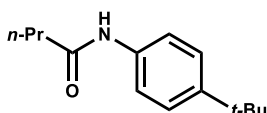
N-(3-(methoxy)phenyl)acetamide (94o):¹⁴⁷ Prepared from triazene **84o** (76 mg, 0.2 mmol) according to the general procedure, obtained as a pale yellow solid (30 mg, 78%). ¹H NMR (CDCl₃, 500 MHz): δ 7.89 (s, 1H), 7.26-7.17 (m, 2H), 6.99-6.97 (m, 1H), 6.67-6.65 (m, 1H), 3.77 (s, 3H), 2.17 (s, 3H); ¹³C NMR (CDCl₃, 125 MHz): δ 169.34, 160.02, 138.78, 129.61, 112.30, 110.20, 106.03, 55.22, 24.31



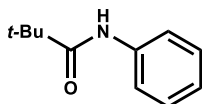
N-(4-(bromo)phenyl)acetamide (94p):¹⁴⁸ Prepared from triazene **84p** (88 mg, 0.2 mmol) according to the general procedure, obtained as a pale yellow solid (30 mg, 61%). ¹H NMR (CDCl₃, 500 MHz): δ 7.57 (s, 1H), 7.40 (s, 4H), 2.17 (s, 3H); ¹³C NMR (CDCl₃, 125 MHz): δ 168.61, 136.82, 131.92, 121.49, 116.96, 24.56



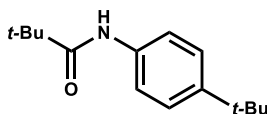
N-(4-*tert*-butylphenyl)butyramide (94r): Prepared from triazene **84d** (69 mg, 0.2 mmol) according to the general procedure, obtained as a colorless solid (29 mg, 77%). $^1\text{H NMR}$ (CDCl_3 , 500 MHz): δ 7.52 (d, $J = 8.0$ Hz, 3H), 7.30 (t, $J = 8.0$ Hz, 2H), 7.09 (t, $J = 7.5$ Hz, 1H), 2.33 (t, $J = 7.5$ Hz, 2H), 1.75 (q, $J = 7.5$ Hz, 2H), 0.99 (t, $J = 7.5$ Hz, 3H); $^{13}\text{C NMR}$ (CDCl_3 , 125 MHz): δ 171.47, 137.95, 128.90, 124.13, 119.86, 39.59, 19.06, 13.70



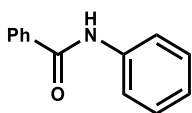
N-(4-*tert*-butylphenyl)butyramide (94s): Prepared from triazene **84c** (82 mg, 0.2 mmol) according to the general procedure, obtained as a colorless solid (48 mg, 95%). $^1\text{H NMR}$ (CDCl_3 , 500 MHz): δ 7.56 (s, 1H), 7.44 (d, $J = 8.6$ Hz, 2H), 7.32 (d, $J = 8.6$ Hz, 2H), 2.33 (t, $J = 7.5$ Hz, 2H), 1.75 (sext, $J = 7.5$ Hz, 2H), 1.29 (s, 9H), 0.99 (t, $J = 7.5$ Hz, 3H); $^{13}\text{C NMR}$ (CDCl_3 , 125 MHz): δ 172.88, 147.93, 134.54, 125.79, 120.34, 39.29, 34.35, 31.26, 19.32, 13.60



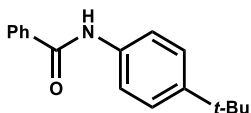
N-(phenyl)trimethylacetamide (94t):¹³⁸ Prepared from triazene **84d** (82 mg, 0.2 mmol) according to the general procedure, obtained as a colorless solid (20 mg, 48%). $^1\text{H NMR}$ (CDCl_3 , 500 MHz): δ 7.53 (d, $J = 8.0$ Hz, 2H), 7.32 (t, $J = 7.5$ Hz, 2H), 7.10 (t, $J = 7.5$ Hz, 1H), 1.32 (s, 9H); $^{13}\text{C NMR}$ (CDCl_3 , 125 MHz): δ 176.60, 137.95, 128.93, 124.21, 119.97, 39.57, 27.60



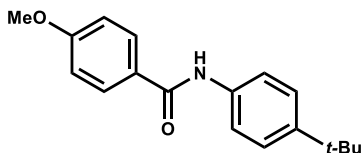
N-(4-*tert*-butylphenyl)trimethylacetamide (94u): Prepared from triazene **84c** (82 mg, 0.2 mmol) according to the general procedure, obtained as a colorless solid (44 mg, 81%). $^1\text{H NMR}$ ($\text{DMSO}-d_6$, 500 MHz): δ 9.11 (s, 1H), 7.53 (d, $J = 8.9$ Hz, 2H), 7.29 (d, $J = 8.9$ Hz, 2H), 1.25 (s, 9H), 1.21 (s, 9H); $^{13}\text{C NMR}$ ($\text{DMSO}-d_6$, 125 MHz): δ 176.24, 145.41, 136.80, 124.96, 119.99, 33.97, 31.23, 27.25



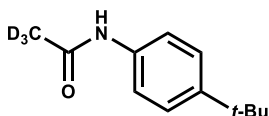
N-(phenyl)phenylformamide (94x):¹⁴⁹ Prepared from triazene **84d** (69 mg, 0.2 mmol) according to the general procedure, obtained as a colorless solid (19 mg, 41%). ¹H NMR (CDCl₃, 500 MHz): δ 7.89-7.86 (m, 2H), 7.81 (s, 1H), 7.66-7.63 (m, 2H), 7.59-7.48 (m, 3H), 7.41-7.36 (m, 2H), 7.19-7.14 (m, 1H); ¹³C NMR (CDCl₃, 125 MHz): δ 166.38, 137.74, 134.83, 132.12, 129.25, 128.96, 127.17, 124.95, 120.57



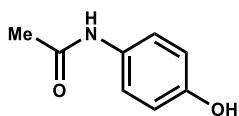
N-(4-tert-butylphenyl)phenylformamide (94y):¹⁵⁰ Prepared from triazene **84c** (82 mg, 0.2 mmol) according to the general procedure, obtained as a colorless solid (26 mg, 44%). ¹H NMR (CDCl₃, 500 MHz): δ 7.87-7.85 (m, 3H), 7.57-7.53 (m, 3H), 7.48 (t, *J* = 7.5 Hz, 2H), 7.39 (d, *J* = 8.6 Hz, 2H), 1.33 (s, 9H); ¹³C NMR (CDCl₃, 125 MHz): δ 165.69, 147.57, 135.23, 135.04, 132.75, 131.73, 128.74, 126.98, 125.89, 120.00, 34.39, 31.34



N-(4-tert-butylphenyl)-4-methoxyformamide (94aa): Prepared from triazene **84c** (82 mg, 0.2 mmol) according to the general procedure, obtained as a colorless solid (20 mg, 31%). ¹H NMR (CDCl₃, 500 MHz): δ 7.83 (d, *J* = 8.6 Hz, 2H), 7.75 (s, 1H), 7.53 (d, *J* = 8.6 Hz, 2H), 7.39 (d, *J* = 8.6 Hz, 2H), 6.98 (d, *J* = 9.2 Hz, 2H), 3.88 (s, 3H), 1.32 (s, 9H); ¹³C NMR (CDCl₃, 125 MHz): δ 162.54, 147.66, 135.13, 128.92, 125.93, 120.19, 114.01, 55.47, 34.41, 31.34



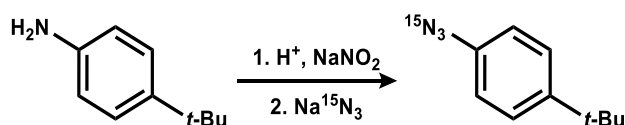
N-(4-(tert-butyl)phenyl)acetamide-d₃ (94c'): Prepared from triazene **84c** (82 mg, 0.2 mmol) according to the general procedure, obtained as a pale yellow solid (29 mg, 65%). ¹H NMR (CDCl₃, 500 MHz): δ 8.30 (s, 1H), 7.42 (d, *J* = 8.6 Hz, 2H), 7.31 (d, *J* = 8.6 Hz, 2H), 1.29 (s, 9H); ¹³C NMR (CDCl₃, 125 MHz): δ 169.51, 147.81, 134.72, 125.75, 120.28, 34.35, 31.28



N-(4-(hydroxy)phenyl)acetamide:¹⁵¹ Prepared from triazene **84g** (382 mg, 1.2 mmol), obtained as a pale yellow solid (92 mg, 53%).

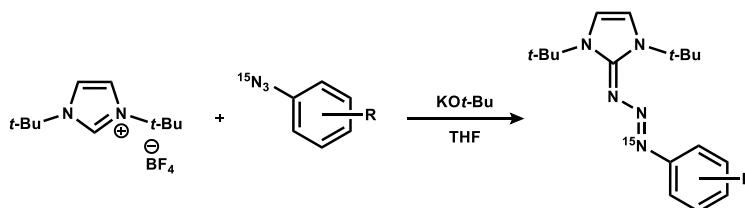
¹H NMR (CDCl₃, 500 MHz): δ 9.65 (s, 1H), 7.33 (d, *J* = 9.2 Hz, 2H), 6.67 (d, *J* = 9.2 Hz, 2H), 1.97 (s, 3H); ¹³C NMR (CDCl₃, 125 MHz): δ 167.58, 153.16, 131.06, 120.86, 115.02, 23.75

Preparation of ¹⁵N Labelled Azide



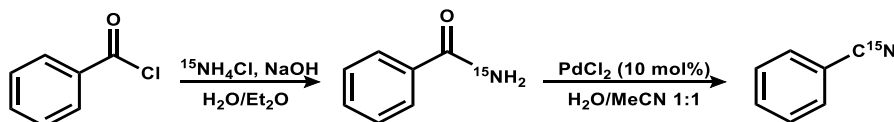
A flask containing 4-*tert*-butylaniline (2.0 mmol) in 17% HCl (12.5 mL) was cooled to 0 °C and then sodium nitrite (3.0 mmol) was added slowly. The mixture was stirred at 0 °C for 20 min and then, ¹⁵N labelled sodium azide (3.0 mmol) was added slowly. The reaction mixture was then stirred at room temperature for 3 h. The reaction mixture was then extracted with ethyl acetate, the organic layer was washed with sodium bicarbonate solution and brine and dried with anhydrous sodium sulfate. The organic layer was then concentrated *in vacuo*. Purification by flash chromatography (SiO₂, EtOAc/hexanes mixtures) provided the pure azide.

Preparation of ^{15}N Labelled Triazene



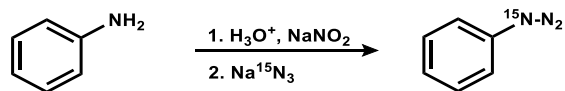
To a flask containing 1,3-ditert-butylimidazolium tetrafluoroborate (0.5 mmol), potassium *tert*-butoxide (0.6 mmol) and dry THF was added (2.5 mL) under Ar. The resulting suspension was stirred for 15 minutes, followed by dropwise addition of ^{15}N labelled azide (0.5 mmol). The resulting mixture was left stirring at room temperature for 12 h. After this time, hexanes (1 mL) were added and the resulting solid precipitate filtered. The filtered solid was dissolved in DCM (5 mL) and the precipitated salts filtered. The resulting solution was then concentrated *in vacuo* and dried under high vacuum, affording the pure triazene.

Preparation of ^{15}N Labelled Benzonitrile

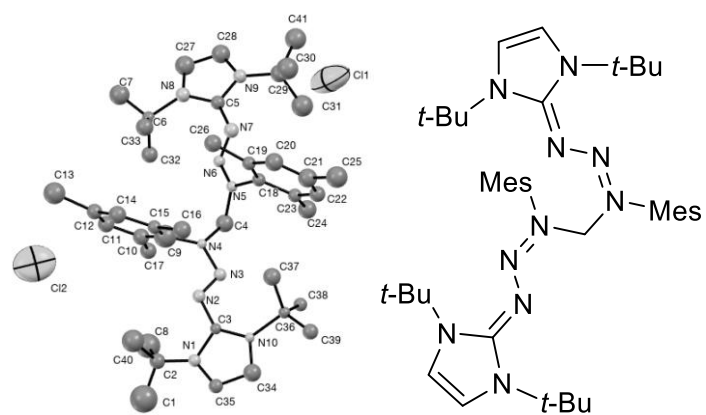


To a flask containing benzoyl chloride (3.0 mmol) in water/ Et_2O 3:2 (1.1 mL) was added $^{15}\text{NH}_4\text{Cl}$ (3.6 mmol) and cooled to 0°C . Ice cold 10 M NaOH (0.5 mL) was added to the mixture and stirred for 20 min. Then the resulting white solid was filtered using a sintered glass funnel and washed with a water/ Et_2O 1:1 mixture, then dried *in vacuo* affording the pure amide. Then, benzamide (1.6 mmol) was dissolved in of 1:1 MeCN/ H_2O (12 mL) and PdCl_2 (0.16 mmol) was added and the mixture was stirred at room temperature for 40 h. Then the mixture was extracted with chloroform, the organic layer was washed with brine and concentrated *in vacuo*. Purification by flash chromatography (SiO_2 , EtOAc/hexanes mixtures) provided the pure aromatic nitrile.

Procedure for the synthesis of ^{15}N labelled 4-*tert*-butylazidobenzene



To a flask containing 4-*tert*-butyl aniline (2.0 mmol), 17% HCl (12.5 mL) was added. Then the flask was cooled to 0 °C in an ice/water bath and NaNO_2 (3.0 mmol) was slowly added and the reaction was left stirring for 20 min. After this time Na^{15}N_3 (3.0 mmol) was slowly added and the reaction was left stirring at room temperature for 2 h. After this time, the reaction mixture was extracted with EtOAc (5 mL) three times and the organic layer was neutralized with NaHCO_3 (5 mL) three times and washed with brine (5 mL). The organic layer was then concentrated *in vacuo* and dried under high vacuum, affording the pure azide.



ORTEP representation of the X-ray crystal structure of a dimer of triazene **84e** showing atom labeling. 50% Probability amplitude displacement ellipsoids are shown. For clarity, all hydrogen atoms are omitted.

Appendix A
List of abbreviations

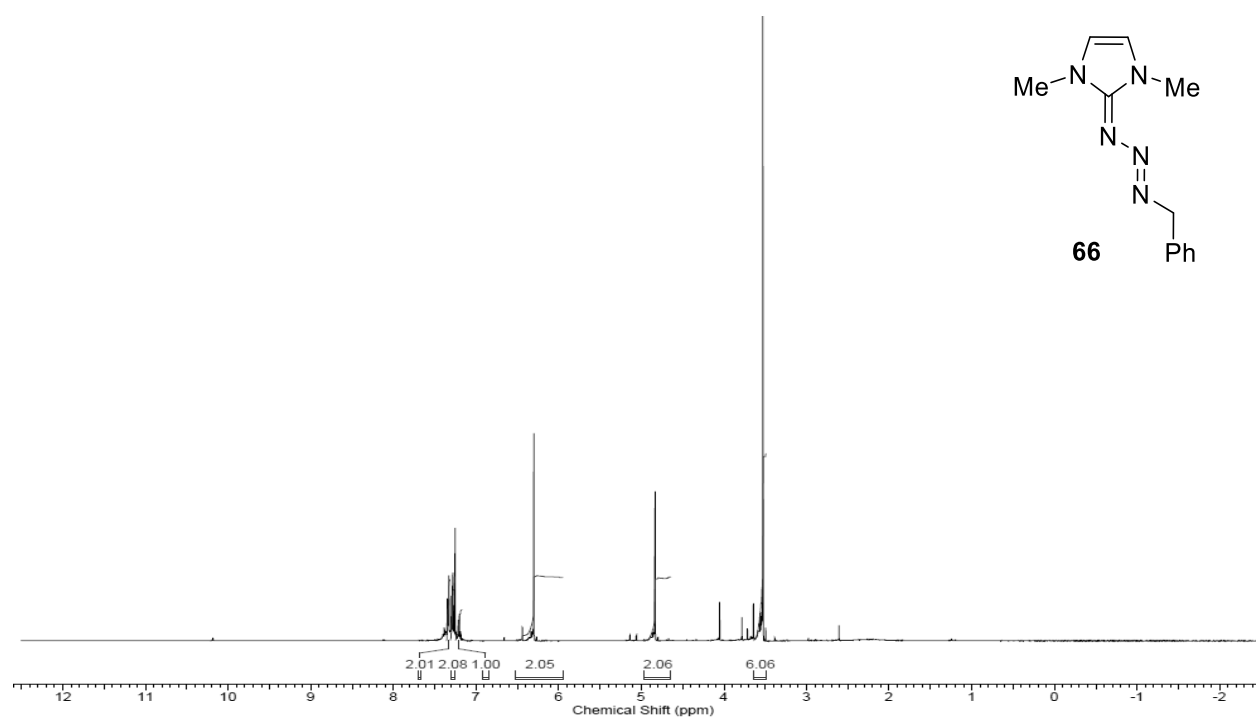
δ : chemical shift (ppm)
[M⁺]: molecular ion
Ac: acyl
Ar: aryl
ATR: Attenuated Total Reflection
Bn: benzyl
Bu: butyl
C: Celsius
calcd: calculated
cat.: catalytic amount
DCM: dichloromethane
DMF: dimethylformamide
DMSO: dimethyl sulfoxide
eq.: equation
equiv.: equivalent
Et: ethyl
ESI: Electrospray ionization
g: gram
GCMS: gas chromatography mass spectrometry
h: hours
HRMS: high resolution mass spectrometry
 $h\nu$: Electromagnetic radiation
Hz: hertz
IR: infrared
 J : coupling constant
M: molar

Me: methyl
Mes: mesityl
MeCN: acetonitrile
MeOH: methanol
EtOH: ethanol
mg: milligram
MHz: megahertz
min.: minutes
mL: milliliter
mmol: millimole
mp: melting point
MW: molecular weight
NHC: *N*-heterocyclic carbene
NMR: Nuclear Magnetic Resonance
RDL: Radiationless Decay
rt: room temperature
*S*1: First excited state
*S*0: Ground state
t-Bu: *tert*-butyl
TFA: Trifluoroacetic acid
TLC: thin layer chromatography
TOF: time of flight
TS: transition state
TsOH: *p*-toluensulfonic acid
UV-Vis Ultraviolet-visible
XPhos: 2-Dicyclohexylphosphino-2',4',6'-triisopropylbiphenyl

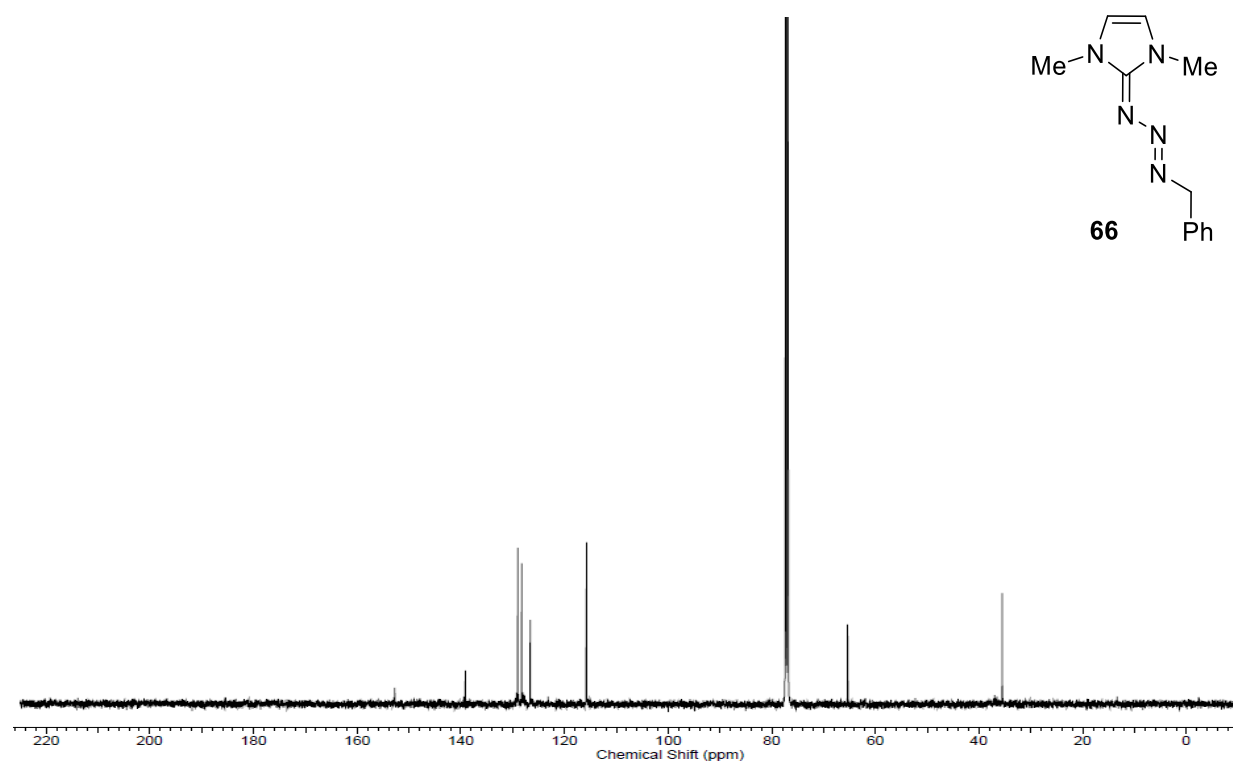
Appendix B

^1H and ^{13}C NMR Spectra

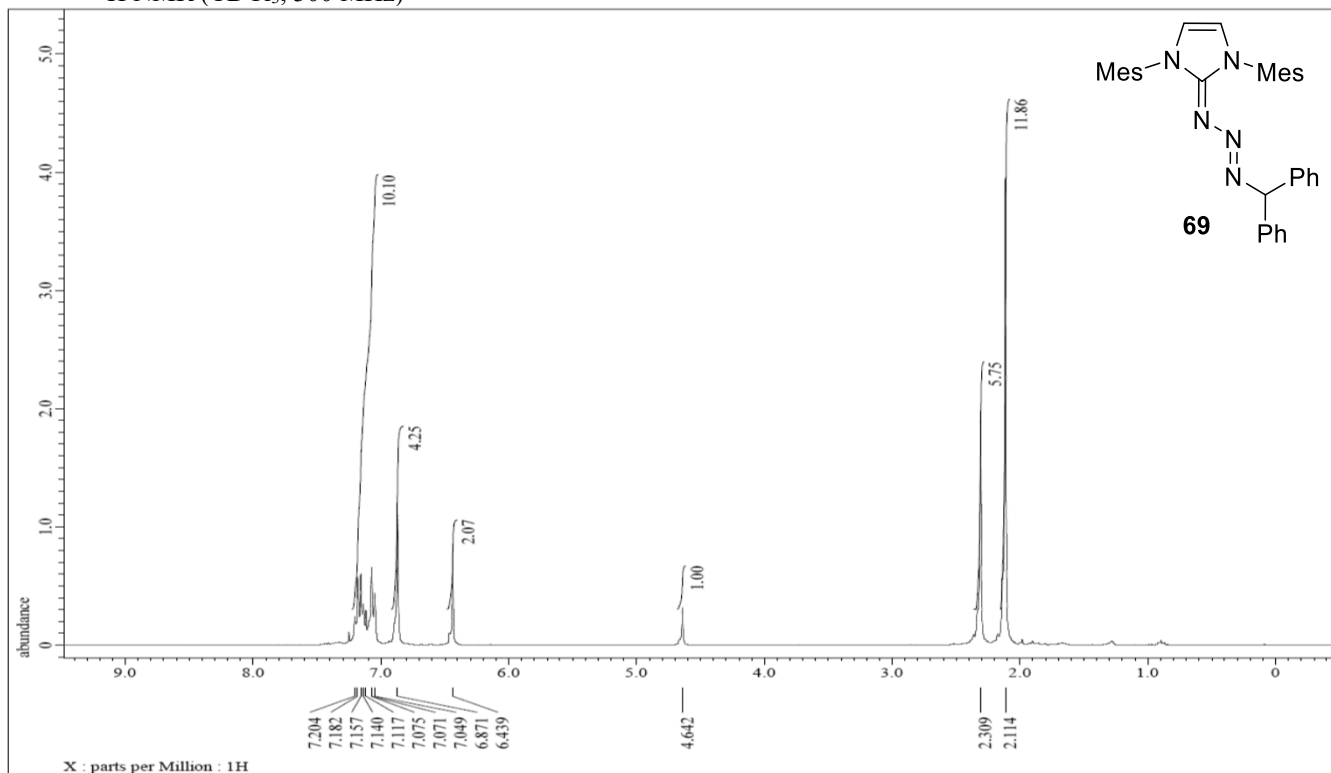
^1H NMR (CDCl_3 , 500 MHz)



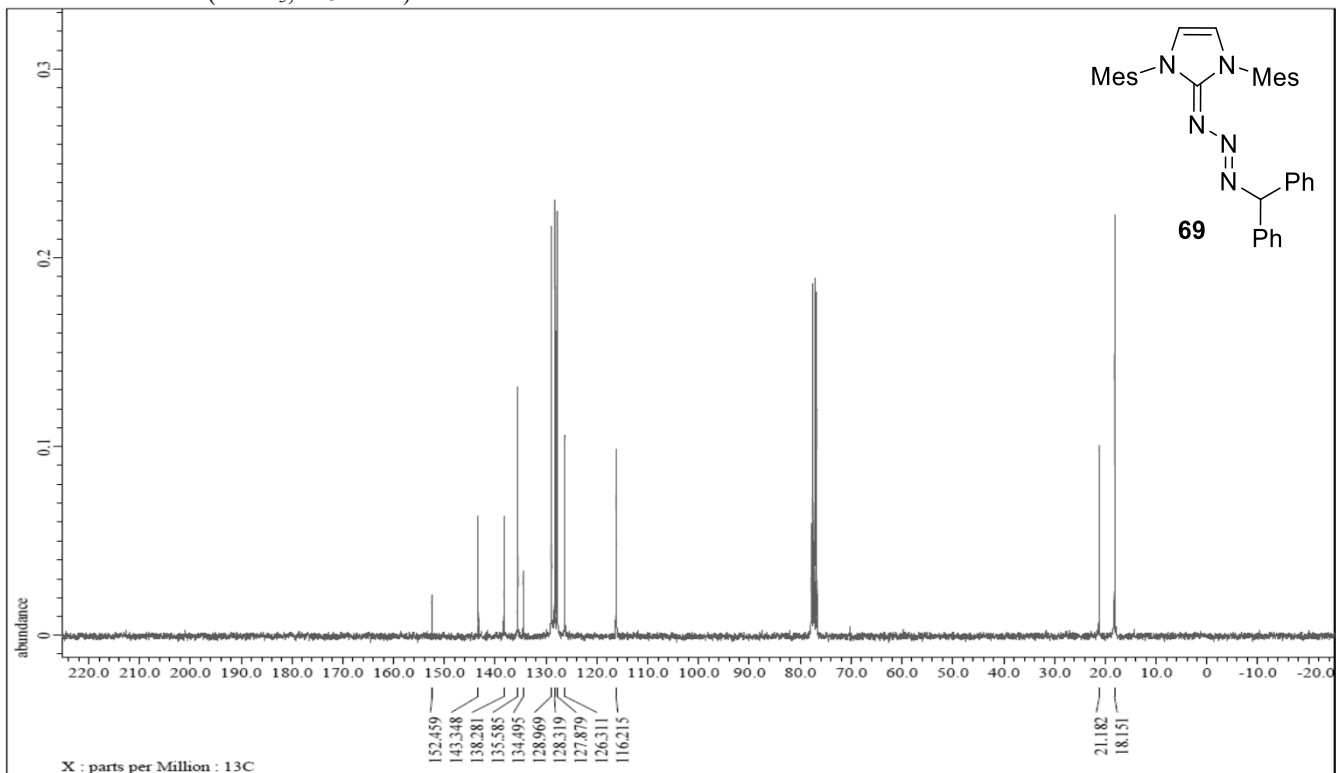
^{13}C NMR (CDCl_3 , 125 MHz)



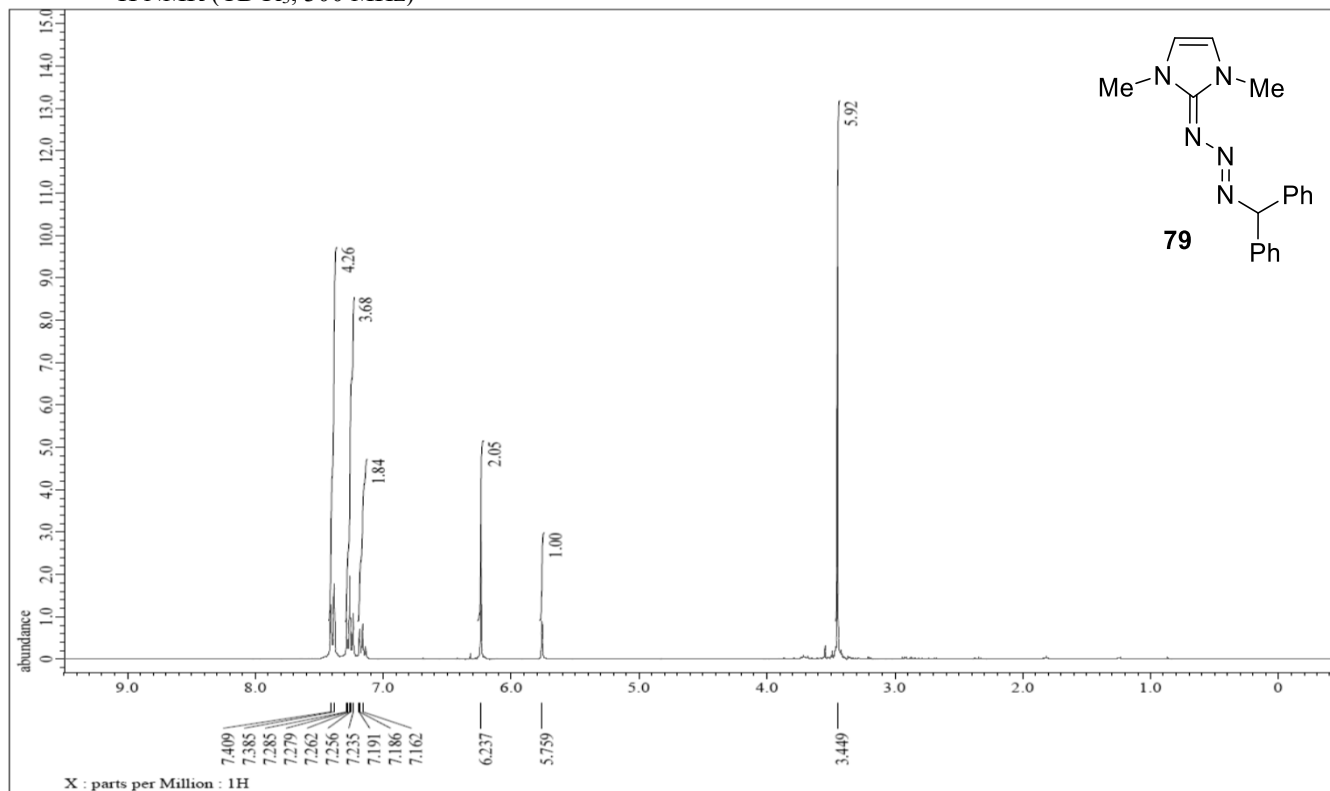
^1H NMR (CDCl_3 , 300 MHz)



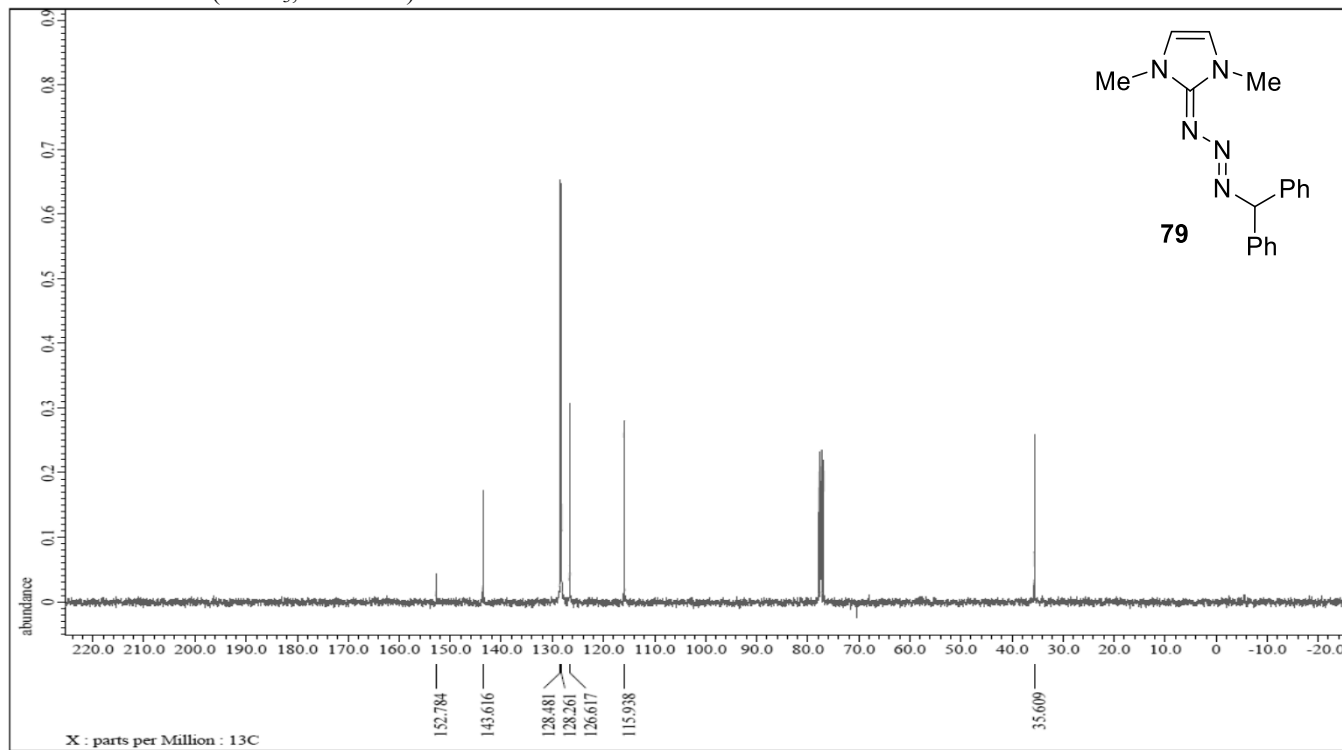
^{13}C NMR (CDCl_3 , 125 MHz)



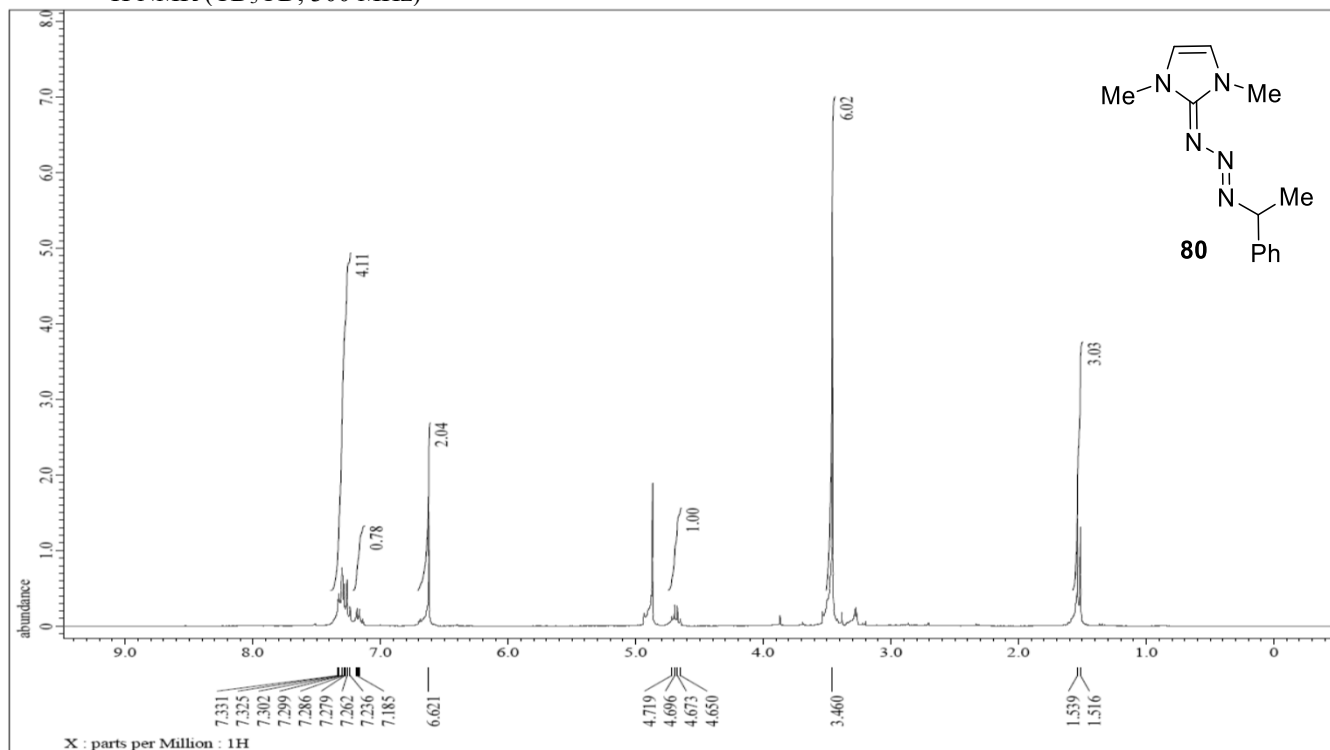
¹H NMR (CDCl₃, 300 MHz)



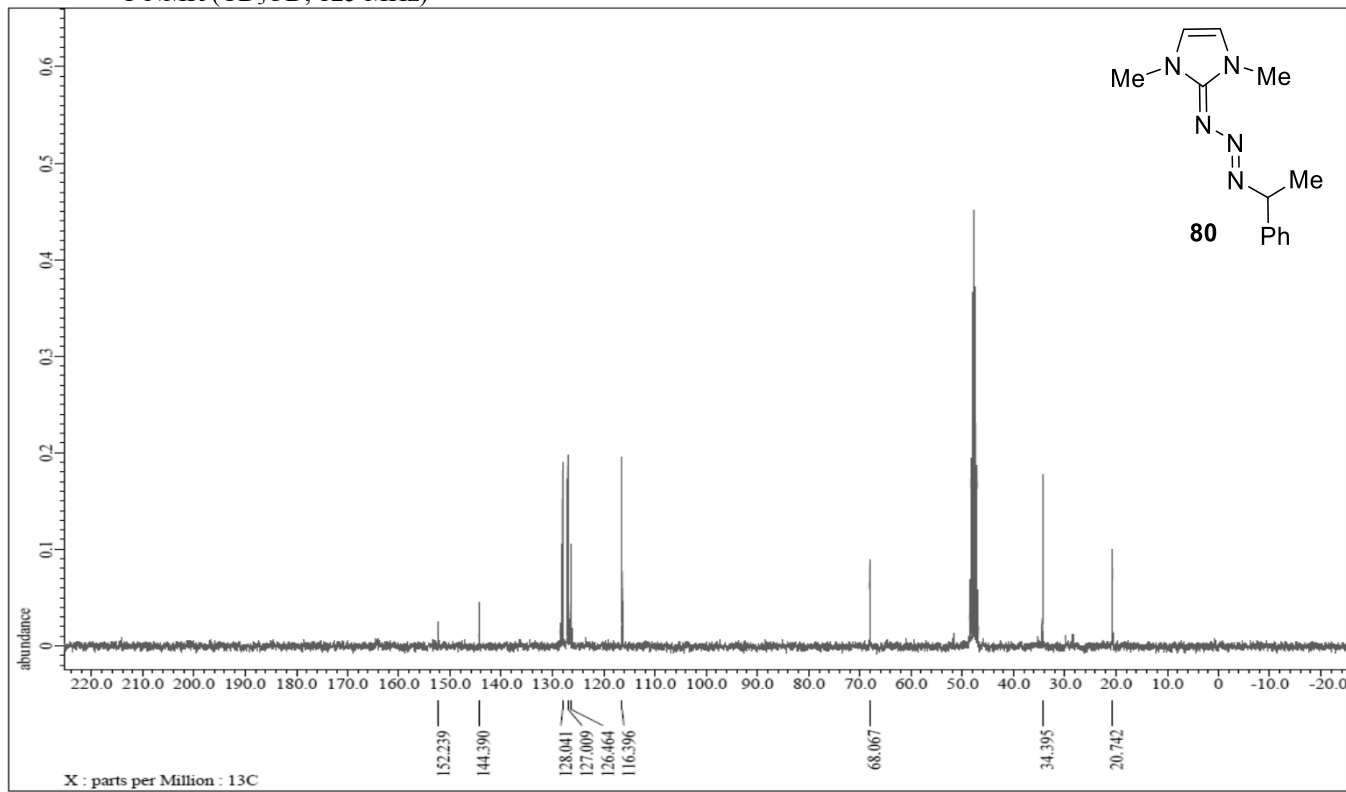
¹³C NMR (CDCl₃, 125 MHz)



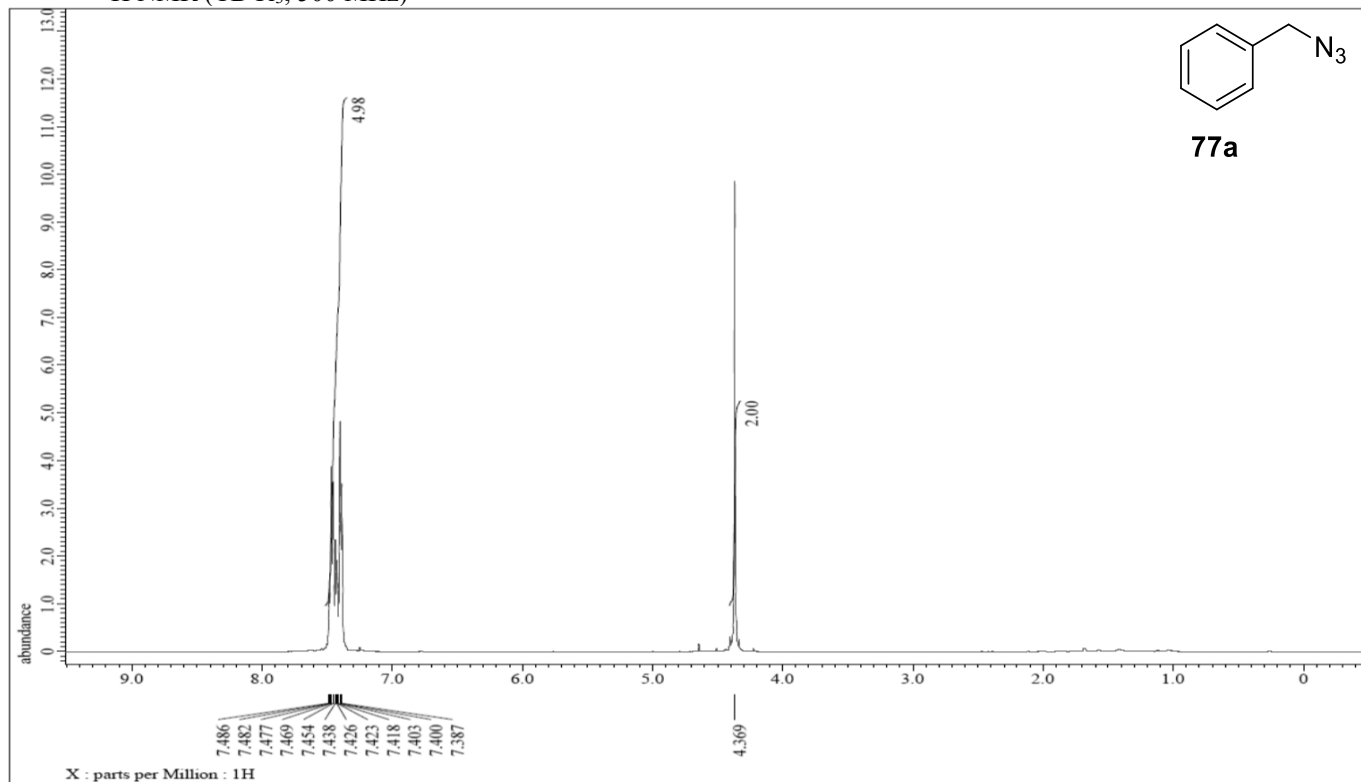
^1H NMR (CD_3OD , 300 MHz)



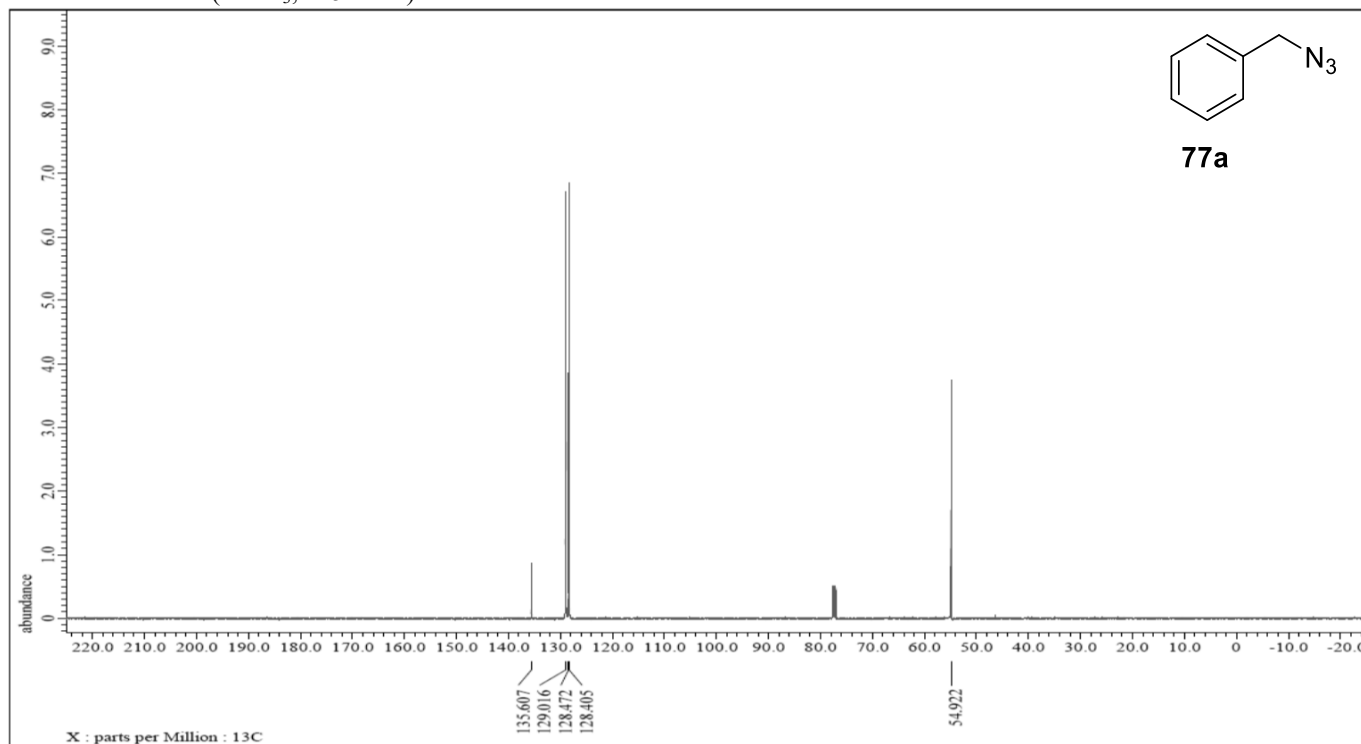
^{13}C NMR (CD_3OD , 125 MHz)



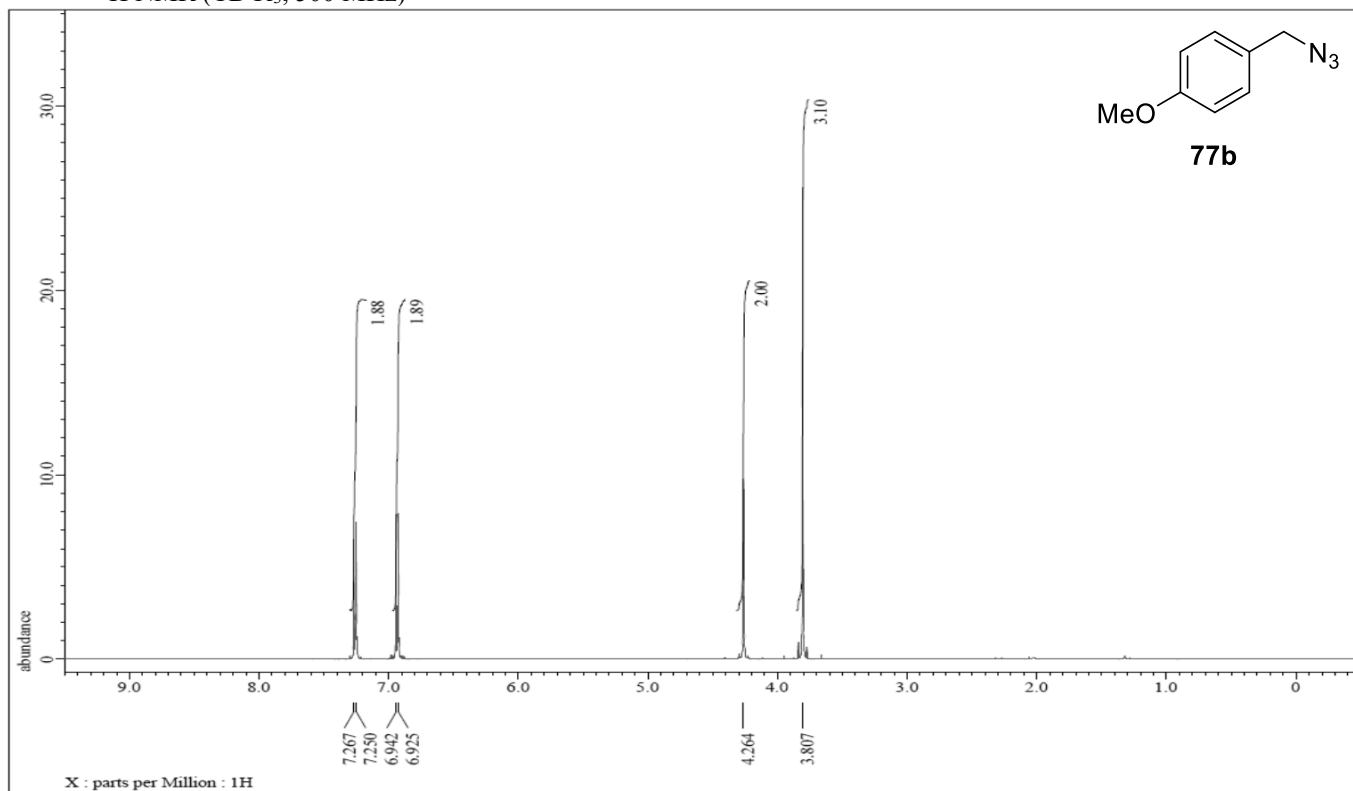
¹H NMR (CDCl₃, 500 MHz)



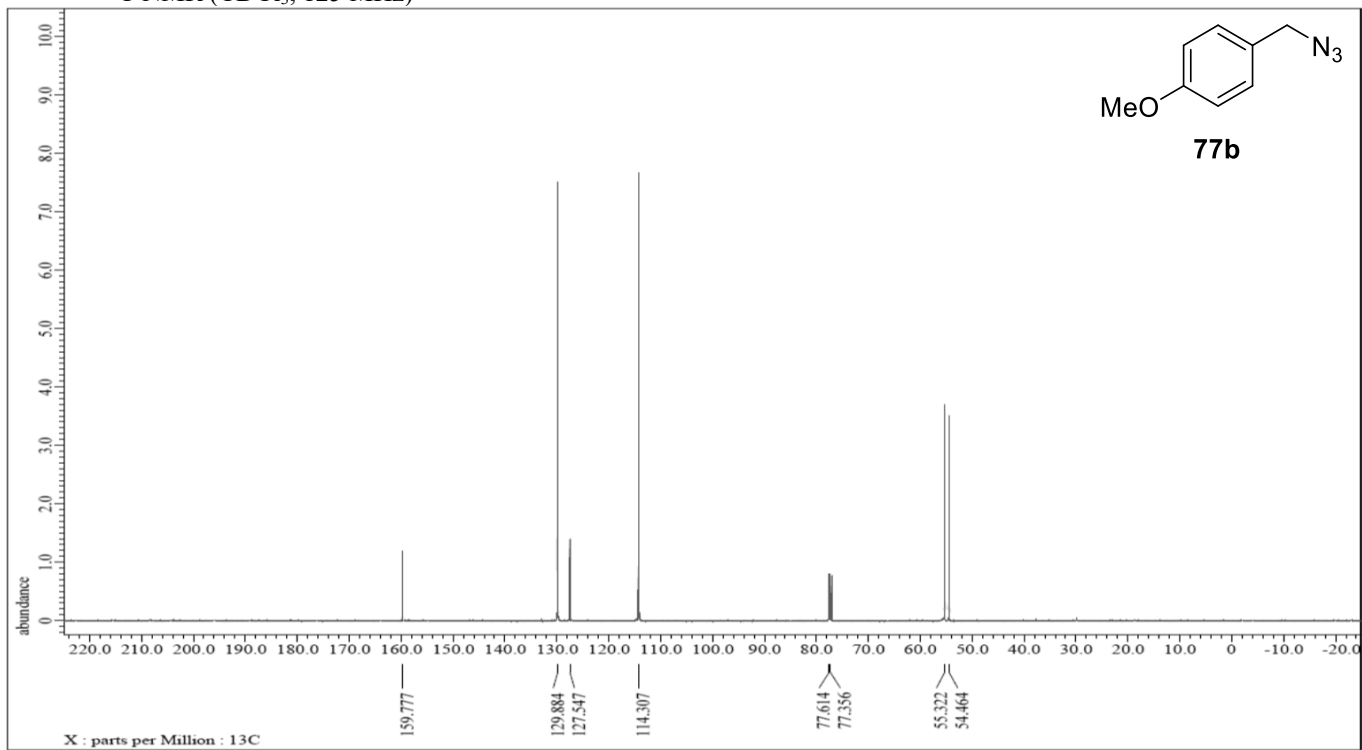
¹³C NMR (CDCl₃, 125 MHz)



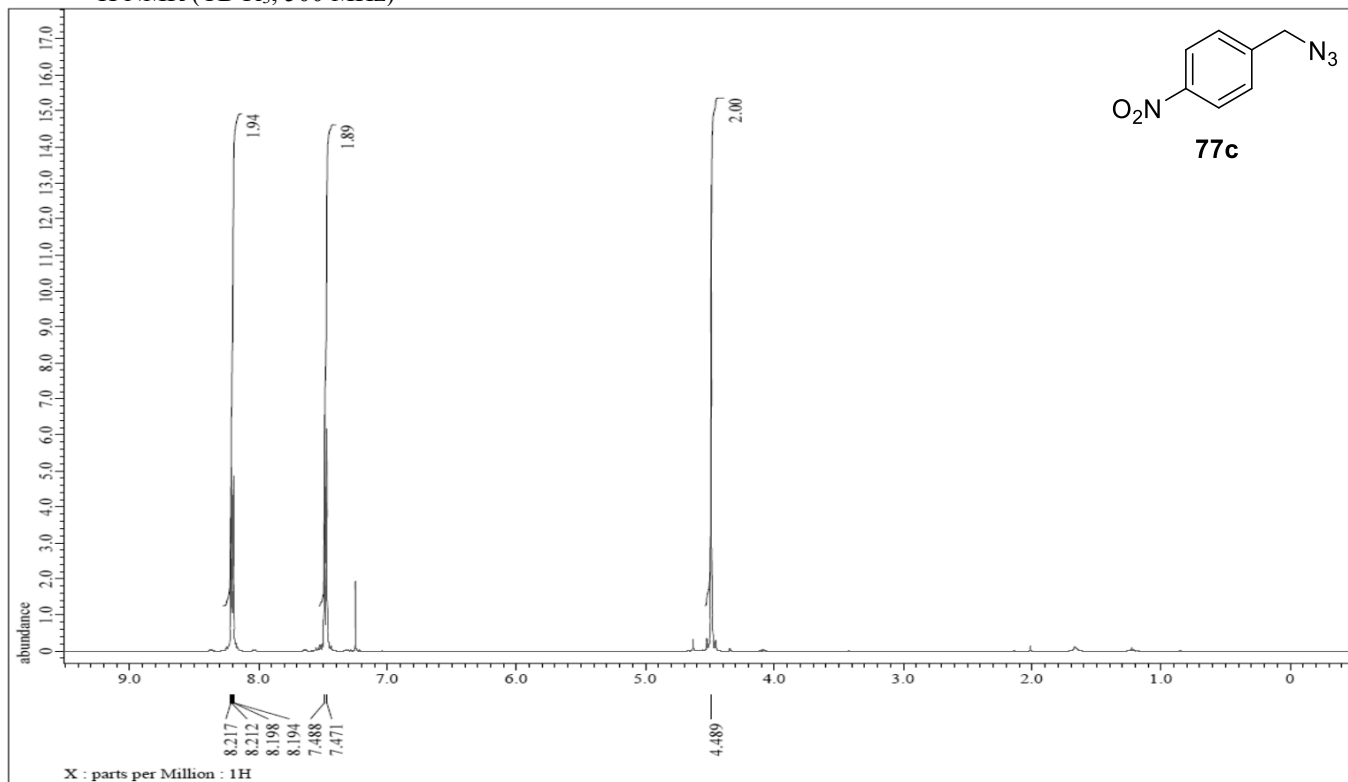
^1H NMR (CDCl_3 , 500 MHz)



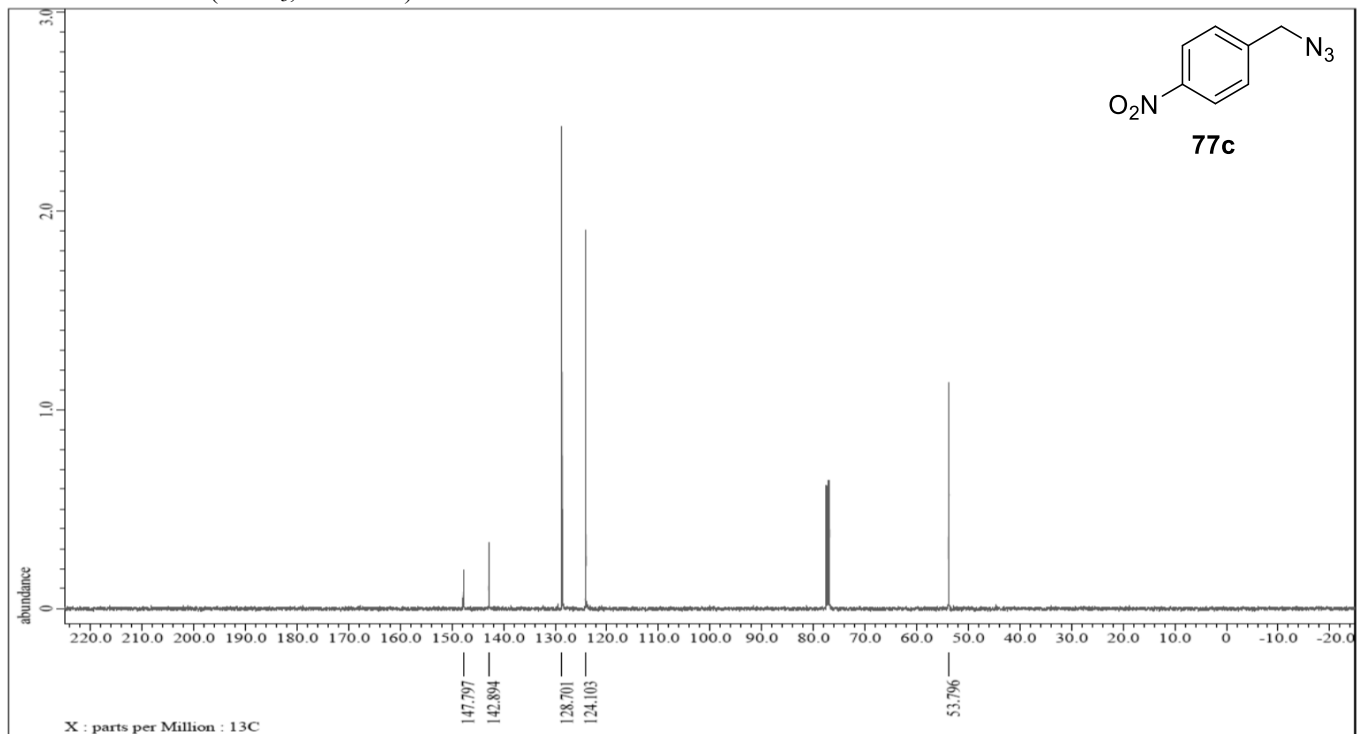
^{13}C NMR (CDCl_3 , 125 MHz)



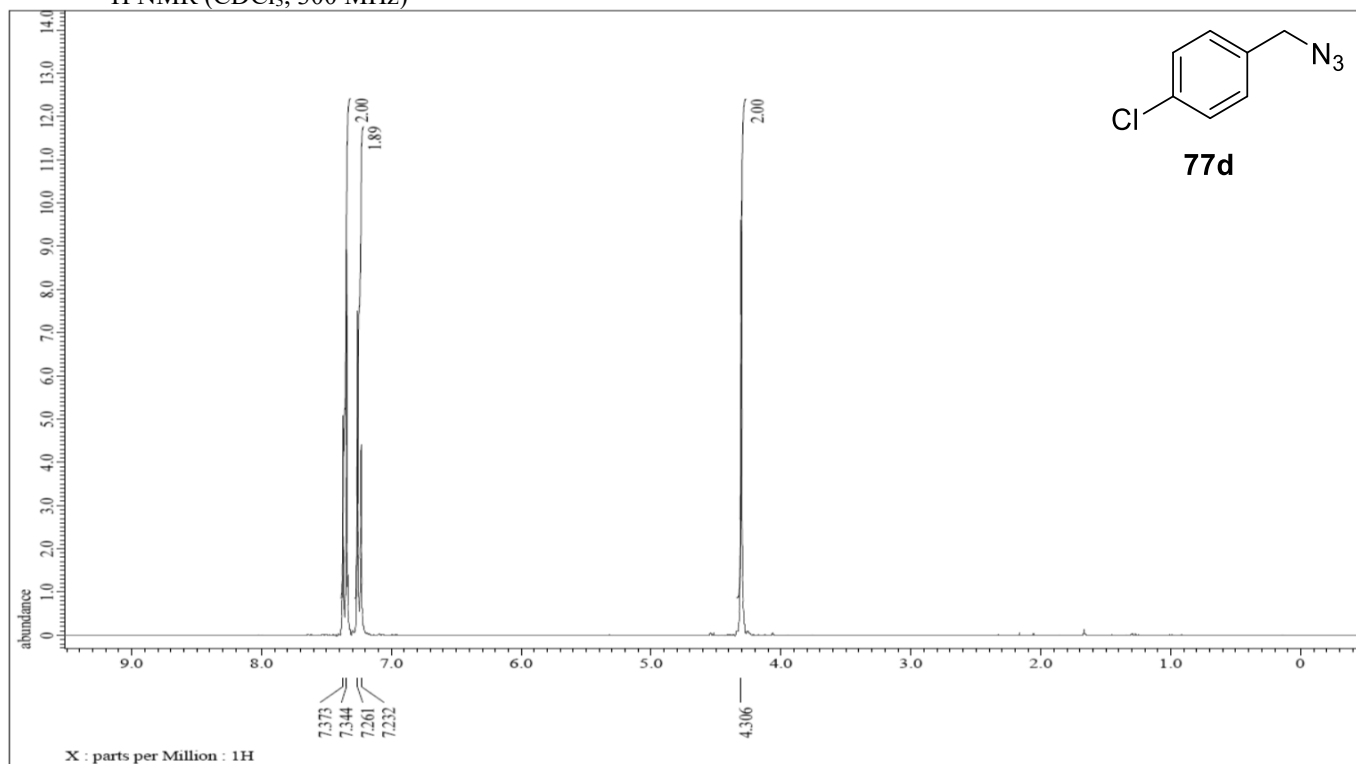
^1H NMR (CDCl_3 , 500 MHz)



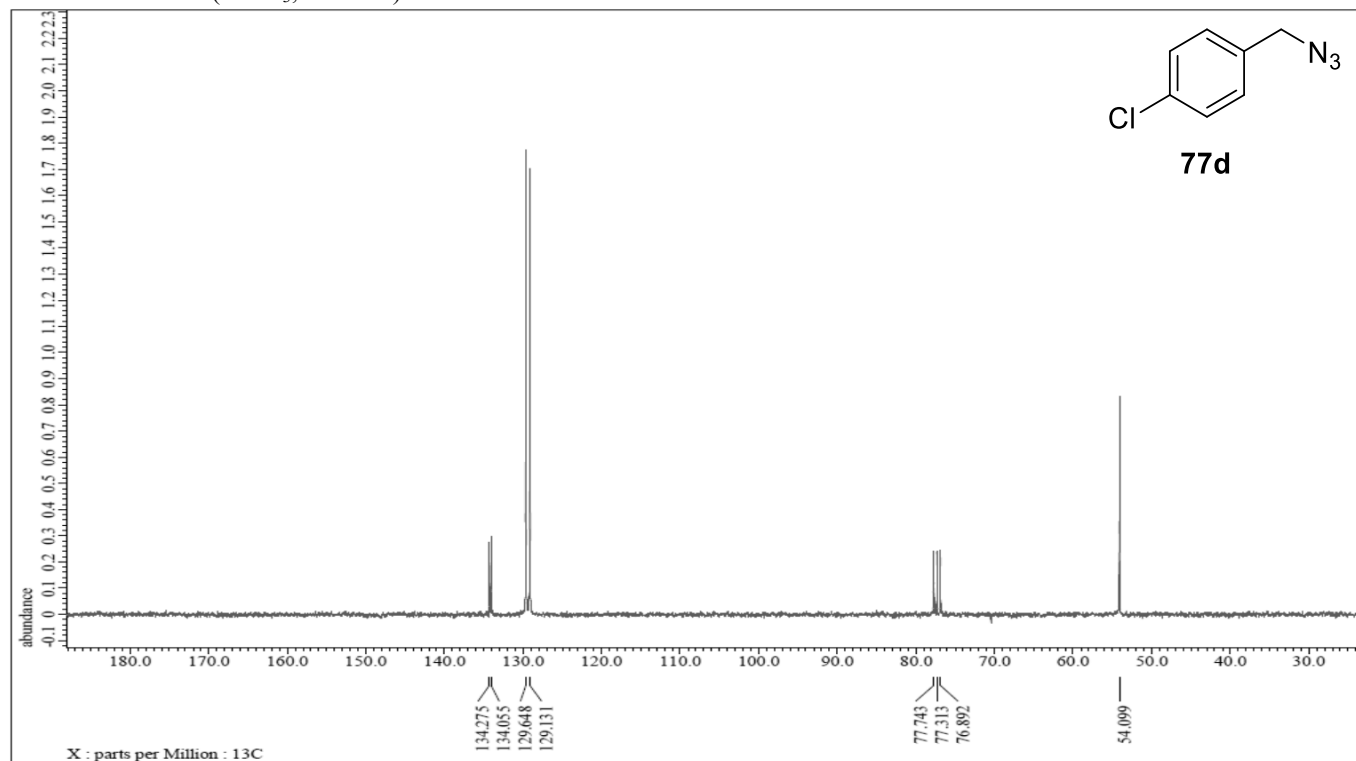
^{13}C NMR (CDCl_3 , 125 MHz)



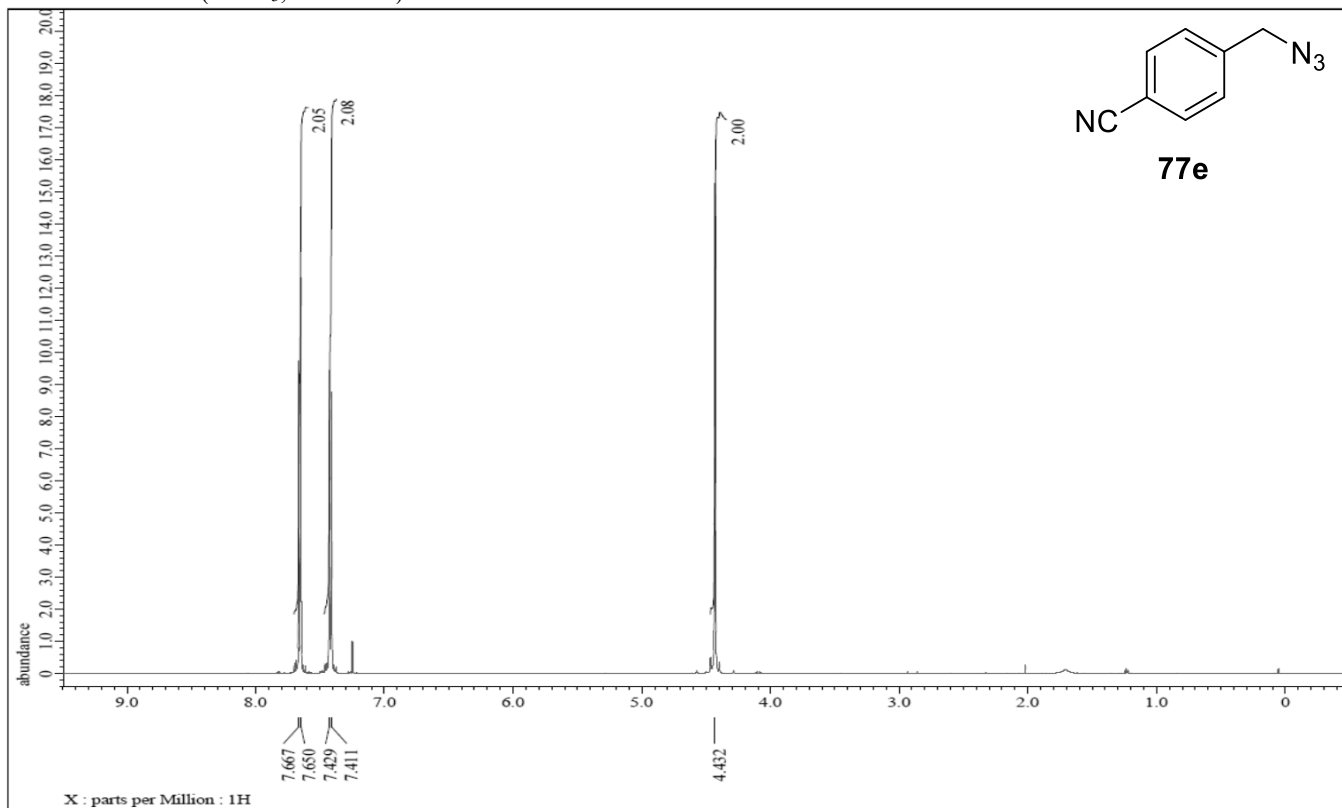
^1H NMR (CDCl_3 , 300 MHz)



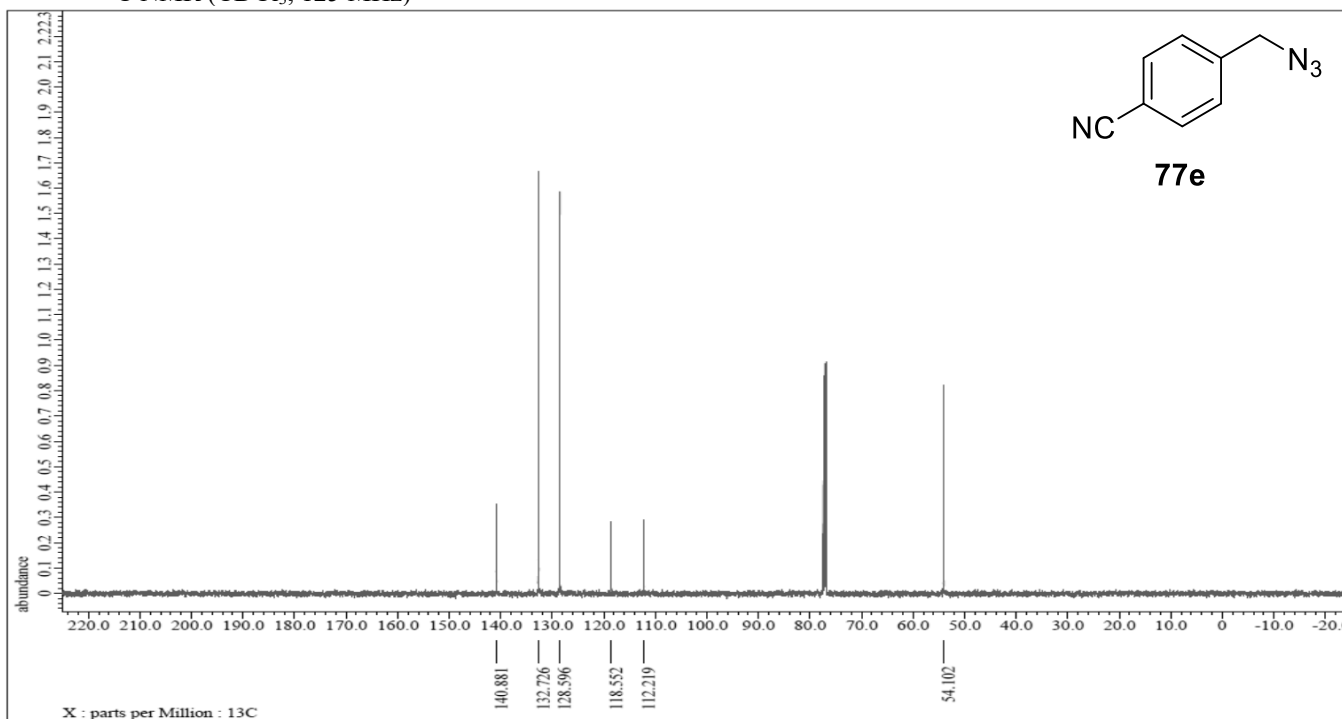
^{13}C NMR (CDCl_3 , 75 MHz)



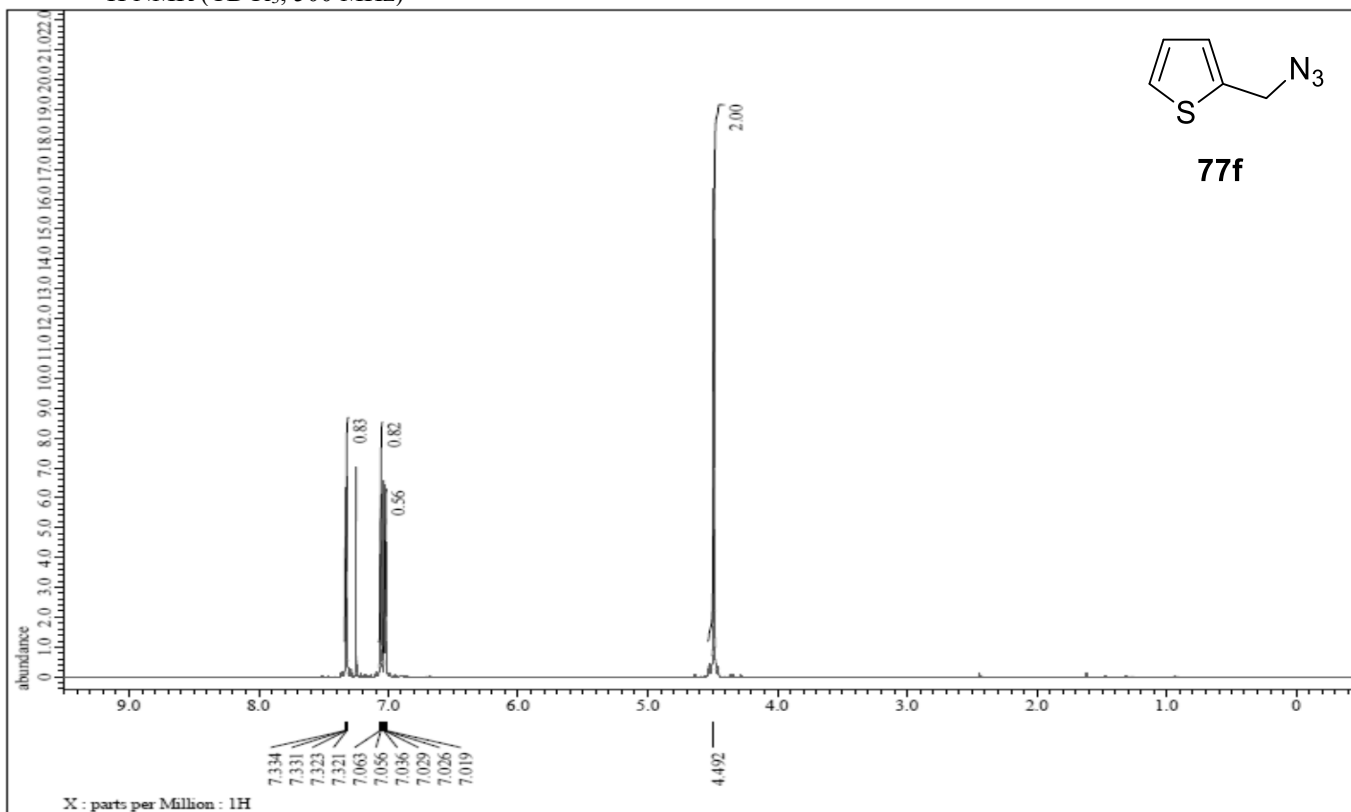
^1H NMR (CDCl_3 , 500 MHz)



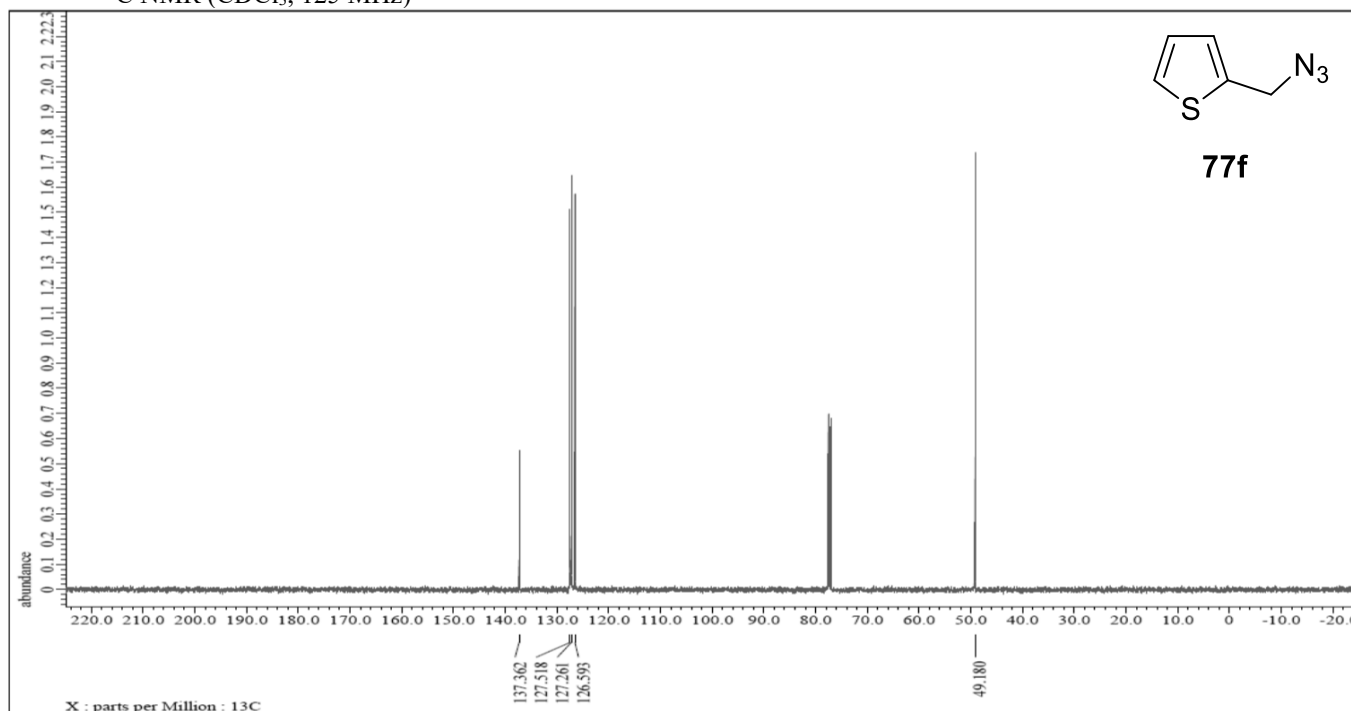
^{13}C NMR (CDCl_3 , 125 MHz)



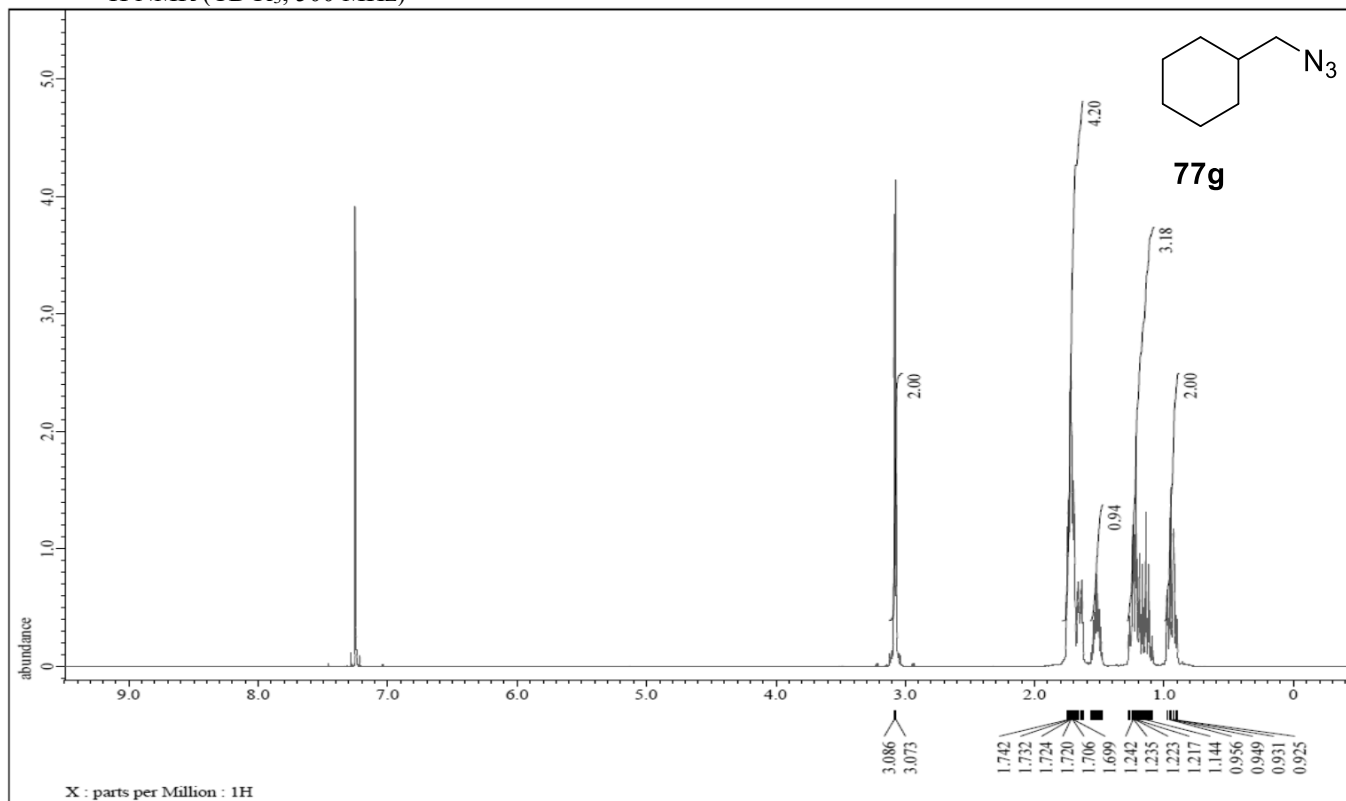
¹H NMR (CDCl₃, 500 MHz)



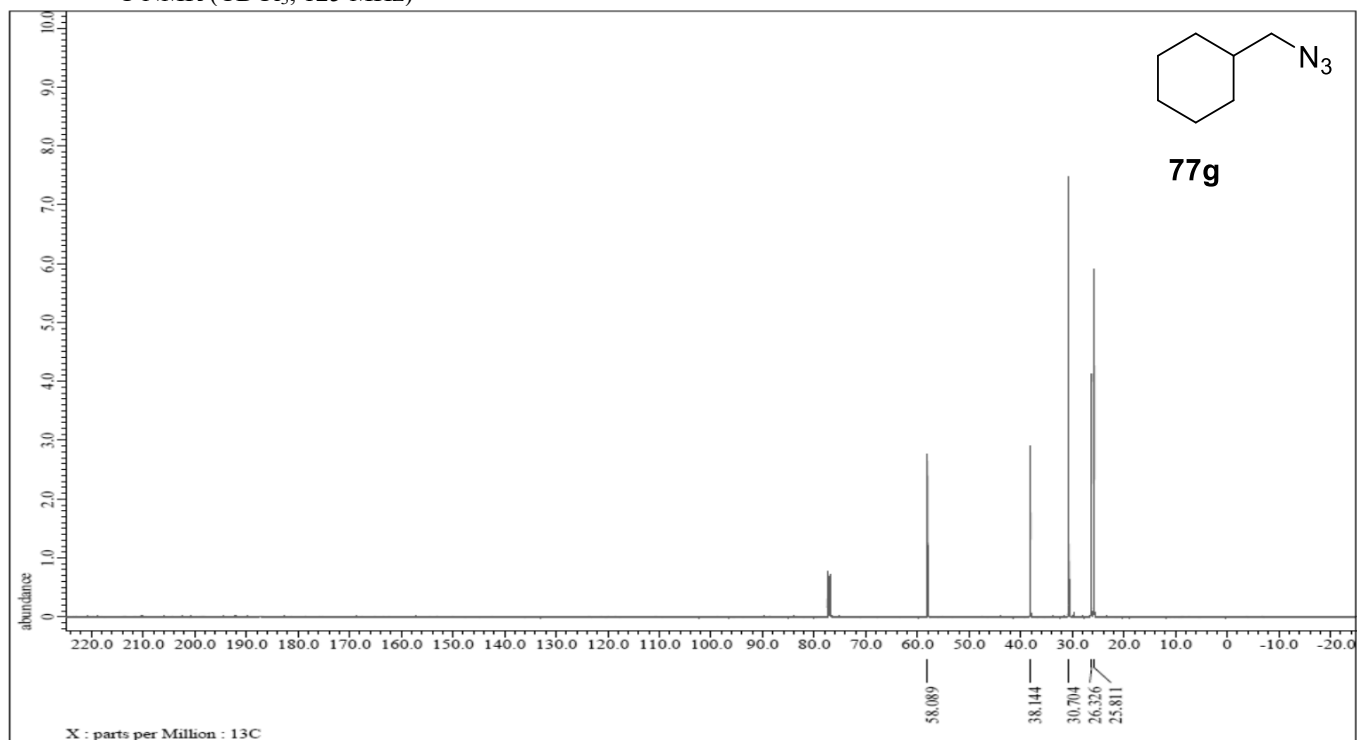
¹³C NMR (CDCl₃, 125 MHz)



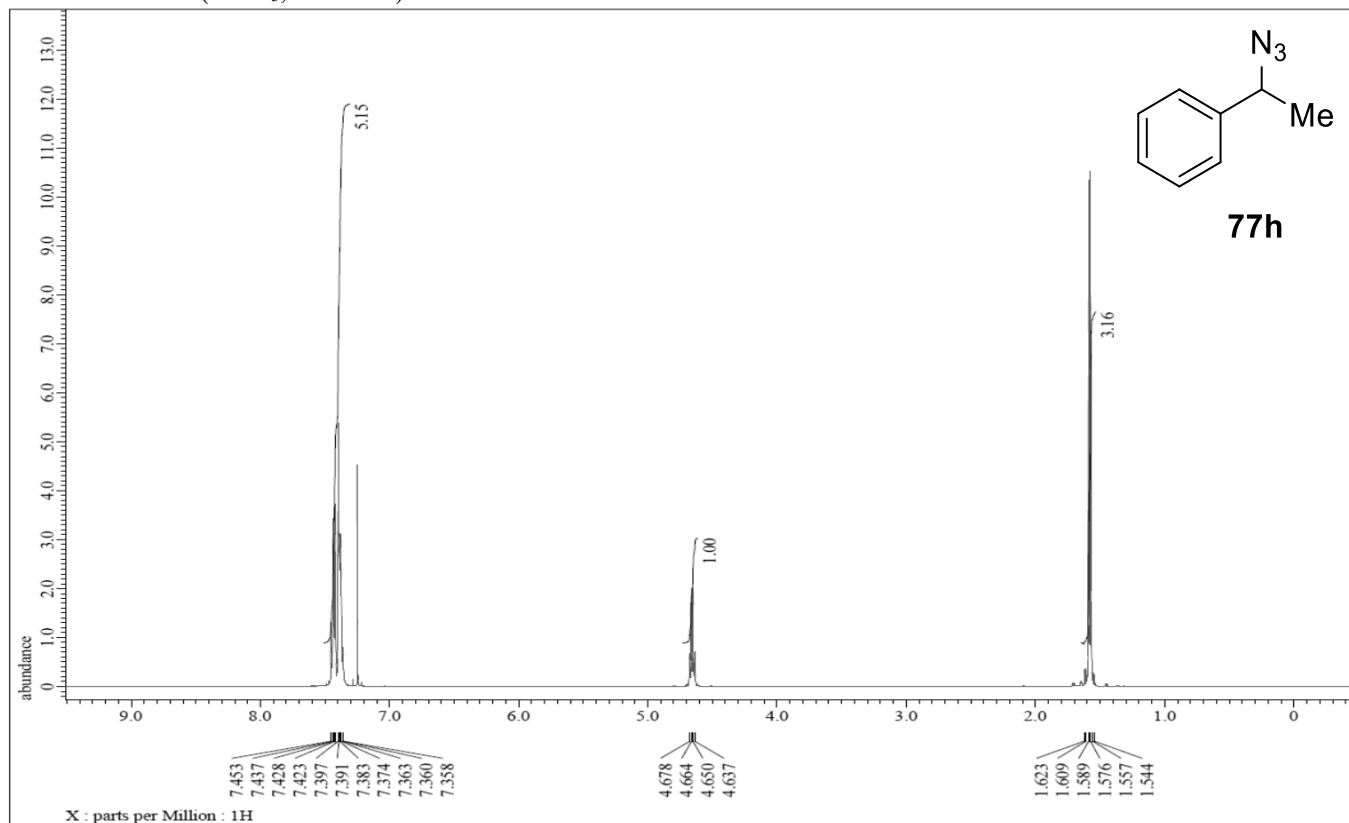
^1H NMR (CDCl_3 , 500 MHz)



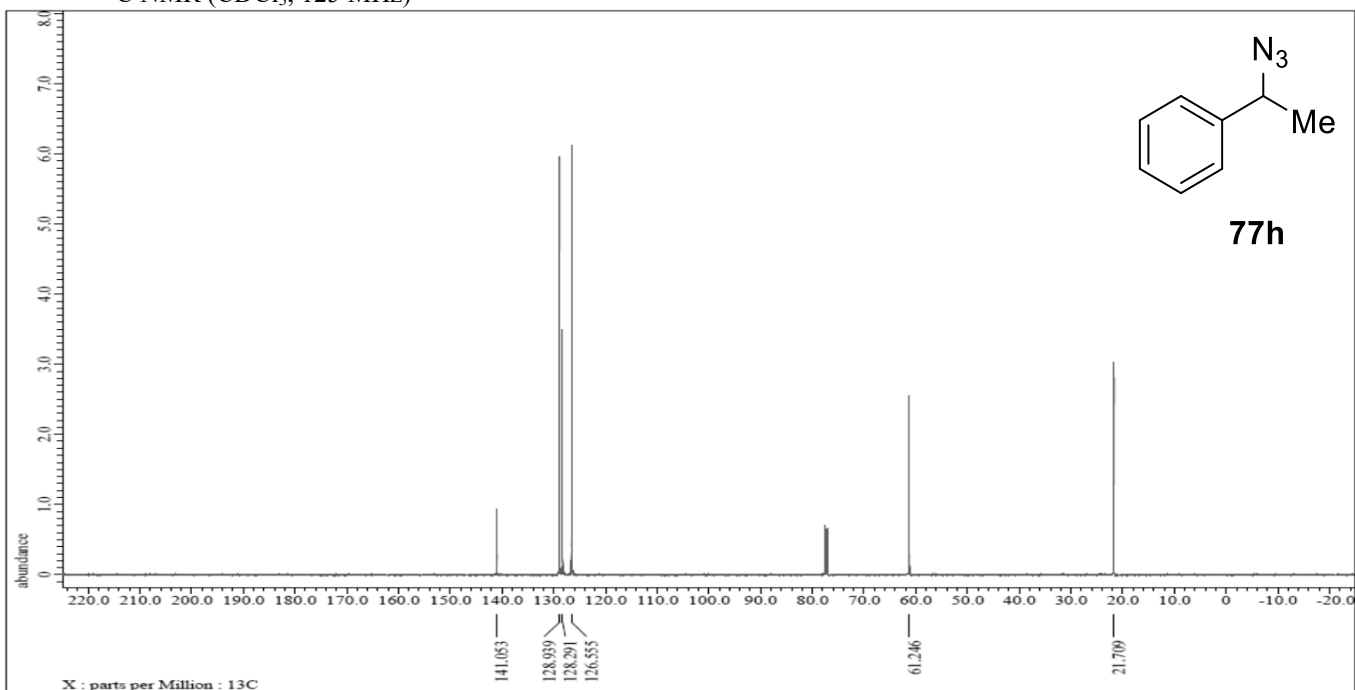
^{13}C NMR (CDCl_3 , 125 MHz)



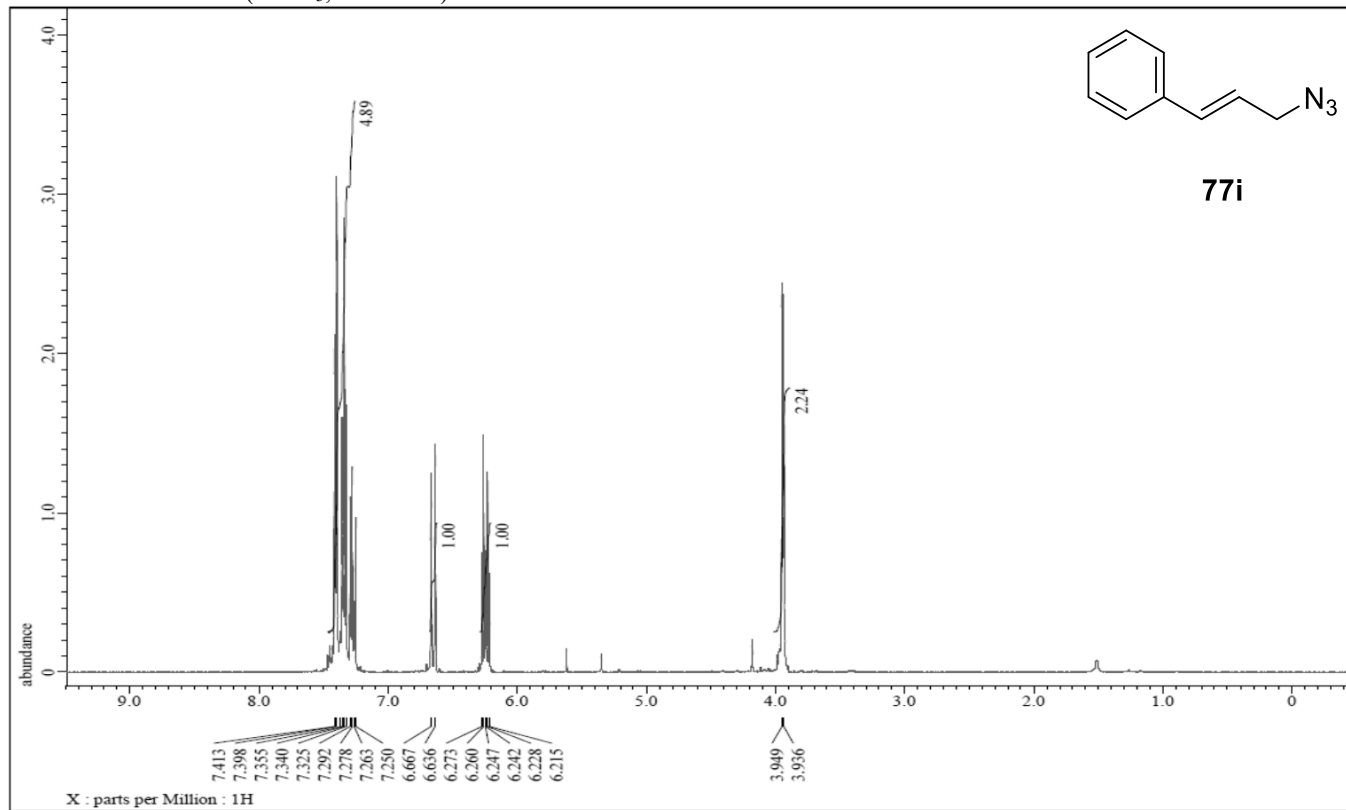
^1H NMR (CDCl_3 , 500 MHz)



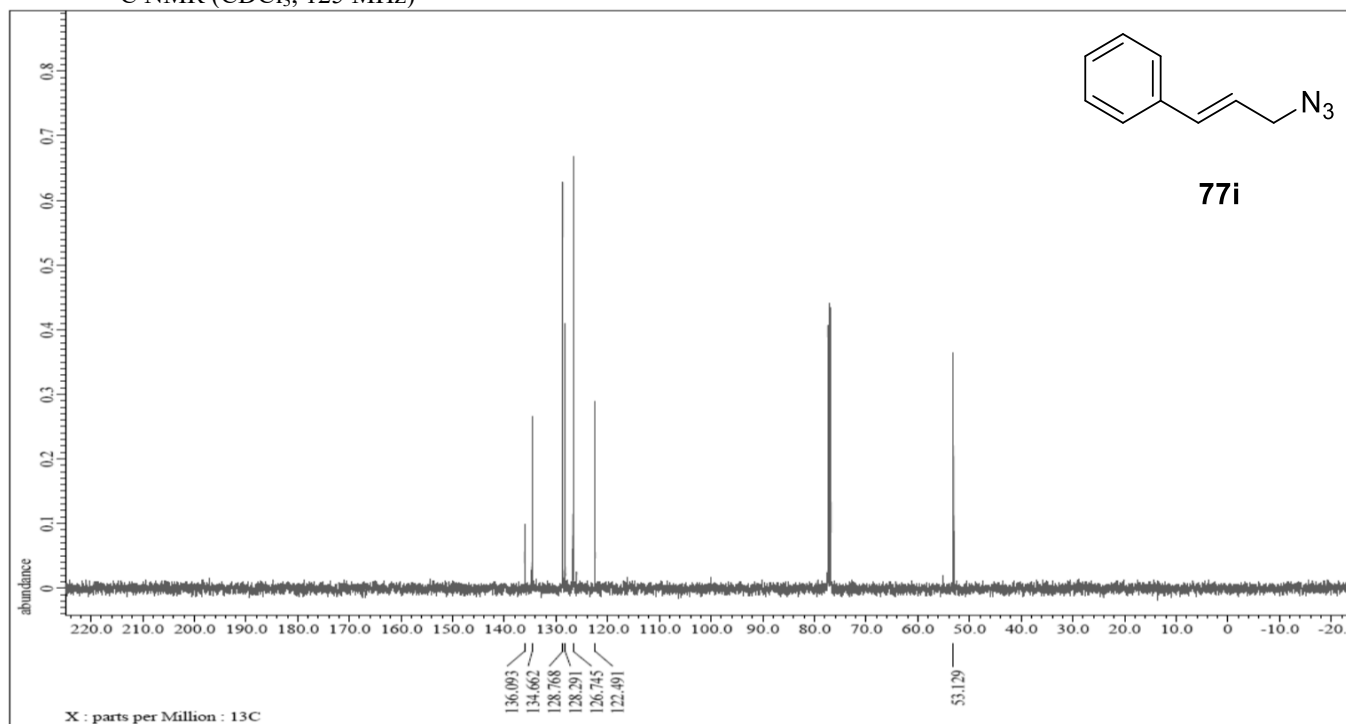
^{13}C NMR (CDCl_3 , 125 MHz)



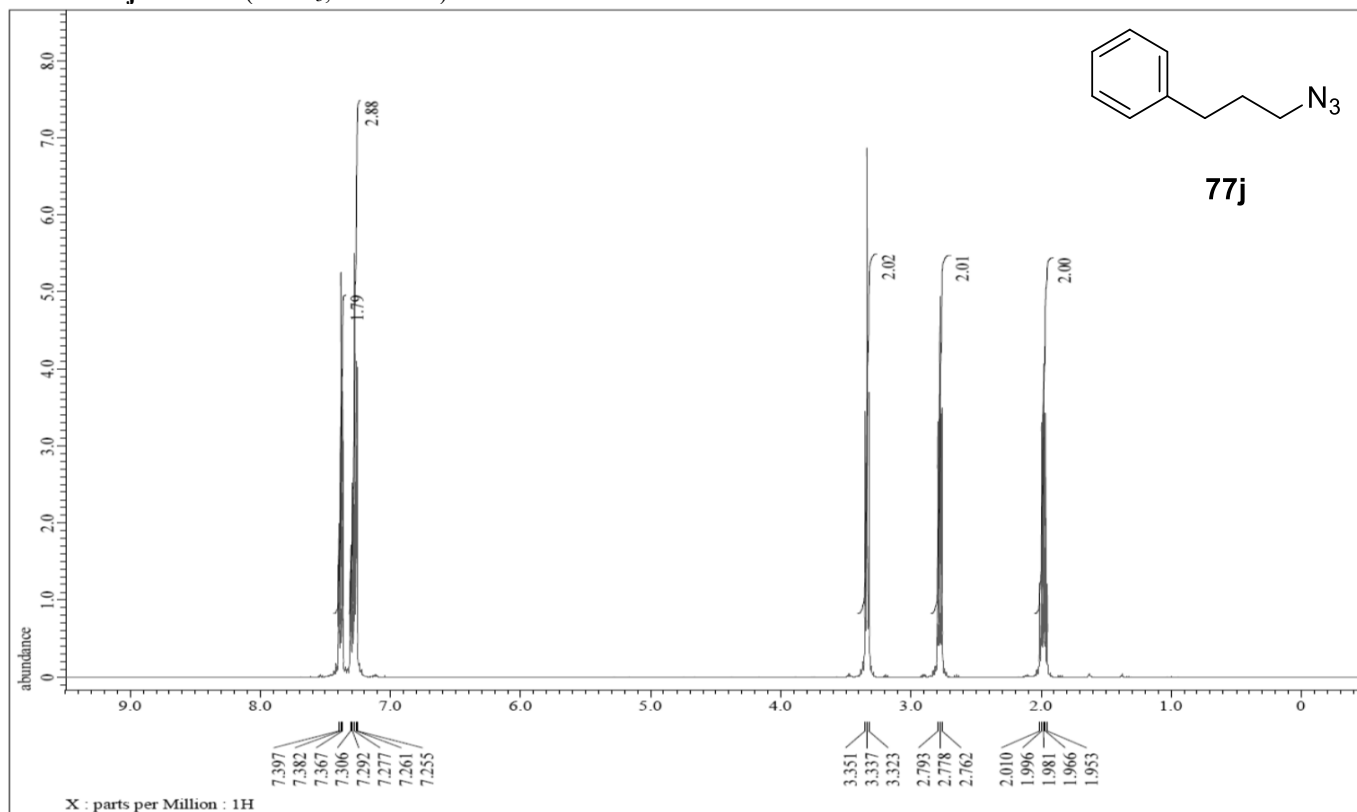
11i ^1H NMR (CDCl_3 , 500 MHz)



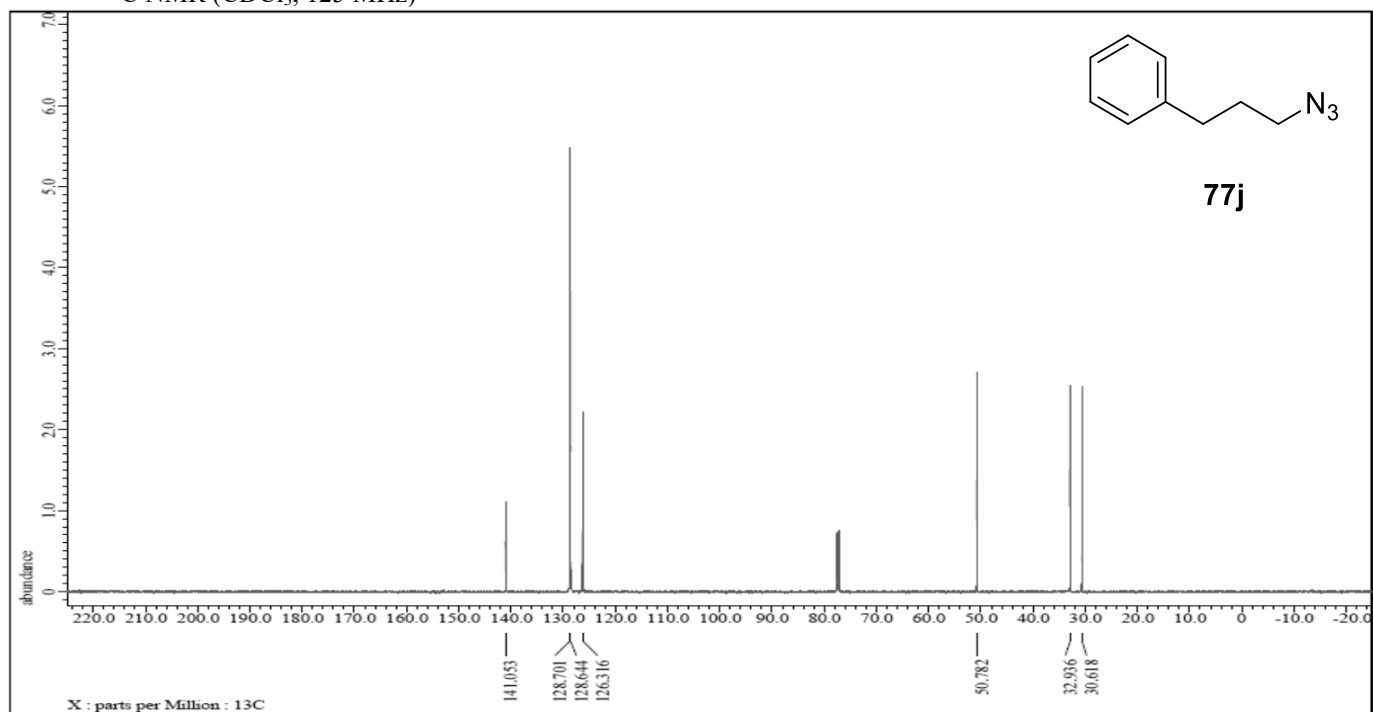
^{13}C NMR (CDCl_3 , 125 MHz)



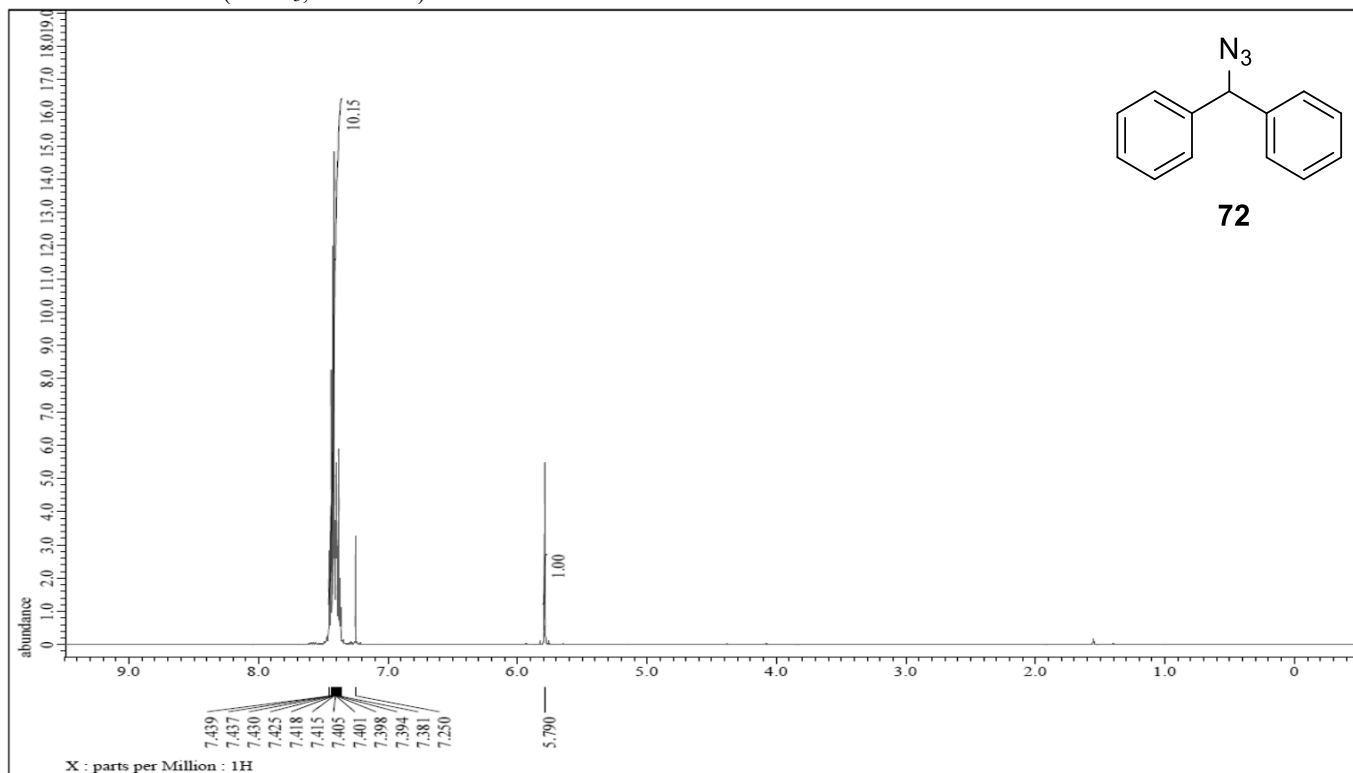
11j ^1H NMR (CDCl_3 , 500 MHz)



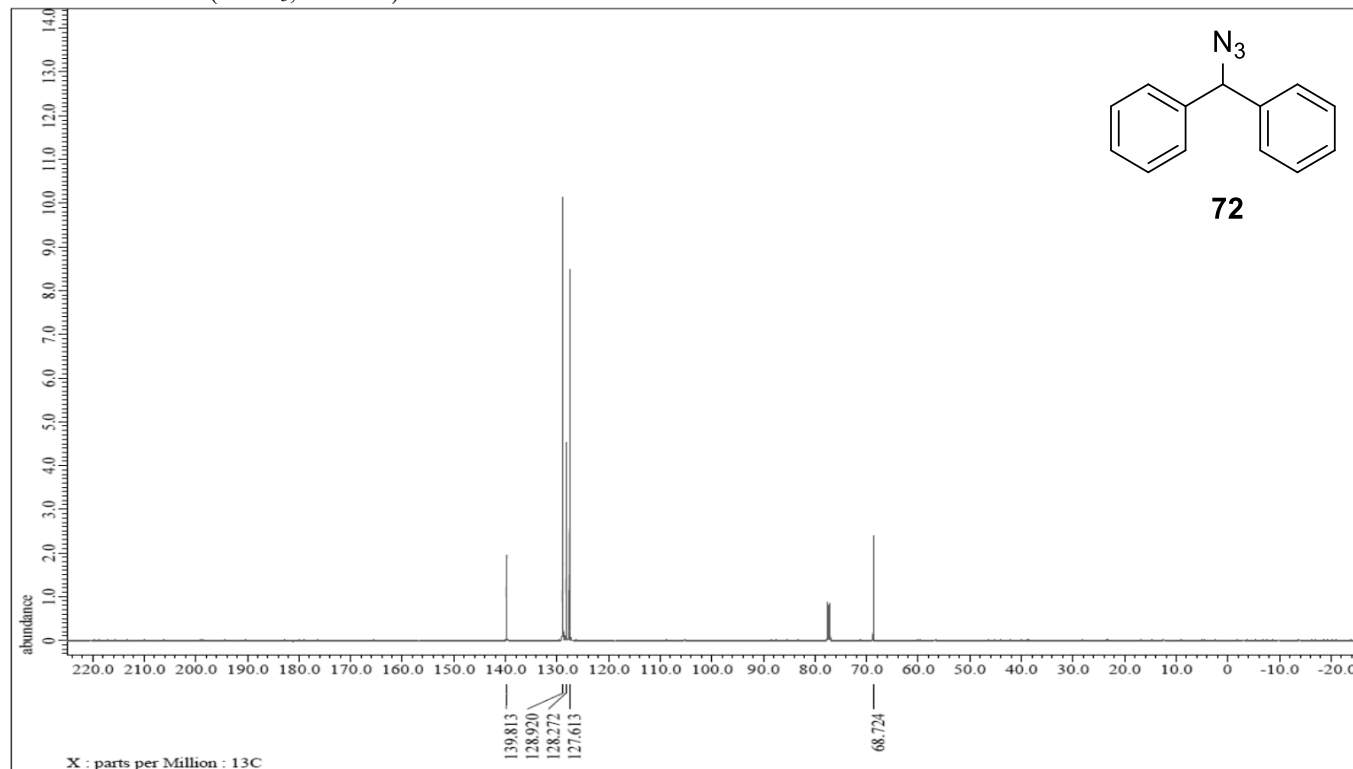
^{13}C NMR (CDCl_3 , 125 MHz)



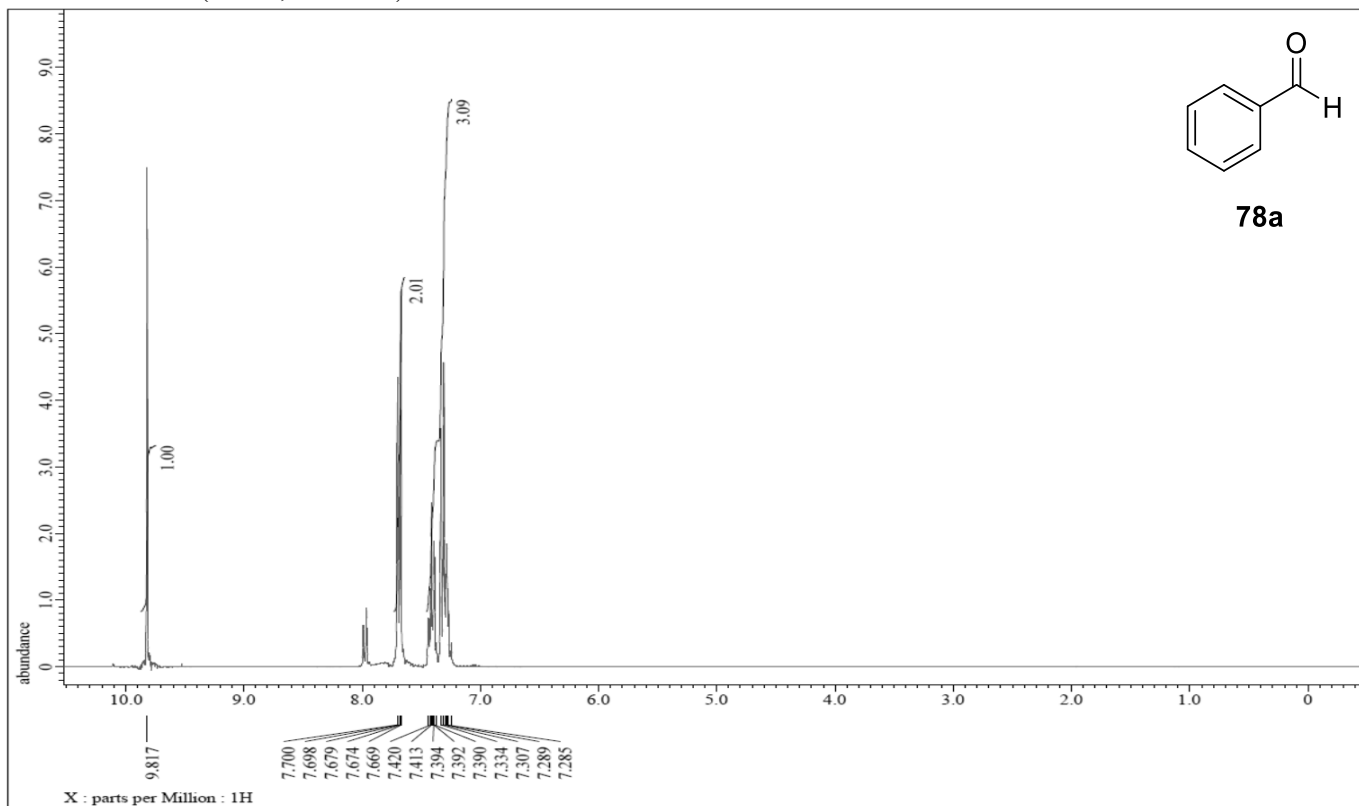
7 ¹H NMR (CDCl₃, 300 MHz)



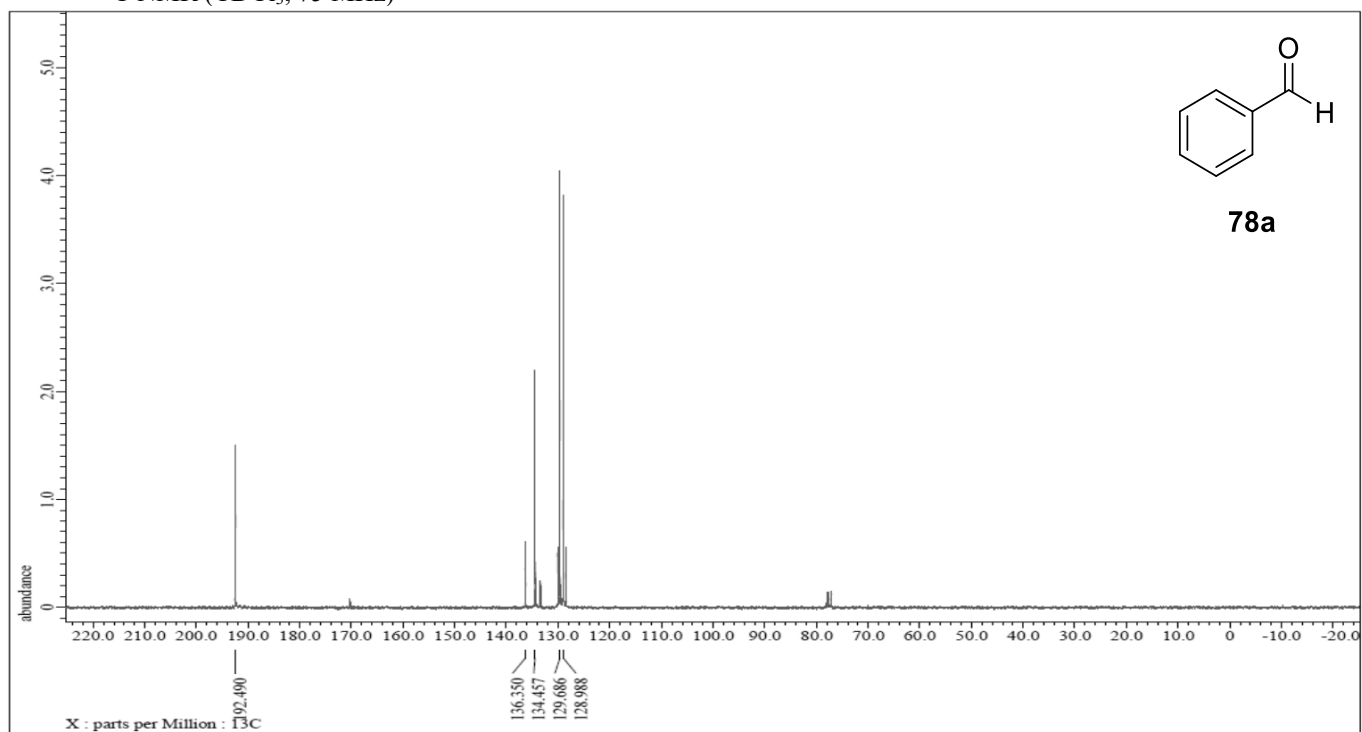
¹³C NMR (CDCl₃, 75 MHz)



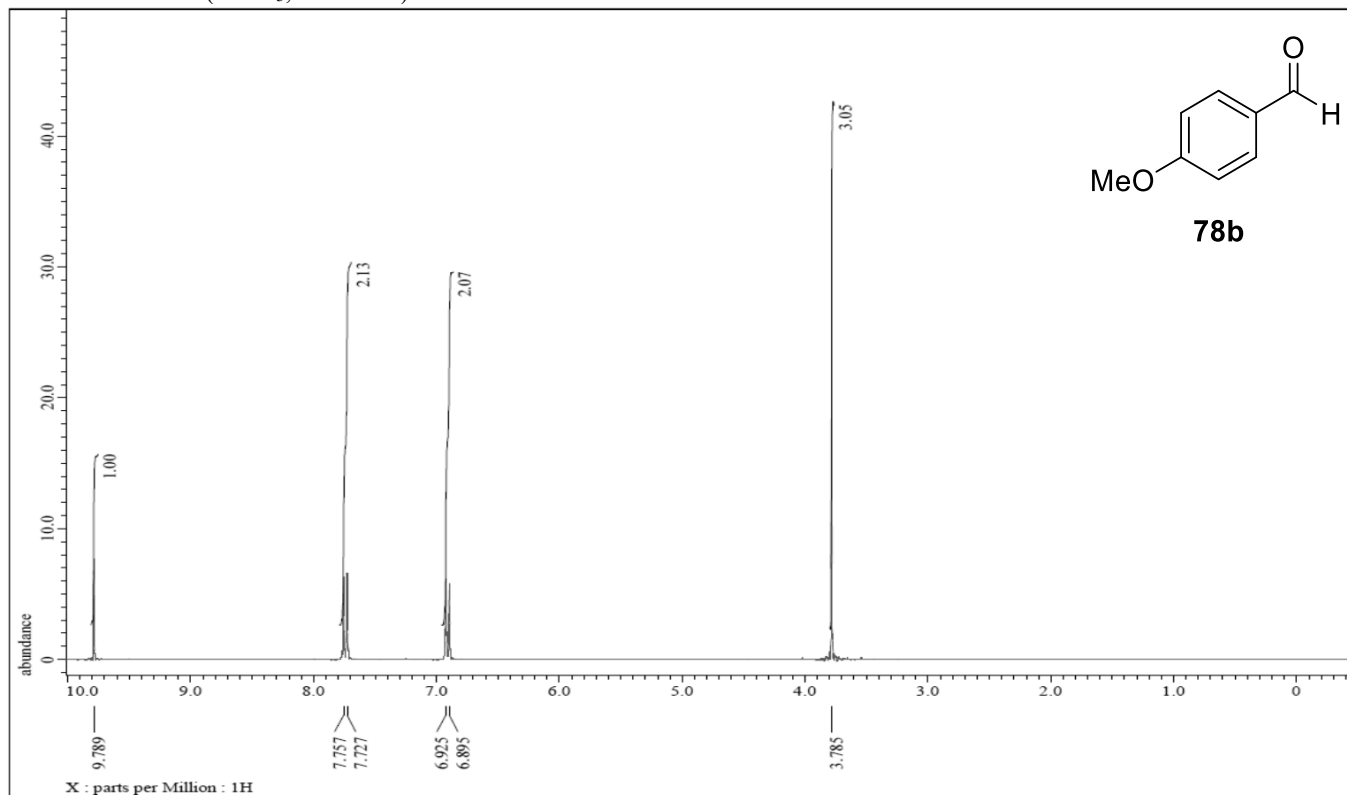
^1H NMR (CDCl_3 , 300 MHz)



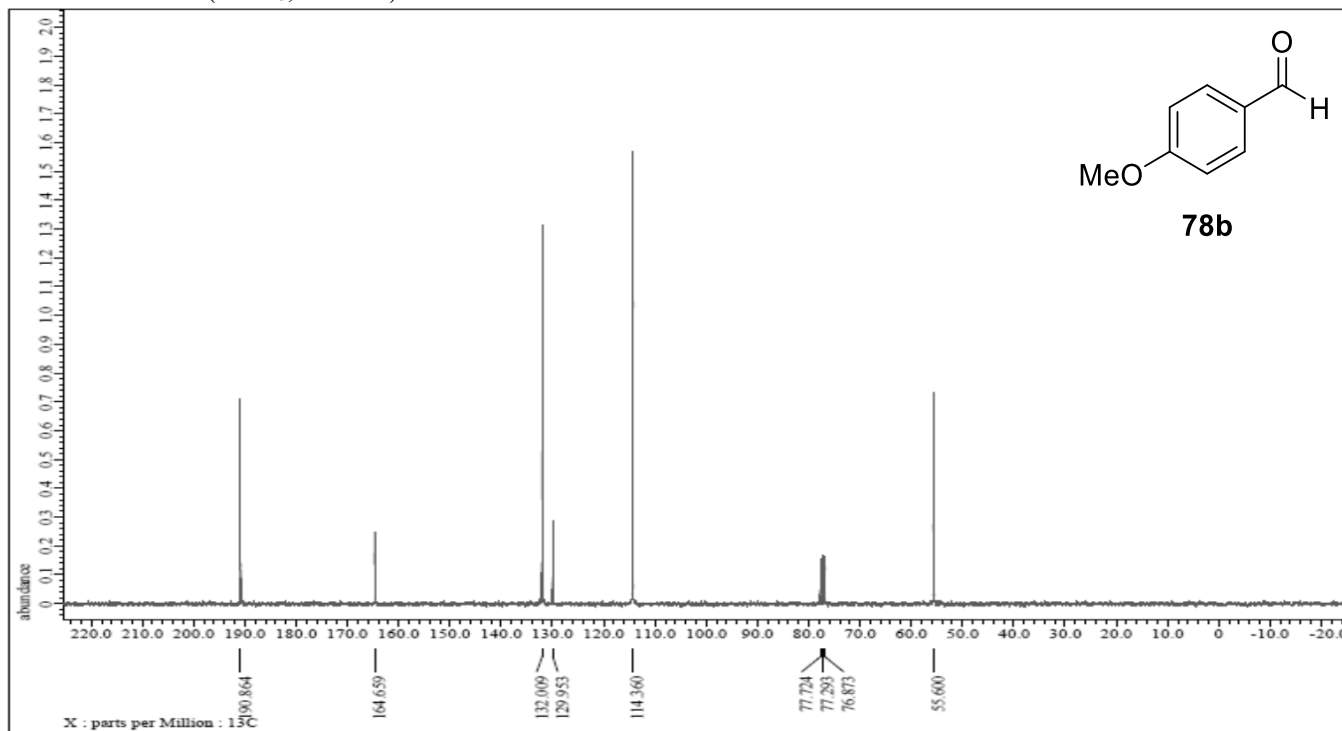
^{13}C NMR (CDCl_3 , 75 MHz)



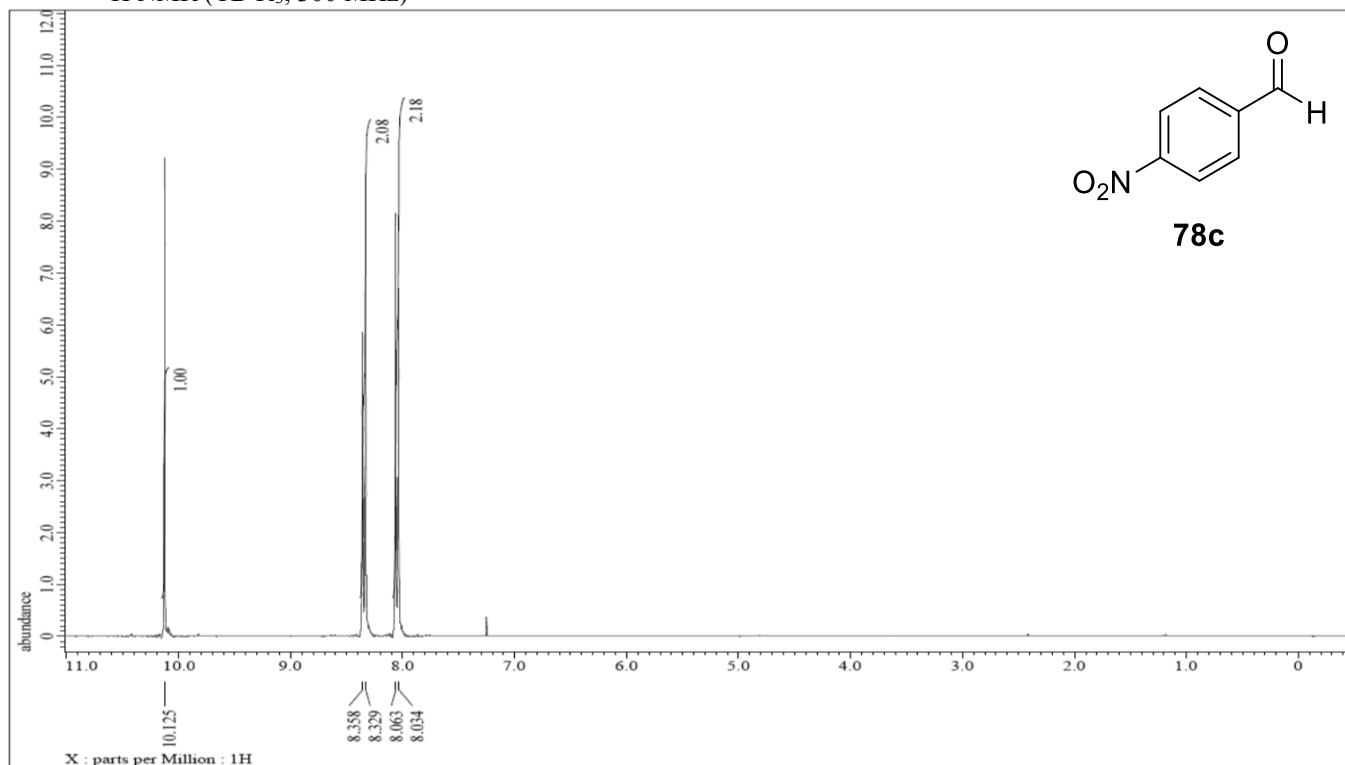
^1H NMR (CDCl_3 , 300 MHz)



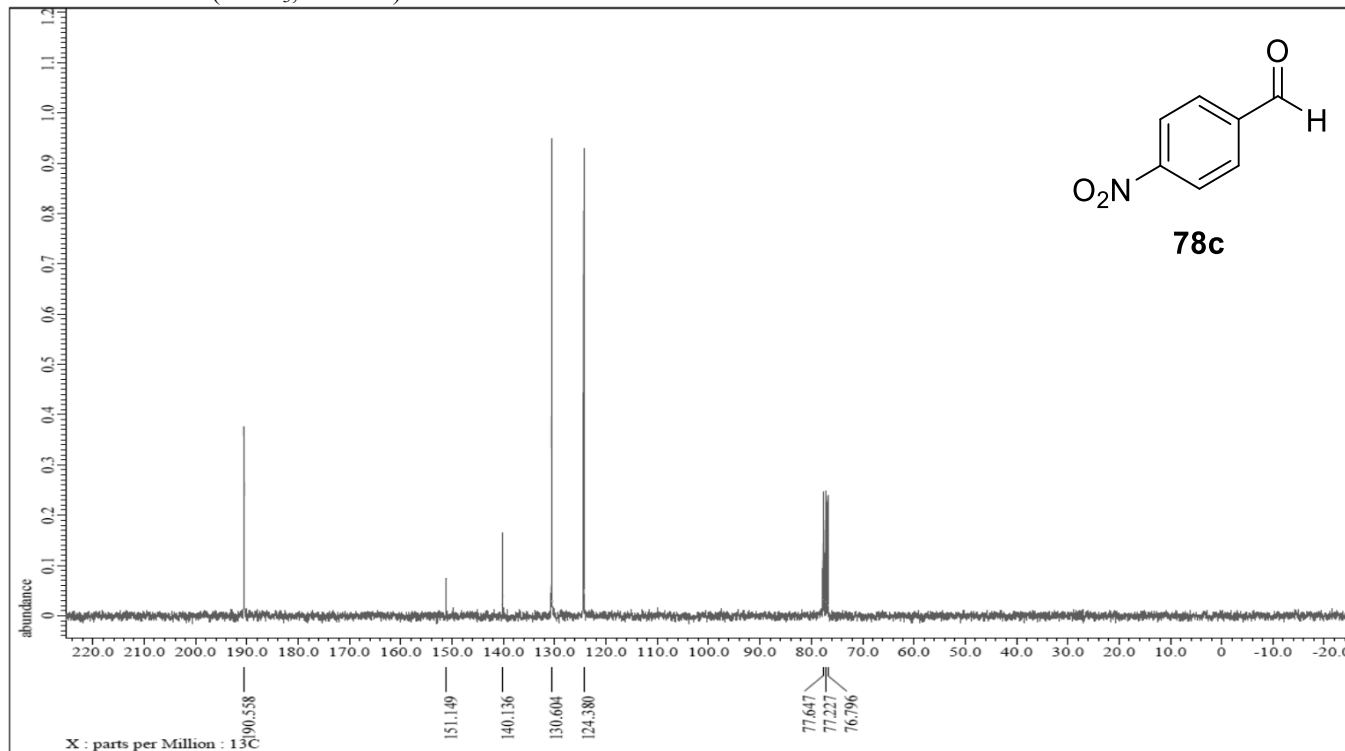
^{13}C NMR (CDCl_3 , 75 MHz)



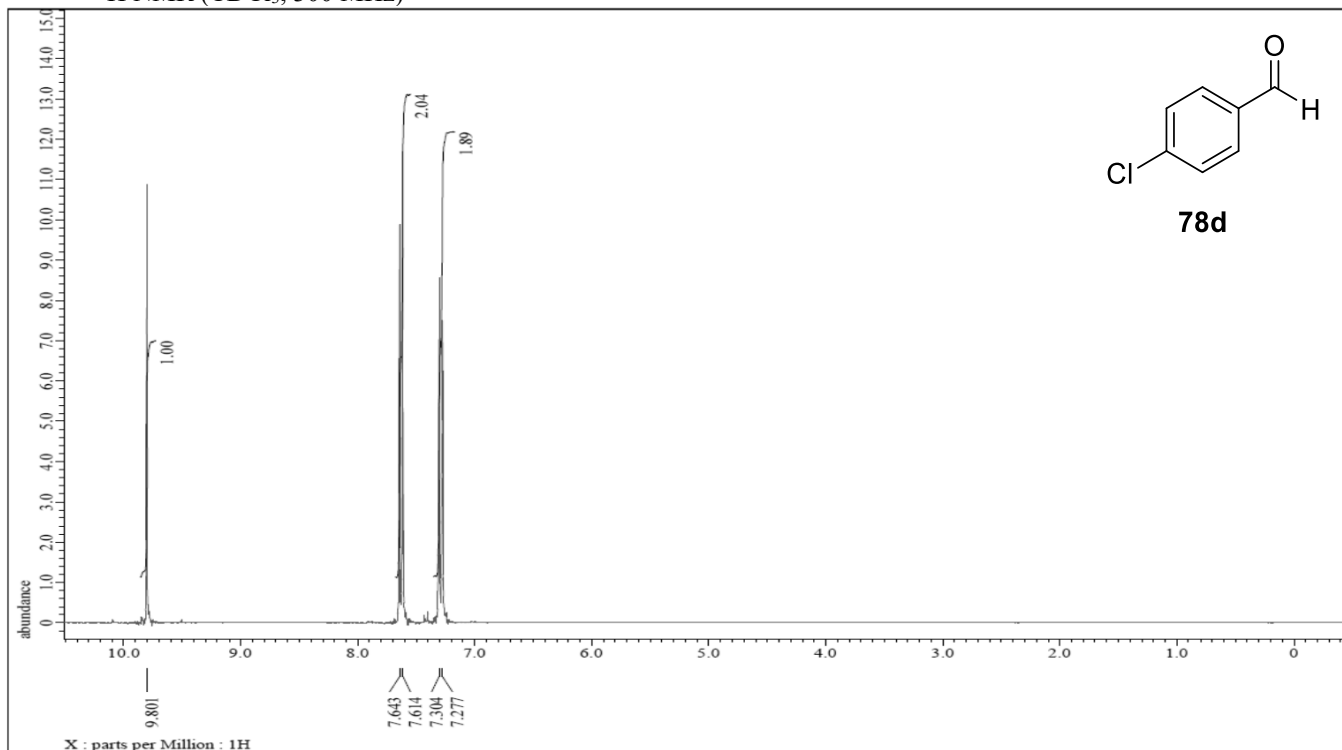
^1H NMR (CDCl_3 , 300 MHz)



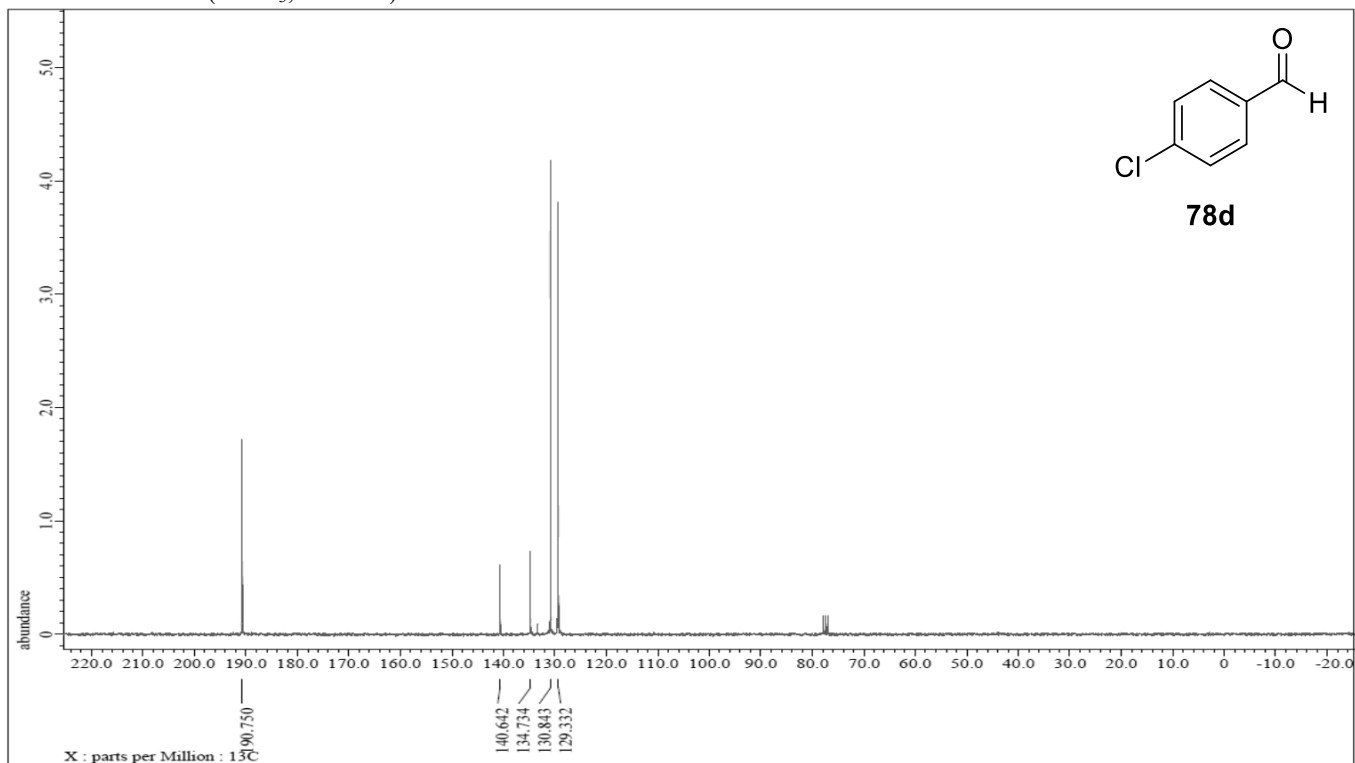
^{13}C NMR (CDCl_3 , 75 MHz)



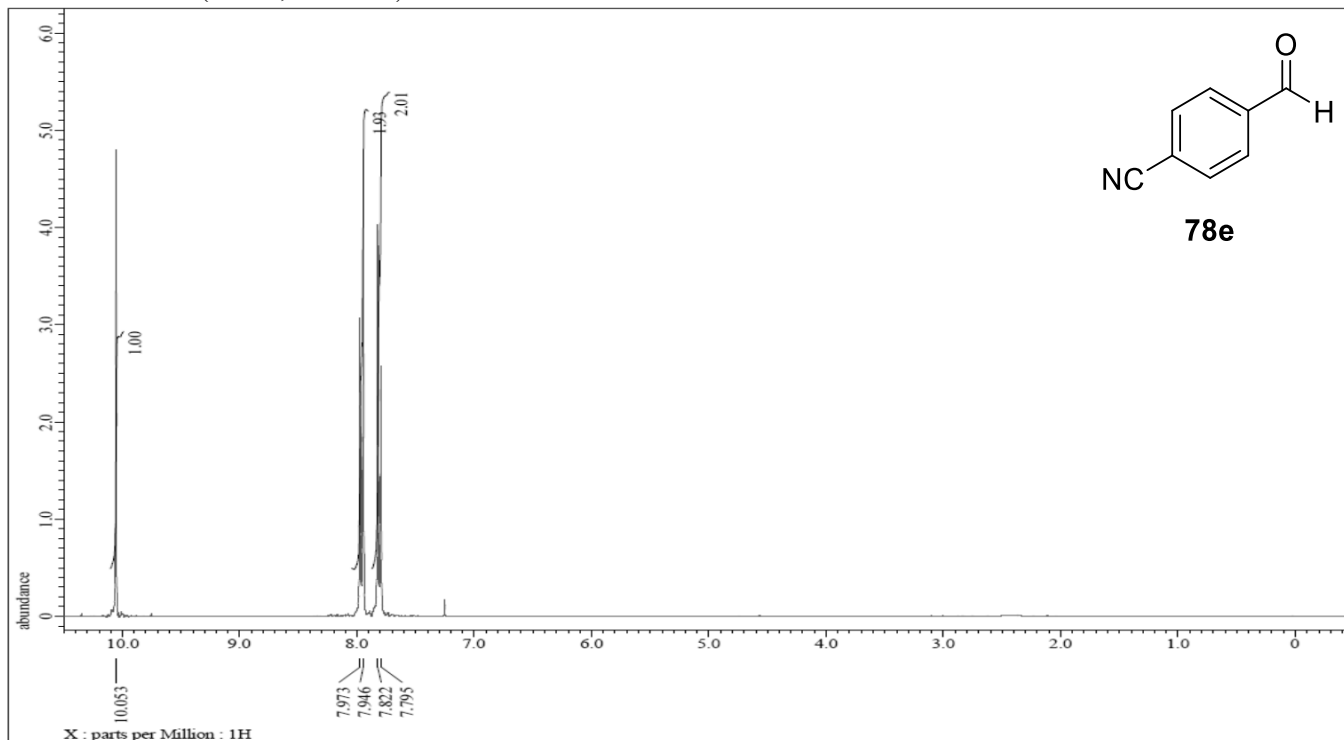
^1H NMR (CDCl_3 , 300 MHz)



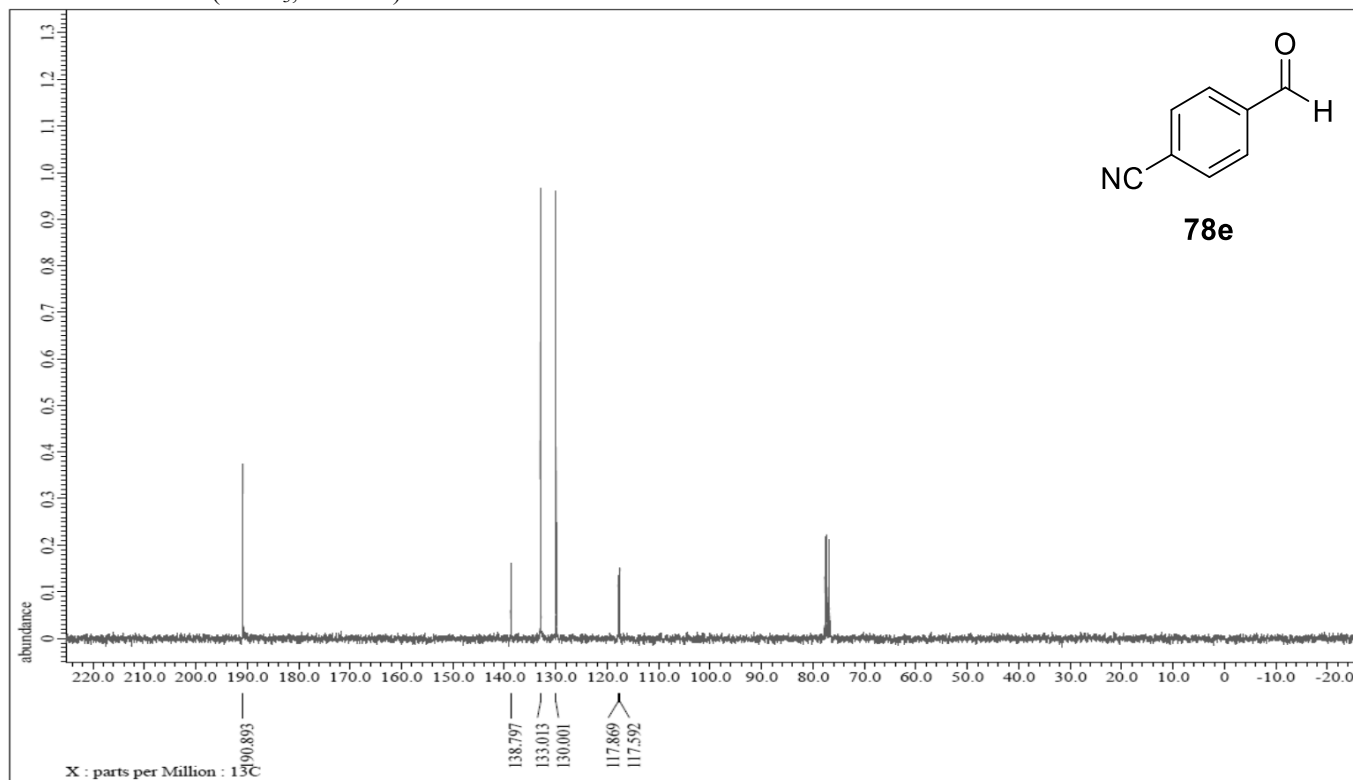
^{13}C NMR (CDCl_3 , 75 MHz)



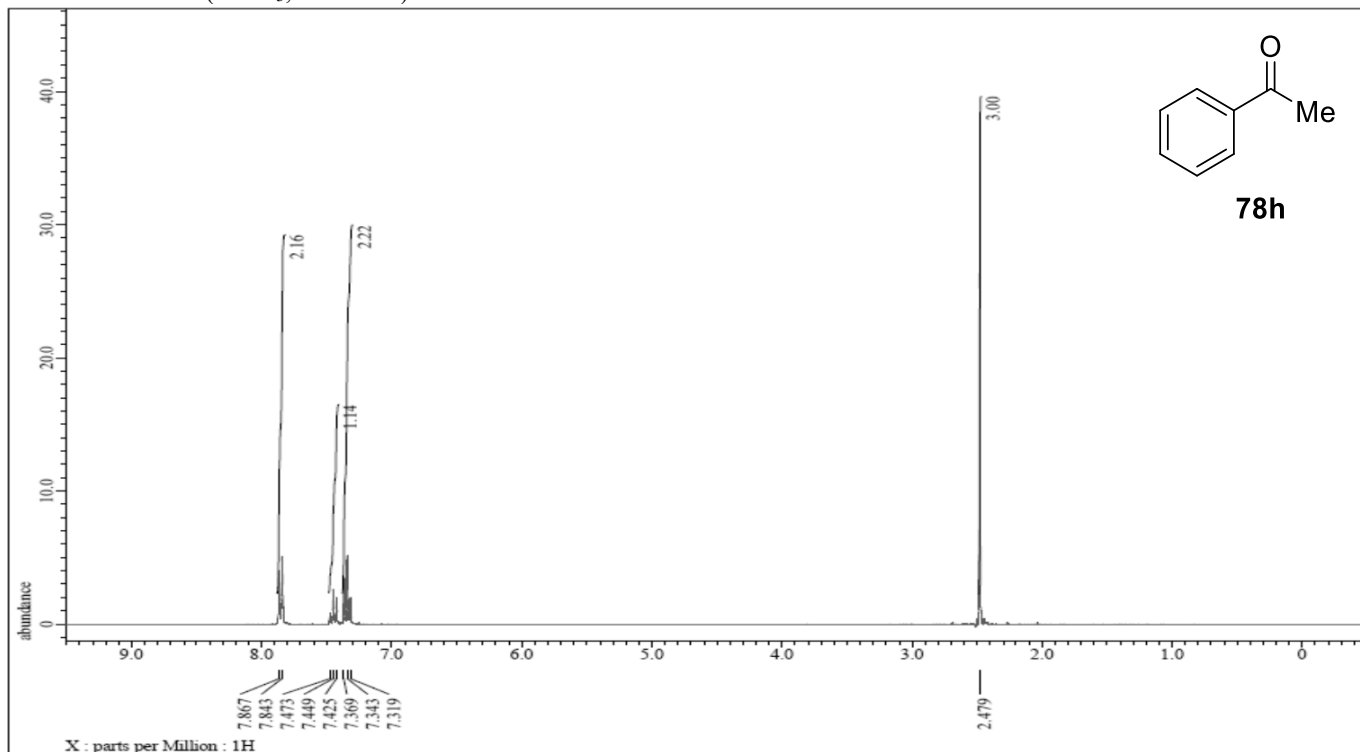
^1H NMR (CDCl_3 , 300 MHz)



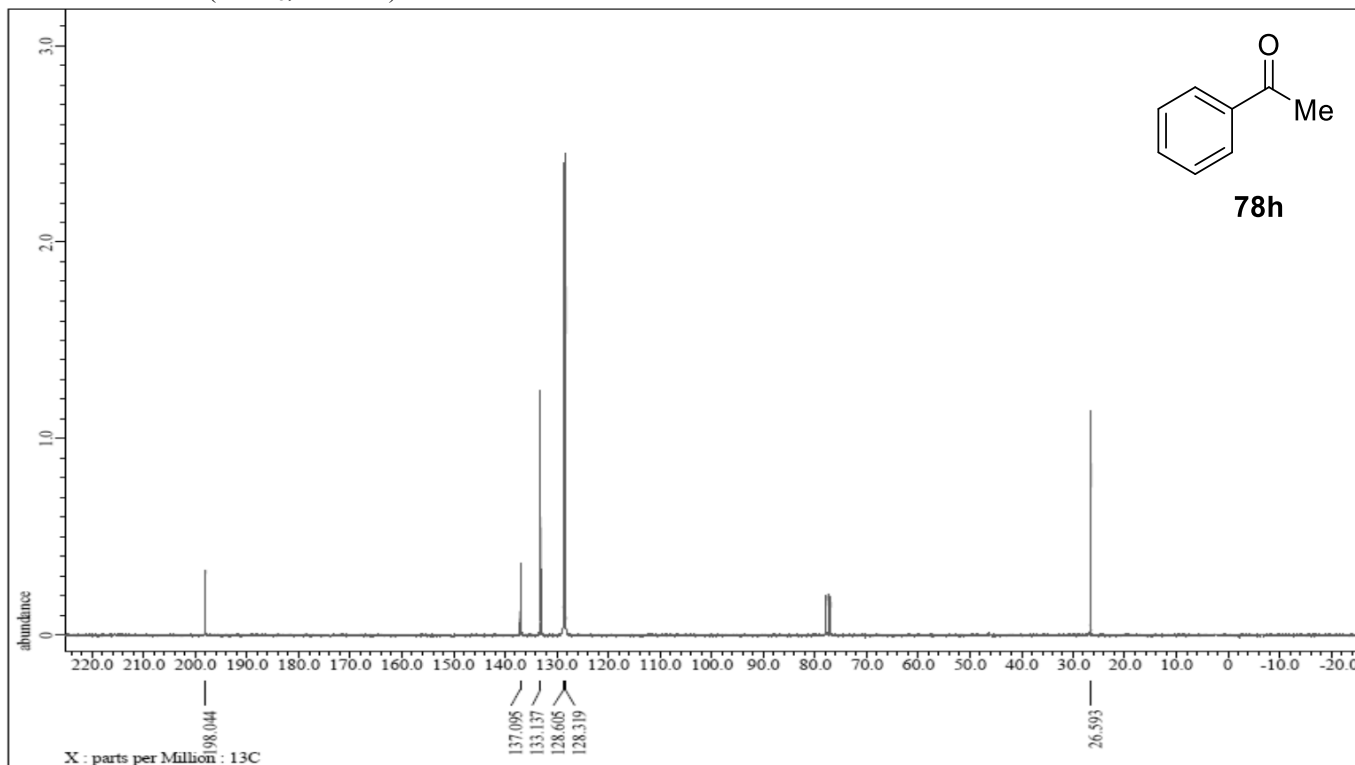
^{13}C NMR (CDCl_3 , 75 MHz)



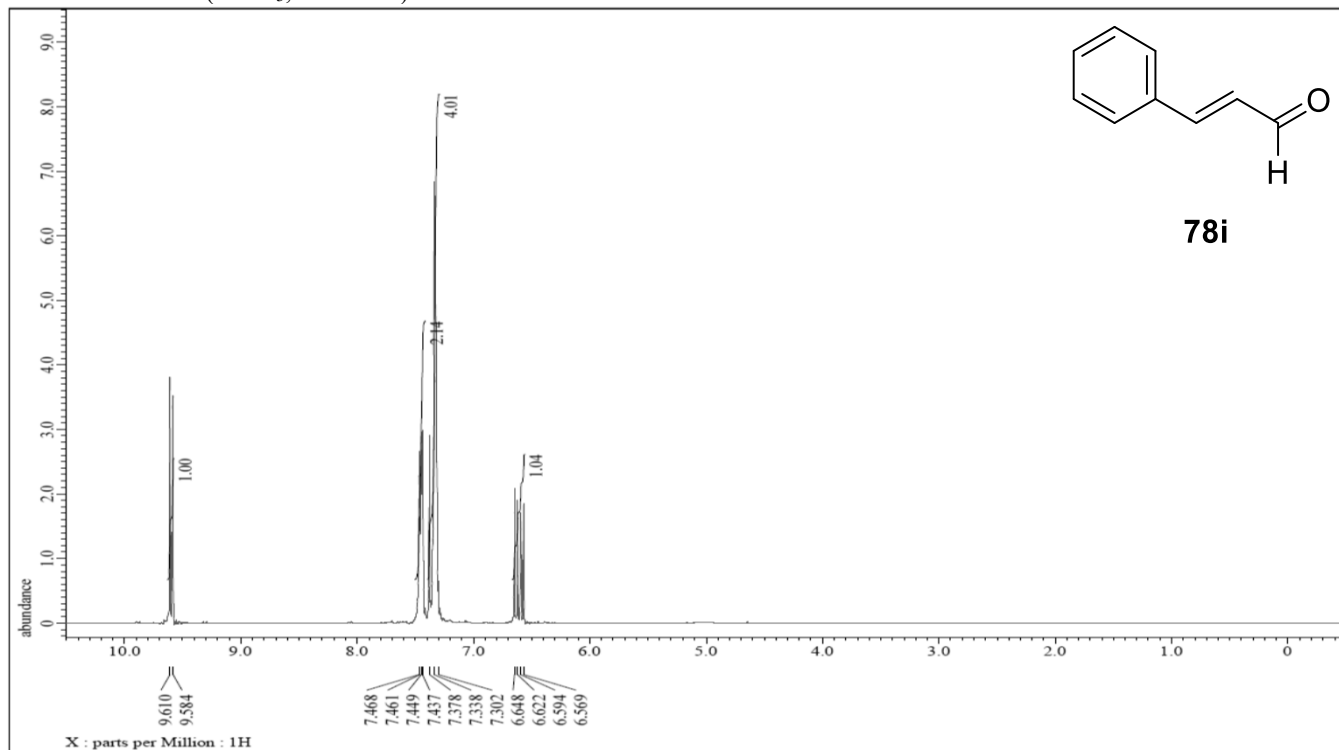
^1H NMR (CDCl_3 , 300 MHz)



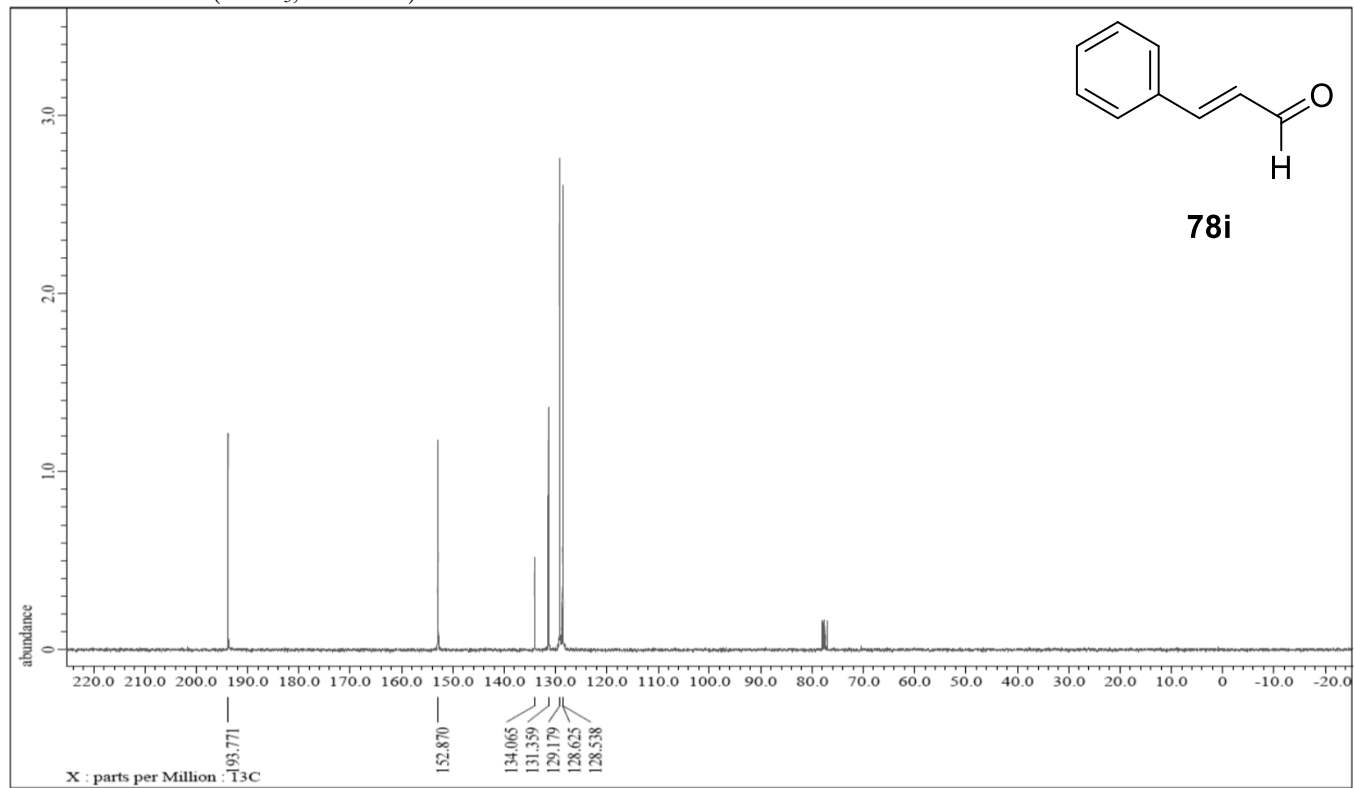
^{13}C NMR (CDCl_3 , 75 MHz)



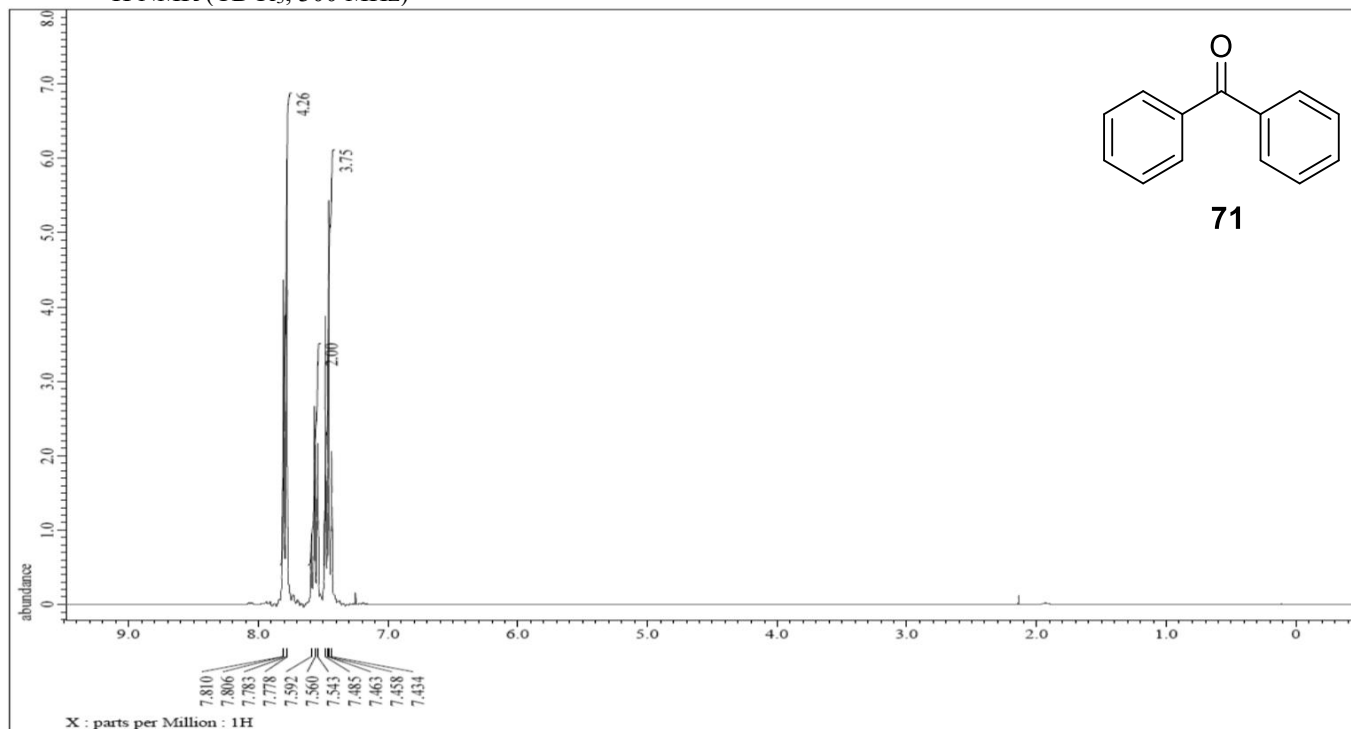
^1H NMR (CDCl_3 , 500 MHz)



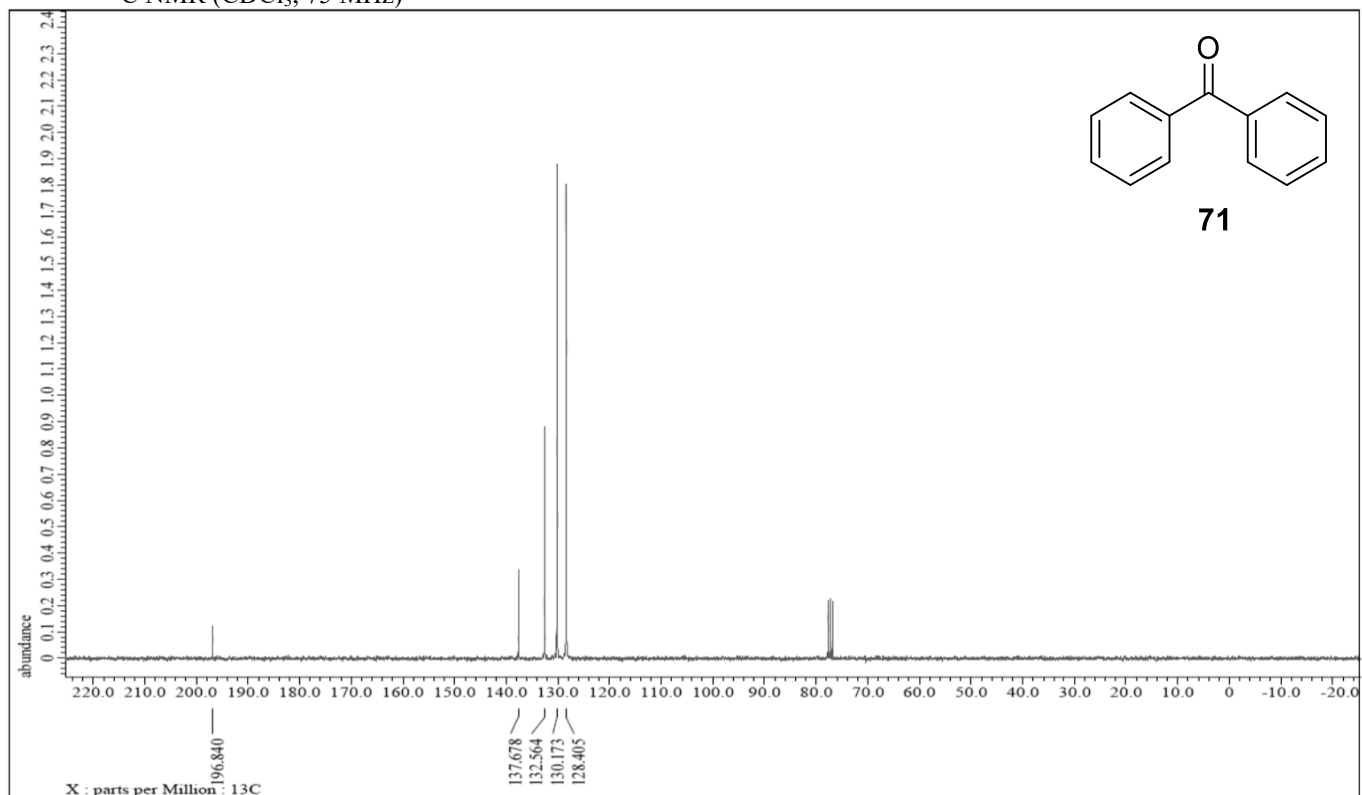
^{13}C NMR (CDCl_3 , 125 MHz)



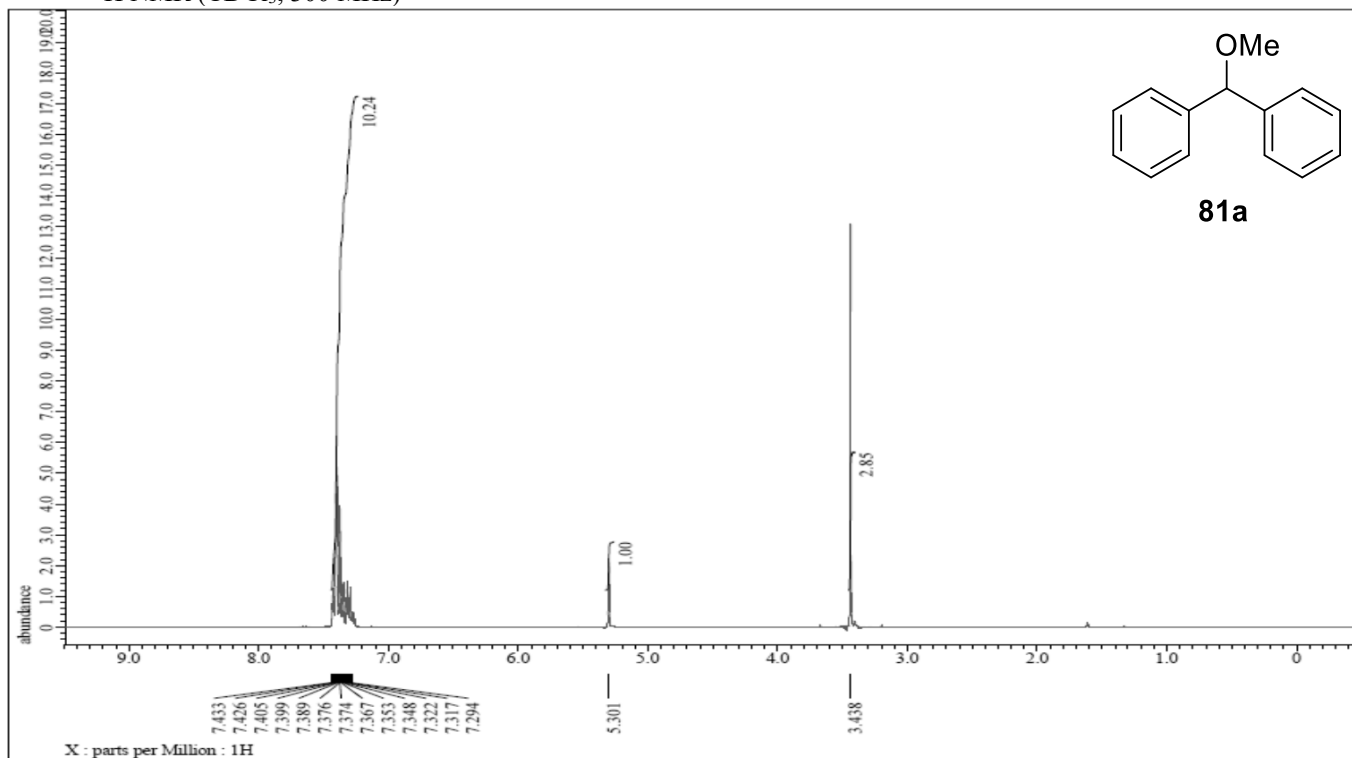
^1H NMR (CDCl_3 , 300 MHz)



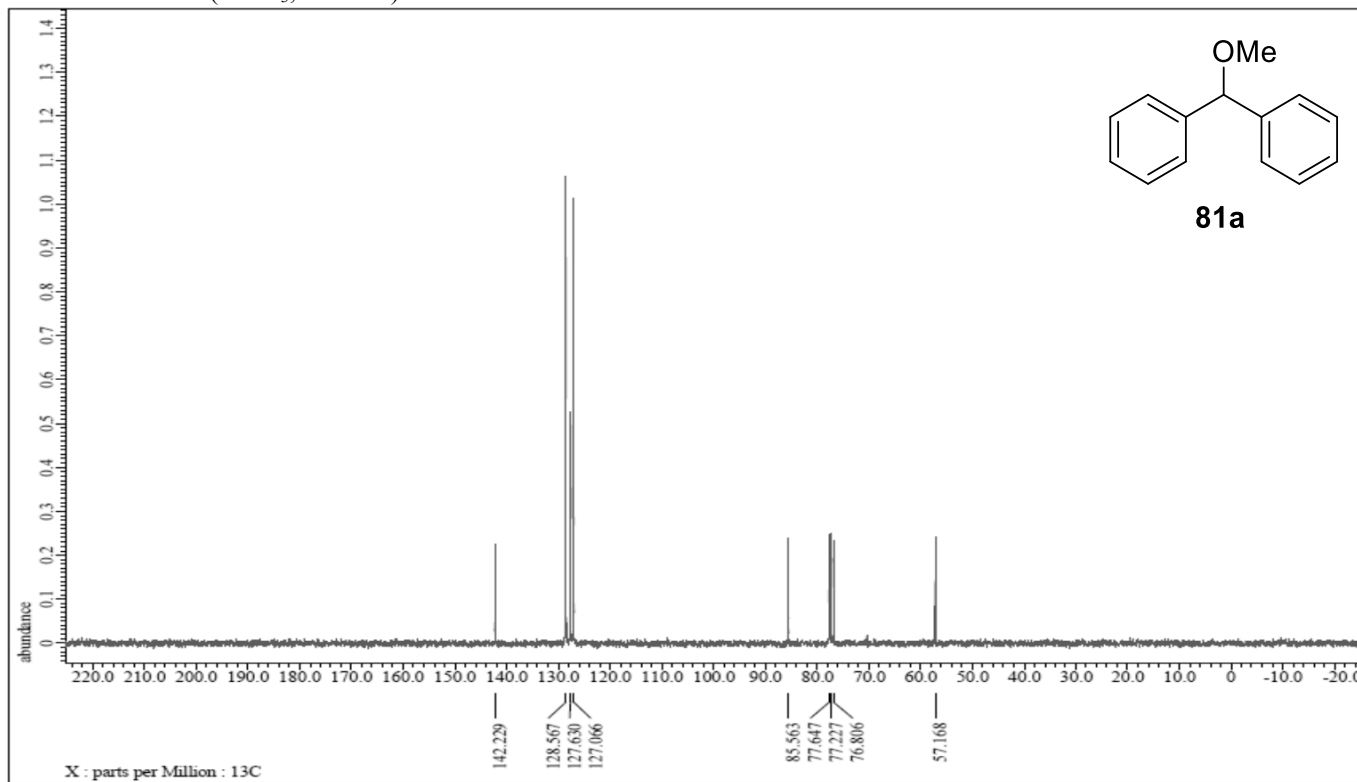
^{13}C NMR (CDCl_3 , 75 MHz)



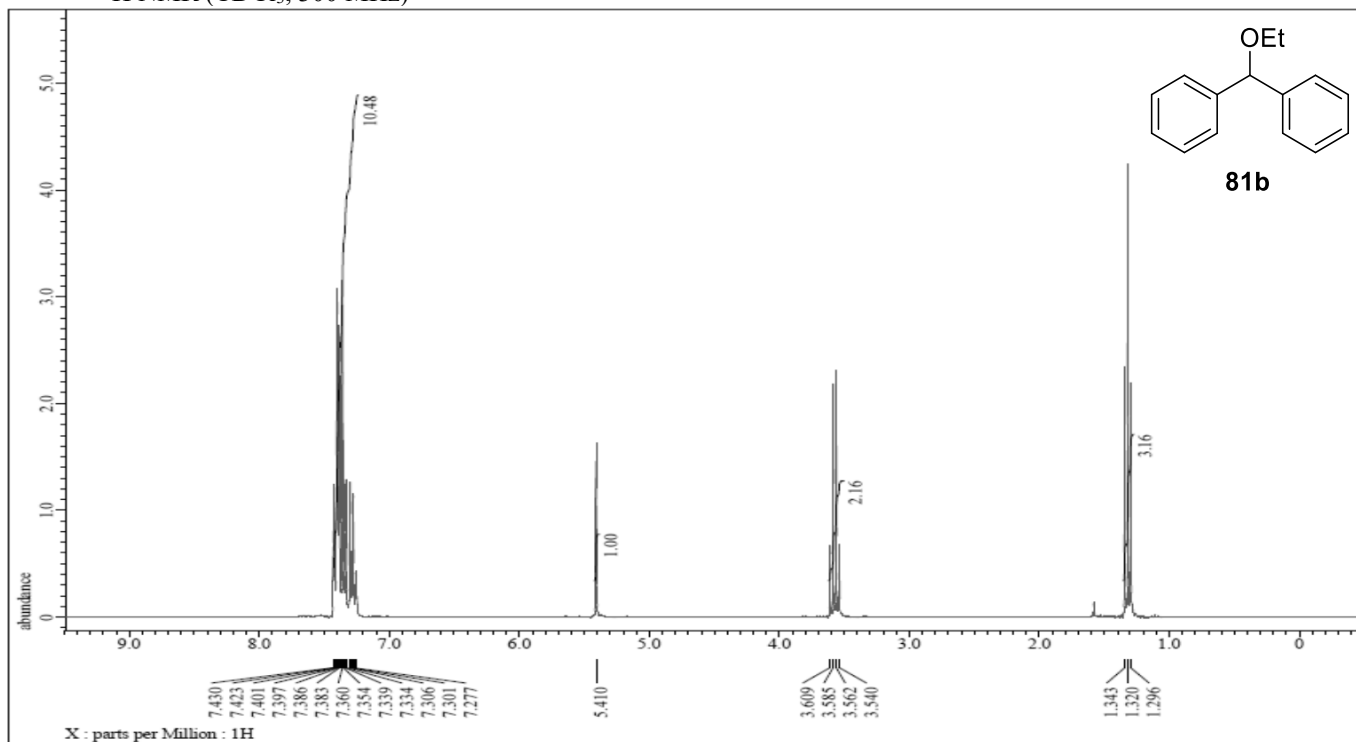
¹H NMR (CDCl₃, 300 MHz)



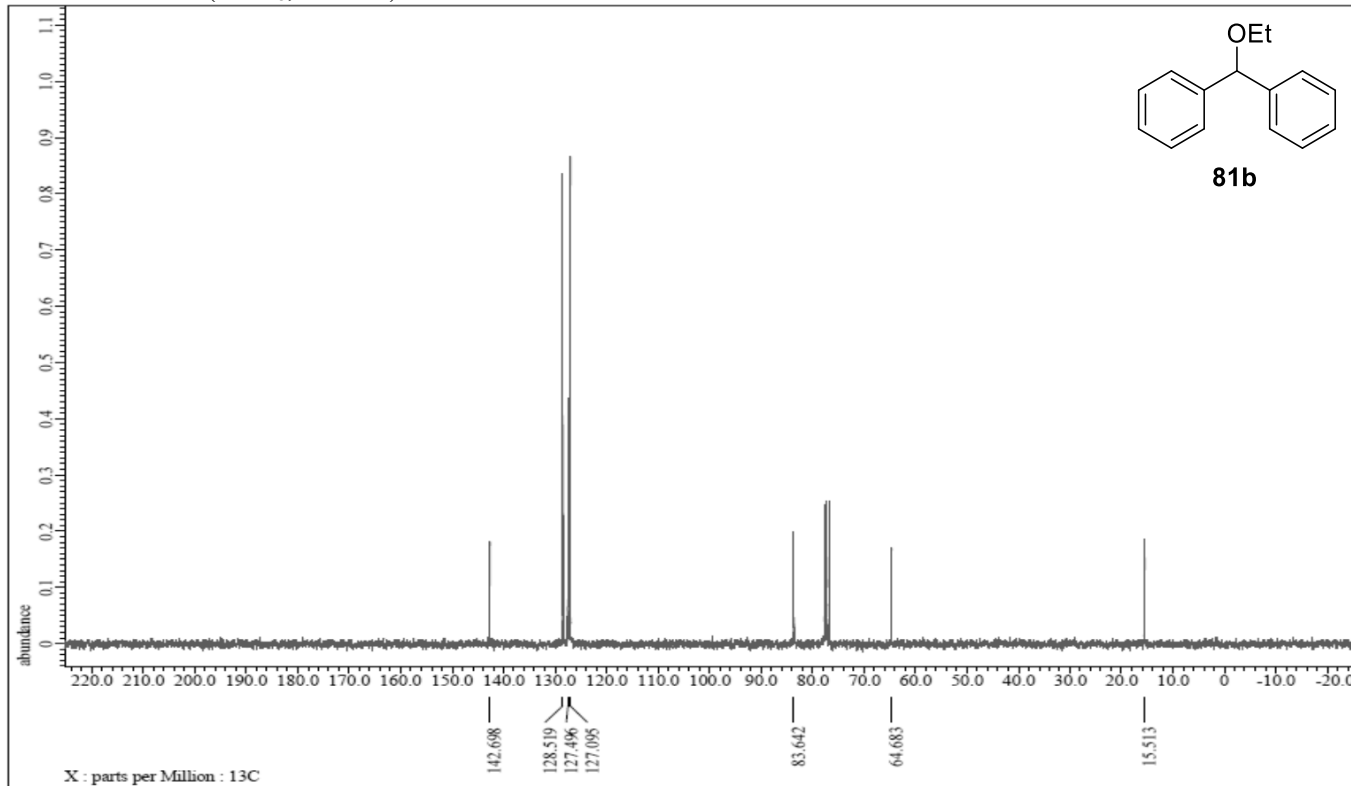
¹³C NMR (CDCl₃, 75 MHz)



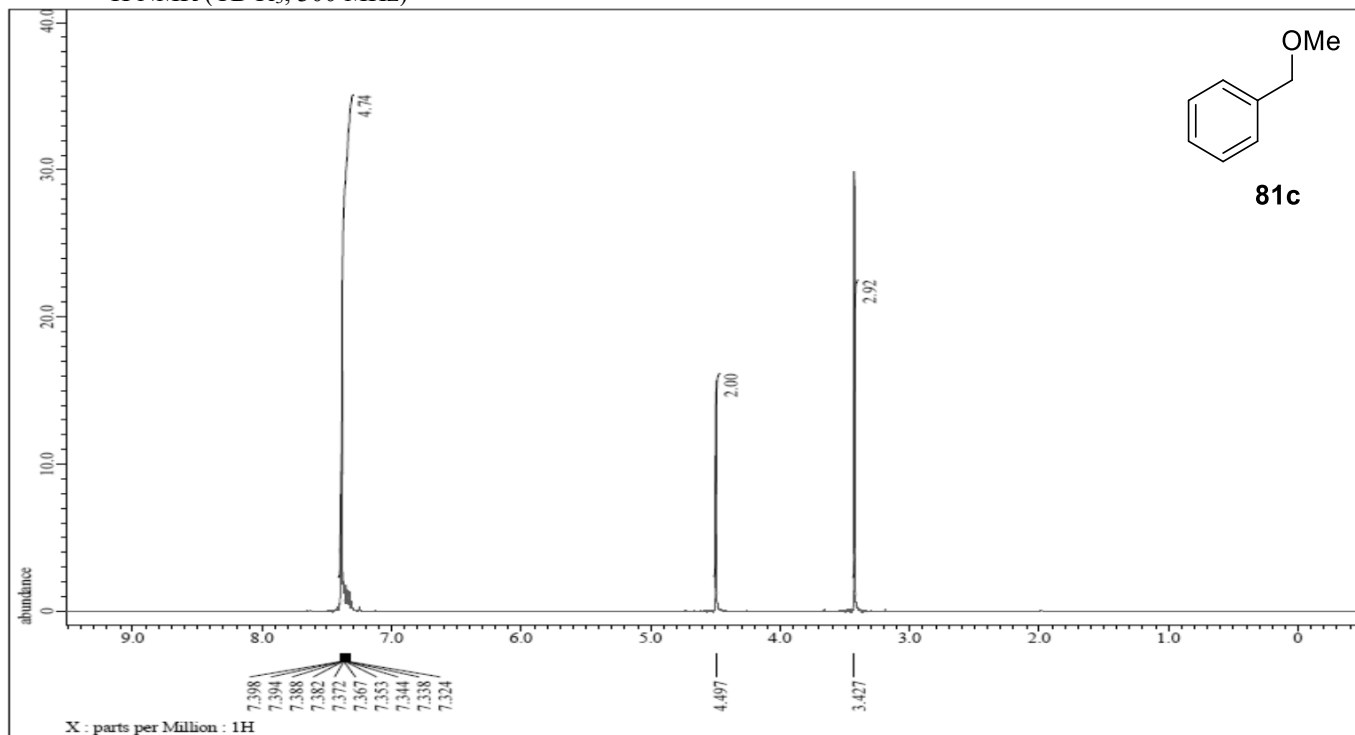
^1H NMR (CDCl_3 , 300 MHz)



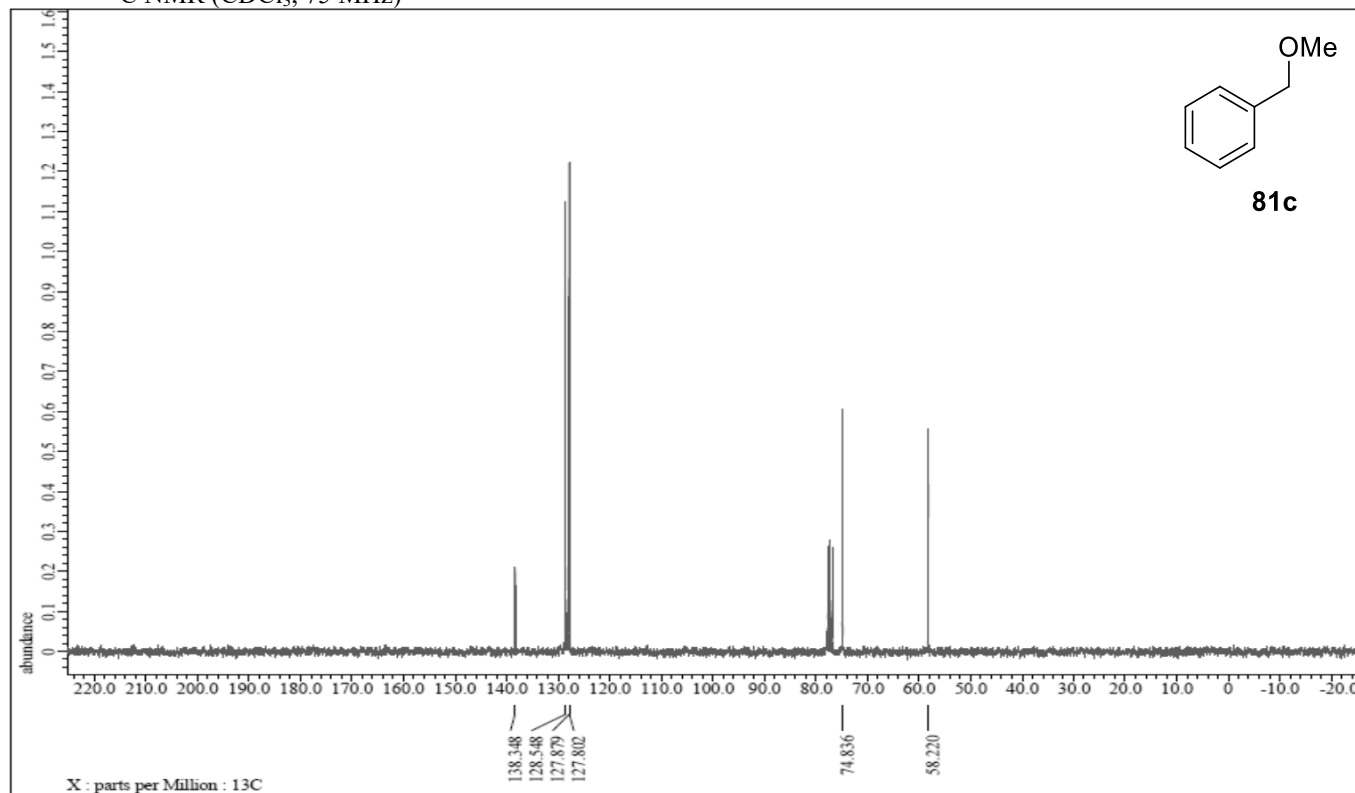
^{13}C NMR (CDCl_3 , 75 MHz)



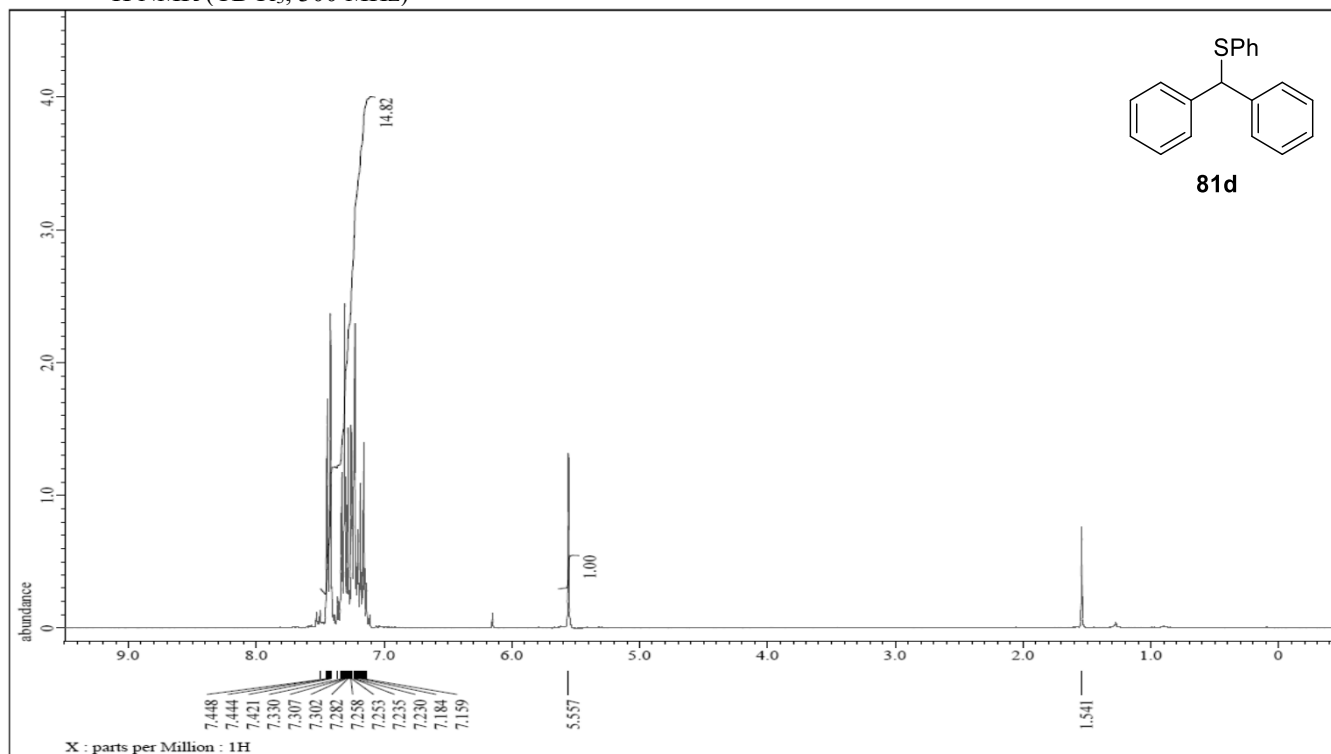
¹H NMR (CDCl₃, 300 MHz)



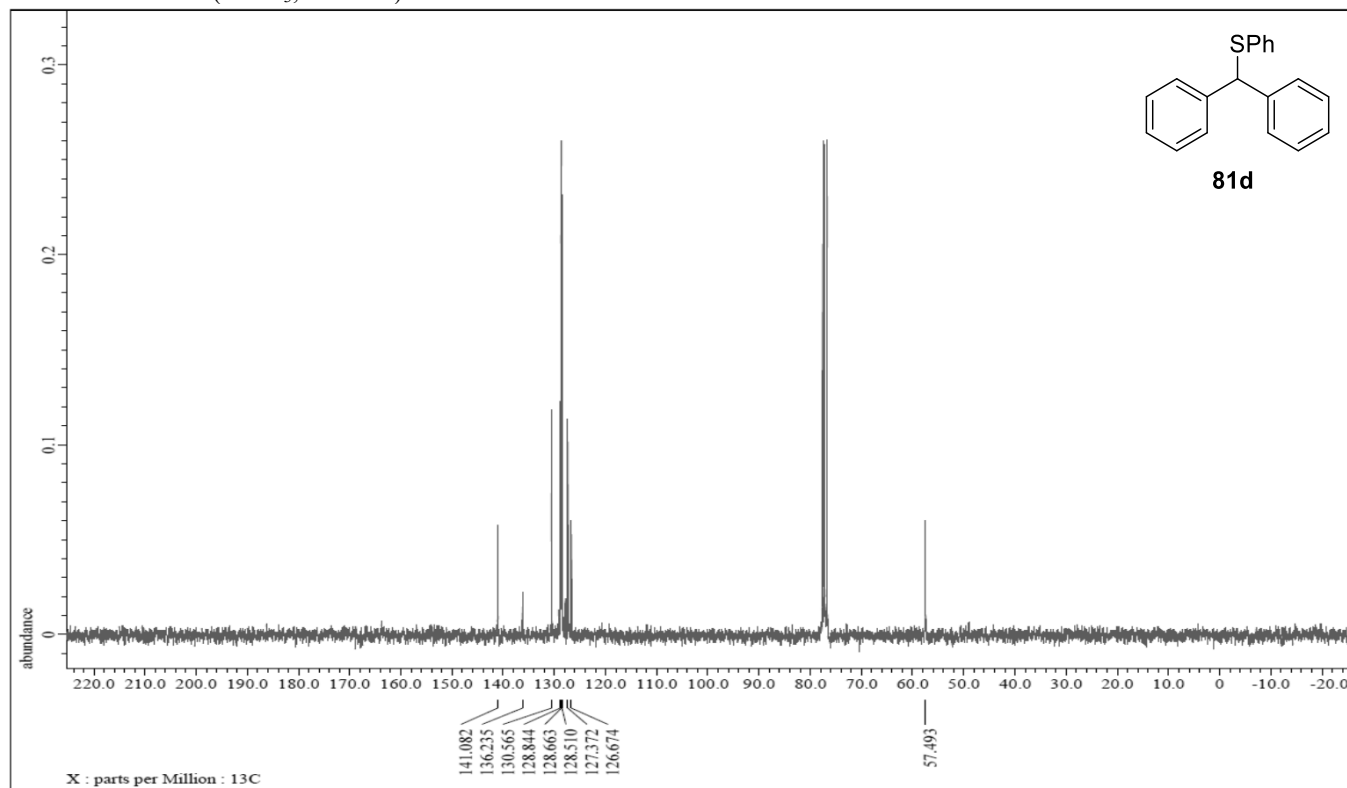
¹³C NMR (CDCl₃, 75 MHz)



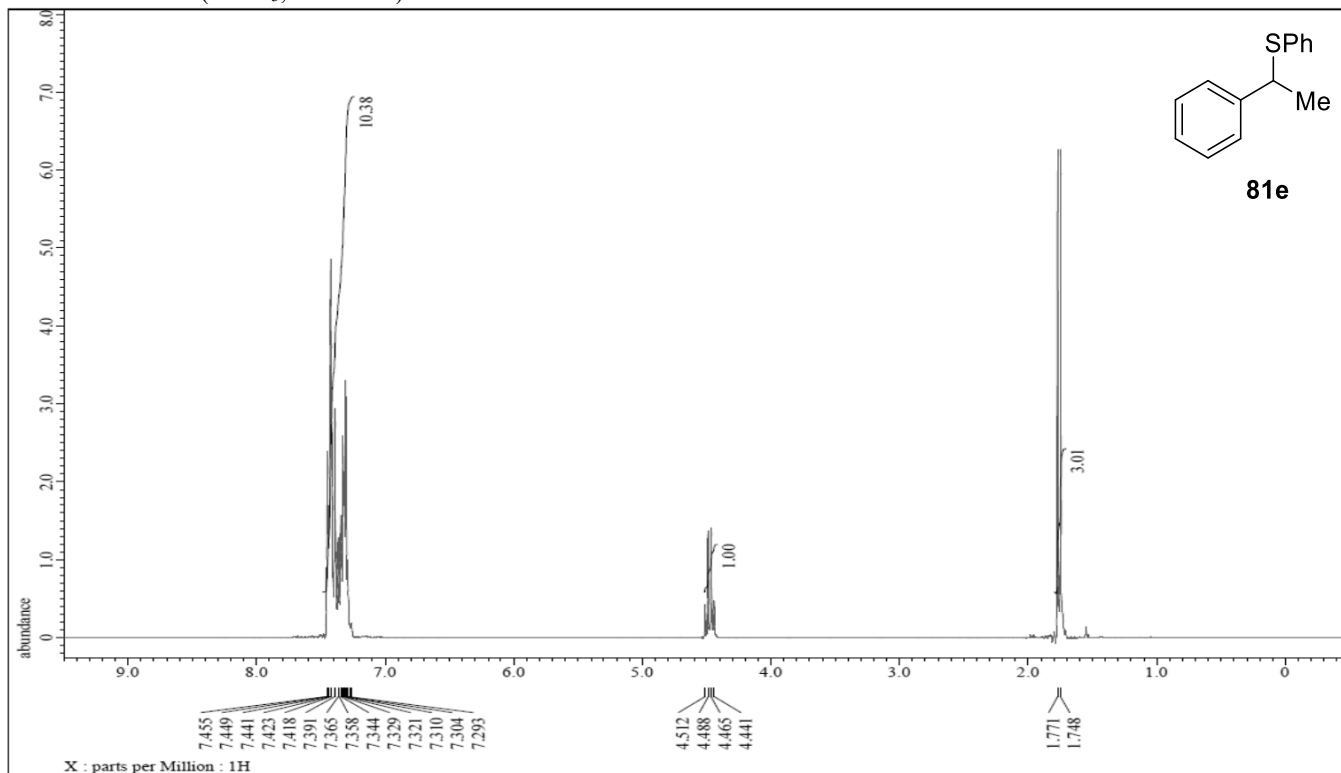
^1H NMR (CDCl_3 , 300 MHz)



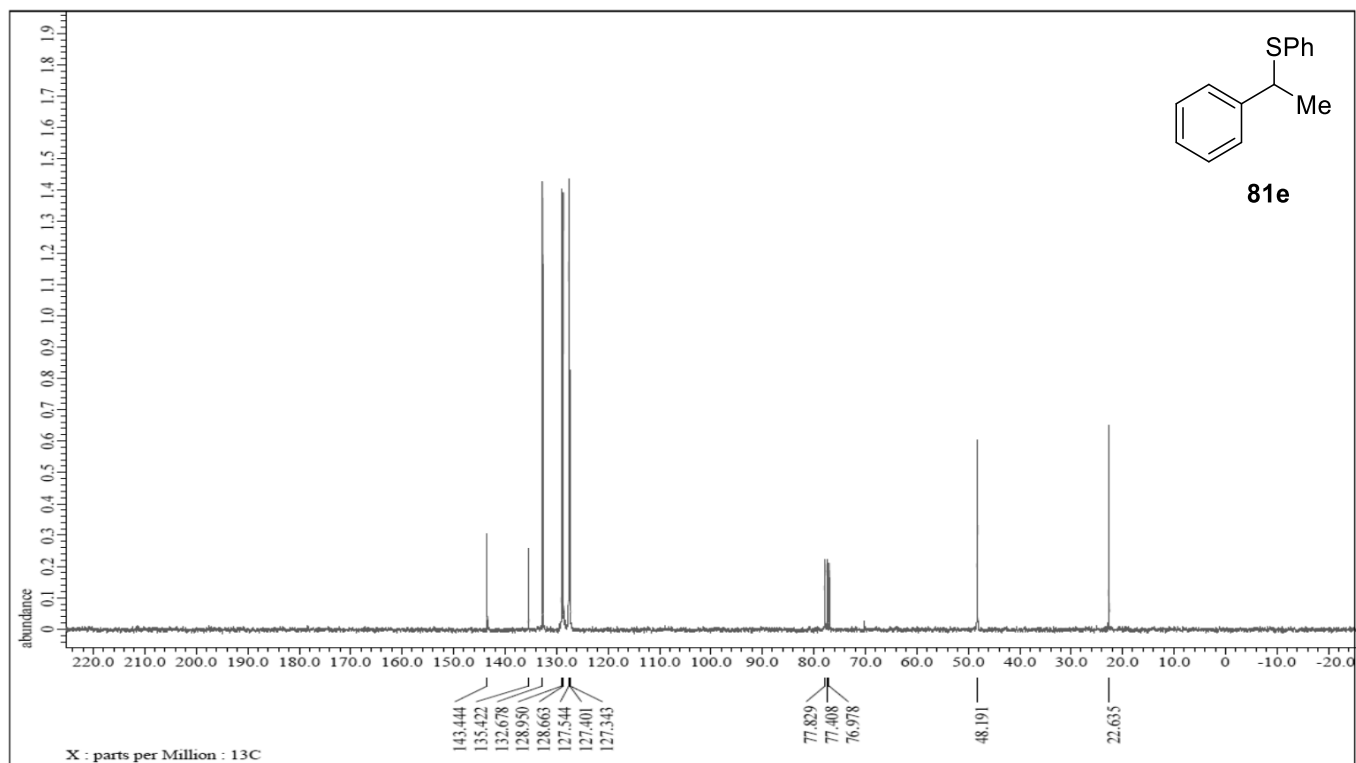
^{13}C NMR (CDCl_3 , 75 MHz)



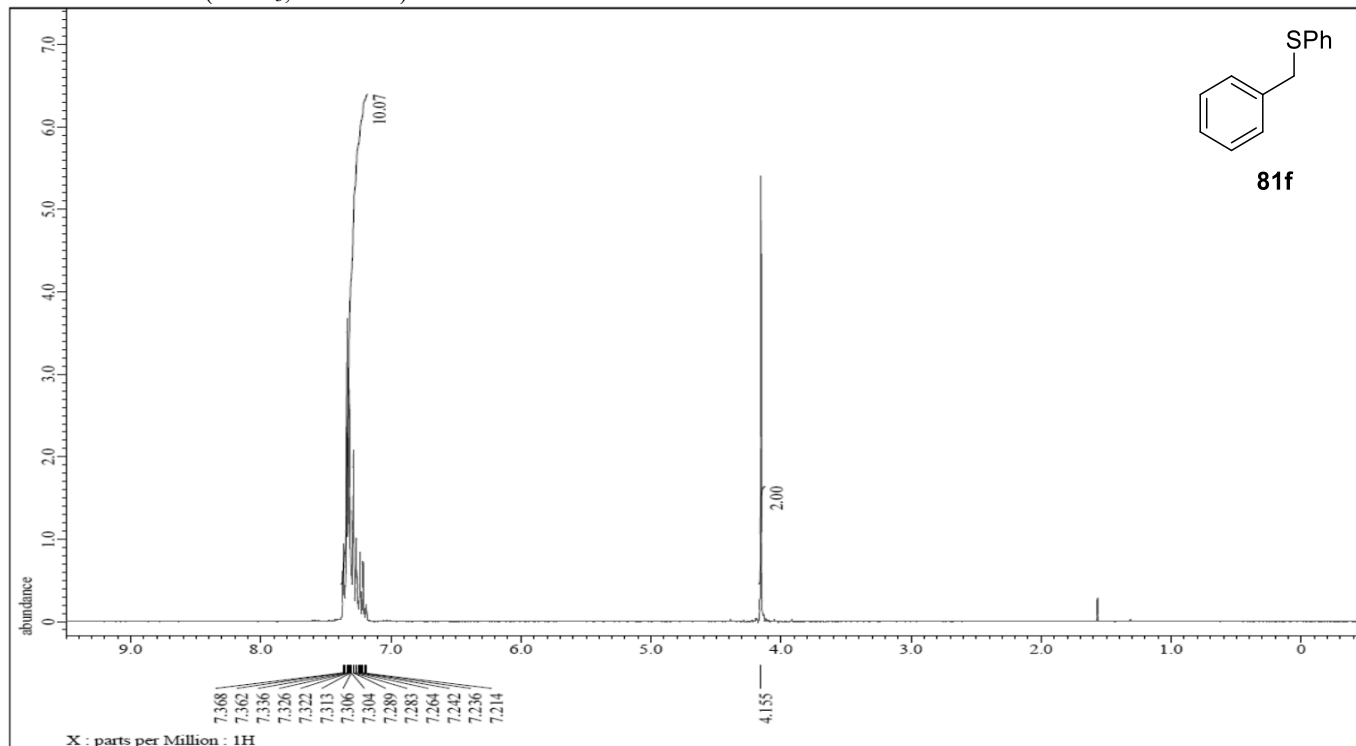
¹H NMR (CDCl₃, 300 MHz)



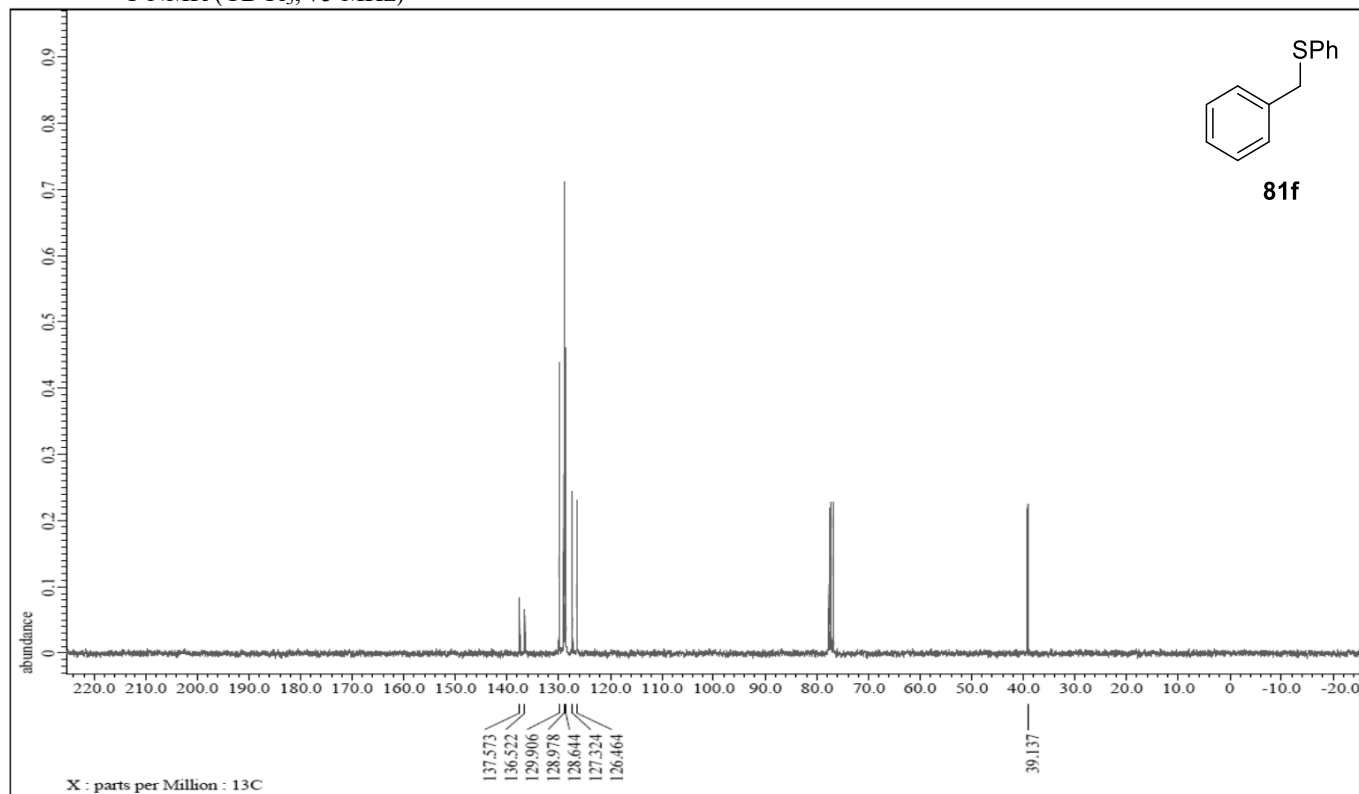
¹³C NMR (CDCl₃, 75 MHz)



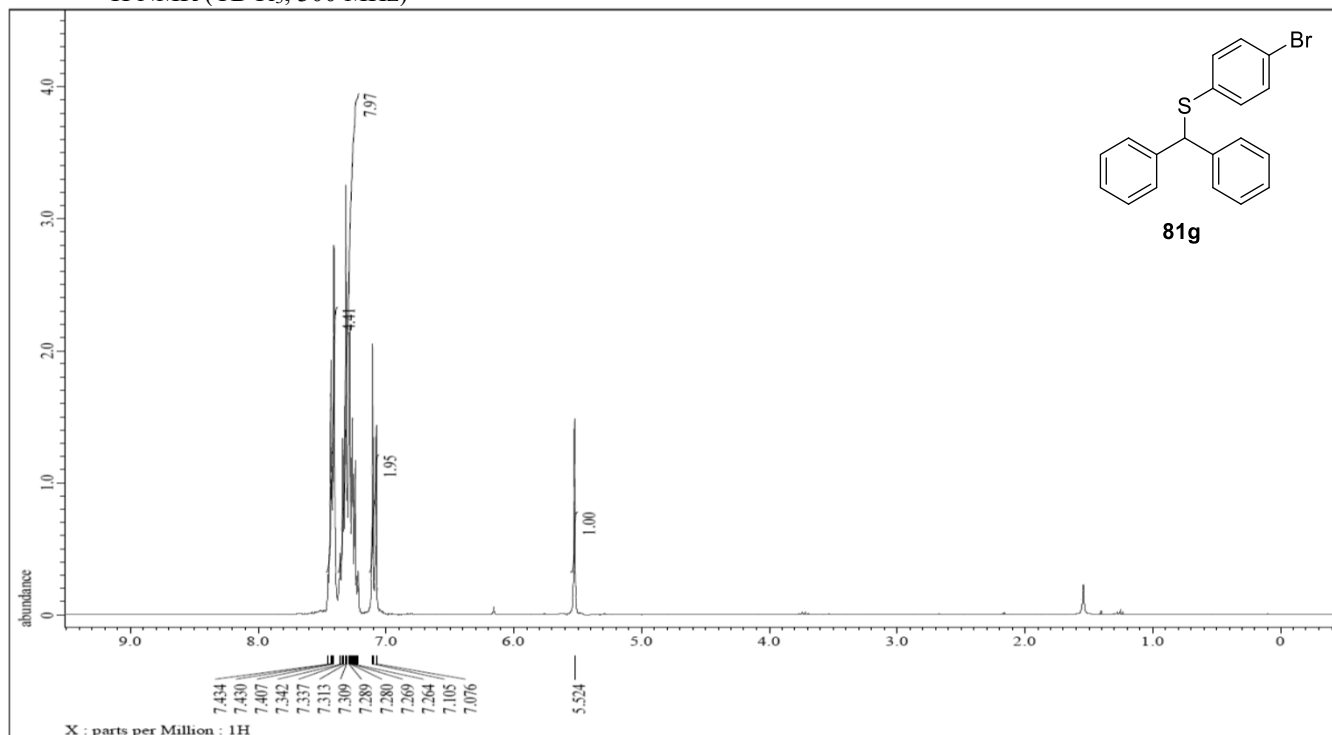
¹H NMR (CDCl₃, 300 MHz)



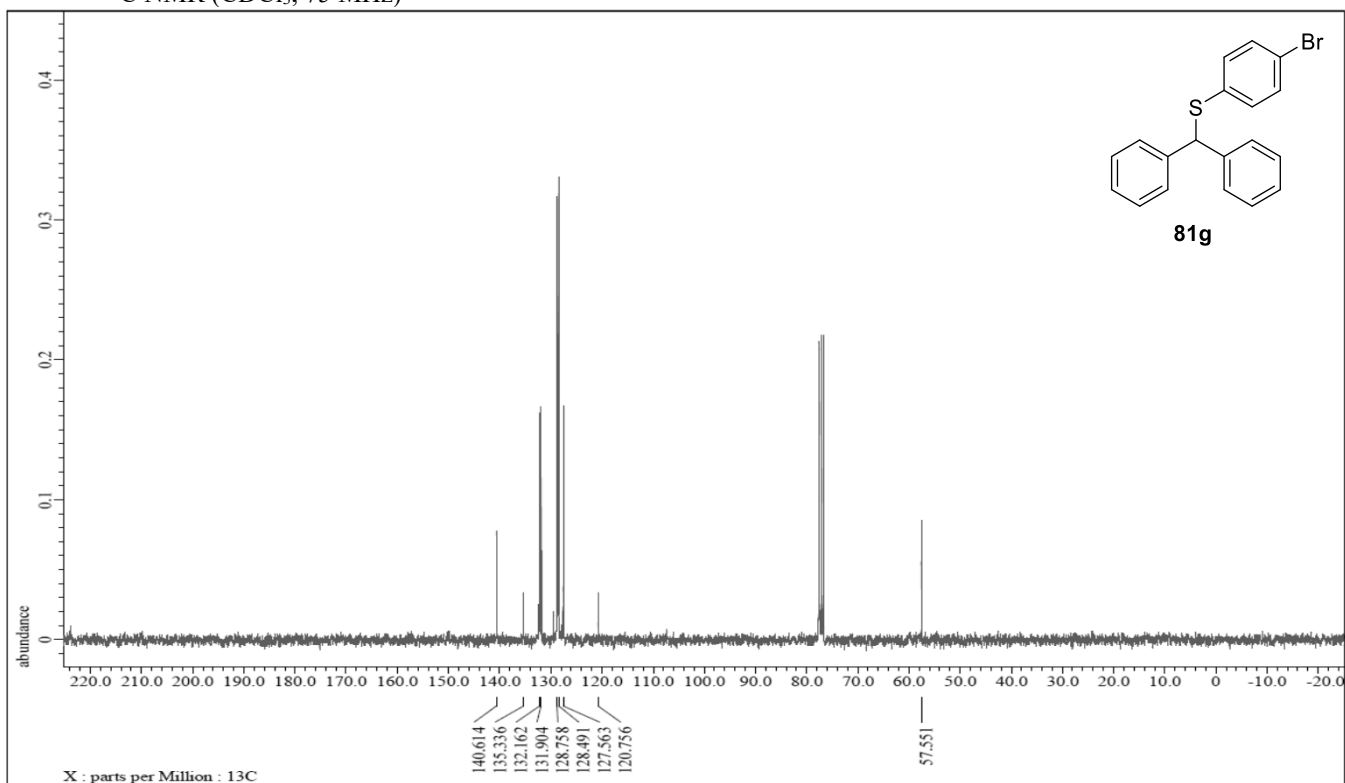
¹³C NMR (CDCl₃, 75 MHz)



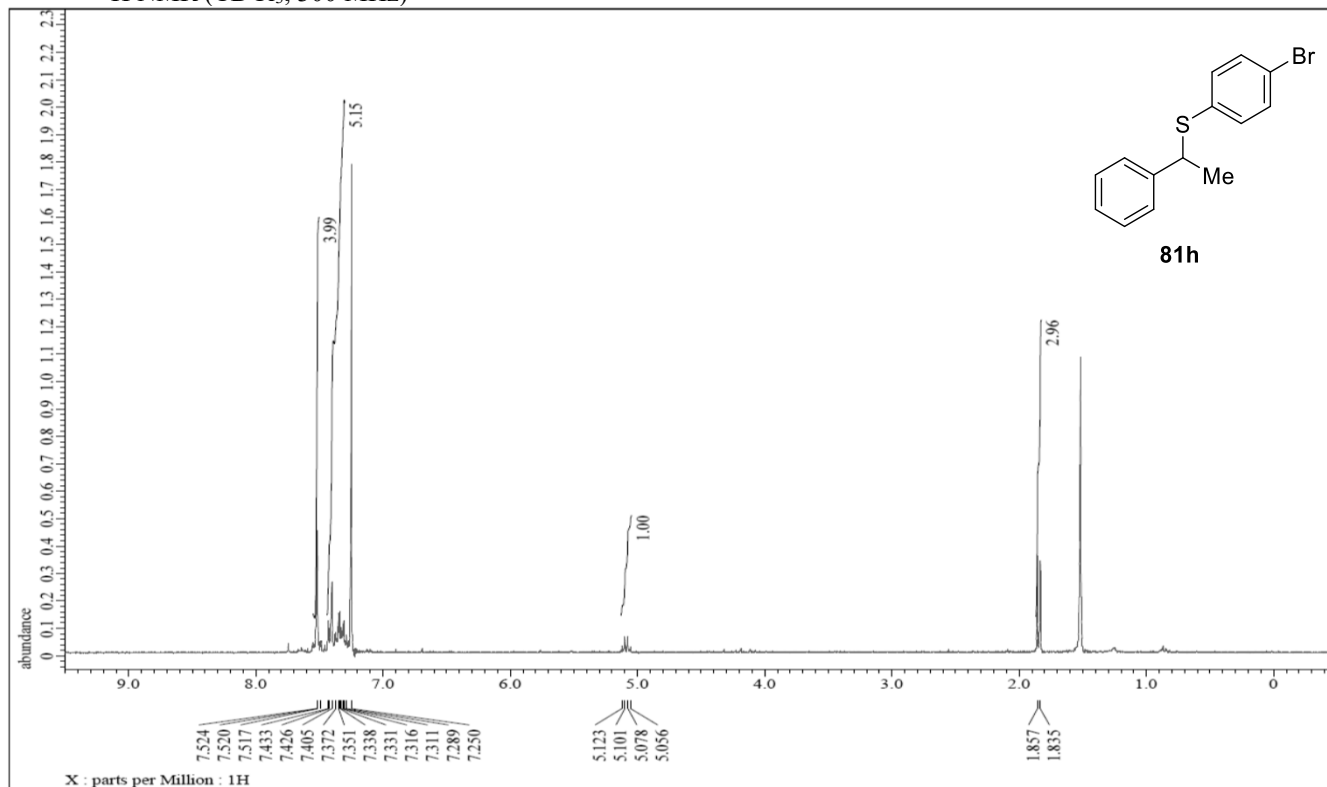
^1H NMR (CDCl_3 , 300 MHz)



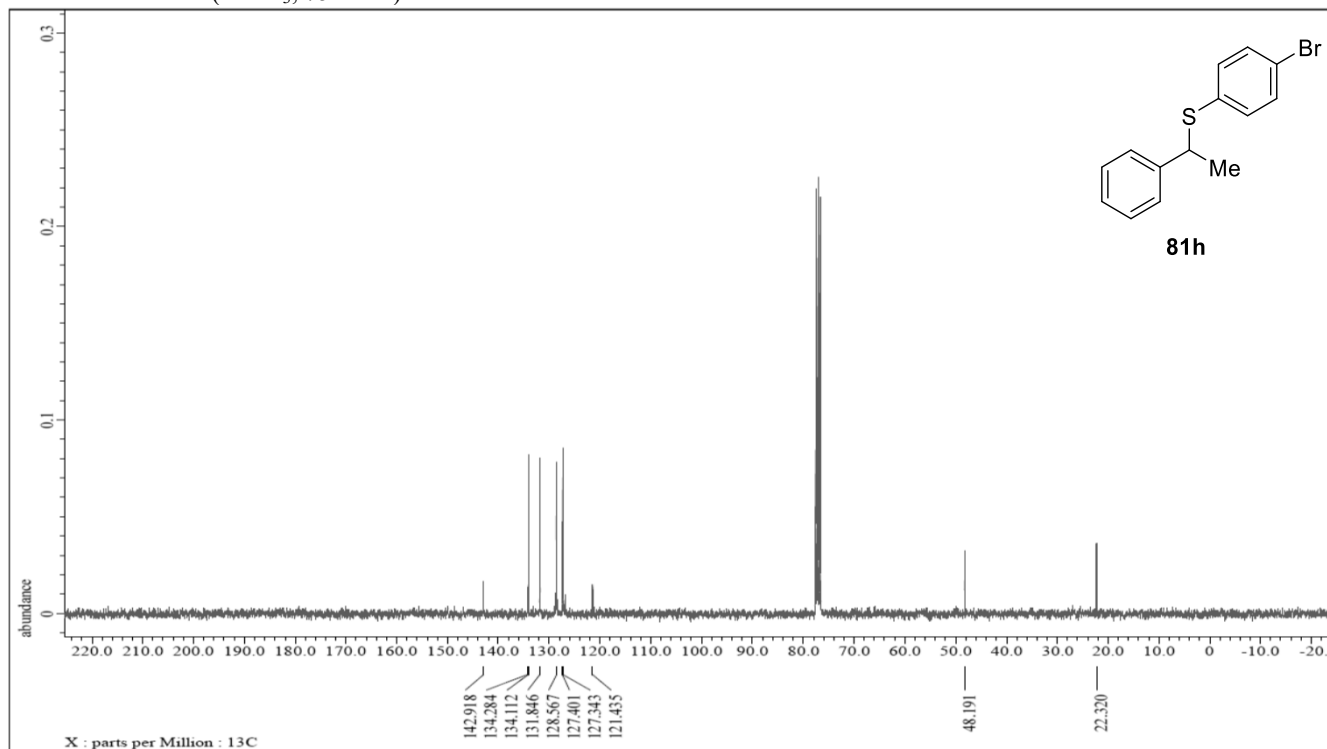
^{13}C NMR (CDCl_3 , 75 MHz)



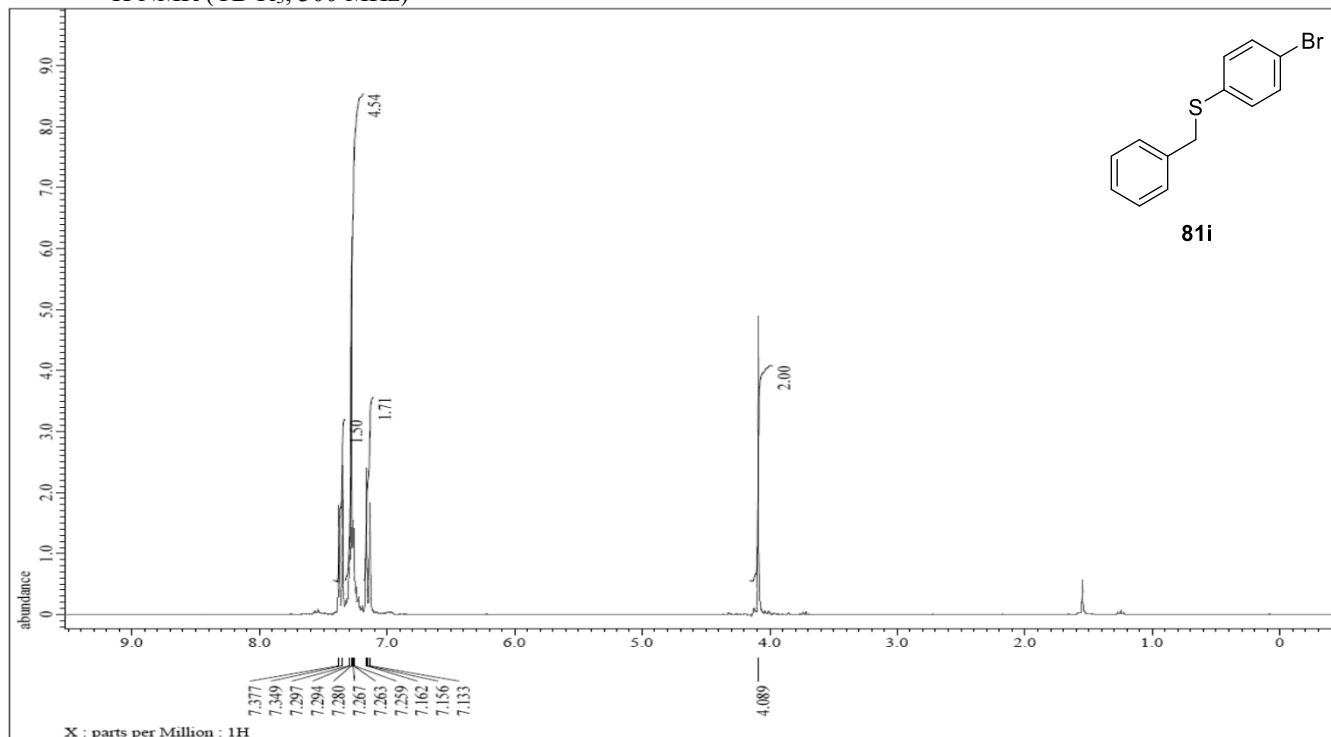
^1H NMR (CDCl_3 , 300 MHz)



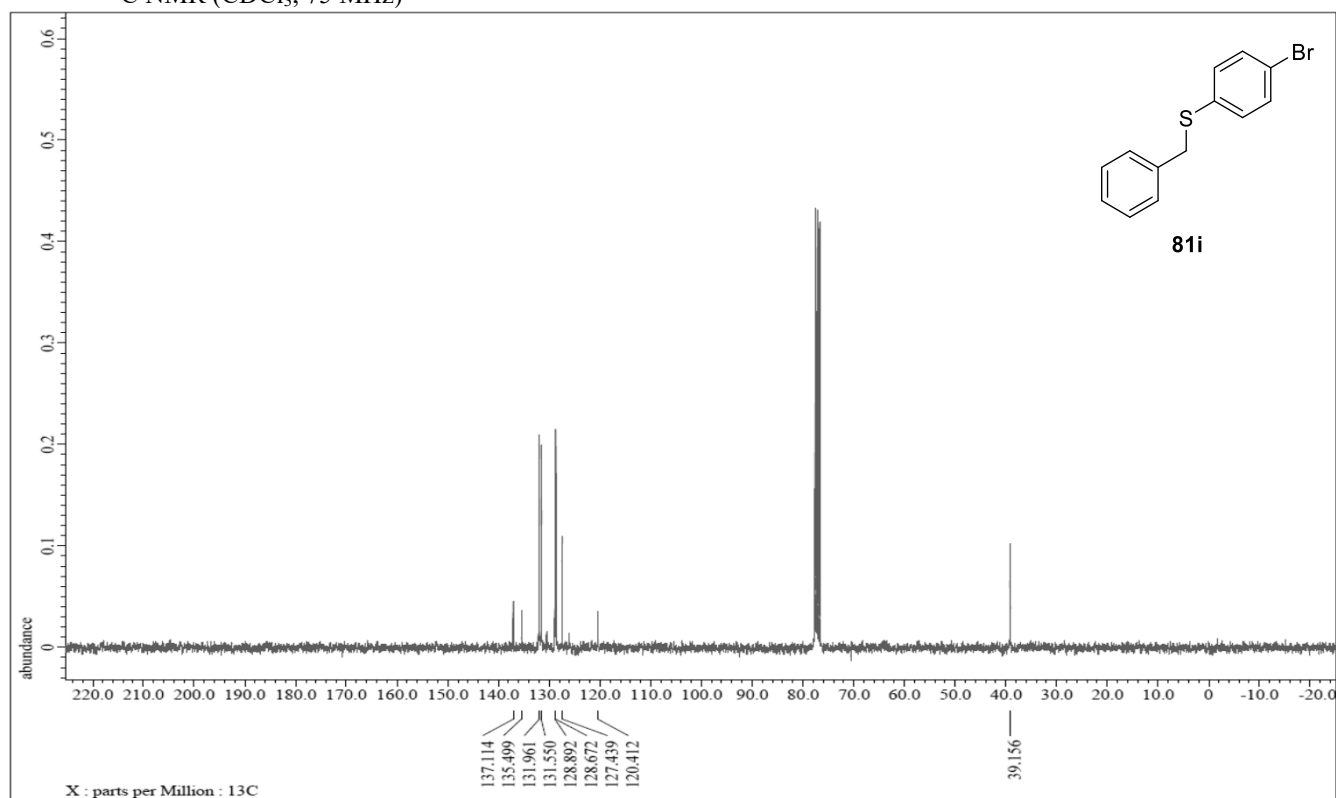
^{13}C NMR (CDCl_3 , 75 MHz)



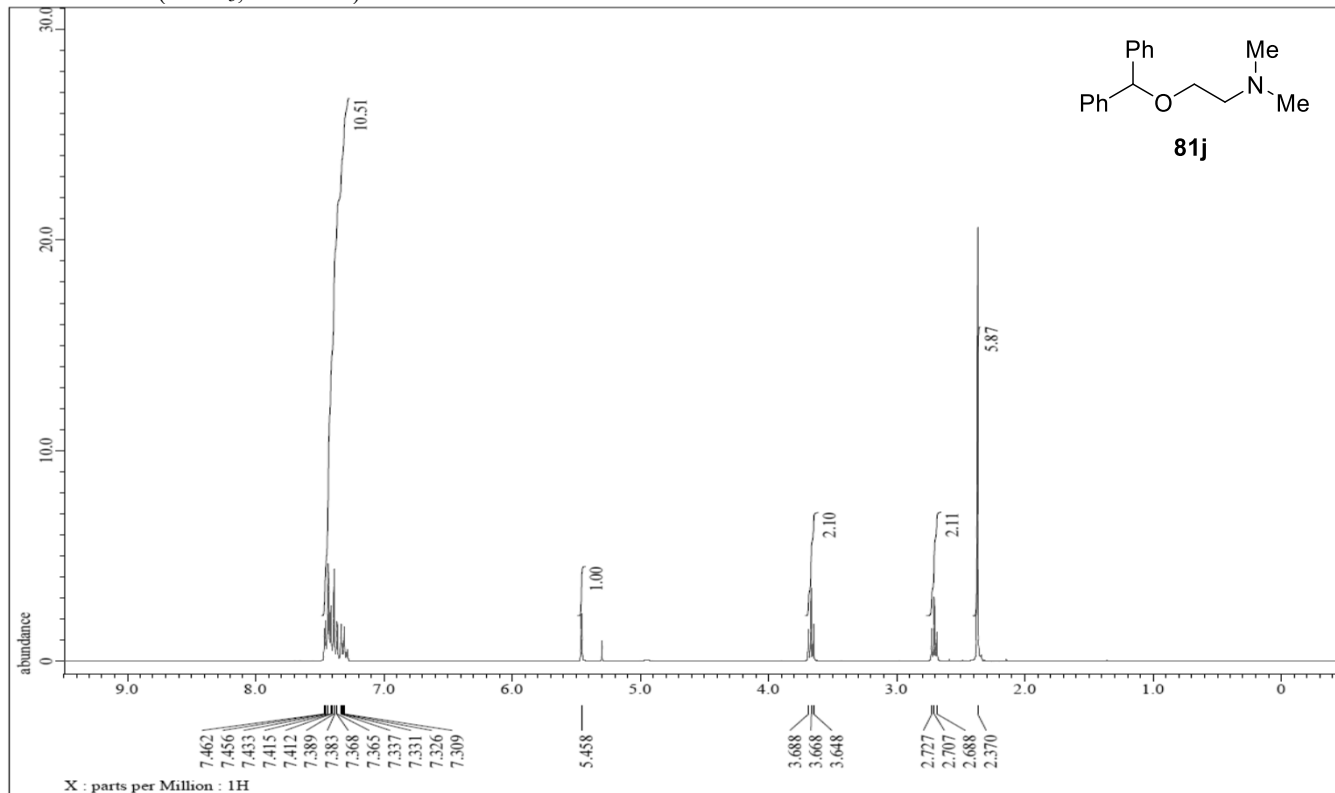
^1H NMR (CDCl_3 , 300 MHz)



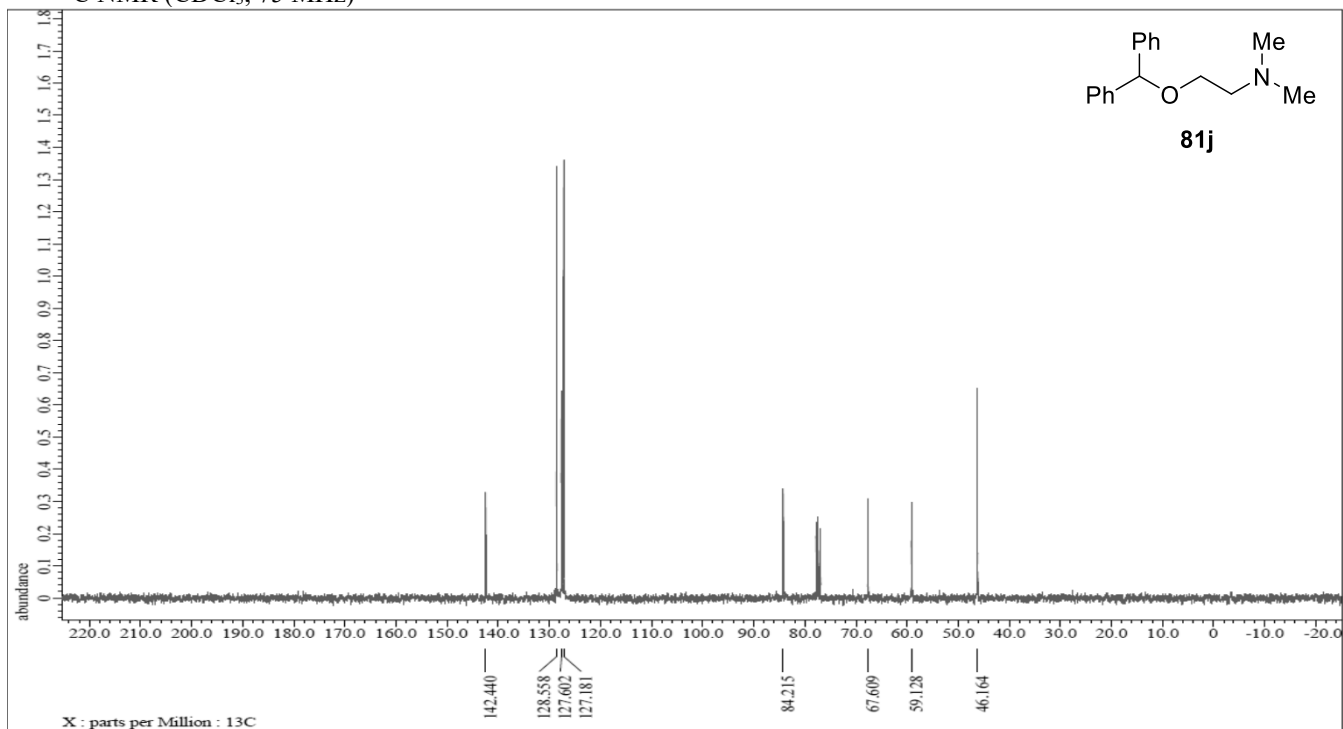
^{13}C NMR (CDCl_3 , 75 MHz)



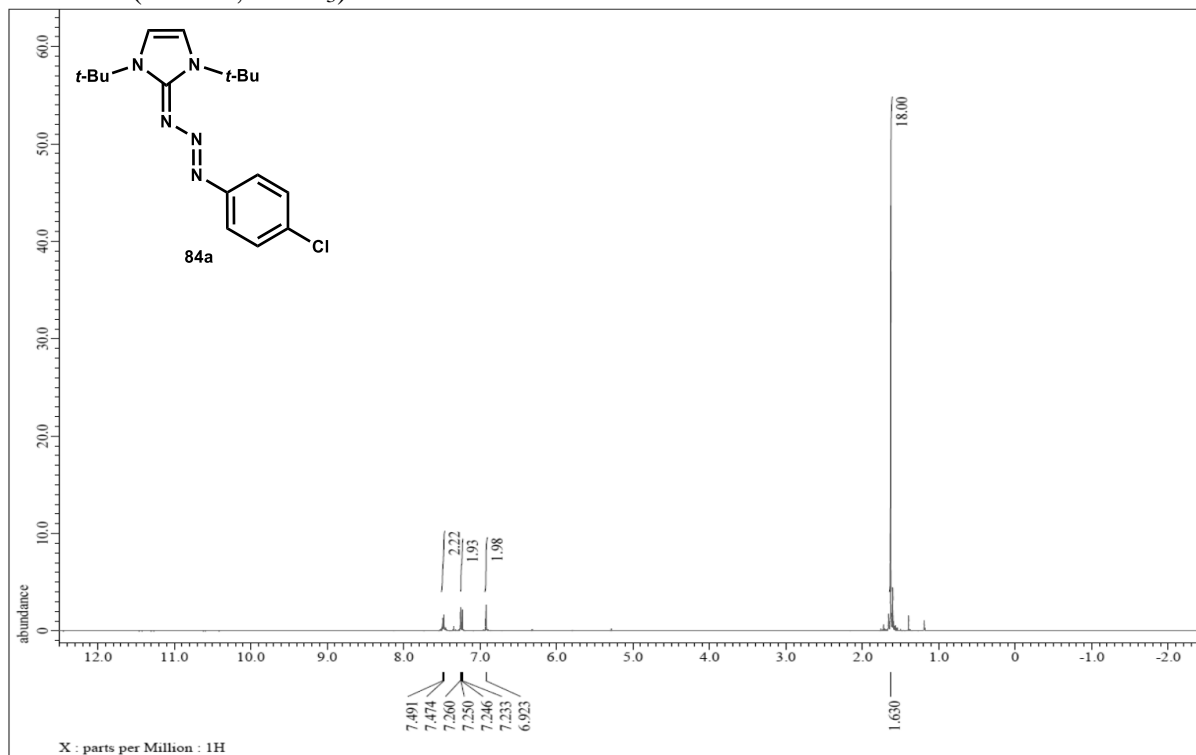
¹H NMR (CDCl₃, 300 MHz)



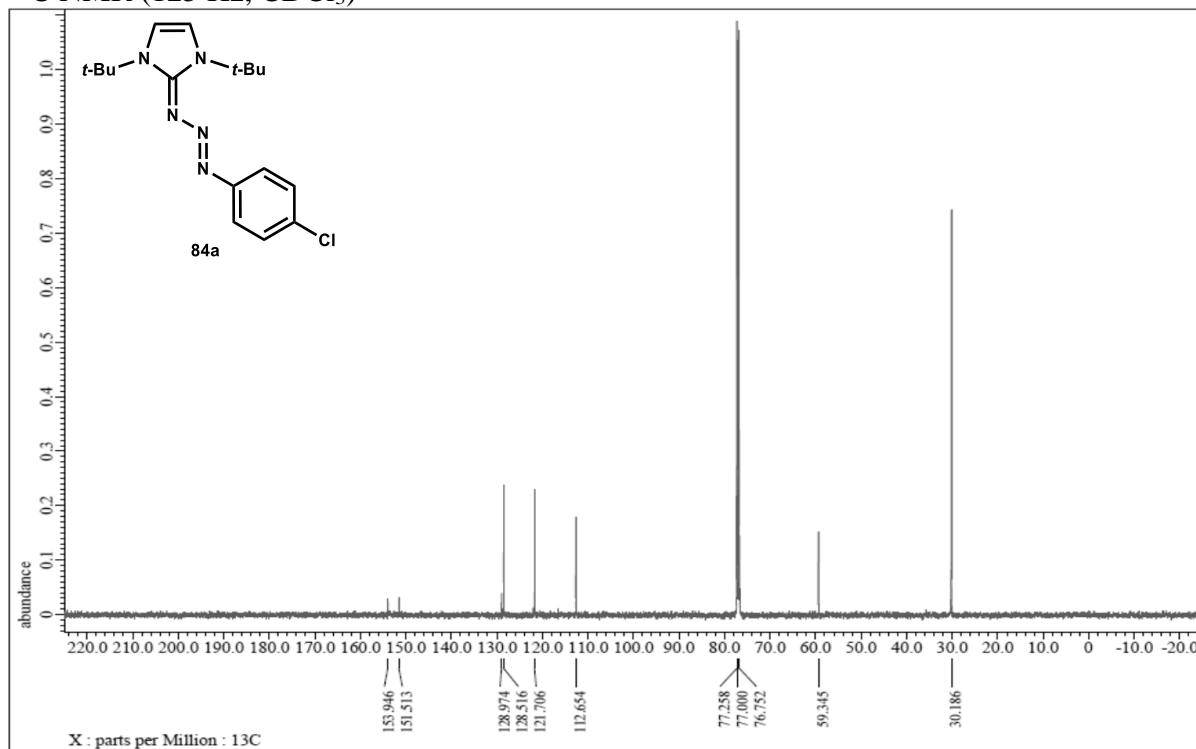
¹³C NMR (CDCl₃, 75 MHz)



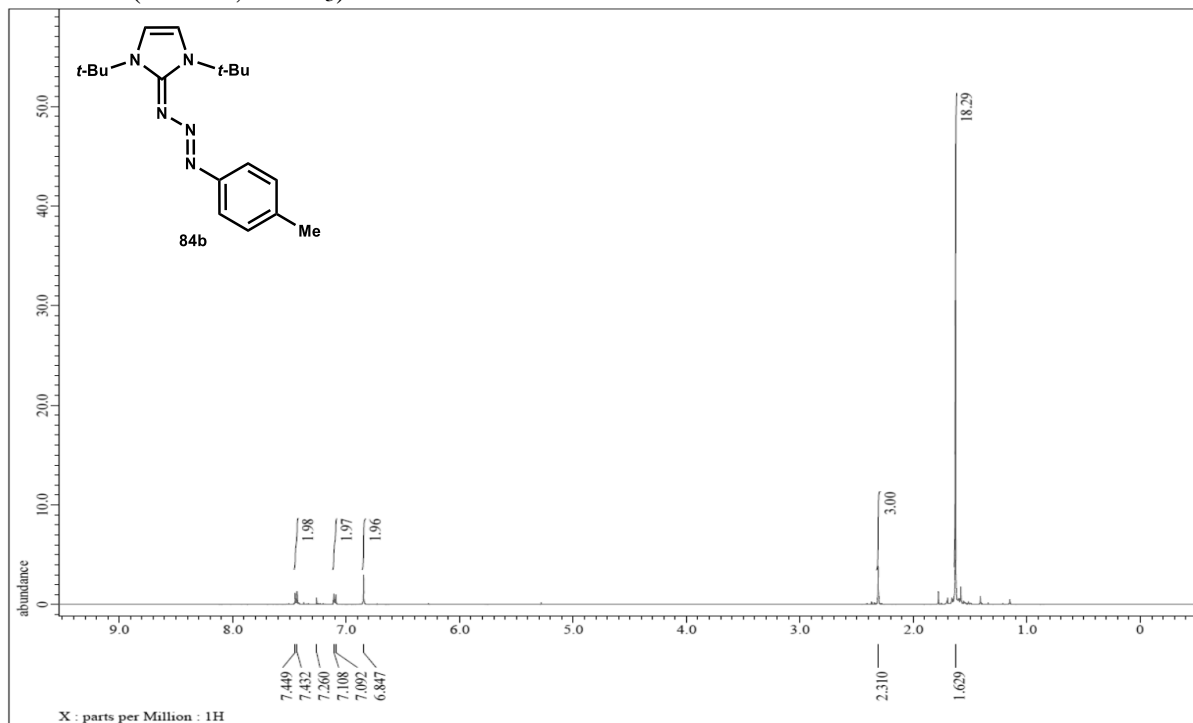
¹H NMR (500 Hz, CDCl₃)



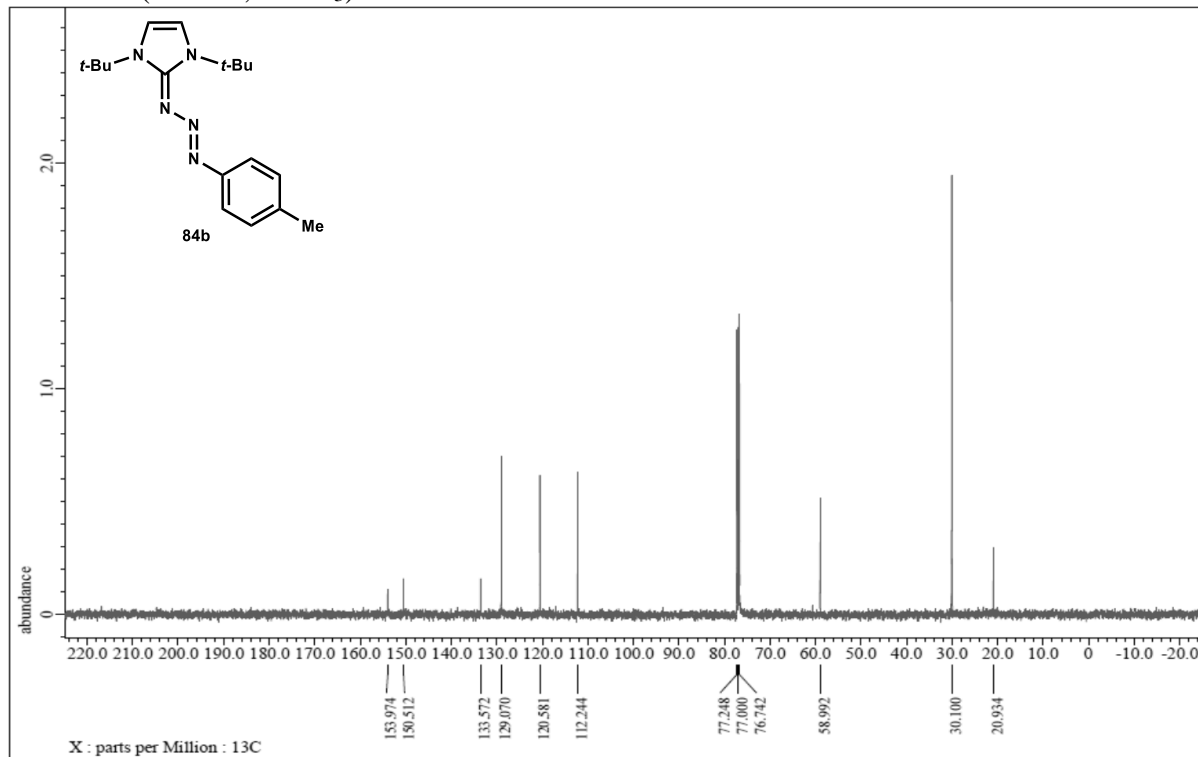
¹³C NMR (125 Hz, CDCl₃)



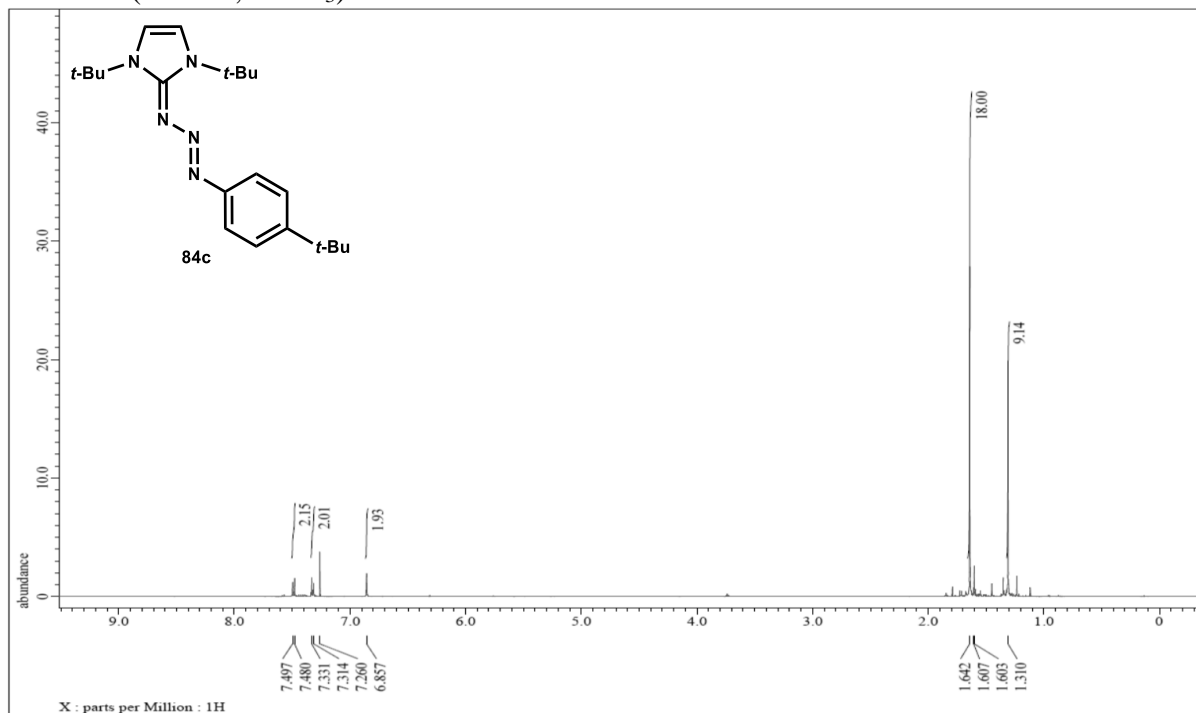
¹H NMR (500 Hz, CDCl₃)



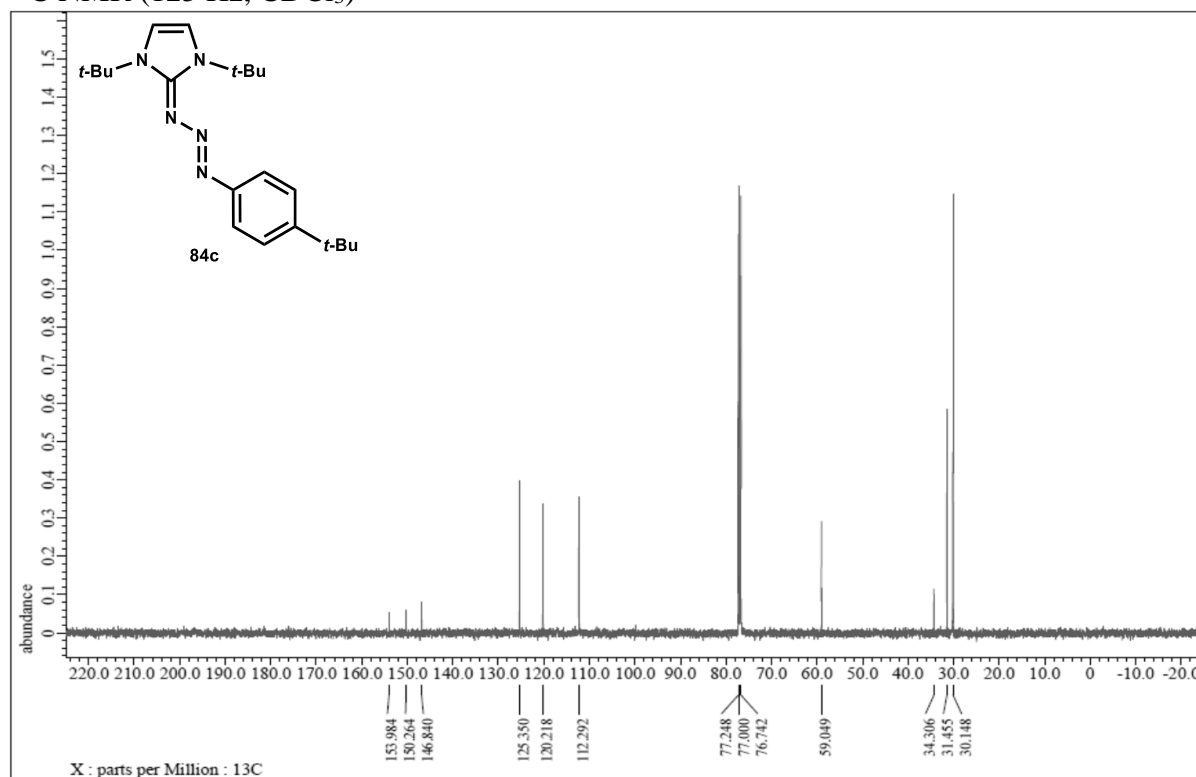
¹³C NMR (125 Hz, CDCl₃)



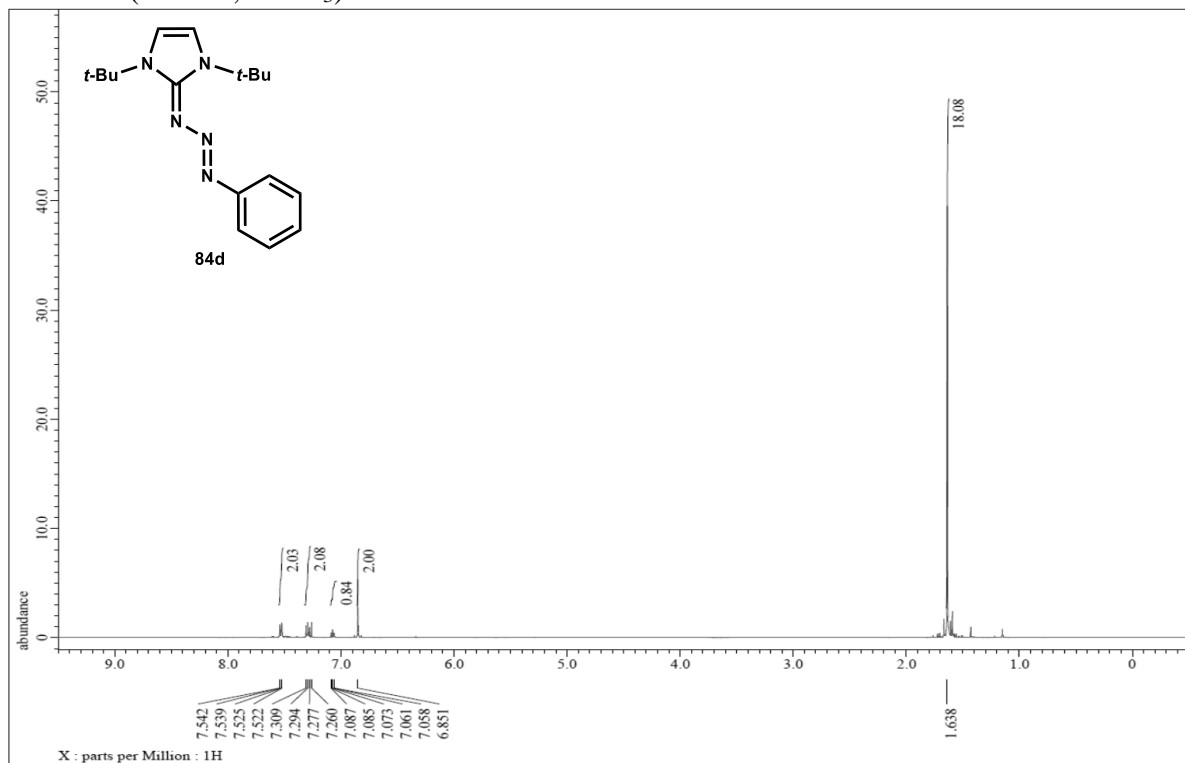
^1H NMR (500 Hz, CDCl_3)



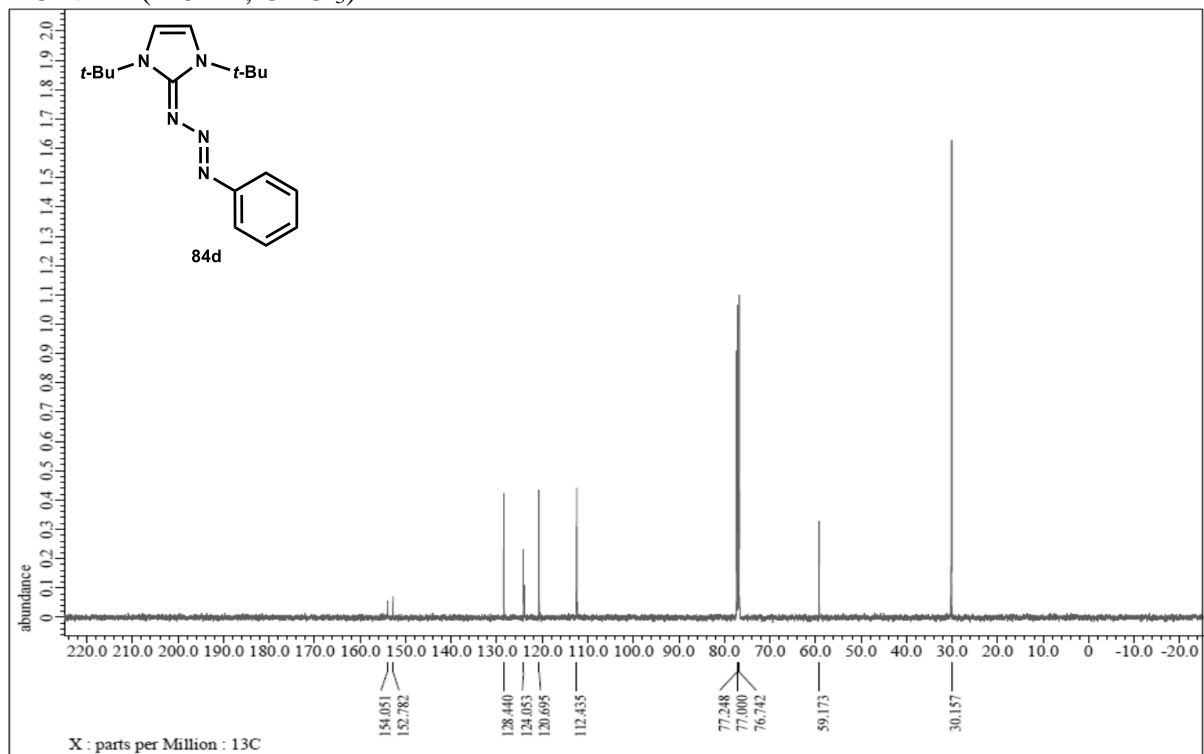
^{13}C NMR (125 Hz, CDCl_3)



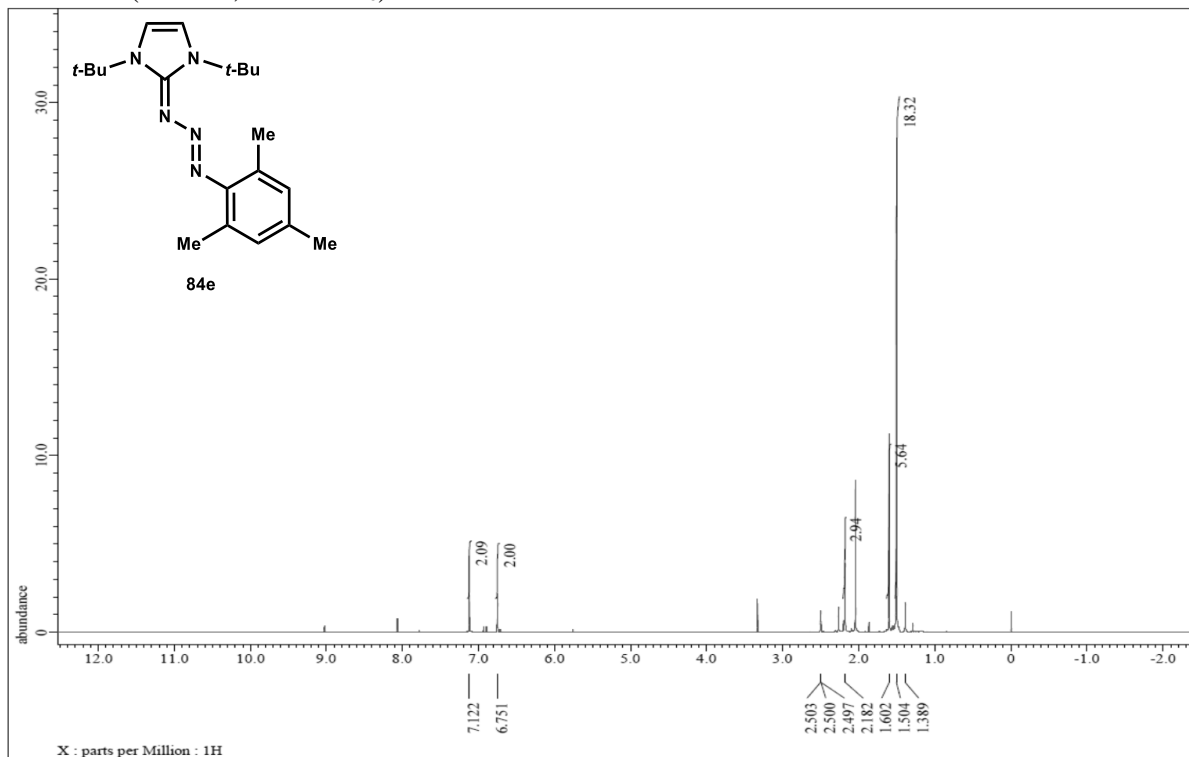
¹H NMR (500 Hz, CDCl₃)



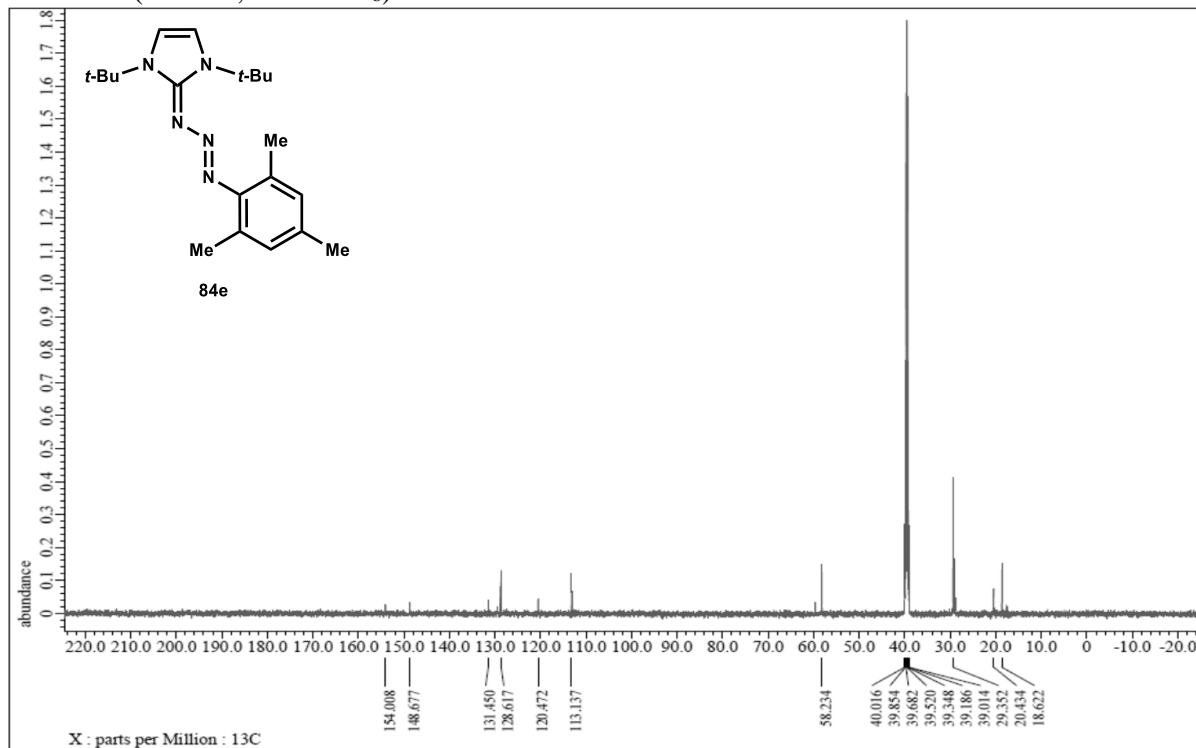
¹³C NMR (125 Hz, CDCl₃)



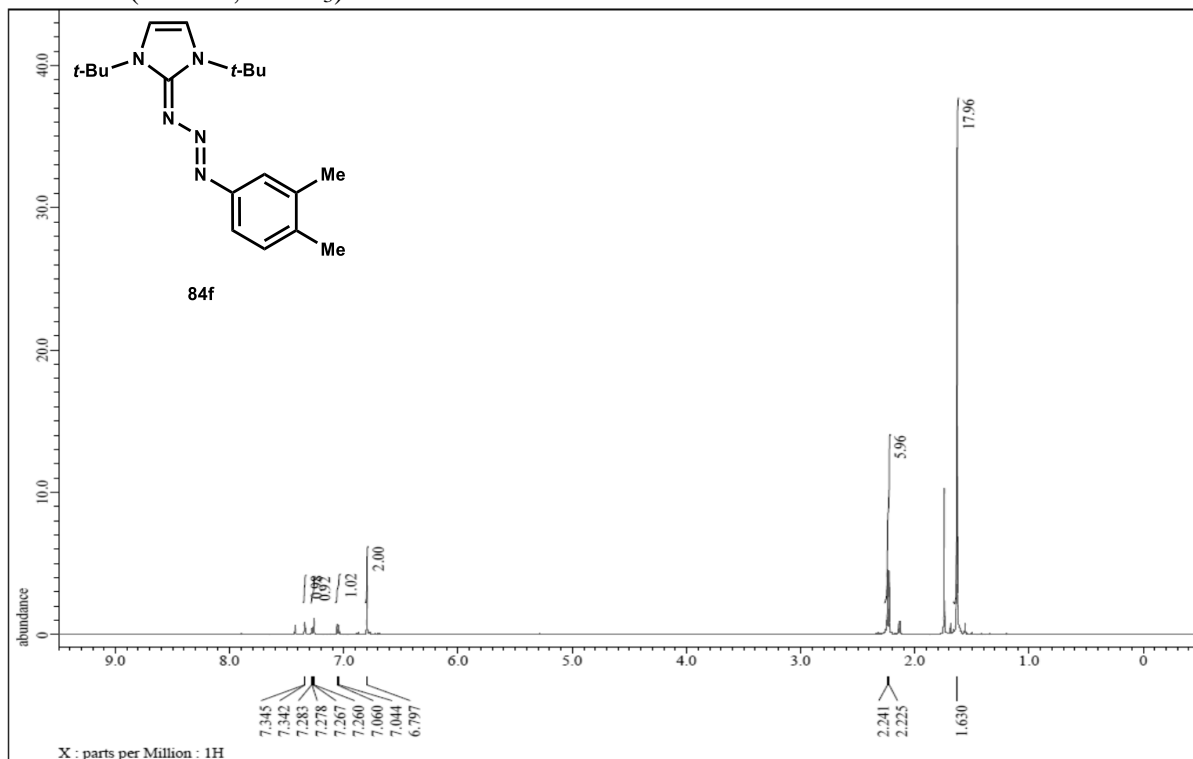
^1H NMR (500 Hz, $\text{DMSO-}d_6$)



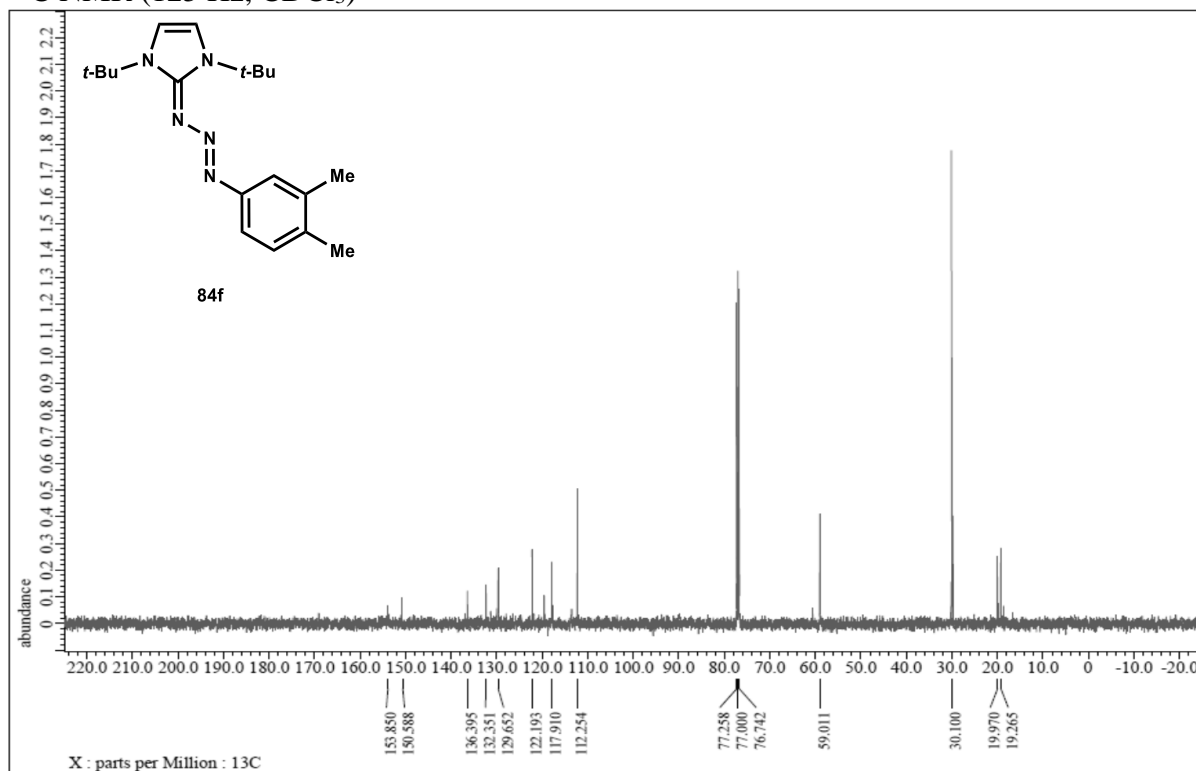
^{13}C NMR (125 Hz, $\text{DMSO-}d_6$)



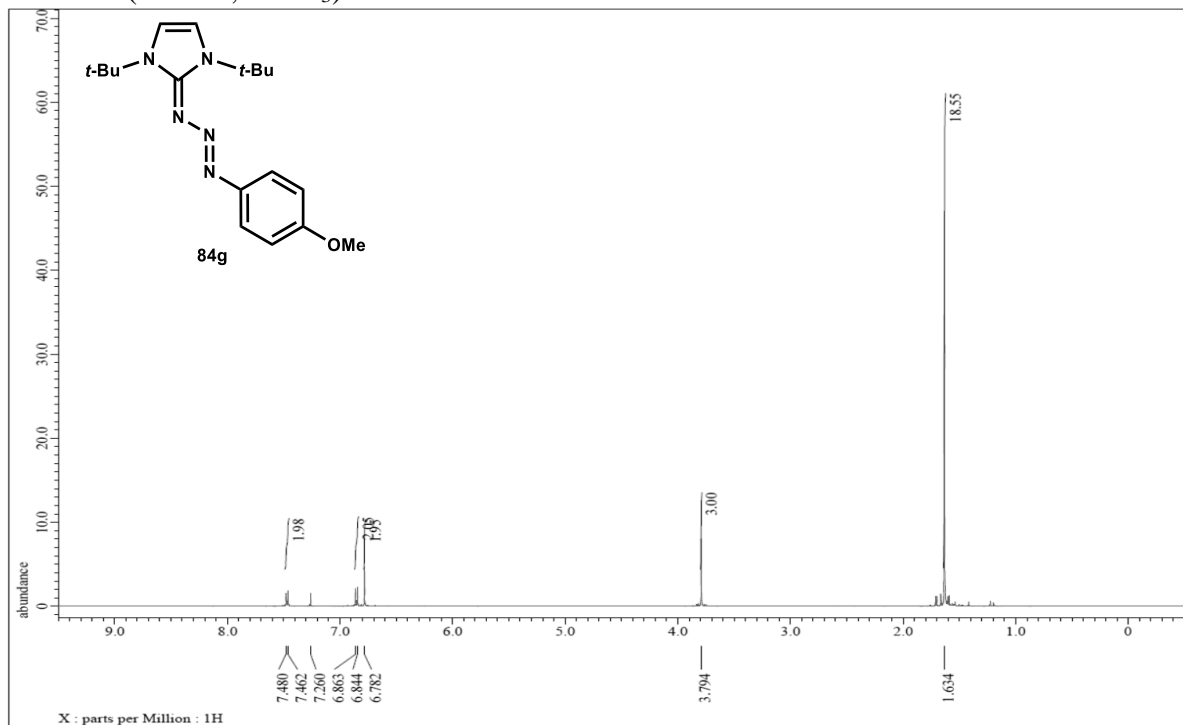
¹H NMR (500 Hz, CDCl₃)



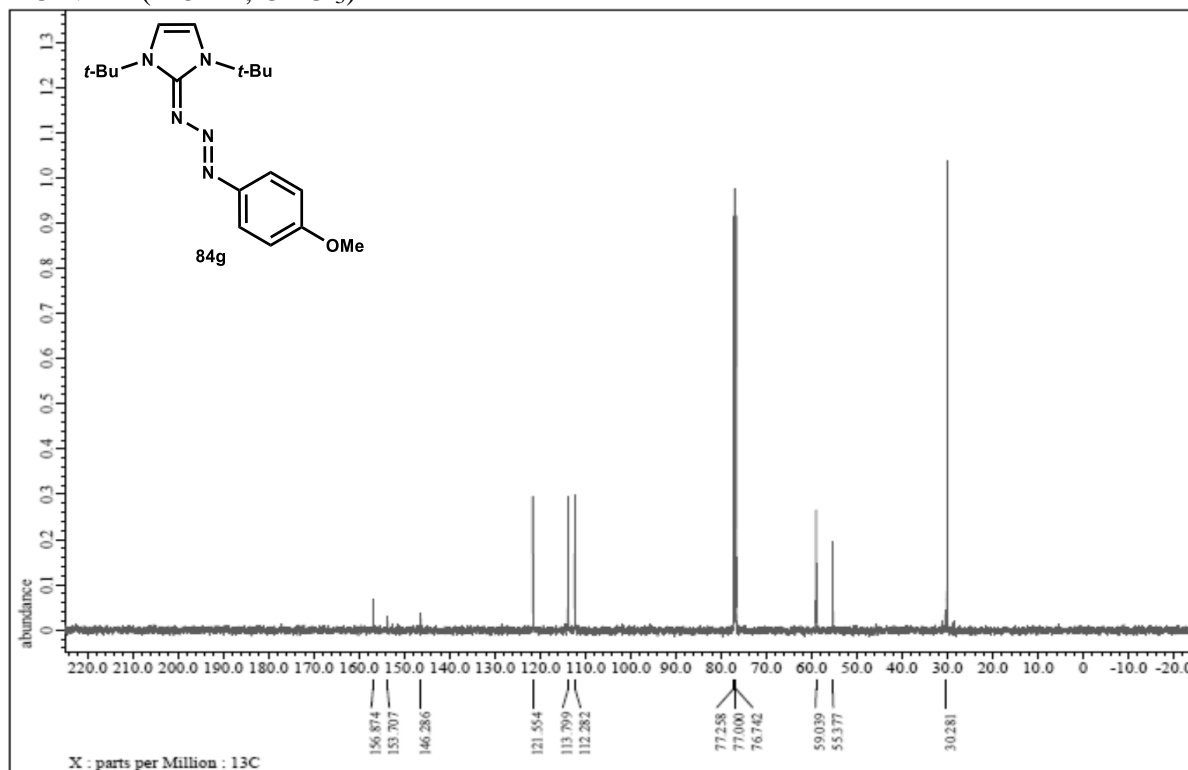
¹³C NMR (125 Hz, CDCl₃)



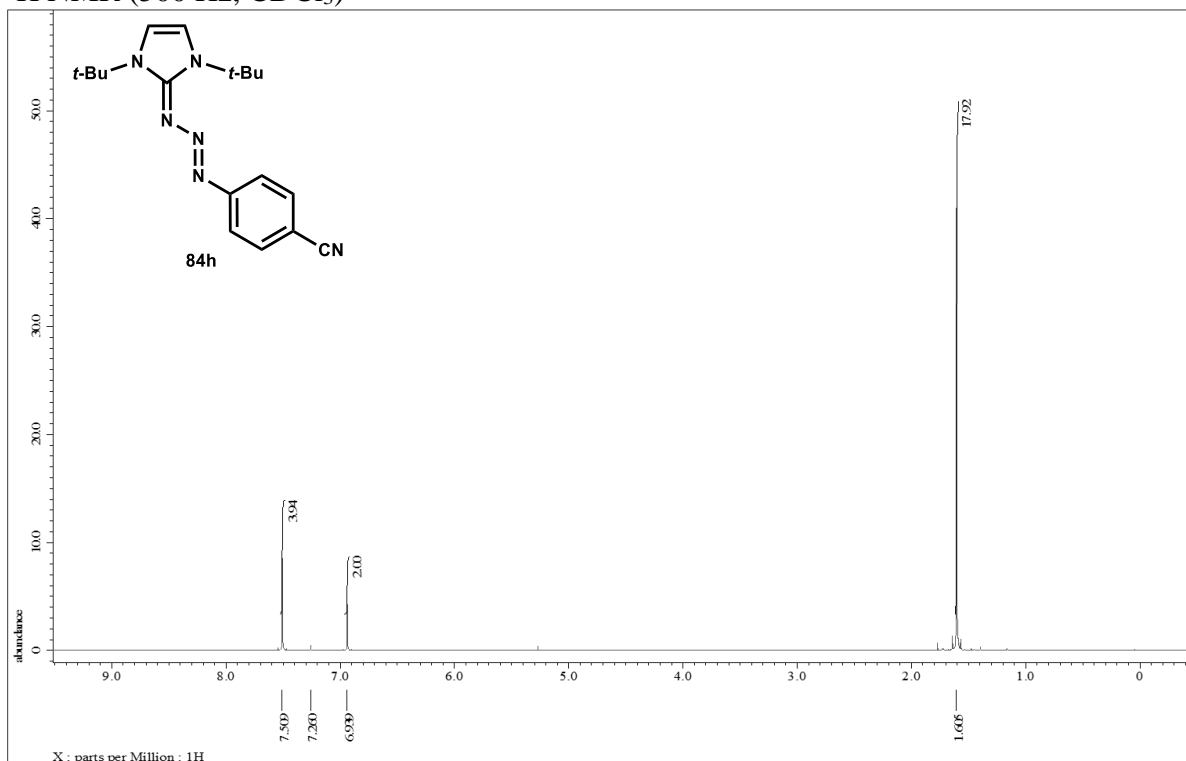
¹H NMR (500 Hz, CDCl₃)



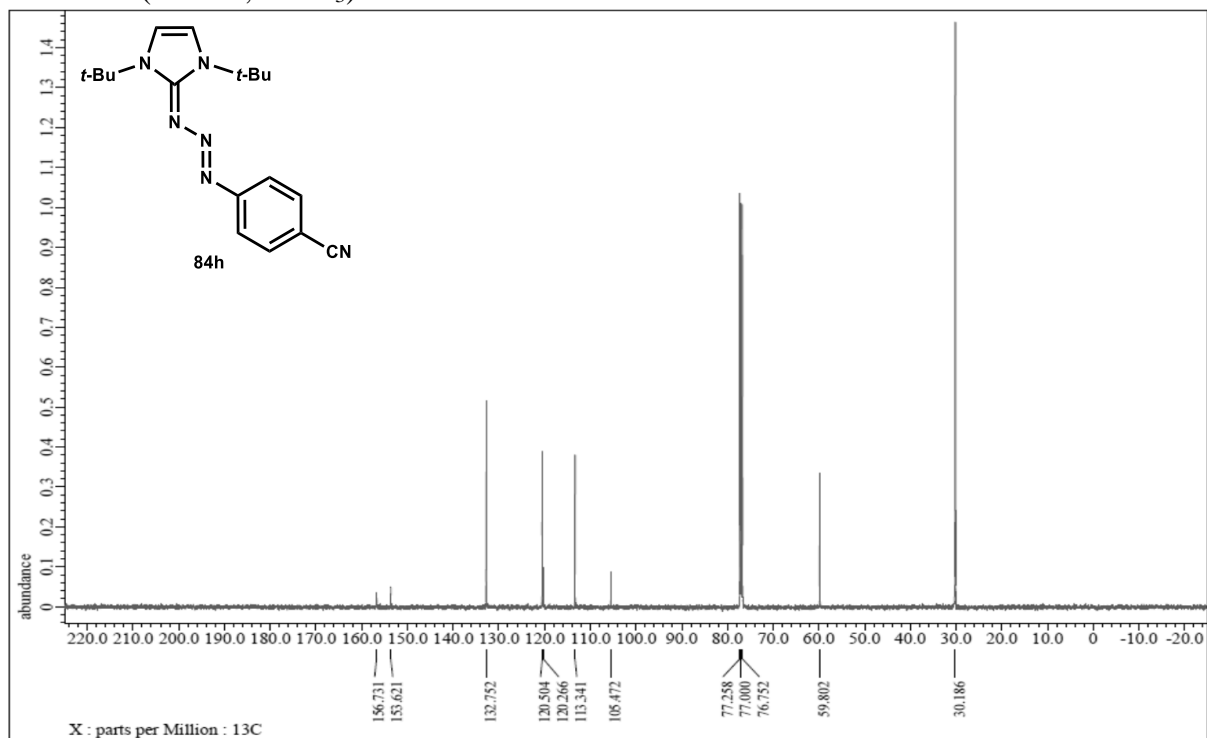
¹³C NMR (125 Hz, CDCl₃)



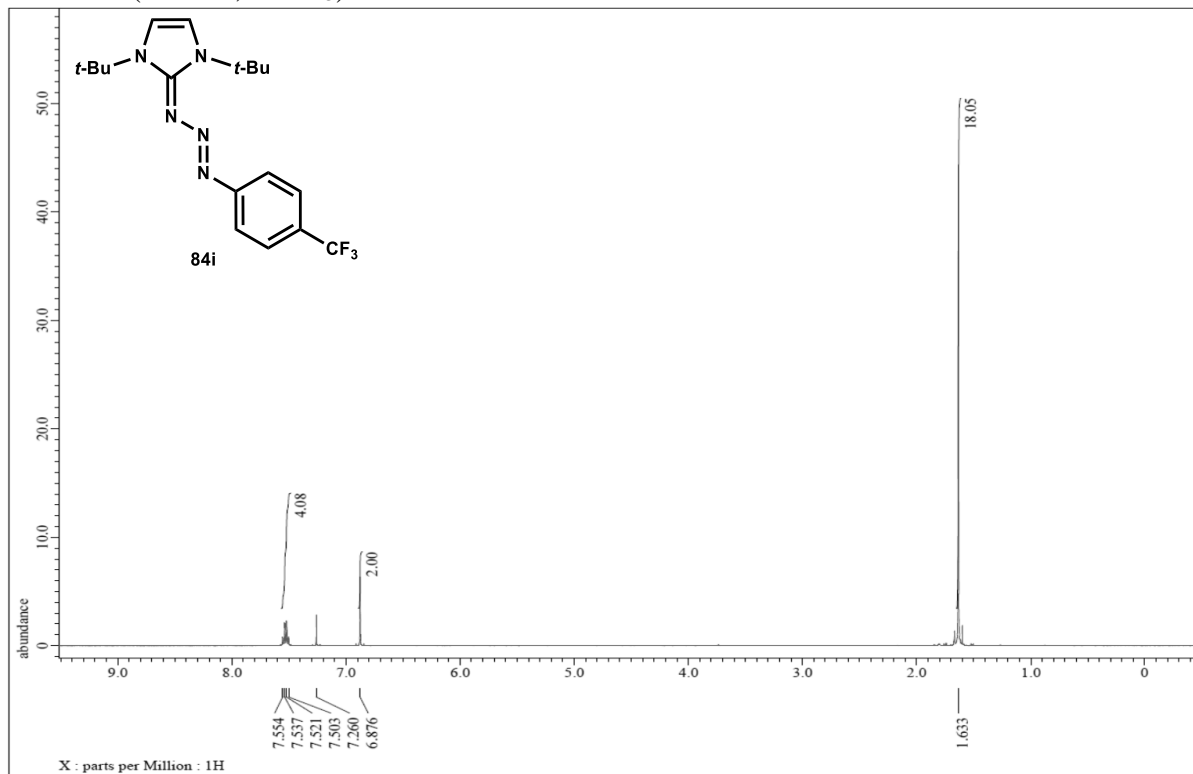
¹H NMR (500 Hz, CDCl₃)



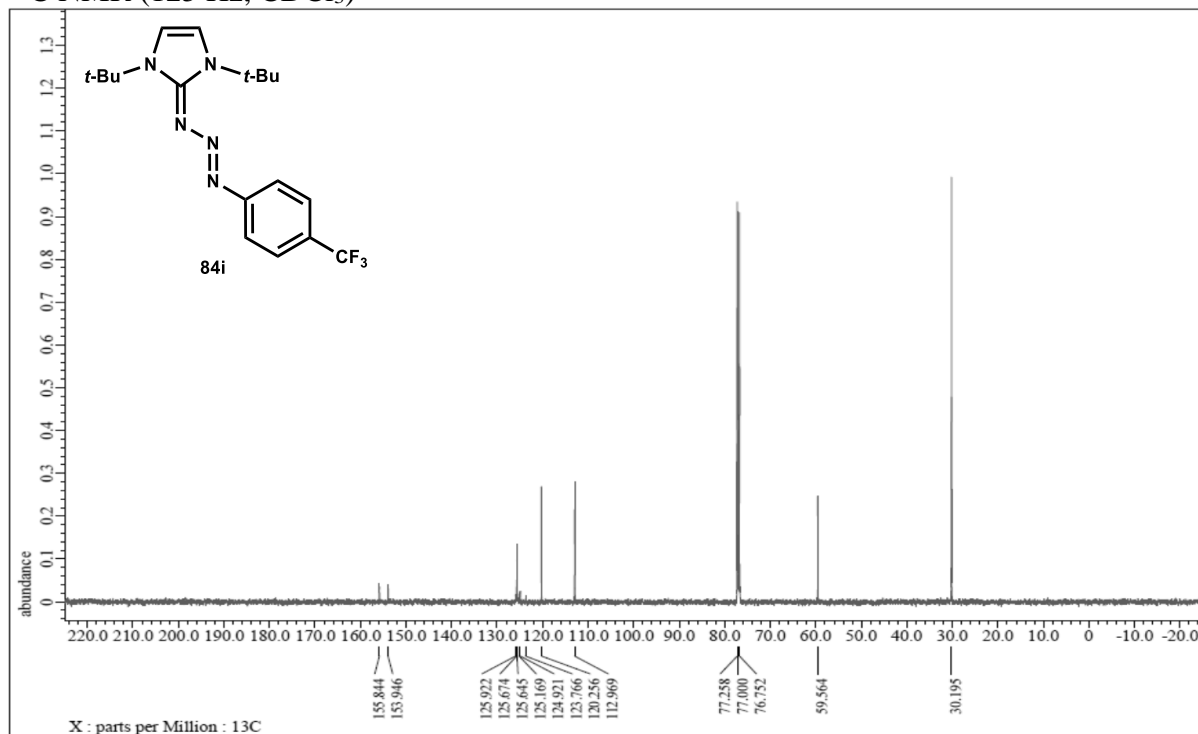
¹³C NMR (125 Hz, CDCl₃)



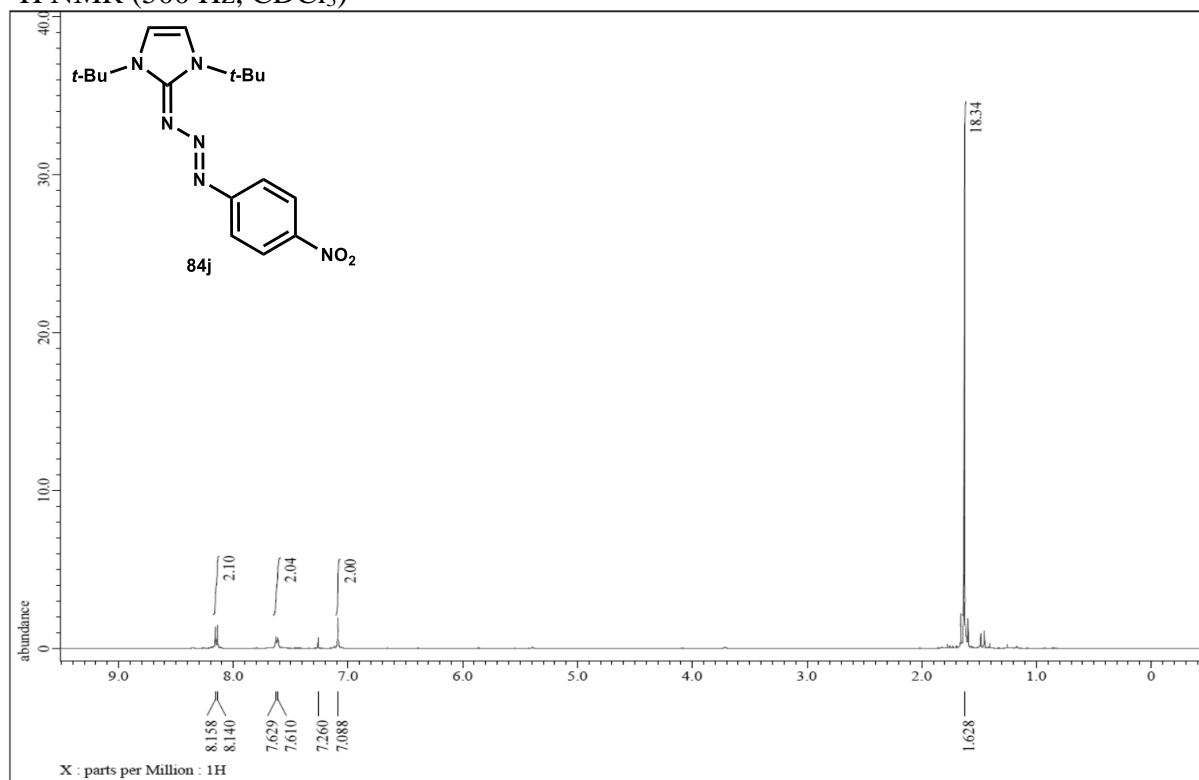
¹H NMR (500 Hz, CDCl₃)



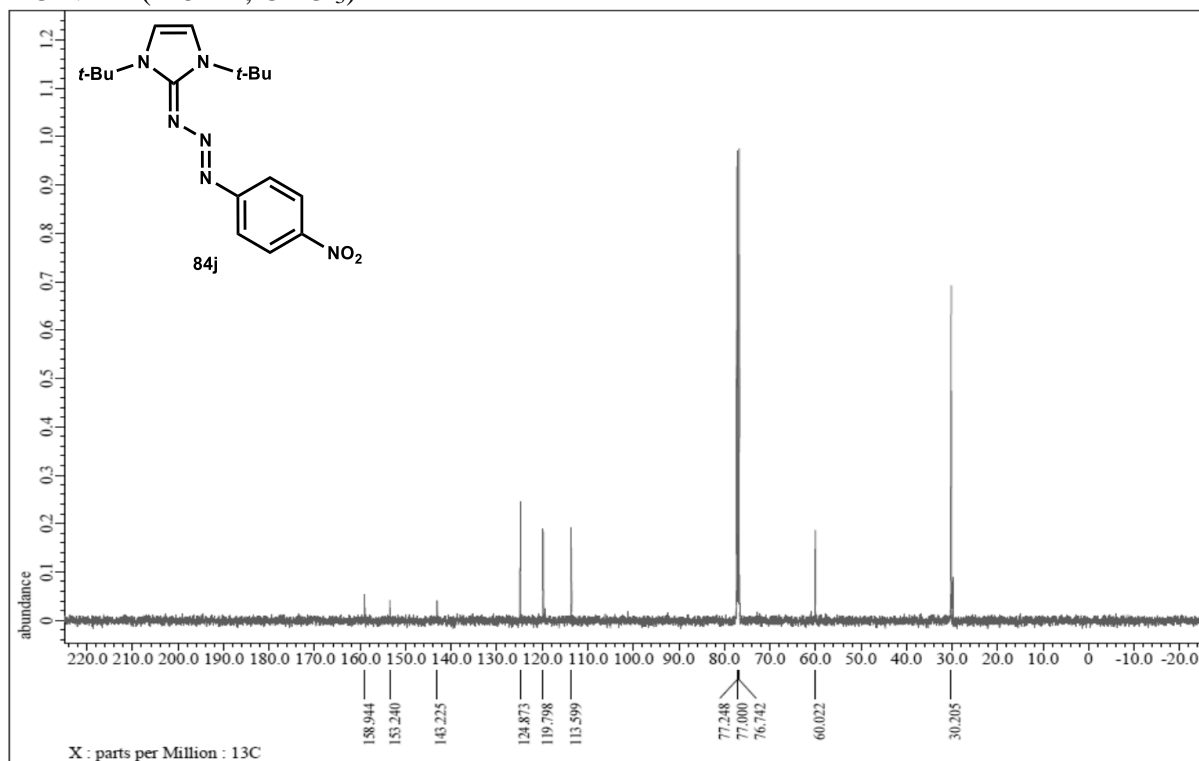
¹³C NMR (125 Hz, CDCl₃)



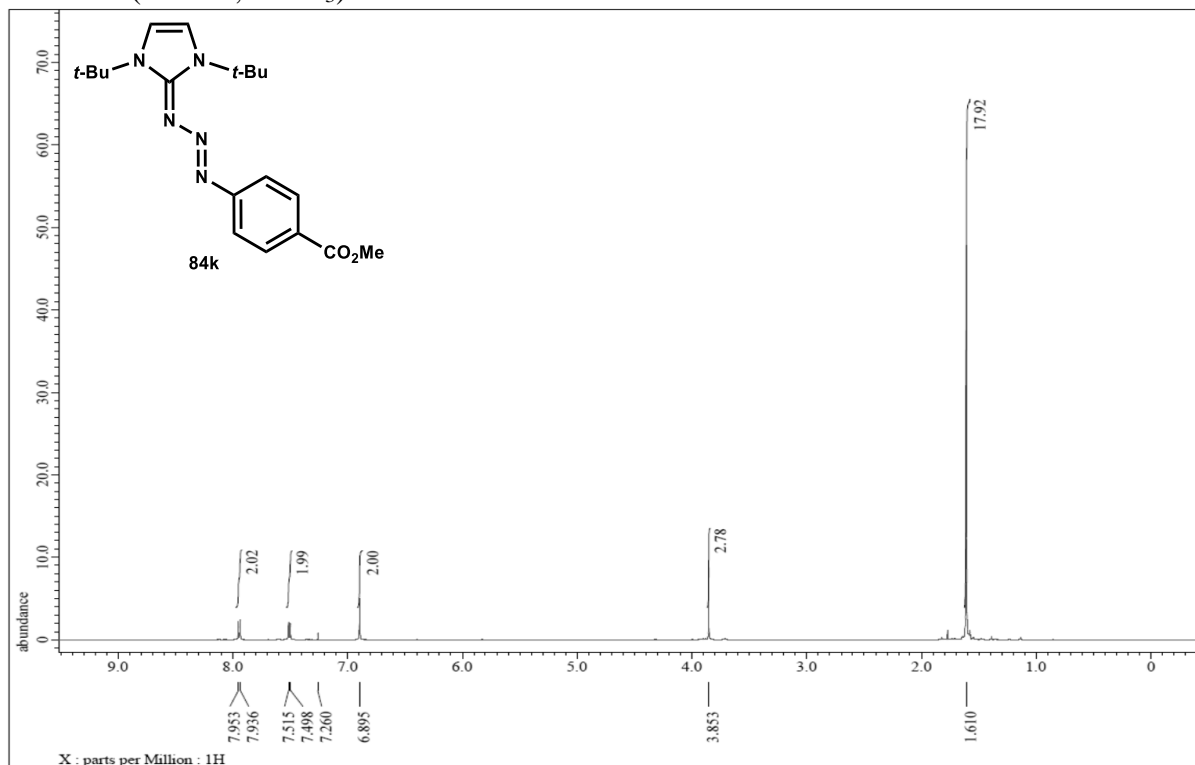
¹H NMR (500 Hz, CDCl₃)



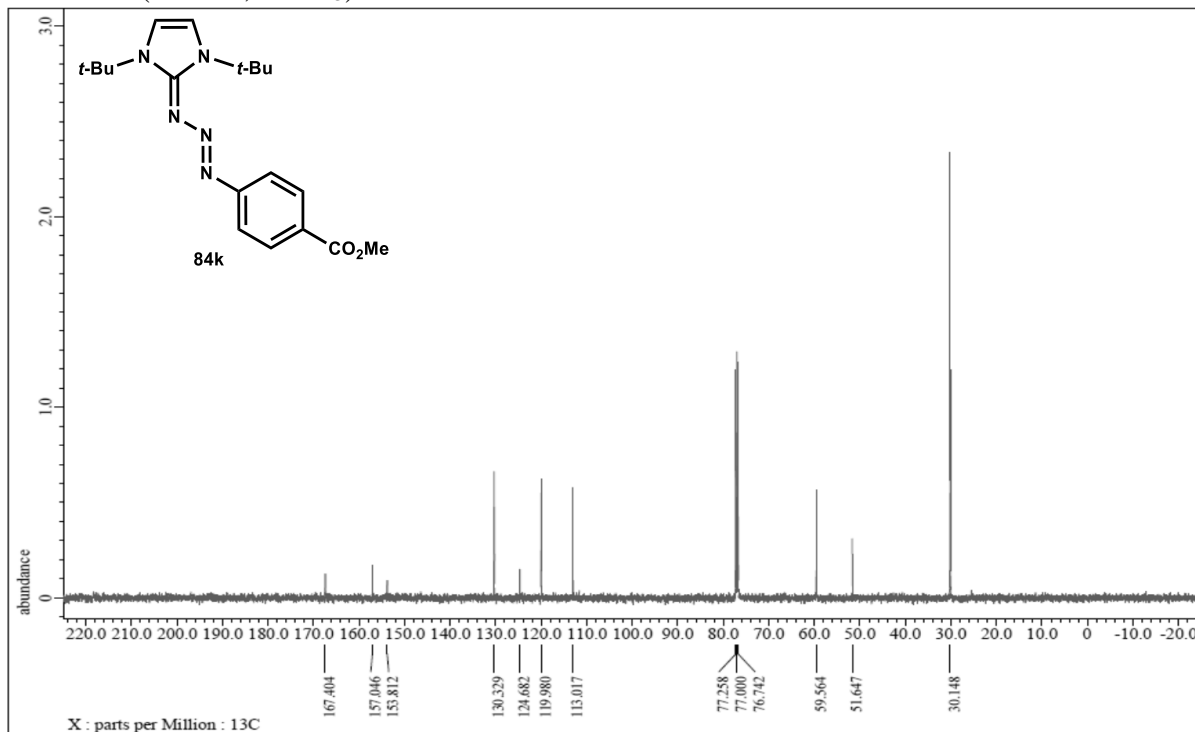
¹³C NMR (125 Hz, CDCl₃)



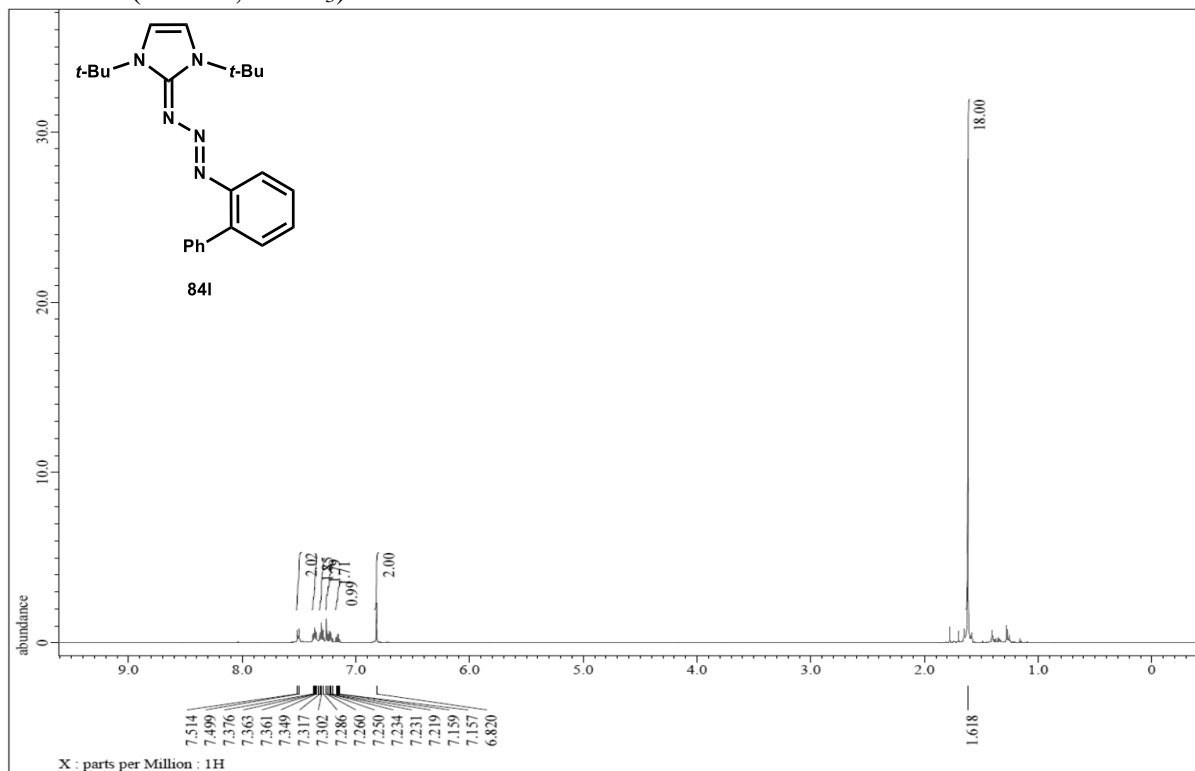
^1H NMR (500 Hz, CDCl_3)



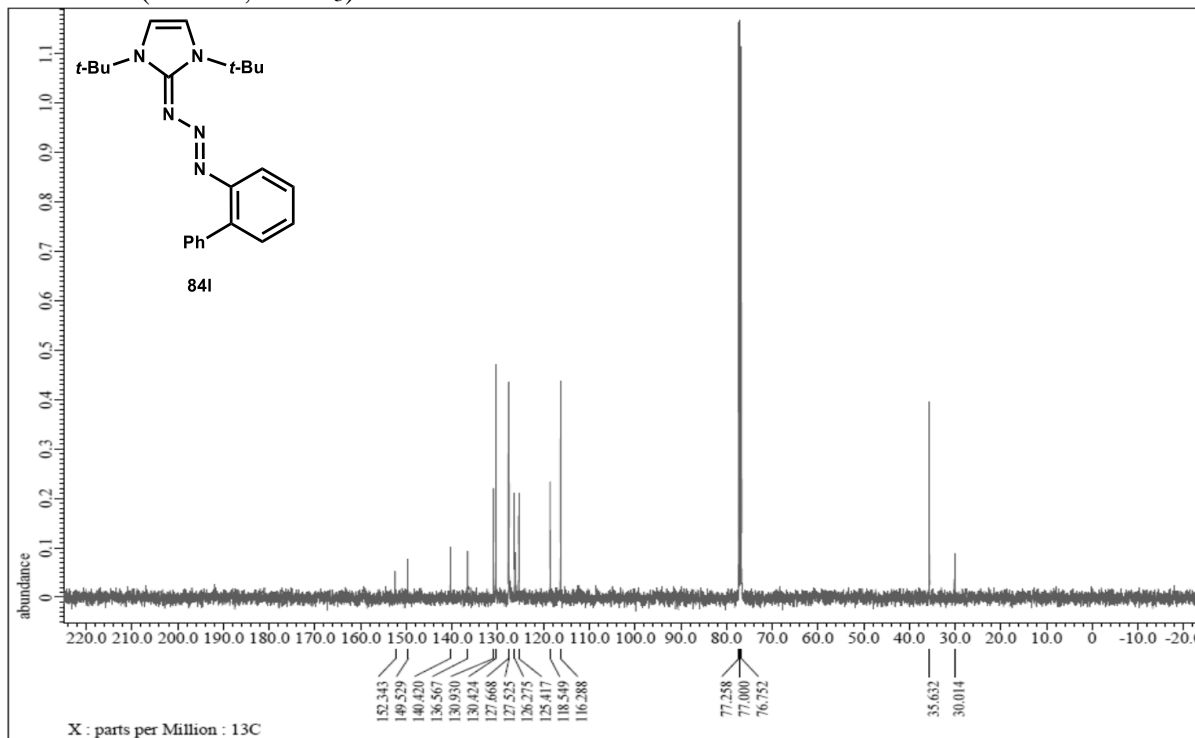
^{13}C NMR (125 Hz, CDCl_3)



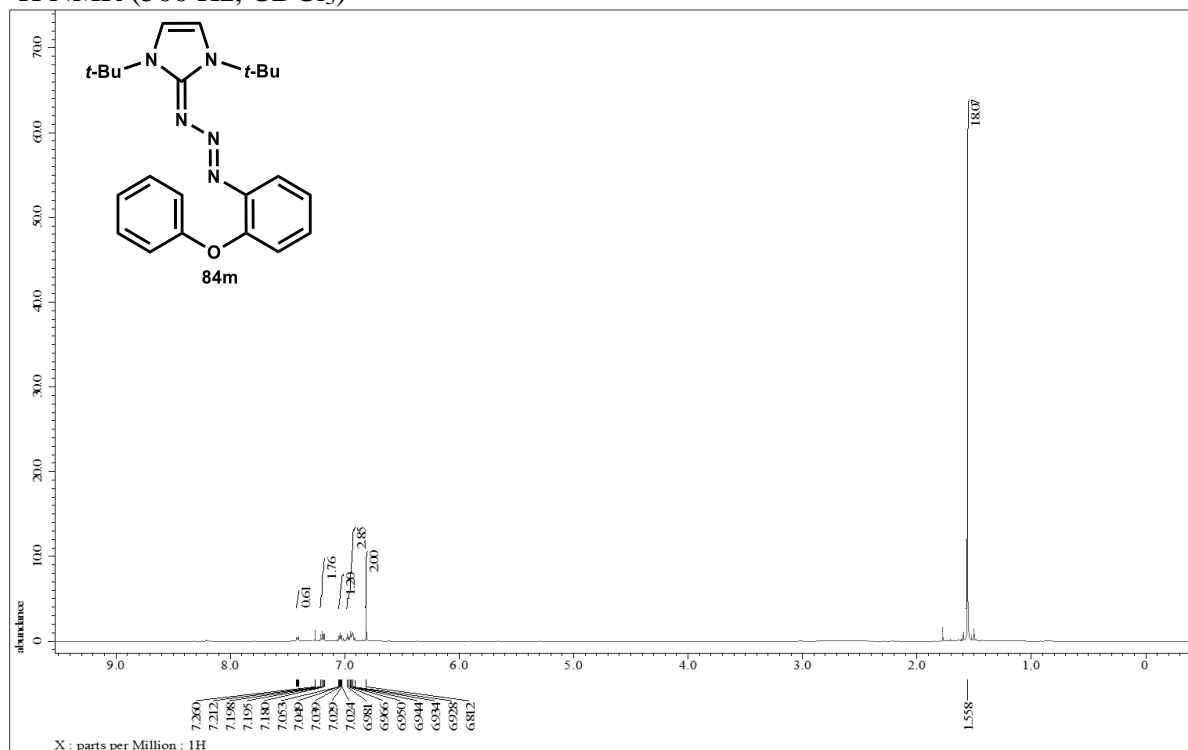
¹H NMR (500 Hz, CDCl₃)



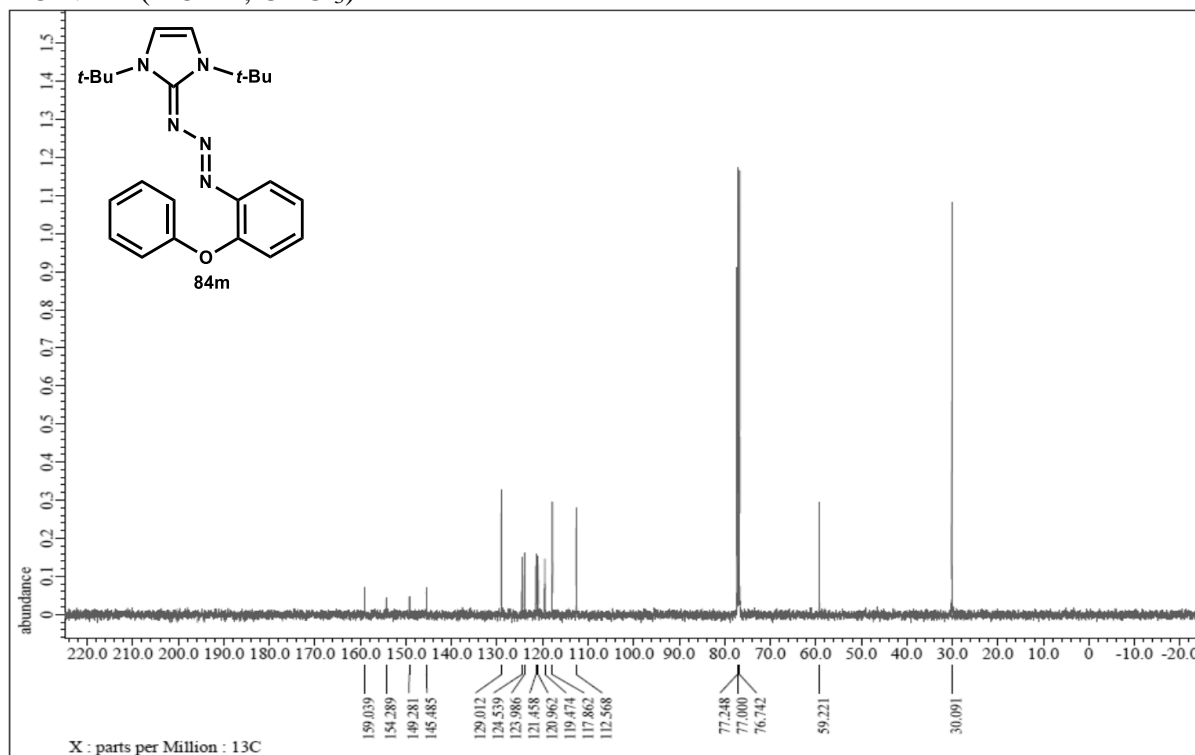
¹³C NMR (125 Hz, CDCl₃)



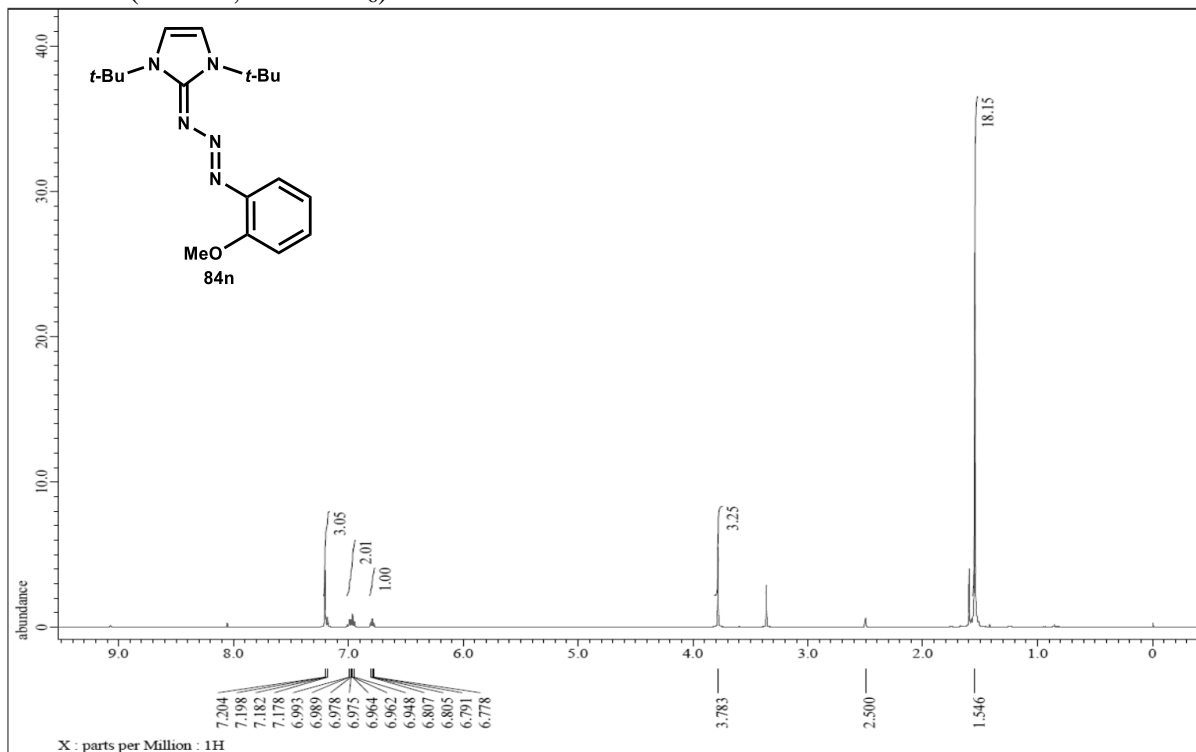
¹H NMR (500 Hz, CDCl₃)



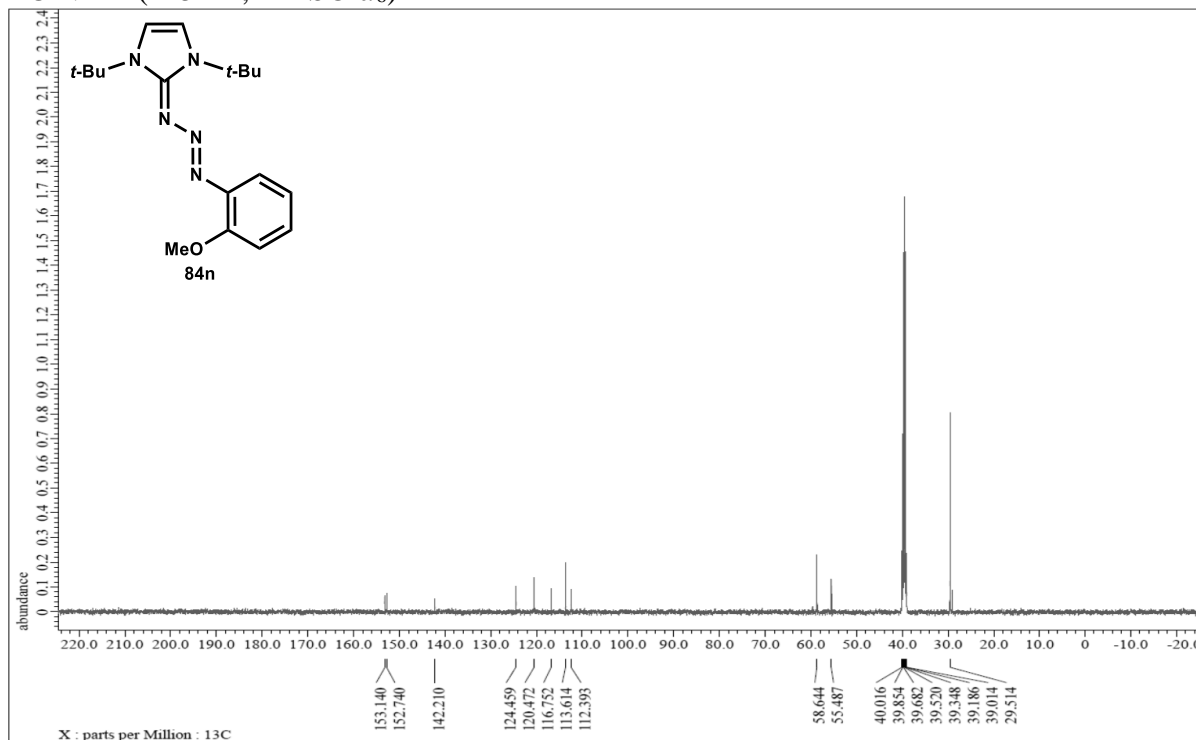
¹³C NMR (125 Hz, CDCl₃)



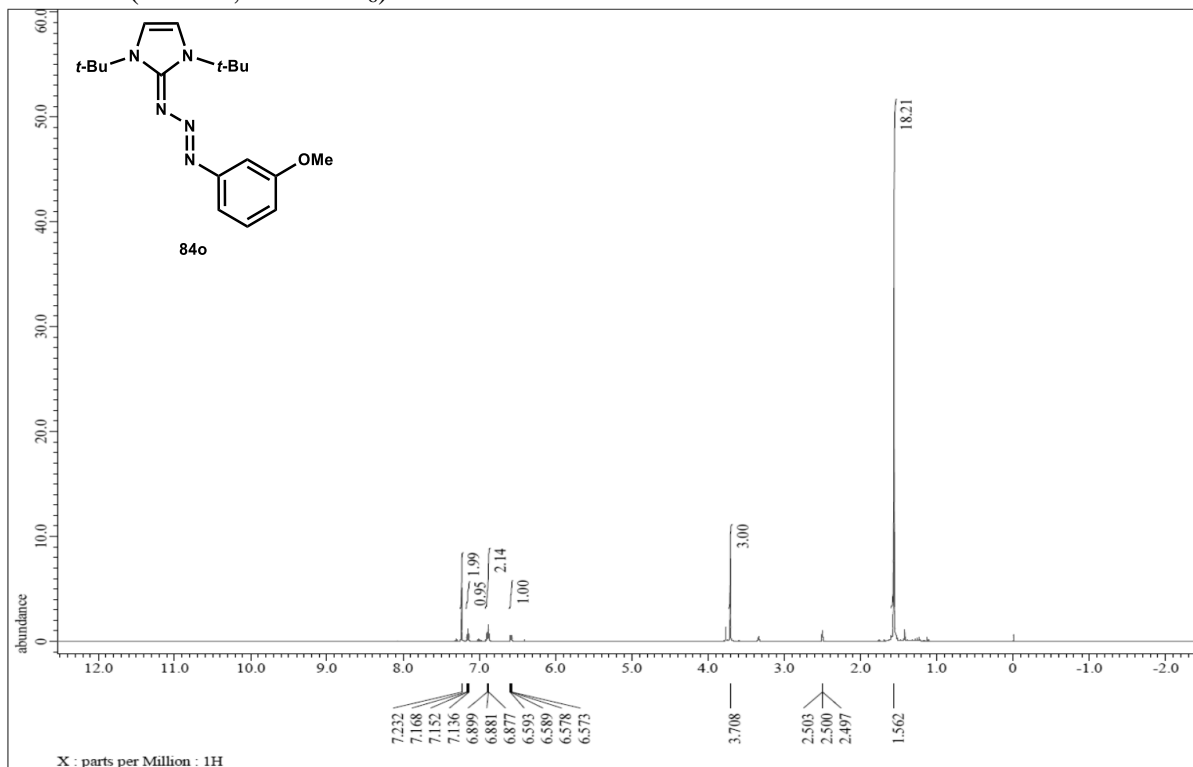
¹H NMR (500 Hz, DMSO-*d*₆)



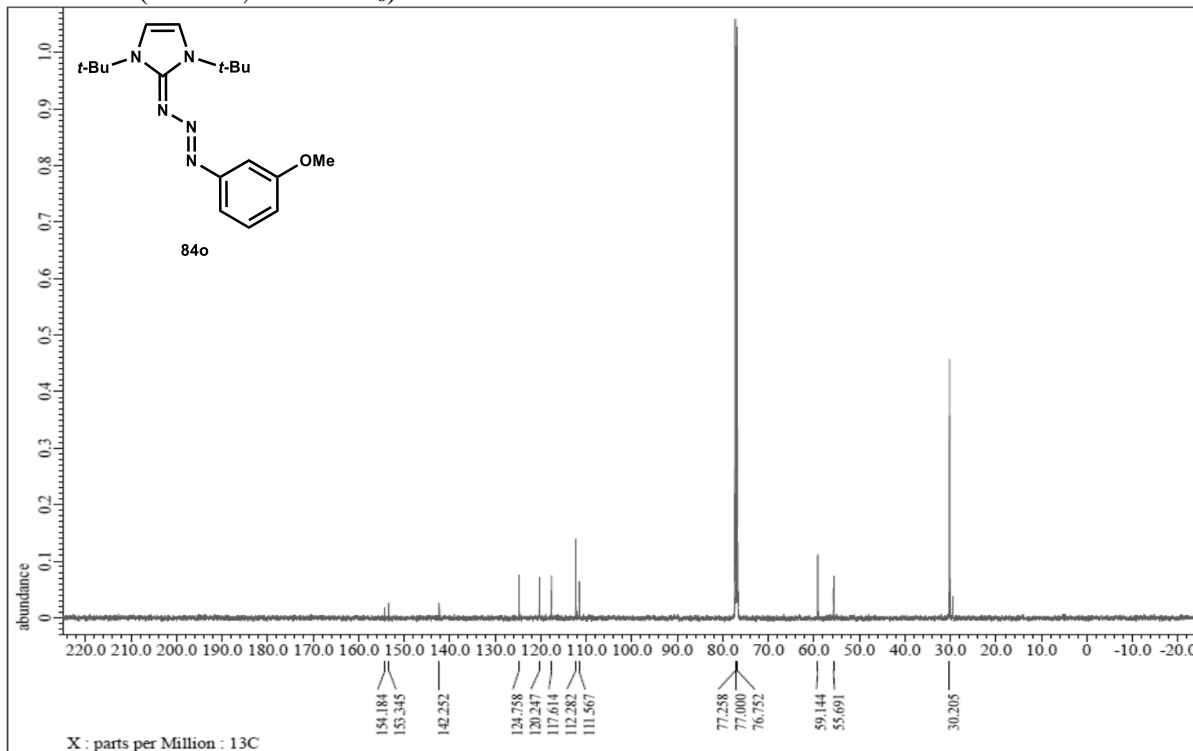
¹³C NMR (125 Hz, DMSO-*d*₆)



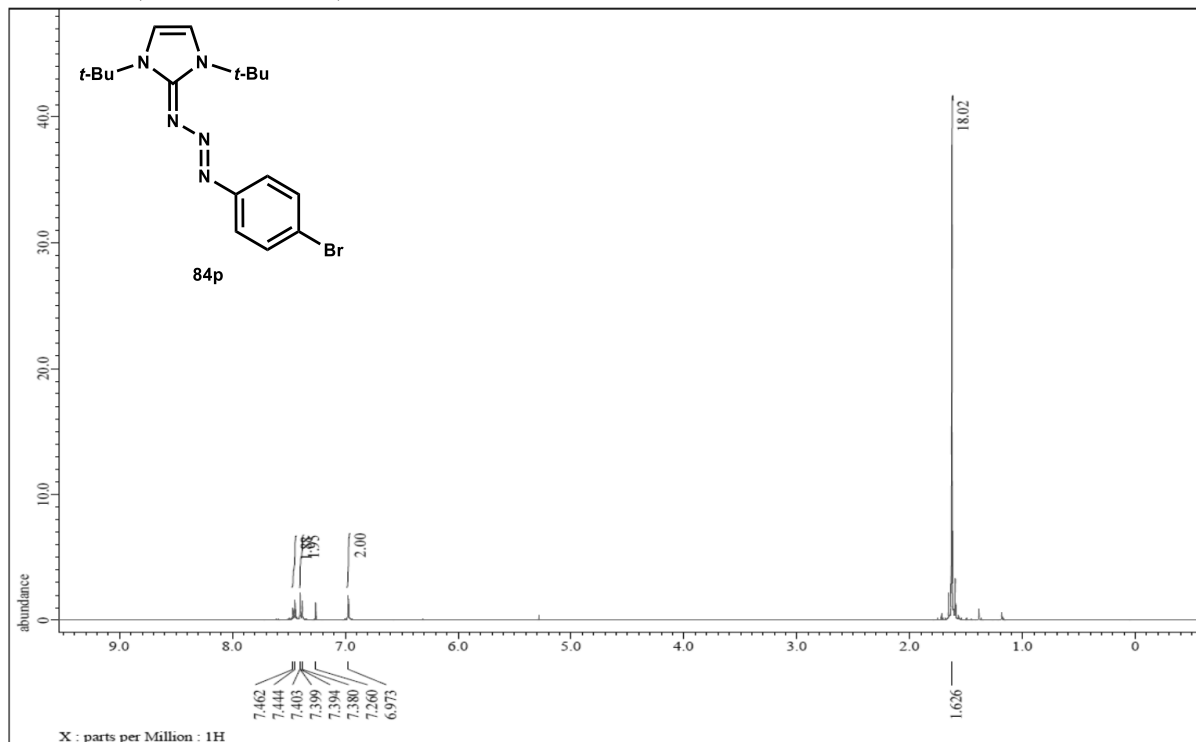
^1H NMR (500 Hz, $\text{DMSO-}d_6$)



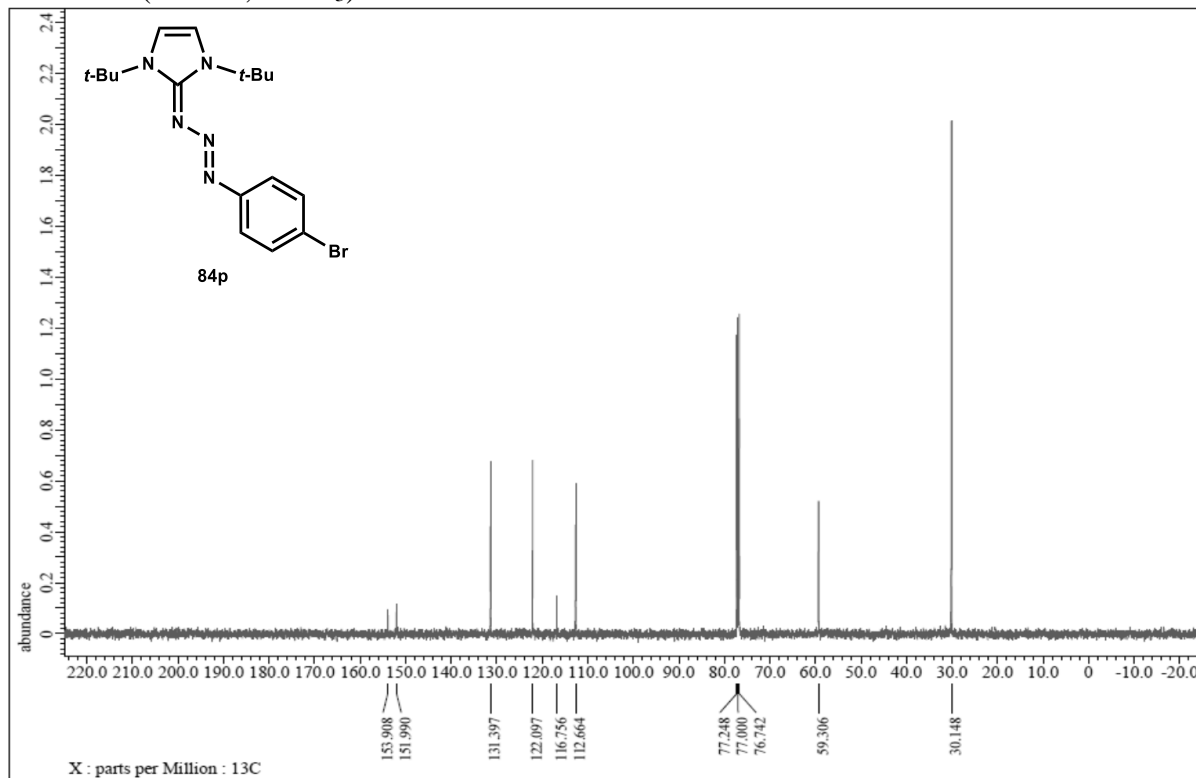
^{13}C NMR (125 Hz, $\text{DMSO-}d_6$)



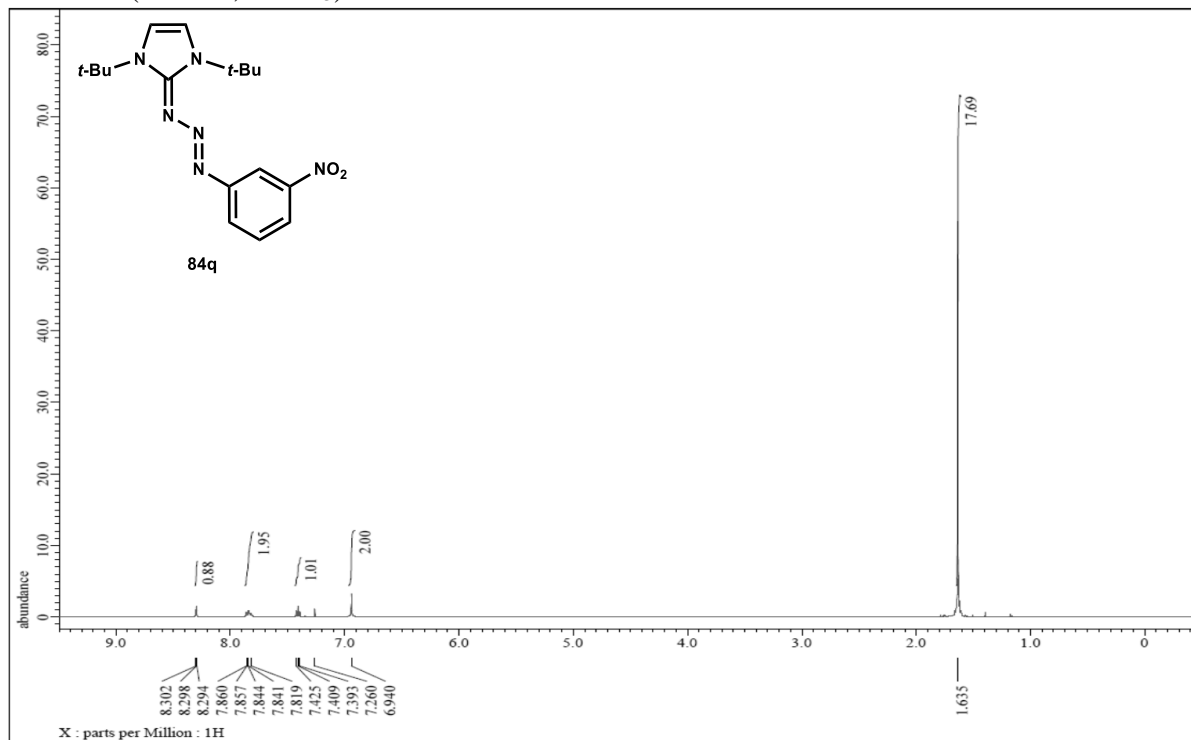
^1H NMR (500 Hz, CDCl_3)



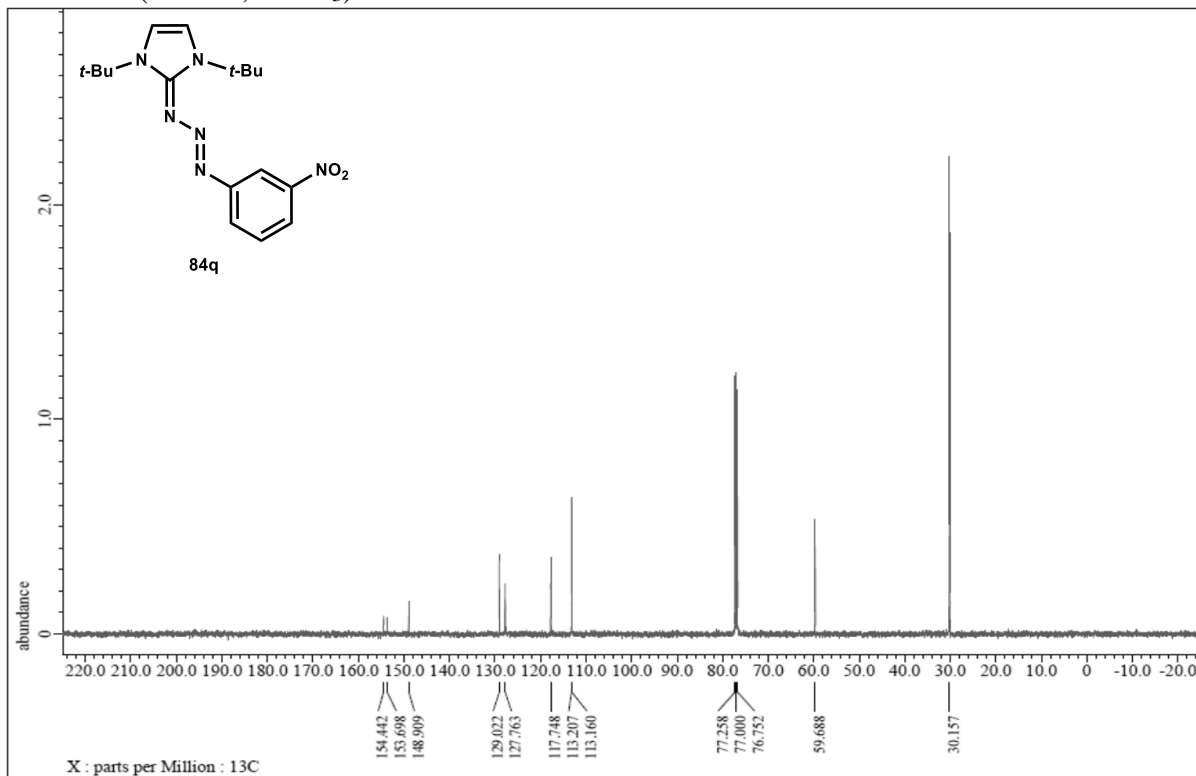
^{13}C NMR (125 Hz, CDCl_3)



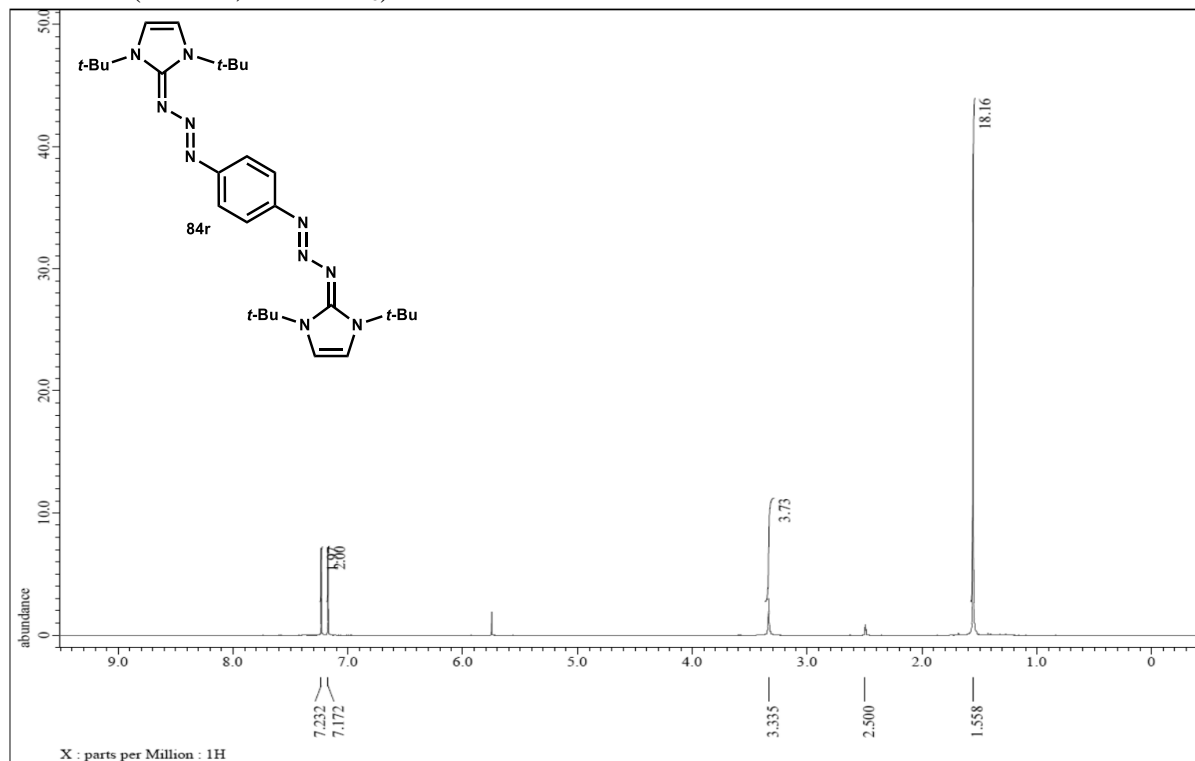
¹H NMR (500 Hz, CDCl₃)



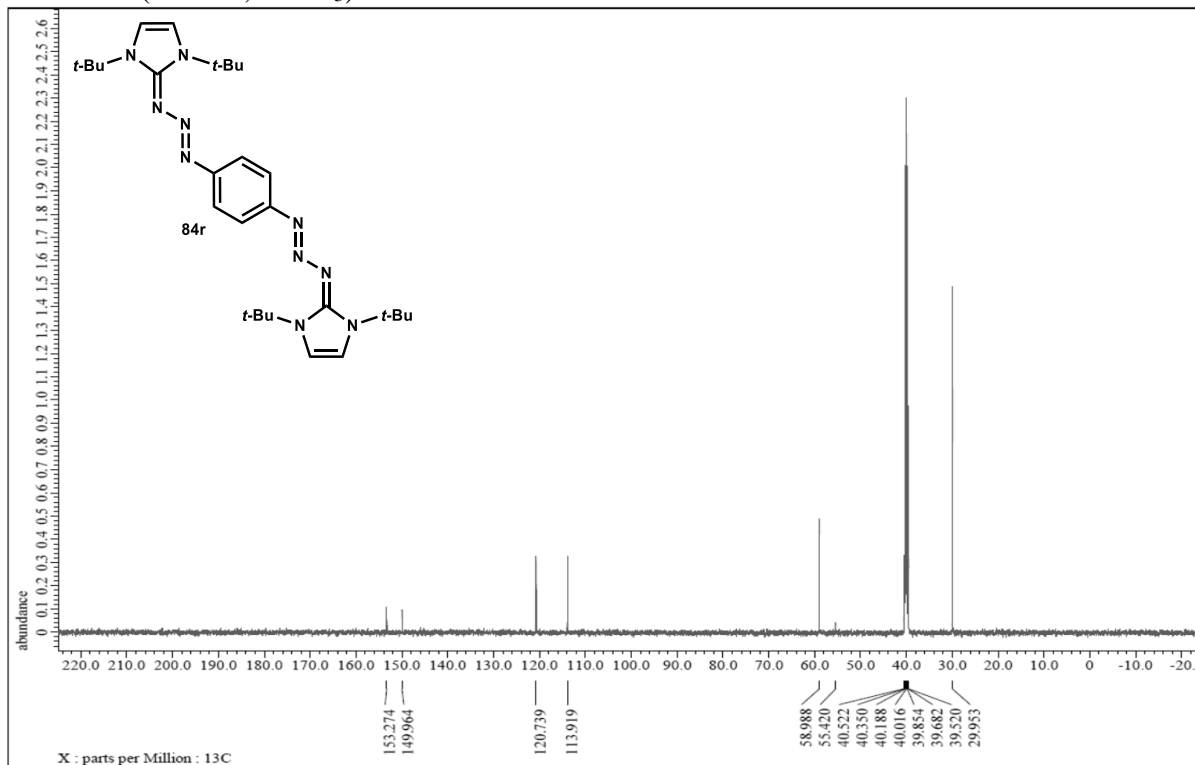
¹³C NMR (125 Hz, CDCl₃)



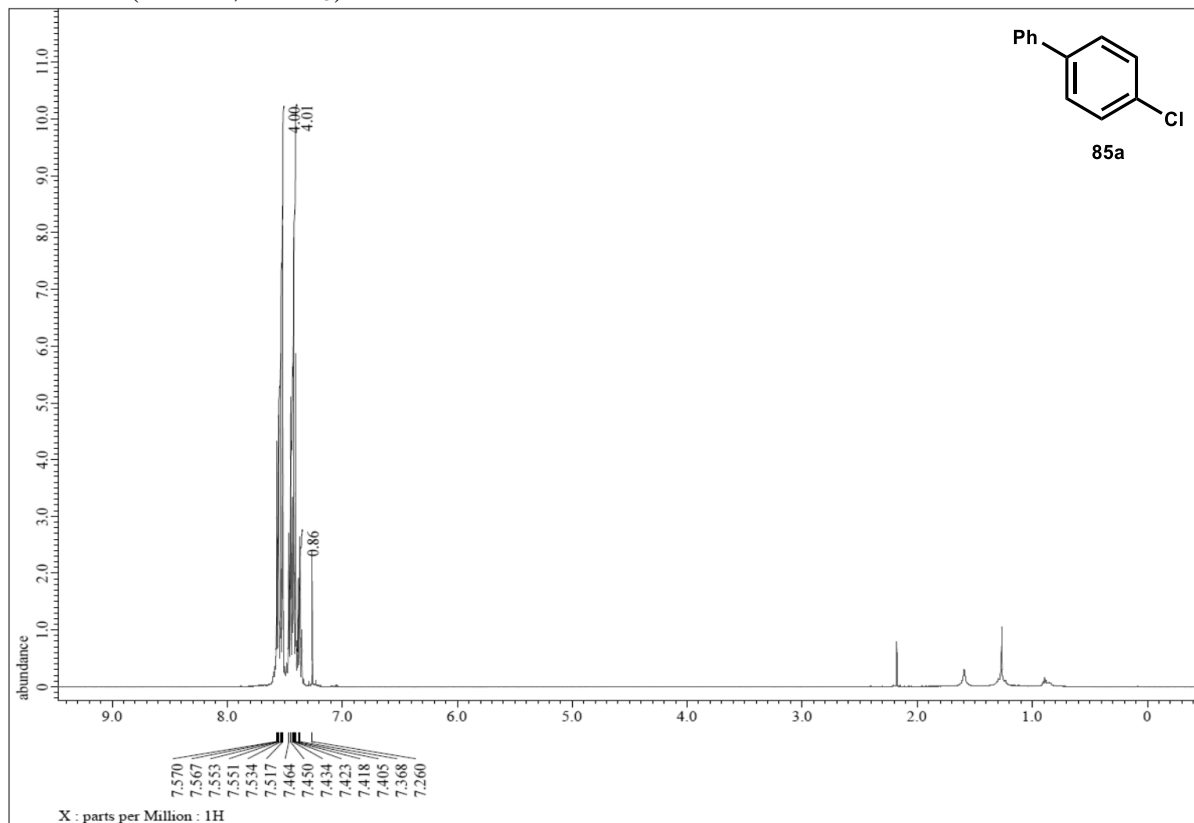
^1H NMR (500 Hz, $\text{DMSO}-d_6$)



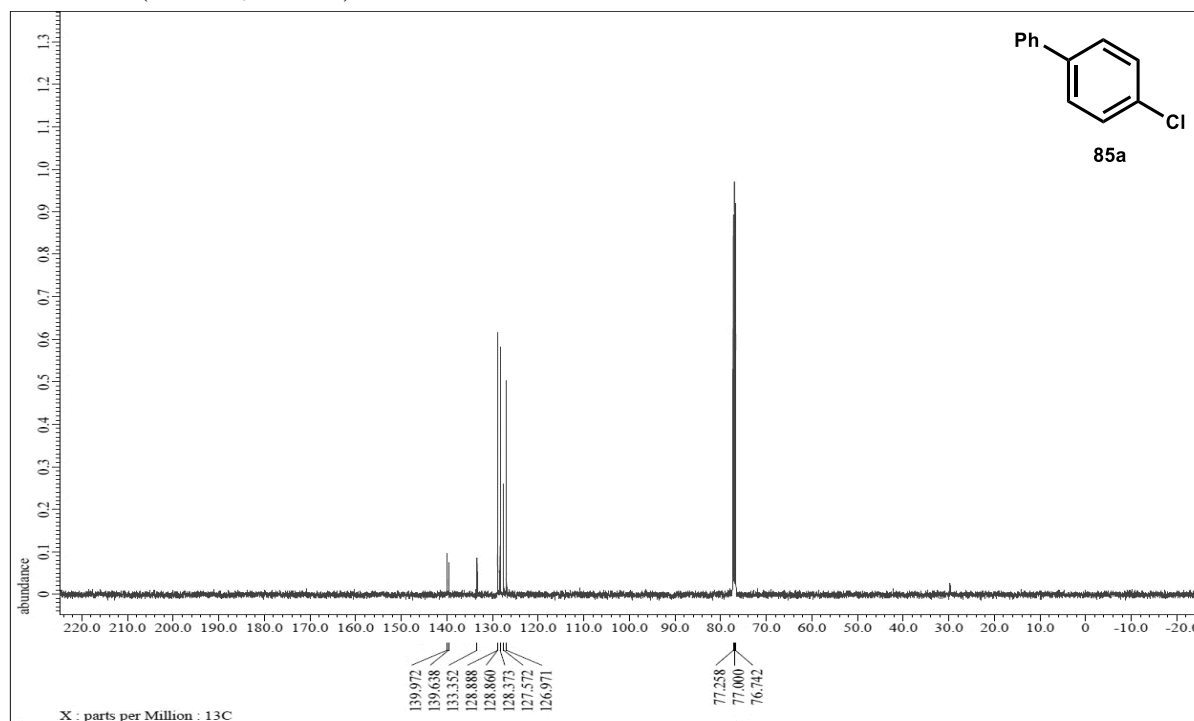
^{13}C NMR (125 Hz, CDCl_3)



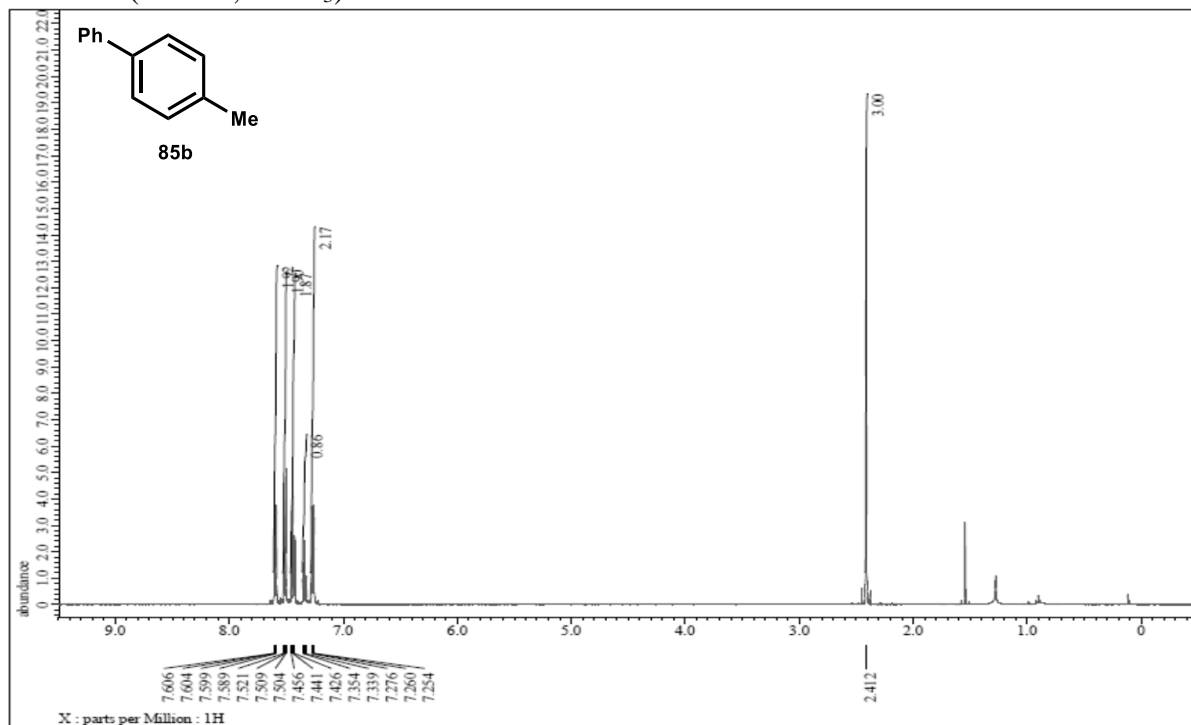
^1H NMR (500 Hz, CDCl_3)



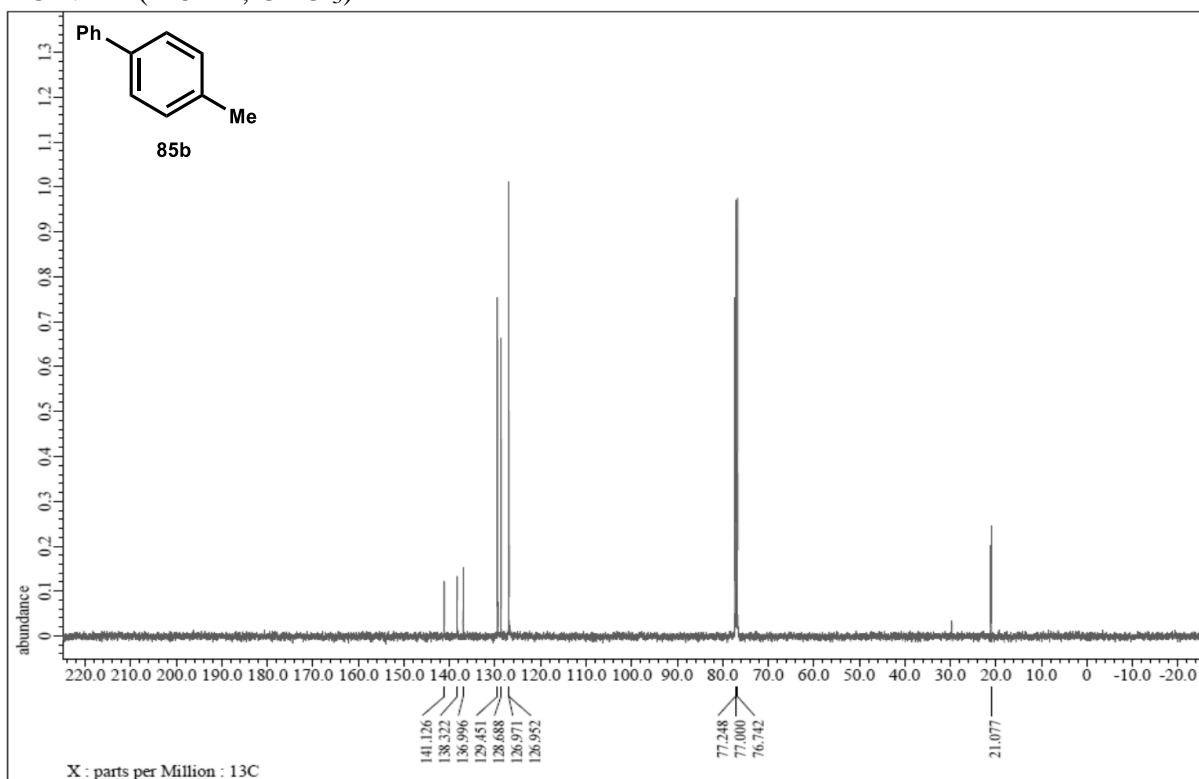
^{13}C NMR (125 Hz, CDCl_3)



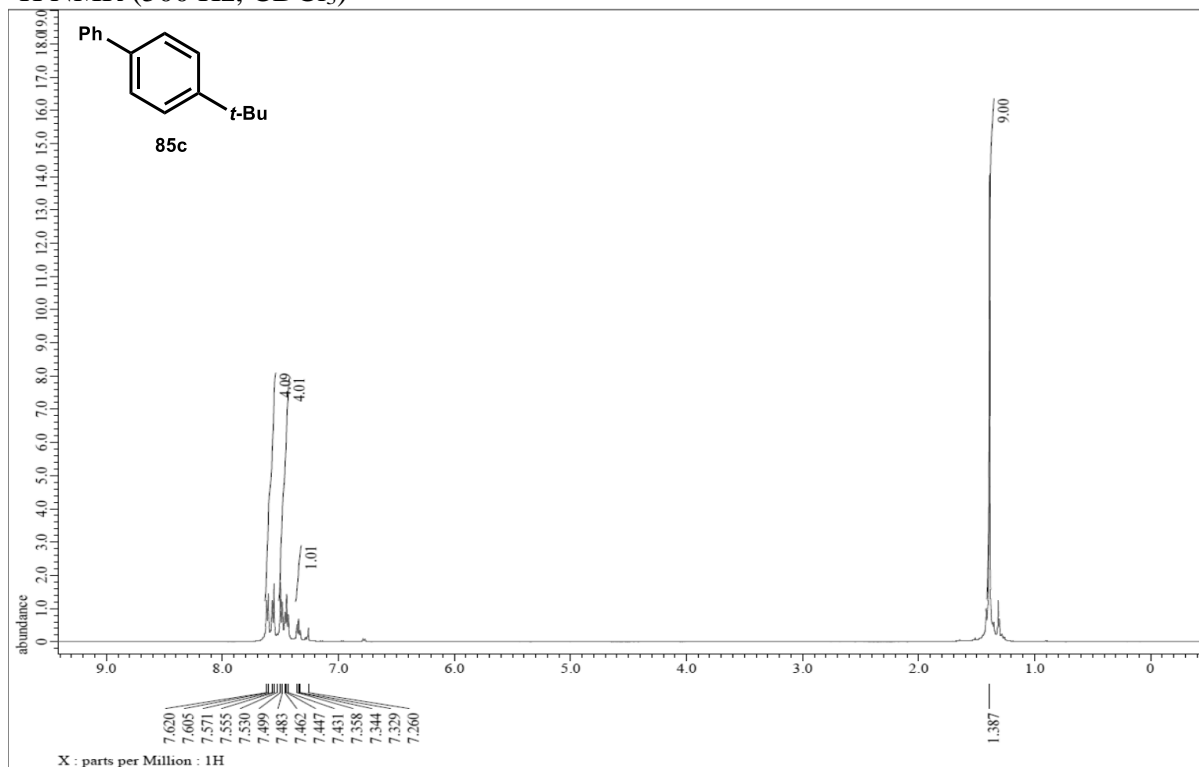
^1H NMR (500 Hz, CDCl_3)



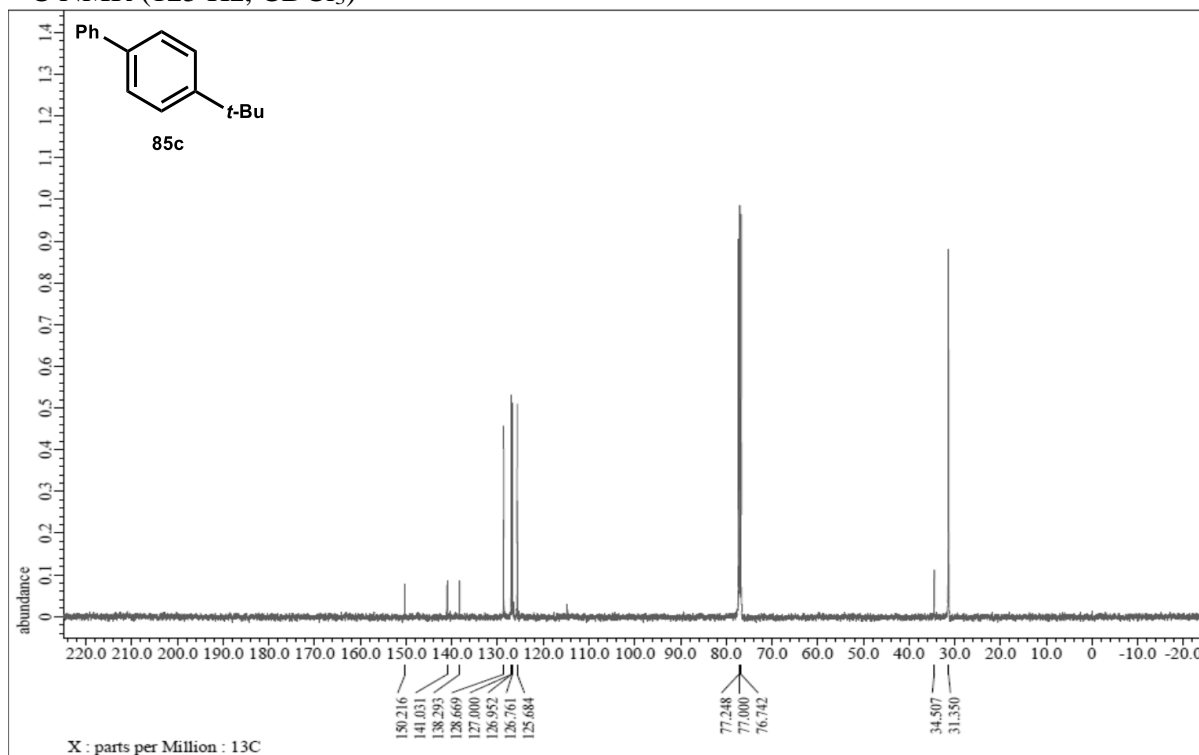
^{13}C NMR (125 Hz, CDCl_3)



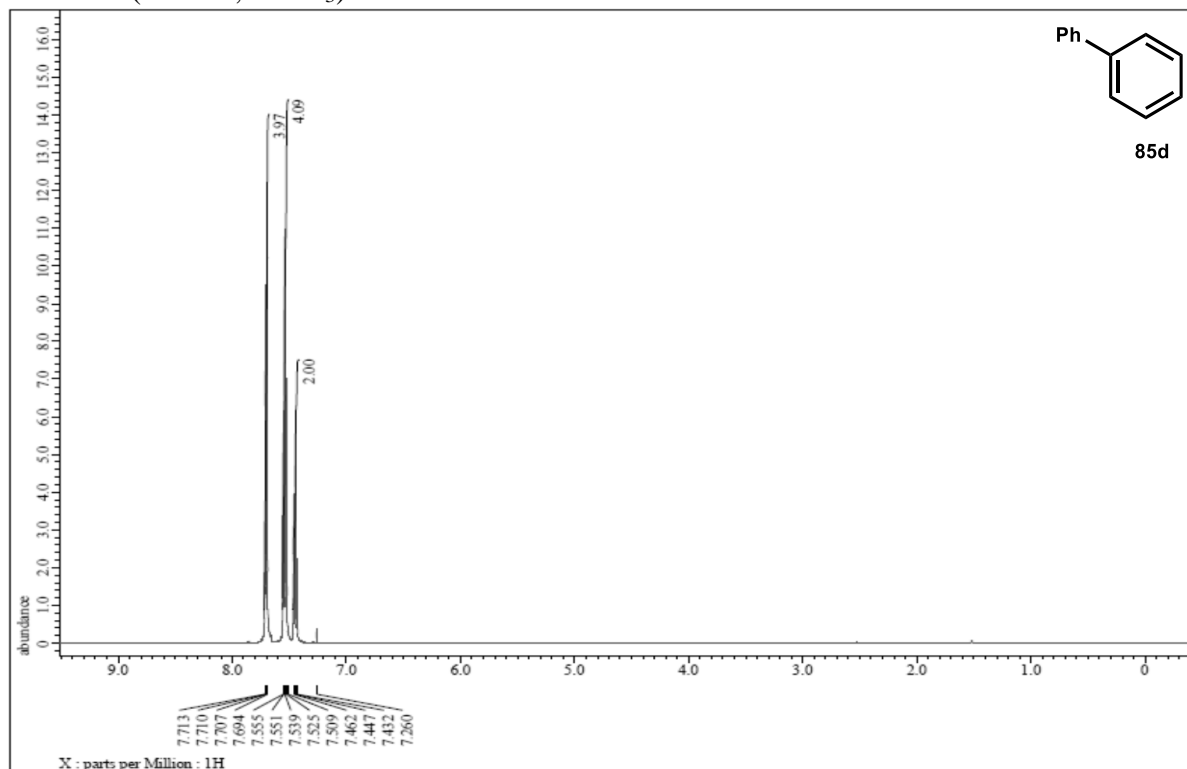
^1H NMR (500 Hz, CDCl_3)



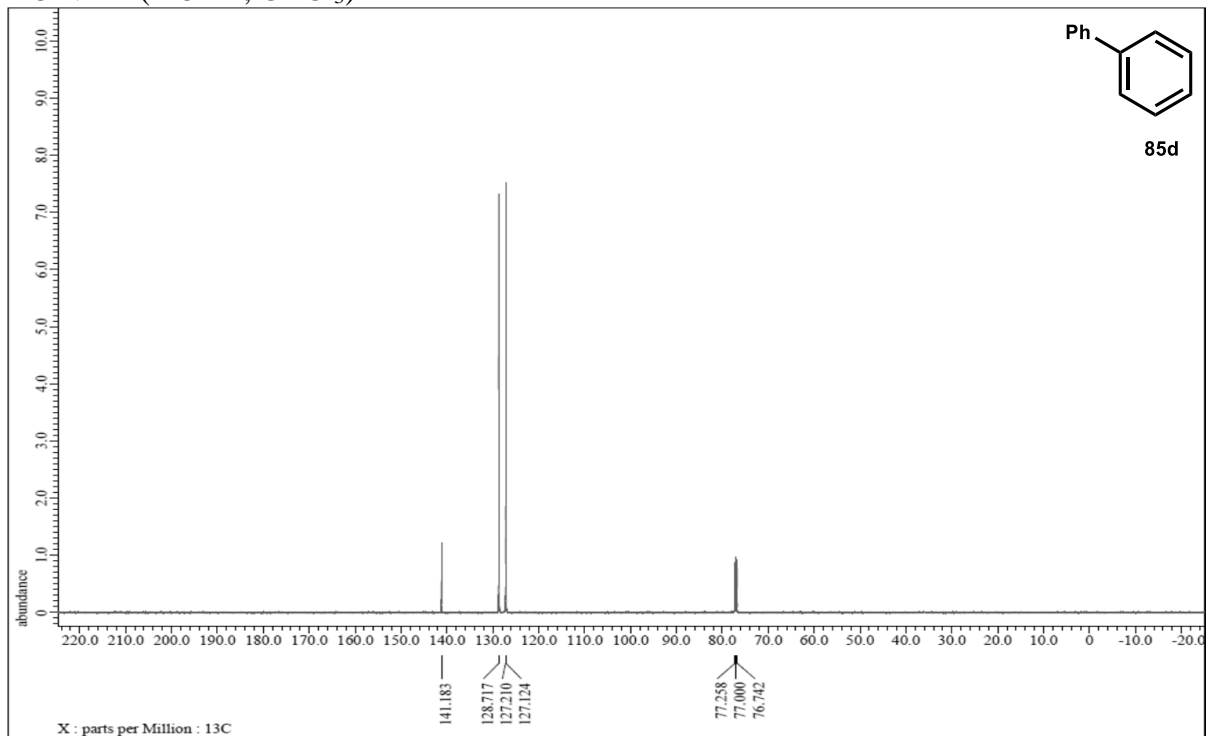
^{13}C NMR (125 Hz, CDCl_3)



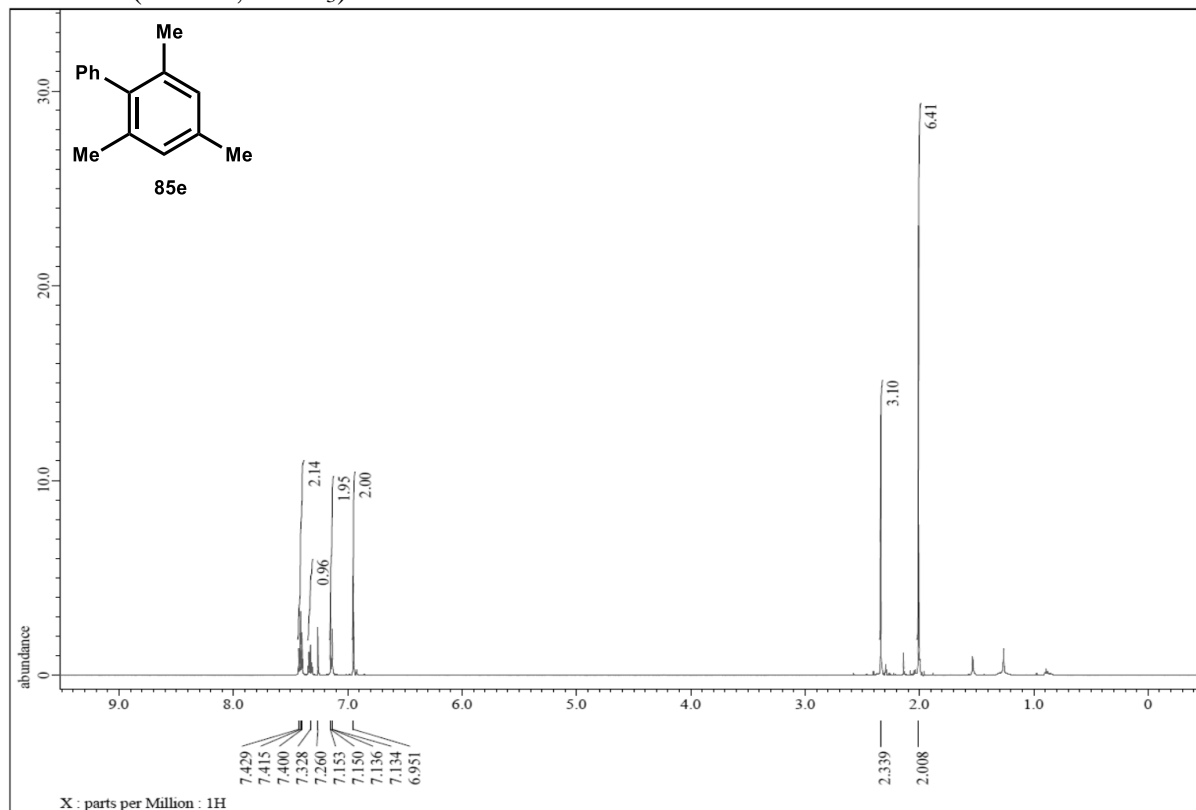
^1H NMR (500 Hz, CDCl_3)



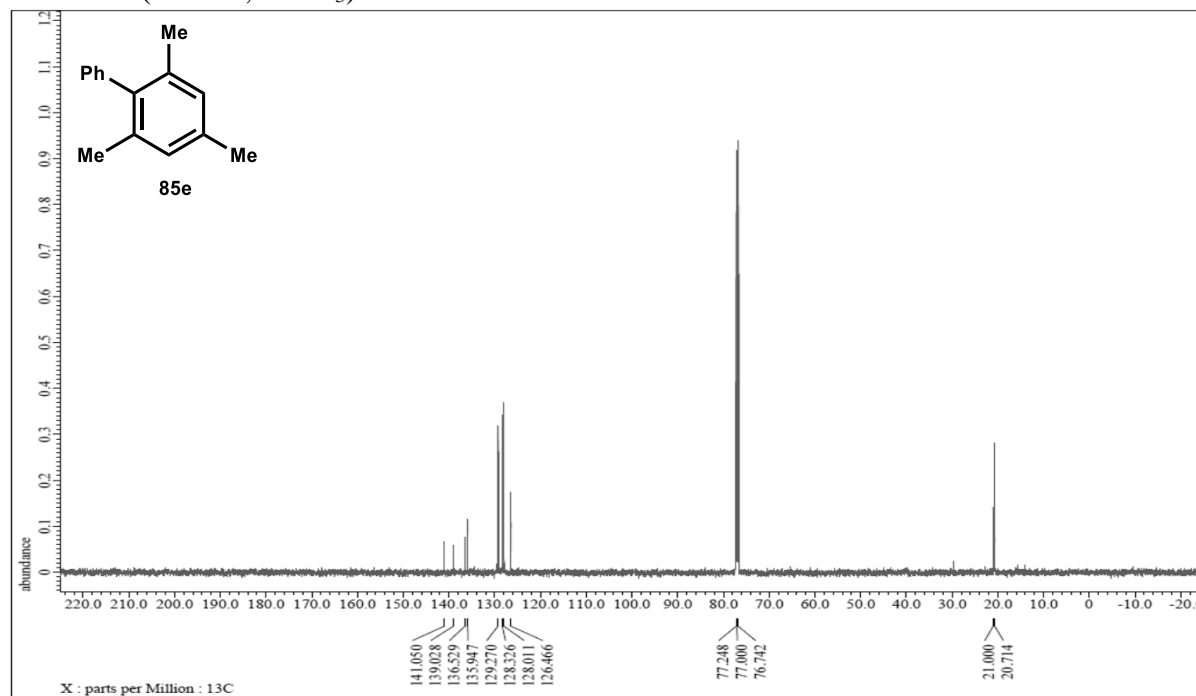
^{13}C NMR (125 Hz, CDCl_3)



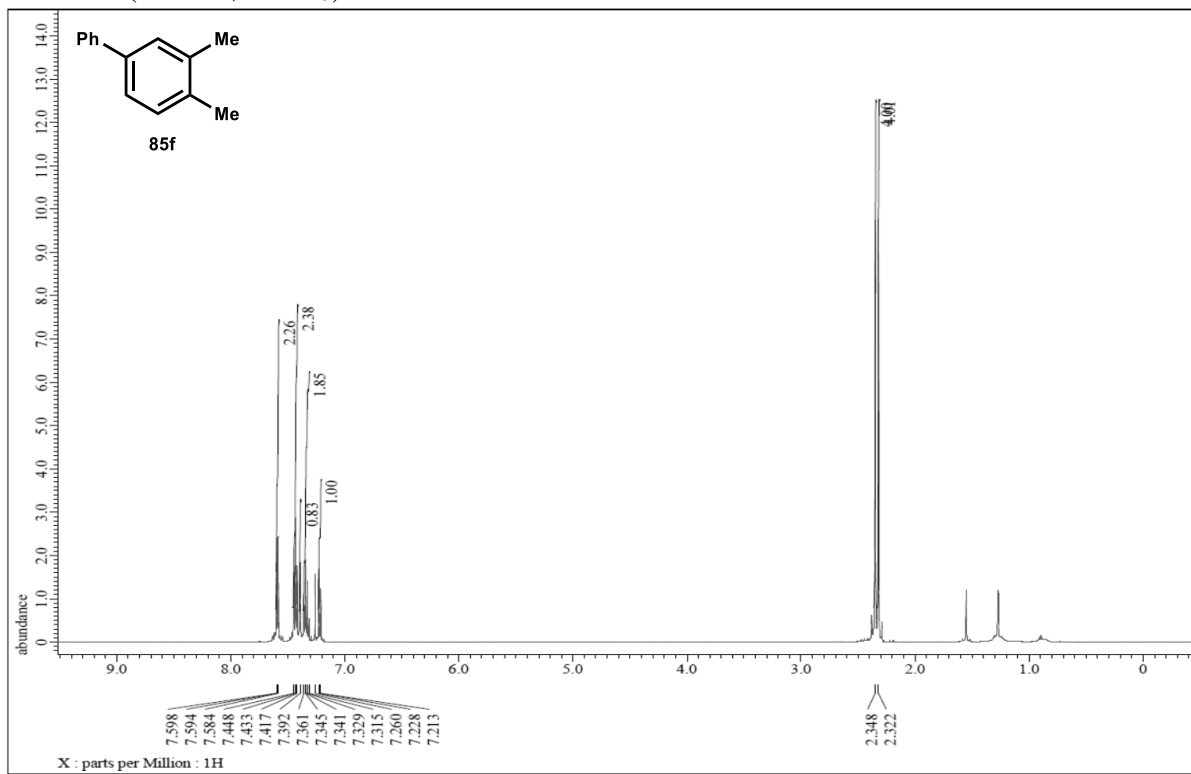
^1H NMR (500 Hz, CDCl_3)



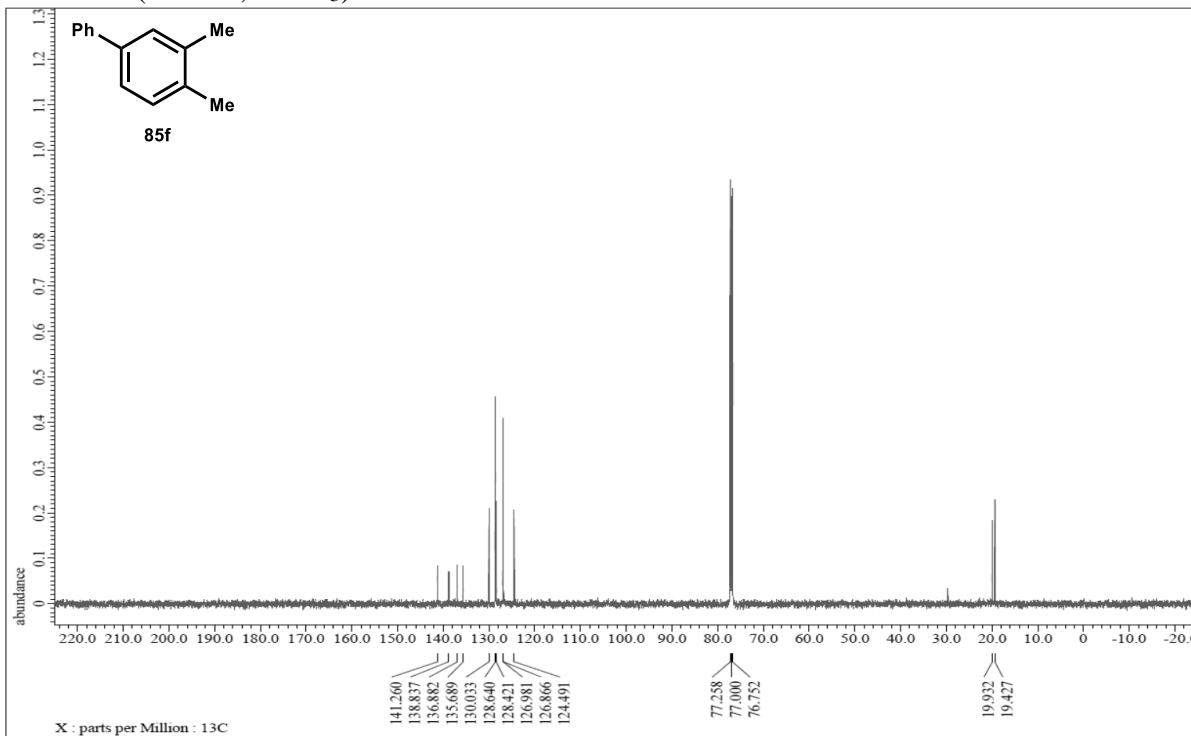
^{13}C NMR (125 Hz, CDCl_3)



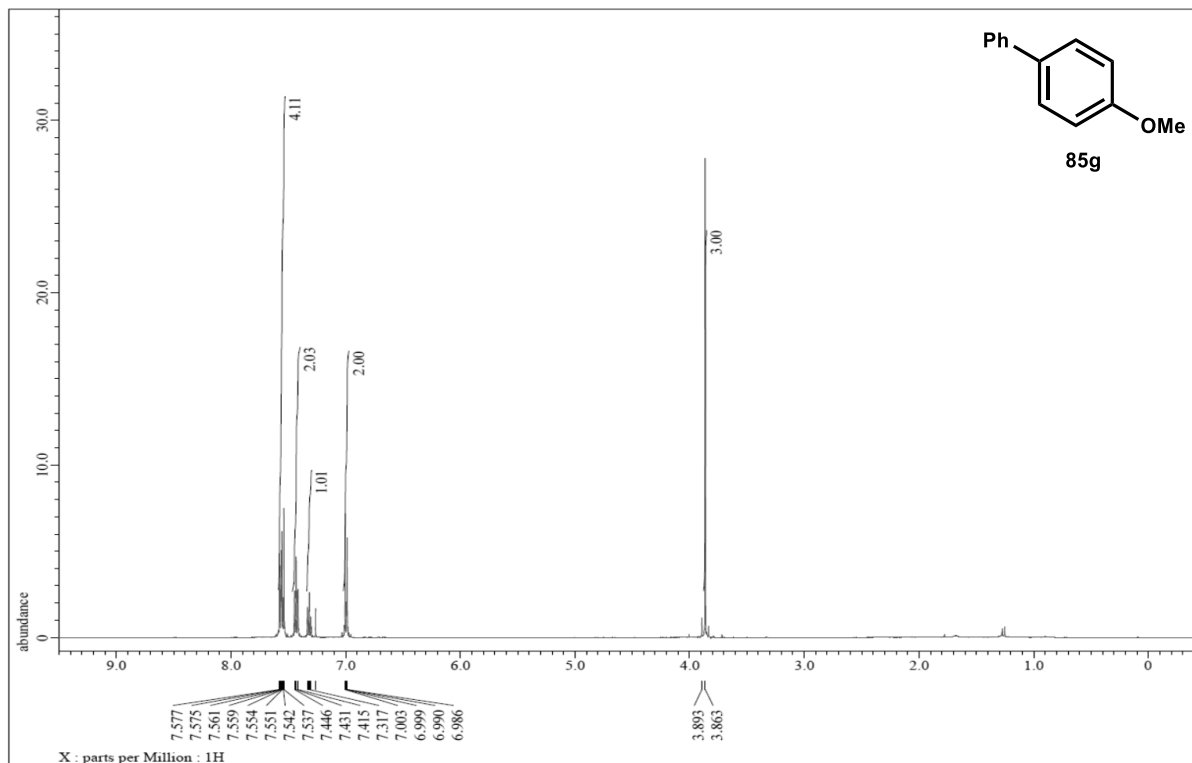
¹H NMR (500 Hz, CDCl₃)



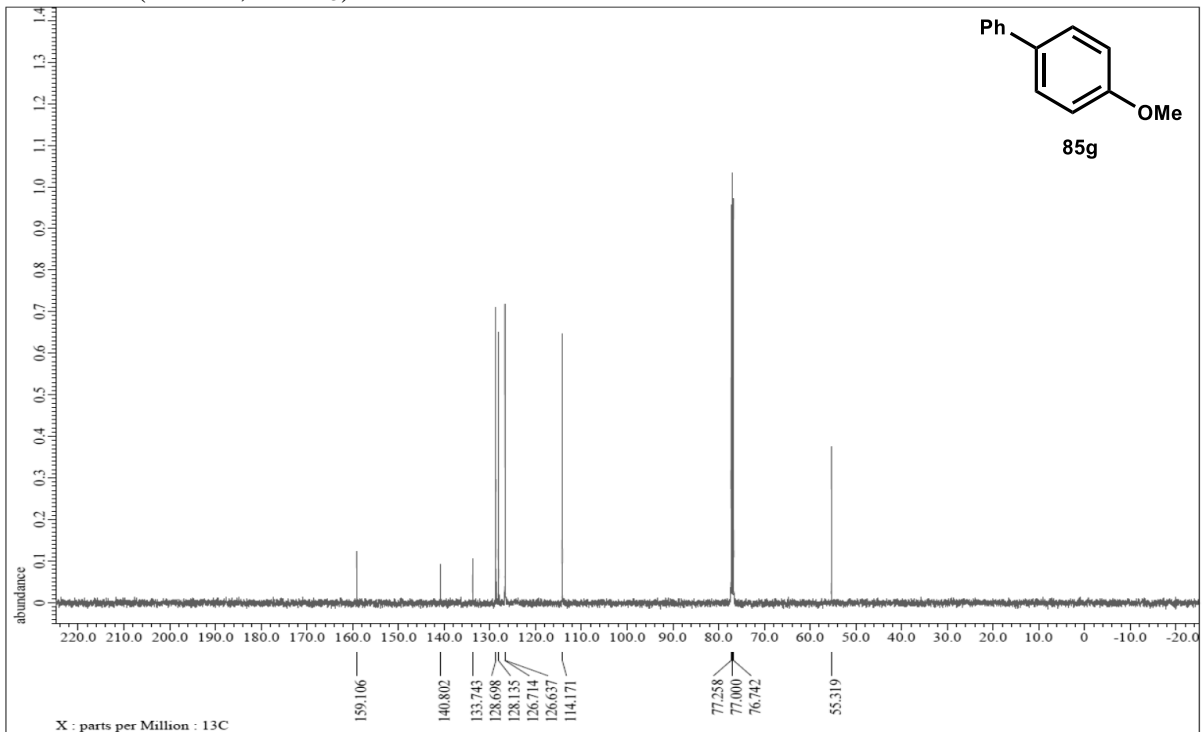
¹³C NMR (125 Hz, CDCl₃)



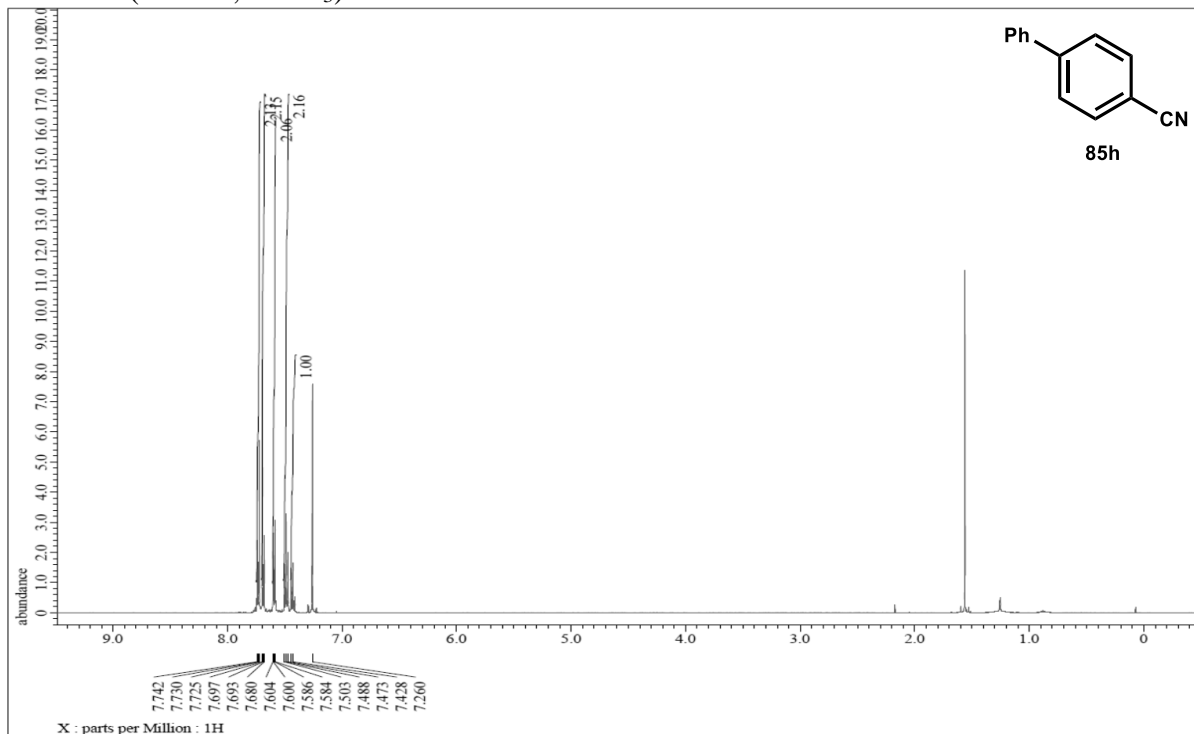
^1H NMR (500 Hz, CDCl_3)



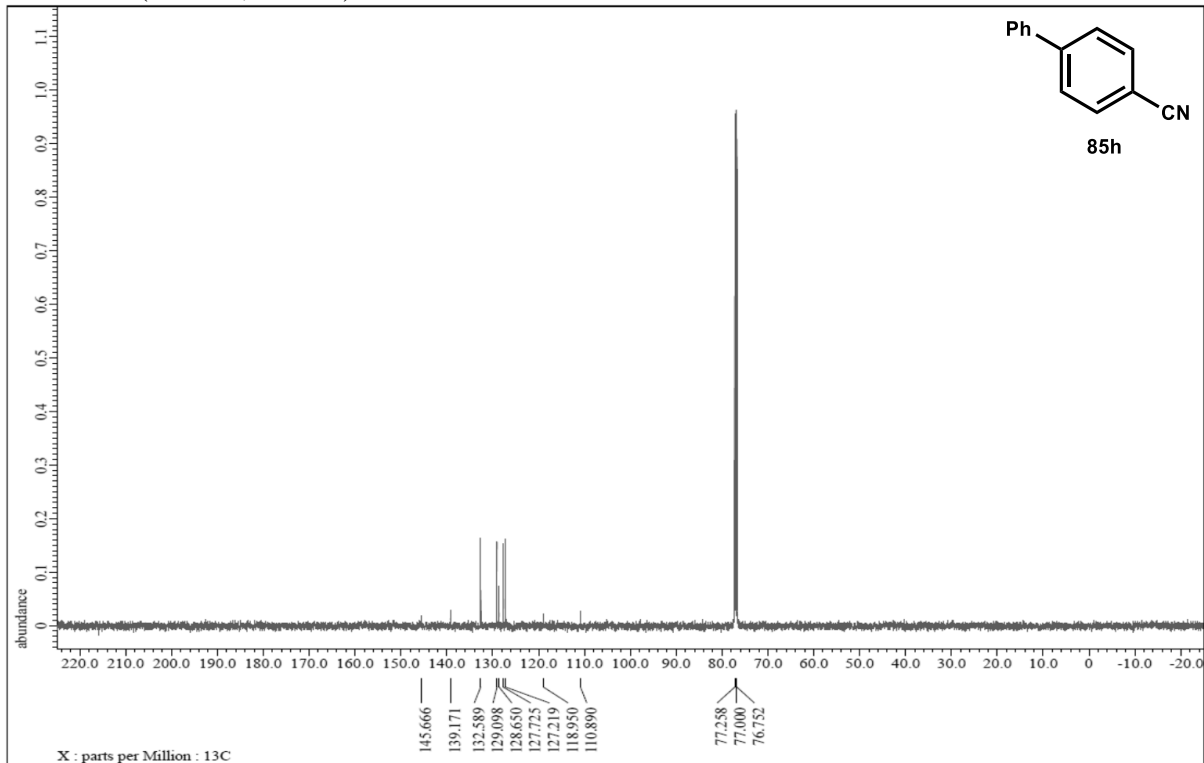
^{13}C NMR (125 Hz, CDCl_3)



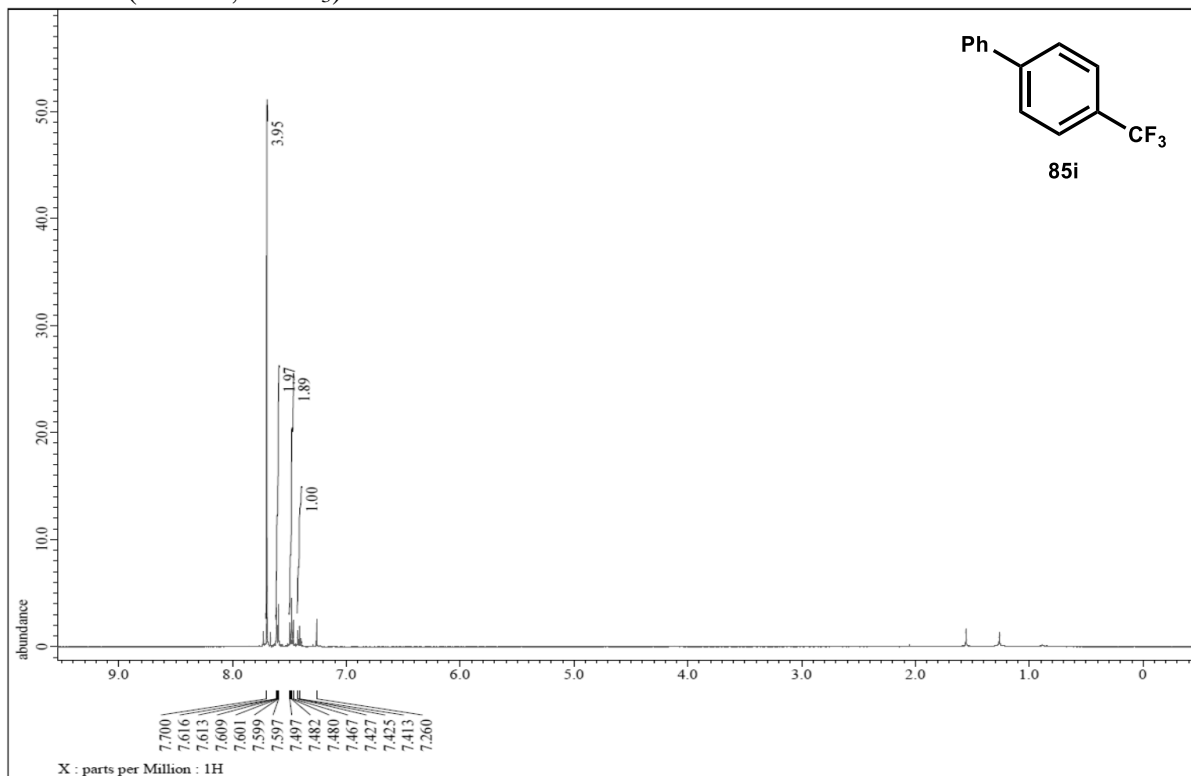
¹H NMR (500 Hz, CDCl₃)



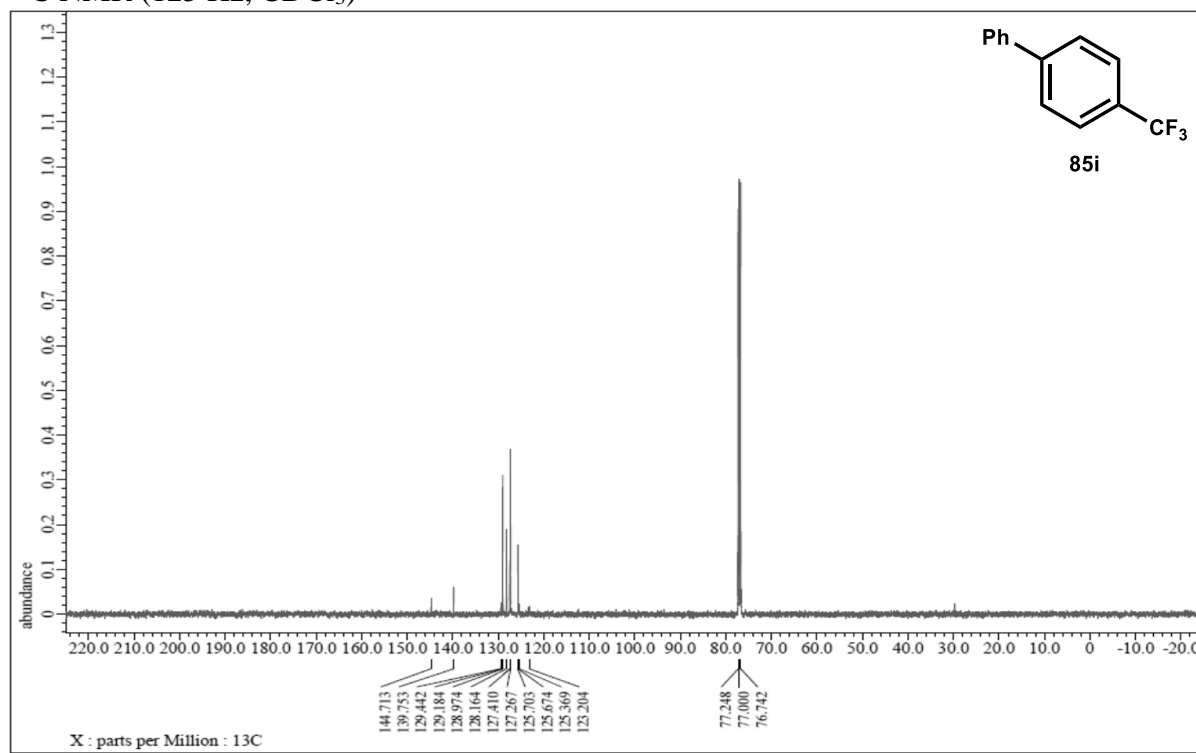
¹³C NMR (125 Hz, CDCl₃)



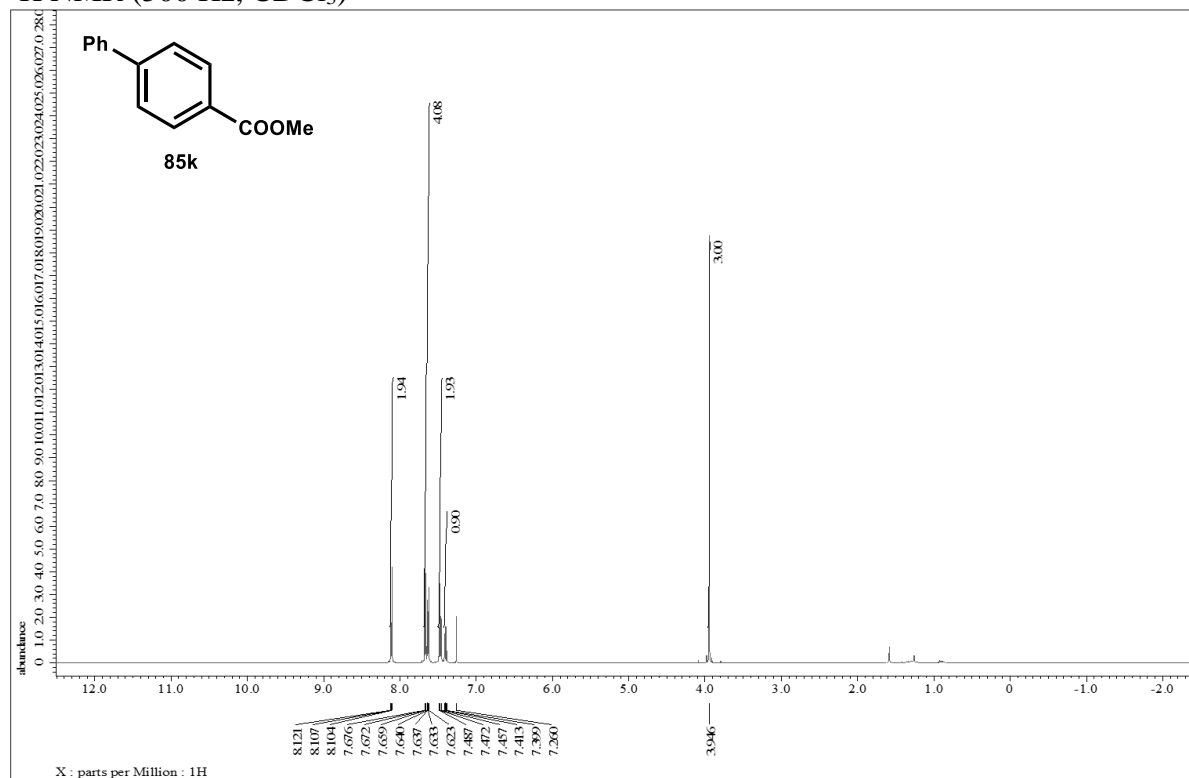
¹H NMR (500 Hz, CDCl₃)



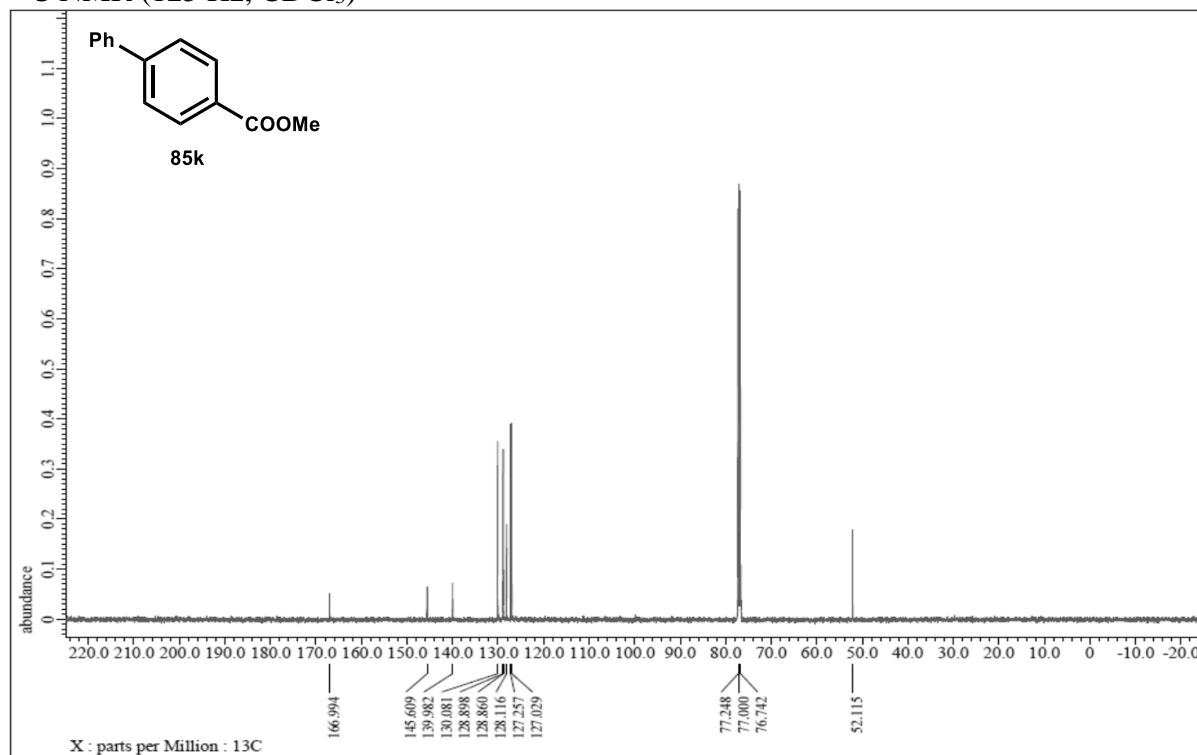
¹³C NMR (125 Hz, CDCl₃)



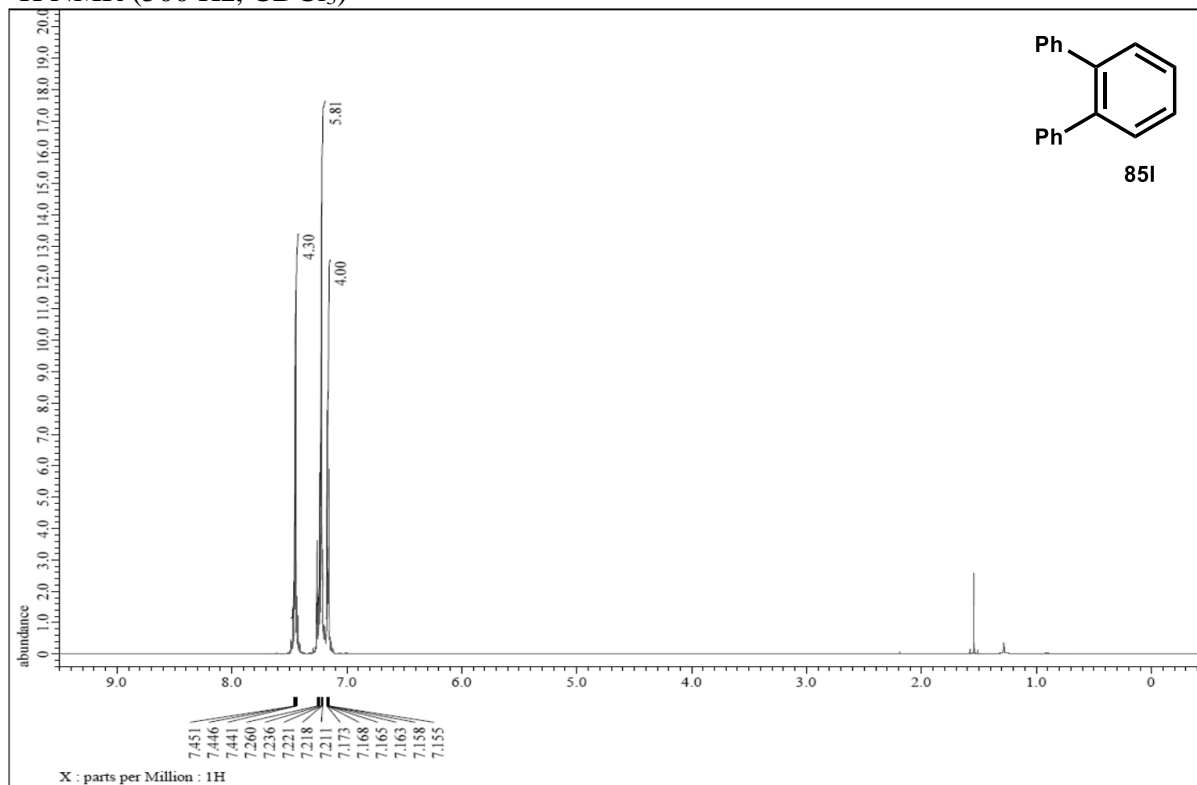
¹H NMR (500 Hz, CDCl₃)



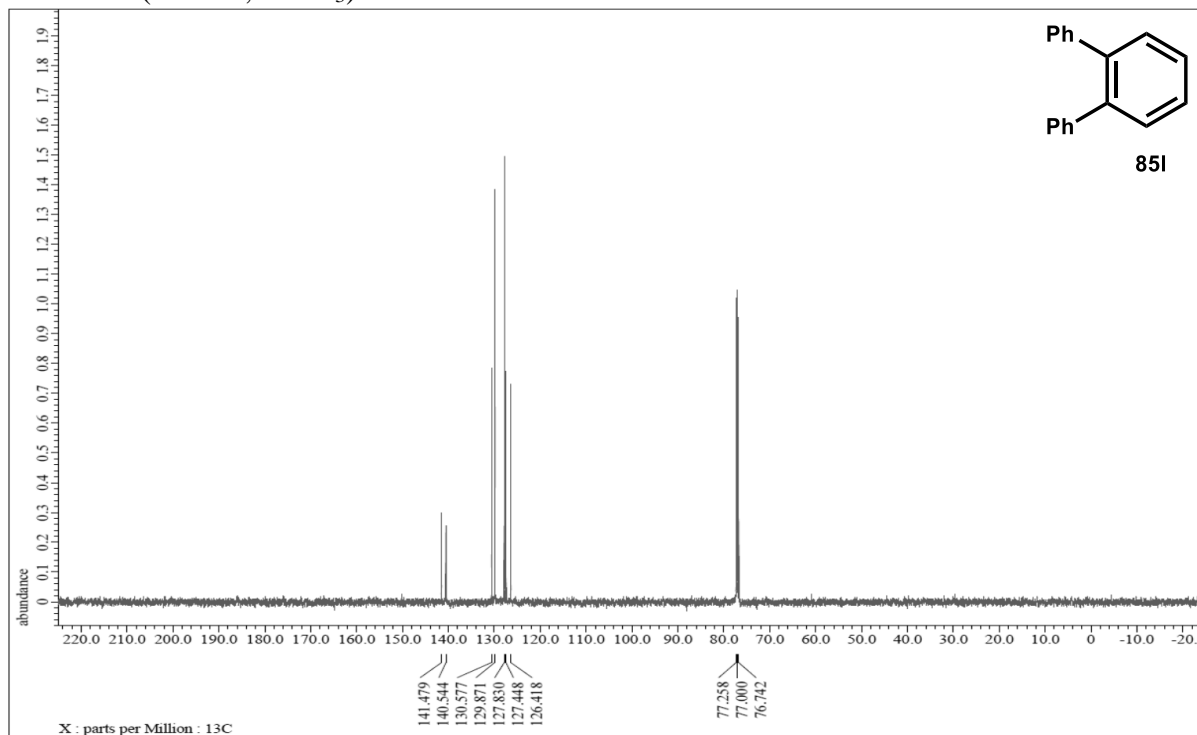
¹³C NMR (125 Hz, CDCl₃)



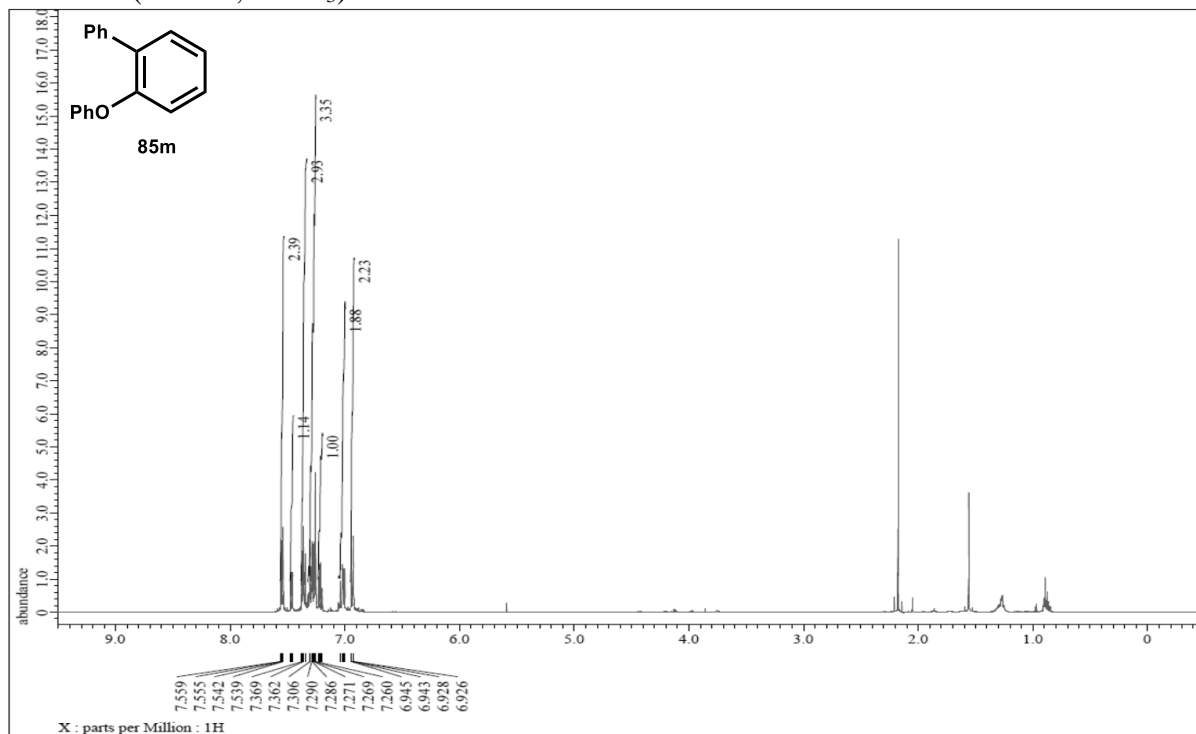
¹H NMR (500 Hz, CDCl₃)



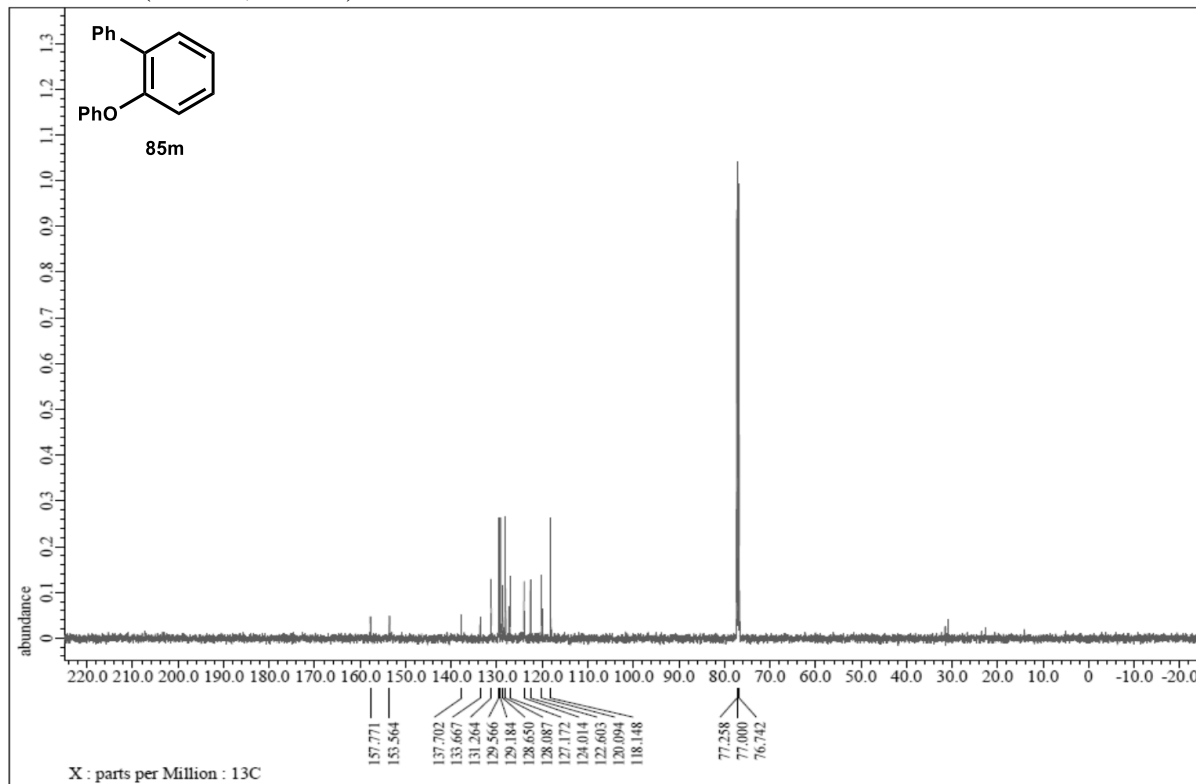
¹³C NMR (125 Hz, CDCl₃)



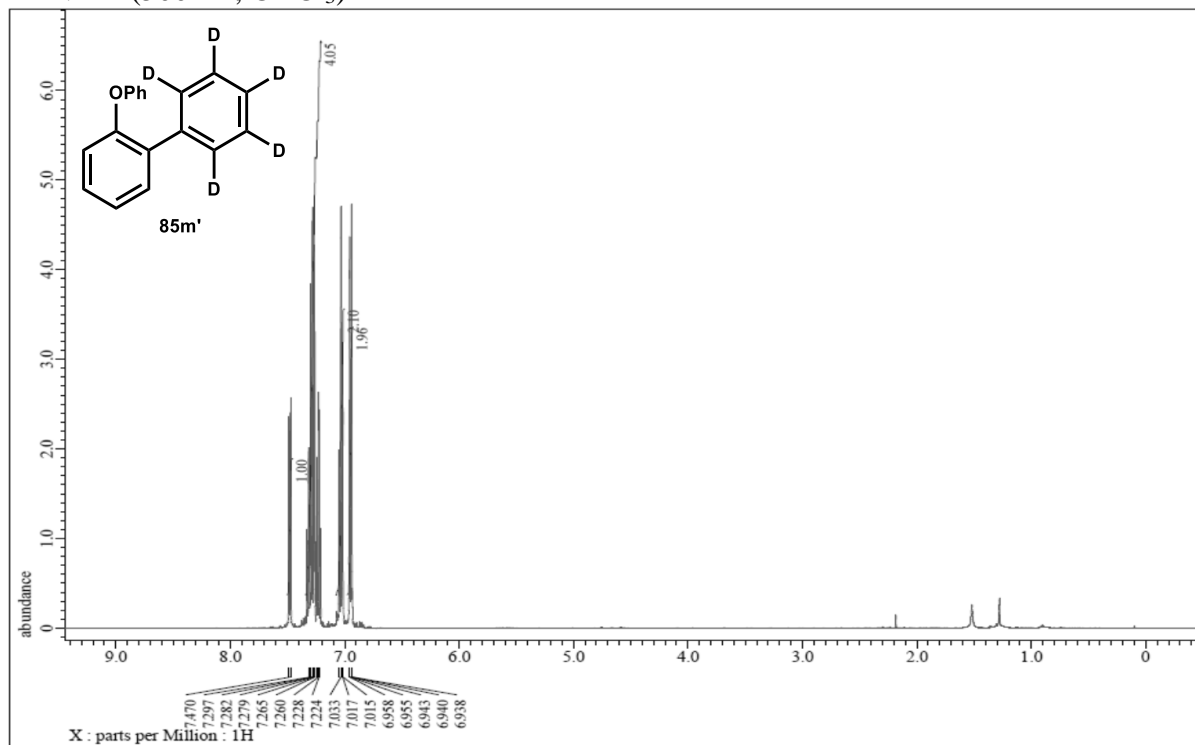
¹H NMR (500 Hz, CDCl₃)



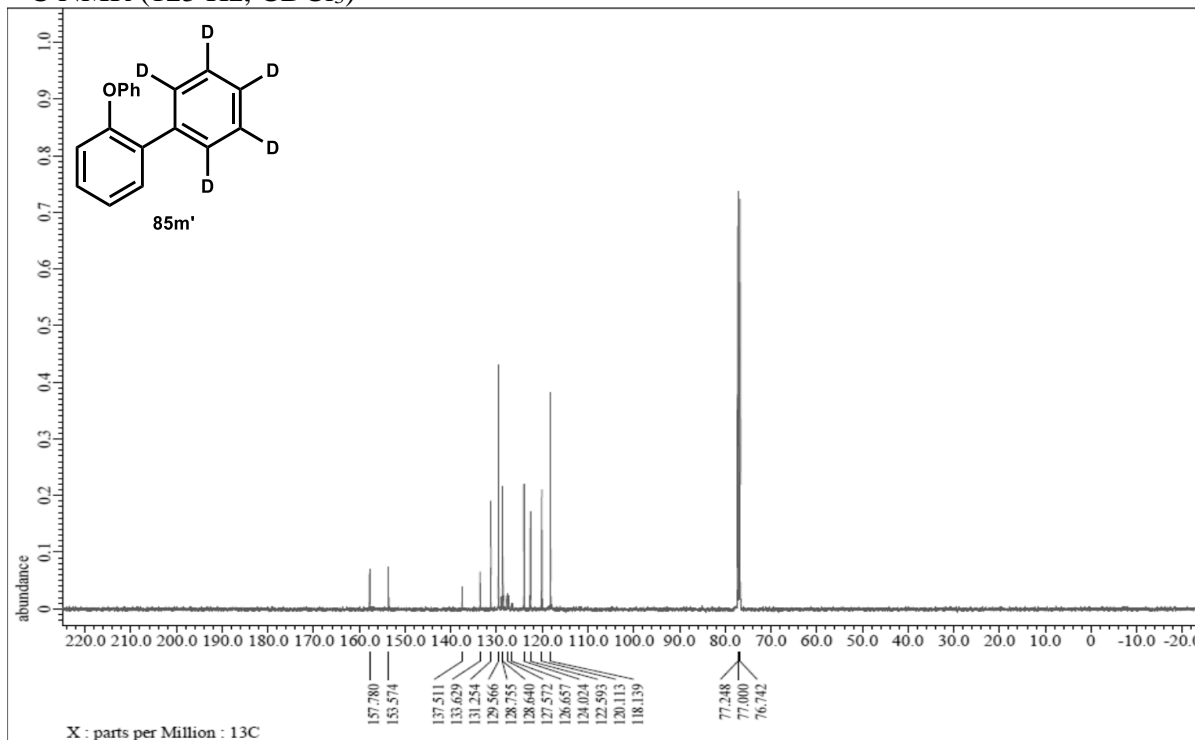
¹³C NMR (125 Hz, CDCl₃)



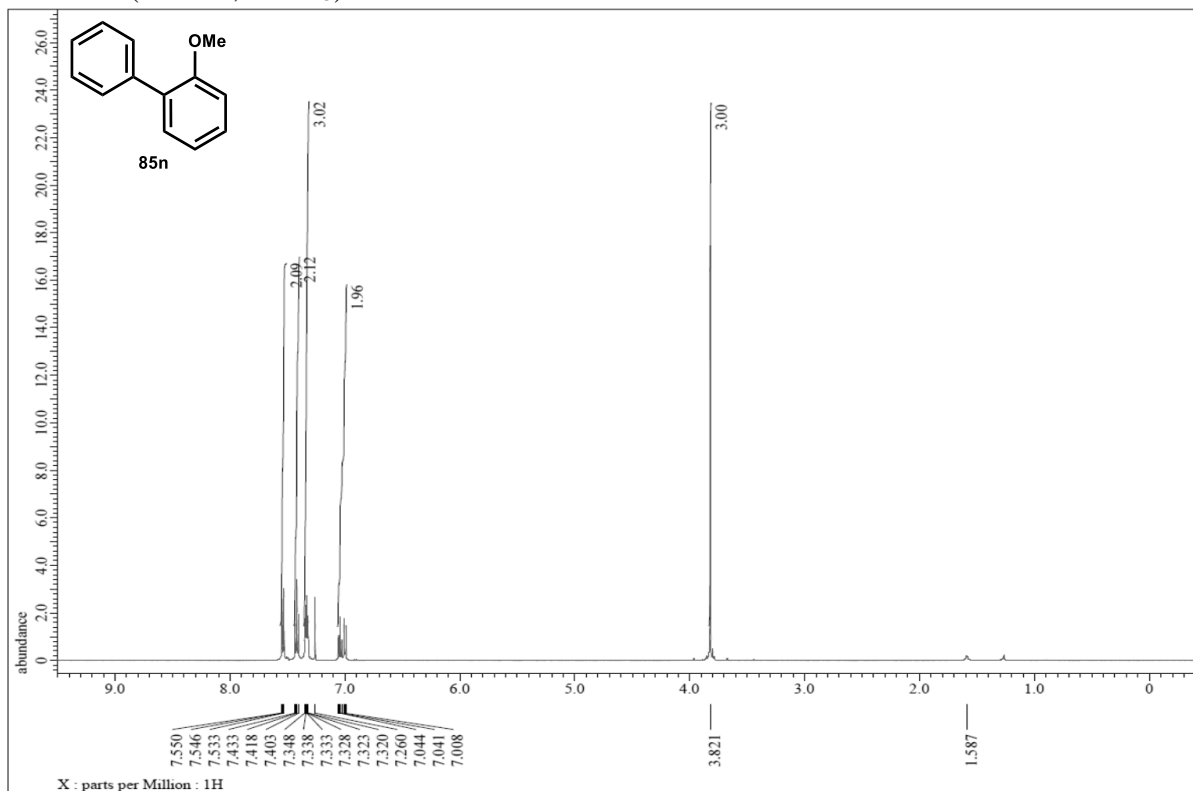
¹H NMR (500 Hz, CDCl₃)



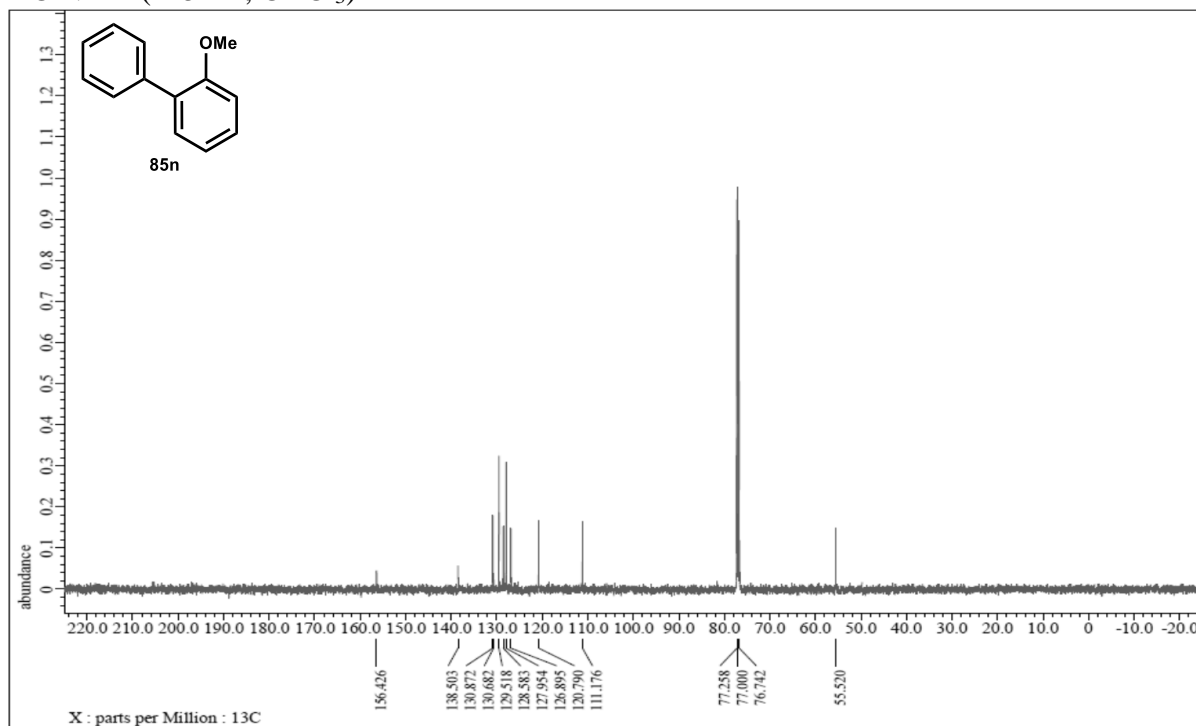
¹³C NMR (125 Hz, CDCl₃)



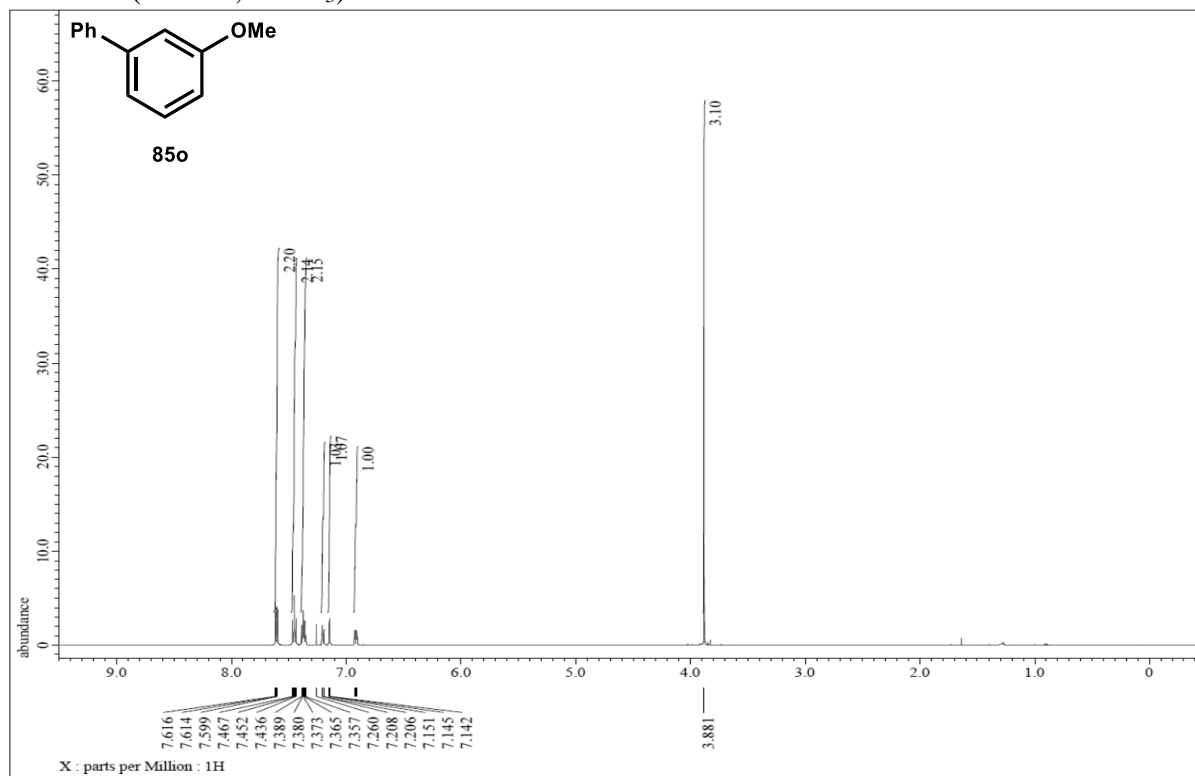
^1H NMR (500 Hz, CDCl_3)



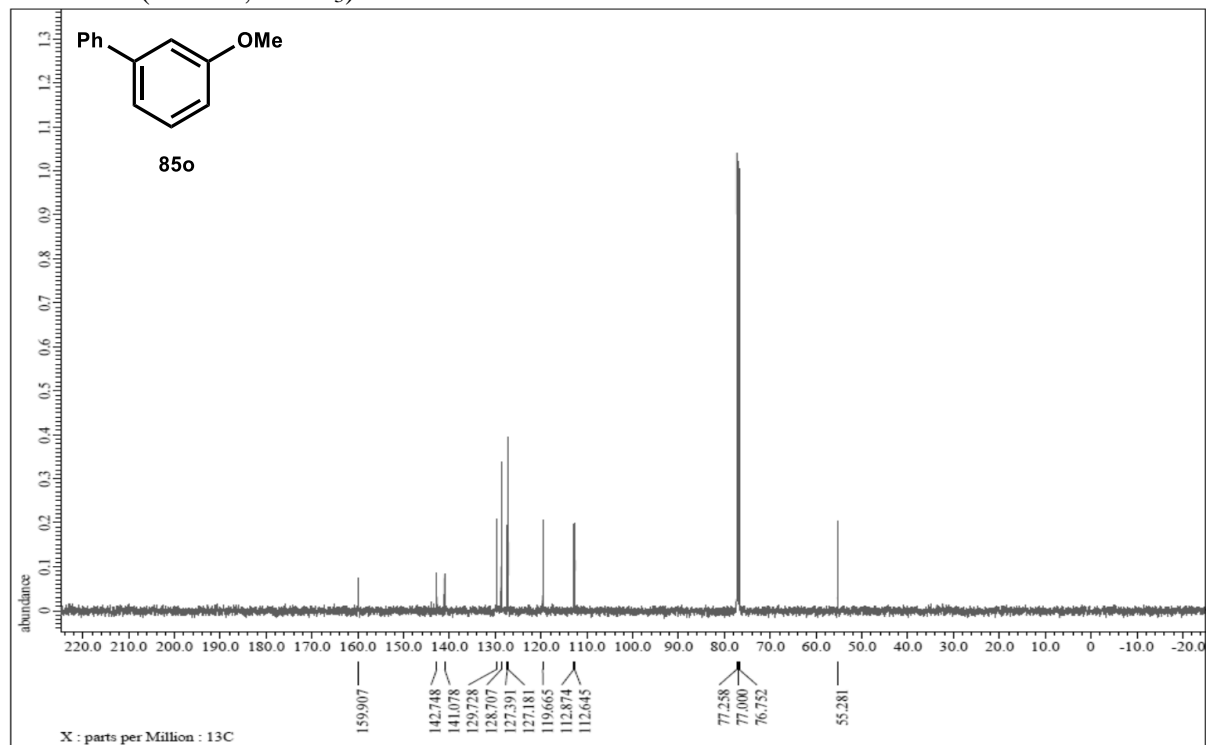
^{13}C NMR (125 Hz, CDCl_3)



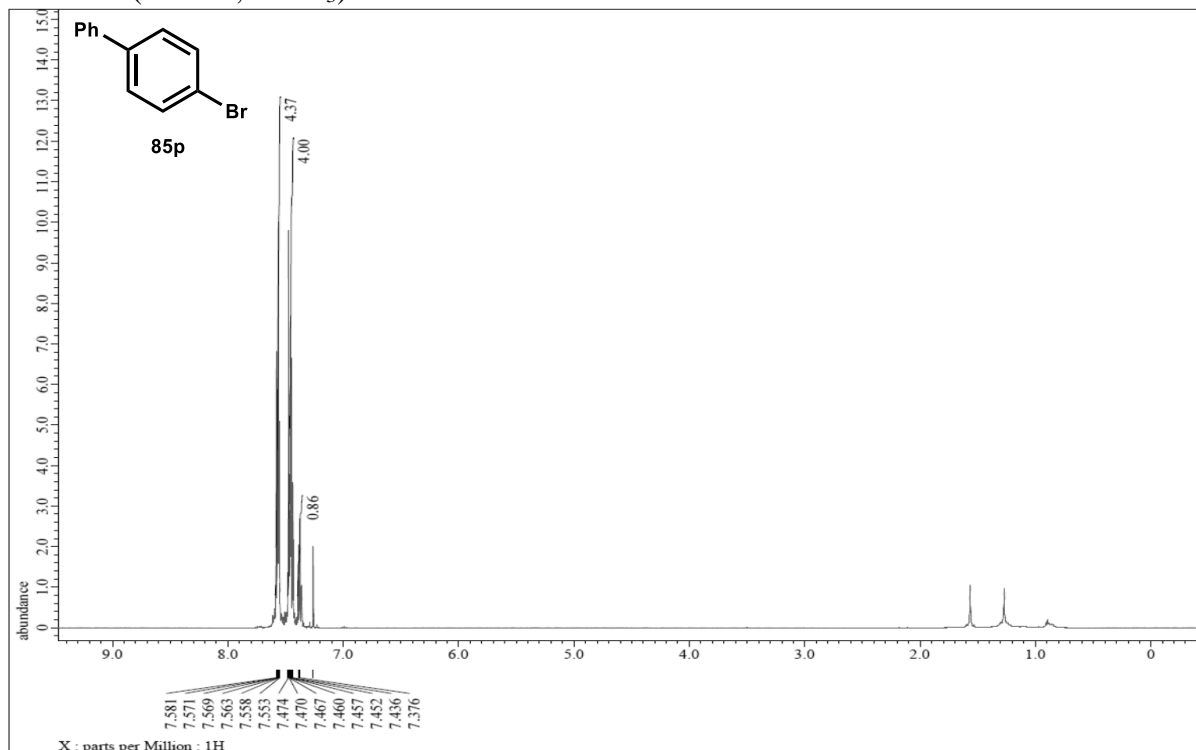
^1H NMR (500 Hz, CDCl_3)



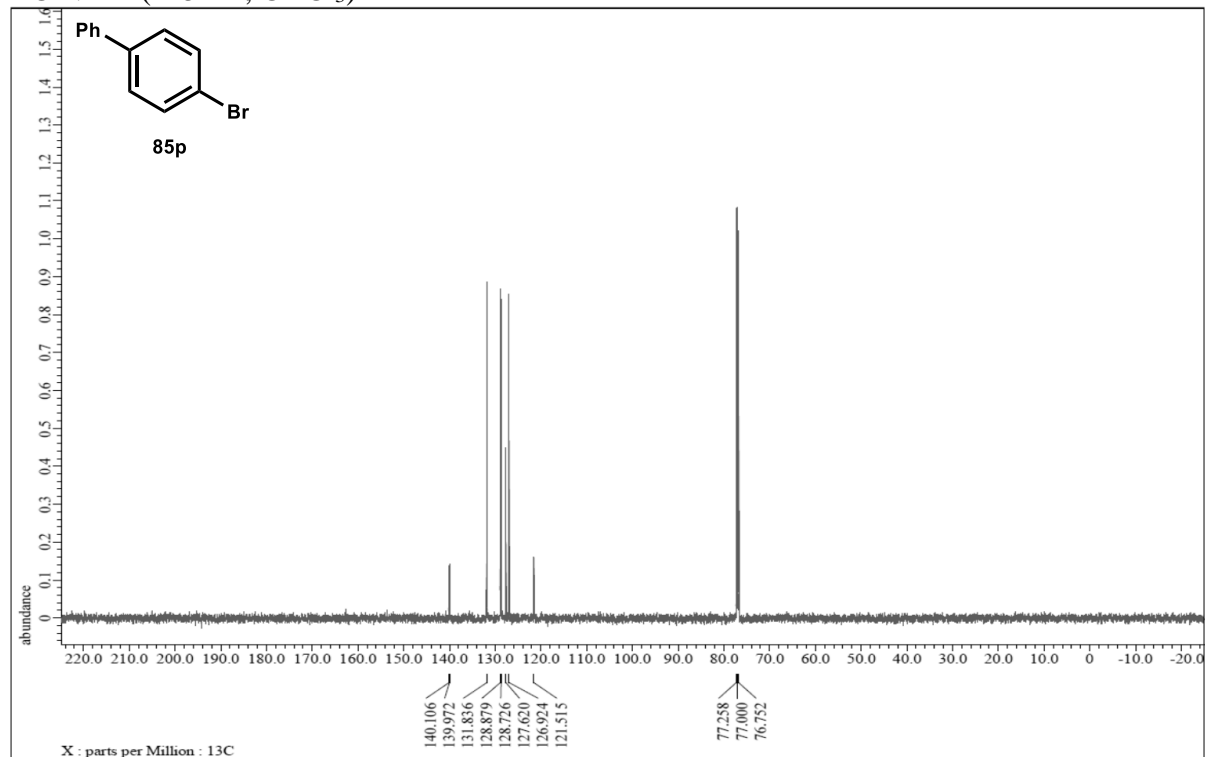
^{13}C NMR (125 Hz, CDCl_3)



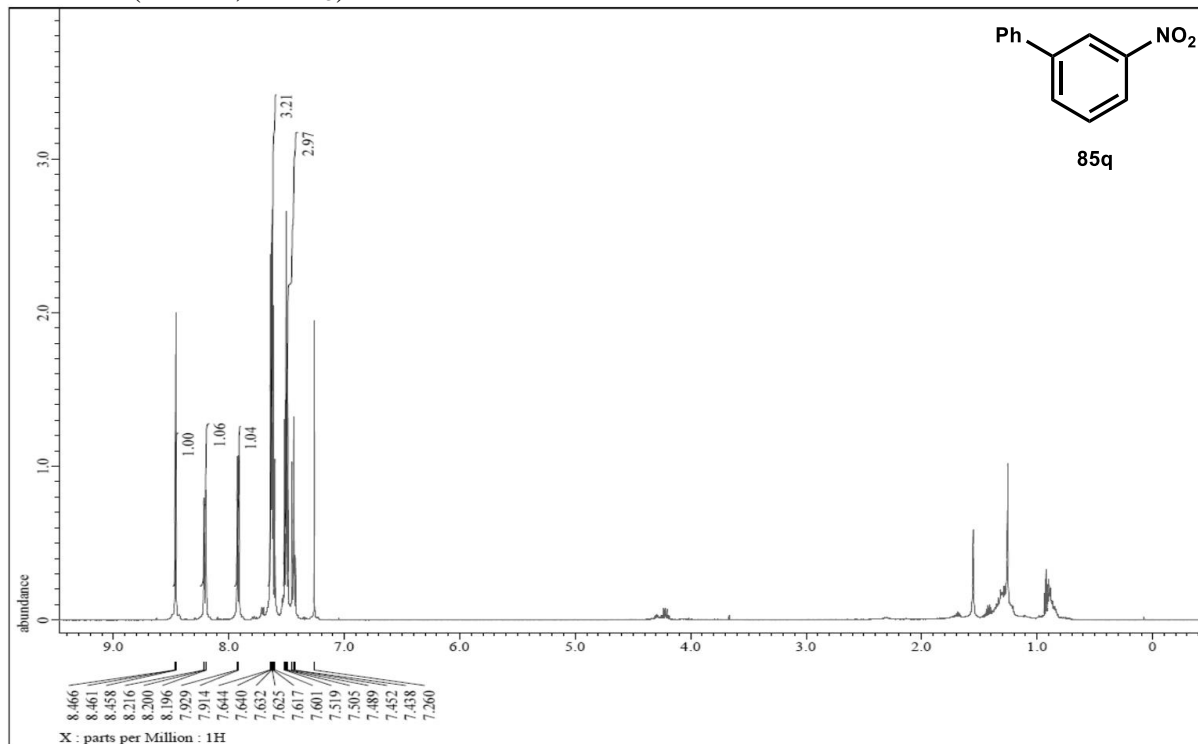
^1H NMR (500 Hz, CDCl_3)



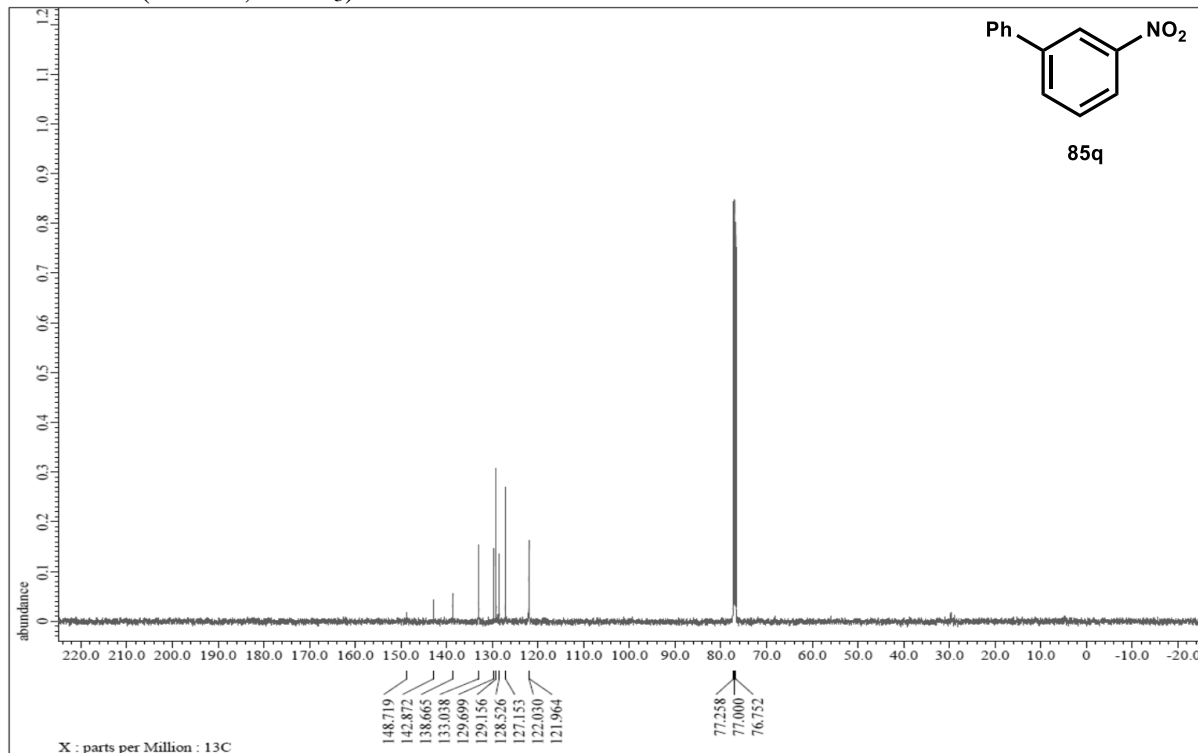
^{13}C NMR (125 Hz, CDCl_3)



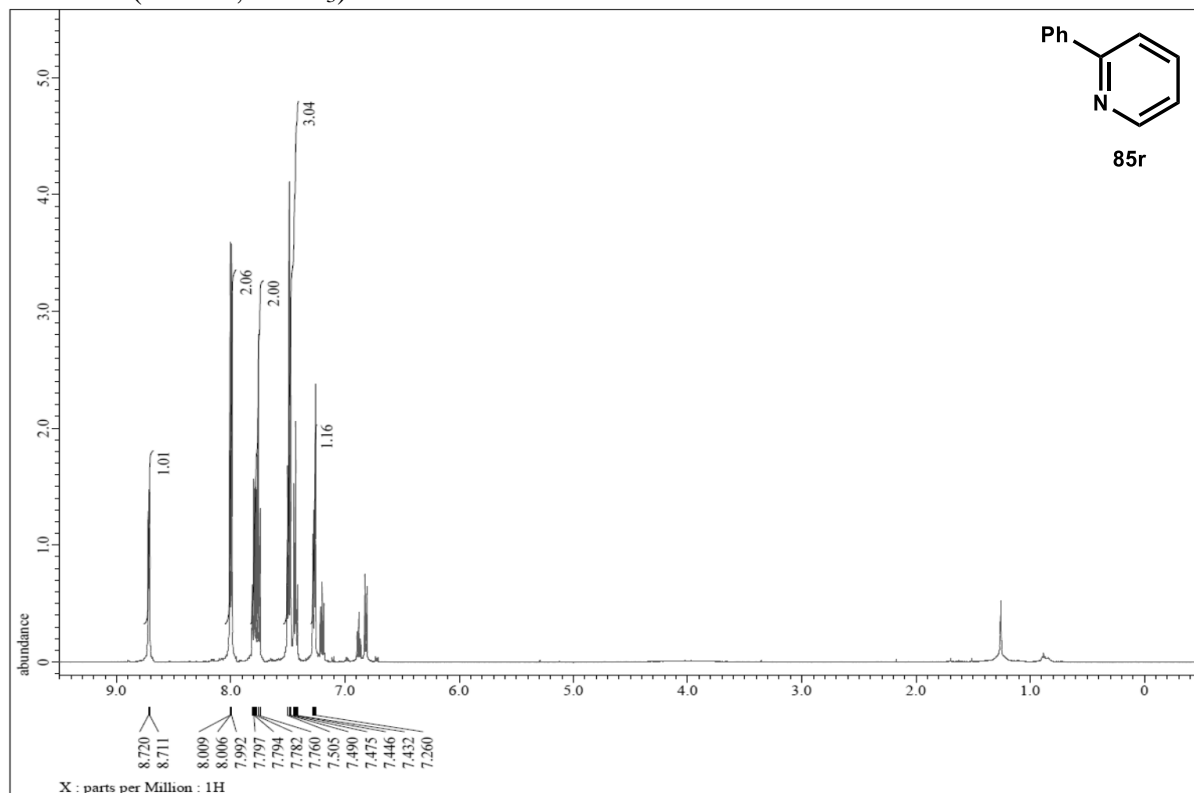
¹H NMR (500 Hz, CDCl₃)



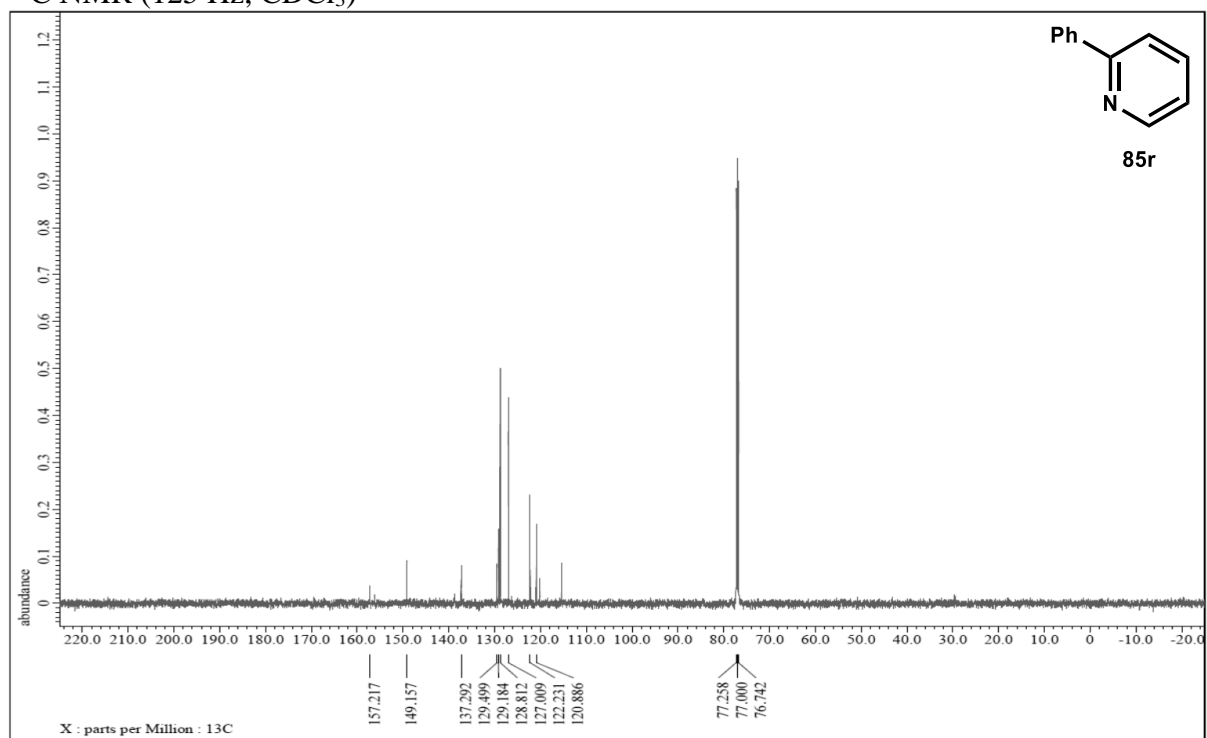
¹³C NMR (125 Hz, CDCl₃)



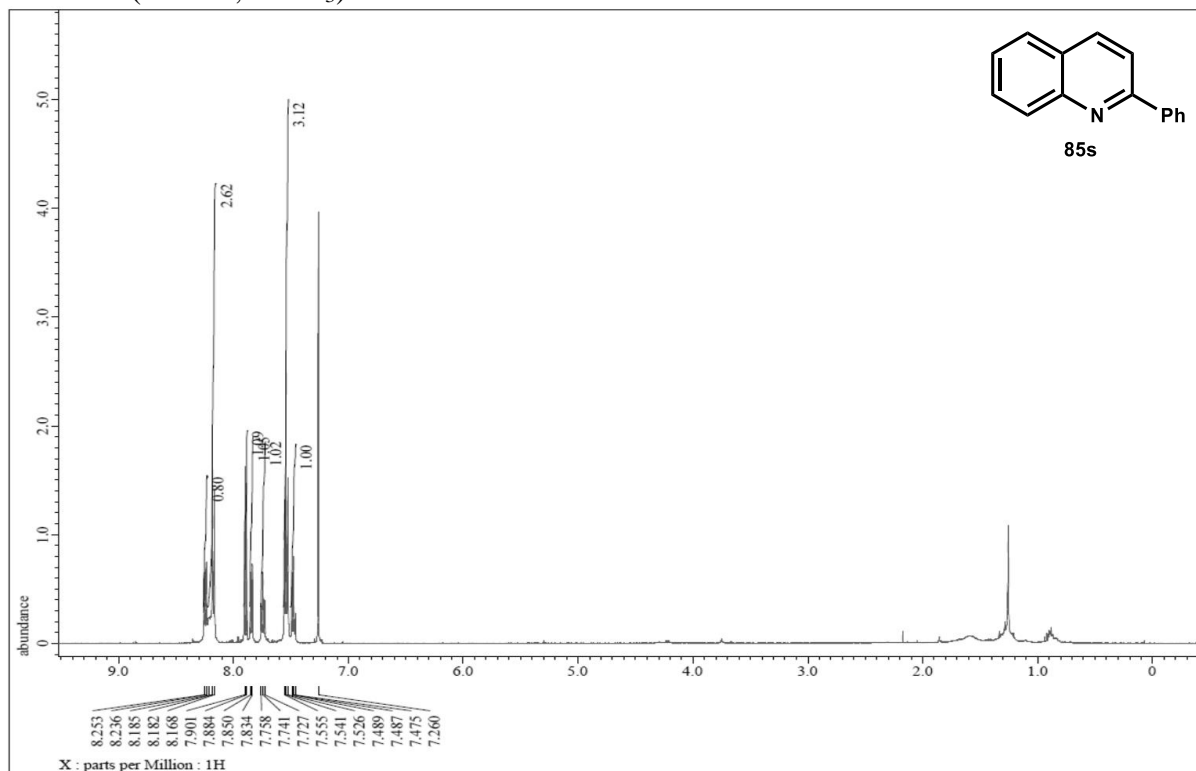
^1H NMR (500 Hz, CDCl_3)



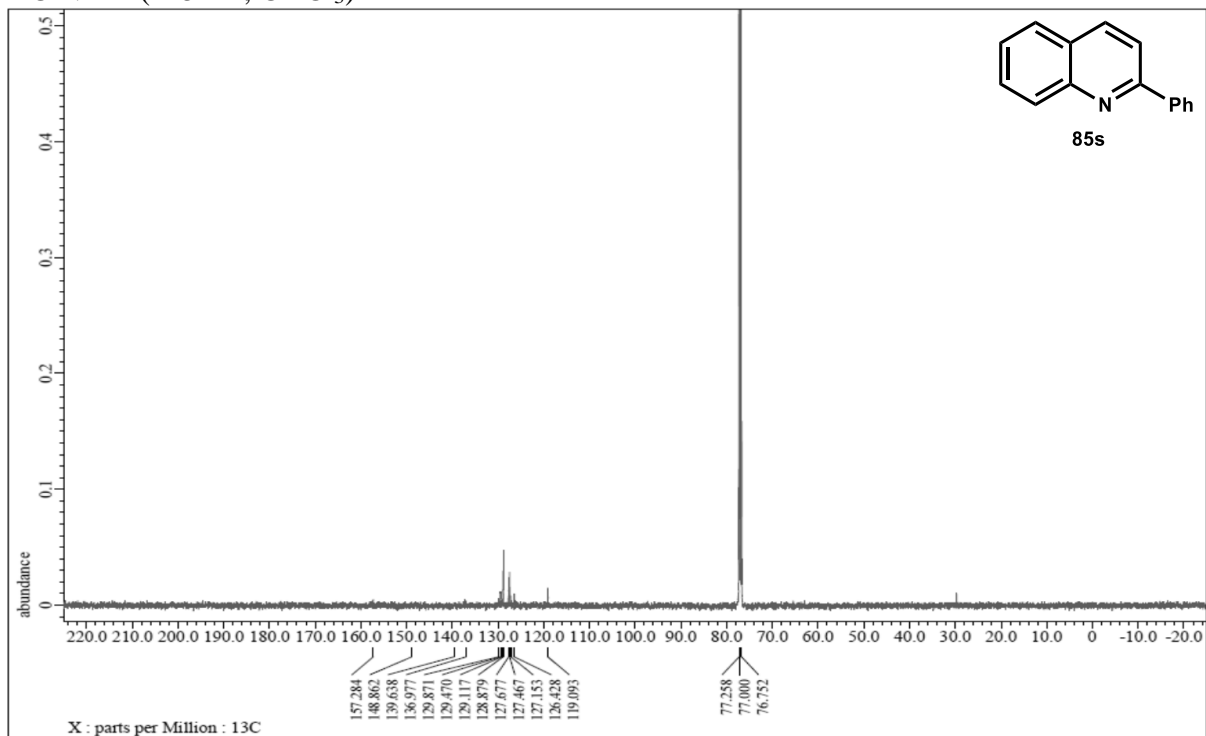
^{13}C NMR (125 Hz, CDCl_3)



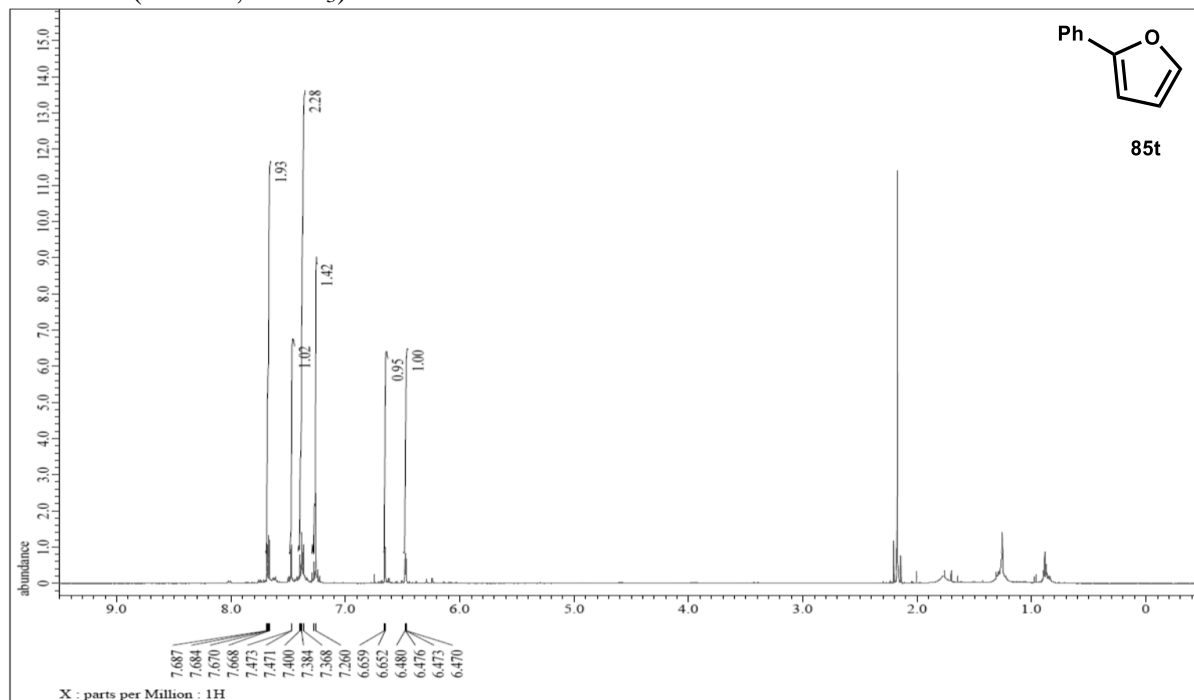
^1H NMR (500 Hz, CDCl_3)



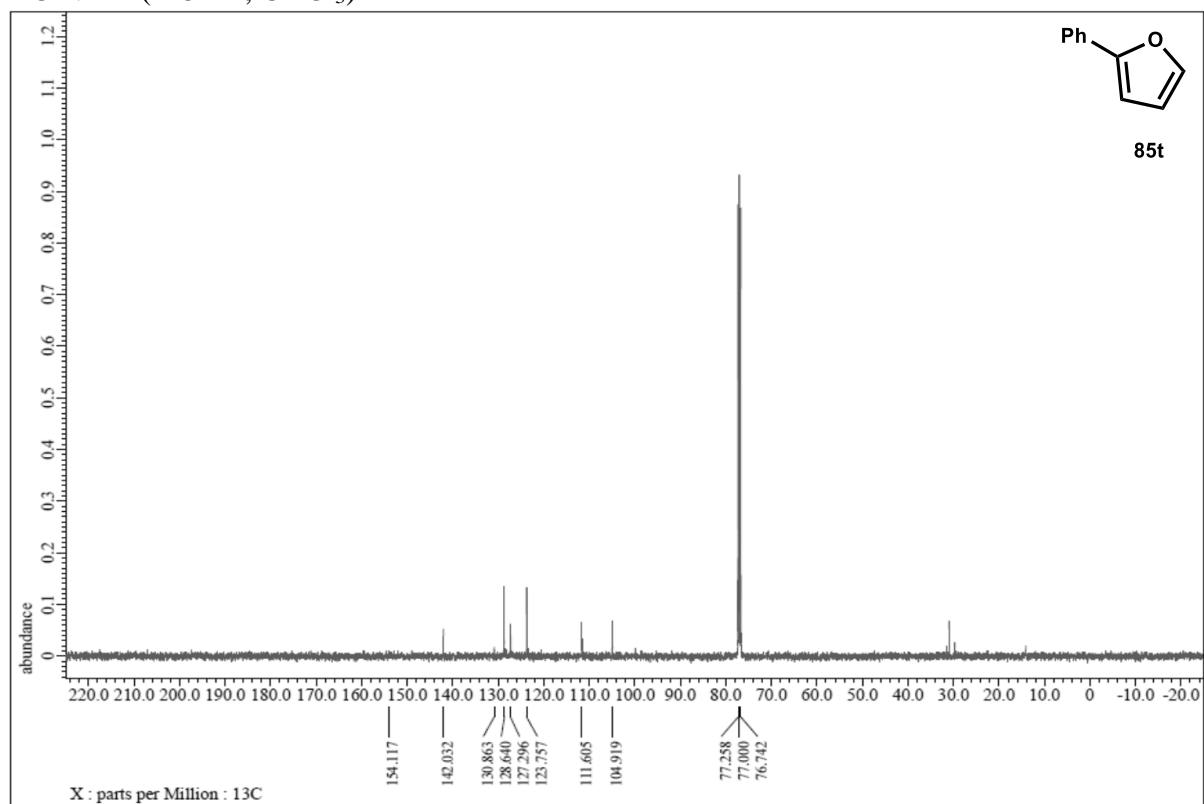
^{13}C NMR (125 Hz, CDCl_3)



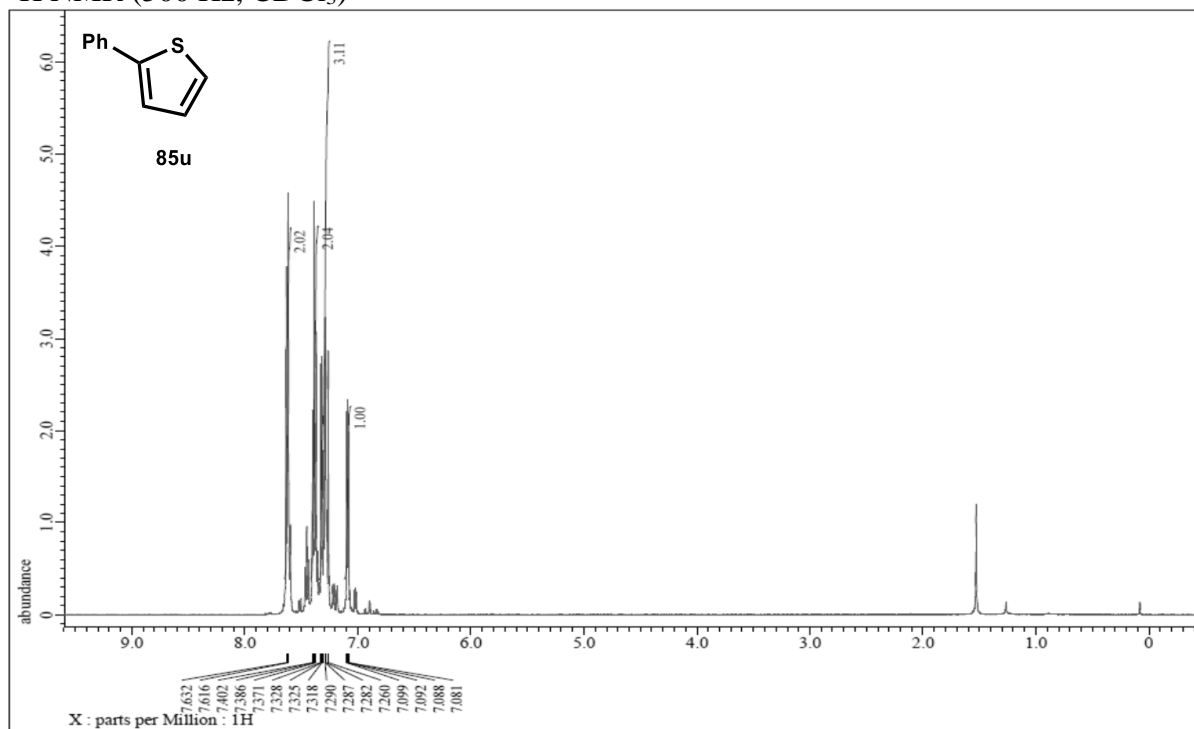
¹H NMR (500 Hz, CDCl₃)



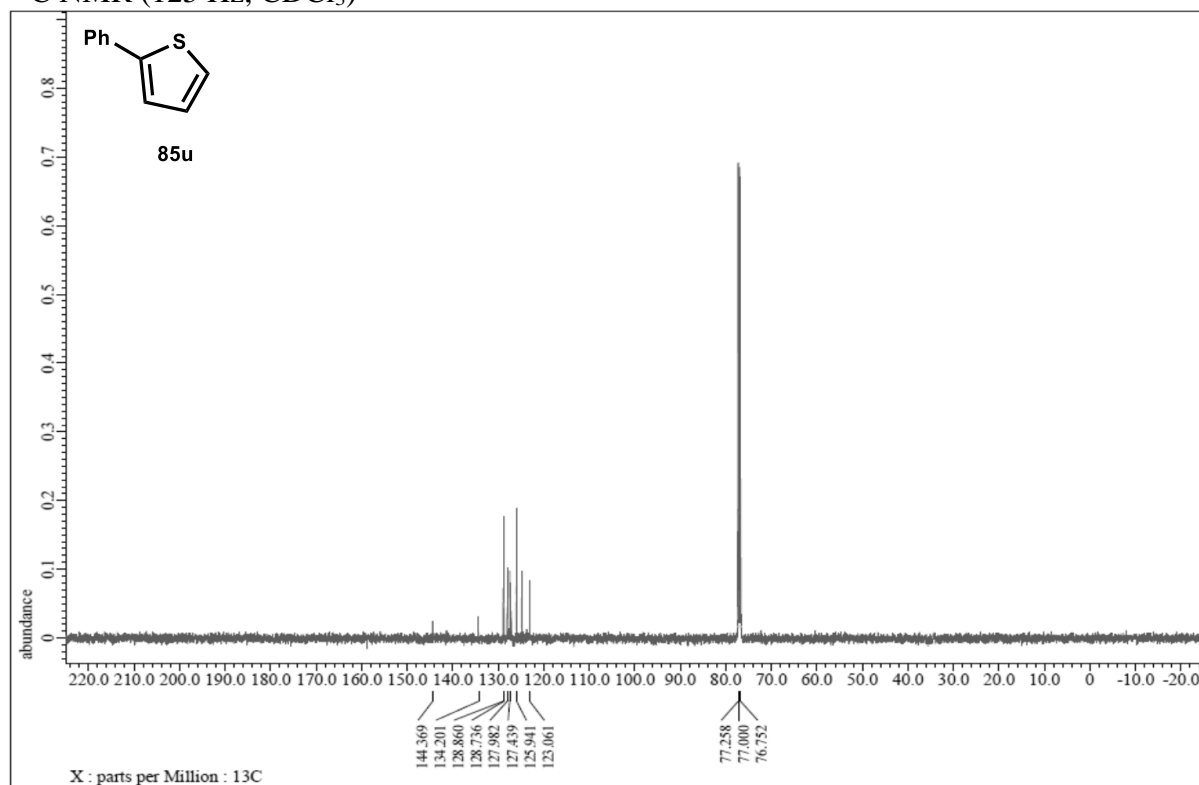
¹³C NMR (125 Hz, CDCl₃)



¹H NMR (500 Hz, CDCl₃)



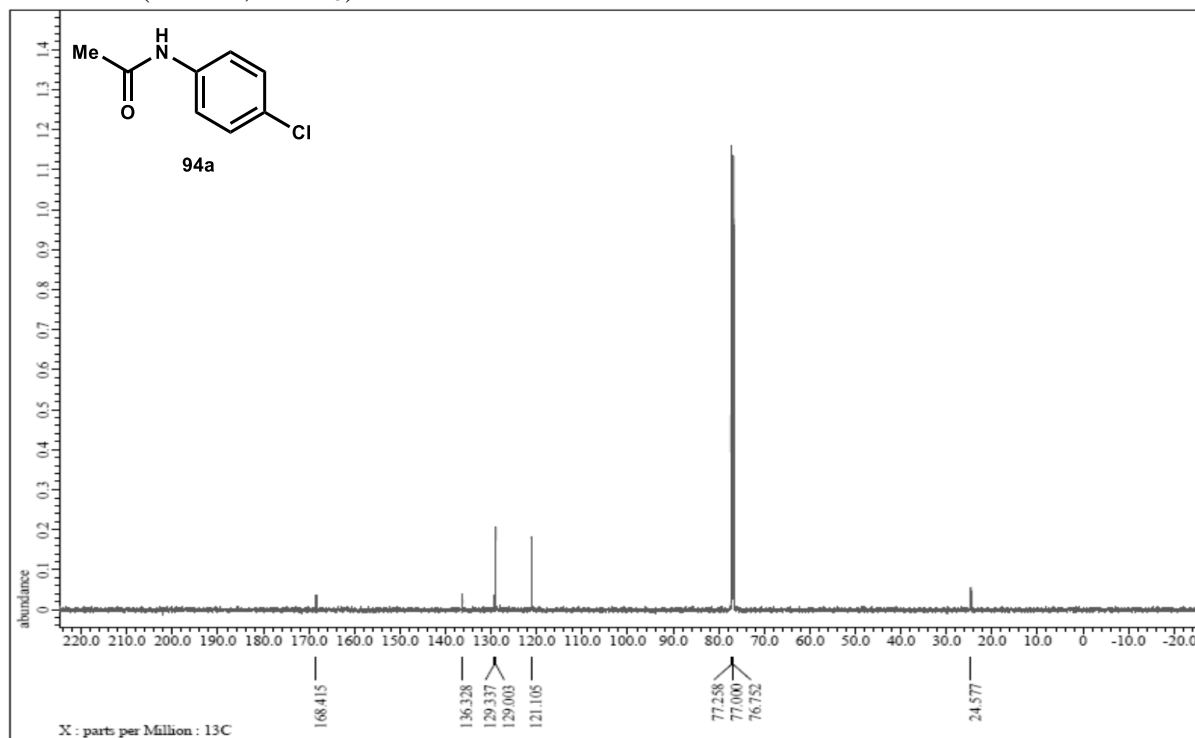
¹³C NMR (125 Hz, CDCl₃)



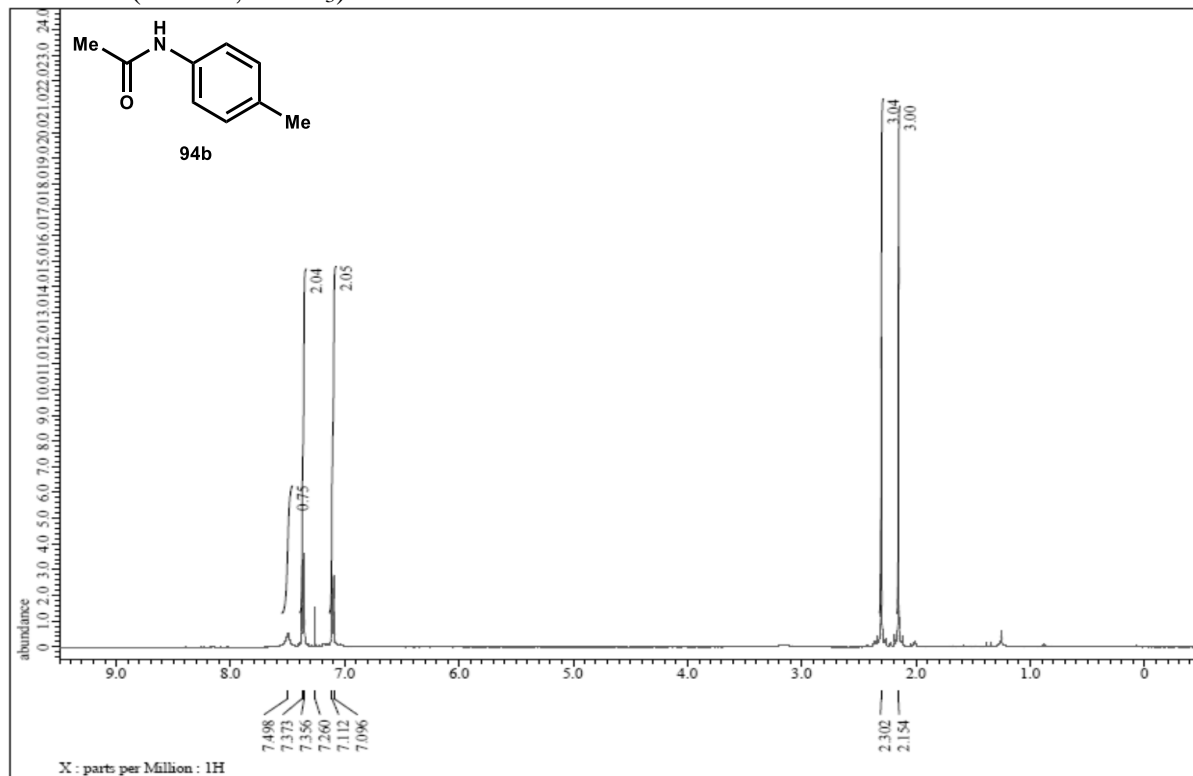
^1H NMR (500 Hz, CDCl_3)



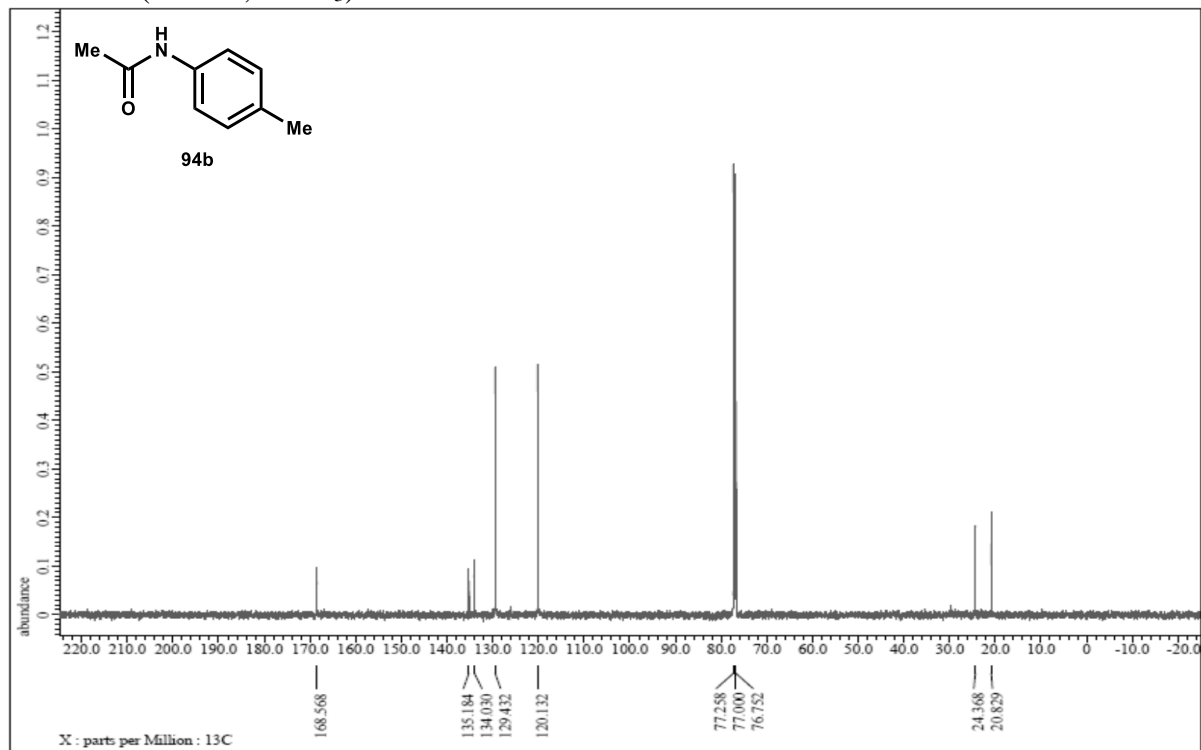
^{13}C NMR (125 Hz, CDCl_3)



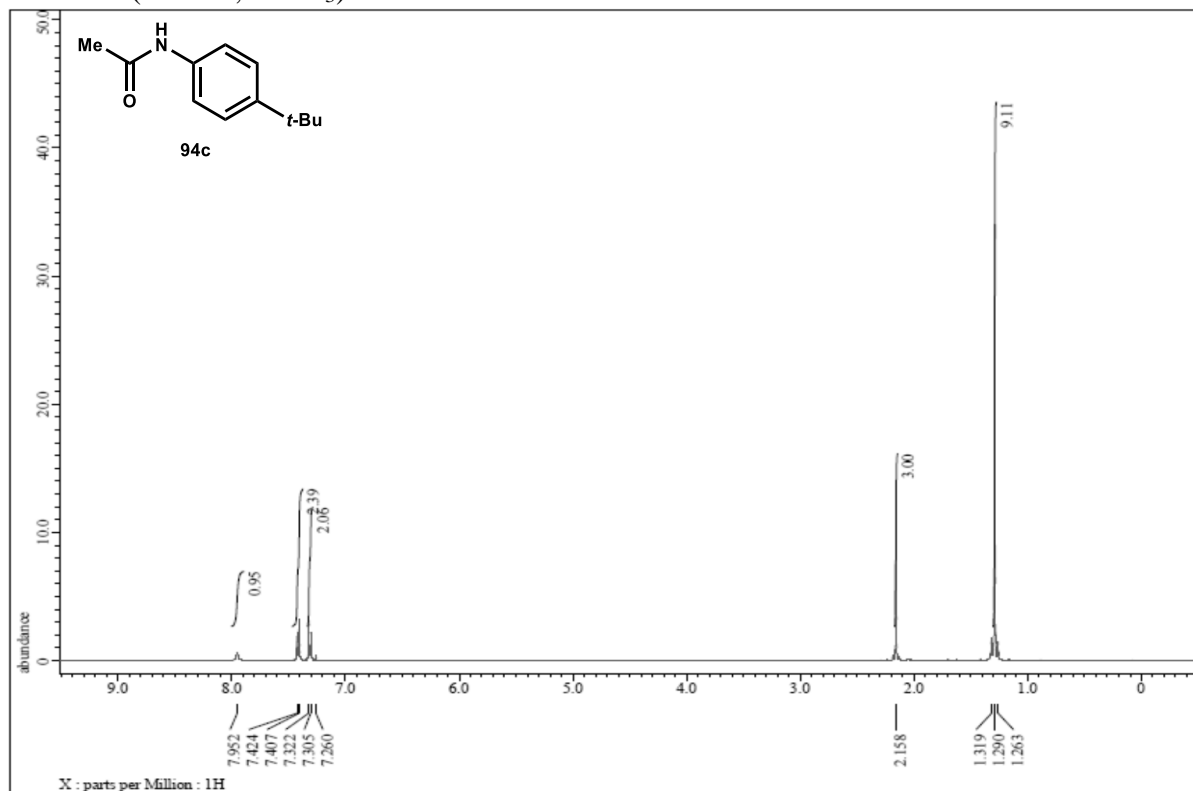
^1H NMR (500 Hz, CDCl_3)



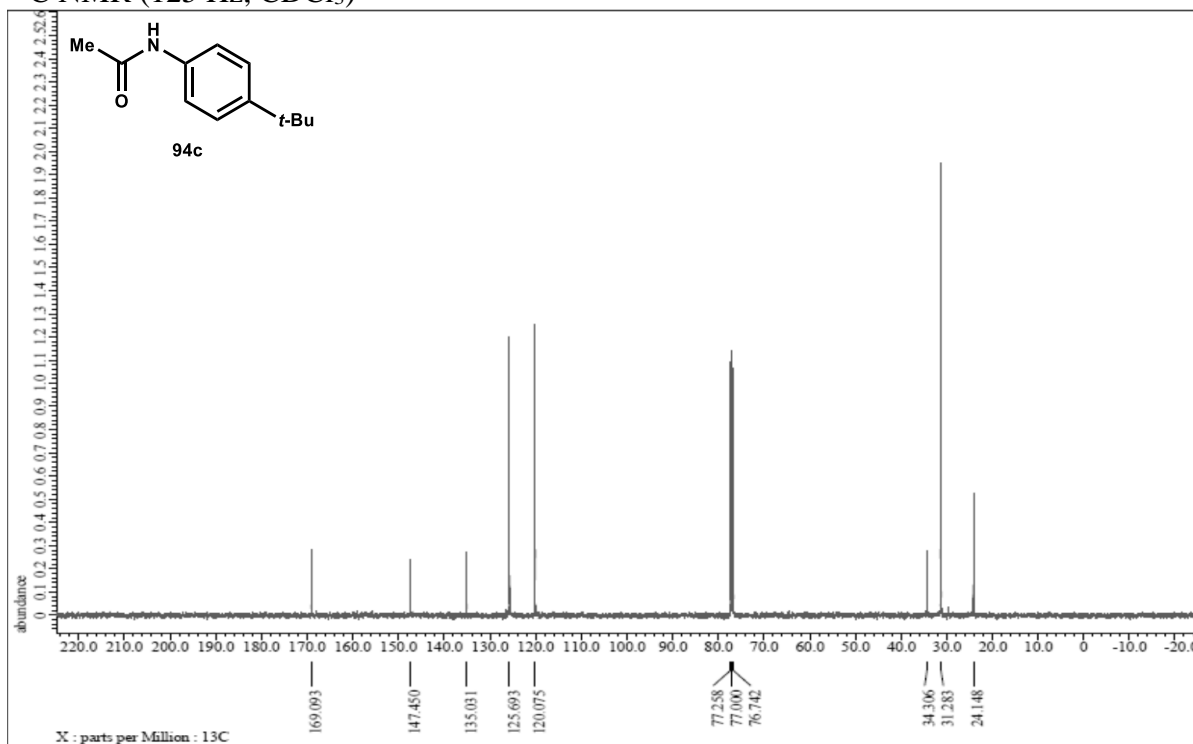
^{13}C NMR (125 Hz, CDCl_3)



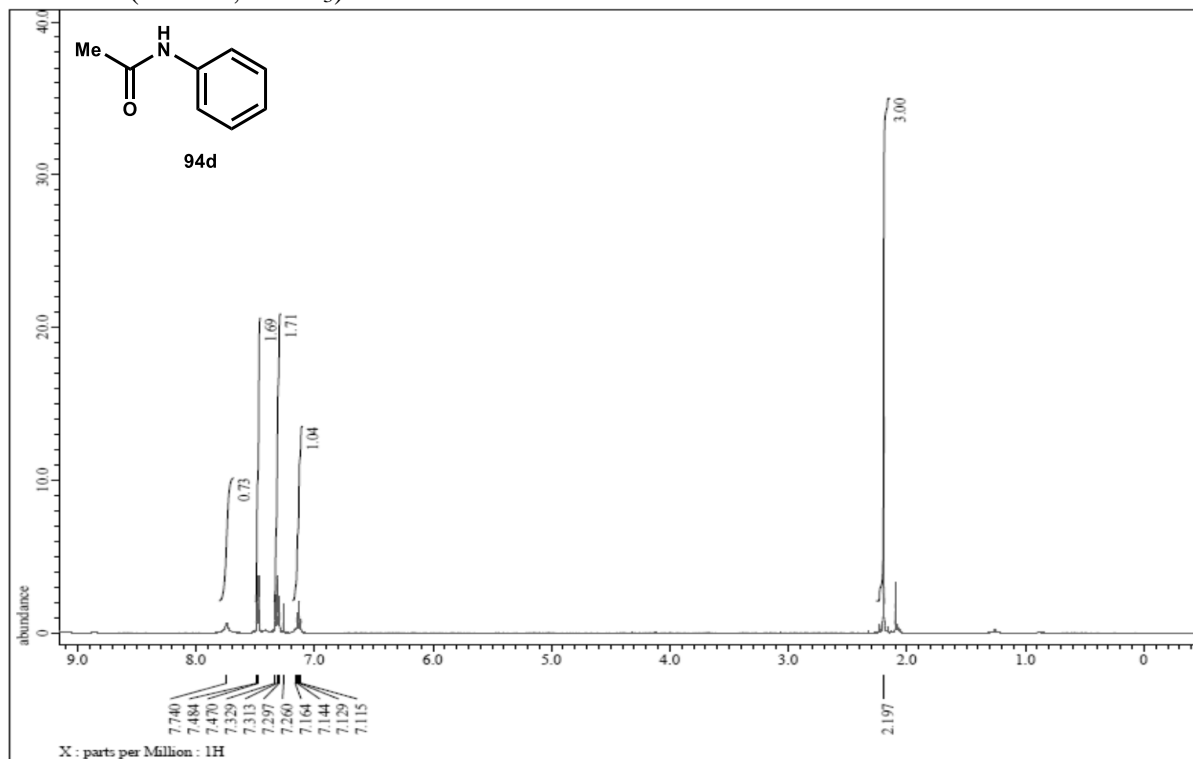
^1H NMR (500 Hz, CDCl_3)



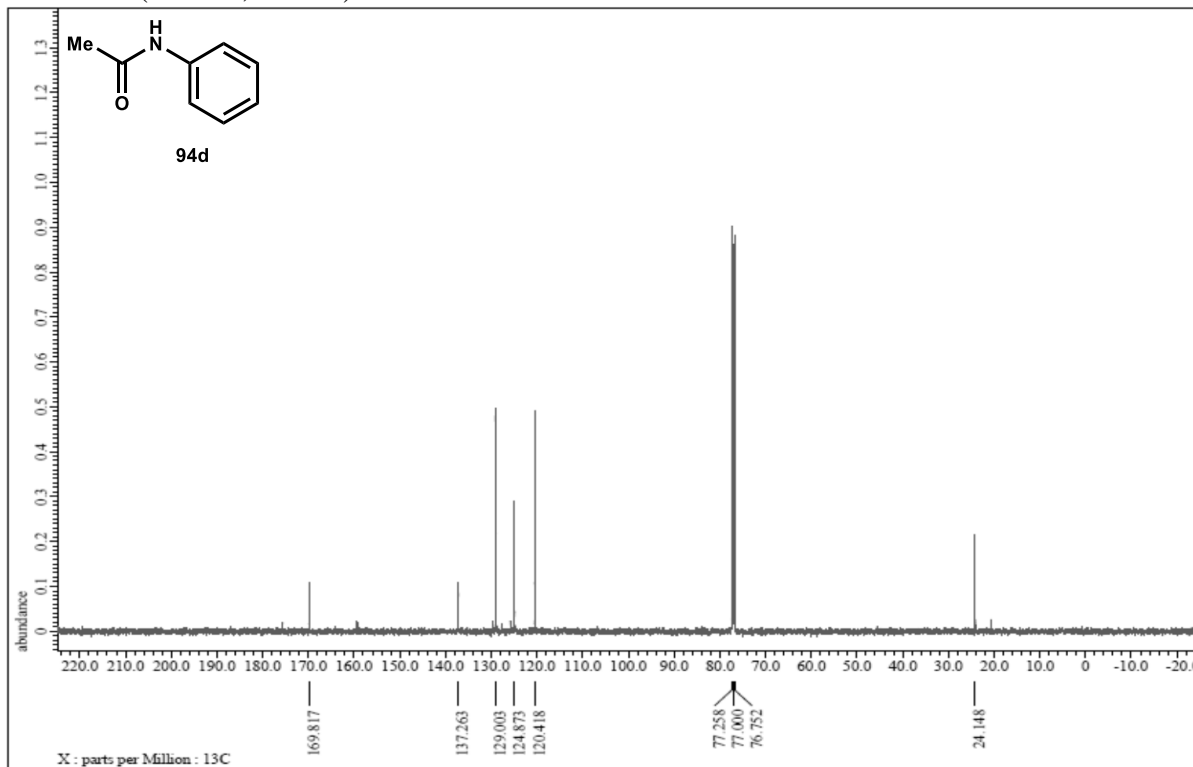
^{13}C NMR (125 Hz, CDCl_3)



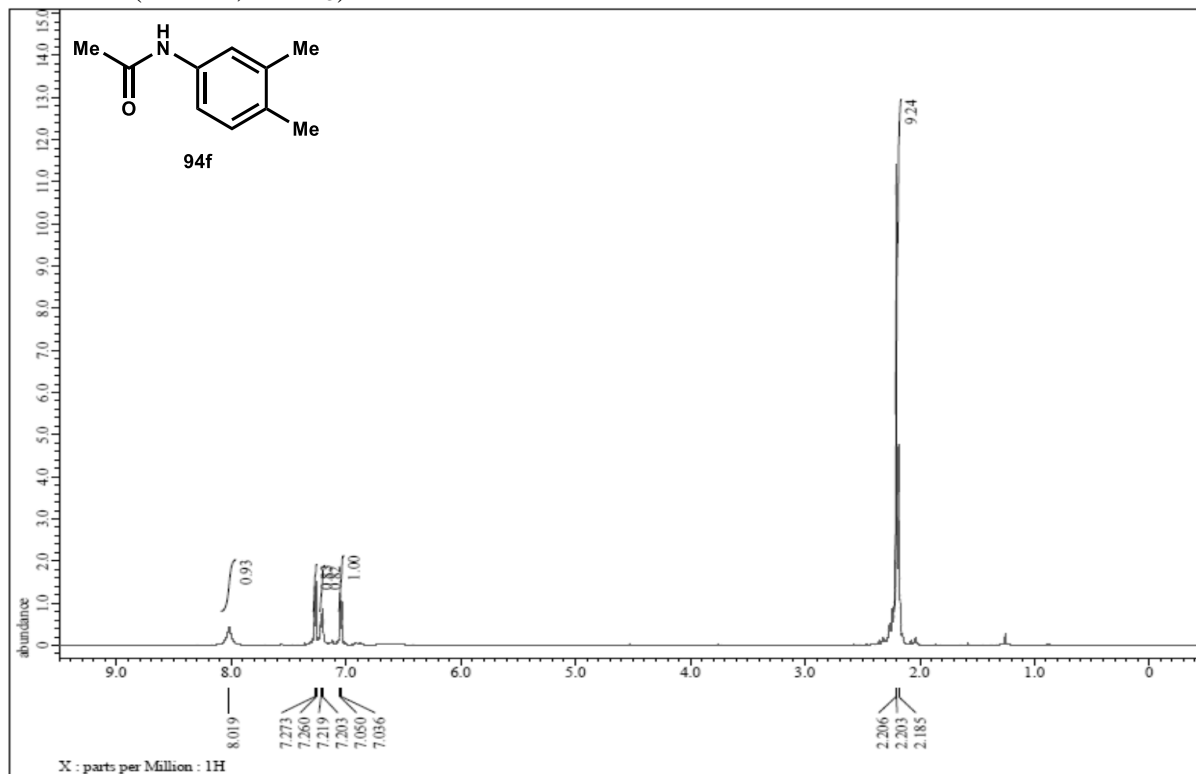
^1H NMR (500 Hz, CDCl_3)



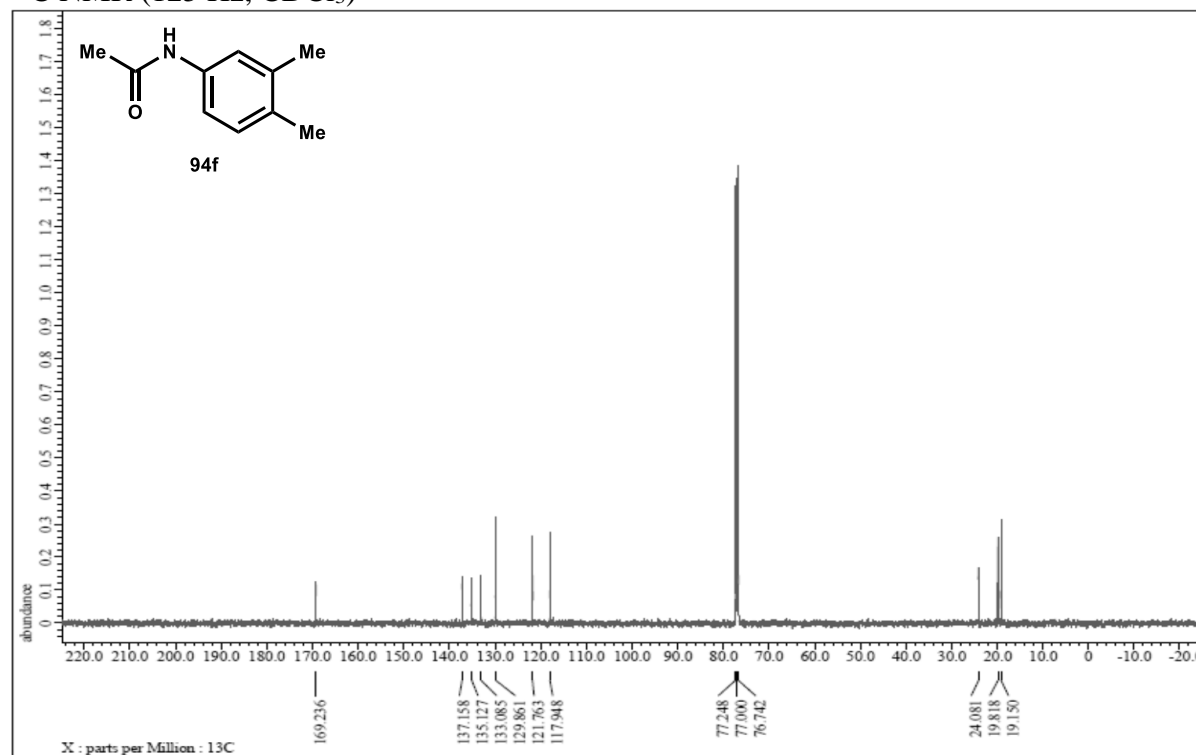
^{13}C NMR (125 Hz, CDCl_3)



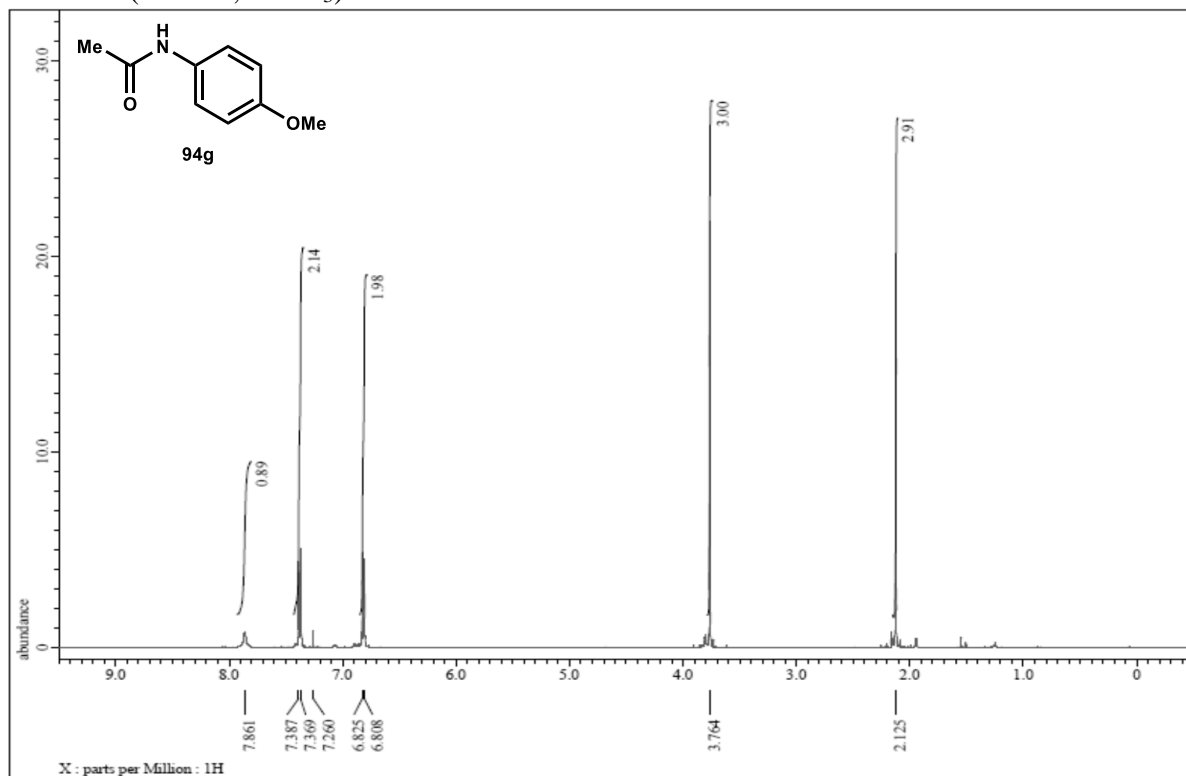
^1H NMR (500 Hz, CDCl_3)



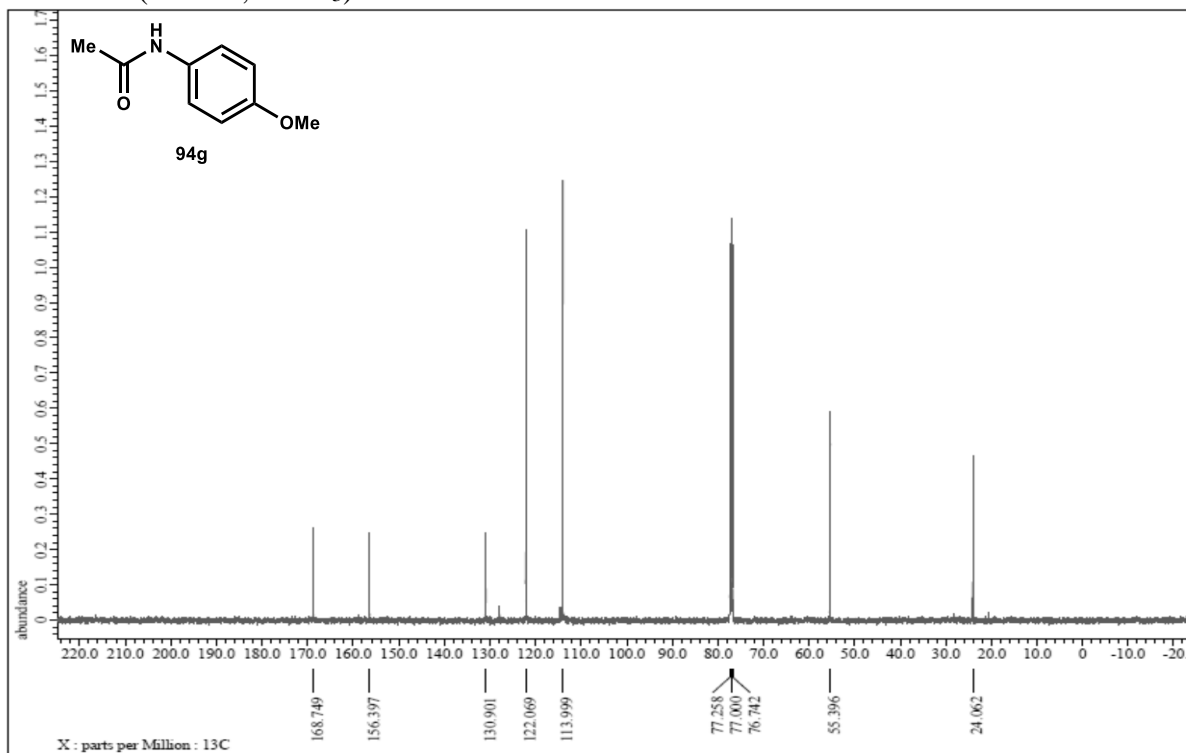
^{13}C NMR (125 Hz, CDCl_3)



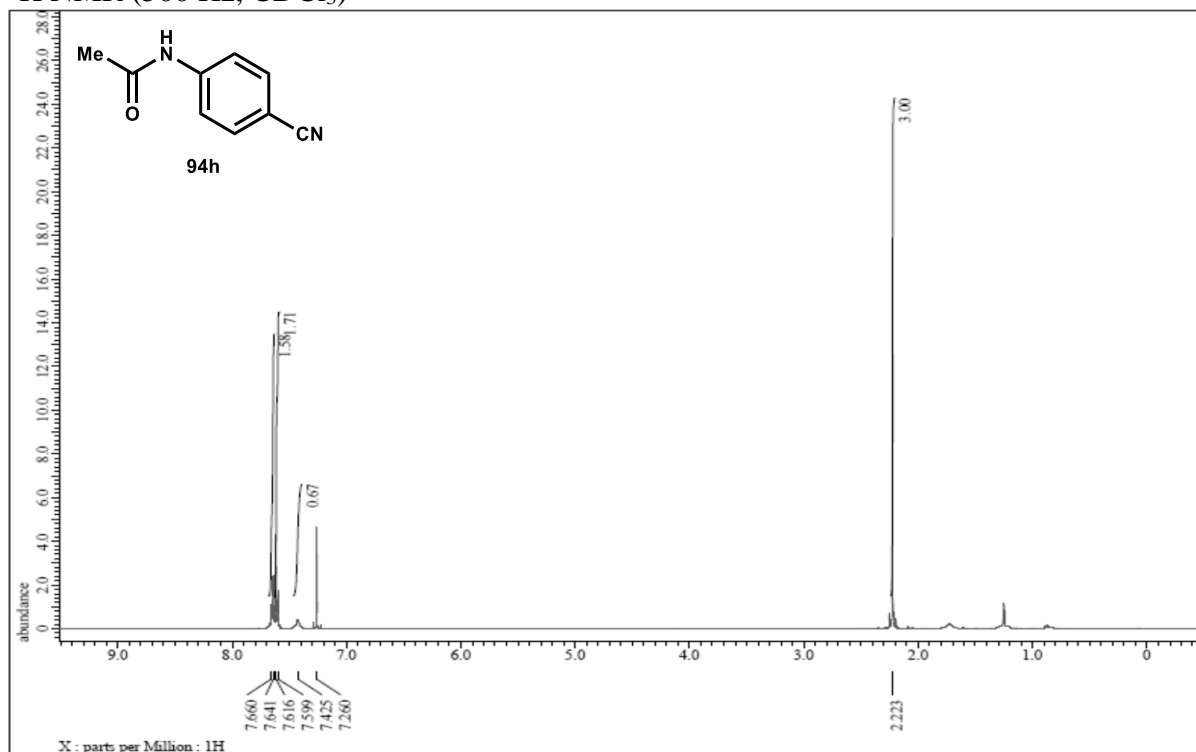
¹H NMR (500 Hz, CDCl₃)



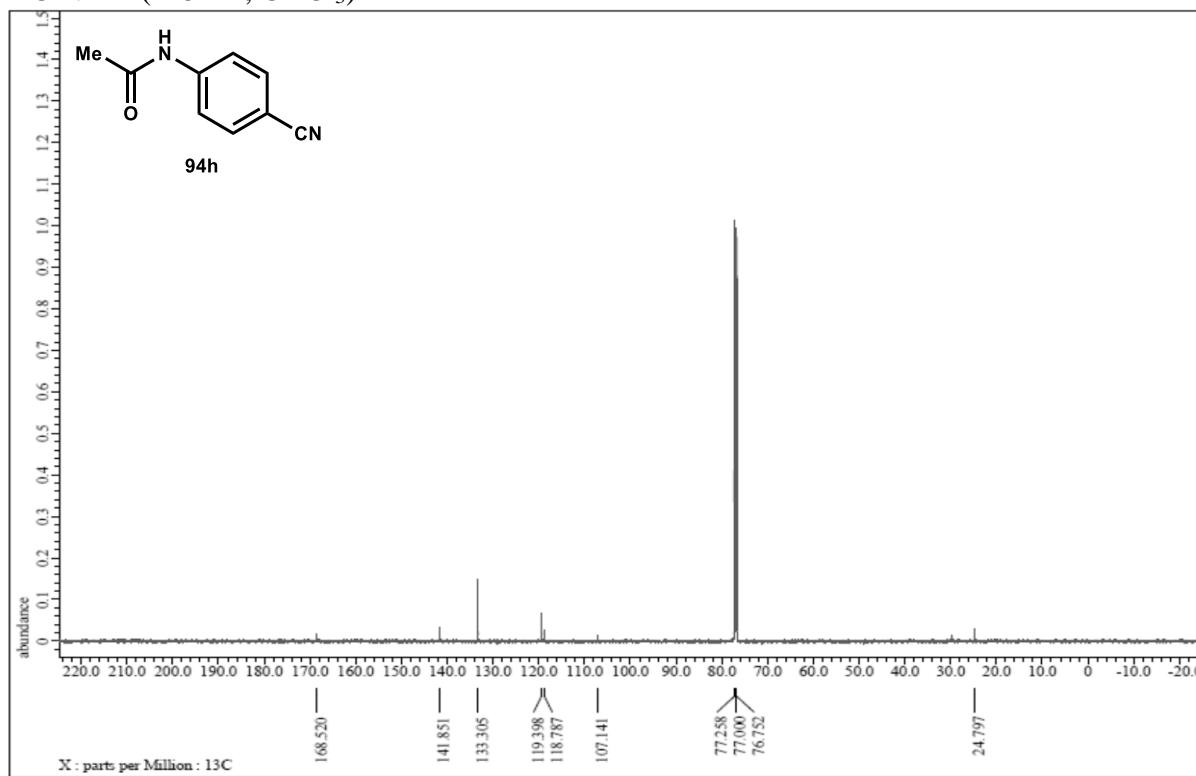
¹³C NMR (125 Hz, CDCl₃)



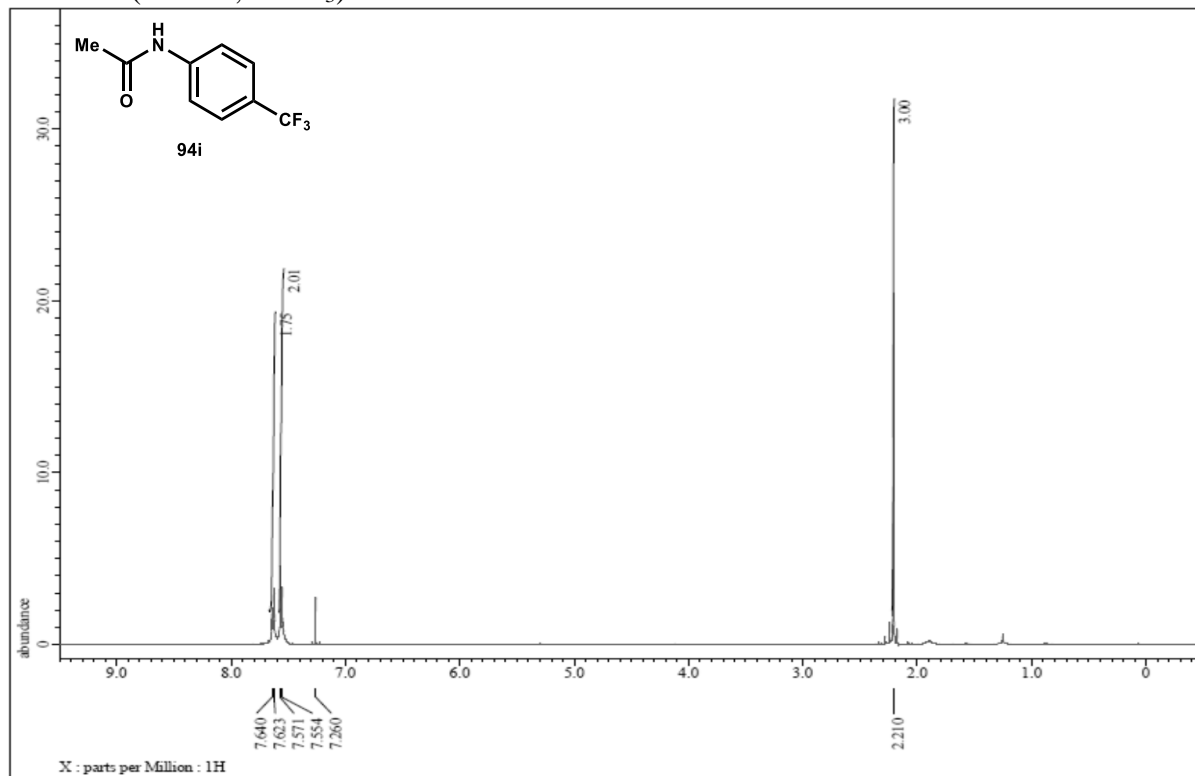
^1H NMR (500 Hz, CDCl_3)



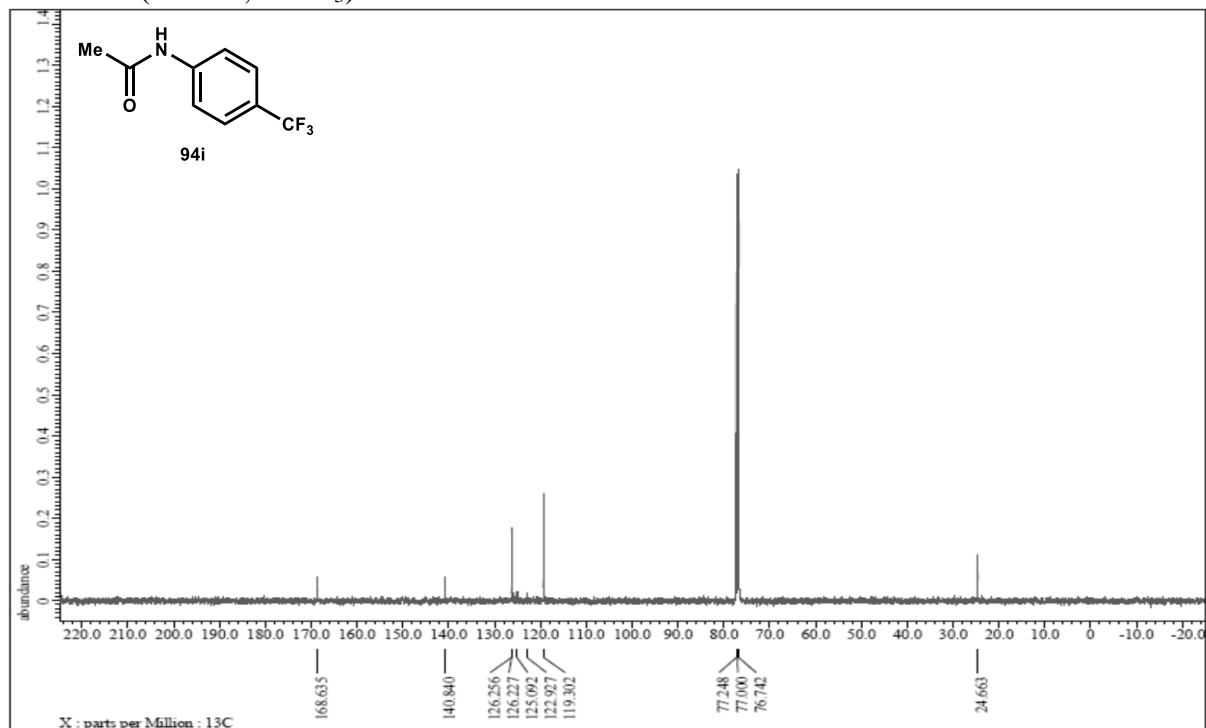
^{13}C NMR (125 Hz, CDCl_3)



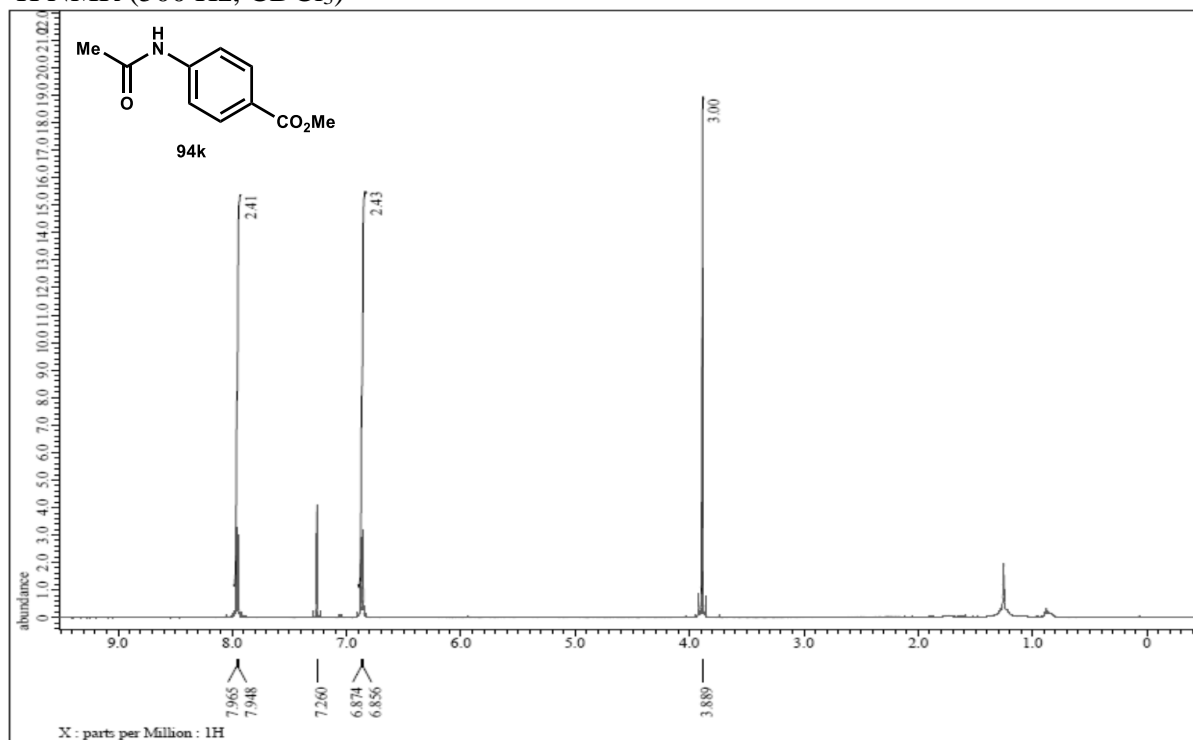
¹H NMR (500 Hz, CDCl₃)



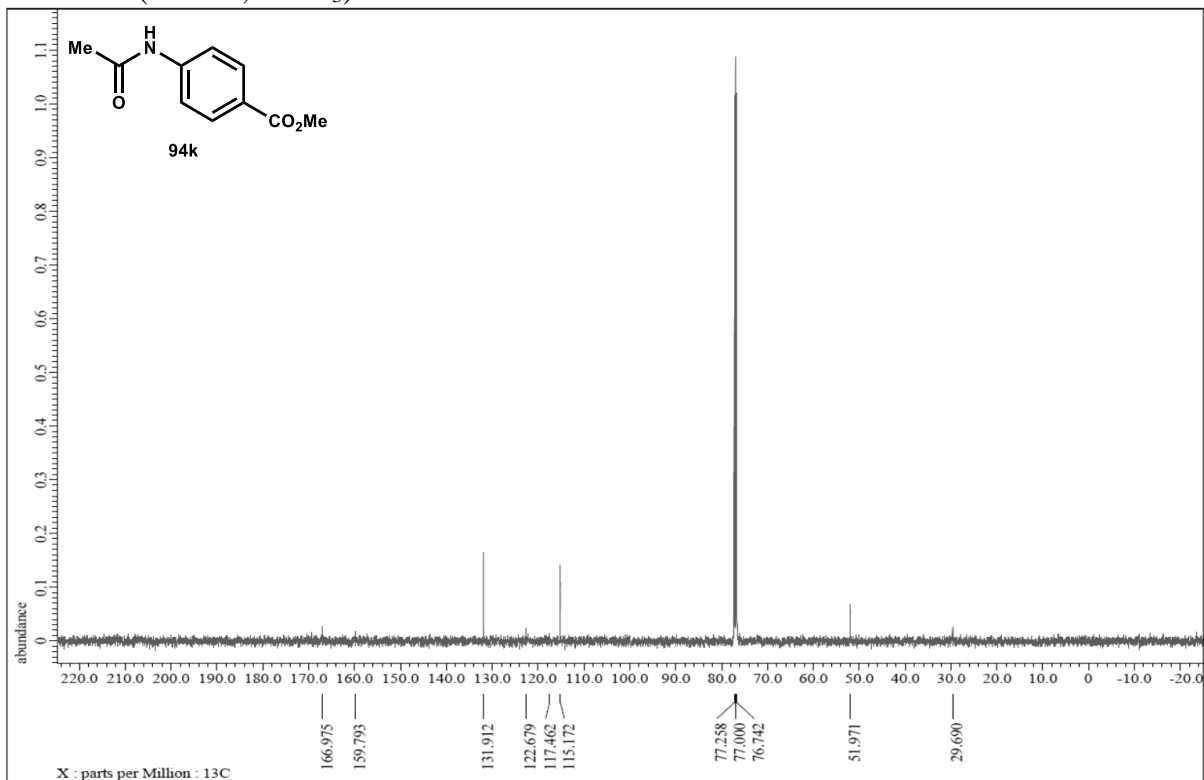
¹³C NMR (125 Hz, CDCl₃)



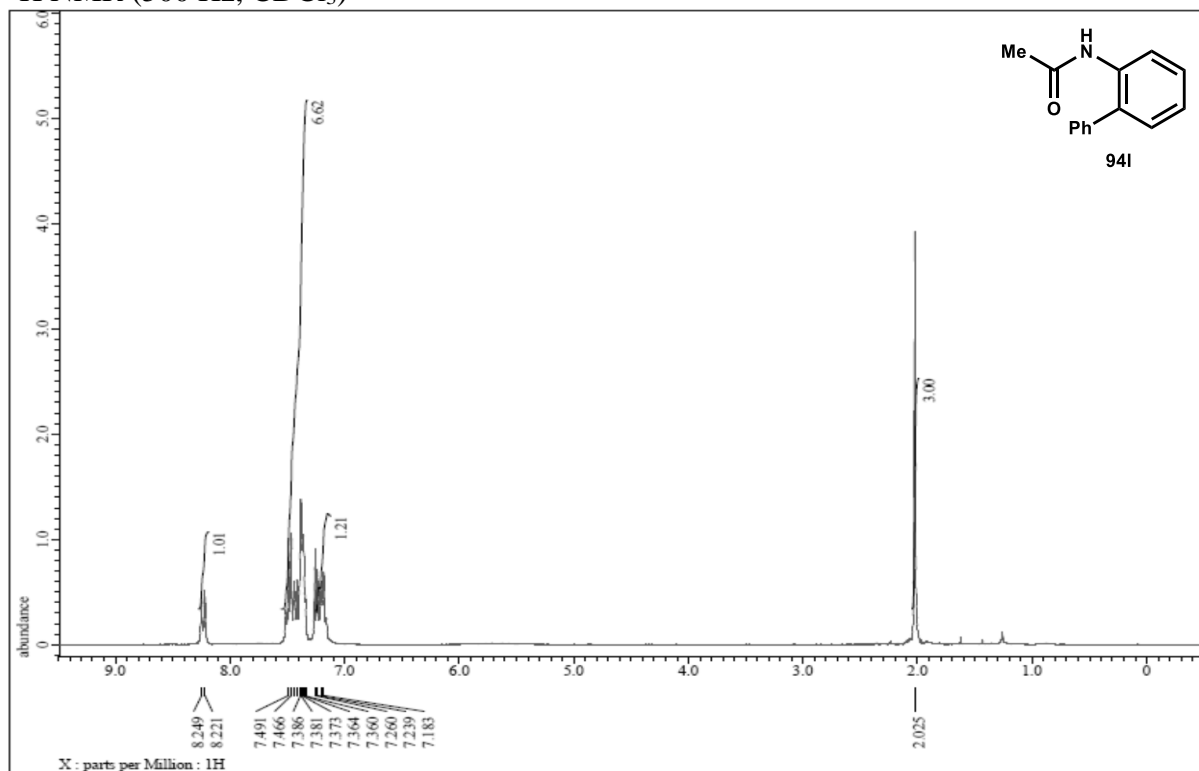
¹H NMR (500 Hz, CDCl₃)



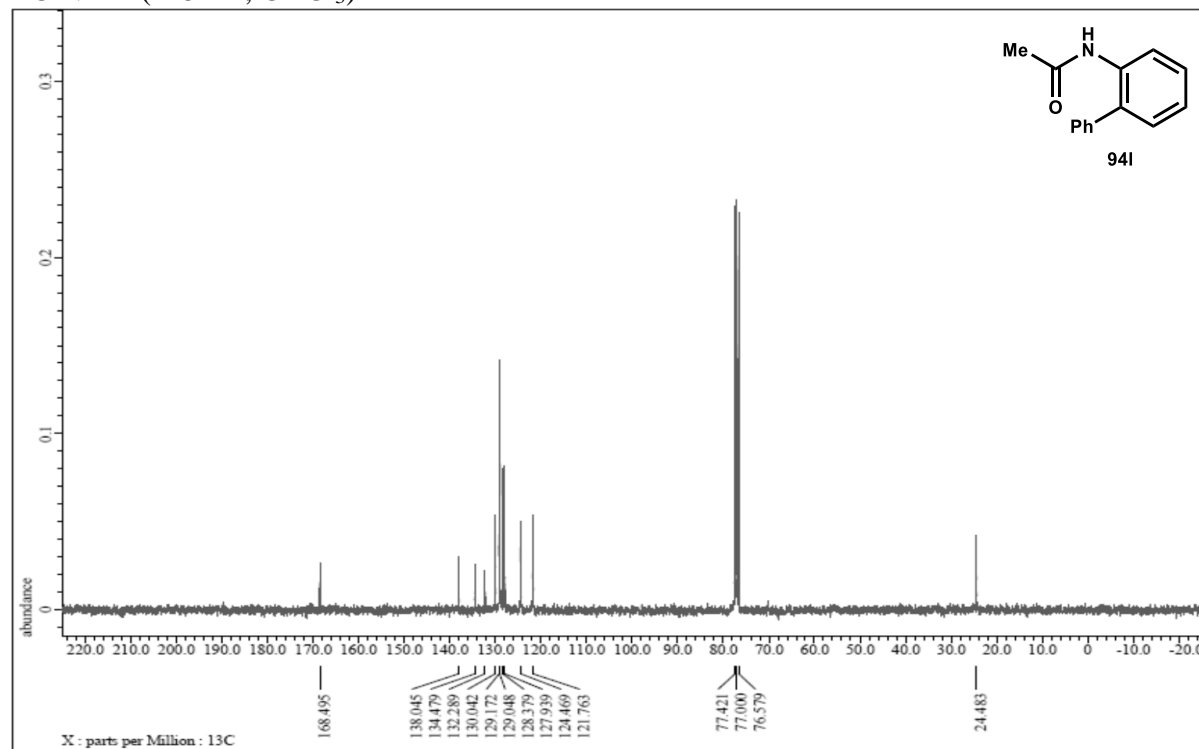
¹³C NMR (125 Hz, CDCl₃)



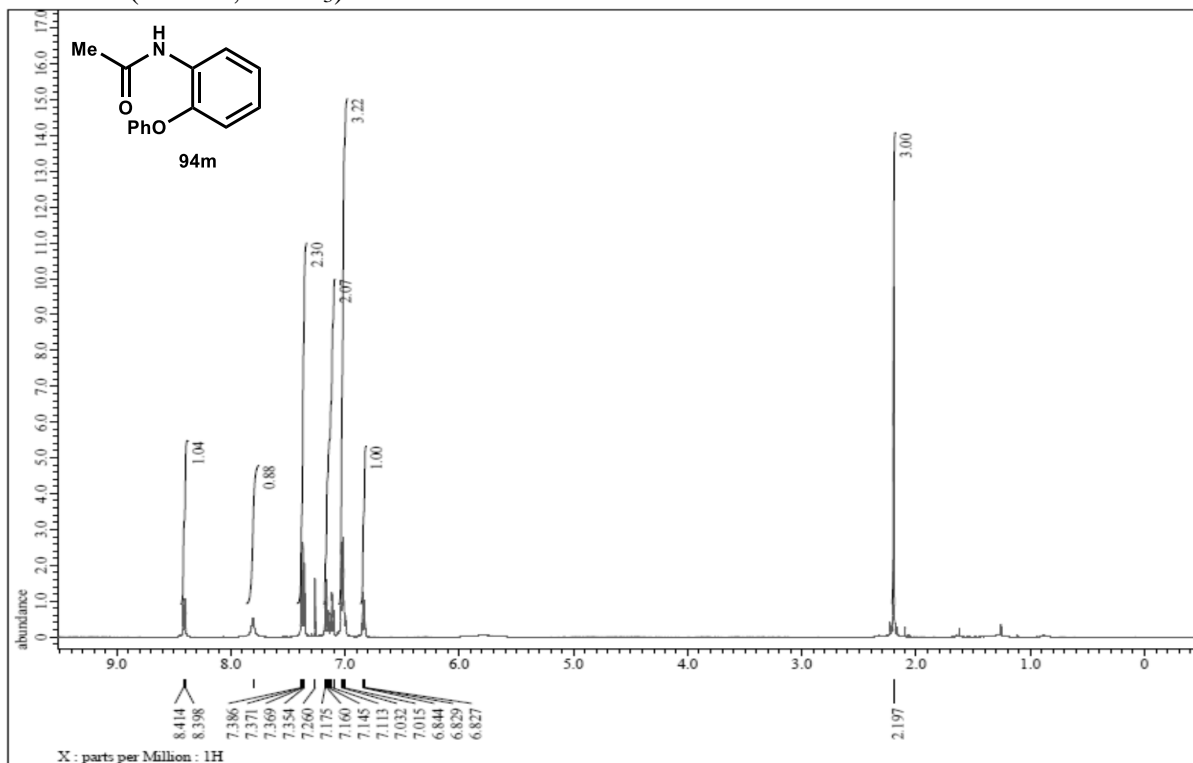
^1H NMR (500 Hz, CDCl_3)



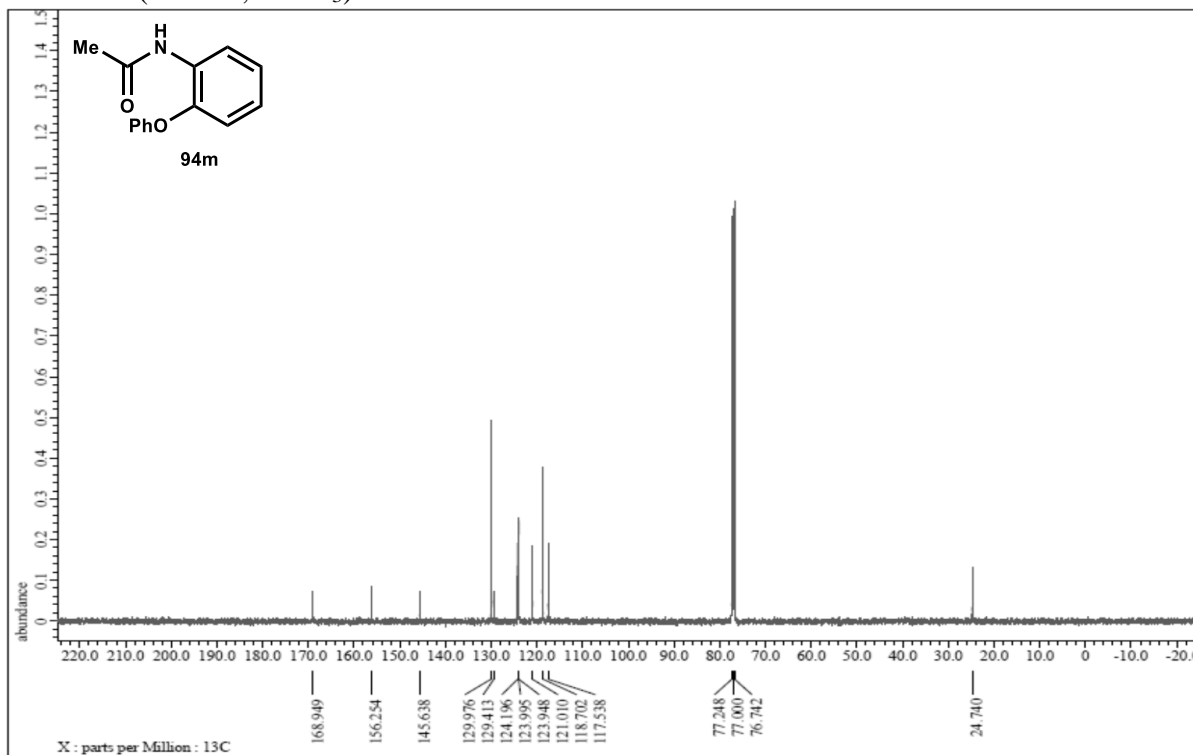
^{13}C NMR (125 Hz, CDCl_3)



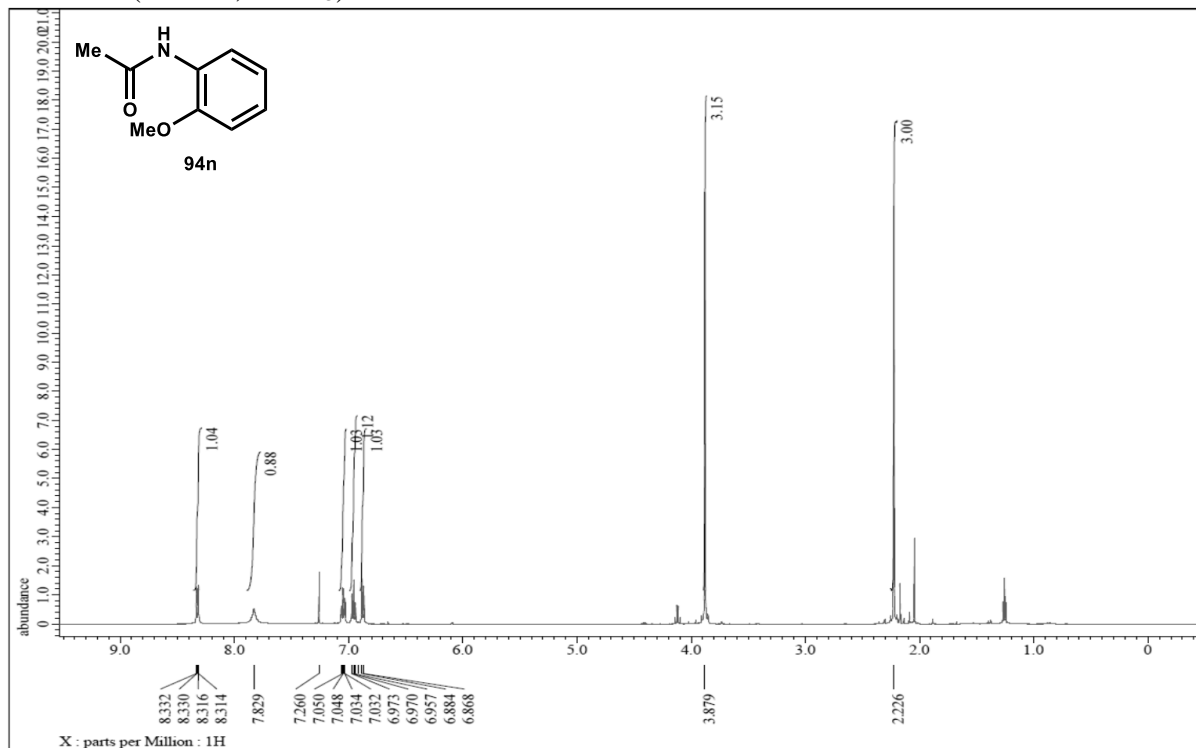
^1H NMR (500 Hz, CDCl_3)



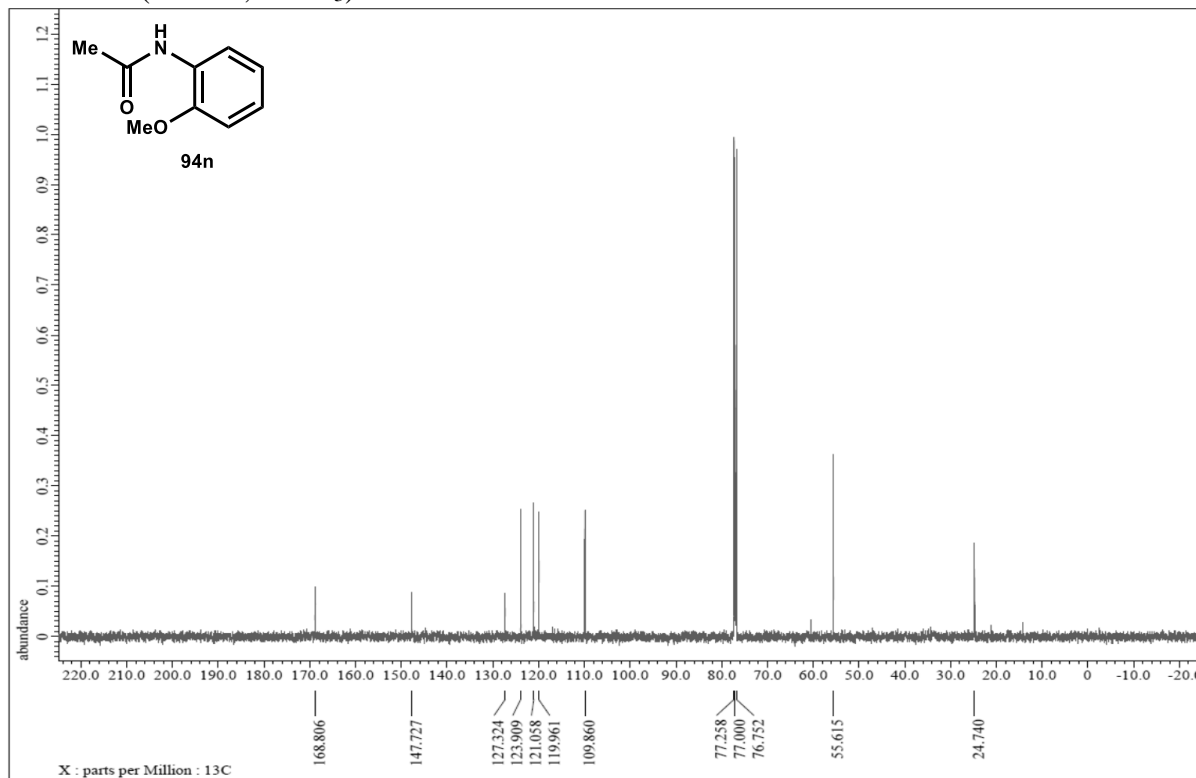
^{13}C NMR (125 Hz, CDCl_3)



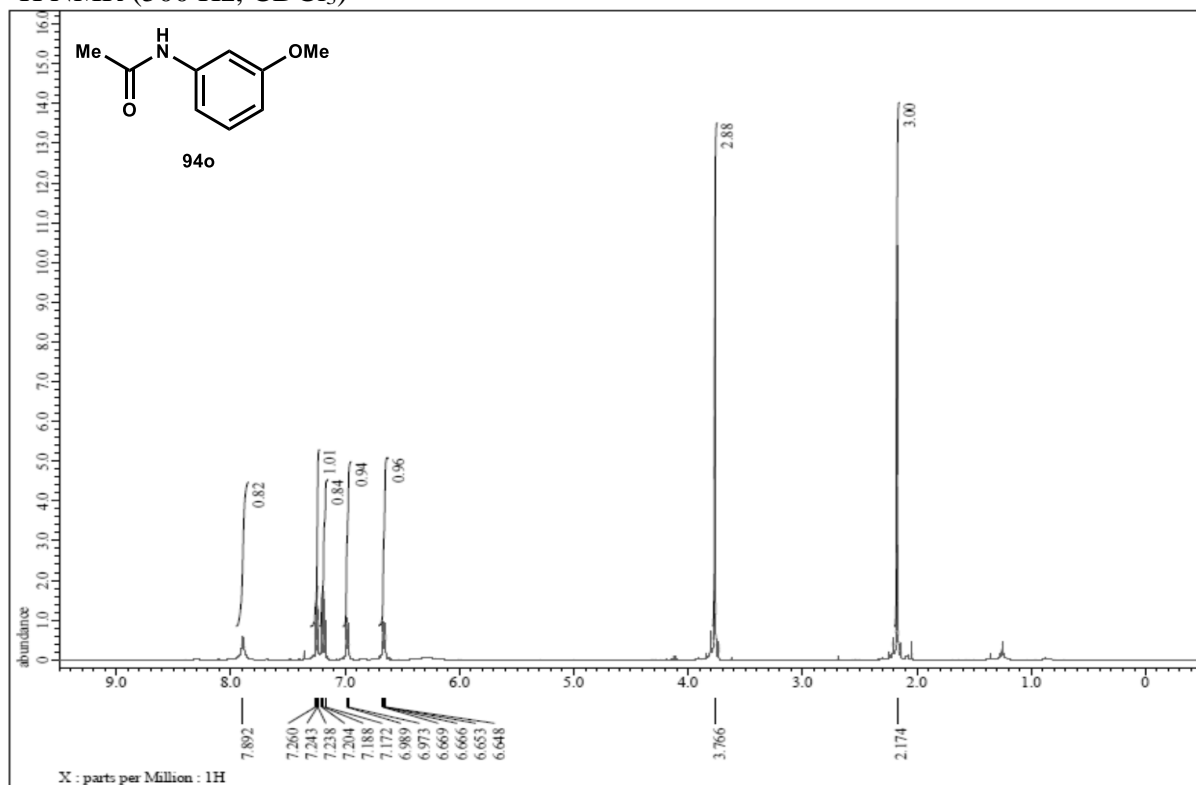
¹H NMR (500 Hz, CDCl₃)



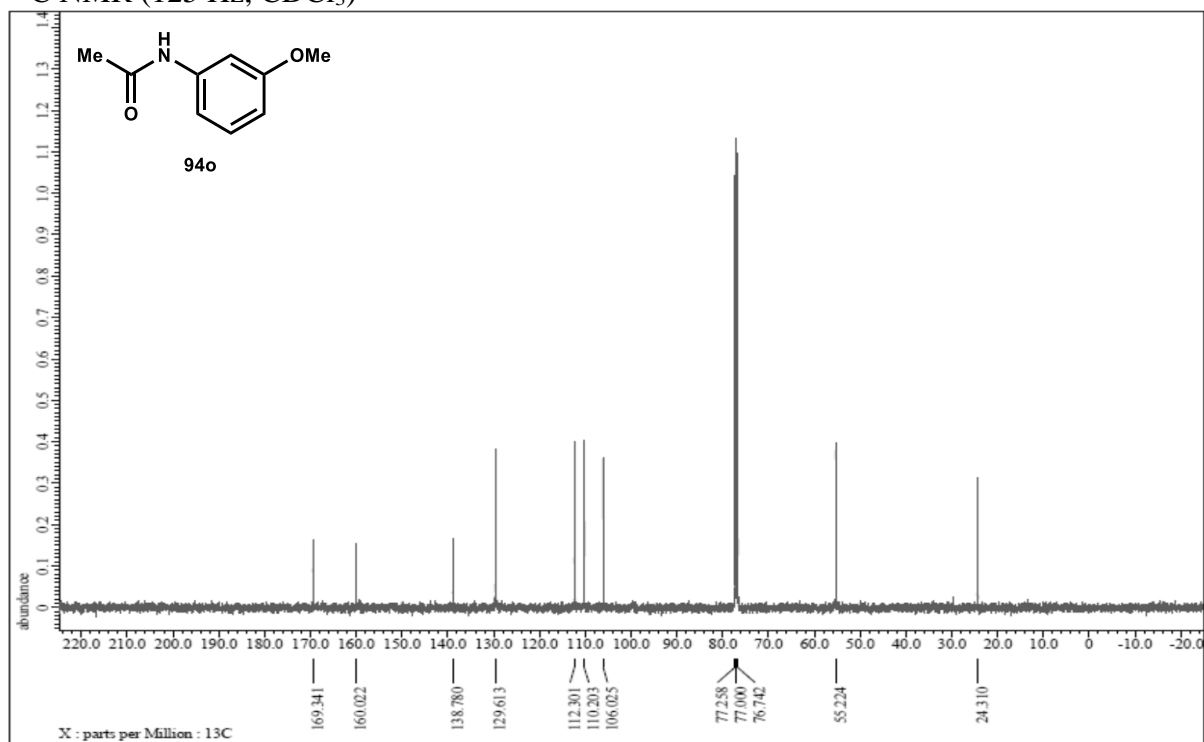
¹³C NMR (125 Hz, CDCl₃)



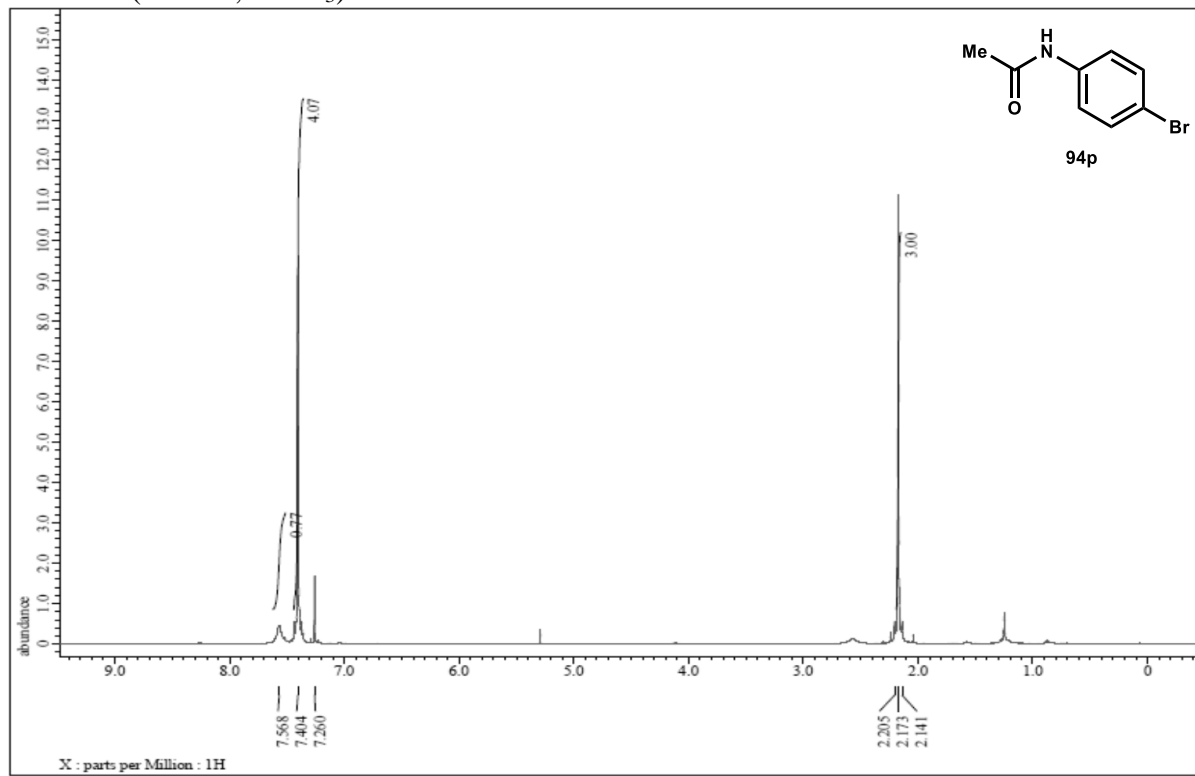
¹H NMR (500 Hz, CDCl₃)



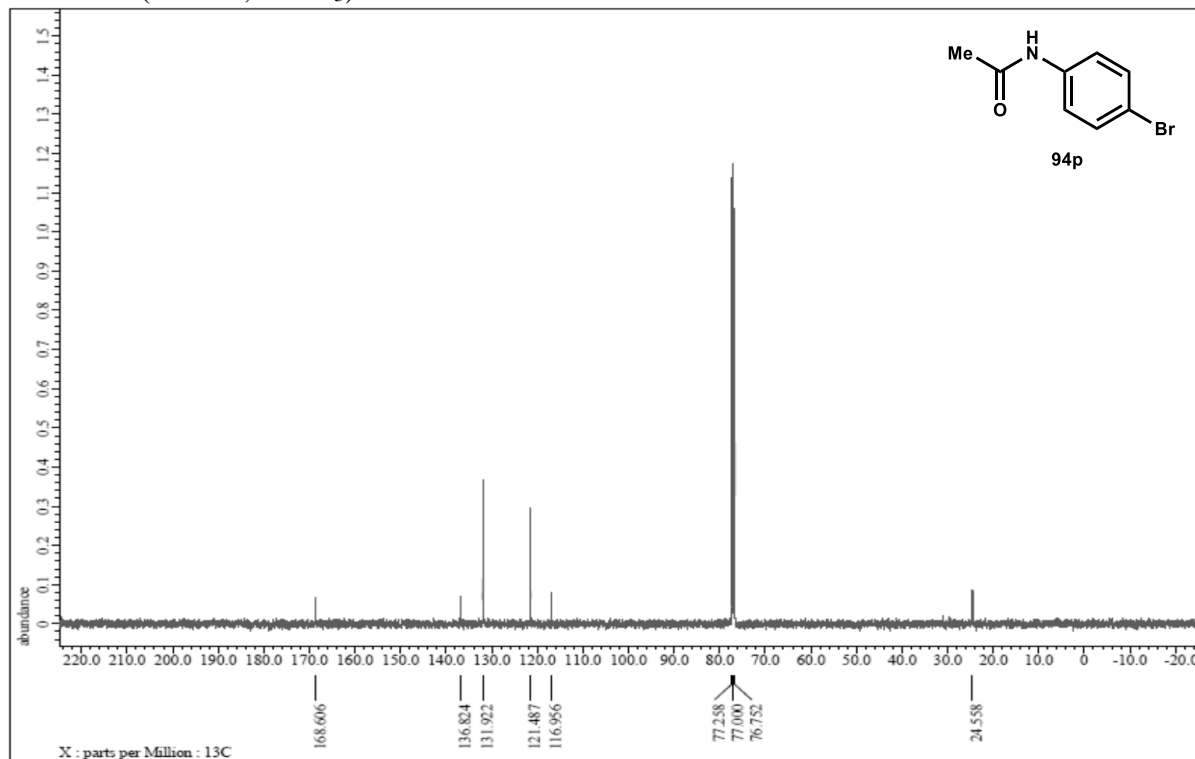
¹³C NMR (125 Hz, CDCl₃)



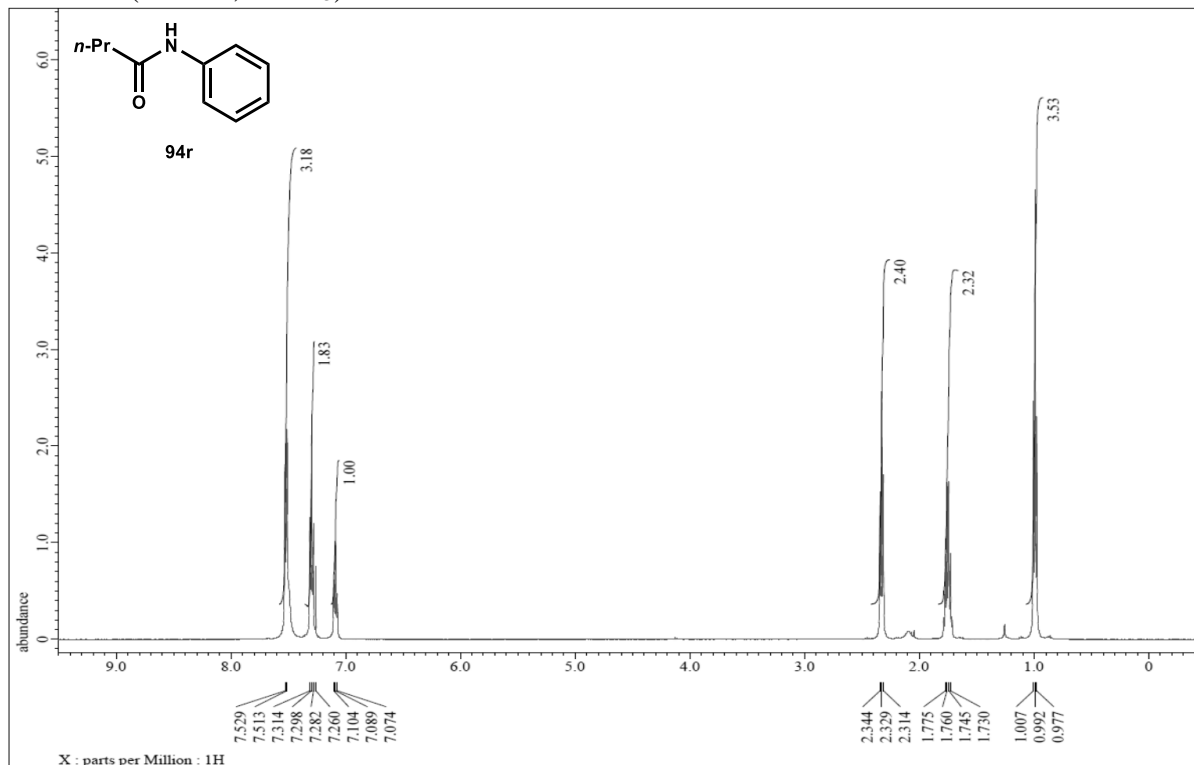
¹H NMR (500 Hz, CDCl₃)



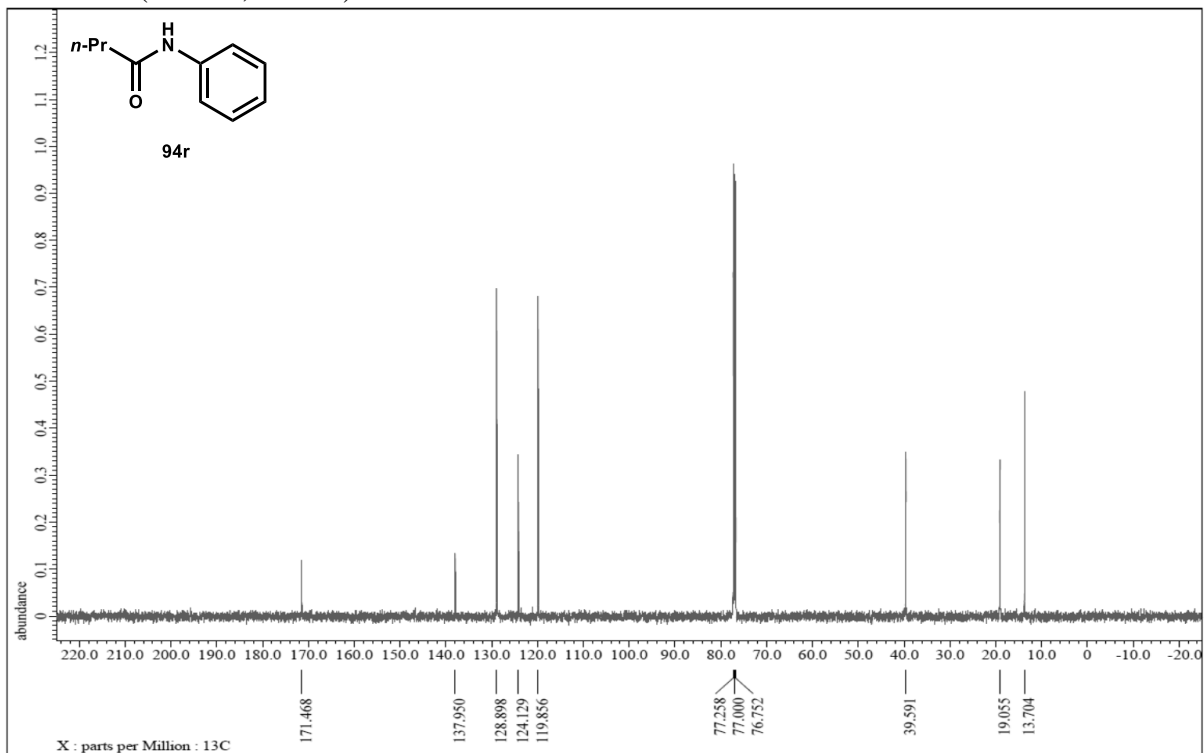
¹³C NMR (125 Hz, CDCl₃)



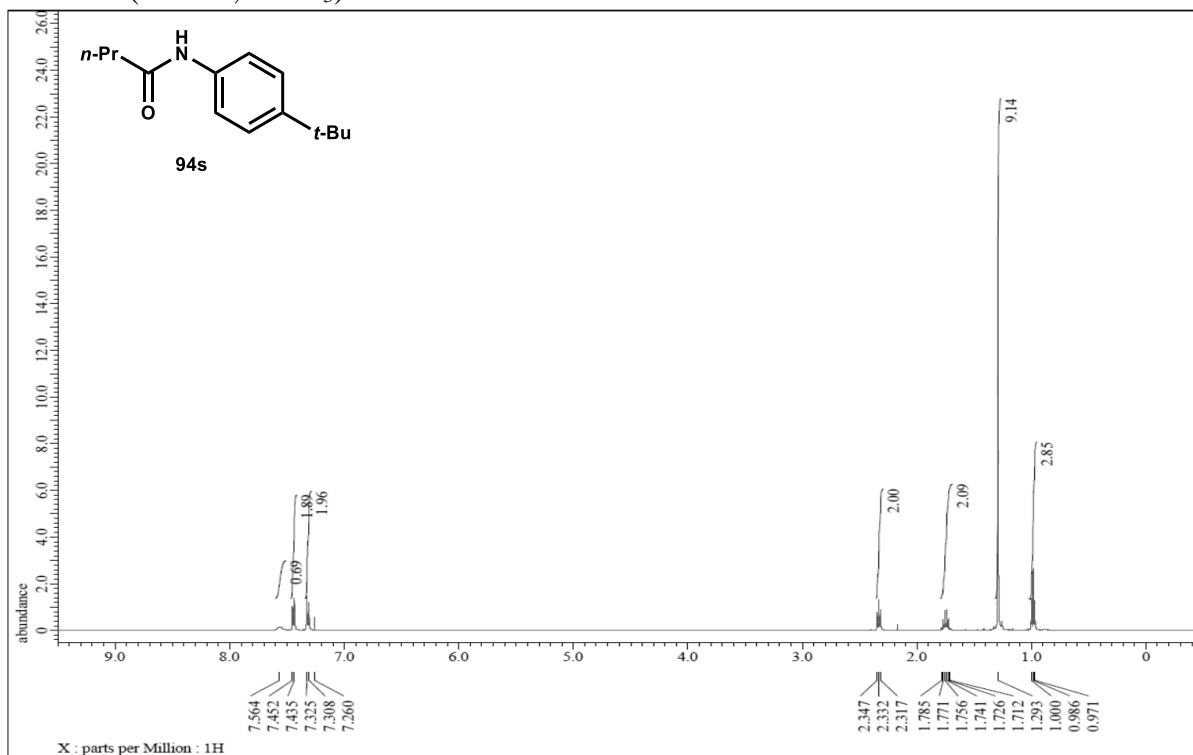
^1H NMR (500 Hz, CDCl_3)



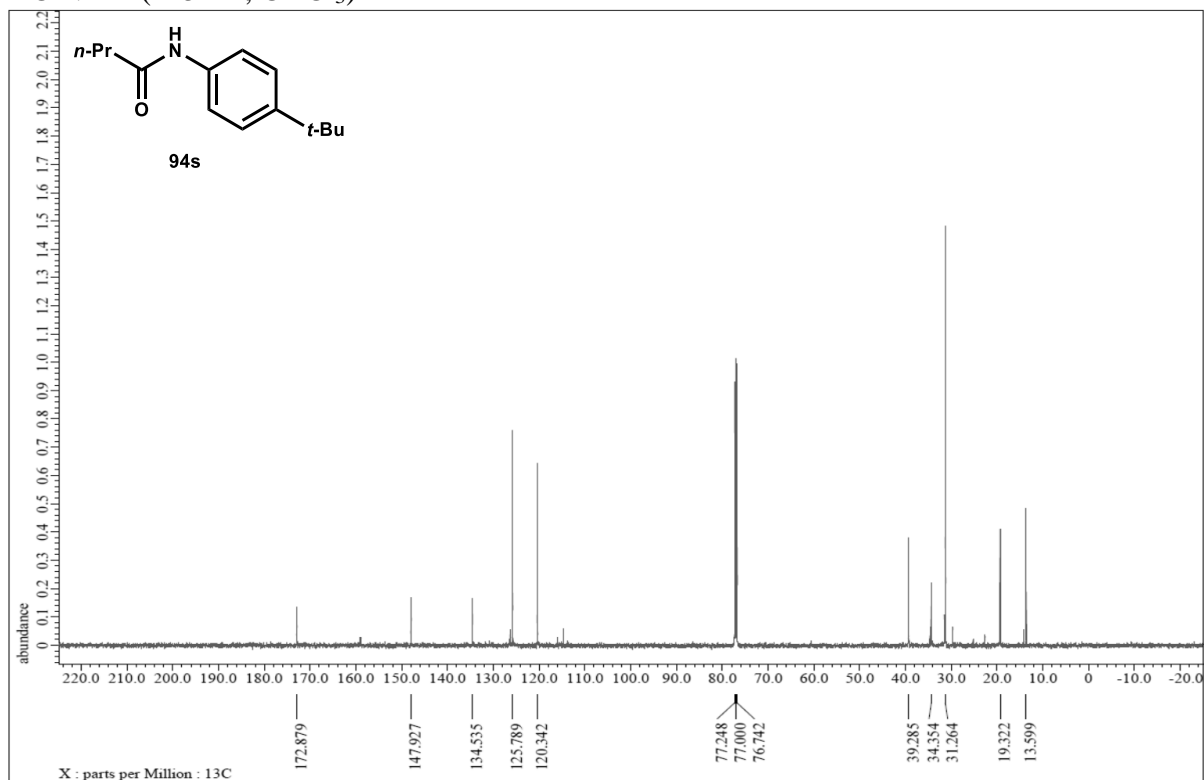
^{13}C NMR (125 Hz, CDCl_3)



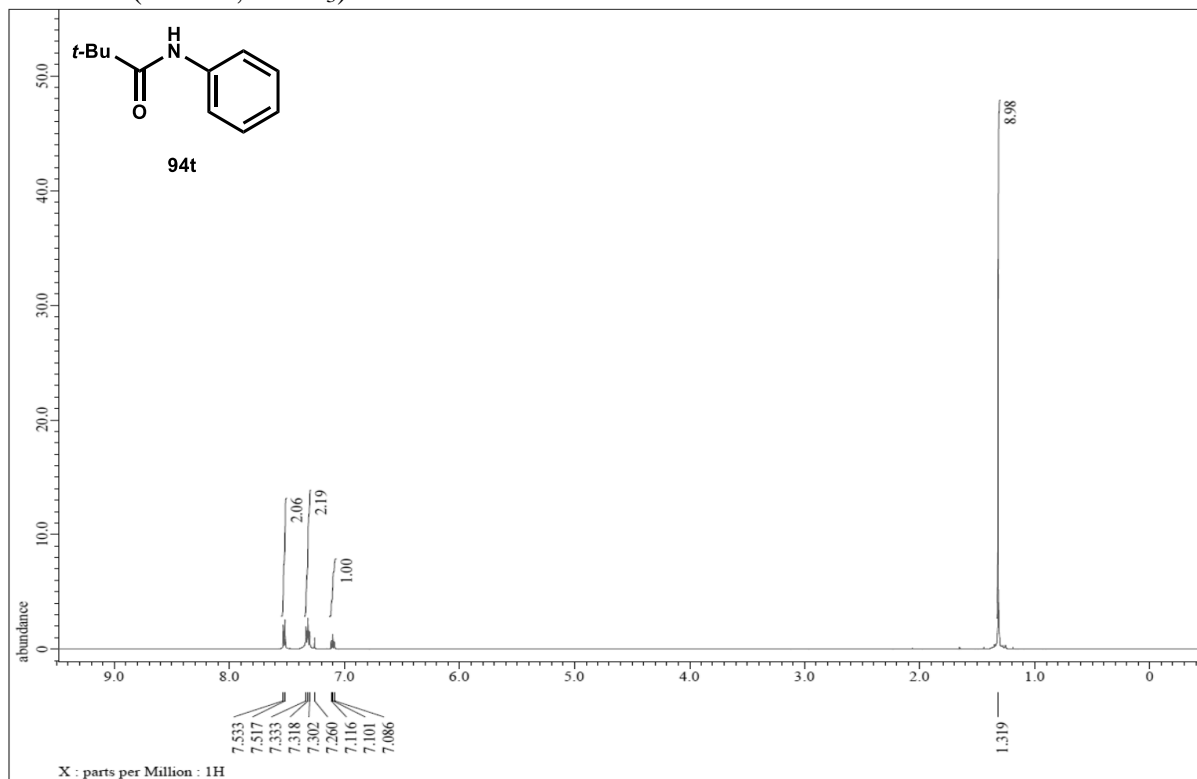
¹H NMR (500 Hz, CDCl₃)



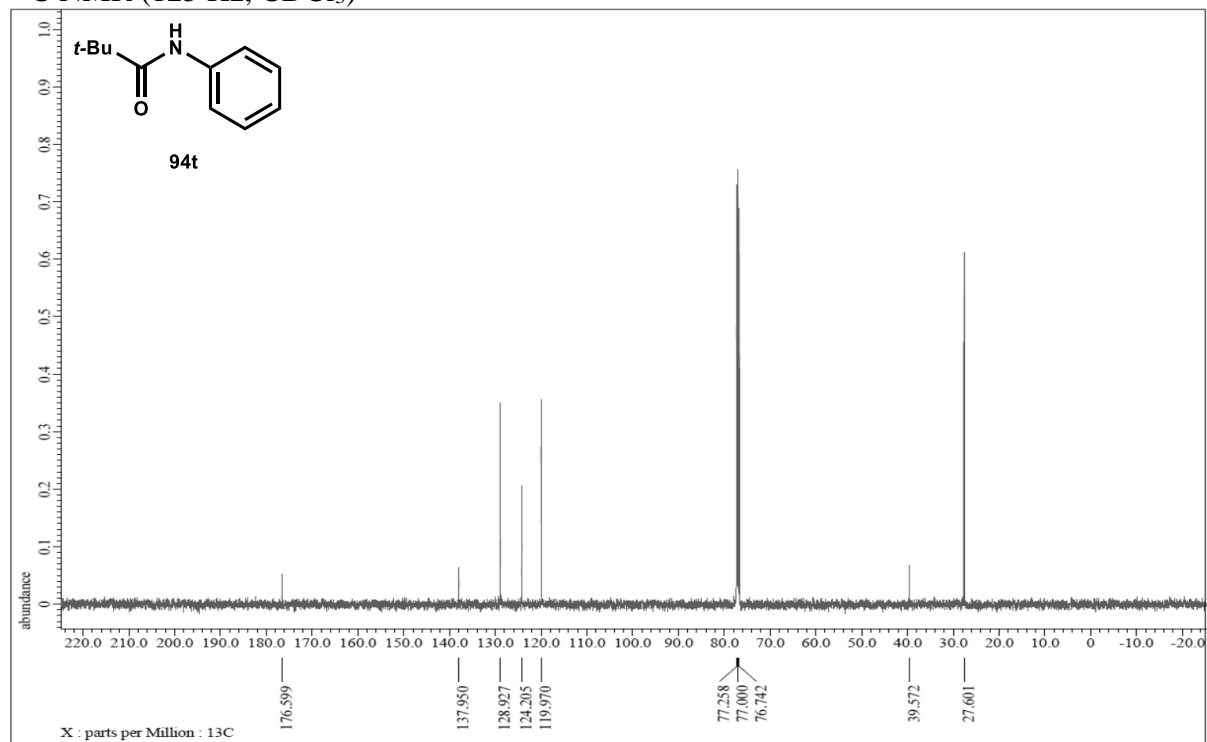
¹³C NMR (125 Hz, CDCl₃)



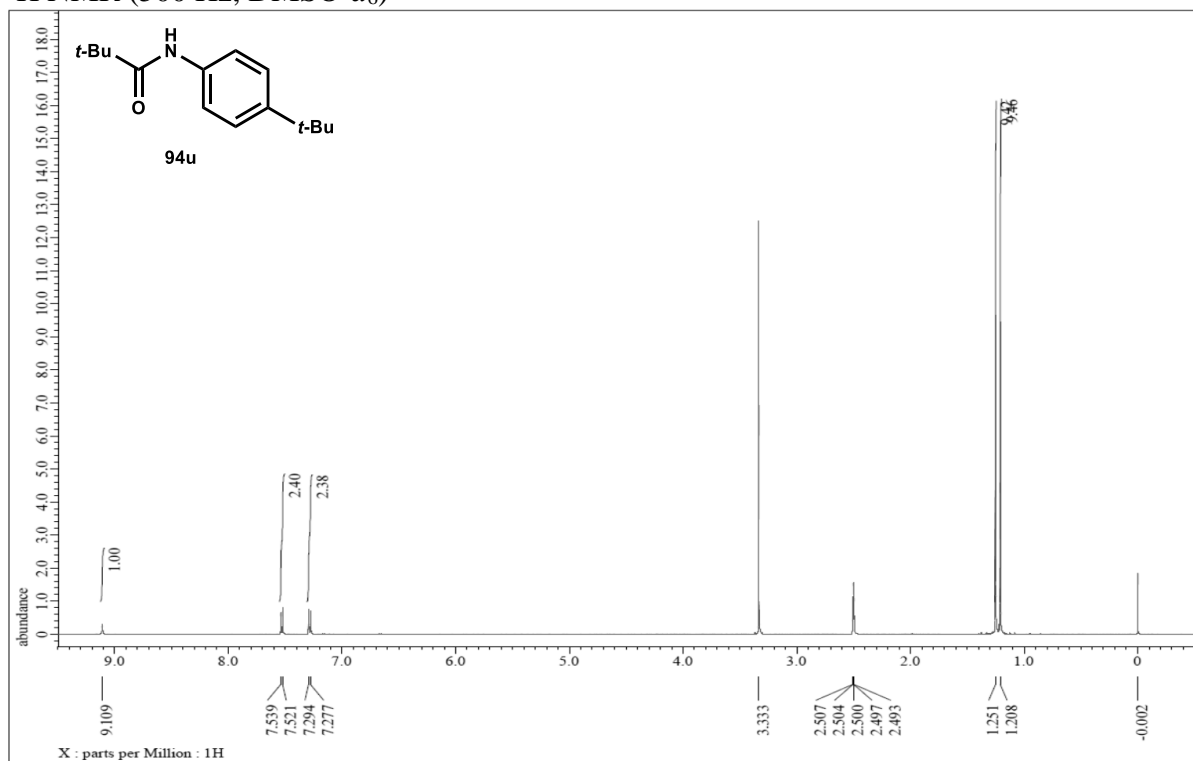
^1H NMR (500 Hz, CDCl_3)



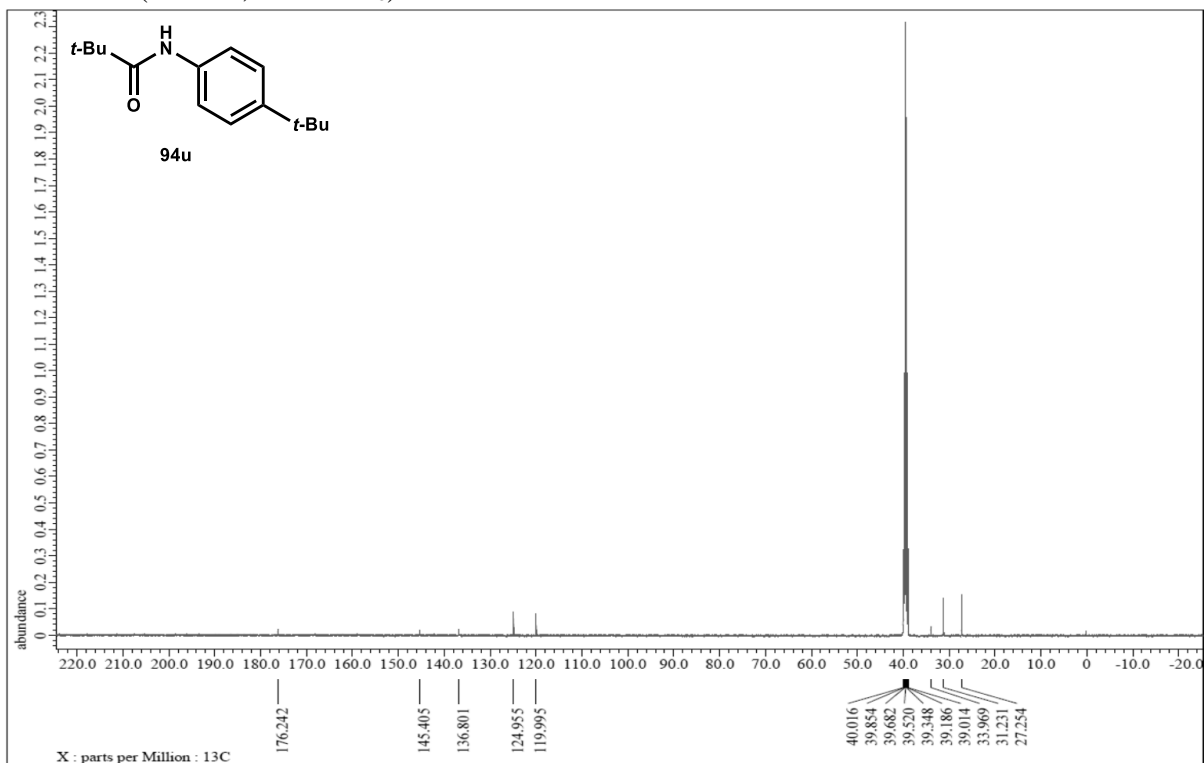
^{13}C NMR (125 Hz, CDCl_3)



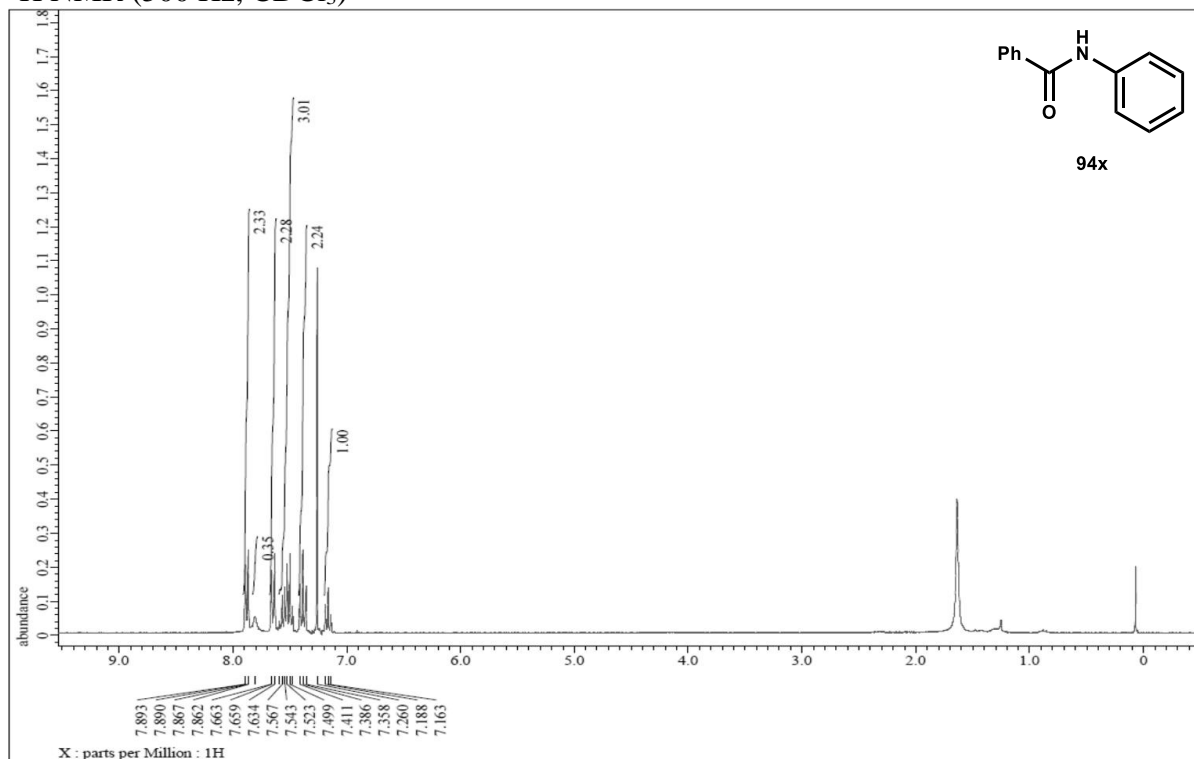
¹H NMR (500 Hz, DMSO-d₆)



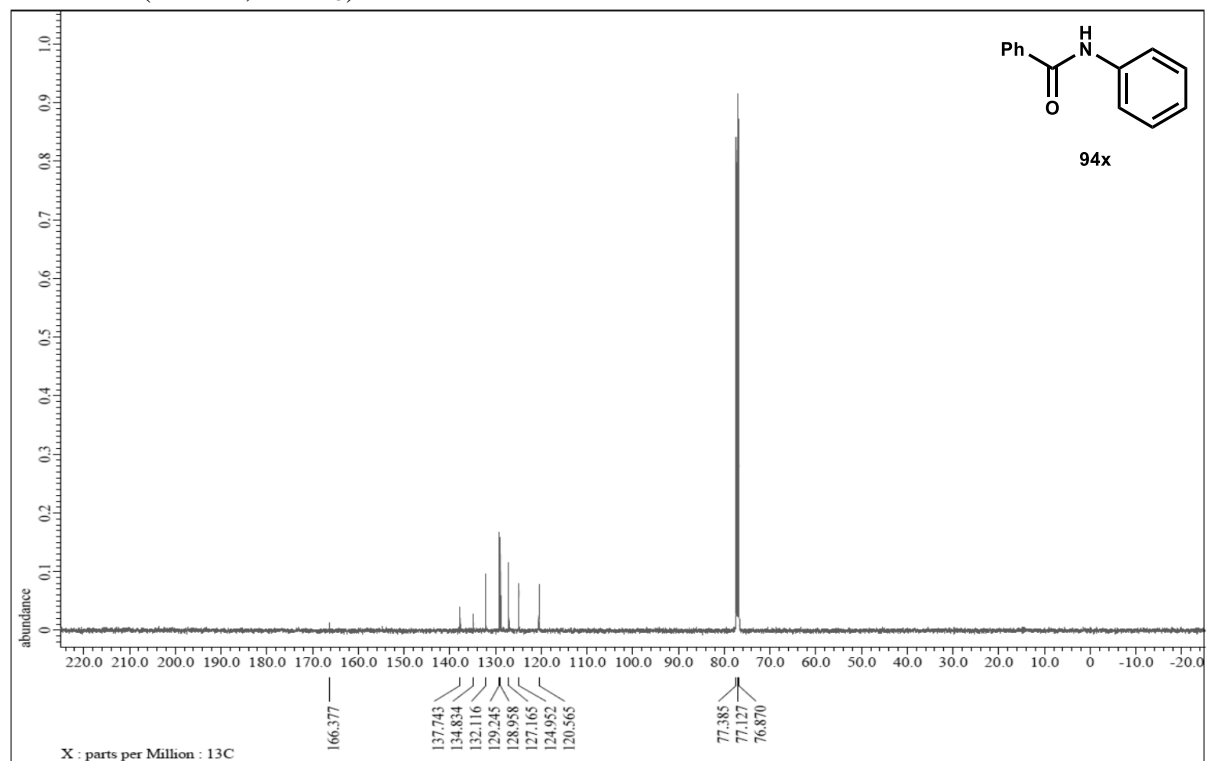
¹³C NMR (125 Hz, DMSO-d₆)



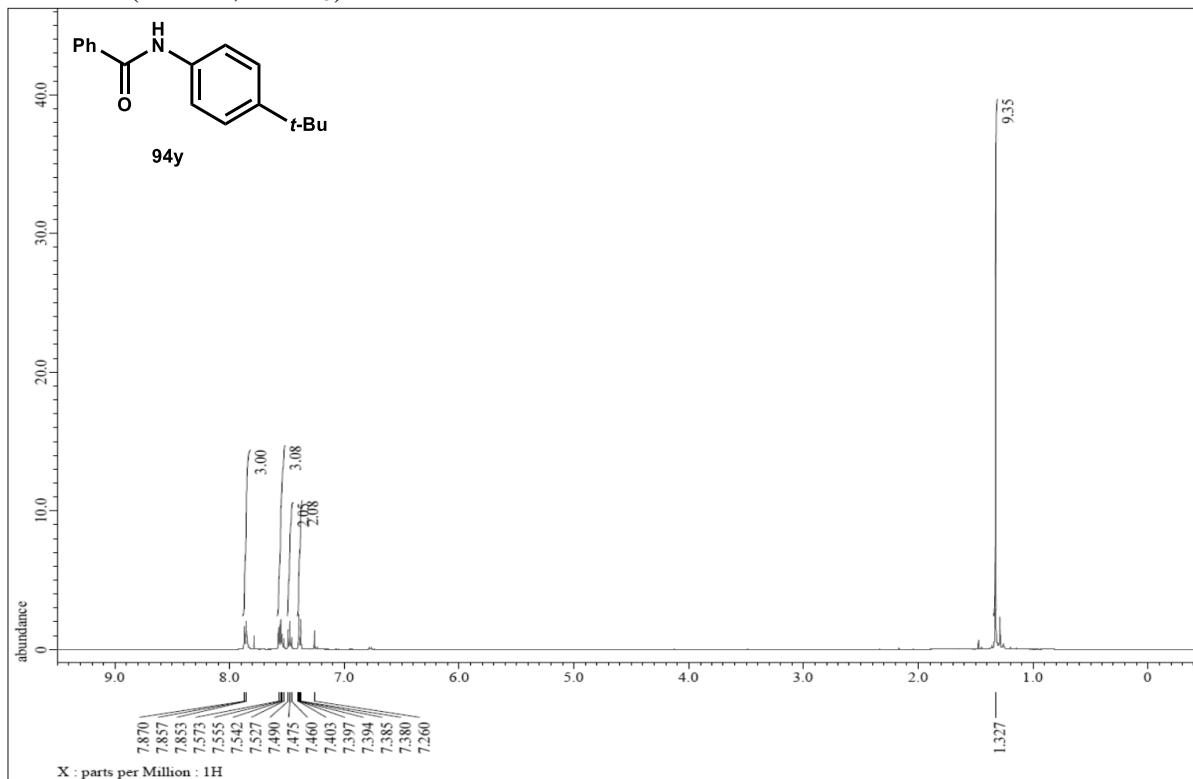
^1H NMR (500 Hz, CDCl_3)



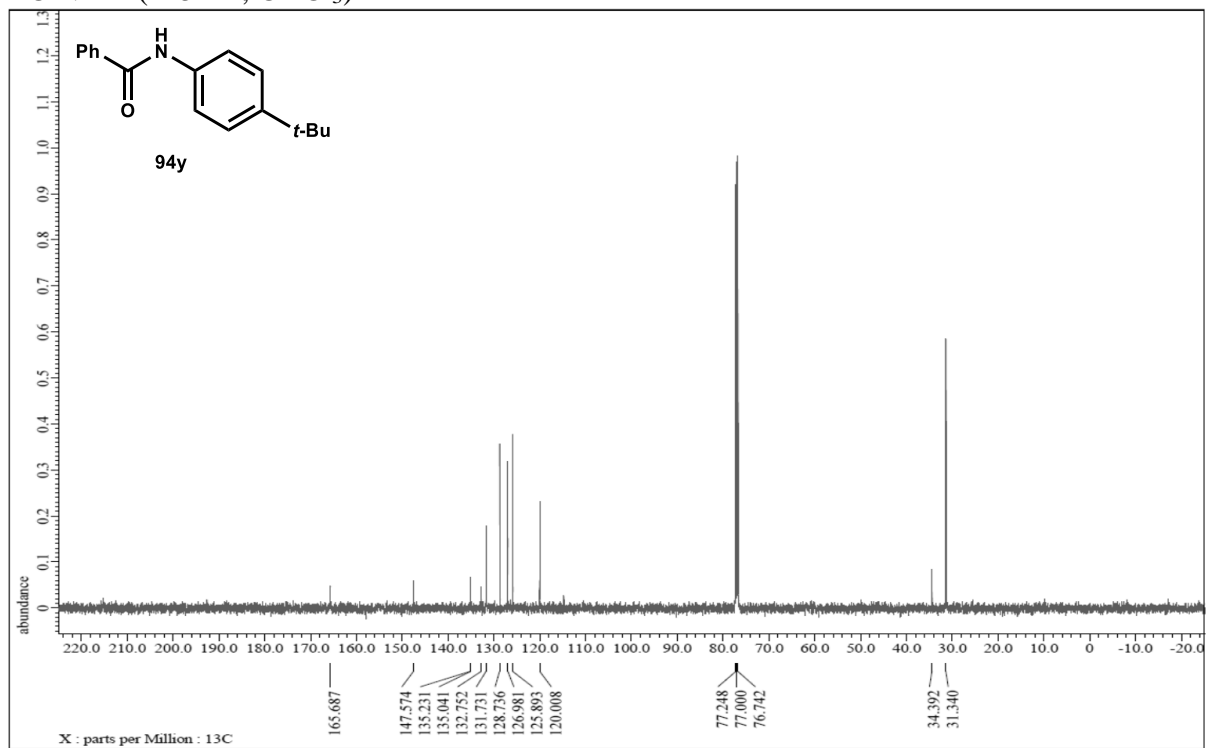
^{13}C NMR (125 Hz, CDCl_3)



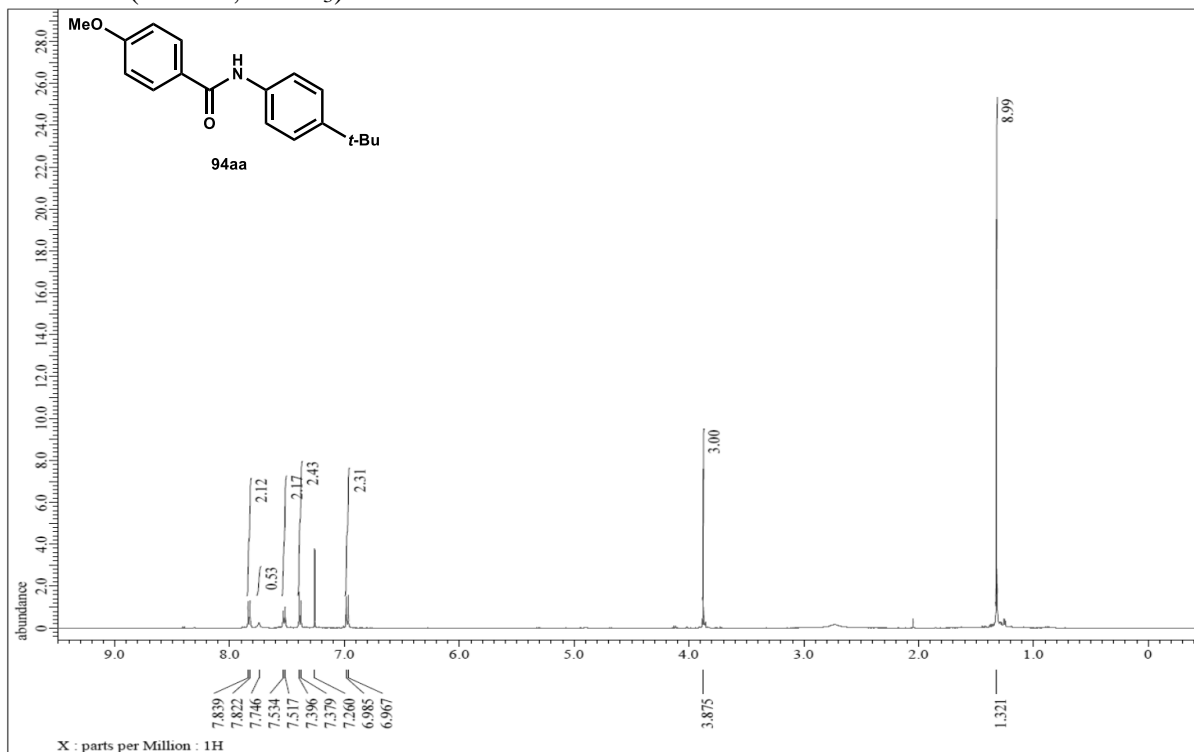
^1H NMR (500 Hz, CDCl_3)



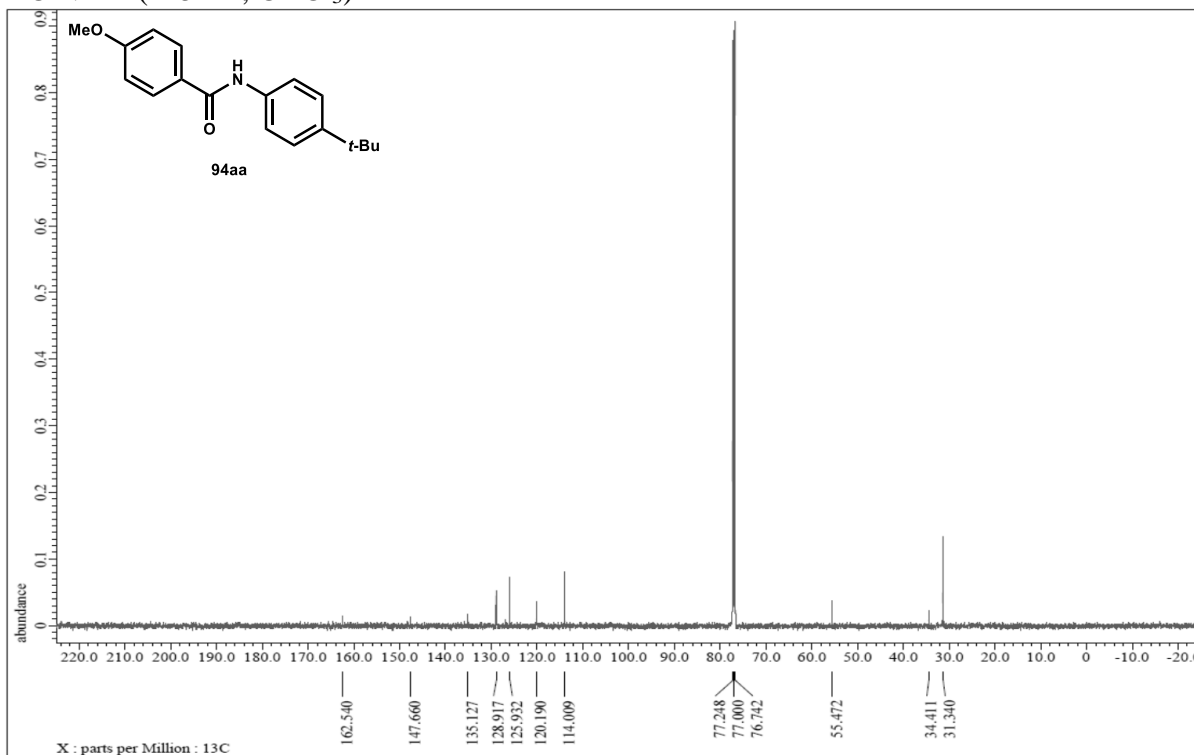
^{13}C NMR (125 Hz, CDCl_3)



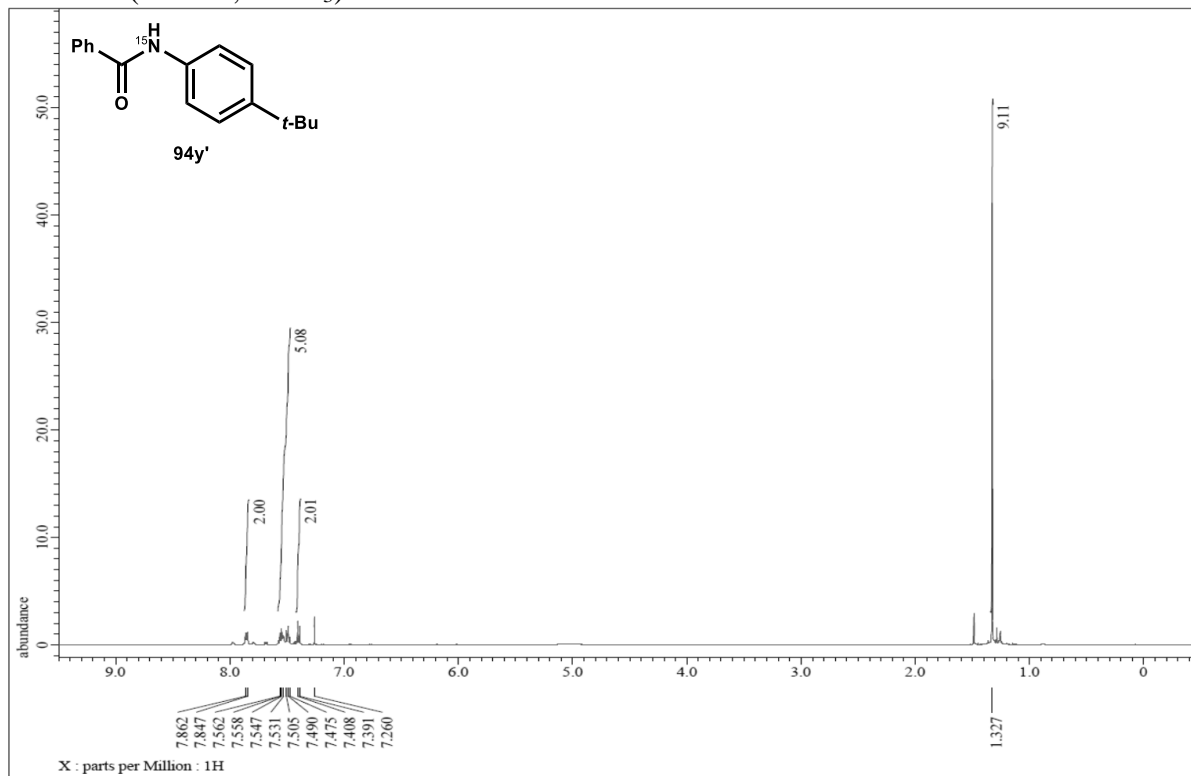
¹H NMR (500 Hz, CDCl₃)



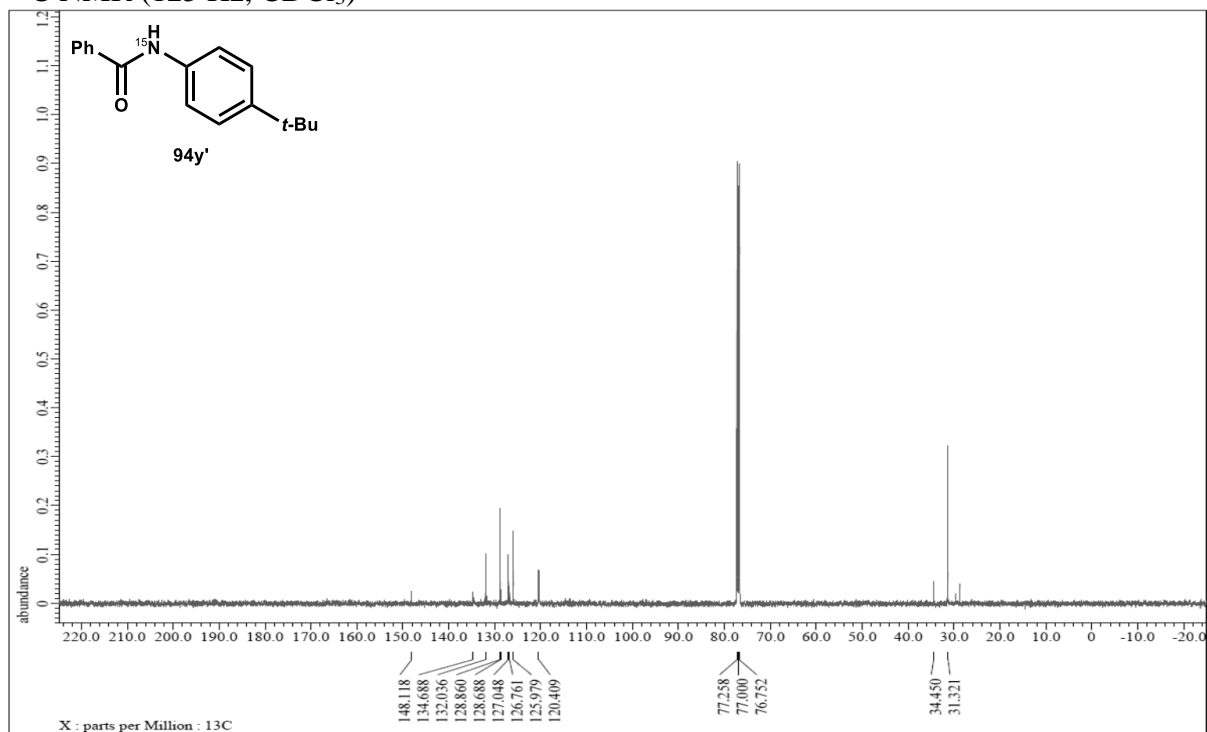
¹³C NMR (125 Hz, CDCl₃)



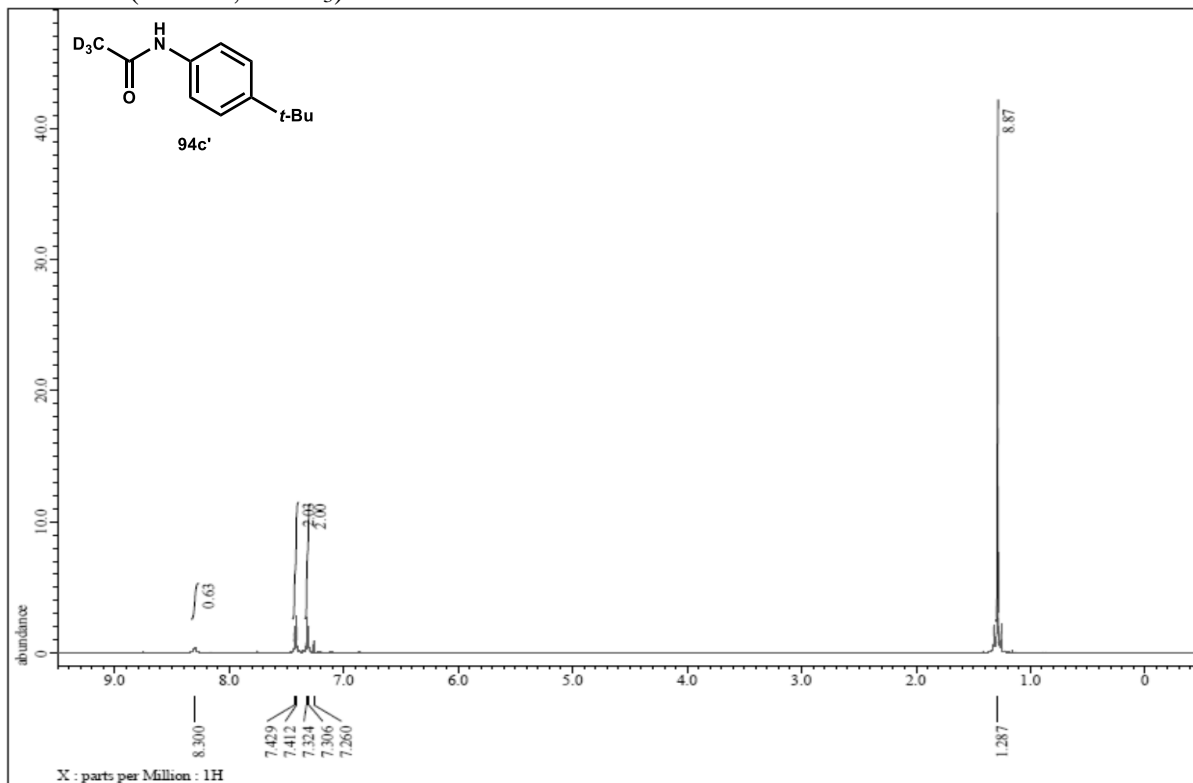
^1H NMR (500 Hz, CDCl_3)



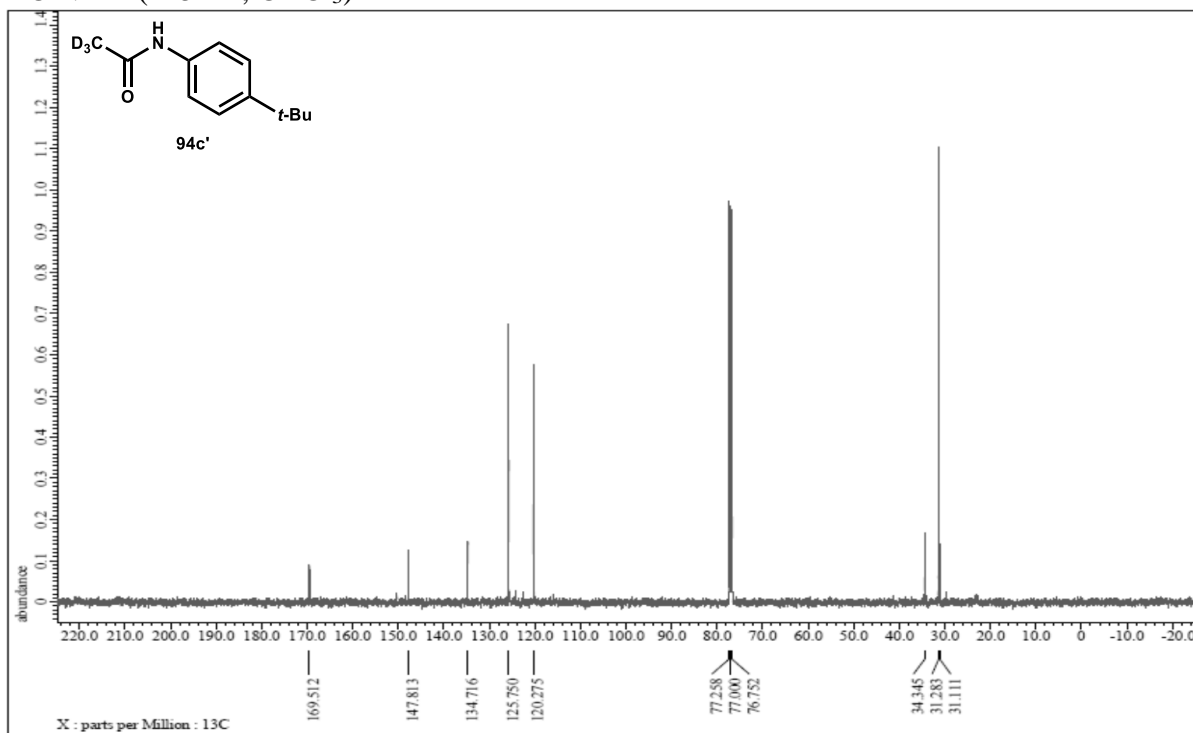
^{13}C NMR (125 Hz, CDCl_3)



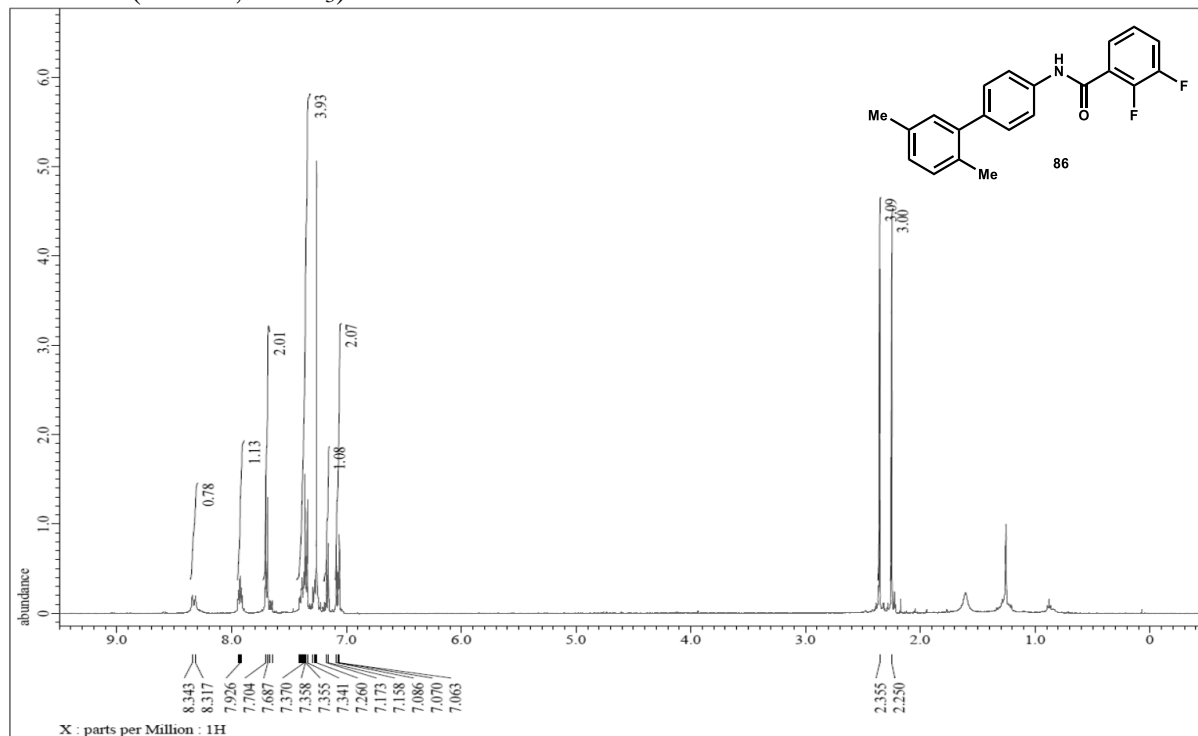
¹H NMR (500 Hz, CDCl₃)



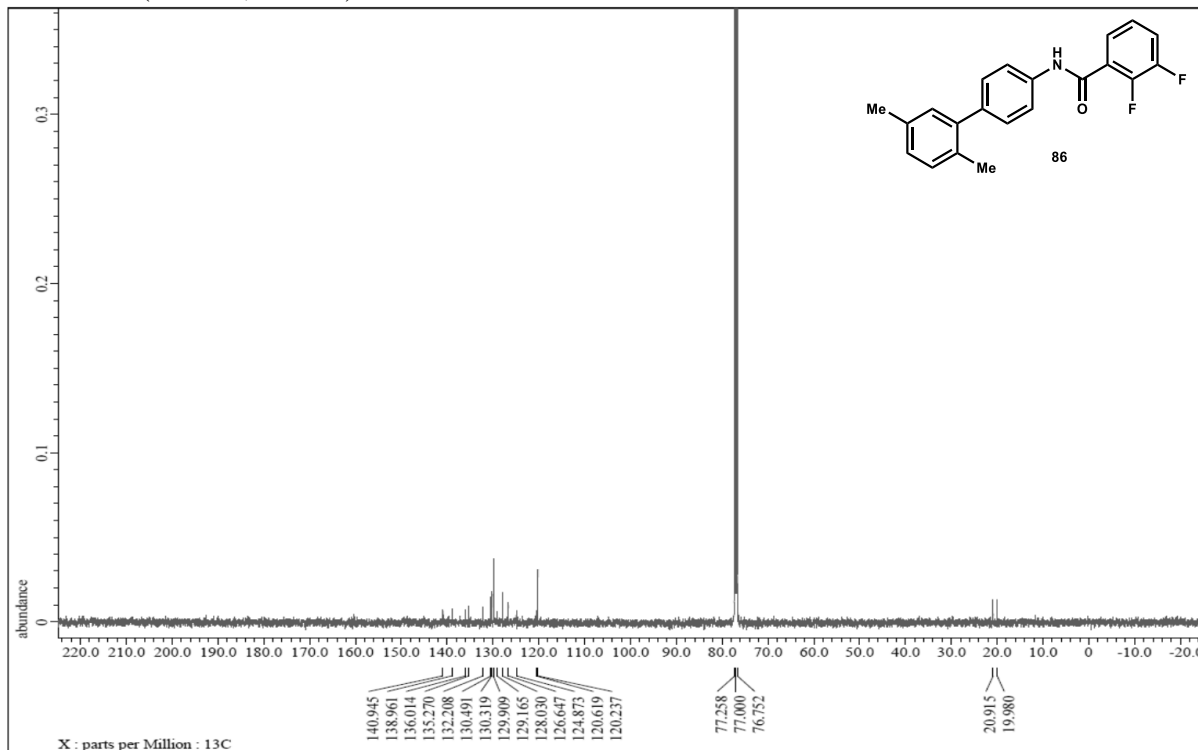
¹³C NMR (125 Hz, CDCl₃)



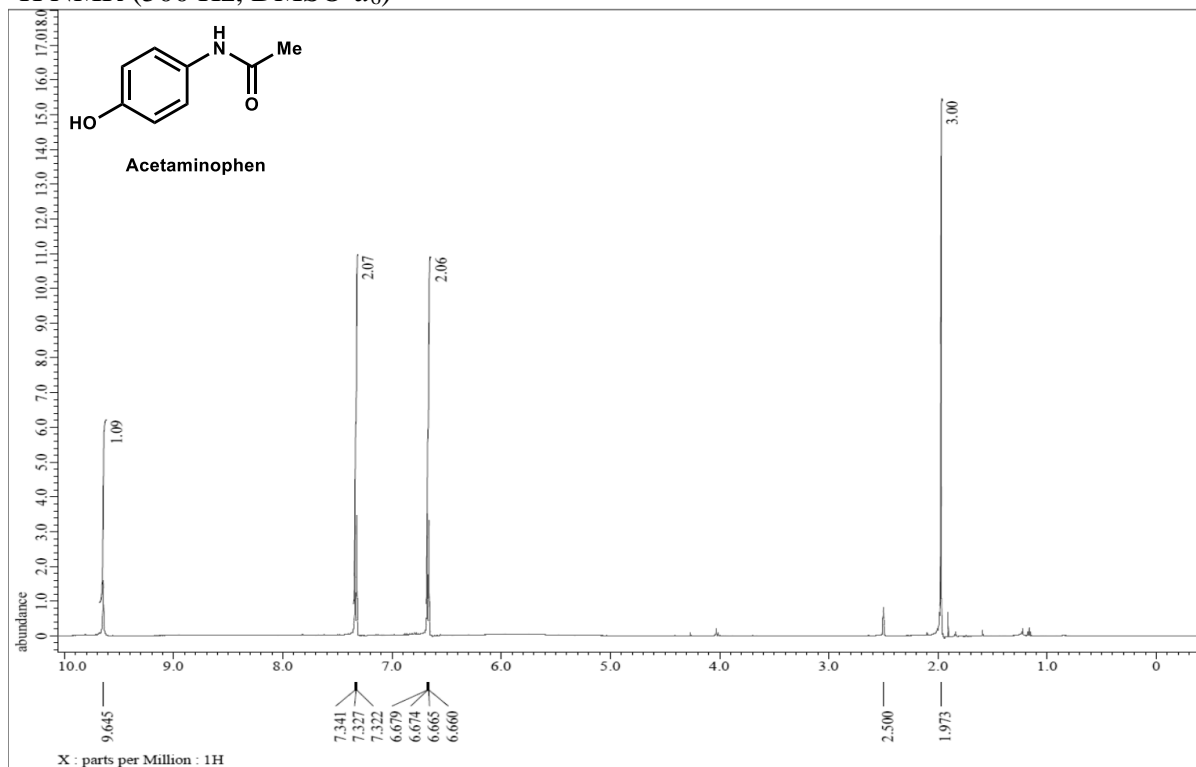
¹H NMR (500 Hz, CDCl₃)



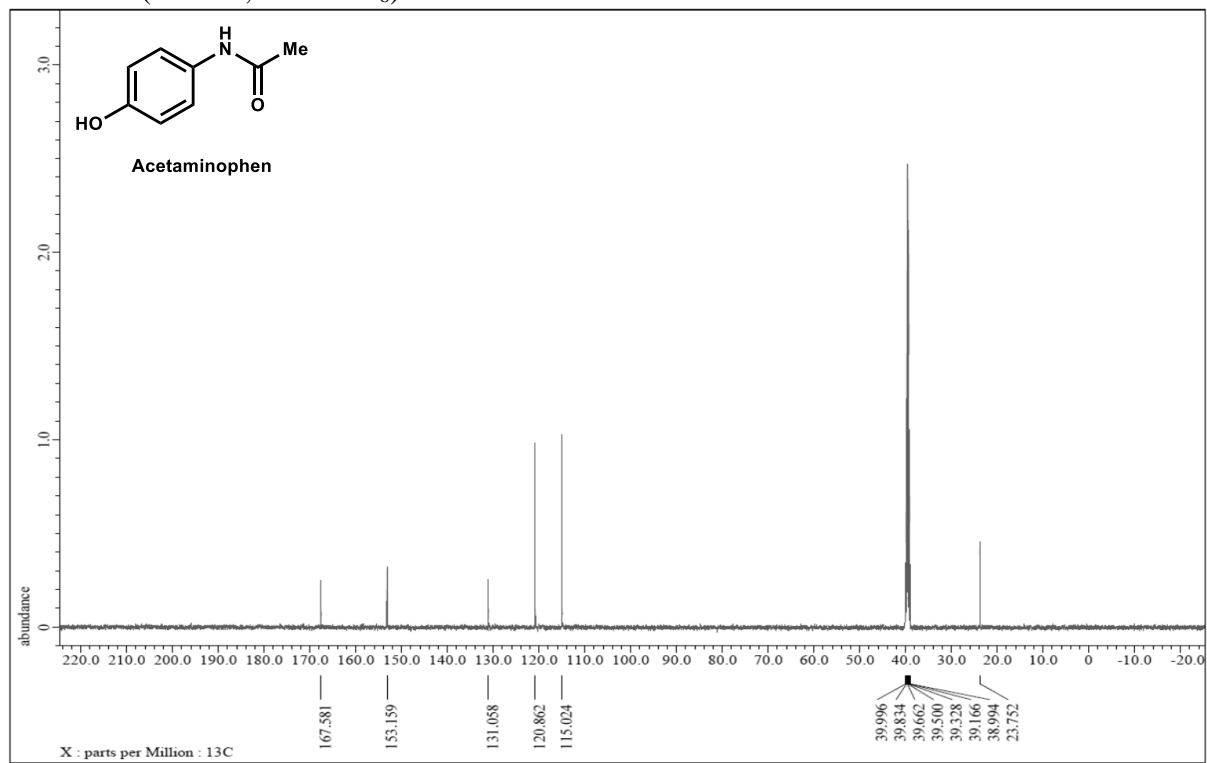
¹³C NMR (125 Hz, CDCl₃)



¹H NMR (500 Hz, DMSO-d₆)

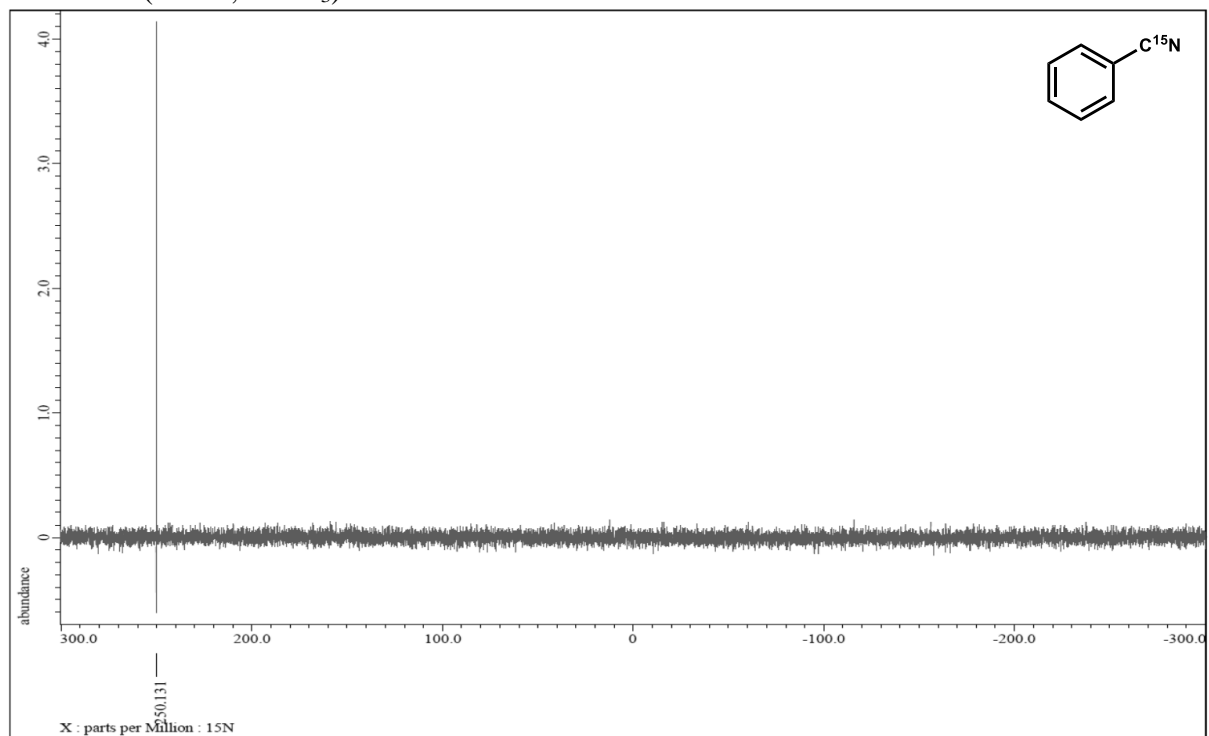


¹³C NMR (125 Hz, DMSO-d₆)

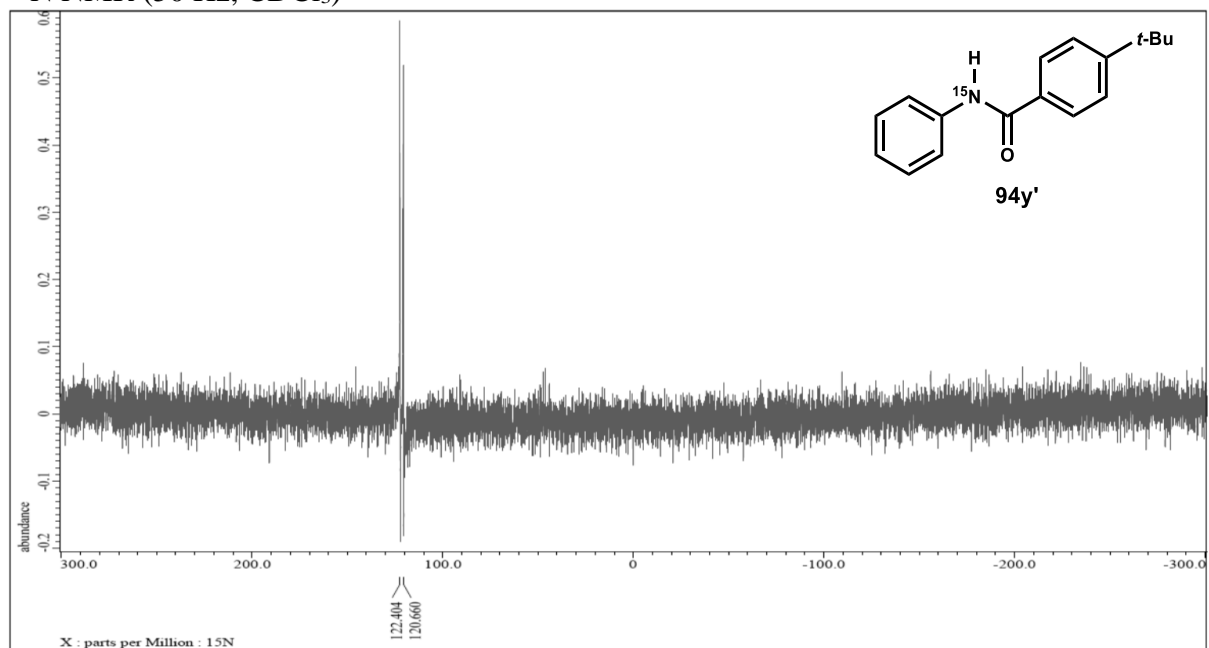


^{15}N NMR Spectra



^{15}N NMR (50 Hz, CDCl_3)



^{15}N NMR (50 Hz, CDCl_3)



NMR Instrument Parameters

	
<pre> ----- PROCESSING PARAMETERS ----- dc_balance(0, FALSE) sexp(0.2[Hz], 0.0[s]) trapezoid3(0[%], 80[%], 100[%]) zerofill(1) fft(1, TRUE, TRUE) machinephase ppm </pre>	<pre> ----- PROCESSING PARAMETERS ----- dc_balance(0, FALSE) sexp(2.0[Hz], 0.0[s]) trapezoid3(0[%], 80[%], 100[%]) zerofill(1) fft(1, TRUE, TRUE) machinephase ppm </pre>
<pre> Filename = EB_II_28_2_SM_Diben Author = delta Experiment = single_pulse.ex2 Sample_Id = S#595737 Solvent = CHLOROFORM-D Actual_Start_Time = 14-APR-2017 23:41:0 Revision_Time = 3-JUN-2017 13:44:0 Comment = single_pulse Data_Format = 1D COMPLEX Dim_Size = 13107 X_Domain = 1H Dim_Title = 1H Dim_Units = [ppm] Dimensions = X Site = ECA 500 Spectrometer = JNM-ECA500 Field_Strength = 11.7473579[T] (500[X_Acq_Duration = 1.74587904[s] X_Domain = 1H X_Freq = 500.15991521[MHz] X_Offset = 5.0[ppm] X_Points = 16384 X_Prescans = 0 X_Resolution = 0.57277737[Hz] X_Sweep = 9.38438438[kHz] Irr_Domain = 1H Irr_Freq = 500.15991521[MHz] Irr_Offset = 5.0[ppm] Tri_Domain = 1H Tri_Freq = 500.15991521[MHz] Tri_Offset = 5.0[ppm] Clipped = FALSE Scans = 6 Total_Scans = 6 Relaxation_Delay = 5[s] Recvr_Gain = 36 Temp_Get = 21[dC] X_90_Width = 12.54[us] X_Acq_Time = 1.74587904[s] </pre>	<pre> Filename = eb_13C_II_142_label Author = delta Experiment = single_pulse_dec Sample_Id = S#434700 Solvent = DMSO-D6 Actual_Start_Time = 25-JUL-2018 19:20:0 Revision_Time = 25-JUL-2018 15:29:3 Comment = single_pulse decoupl Data_Format = 1D COMPLEX Dim_Size = 26214 X_Domain = 13C Dim_Title = 13C Dim_Units = [ppm] Dimensions = X Site = ECA 500 Spectrometer = JNM-ECA500 Field_Strength = 11.7473579[T] (500[X_Acq_Duration = 0.83361792[s] X_Domain = 13C X_Freq = 125.76529768[MHz] X_Offset = 100[ppm] X_Points = 32768 X_Prescans = 4 X_Resolution = 1.19959034[Hz] X_Sweep = 39.3081761[kHz] Irr_Domain = 1H Irr_Freq = 500.15991521[MHz] Irr_Offset = 5.0[ppm] Clipped = FALSE Scans = 110 Total_Scans = 110 Relaxation_Delay = 2[s] Recvr_Gain = 50 Temp_Get = 22.9[dC] X_90_Width = 10.73[us] X_Acq_Time = 0.83361792[s] X_Angle = 30[deg] X_Atn = 9[dB] X_Pulse = 3.57666667[us] </pre>

¹H NMR

¹³C NMR

References

1. Bada, J. L., Biogeochemistry of Organic Nitrogen Compounds. In *Nitrogen-Containing Macromolecules in the Bio- and Geosphere*, American Chemical Society: 1998; Vol. 707, pp 64-73.
2. Quin, L. D.; Tyrell, J. A., *Fundamentals of Heterocyclic Chemistry: Importance in Nature and in the Synthesis of Pharmaceuticals*. John Wiley and Sons. Ltd.: 2010.
3. Patil, S.; Bugarin, A. *Eur. J. Org. Chem.* **2016**, 2016, 860-870.
4. Kimball, D. B.; Haley, M. M., *Angew. Chem. Int. Ed.* **2002**, 41, 3338-3351.
5. Rouzer, C. A.; Sabourin, M.; Skinner, T. L.; Thompson, E. J.; Wood, T. O.; Chmurny, G. N.; Klose, J. R.; Roman, J. M.; Smith, R. H.; Michejda, C. J. *Chem. Res. Toxicol.* **1996**, 9, 172-178.
6. Marchesi, F.; Turriziani, M.; Tortorelli, G.; Avvisati, G.; Torino, F.; De Vecchis, L. *Pharmacol. Res.* **2007**, 56, 275-287.
7. Al-Badr, A. A.; Alodhaib, M. M., Chapter Four - Dacarbazine. In *Profiles of Drug Substances, Excipients and Related Methodology*, Brittain, H. G., Ed. Academic Press: 2016; Vol. 41, pp 323-377.
8. Hejesen, C.; Petersen, L. K.; Hansen, N. J. V.; Gothelf, K. V. *Org. Biomol. Chem.* **2013**, 11, 2493-2497.
9. Gross, M. L.; Blank, D. H.; Welch, W. M. *J. Org. Chem.* **1993**, 58, 2104-2109.
10. Wang, C.; Sun, H.; Fang, Y.; Huang, Y. *Angew. Chem. Int. Ed.* **2013**, 52, 5795-5798.
11. Hegi, M. E.; Diserens, A.-C.; Gorlia, T.; Hamou, M.-F.; de Tribolet, N.; Weller, M.; Kros, J. M.; Hainfellner, J. A.; Mason, W.; Mariani, L.; Bromberg, J. E. C.; Hau, P.; Mirimanoff, R. O.; Cairncross, J. G.; Janzer, R. C.; Stupp, R. N. *Engl. J. Med.* **2005**, 352, 997-1003.
12. Winberg, H. E.; Coffman, D. D. *J. Am. Chem. Soc.* **1965**, 87, 2776-2777.
13. Coady, D. J.; Khramov, D. M.; Norris, B. C.; Tennyson, A. G.; Bielawski, C. W. *Angew. Chem. Int. Ed.* **2009**, 48, 5187-5190.
14. Kimani, F. W.; Jewett, J. C. *Angew. Chem. Int. Ed.* **2015**, 54, 4051-4054.
15. He, J.; Kimani, F. W.; Jewett, J. C. *J. Am. Chem. Soc.* **2015**, 137, 9764-9767.
16. Khramov, D. M.; Bielawski, C. W. *Chem. Commun.* **2005**, 4958-4960.
17. Khramov, D. M.; Bielawski, C. W. *J. Org. Chem.* **2007**, 72, 9407-9417.
18. Liu, Y.; Lindner, P. E.; Lemal, D. M. *J. Am. Chem. Soc.* **1999**, 121, 10626-10627.
19. Patil, S.; White, K.; Bugarin, A. *Tetrahedron Lett.* **2014**, 55, 4826-4829.
20. Patil, S.; Bugarin, A. *Acta Cryst. E* **2014**, 70, 224-227.
21. Neilson, B. M.; Tennyson, A. G.; Bielawski, C. W. *J. Phys. Org. Chem.* **2012**, 25, 531-543.

22. Hopkins, J. M.; Bowdridge, M.; Robertson, K. N.; Cameron, T. S.; Jenkins, H. A.; Clyburne, J. A. C. *J. Org. Chem.* **2001**, *66*, 5713-5716.
23. Kunetskiy, R. A.; Císařová, I.; Šaman, D.; Lyapkalo, I. M. *Chem. Eur. J.* **2009**, *15*, 9477-9485.
24. Lysenko, S.; Daniliuc, C. G.; Jones, P. G.; Tamm, M. *J. Organomet. Chem.* **2013**, *744*, 7-14.
25. Regitz, M. *Angew. Chem. Int. Ed.* **1967**, *6*, 733-749.
26. Kitamura, M.; Tashiro, N.; Okauchi, T. *Synlett* **2009**, *2009*, 2943-2944.
27. Kitamura, M.; Yano, M.; Tashiro, N.; Miyagawa, S.; Sando, M.; Okauchi, T. *Eur. J. Org. Chem.* **2011**, *2011*, 458-462.
28. Jishkariani, D.; Hall, C. D.; Demircan, A.; Tomlin, B. J.; Steel, P. J.; Katritzky, A. R. *J. Org. Chem.* **2013**, *78*, 3349-3354.
29. Tennyson, A. G.; Moorhead, E. J.; Madison, B. L.; Er, J. A. V.; Lynch, V. M.; Bielawski, C. W. *Eur. J. Org. Chem.* **2010**, *2010*, 6277-6282.
30. Felzmann, W.; Castagnolo, D.; Rosenbeiger, D.; Mulzer, J. *J. Org. Chem.* **2007**, *72*, 2182-2186.
31. Cowper, P.; Jin, Y.; Turton, M. D.; Kociok-Köhn, G.; Lewis, S. E. *Angew. Chem. Int. Ed.* **2016**, *55*, 2564-2568.
32. (a) Charpentier, J.; Früh, N.; Togni, A. *Chem. Rev.* **2015**, *115*, 650-682; (b) Jia, Z.; Gálvez, E.; Sebastián, R. M.; Pleixats, R.; Álvarez-Larena, Á.; Martín, E.; Vallribera, A.; Shafir, A. *Angew. Chem. Int. Ed.* **2014**, *53*, 11298-11301.
33. (a) Mal, K.; Kaur, A.; Haque, F.; Das, I. *J. Org. Chem.* **2015**, *80*, 6400-6410; (b) Chen, J.-Y.; Chen, X.-L.; Li, X.; Qu, L.-B.; Zhang, Q.; Duan, L.-K.; Xia, Y.-Y.; Chen, X.; Sun, K.; Liu, Z.-D.; Zhao, Y.-F. *Eur. J. Org. Chem.* **2015**, *2015*, 314-319; (c) Diao, T.; Pun, D.; Stahl, S. S. *J. Am. Chem. Soc.* **2013**, *135*, 8205-8212.
34. (a) Li, Y.; Xue, D.; Lu, W.; Wang, C.; Liu, Z.-T.; Xiao, J. *Org. Lett.* **2014**, *16*, 66-69; (b) Ding, S.; Jiao, N. *Angew. Chem. Int. Ed.* **2012**, *51*, 9226-9237.
35. (a) Bräse, S.; Gil, C.; Knepper, K.; Zimmermann, V. *Angew. Chem. Int. Ed.* **2005**, *44*, 5188-5240; (b) Scriven, E. F. V.; Turnbull, K. *Chem. Rev.* **1988**, *88*, 297-368.
36. (a) Thirumurugan, P.; Matosiuk, D.; Jozwiak, K. *Chem. Rev.* **2013**, *113*, 4905-4979; (b) Tiwari, V. K.; Mishra, B. B.; Mishra, K. B.; Mishra, N.; Singh, A. S.; Chen, X. *Chem. Rev.* **2016**, *116*, 3086-3240.
37. (a) Adam, G.; Andrielix, J.; Plat, M. *Tetrahedron Lett.* **1981**, *22*, 3181-3184; (b) Tanimoto, H.; Kakiuchi, K., *Nat. Prod. Commun.* **2013**, *8*, 1021-1034.
38. (a) Hu, B.; DiMagno, S. G. *Org. Biomol. Chem.* **2015**, *13*, 3844-3855; (b) Cramer, S. A.; Jenkins, D. M. *J. Am. Chem. Soc.* **2011**, *133*, 19342-19345.

39. (a) Myers, E. L.; Raines, R. T. *Angew. Chem. Int. Ed.* **2009**, *48*, 2359-2363; (b) van Kalker, H. A.; Bruins, J. J.; Rutjes, F. P. J. T.; van Delft, F. L. *Adv. Synth. Cat.* **2012**, *354*, 1417-1421.
40. (a) Dequierez, G.; Pons, V.; Dauban, P. *Angew. Chem. Int. Ed.* **2012**, *51*, 7384-7395; (b) Koga, G.; Anselme, J. P. *J. Org. Chem.* **1970**, *35*, 960-964.
41. Alagiri, K.; Prabhu, K. R. *Tetrahedron* **2011**, *67*, 8544-8551.
42. (a) Kornblum, N.; Jones, W. J.; Anderson, G. J. *J. Am. Chem. Soc.* **1959**, *81*, 4113-4114; (b) Kornblum, N.; Powers, J. W.; Anderson, G. J.; Jones, W. J.; Larson, H. O.; Levand, O.; Weaver, W. M. *J. Am. Chem. Soc.* **1957**, *79*, 6562-6562.
43. Bull, J. A.; Croft, R. A.; Davis, O. A.; Doran, R.; Morgan, K. F. *Chem. Rev.* **2016**, *116*, 12150-12233.
44. Gutmann, B.; Cantillo, D.; Kappe, C. O. *Angew. Chem. Int. Ed.* **2015**, *54*, 6688-6728.
45. (a) Sharma, A. K.; Ku, T.; Dawson, A. D.; Swern, D. *J. Org. Chem.* **1975**, *40*, 2758-2764; (b) Sharma, A. K.; Swern, D. *Tetrahedron Lett.* **1974**, *15*, 1503-1506; (c) Omura, K.; Sharma, A. K.; Swern, D. *J. Org. Chem.* **1976**, *41*, 957-962.
46. (a) Arterburn, J. B. *Tetrahedron* **2001**, *57*, 9765-9788; (b) Epstein, W. W.; Sweat, F. W. *Chem. Rev.* **1967**, *67*, 247-260.
47. (a) Joo, C.; Kang, S.; Kim, S. M.; Han, H.; Yang, J. W. *Tetrahedron Lett.* **2010**, *51*, 6006-6007; (b) Wang, X.; Wang, D. Z. *Tetrahedron* **2011**, *67*, 3406-3411.
48. González-Calderón, D.; Morales-Reza, M. A.; Díaz-Torres, E.; Fuentes-Benites, A.; González-Romero, C. *RSC Adv.* **2016**, *6*, 83547-83550.
49. (a) Albini, A.; Fagnoni, M. *ChemSusChem* **2008**, *1*, 63-66; (b) Albini, A.; Fagnoni, M. *Green Chem.* **2004**, *6*, 1-6; (c) Roth, H. D. *Angew. Chem. Int. Ed.* **1989**, *28* (9), 1193-1207.
50. Ciamician, G. *Science* **1912**, *36*, 385-394.
51. Klán, P.; Wirz, J., *Photochemistry of Organic Compounds*. John Wiley & Sons Ltd.: 2009.
52. Romero, N. A.; Nicewicz, D. A. *Chem. Rev.* **2016**, *116*, 10075-10166.
53. Waldeck, D. H. *Chem. Rev.* **1991**, *91*, 415-436.
54. (a) Bach, T. *Synthesis* **1998**, *1998*, 683-703; (b) Crimmins, M. T., *Chem. Rev.* **1988**, *88*, 1453-1473.
55. Klán, P.; Šolomek, T.; Bochet, C. G.; Blanc, A.; Givens, R.; Rubina, M.; Popik, V.; Kostikov, A.; Wirz, J. *Chem. Rev.* **2013**, *113*, 119-191.
56. (a) Peng, L.; Li, Z.; Yin, G. *Org. Lett.* **2018**, *20*, 1880-1883; (b) Yu, X.-Y.; Chen, J.-R.; Wang, P.-Z.; Yang, M.-N.; Liang, D.; Xiao, W.-J. *Angew. Chem. Int. Ed.* **2018**, *57*, 738-743.

57. Hassan, J.; Sévignon, M.; Gozzi, C.; Schulz, E.; Lemaire, M. *Chem. Rev.* **2002**, *102*, 1359-1470.
58. (a) Ackermann, L.; Potukuchi, H. K.; Althammer, A.; Born, R.; Mayer, P. *Org. Lett.* **2010**, *12*, 1004-1007; (b) Gurung, S. K.; Thapa, S.; Kafle, A.; Dickie, D. A.; Giri, R. *Org. Lett.* **2014**, *16*, 1264-1267; (c) Han, J.; Liu, Y.; Guo, R. *J. Am. Chem. Soc.* **2009**, *131*, 2060-2061; (d) Kwong, F. Y.; Chan, K. S.; Yeung, C. H.; Chan, A. S. C. *Chem. Commun.* **2004**, 2336-2337.
59. (a) Negishi, E.; King, A. O.; Okukado, N. *J. Org. Chem.* **1977**, *42*, 1821-1823; (b) Negishi, E.-i. *Angew. Chem. Int. Ed.* **2011**, *50*, 6738-6764; (c) Zhang, X.-Q.; Wang, Z.-X. *J. Org. Chem.* **2012**, *77*, 3658-3663.
60. (a) Li, J.-H.; Liang, Y.; Wang, D.-P.; Liu, W.-J.; Xie, Y.-X.; Yin, D.-L. *J. Org. Chem.* **2005**, *70*, 2832-2834; (b) Mee, S. P. H.; Lee, V.; Baldwin, J. E. *Angew. Chem. Int. Ed.* **2004**, *43*, 1132-1136.
61. (a) Alacid, E.; Nájera, C. *J. Org. Chem.* **2008**, *73*, 2315-2322; (b) McLaughlin, M. G.; McAdam, C. A.; Cook, M. J. *Org. Lett.* **2015**, *17*, 10-13.
62. Friedman, D.; Masciangioli, T.; Olson, S., *The Role of the Chemical Sciences in Finding Alternatives to Critical Resources*. National Academy Press: 2012.
63. Dach, R.; Song, J. J.; Roschangar, F.; Samstag, W.; Senanayake, C. H. *Org. Process Res. Dev.* **2012**, *16*, 1697-1706.
64. Dewanji, A.; Murarka, S.; Curran, D. P.; Studer, A. *Org. Lett.* **2013**, *15*, 6102-6105.
65. Storr, T. E.; Greaney, M. F. *Org. Lett.* **2013**, *15*, 1410-1413.
66. Hofmann, J.; Gans, E.; Clark, T.; Heinrich, M. R. *Chem. Eur. J.* **2017**, *23*, 9647-9656.
67. (a) Wassmundt, F. W.; Kiesman, W. F. *J. Org. Chem.* **1997**, *62*, 8304-8308; (b) Pazo-Llorente, R.; Maskill, H.; Bravo-Diaz, C.; Gonzalez-Romero, E. *Eur. J. Org. Chem.* **2006**, *2006*, 2201-2209.
68. Galli, C. *Chem. Rev.* **1988**, *88*, 765-792.
69. Agrawal, J. P.; Hodgson, R., *Organic Chemistry of Explosives*. John Wiley and Sons, Ltd.: 2007.
70. Barragan, E.; Bugarin, A. *J. Org. Chem.* **2017**, *82*, 1499-1506.
71. Fabre, I.; Perego, L. A.; Bergès, J.; Ciofini, I.; Grimaud, L.; Taillefer, M. *Eur. J. Org. Chem.* **2016**, *2016*, 5887-5896.
72. Roman, D. S.; Takahashi, Y.; Charette, A. B. *Org. Lett.* **2011**, *13*, 3242-3245.
73. Caron, S., *Practical Synthetic Organic Chemistry*. John Wiley and Sons, Ltd.: 2011.
74. Gan, Z.; Epifanovsky, E.; Gilbert, A. T. B.; Wormit, M.; Kussmann, J.; Lange, A. W.; Behn, A.; Deng, J.; Feng, X.; Ghosh, D.; Goldey, M.; Horn,

- P. R.; Jacobson, L. D.; Kaliman, I.; Khaliullin, R. Z.; Kuś, T.; Landau, A.; Liu, J.; Proynov, E. I.; Rhee, Y. M.; Richard, R. M.; Rohrdanz, M. A.; Steele, R. P.; Sundstrom, E. J.; Woodcock, H. L.; Zimmerman, P. M.; Zuev, D.; Albrecht, B.; Alguire, E.; Austin, B.; Beran, G. J. O.; Bernard, Y. A.; Berquist, E.; Brandhorst, K.; Bravaya, K. B.; Brown, S. T.; Casanova, D.; Chang, C.-M.; Chen, Y.; Chien, S. H.; Closser, K. D.; Crittenden, D. L.; Diedenhofen, M.; DiStasio, R. A.; Do, H.; Dutoi, A. D.; Edgar, R. G.; Fatehi, S.; Fusti-Molnar, L.; Ghysels, A.; Golubeva-Zadorozhnaya, A.; Gomes, J.; Hanson-Heine, M. W. D.; Harbach, P. H. P.; Hauser, A. W.; Hohenstein, E. G.; Holden, Z. C.; Jagau, T.-C.; Ji, H.; Kaduk, B.; Khistyayev, K.; Kim, J.; Kim, J.; King, R. A.; Klunzinger, P.; Kosenkov, D.; Kowalczyk, T.; Krauter, C. M.; Lao, K. U.; Laurent, A. D.; Lawler, K. V.; Levchenko, S. V.; Lin, C. Y.; Liu, F.; Livshits, E.; Lochan, R. C.; Luenser, A.; Manohar, P.; Manzer, S. F.; Mao, S.-P.; Mardirossian, N.; Marenich, A. V.; Maurer, S. A.; Mayhall, N. J.; Neuscamman, E.; Oana, C. M.; Olivares-Amaya, R.; O'Neill, D. P.; Parkhill, J. A.; Perrine, T. M.; Peverati, R.; Prociuk, A.; Rehn, D. R.; Rosta, E.; Russ, N. J.; Sharada, S. M.; Sharma, S.; Small, D. W.; Sodt, A.; Stein, T.; Stück, D.; Su, Y.-C.; Thom, A. J. W.; Tsuchimochi, T.; Vanovschi, V.; Vogt, L.; Vydrov, O.; Wang, T.; Watson, M. A.; Wenzel, J.; White, A.; Williams, C. F.; Yang, J.; Yeganeh, S.; Yost, S. R.; You, Z.-Q.; Zhang, I. Y.; Zhang, X.; Zhao, Y.; Brooks, B. R.; Chan, G. K. L.; Chipman, D. M.; Cramer, C. J.; Goddard, W. A.; Gordon, M. S.; Hehre, W. J.; Klamt, A.; Schaefer, H. F.; Schmidt, M. W.; Sherrill, C. D.; Truhlar, D. G.; Warshel, A.; Xu, X.; Aspuru-Guzik, A.; Baer, R.; Bell, A. T.; Besley, N. A.; Chai, J.-D.; Dreuw, A.; Dunietz, B. D.; Furlani, T. R.; Gwaltney, S. R.; Hsu, C.-P.; Jung, Y.; Kong, J.; Lambrecht, D. S.; Liang, W.; Ochsenfeld, C.; Rassolov, V. A.; Slipchenko, L. V.; Subotnik, J. E.; Van Voorhis, T.; Herbert, J. M.; Krylov, A. I.; Gill, P. M. W.; Head-Gordon, M., Advances in molecular quantum chemistry contained in the Q-Chem 4 program package AU - Shao, Yihan. *Mol. Phys.* **2015**, *113*, 184-215.
75. (a) Barone, V.; Cossi, M., Quantum Calculation of Molecular Energies and Energy Gradients in Solution by a Conductor Solvent Model. *J. Phys. Chem. A* **1998**, *102*, 1995-2001; (b) Cossi, M.; Rega, N.; Scalmani, G.; Barone, V. *J. Comput. Chem.* **2003**, *24*, 669-681.
76. (a) Feyereisen, M.; Fitzgerald, G.; Komornicki, A. *Chem. Phys. Lett.* **1993**, *208*, 359-363; (b) Dunlap, B. I. *Phys. Chem. Chem. Phys.* **2000**, *2*, 2113-2116; (c) Jung, Y.; Sodt, A.; Peter, M. W. G.; Head-Gordon, M.; Berne, B. *J. Proc. Natl. Acad. Sci. U. S. A.* **2005**, *102*, 6692-6697.
77. (a) Cave, R. J.; Newton, M. D. *Chem. Phys. Lett.* **1996**, *249*, 15-19; (b) Cave, R. J.; Newton, M. D. *J. Chem. Phys.* **1997**, *106*, 9213-9226.
78. Hodgson, H. H. *Chem. Rev.* **1947**, *40*, 251-277.

79. Beadle, J. R.; Korzeniowski, S. H.; Rosenberg, D. E.; Garcia-Slanga, B. J.; Gokel, G. W. *J. Org. Chem.* **1984**, *49*, 1594-1603.
80. Greenberg, A., *The Amide Linkage: Structural Significance in Chemistry, Biochemistry and Materials Science*. John Wiley & Sons: 2000.
81. Wieland, T.; Bodanszky, M., *The World of Peptides: A Brief History of Peptide Chemistry*. Springer: 1991.
82. Ghose, A. K.; Viswanadhan, V. N.; Wendoloski, J. J. *J. Comb. Chem.* **1999**, *1*, 55-68.
83. Constable, D. J. C.; Dunn, P. J.; Hayler, J. D.; Humphrey, G. R.; Leazer, J. J. L.; Linderman, R. J.; Lorenz, K.; Manley, J.; Pearlman, B. A.; Wells, A.; Zaks, A.; Zhang, T. Y. *Green Chem.* **2007**, *9*, 411-420.
84. Brown, M. J. B. In *Green and Sustainable Medicinal Chemistry: Methods, Tools and Strategies for the 21st Century Pharmaceutical Industry*, The Royal Society of Chemistry: 2016; pp 7-18.
85. Ulijn, R. V.; Moore, B. D.; Janssen, A. E. M.; Halling, P. J. *J. Chem. Soc., Perkin Trans. 2* **2002**, 1024-1028.
86. (a) Lee, J. B. *J. Am. Chem. Soc.* **1966**, *88*, 3440-3441; (b) Carpino, L. A.; Beyermann, M.; Wenschuh, H.; Bienert, M., Peptide Synthesis via Amino Acid Halides. *Acc. Chem. Res.* **1996**, *29*, 268-274.
87. (a) Schlama, T.; Gouverneur, V.; Mioskowski, C. *Tetrahedron Lett.* **1996**, *37*, 7047-7048; (b) Wittenberger, S. J.; McLaughlin, M. A. *Tetrahedron Lett.* **1999**, *40*, 7175-7178.
88. (a) Klausner, Y. S.; Bodanszky, M. *Synthesis* **1974**, *1974*, 549-559; (b) Th., C., Synthetische Versuche mit Hippurazid. *Ber. Dtsch. Chem. Ges.* **1902**, *35*, 3226-3228.
89. (a) Chakrabarti, J. K.; Hotten, T. M.; Pullar, I. A.; Tye, N. C. *J. Med. Chem.* **1989**, *32*, 2573-2582; (b) Adamczyk, M.; Grote, J. *Bioorg. Med. Chem. Lett.* **2000**, *10*, 1539-1541.
90. (a) Paul, R.; Anderson, G. W. *J. Am. Chem. Soc.* **1960**, *82*, 4596-4600; (b) Dale, D. J.; Dunn, P. J.; Golightly, C.; Hughes, M. L.; Levett, P. C.; Pearce, A. K.; Searle, P. M.; Ward, G.; Wood, A. S. *Org. Process Res. Dev.* **2000**, *4*, 17-22.
91. Montalbetti, C. A. G. N.; Falque, V. *Tetrahedron* **2005**, *61*, 10827-10852.
92. Luknitskii, F. I.; Vovsi, B. A. *Usp. Khim.* **1969**, *38*, 1072-1088.
93. Curt, W.; Holger, B. *Eur. J. Org. Chem.* **2005**, *2005*, 4521-4524.
94. (a) Ishihara, K.; Ohara, S.; Yamamoto, H. *J. Org. Chem.* **1996**, *61*, 4196-4197; (b) Lanigan, R. M.; Starkov, P.; Sheppard, T. D. *J. Org. Chem.* **2013**, *78*, 4512-4523; (c) Starkov, P.; Sheppard, T. D. *Org. Biomol. Chem.* **2011**, *9*, 1320-1323.

95. (a) Nordstrøm, L. U.; Vogt, H.; Madsen, R. *J. Am. Chem. Soc.* **2008**, *130*, 17672-17673; (b) Gunanathan, C.; Ben-David, Y.; Milstein, D.. *Science* **2007**, *317*, 790-792.
96. (a) Li, X.; Danishefsky, S. J. *J. Am. Chem. Soc.* **2008**, *130*, 5446-5448; (b) Rao, Y.; Li, X.; Danishefsky, S. J. *J. Am. Chem. Soc.* **2009**, *131*, 12924-12926.
97. Crich, D.; Sasaki, K. *Org. Lett.* **2009**, *11*, 3514-3517.
98. Shanguan, N.; Katukojvala, S.; Greenberg, R.; Williams, L. J. *J. Am. Chem. Soc.* **2003**, *125*, 7754-7755.
99. Crich, D.; Sana, K.; Guo, S. *Org. Lett.* **2007**, *9*, 4423-4426.
100. Burgos, C. H.; Barder, T. E.; Huang, X.; Buchwald, S. L. *Angew. Chem. Int. Ed.* **2006**, *45*, 4321-4326.
101. Pattabiraman, V. R.; Bode, J. W. *Nature* **2011**, *480*, 471.
102. (a) Huang, X.; Fulton, B.; White, K.; Bugarin, A. *Org. Lett.* **2015**, *17*, 2594-2597; (b) Bugarin, A.; Barragan, E., Noonikara Poyil, A.; Yang, C.-H.; Wang, H. *Org. Chem. Front.* **2019**, *6*, 152-161; (c) Huang, X.; Bugarin, A. *Chem. Eur. J.* **2016**, *22*, 12696-12700.
103. Ritter, J. J.; Minieri, P. P. *J. Am. Chem. Soc.* **1948**, *70*, 4045-4048.
104. Fanghänel, E.; Ortmann, W.; Hennig, A. *J. Prakt. Chem.* **1988**, *330*, 27-34.
105. Heinrich, Z. *Angew. Chem. Int. Ed.* **1978**, *17*, 141-150.
106. Singh, S.; Roy, K. K.; Khan, S. R.; Kashyap, V. K.; Sharma, A.; Jaiswal, S.; Sharma, S. K.; Krishnan, M. Y.; Chaturvedi, V.; Lal, J.; Sinha, S.; Dasgupta, A.; Srivastava, R.; Saxena, A. K. *Bioorg. Med. Chem.* **2015**, *23*, 742-752.
107. Colombano, G.; Albani, C.; Ottonello, G.; Ribeiro, A.; Scarpelli, R.; Tarozzo, G.; Daglian, J.; Jung, K.-M.; Piomelli, D.; Bandiera, T. *ChemMedChem* **2015**, *10*, 380-395.
108. Yang, S.; Li, X.; Hu, F.; Li, Y.; Yang, Y.; Yan, J.; Kuang, C.; Yang, Q. *J. Med. Chem.* **2013**, *56*, 8321-8331.
109. Elson, K. E.; Jenkins, I. D.; Loughlin, W. A.. *Org. Biomol. Chem.* **2003**, *1*, 2958-2965.
110. Kamal, A.; Ramesh, G.; Laxman, N. *Synth. Commun.* **2001**, *31*, 827-833.
111. Suzuki, T.; Ota, Y.; Kasuya, Y.; Mutsuga, M.; Kawamura, Y.; Tsumoto, H.; Nakagawa, H.; Finn, M. G.; Miyata, N. *Angew. Chem. Int. Ed.* **2010**, *49*, 6817-6820.
112. Alonso, F.; Melkonian, T.; Moglie, Y.; Yus, M. *Eur. J. Org. Chem.* **2011**, *2011*, 2524-2530.
113. Jeon, K. O.; Jun, J. H.; Yu, J. S.; Lee, C. K. *J. Heterocycl. Chem.* **2003**, *40*, 763-771.
114. Abraham, R. J.; Mobli, M.; Smith, R. J. *Magn. Reson. Chem.* **2003**, *41*, 26-36.

115. Iinuma, M.; Moriyama, K.; Togo, H. *Tetrahedron* **2013**, *69*, 2961-2970.
116. Kornblum, N.; Fifolt, M. J. *Tetrahedron* **1989**, *45*, 1311-1322.
117. Jiang, N.; Ragauskas, A. J. *Org. Lett.* **2005**, *7*, 3689-3692.
118. Phan, T. B.; Nolte, C.; Kobayashi, S.; Ofial, A. R.; Mayr, H. *J. Am. Chem. Soc.* **2009**, *131*, 11392-11401.
119. Davis, P. J.; Harris, L.; Karim, A.; Thompson, A. L.; Gilpin, M.; Moloney, M. G.; Pound, M. J.; Thompson, C. *Tetrahedron Lett.* **2011**, *52*, 1553-1556.
120. Tsai, C.-Y.; Sung, R.; Zhuang, B.-R.; Sung, K. *Tetrahedron* **2010**, *66*, 6869-6872.
121. Shirakawa, S.; Kobayashi, S., *Org. Lett.* **2007**, *9*, 311-314.
122. Yadav, L. D. S.; Garima; Kapoor, R. *Synth. Commun.* **2010**, *41*, 100-112.
123. Itoh, T.; Mase, T. *Org. Lett.* **2004**, *6*, 4587-4590.
124. Ham, J.; Yang, I.; Kang, H. *J. Org. Chem.* **2004**, *69*, 3236-3239.
125. Bai, L.; Wang, J.-X. *Adv. Synth. Cat.* **2008**, *350*, 315-320.
126. Bandari, R.; Höche, T.; Prager, A.; Dirnberger, K.; Buchmeiser, M. R. *Chem. Eur. J.* **2010**, *16*, 4650-4658.
127. Li, H.; Sun, C.-L.; Yu, M.; Yu, D.-G.; Li, B.-J.; Shi, Z.-J. *Chem. Eur. J.* **2011**, *17*, 3593-3597.
128. Hatakeyama, T.; Nakamura, M., *J. Am. Chem. Soc.* **2007**, *129*, 9844-9845.
129. Jin, J.; Cai, M.-M.; Li, J.-X. *Synlett* **2009**, *2009*, 2534-2538.
130. Schulman, E. M.; Christensen, K. A.; Grant, D. M.; Walling, C. *J. Org. Chem.* **1974**, *39*, 2686-2690.
131. Ackermann, L.; Kapdi, A. R.; Fenner, S.; Kornhaaß, C.; Schulzke, C. *Chem. Eur. J.* **2011**, *17*, 2965-2971.
132. Stevens, P. D.; Fan, J.; Gardimalla, H. M. R.; Yen, M.; Gao, Y. *Org. Lett.* **2005**, *7*, 2085-2088.
133. Lau, K. C. Y.; He, H. S.; Chiu, P.; Toy, P. H. *J. Comb. Chem.* **2004**, *6*, 955-960.
134. Sprouse, S.; King, K. A.; Spellane, P. J.; Watts, R. J. *J. Am. Chem. Soc.* **1984**, *106*, 6647-6653.
135. Steel, P. J.; Caygill, G. B. *J. Organomet. Chem.* **1990**, *395*, 359-373.
136. Egi, M.; Azechi, K.; Akai, S. *Org. Lett.* **2009**, *11*, 5002-5005.
137. Lois, S.; Florès, J.-C.; Lère-Porte, J.-P.; Serein-Spirau, F.; Moreau, J. J. E.; Miqueu, K.; Sotiropoulos, J.-M.; Baylère, P.; Tillard, M.; Belin, C. *Eur. J. Org. Chem.* **2007**, *2007*, 4019-4031.
138. Gowda, B. T.; Usha, K. M.; Jayalakshmi, K. L., *Z. Naturforsch* **2003**, *58*, 801-806.
139. Thopate, S. R.; Kote, S. R.; Rohokale, S. V.; Thorat, N. M. **2011**, *35*, 124-125.
140. Taylor, J. E.; Jones, M. D.; Williams, J. M. J.; Bull, S. D. *J. Org. Chem.* **2012**, *77*, 2808-2818.

141. Lee, Y. M.; Moon, M. E.; Vajpayee, V.; Filimonov, V. D.; Chi, K.-W. *Tetrahedron* **2010**, *66*, 7418-7422.
142. Zhang, G.; Ren, X.; Chen, J.; Hu, M.; Cheng, J. *Org. Lett.* **2011**, *13*, 5004-5007.
143. Morimoto, H.; Tsubogo, T.; Litvinas, N. D.; Hartwig, J. F. *Angew. Chem. Int. Ed.* **2011**, *50*, 3793-3798.
144. Augustine, J. K.; Kumar, R.; Bombrun, A.; Mandal, A. B. *Tetrahedron Lett.* **2011**, *52*, 1074-1077.
145. Yang, S.; Li, B.; Wan, X.; Shi, Z. *J. Am. Chem. Soc.* **2007**, *129*, 6066-6067.
146. Gao, K.; Yu, C.-B.; Li, W.; Zhou, Y.-G.; Zhang, X. *Chem. Commun.* **2011**, *47*, 7845-7847.
147. Furuya, Y.; Ishihara, K.; Yamamoto, H. *J. Am. Chem. Soc.* **2005**, *127*, 11240-11241.
148. Chrétien, J.-M.; Zammattio, F.; Le Grogneq, E.; Paris, M.; Cahingt, B.; Montavon, G.; Quintard, J.-P. *J. Org. Chem.* **2005**, *70*, 2870-2873.
149. Bradamante, S.; Pagani, G. A. *J. Org. Chem.* **1980**, *45*, 114-122.
150. Dooleweerd, K.; Fors, B. P.; Buchwald, S. L. *Org. Lett.* **2010**, *12*, 2350-2353.
151. Lewis, E. A.; Adamek, T. L.; Vining, L. C.; White, R. L. *J. Nat. Prod.* **2003**, *66*, 62-66.

Biographical information

Horacio Enrique Barragan Peyrani was born in Monterrey, Mexico in 1989. He obtained his bachelor degree in Industrial Chemistry from Universidad Autonoma de Nuevo Leon in 2011. After working in joint research projects between university and industry, he decided to pursue higher education studies in the United States and obtained his PhD in Chemistry from the University of Texas at Arlington in 2019. His area of specialty is Organic Chemistry and his research interests include: methodology development of new synthetic reactions under mild conditions, small molecule synthesis, triazene chemistry and chemistry of organic nitrogen-containing molecules. His plans for the future are to work in the pharmaceutical or agrochemical industry to continue developing his research and organic chemistry skills and apply them for the synthesis of molecules with significant applications.